frontiers | Research Topics

Ionizing radiation reprograms tumor immune microenvironment by inducing immunogenic cell death

Edited by
Fei Yu, Shaoli Song, Haojun Chen, Kuangyu Shi and Weijun Wei

Published in
Frontiers in Immunology

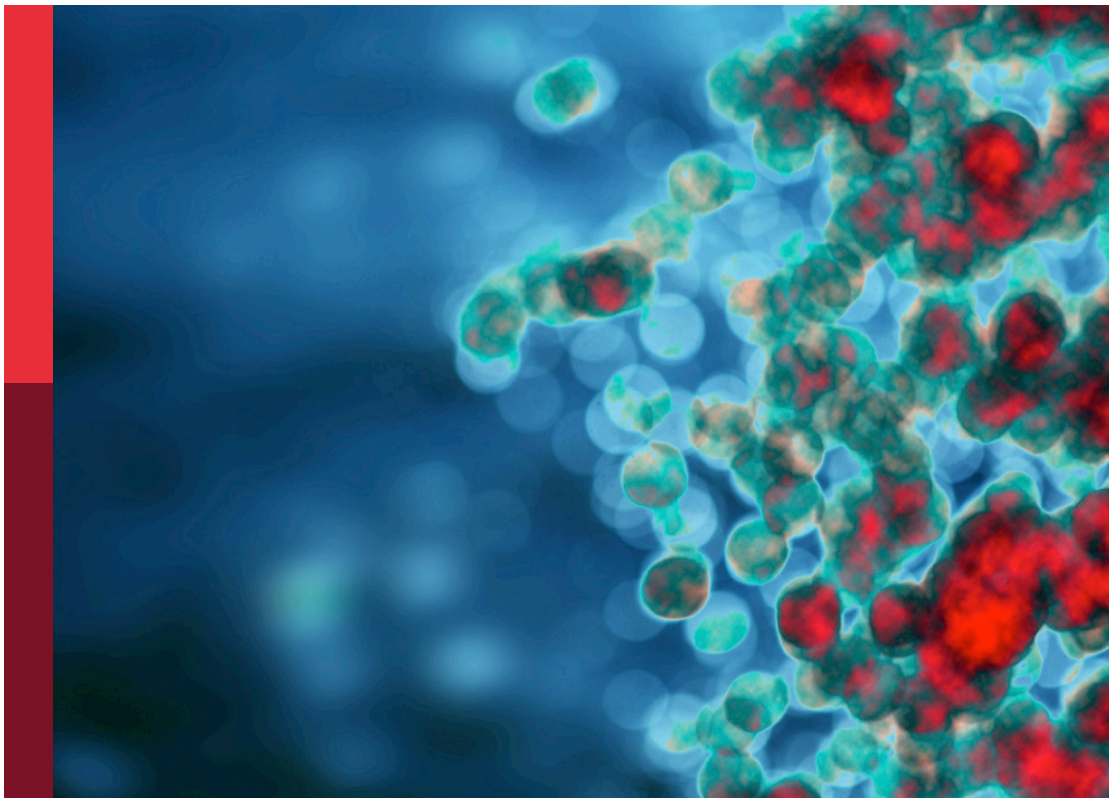

ISSN 1664-8714
ISBN 978-2-8325-3411-3
DOI 10.3389/978-2-8325-3411-3

About Frontiers

Frontiers is more than just an open access publisher of scholarly articles: it is a pioneering approach to the world of academia, radically improving the way scholarly research is managed. The grand vision of Frontiers is a world where all people have an equal opportunity to seek, share and generate knowledge. Frontiers provides immediate and permanent online open access to all its publications, but this alone is not enough to realize our grand goals.

Frontiers journal series

The Frontiers journal series is a multi-tier and interdisciplinary set of open-access, online journals, promising a paradigm shift from the current review, selection and dissemination processes in academic publishing. All Frontiers journals are driven by researchers for researchers; therefore, they constitute a service to the scholarly community. At the same time, the *Frontiers journal series* operates on a revolutionary invention, the tiered publishing system, initially addressing specific communities of scholars, and gradually climbing up to broader public understanding, thus serving the interests of the lay society, too.

Dedication to quality

Each Frontiers article is a landmark of the highest quality, thanks to genuinely collaborative interactions between authors and review editors, who include some of the world's best academicians. Research must be certified by peers before entering a stream of knowledge that may eventually reach the public - and shape society; therefore, Frontiers only applies the most rigorous and unbiased reviews. Frontiers revolutionizes research publishing by freely delivering the most outstanding research, evaluated with no bias from both the academic and social point of view. By applying the most advanced information technologies, Frontiers is catapulting scholarly publishing into a new generation.

What are Frontiers Research Topics?

Frontiers Research Topics are very popular trademarks of the *Frontiers journals series*: they are collections of at least ten articles, all centered on a particular subject. With their unique mix of varied contributions from Original Research to Review Articles, Frontiers Research Topics unify the most influential researchers, the latest key findings and historical advances in a hot research area.

Find out more on how to host your own Frontiers Research Topic or contribute to one as an author by contacting the Frontiers editorial office: frontiersin.org/about/contact

Ionizing radiation reprograms tumor immune microenvironment by inducing immunogenic cell death

Topic editors

Fei Yu — Tongji University School of Medicine, China
Shaoli Song — Fudan University, China
Haojun Chen — First Affiliated Hospital of Xiamen University, China
Kuangyu Shi — University of Bern, Switzerland
Weijun Wei — Shanghai Jiao Tong University, China

Citation

Yu, F., Song, S., Chen, H., Shi, K., Wei, W., eds. (2023). *Ionizing radiation reprograms tumor immune microenvironment by inducing immunogenic cell death*. Lausanne: Frontiers Media SA. doi: 10.3389/978-2-8325-3411-3

Table of contents

frontiers | Frontiers in Immunology

TYPE Editorial
PUBLISHED 20 June 2023
DOI 10.3389/fimmu.2023.1235024

OPEN ACCESS

EDITED AND REVIEWED BY
Weiyu Chen,
Zhejiang University, China

*CORRESPONDENCE
Fei Yu
yufei_021@163.com

RECEIVED 05 June 2023
ACCEPTED 13 June 2023
PUBLISHED 20 June 2023

CITATION
Yu F, Shi K, Song S, Chen H and Wei W (2023) Editorial: Ionizing radiation reprograms tumor immune microenvironment by inducing immunogenic cell death.
Front. Immunol. 14:1235024.
doi: 10.3389/fimmu.2023.1235024

Editorial: Ionizing radiation reprograms tumor immune microenvironment by inducing immunogenic cell death

Fei Yu[1,2]*, Kuangyu Shi[3,4], Shaoli Song[5,6], Haojun Chen[7] and Weijun Wei[8]

[1]Department of Nuclear Medicine, Shanghai Tenth People's Hospital, Tongji University School of Medicine, Shanghai, China, [2]Institute of Nuclear Medicine, Tongji University School of Medicine, Shanghai, China, [3]Department of Nuclear Medicine, Inselspital, Bern University Hospital, University of Bern, Bern, Switzerland, [4]Computer Aided Medical Procedures and Augmented Reality, Institute of Informatics I16, Technical University of Munich, Munich, Germany, [5]Department of Nuclear Medicine, Fudan University Shanghai Cancer Center, Shanghai, China, [6]Shanghai Engineering Research Center of Molecular Imaging Probes, Shanghai, China, [7]Department of Nuclear Medicine and Minnan PET Center, The First Affiliated Hospital of Xiamen University, Xiamen, China, [8]Department of Nuclear Medicine, Institute of Clinical Nuclear Medicine, Renji Hospital, Shanghai Jiao Tong University School of Medicine, Shanghai, China

KEYWORDS

ionizing radiation, tumor immune microenvironment, immunogenic cell death, immunotharapy, biomarker

Editorial on the Research Topic

Ionizing radiation reprograms tumor immune microenvironment by inducing immunogenic cell death

Internal irradiation (IRT) and external-beam radiotherapy (EBRT) are two types of radiotherapy that use radiation beams like X-rays, gamma rays, or gamma rays to kill cancer cells directly and alter the tumor immunological microenvironment. Studies have currently shown a connection between radiotherapy and the tumor immune microenvironment, but further research is still required. In order to improve the efficacy of treatment, more information regarding the underlying mechanisms and how to improve the sensitivity of radiotherapy is required. Immune checkpoint blocking therapy (ICB) still has a low response rate due to the cold tumor microenvironment, which may be overcome so that the efficacy could be further increased when ICB is combined with other treatments. To assess the effectiveness and determine the prognosis, it will be helpful to search for the corresponding biomarkers.

As a result, the relationship between radiotherapy and the tumor immune microenvironment was revealed in the current Research Topic. Additionally, new techniques to increase the sensitivity of radiotherapy therapy were developed, and biomarkers to assess therapeutic efficacy and forecast therapeutic prognosis were investigated. The intricacy of the systemic and local immune environments in various cancer types is examined by Iliadi et al. How radiation shapes the immune landscape is focused on. Radiation was found to directly influence tumor cells and their surroundings, which mostly primes the immune response but may potentially inhibit it. When combined with immunotherapy, radiation causes an increase in infiltrating T cells and the production

of programmed death ligand 1, which may be beneficial for the patient. Radiation causes an increase in immunosuppressive populations, particularly pro-tumoral M2 macrophages and myeloid-derived suppressor cells (MDSCs), in a number of malignancies. They also reveal potential prognostic and predictive information gleaned from the patient's iTME and systemic immune profile to direct therapy choices. Zhu et al. found that the radio-sensitivity of TIME and circulating lymphocytes must be carefully taken into account when choosing the most appropriate radiotherapy regimen for combination with immunotherapy because different immune cell types, with different states of differentiation, exhibit different radio-sensitivities. The benefits of low-dose radiation (LDRT) over high-dose radiotherapy (HDRT) were highlighted by Ji et al. Firstly, LDRT has a low level of toxicity. It is challenging to reach the dosage limit for the organ at risk with SBRT, whereas dose restrictions will be easier to satisfy with LDRT, if radiotherapy is to be delivered simultaneously to many lesions within an organ. Secondly, LDRT is more secure for individuals who have previously undergone radiation treatment. When re-radiation is carried out with LDRT, there is a very little chance that the normal tissue dosage limitations will be exceeded. Finally, it is simpler to deliver LDRT. LDRT can be carried out in clinical settings using three-dimensional technology, but HDRT necessitates specialist imaging, respiratory gating, and even the implantation of gold fiducials.

The potential for radiotherapy to induce an immunogenic cell death (ICD) is supported by Mariampillai et al. They also demonstrate that using radiotherapy in combination with ATR inhibition boosts this potential. Additionally, they discovered that pan-caspase inhibition eliminates HMGB1 release, marginally boosts ATP secretion, and has little or no impact on ecto-CALR. Understanding these pathways will also probably make it easier to take advantage of the combined therapy's immunostimulatory effects, perhaps by administering immune checkpoint blockade therapy afterward. Besides, Yuan et al. found that the gut microbiota may also be a common biological target for minimizing the side effects of radioimmunotherapy, inhibiting the target may improve efficacy and point patients with CRC in the right direction for achieving a longer survival and a higher quality of life after treatment. In order to achieve multimodal imaging and theranostics of lymph node metastasis, the Zhang et al. developed a nanoprobe conjugated trastuzumab based on upconversion nanoparticles, further developed a nanonuclear drug labeled ^{68}Ga or ^{177}Lu, and adopted a new imaging and theranostic strategy for lymphatic targeting. It is intended to direct research into and advancements in more potent theranostic methods for treating malignancies.

According to Gao et al., the parameters of ^{18}F-fluorodeoxyglucose PET/CT served as biomarkers and were crucial in the treatment of ICIs, allowing for the assessment of the tumor microenvironment, the identification of immune-related adverse events, the evaluation of therapeutic efficacy, and the prognosis of the treatment. Transient receptor potential channels (TRPC) are essential regulators of the development and spread of cancer. Wang et al. created a unique risk score for colorectal cancer prognosis using eight TRPCG with excellent discrimination and calibration. A promising biomarker for ICIs and neoadjuvant therapy in the management of colorectal cancer could be the present TRPCRS. Fatty acid metabolism (FAM) is closely linked to the development of cancer and carcinogenesis.

In the context of cancer, Zhou et al. investigated the critical impact of FAM on the gut flora and metabolism. Patients with high-risk scores were closely associated with activating type I interferon response and inflammation-promoting actions, according to an extensive analysis of the tumor microenvironment based on the FAM-related signature. In patients with locally advanced rectal cancer, their findings suggest that FAM may be able to predict the outcome of neoadjuvant chemotherapy and radiation therapy as well as the prognosis of disease-free survival (DFS) and overall survival (OS). Finding precise biomarkers may aid in risk classification and treatment choices for locally advanced rectal cancer, according to Wang et al.

Altogether, after having seen all individual contributions to this Research Topic, we see that the topic of "*Ionizing Radiation Reprograms Tumor Immune Microenvironment by Inducing Immunogenic Cell Death*" is broad and has its roots in an active research field. The far-reaching implications of ionizing radiation-related tumor immune microenvironment make this an intriguing subject important for future studies to gain a better understanding.

Author contributions

FY wrote the paper. All authors listed have made a substantial, direct and intellectual contribution to the work, and approved it for publication.

Acknowledgments

We thank the authors of the 10 publications of the Research Topic for their high-quality work. We thank the Frontiers in Immunology Editorial Office and the Editor for their support.

Conflict of interest

WW is a consultant of Alpha Nuclide Ningbo Medical Technology Co., Ltd.

The remaining authors declare that the research was conducted in the absence of any commercial or financial relationships that could be construed as a potential conflict of interest.

Publisher's note

frontiers | Frontiers in Immunology

TYPE Original Research
PUBLISHED 18 October 2022
DOI 10.3389/fimmu.2022.1014834

OPEN ACCESS

EDITED BY
Haojun Chen,
First Affiliated Hospital of Xiamen University, China

REVIEWED BY
Di Fan,
Capital Medical University, China
Shaobo Yao,
First Affiliated Hospital of Fujian Medical University, China

*CORRESPONDENCE
Junxin Wu
junxinwufj@aliyun.com
Gang Chen
naichengang@126.com

†These authors have contributed equally to this work

SPECIALTY SECTION
This article was submitted to Cancer Immunity and Immunotherapy, a section of the journal Frontiers in Immunology

RECEIVED 09 August 2022
ACCEPTED 23 September 2022
PUBLISHED 18 October 2022

CITATION
Wang L, Chen X, Zhang H, Hong L, Wang J, Shao L, Chen G and Wu J (2022) Comprehensive analysis of transient receptor potential channels-related signature for prognosis, tumor immune microenvironment, and treatment response of colorectal cancer.
Front. Immunol. 13:1014834.
doi: 10.3389/fimmu.2022.1014834

Comprehensive analysis of transient receptor potential channels-related signature for prognosis, tumor immune microenvironment, and treatment response of colorectal cancer

Lei Wang[1†], Xingte Chen[1†], Hejun Zhang[2†], Liang Hong[1], Jianchao Wang[2], Lingdong Shao[1], Gang Chen[2*] and Junxin Wu[1*]

[1]Department of Radiation Oncology, Clinical Oncology School of Fujian Medical University, Fujian Cancer Hospital, Fuzhou, China, [2]Department of Pathology, Clinical Oncology School of Fujian Medical University, Fujian Cancer Hospital, Fuzhou, China

Background: Transient receptor potential channels (TRPC) play critical regulatory functions in cancer occurrence and progression. However, knowledge on its role in colorectal cancer (CRC) is limited. In addition, neoadjuvant treatment and immune checkpoint inhibitors (ICIs) have increasing roles in CRC management, but not all patients benefit from them. In this study, a TRPC related signature (TRPCRS) was constructed for prognosis, tumor immune microenvironment (TIME), and treatment response of CRC.

Methods: Data on CRC gene expression and clinical features were retrospectively collected from TCGA and GEO databases. Twenty-eight TRPC regulators (TRPCR) were retrieved using gene set enrichment analysis. Different TRPCR expression patterns were identified using non-negative matrix factorization for consensus clustering, and a TRPCRS was established using LASSO. The potential value of TRPCRS was assessed using functional enrichment analysis, tumor immune analysis, tumor somatic mutation analysis, and response to preoperative chemoradiotherapy or ICIs. Moreover, an external validation was conducted using rectal cancer samples that received preoperative chemoradiotherapy at Fujian Cancer Hospital (FJCH) *via* qRT-PCR.

Results: Among 834 CRC samples in the TCGA and meta-GEO cohorts, two TRPCR expression patterns were identified, which were associated with various immune infiltrations. In addition, 266 intersected genes from 5564 differentially expressed genes (DEGs) between two TRPC subtypes, 4605 DEGs between tumor tissue and adjacent non-tumor tissue (all FDR< 0.05, adjusted P< 0.001),

and 1329 prognostic related genes (P< 0.05) were identified to establish the TRPCRS, which was confirmed in the TCGA cohort, two cohorts from GEO, and one qRT-PCR cohort from FJCH. According to the current signature, the high-TRPC score group had higher expressions of PD-1, PD-L1, and CTLA4, lower TIDE score, and improved response to anti-PD-1 treatment with better predictive ability. Compared to the high-TRPC score group, the low-TRPC score group comprised an immunosuppressive phenotype with increased infiltration of neutrophils and activated MAPK signaling pathway, but was more sensitive to preoperative chemoradiotherapy and associated with improved prognosis

Conclusions: The current TRPCRS predicted the prognosis of CRC, evaluated the TIME in CRC, and anticipated the response to immune therapy and neoadjuvant treatment.

KEYWORDS

transient receptor potential channels, colorectal cancer, prognosis, immune checkpoint inhibitor, neoadjuvant treatment

Introduction

Colorectal cancer (CRC) is one of the most common cancers worldwide (1), with 151,030 cases diagnosed annually in the United States (2). Currently, its incidence is increasing worldwide (1). Moreover, CRC is the third leading cause of cancer mortality worldwide (1), with 0.9 million deaths in the United States yearly. Current plights of the CRC are as followed: 1) lack of specific markers of early screening, regardless of promotion of colonoscopy (3); 2) inaccuracy of the current staging systems on prognosis and management (4, 5), and 3) short of biomarkers for both local and systematic treatment in the era of precision medicine and individualized therapy (4, 5). Hence, early diagnosis biomarkers, accurate prognosis prediction, and precise direct management for CRC are urgently required (3).

Transient receptor potential channels (TRPC) was first reported in 1969 (6). Numerous homologous TRPC family genes are identified as TRPC regulators (TRPCR) (7, 8). In 2021, Ardem Patapoutian and David Julius were awarded the Nobel Prize in Physiology or Medicine for the discovery of TRPC (9), which are multifunctional signaling molecules investigated in channelopathy-related diseases including neurodegenerative (10), cardiovascular (11), and metabolic diseases (12). However, increasing reports support their roles in carcinogenesis, tumor invasion, migration, angiogenesis, and prognosis (13–15). There were differences in expression of several TRPCR, such as TRPV1, TRPV6, TRPM4, and TRPC6 between CRC and normal tissues (16, 17). Some TRPCR, such as TRPM6 and TRPC1, are associated with the prognosis of patients with CRC (16, 17). However, a comprehensive analysis of TRPCR on CRC prognosis and management is inadequate.

Although neoadjuvant treatment and immune checkpoint inhibitors (ICIs) play an increasing role in CRC management, not all patients benefit from them (18, 19). In addition, no biomarkers exist to screen their potential benefit (18). Evidence showed that tumor immune microenvironment (TIME) (20), which is associated with TRPC *via* polarization of macrophages, recruitment of chemokines, and activation of effector cells, strongly influences cancer treatment response (20, 21). In the present study, non-negative matrix factorization (NMF) clustering was adopted to identify the correlations between TRPCR and immune infiltration, and a TRPC-related signature (TRPCRS) was established to predict the prognosis of CRC, and explore the intrinsic connections between TRPCRS and TIME. Furthermore, correlations between TRPCRS and response to neoadjuvant treatment or ICIs were conducted to determine the potential value of the current signature.

Methods

Patients and data source

The analytical process of the study is provided in Figure 1. Data on CRC gene expression and clinical features were retrospectively collected from The Cancer Genome Atlas

10.3389/fimmu.2022.1014834

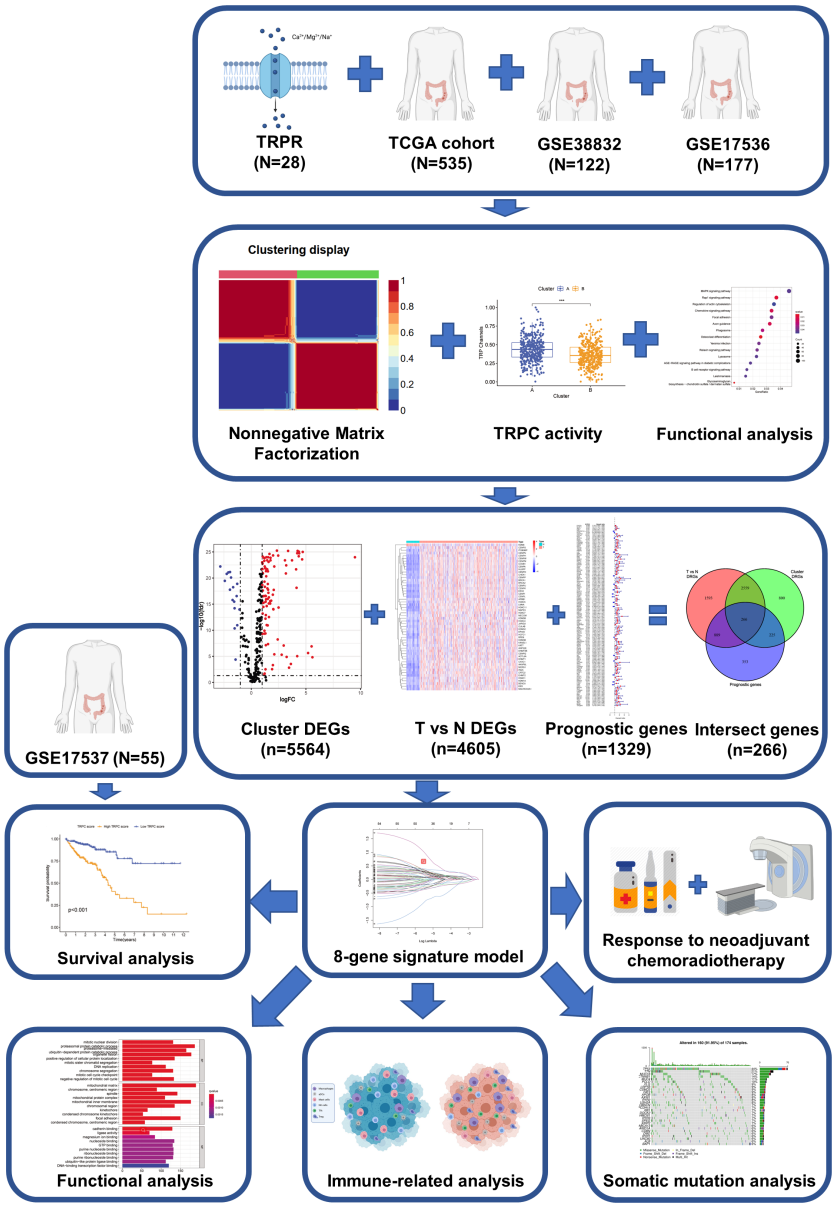

FIGURE 1
The flow-chart of this study.

(TCGA, https://cancergenome.nih.gov/) and Gene Expression Omnibus (GEO) databases (https://www.ncbi.nlm.nih.gov/geo/). TCGA RNA sequencing data were converted from fragments per kilobase of exon model per million mapped fragments (FPKM) format to millions of transcripts per kilobase (TPM). Batch effects among TCGA-COAD, TCGA-READ, and GEO datasets were eliminated using "ComBat" method in "sva" R package, and TCGA-COAD-READ and meta-GEO (GSE38832 (22) and GSE17536 (23)) datasets were constructed. Genomic mutation data of TCGA-COAD-READ, including somatic mutations and copy number variations, were obtained from UCSC's Xena database. Copy number changes of 28 TRPCR in human chromosomes were mapped using the R package "rcircos". The corresponding TRPCR were extracted from the Gene Set Enrichment Analysis (GSEA) website (https://www.gsea-msigdb.org/GSEA/index.jsp, Table S1). Moreover, 85 frozen rectal cancer samples that received both, neoadjuvant treatment and radical surgery, at Fujian Cancer Hospital (FJCH) between March 2016 - March 2021 were added to conduct external validation. This study was approved by the Ethics Committee of FJCH (K2021-03-017).

The baseline characteristics of patients in the cohort are presented in Table 1.

Consensus molecular clustering of 28 TRPCR

Different TRPCR expression patterns were identified using NMF based on the expressions of 28 TRPCR using the R package "NMF" (version 0.22.0) (24). The expressions of 28 TRPCR (matrix A) were decomposed into two non-negative matrices, W and H (i.e., A≈WH). Matrix A was repeatedly decomposed, and its output was aggregated to obtain a consistent cluster of CRC samples (TCGA-COAD-READ and meta-GEO). The optimal k of clusters was selected according to apparent, discrete, and silhouette coefficients. Brunet algorithm and 200 nrun were used for consensus clustering.

Identification of differentially expressed genes and enriched pathways

Differentially expressed genes (DEGs) among TRPC subtypes (DEG_a, false discovery rate< 0.05, adjusted P< 0.001) were obtained using the "limma" R package. The pathway activity of "REACTINE_TRP_CHANNELS" in each sample was calculated using "GSVA" packages, and the differences among various TRPC subtypes were analyzed.

Construction of TRPCRS

DEGs between tumor tissues and adjacent non-tumor tissues (DEGb, FDR< 0.05, adjusted P< 0.001) were determined using the "limma" R package. Prognostic genes were screened using the "survival" R package *via* univariate Cox regression analysis (P< 0.05). The overlapped genes among DEGa, DEGb, and prognostic genes were identified as candidate TRPC-related genes (TRPCGs). These candidate genes were screened again based on the least absolute shrinkage and selection operator (LASSO) (25) estimation to avoid over-fitting the model. The optimal value of the penalty coefficient lambda was selected after running the cross-validation probability 1000 times through the "glmnet" software package. Considering that the genes included in the gene signature were derived from DEGa between two clusters with significantly different TRPC, the resulting gene signature was called TRPCRS. Thus, the equation was established as follows:

$$TRPC\ score = \sum_{i=1}^{n} Coef(i) \times x(i)$$

According to the corresponding median of TRPCRS in each dataset, patients were divided into low TRPC score and high TRPC score groups.

Validation of TRPC score model

The TRPC score was validated in TCGA-COAD-READ, meta-GEO, and an external validation set of GSE17537 (26). The survival difference between the two groups was visually displayed using the receiver operator characteristic (ROC) curves and "survival" R package. The significance of the TRPC score was further analyzed using the multivariate Cox regression model, and the relationships between the TRPC score and clinical features were evaluated using the Wilcox test.

Function analysis

The Gene Ontology (GO) and Kyoto Encyclopedia of Genes and Genomes (KEGG) enrichment analyses were conducted on DEG_a using the "clusterProfiler" R package (27). Stromal and immune cells infiltrated in malignant tumors were estimated using the ESTIMATE algorithm, utilizing the unique properties of transcription profiles to infer tumor cell count and tumor purity.

Immune-related analysis

The relative abundance of 28 immune cells in TIME was evaluated using the "GSVA" package (28). Differences in the immune cells and immune checkpoint genes were compared between high- and low-TRPC scores. Scores of tumor immune dysfunction and exclusion (TIDE), microsatellite instability (MSI) expression, dysfunction, and rejection were calculated using http://tide.harvard.edu, and the differences were compared between the two groups. In addition, the prediction value of the TRPC score for immunotherapy was estimated using the "IMvigor 210" dataset package (29).

Somatic mutation analysis

Quantity and quality of mutations in high- and low- TRPC scores were calculated using the "Maftools" R package. Missense, nonsense, continuous and silent, and frameshift/in-box insertion and deletion mutations were counted after excluding germline mutations without somatic mutations. Tumor mutation burden (TMB) is defined as the total number of somatic mutations.

Development of risk prediction model

In addition to TRPC scores and clinical features, a nomogram predicting 1-year, 3-year, and 5-year overall survival (OS) of patients with CRC was established using the "RMS" R package. The nomogram prediction was evaluated using the calibration curve, restricted mean survival (RMS), C index, ROC curve, and decision curve analysis (DCA).

Response prediction of neoadjuvant therapy

GSE45404 (30) and GSE87211 (31) were administrated to conduct external validation, among which patients with rectal cancer received neoadjuvant treatment. GSE45404 contained data on response to neoadjuvant treatment and was graded using the Mandard tumor regression grade (TRG), while GSE87211 contained data on clinicopathological characteristics and survival. "REACTINE_TRP_CHANNELS", "KEGG_MISMATCH_REPAIR", "KEGG_MAPK_SIGNALING_PATHWAY", and "KEGG_B_CELL_SIGNALING_PATHWAY" of each sample were calculated using "GSVA" R package, and the infiltration situation of 28 immune cells in the TIME were plotted using "ggplot2" and "corrplot" R packages, respectively.

Quantitative real time polymerase chain reaction

Quantitative real time polymerase chain reaction (qRT-PCR) was performed on 85 samples by the Department of Pathology Department of FJCH. RNA was extracted using TRIzol (Takara, Kusatsu, Shiga, Japan), and random primers were reverse transcribed using a cDNA synthesis kit (Thermo Fisher Scientific, Waltham, MA, USA). In addition, mRNA expression levels were detected using Roche LightCycler 480 (Basel, Switzerland) and FastStart Essential DNA Green Master Mix (Thermo Fisher Scientific). The mRNA expressions of each hub gene were normalized to that of β-actin. All qRT-PCR analyses were conducted in triplicates, and the average value was calculated using the Livak method. The primers used in this study were synthesized using Sunya Biotech (Fuzhou, China) and are listed in Supplementary Table 2.

Statistical analyses

All analyses in this study were performed using R-3.6.1. Normally distributed variables were compared using Student's t-test, while non-normally distributed variables were compared using the Wilcoxon rank sum test. All tests were two-sided, and $P< 0.05$ was considered to be statistically significant.

Results

Genetic alteration landscape of TRPCR in CRC

In the present study, TRPCR were widely located in almost all human chromosomes (Supplementary Figure 1A). Supplementary Figure 1B depicts interactions of 28 TRPCR expressions, and TRPC1, TRPA1, and RIPK as the top three TRPCR. Furthermore, analysis of 28 TRPCR revealed that copy number variations (CNV) mutations were prevalent. TRPC4AP, TRPC4, TRPA1, TRPV6, TRPC1, TRPC5, TRPV3, TRPV1, and TRPM6 showed widespread CNV amplification. In contrast, TRPV5, MCOLN3, TRPM8, RIPK3, TRPM2, RIPK1, TRPC6, TRPM1, MCOLN1, TRPC3, TRPC7, TRPV4, TRPM7, TRPM4, TRPM3, MLKL, and TRPV2 showed prevalent CNV deletions (Supplementary Figure 1C). TRPCR mutations were detected in 137 (34.34%) patients from 399 samples. Supplementary Figure 1D exhibited the landscape of the mutations, with TRPM5, TRPC3, and TRPC7 as the top three mutations.

Almost all TRPCR were downregulated, while MLKL, TRPC4AP, TRPM2, and TRPV4 were upregulated in the CRC tissues compared with normal tissues ($P< 0.05$, Supplementary Figure 1E). No significant differences were observed in MCOLN3, TRPC4, TRPM1, TRPM8, TRPV1, and TRPV5 ($P > 0.05$, Supplementary Figure 1E). Unfortunately, only two TRPCR, including TRPM5 and TRPV4 ($HR > 1$, $P< 0.01$), were associated with the OS of patients with CRC (Supplementary Figure 1F).

Unsupervised clustering of 28 TRPCR and differences between two clusters

As shown in Supplementary Figure 2, the highest intra-group correlations and lowest inter-group correlations were observed when $k = 2$ in the TCGA and meta-GEO cohorts, indicating that patients can be divided into cluster A and cluster B based on 28 TRPC-associated DEGs (DEG_a). Figure 2A exhibited two distinct patterns of CRC samples, which had two apparently different Kaplan–Meier survival curves ($P< 0.05$, Figure 2B). The silhouette plot of the two clusters is shown in Figure 2C. Interestingly, TRPC was more enriched in cluster A compared with cluster B ($P< 0.05$, Figure 2D). The single sample gene set enrichment analysis (ssGSEA) scores of

10.3389/fimmu.2022.1014834

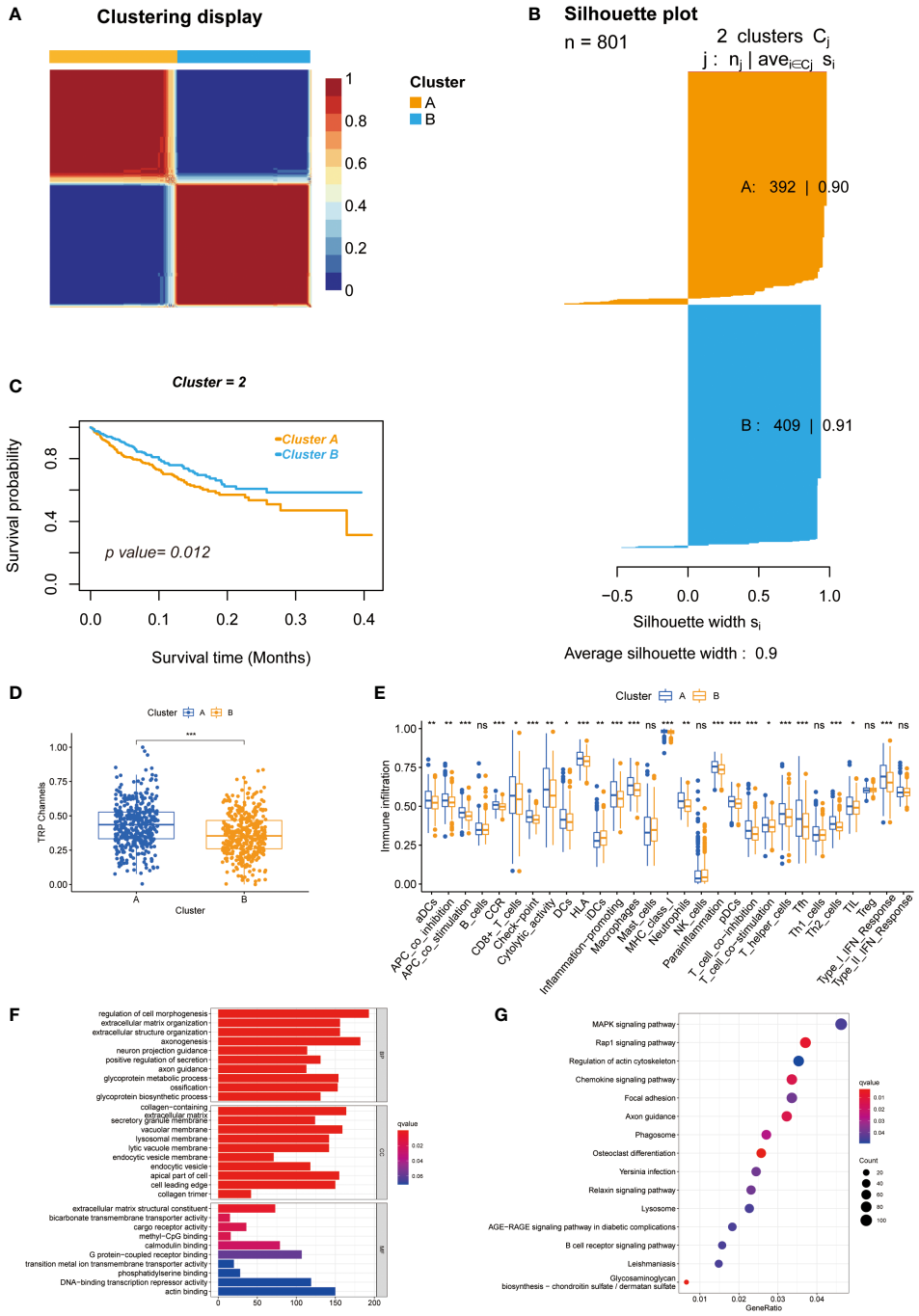

FIGURE 2
Unsupervised clustering of 28 TRPCR and differences between two clusters. **(A)** Heatmap representation of NMF clustering for TRPCR. **(B)** Kaplan-Meier curves of OS with two TRPC clusters. **(C)** Silhouette plot of the two clusters. **(D)** The TRPC activity between two clusters. **(E)** The ssGSEA scores of immune cells and immune-related functions with two clusters. **(F, G)** Functional annotation for TRPC clusters using GO and KEGG enrichment analysis. GO, Gene Ontology; KEGG, Kyoto Encyclopedia of Genes and Genomes; OS, overall survival; ssGSEA, single sample gene set enrichment analysis; TRPC, transient receptor potential channels; TRPCR, transient receptor potential channels regulators; ns, not significant; *P< 0.05; **P< 0.01; ***P< 0.001.

aDCS, antigen-presenting cells (APC) co-inhibition, APC co-stimulation, chemokine receptor (CCR), $CD8^+$ T-cells, immune checkpoint, cytolytic activity, dendritic cells (DCs), human leukocyte antigen (HLA), inflammation-promoting, macrophages, major histocompatibility complex (MHC) class I, neutrophils, parainflammation, plasmacytoid dendritic cell (pDCs), T cell co-inhibition, T cell co-stimulation, T helper (Th) cells, follicular helper T cell (Tfh), Th2 cells, tumor infiltrating lymphocyte (TIL), and Type I interferon (INF) response were significantly higher in cluster A than that in cluster B; while it was on the contrary in terms of iDCs ($P< 0.05$, Figure 2E). GO membrane-related pathways were enriched in cellular components (CC) (Figure 2F), and KEGG enrichment analysis showed that MAPK ranked first among the enriched signaling pathways (Figure 2G).

Screening of characteristic predictors and prognostic value of TRPCRS

A total of 5564 genes were identified as DEG_a (Table S3), 4605 as DEG_b (Table S4), and 1329 as prognostic-related genes (Table S5). Among these, 266 intersected genes were selected as candidate genes. Supplementary Figure 3A shows the coefficients of all 266 intersected genes TRPCG according to lambda.min criteria. Using the LASSO regression analysis, 8 gene signatures (UCN, FJX1, TIPM1, PCOLCE2, CD177, PPARGC1A, CLDN23, and MTOR4) were optimal with a minimum lambda (Supplementary Figure 3B). Among these 8 genes, 4 were risk factors (UCN, FJX1, TIPM1, and PCOLCE2), and 4 were protective factors (CD177, PPARGC1A, CLDN23, and MTOR4) (Figure 3A). The correlations between 8 TRPCG and 28 TRPCR are shown in Figure 3B. The

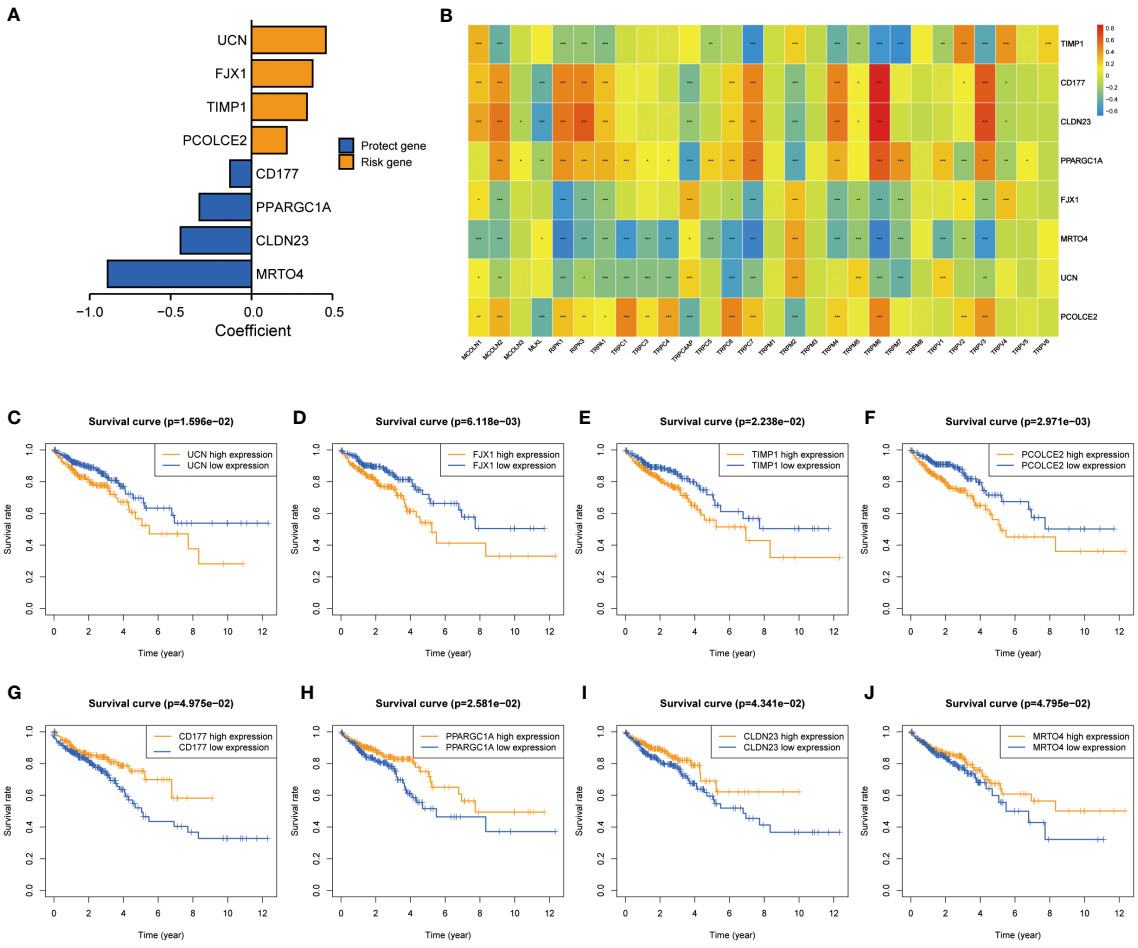

FIGURE 3
Screening of characteristic predictors and prognostic value of TRPCRS. **(A)** The coefficient value of the 8 TRPCGs associated with the TRPC score in CRC. **(B)** The correlation between 8 TRPCGs and 28 TRPCR. **(C–J)** Survival curve analysis of CRC patients based on the expression status of UCN, FJX1, TIMP1, PCOLCE2, CD177, PPARGC1A, CLDN23, MRTO4 genes. CRC, colorectal cancer; TRPCGs, transient receptor potential channels-related genes; TRPCR, transient receptor potential channels regulators; TRPCRS, transient receptor potential channels related signature; ns, not significant; *P< 0.05; **P< 0.01; ***P< 0.001.

apparent Kaplan–Meier survival curves between different groups stratified by the expression of 8 genes are shown in Figures 3C–J ($P< 0.05$). TRPC scores were calculated according to the following formula: TRPC score = [UCN expression×(0.4591)] + [FJX1 expression×(0.3770)] + [TIMP1 expression×(0.3425)] + [PCOLCE2 expression×(0.2178)] + [CD177 expression×(−0.1330)] + [PPARGC1A expression×(−0.3223)] + [CLDN23 expression×(−0.4393)] + [MRTO4 expression×(−0.8897)]. Interestingly, Gene set variation analysis (GSVA) showed that TRPC activity was positively correlated with the TRPC score (Supplementary Figure 3C).

Prognostic analysis of TRPC scores

Considering the median score as the cut-off value, patients in the TCGA cohort were divided into low- and high-TRPC score subgroups. The Kaplan–Meier survival curve showed that the median OS was significantly shorter in the high-TRPC score subgroup than in the low-TRPC score subgroup (high vs. low, HR = 2.33, 95% confidence interval: 1.64–3.31, $P< 0.001$, Figure 4A). The area under the curve (AUC) at 1-year, 3-year, and 5-year were 0.713, 0.700, and 0.801, respectively (Figure 4D). The distinct distribution status of patients between the high- and low-TRPC score subgroups is shown in Figure 4G. Univariate Cox regression analysis showed that TRPC score was negatively associated with OS of patients with CRC. Additionally, multivariate Cox regression analysis showed that TRPC score was an independent risk factor for OS (both $P< 0.05$, Figure 4J). Similar findings were observed in the meta-GEO (Figure 4B, E, H, K) and GSE17537 cohorts (Figures 4C, F, I, L).

Subgroup analyses stratified by different characteristics were conducted to evaluate the correlations between the current TRPC score and other clinicopathological characteristics (Supplementary Figure 4A). No significant differences were observed in TRPC scores stratified by sex (female vs. male, $P > 0.05$, Supplementary Figure 4B) and age (≤65 vs. >65, $P > 0.05$, Supplementary Figure 4C). No significant differences were observed among all subgroups stratified by stage ($P > 0.05$). However, patients in stage IV had higher TRPC scores than those in other stage groups (all $P< 0.05$, Supplementary Figure 4D). Interestingly, patients with microsatellite stability (MSS) had lower TRPC scores than those with microsatellite instability-low (MSI-L) and microsatellite instability-high (MSI-H), but no differences were observed between MSI-L and MSI-H ($P > 0.05$, Supplementary Figure 4E).

GO and KEGG analyses

GO analysis showed that replication-related biological processes (BP), mitochondria-related CC, and division-related molecular functions (MF) were enriched in the TCGA cohort (Supplementary Figure 5A). Enriched signaling pathways associated with CRC and mismatch repair were identified using KEGG analysis (Supplementary Figure 5B). Furthermore, membrane-related CC was enriched in the meta-GEO cohort (Supplementary Figure 5C), and PI3K-AKT and PPAR signaling pathways were identified using KEGG analysis (Supplementary Figure 5D).

Immune landscapes and prediction of immunotherapeutic benefits

The association between TRPC and estimation of stromal and immune cells in malignant tumour tissues using expression data (ESTIMATE) scores was investigated using the ESTIMATE algorithm, which showed that stromal, immune, and ESTIMATE scores were positively correlated with TRPC score ($P< 0.05$, Figures 5A–C). Further, neutrophils, and regulatory T cells (Treg) were negatively associated with TRPC score ($P< 0.05$, Figure 5D). However, immune checkpoint, HLA, macrophages, pDCs, and T helper_cells were positively associated with the TRPC score ($P< 0.05$, Figure 5D).

In addition, significant differences were detected between the low- and high-TRPC score subgroups in most immune checkpoints ($P< 0.05$, Figure 5E). Compared with the low-TRPC score group, the high-TRPC score group had lower TIDE, dysfunction, and exclusion scores, while higher MSI expression score ($P< 0.05$; Figure 5F).

The IMvigor 210 dataset (29), including clinical information and RNA-seq data of patients with metastatic uroepithelial carcinoma treated with atezolizumab (a PD-L1 inhibitor), was used as an external cohort to test the predictive value of TRPC score for immunotherapy efficacy. The results showed that TRPC score was significantly higher in the response group than that in the non-response group ($P< 0.001$, Figure 5G). According to the current TRPC score, the response rate in the low-TRPC score group was significantly lower than that in the high-TRPC score group ($P< 0.05$, Figure 5H). The AUC of the current TRPC score to predict the response of atezolizimab was 0.632, which was higher than that of PDCD1 (PD-1), CD274 (PD-L1), and CTLA4 (Figure 5I).

Summary of CRC mutation of TRPC score groups

As shown in Supplementary Figure 6A, somatic mutations occurred in 160 (96.39%) of 166 samples with high TRPC score. The detailed mutations, including variant classification, single-nucleotide polymorphism (SNP) type, and single-nucleotide variant (SNV) class, were depicted in Supplementary

Figure 7A. Further, somatic mutations occurred in 143 (97.28%) of 147 samples with low TRPC score (Supplementary Figure 6B), and the corresponding mutations were summarized in Supplementary Figure 7B. TMB was positively associated with TRPC score (R = 0.14, P< 0.05, Supplementary Figure 6C), and Kaplan–Meier survival curve showed that patients with low TMB had a worse OS than those with high TMB (P< 0.05, Supplementary Figure 6D). Significant survival differences were observed between patients with high and low TMB stratified by TRPC score (P< 0.05, Supplementary Figures 6E, F).

Development of a nomogram

A nomogram including age, stage, and TRPC score was developed to predict the OS of patients with CRC in the TCGA cohort (Figure 6A). Good calibrations were observed in the 1-year, 3-year, and 5-year predicted vs. observed survival rates (Figure 6B). The RMS of the TRPC nomogram was higher than that of the TRPC score and published models of Yang (32), Liu (33), and Cao (34) (P< 0.05, Figure 6C). The C-index of the TRPC nomogram was 0.779, which was higher than that of the TRPC

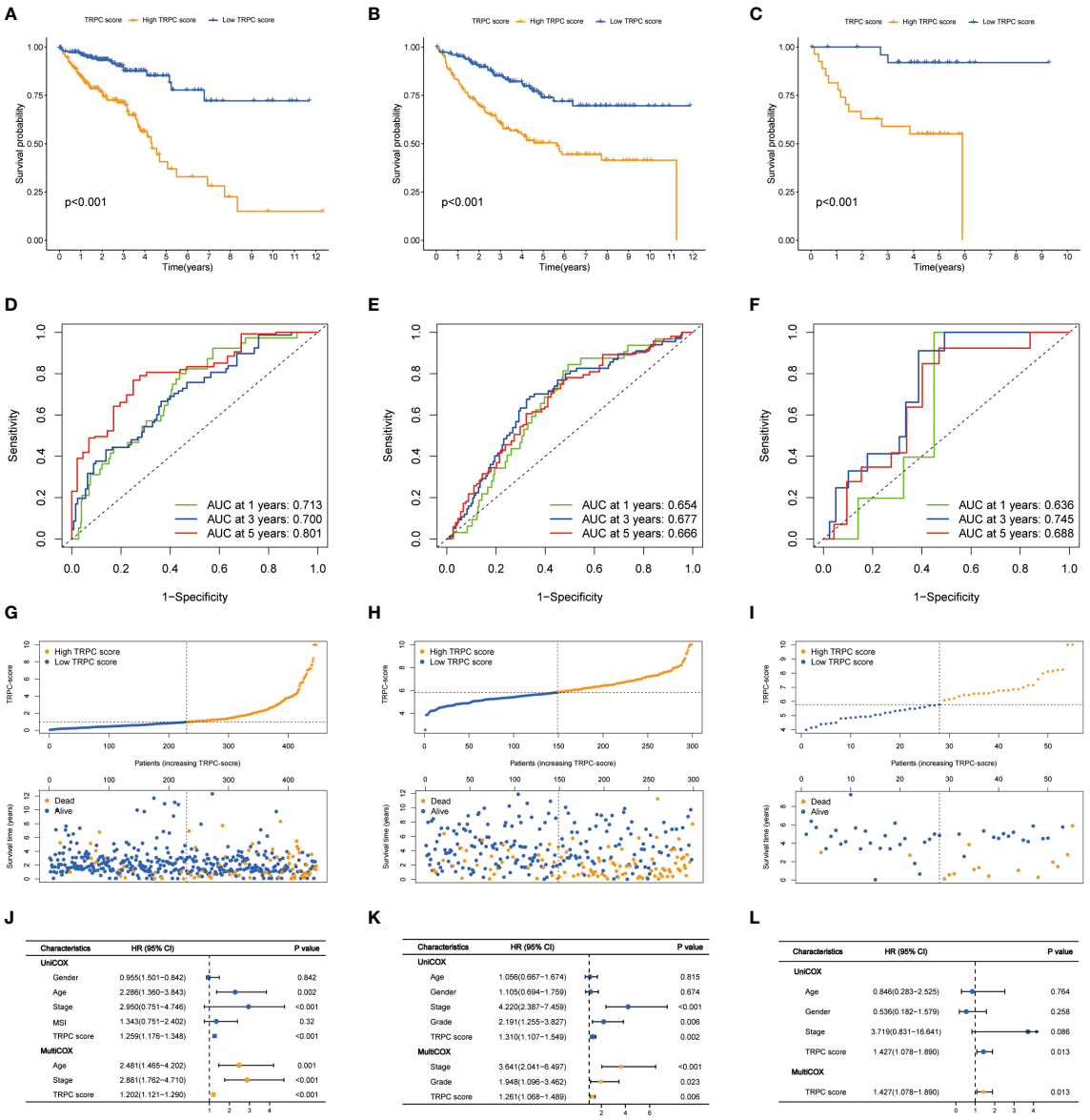

FIGURE 4
Prognostic analysis of TRPC scores. Kaplan–Meier curves **(A-C)**, time-dependent ROC curves **(D-F)**, risk plot distribution and survival status **(G-I)**, univariate and multivariate Cox regression analysis **(J-L)** of the TCGA cohort, the meta-GEO cohort, and the GSE17537 cohort. ROC, receiver operator characteristic; TRPC, transient receptor potential channels.

10.3389/fimmu.2022.1014834

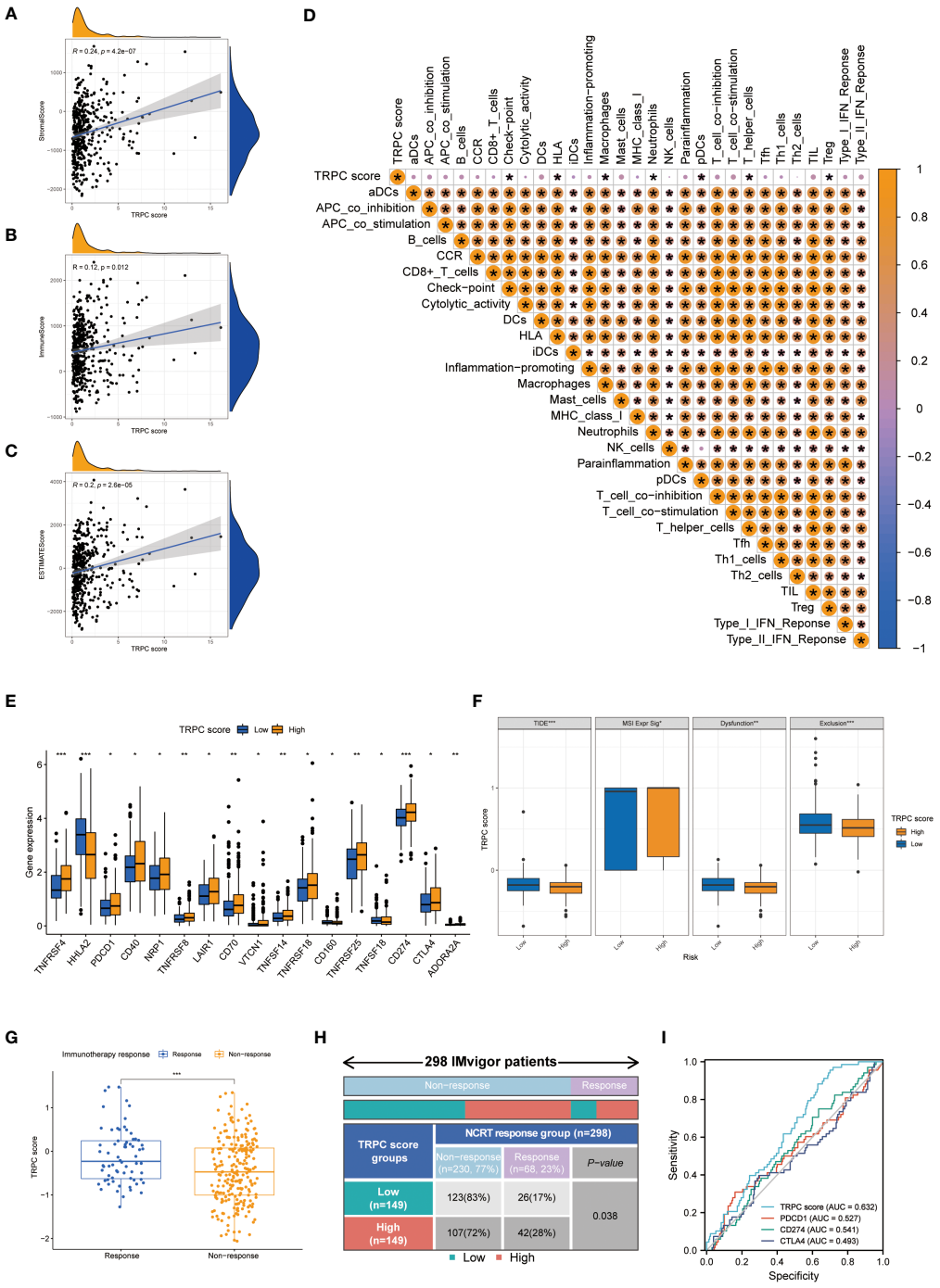

FIGURE 5
Immune landscapes and prediction of immunotherapeutic benefits. Scatter plot showed the association between TRPC score and stromal score **(A)**, immune score **(B)** and ESTIMATE score **(C, D)** Heat map of correlation between TRPC score and immune infiltration. **(E)** The association of the immune check-points between low-and high-TRPC score groups. **(F)** The differences of TIDE score, MSI expression signature score, dysfunction score and immune exclusion score between low- and high-TRPC score groups. The scatter diagram of the TRPC score between response and non-response group **(G)**, and fourfold table between TRPC score and immunotherapy response **(H)** in the IMvigor dataset. **(I)** ROC curves to predict the response of atezolizumab in IMvigor dataset by TRPC score, PDCD1, CD274, and CTLA4. **ESTIMATE:** estimation of stromal and immune cells in malignant tumour tissues using expression data; MSI, microsatellite instability; ROC, receiver operator characteristic; TIDE, tumor immune dysfunction and exclusion; TRPC, transient receptor potential channels; ns, not significant; *P< 0.05; **P< 0.01; ***P< 0.001.

10.3389/fimmu.2022.1014834

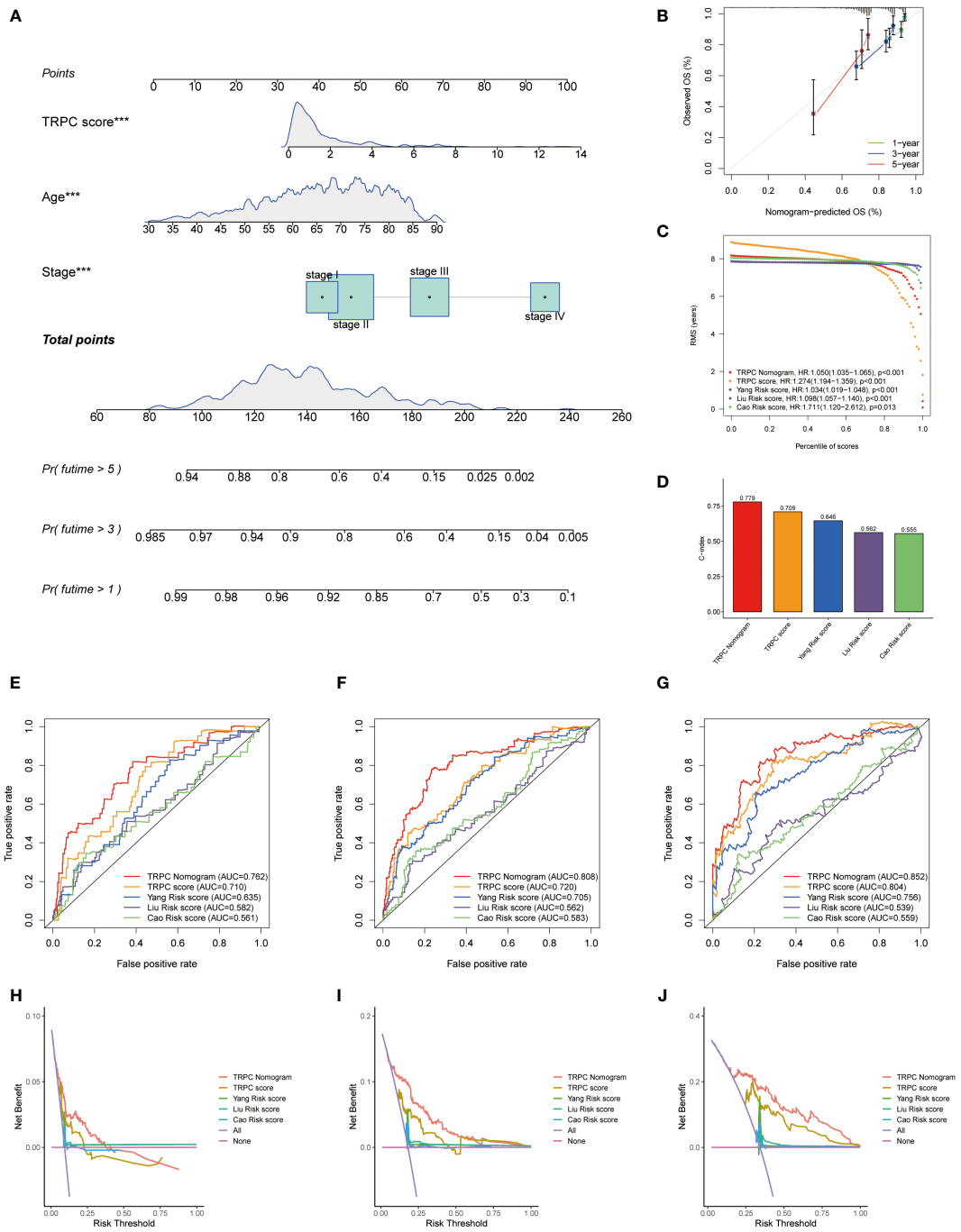

FIGURE 6
Development of a nomogram. **(A)** Nomogram to predict the survival of CRC patients based on the TRPC score. **(B)** Calibration plots of the nomogram for predicting the probability of OS in the 1-year, 3-year, and 5-years. Comparison of RMS **(C)** and C-index **(D)** among the TRPC nomogram, TRPC score, and published models of Yang, Liu, and Cao. The ROC curves **(E-G)** and decision curve analysis **(H-J)** at 1-, 3-, and 5-year OS for TRPC nomogram, TRPC score, and published models of Yang, Liu, and Cao. CRC, colorectal cancer; OS, overall survival; RMS, restricted mean survival; ROC, receiver operator characteristic; TRPC, transient receptor potential channels; ***P< 0.001.

score and published models of Yang (32), Liu (33), and Cao (34) (Figure 6D). ROC curves revealed that the TRPC nomogram predicted the 1-year, 3-year, and 5-year OS more efficiently than the TRPC score and published models of Yang (32), Liu (33), and Cao (34) (Figures 6E–G). As shown in Figures 6H–J, DCA curves showed that the TRPC nomogram had better 1-year, 3-year, and 5-year OS net benefit than the TRPC score and published models of Yang (32), Liu (33), and Cao (34).

Correlation between TRPC score and response to neoadjuvant chemoradiotherapy in the GSE45404 cohort

Figure 7A shows that TRPC score was significantly lower in the response group than that in the non-response group (P< 0.05). According to the current TRPC score, the response rate in the low-TRPC score group was significantly higher than that in the high-TRPC score group (P< 0.05, Figure 7B). Further analysis showed that the current TRPC score had a promising predictive power of neoadjuvant chemoradiotherapy (NCRT) response (Figure 7C). GSVA showed that TRPC activity was significantly lower in the response group than that in the non-response group (P< 0.05, Figure 7D), and positively correlated with the TRPC score (P< 0.05, Figure 7E). B-cells, $CD8^+$ T-cells, mast cells, and Tfh were negatively correlated, whereas immune checkpoint and neutrophils were positively correlated with TRPC activity (Figure 7F). Significantly increased proportions of B-cells, $CD8^+$ T-cells, cytolytic activity, HLA, inflammation-promoting, mast cells, Th1 cells, and Th2 cells were detected in the response group. While, immune checkpoint and neutrophils were significantly increased in the non-response group (P< 0.001, Figure 7G). Further analysis showed that immune checkpoints, including PDCD1 (PD-1), CD274 (PD-L1), and CTLA4, and signaling pathway activities, including mismatch repair, MAPK, and B-cell receptors, were associated with TRPC activity (P< 0.05, Figures 7H–M).

Correlation between TRPC score and prognosis of patients who received NCRT in the GSE87211 cohort

The GSE87211 cohort tested the prognosis prediction capacity of TRPC score in patients who received NCRT. Results of this cohort showed that patients with low-TRPC scores had a longer OS and disease-free survival (DFS) than those with high-TRPC scores (P< 0.05, Figures 8A, B). Significant survival benefits in OS were observed in almost all subgroups (age≤65, Figure 8C; female, Figure 8G; male, Figure 8H; stage II, Figure 8K; stage III, Figure 8L; mutation, Figure 8O; wild type, Figure 8P; P< 0.05). However, there was no significant difference in age> 65 subgroup (Figure 8D, P>0.05). Similar findings were observed in DFS (age, Figures 8E, F; gender, Figures 8I, J; stage, Figures 8M, N; KRAS status, Figures 8Q, R).

Validation of TRPC score in the Fujian Cancer Hospital cohort

A total of 85 samples were used from FJCH to verify the clinical value of the current TRPC score. Kaplan–Meier survival curve showed distinct survival differences between groups of high- and low-TRPC scores, according to the current TRPC scores (P< 0.05, Figure 9A). It also exhibited excellent prognosis prediction with a 5-year AUC of 0.782 (Figure 9B). Multivariate regression analysis showed that TRPC score was the only independent risk factor of OS (P< 0.05, Figure 9C). Furthermore, the TRPC score was significantly lower in the response group to neoadjuvant treatment than that in the non-response group (P< 0.05, Figure 9D). The response rate in the low-TRPC score group was significantly higher than that in the high-TRPC score group (P< 0.05, Figure 9E). The current TRPC score had inspiring predictive ability of response to neoadjuvant treatment with AUC of 0.709 (Figure 9F).

Discussion

Ion channels, particularly TRPC, are crucial in cancer pathophysiology (7). TRPC are often dysregulated in CRC, resulting in alterations in cancer hallmark functions (16, 17). To the best of our knowledge, the present study is the first to systematically evaluate TRPC in CRC. A risk score incorporating 8 TRPCG was established to predict the OS of patients with CRC using the TCGA cohort, and was validated using the GSE38832, GSE17536, and GSE17537 datasets. Furthermore, the TRPC score was associated with other clinicopathological characteristics of patients with CRC and tumor immunity.

Since 1969, many TRPC family members have been identified, regulating numerous cellular, physiological, and pathophysiological functions in tumors (6–8, 13). Previous studies revealed that TRPC1 (35), TRPV6 (36, 37), and TRPM8 (38) were upregulated in CRC tissues compared with normal mucosa, whereas TRPV3 (39), TRPV4 (40), TRPV5 (39), TRPM6 (41), and TRPC6 (39) were downregulated in CRC tissues. However, no systematic study on the role of TRPC in the prognosis of CRC has been reported yet. In the current study, 28 TRPCR were identified from TCGA, showing that almost all 28 TRPCR were dysregulated in CRC tissues than that in normal tissues. However, TRPM5, TRPV4, and TRPC1 were associated with OS of patients with CRC (P< 0.05). Two clusters with distinct prognoses were identified using NMF (P< 0.05), and TRPC were enriched between clusters A and B. Further,

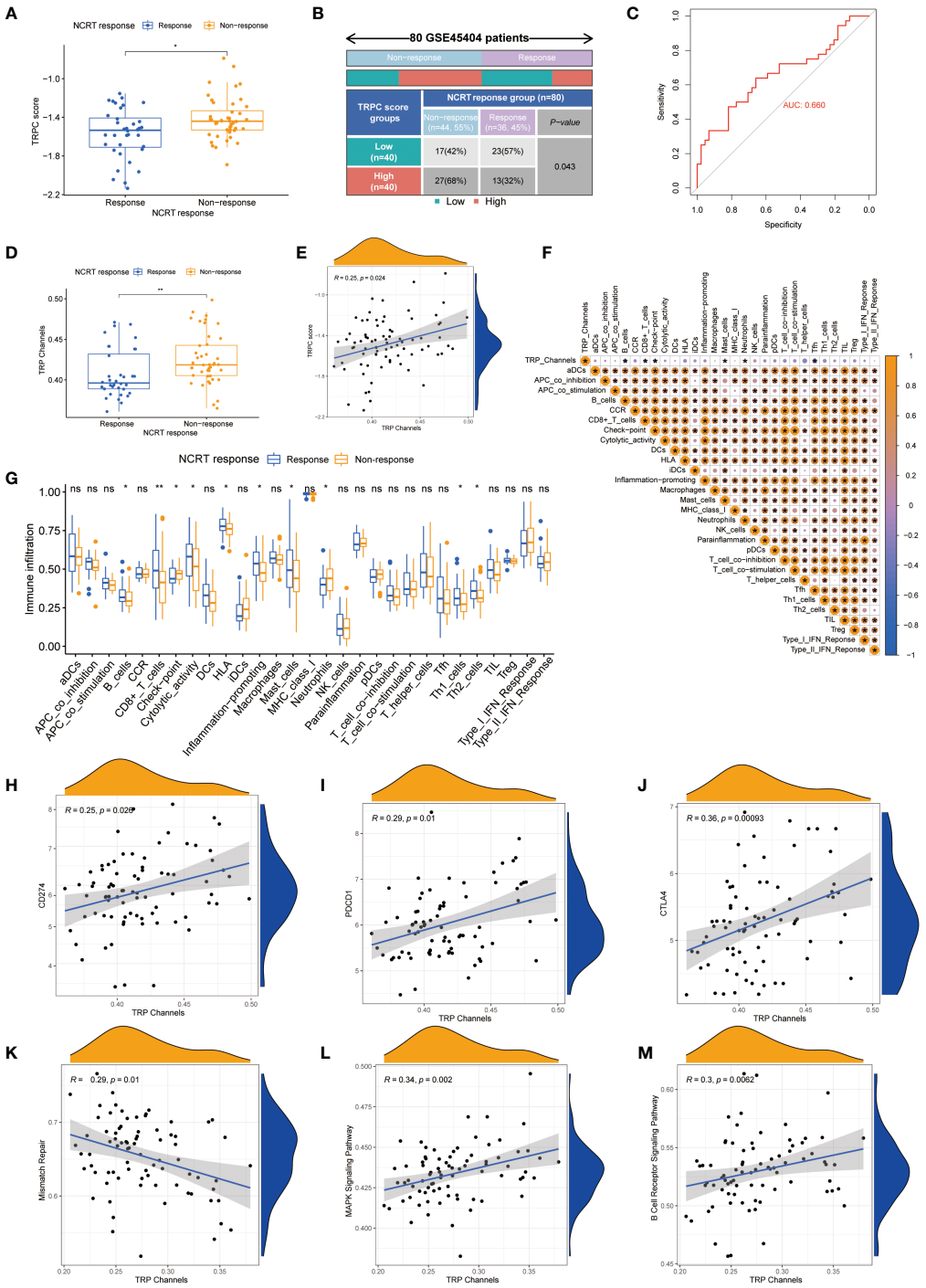

FIGURE 7
Correlation between TRPC score and response to NCRT in the GSE45404 cohort. The scatter diagram of the TRPC score between response and non-response group **(A)**, and fourfold table between TRPC score and NCRT response **(B)**. **(C)** ROC curve of TRPC score to predict NCRT response. **(D)** The distribution of the TRPC activity between response and non-response group. **(E)** Scatter plot showed the association between the TRPC activity and TRPC score. **(F)** Heat map of correlation between the TRPC activity and immune infiltration. **(G)** ssGSEA scores of immune cells and immune-related functions between response and non-response group. **(H-J)** Scatter plot showed the association between immune checkpoints (e.g., PD-1, PD-L1, and CTLA4) and the TRPC activity. **(K-M)** Scatter plot showed the association between signaling pathway (e.g., mismatch repair, MAPK signaling pathway, and B cell receptor signaling pathway) and the TRPC activity. NCRT, neoadjuvant chemoradiotherapy; ROC, receiver operator characteristic; ssGSEA, single sample gene set enrichment analysis; TRPC, transient receptor potential channels; ns, not significant; *P< 0.05; **P< 0.01.

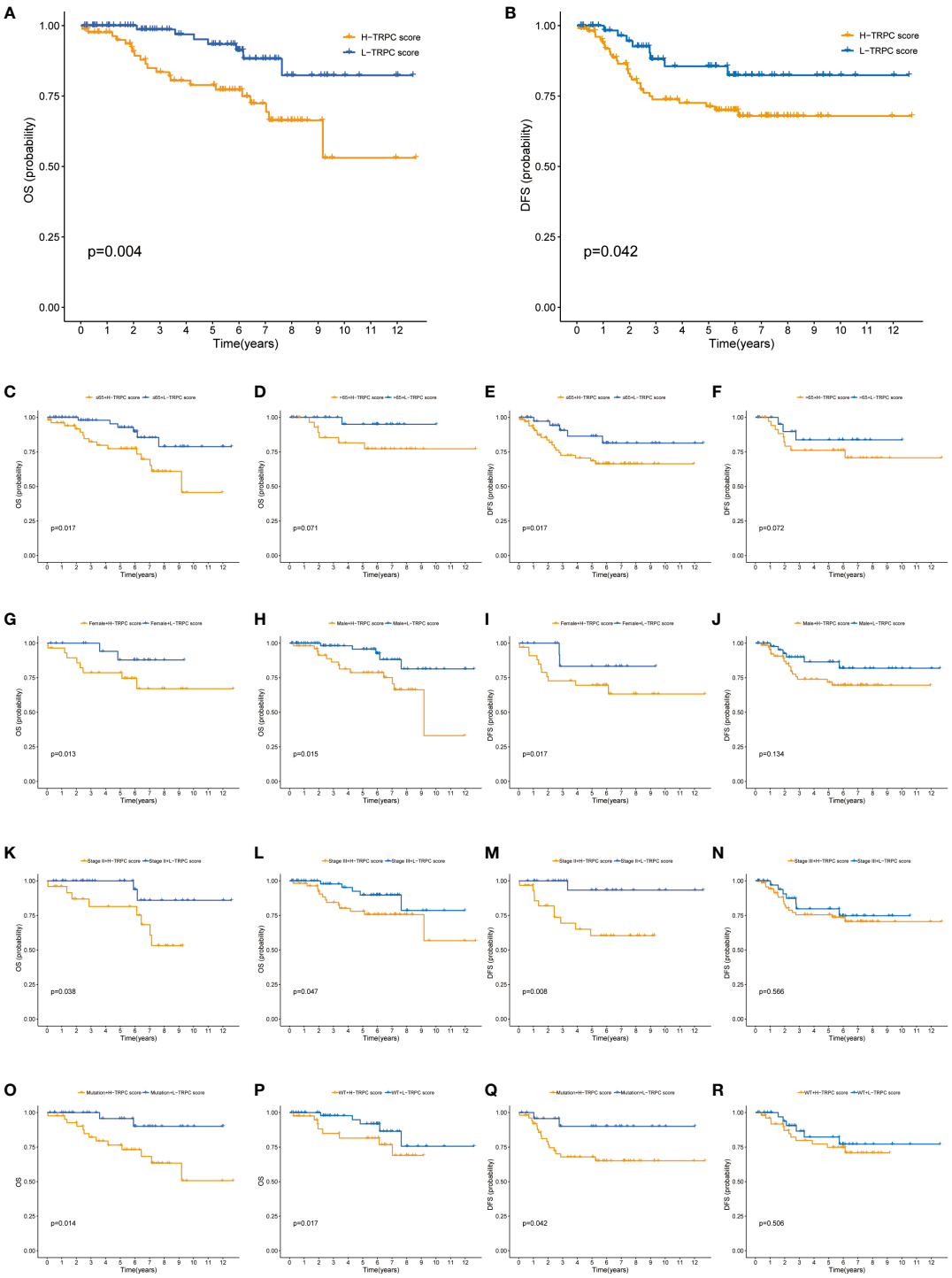

FIGURE 8
Correlation between TRPC score and prognosis of patients who received NCRT in the GSE87211 cohort. **(A)** The Kaplan-Meier curves of OS for patients in the high- and low-TRPC score groups. The Kaplan-Meier curves of OS for supplement clinicopathological characteristics, including age **(C, D)**, gender **(G, H)**, stage **(K, L)**, and KRAS mutation status **(O, P)** in the high- and low-TRPC score groups. **(B)** The Kaplan-Meier curves of DFS for patients in the high- and low-TRPC score groups. The Kaplan-Meier curves of DFS for supplement clinicopathological characteristics, including age **(E, F)**, gender **(I, J)**, stage **(M, N)**, and KRAS mutation status **(Q, R)** in the high- and low-TRPC score groups. NCRT, neoadjuvant chemoradiotherapy; OS, overall survival; TRPC, transient receptor potential channels.

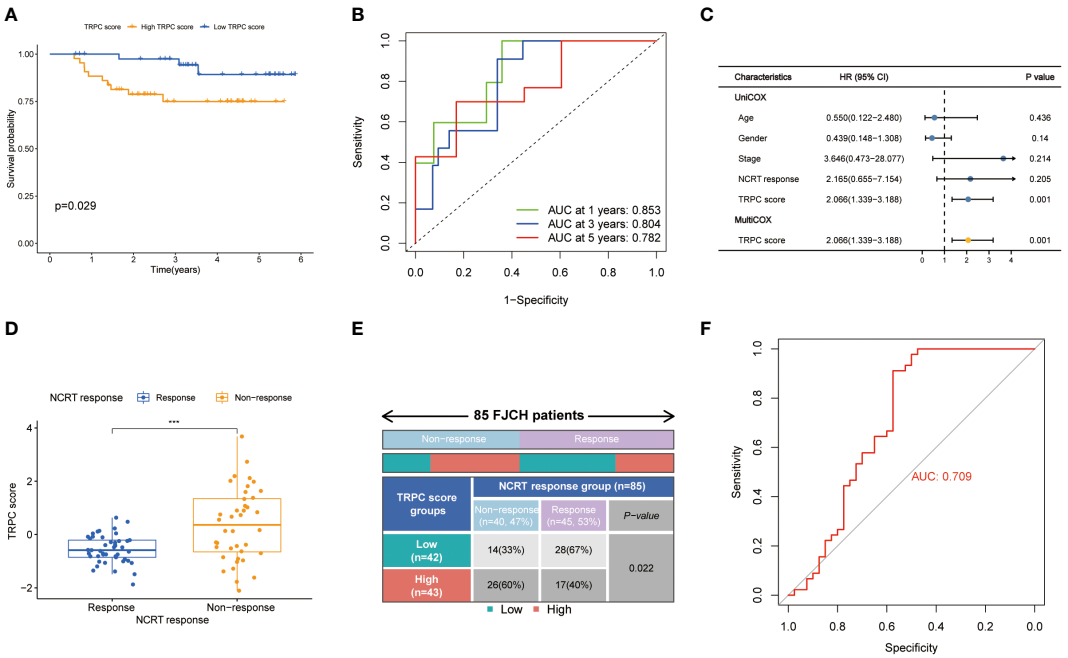

FIGURE 9
Validation of TRPC score in the Fujian Cancer Hospital cohort. Kaplan-Meier curve **(A)**, 1-year, 2-year, and 3-year ROC curves **(B)** and univariate and multivariate Cox regression analysis **(C)** according to the TRPC score. The scatter diagram of the TRPC score between response and non-response group **(D)**, and fourfold table between TRPC score and NCRT response **(E)**. **(F)** ROC curve of TRPC score to predict NCRT response. NCRT, neoadjuvant chemoradiotherapy; ROC, receiver operator characteristic; TRPC, transient receptor potential channels; ***P< 0.001.

immunophenotypes differed significantly between the two clusters, indicating that TRPC might regulate the immune system as reported previously (20, 41).

Considering that studies on TRPCR are scarce, we identified TRPCG, which were not only DEGs between two clusters, but also between tumor and normal samples. In addition, TRPCR were associated with prognosis, and all candidate genes strongly associated with TRPCR. The current TRPC score exhibited excellent prognosis predictive ability in the TCGA, meta-GEO, GSE17537, GSE87211, and FJCH cohorts, and was identified as an independent risk factor of OS (P< 0.05). Furthermore, a nomogram based on the current TRPC score showed higher C-index and AUC of prognosis prediction compared with published risk scores of previous studies by Yang et al. (32), Liu et al. (33), and Cao et al. (34), and improved net benefits. Moreover, the current TRPC score correlated with clinicopathological characteristics, including TNM stages and microsatellite status.

Among the 8 TRPCG, UCN, FJX1, TIPM1, and PCOLCE2 were negatively associated with OS of CRC patients (HR > 1), while CD177, PPARGC1A, CLDN23, and MTOR4 were positively associated with OS of CRC patients (HR< 1). Song et al. (42) reported that TIMP1 expression was significantly associated with regional lymph node and distant metastasis, and was an independent prognostic indicator of colon cancer progression and metastasis through FAk-PI3K/AKT and MAPK signaling pathways (42, 43). FJX1 was reportedly upregulated in the epithelium of CRC, and contributed to poor prognosis in patients with CRC *via* angiogenesis (44). CLDN23 and PPARGC1A were significantly downregulated in CRC tissues, and their reduced levels were associated with shorter OS in patients with CRC (45–47). PPARGC1A reduced the risk of CRC disease and progression through mitochondrial biogenesis, antioxidant system, reactive oxygen species, lipid synthesis, and glycolysis pathway (46). CD177 is mainly expressed by neutrophils, and CRC patients with high density CD177+ neutrophils showed longer OS and DFS (48). Although UCN, PCOLCE2, and MRTO4 are potential prognostic markers of CRC, their action mechanisms remain unclear. In summary, several candidate genes were first considered as prognostic biomarkers for CRC, however, they require further validation.

With promising results of clinical trial of pembrolizumab (49), ICI monotherapy or combination therapy has been well examined in CRC management (50, 51). In recent years, deficient mismatch repair (dMMR) showed the objective response rate of 20–40%, regardless of stages (50, 51). However, the incidence of patients with dMMR account for approximately 15% of CRC (52), and selected patients with proficient mismatch repair MSS precisely could benefit from ICIs (50, 53, 54). In the present study, TRPCR-

10.3389/fimmu.2022.1014834

TABLE 1 Clinical characteristics of the CRC patients used in this study.

	TCGA-COAD-READ cohort	Meta-GEO cohort		GSE17537 cohort	GSE45404 cohort	GSE87211 cohort	FJCH cohort
		GSE38832 cohort	GSE17536 cohort				
No. of patients	535	122	177	55	80	203	85
Age							
≤65	297 (55.5%)	NA	83 (46.9%)	33 (60.0%)	49 (61.3%)	128 (63.1%)	65 (76.5%)
>65	236 (44.1%)	NA	94 (53.1%)	22 (40.0%)	31 (38.7%)	74 (36.4.0%)	20 (23.5%)
unknown	2 (0.4%)	NA	0 (0.0%)	0 (0.0%)	0 (0.0%)	1 (0.5%)	0 (0.0%)
Gender							
Female	259 (48.4%)	NA	81 (45.8%)	29 (52.7%)	31 (38.7%)	61 (30.0%)	30 (35.3%)
Male	265 (49.5%)	NA	96 (54.2%)	26 (47.3%)	49 (61.3%)	142 (70.0%)	55 (64.7%)
unknown	11 (2.1%)	NA	0 (0.0%)	0 (0.0%)	0 (0.0%)	0 (0.0%)	0 (0.0%)
Stage							
I	96 (18.0%)	18 (14.7%)	24 (13.6%)	4 (7.3%)	NA	0 (0.0%)	0 (0.0%)
II	191 (35.7%)	35 (28.7%)	57 (32.2%)	15 (27.3%)	NA	63 (31.0%)	43 (50.6%)
III	150 (28.0%)	39 (32.0%)	57 (32.2%)	19 (34.5%)	NA	125 (61.6%)	42 (49.4%)
IV	76 (14.2%)	30 (24.6%)	39 (22.0%)	17 (30.9%)	NA	12 (5.9%)	0 (0.0%)
unknown	22 (4.1%)	0 (0.0%)	0 (0.0%)	0 (0.0%)	NA	3 (1.5%)	0 (0.0%)
Grade							
Grade 1	NA	NA	16 (9.0%)	NA	NA	NA	2 (9.4%)
Grade 2	NA	NA	134 (75.7%)	NA	NA	NA	74 (87.1%)
Grade 3	NA	NA	27 (15.3%)	NA	NA	NA	2 (9.3%)
Grade 4	NA	NA	0 (0.0%)	NA	NA	NA	3 (3.5%)
unknown	NA	NA	NA	NA	NA	NA	4 (4.7%)
MSI							
MSI-H	60 (11.2%)	NA	NA	NA	NA	NA	0 (0.0%)
MSI-L	72 (13.5%)	NA	NA	NA	NA	NA	0 (0.0%)
MSS	287 (53.6%)	NA	NA	NA	NA	NA	49 (57.6%)
unknown	116 (21.7%)	NA	NA	NA	NA	NA	36 (42.4%)
KRAS status							
Mutation	NA	NA	NA	NA	NA	84 (41.4%)	8 (9.4%)
WT	NA	NA	NA	NA	NA	109 (53.7%)	17 (20.0%)
unknown	NA	NA	NA	NA	NA	10 (4.9%)	60 (70.6%)
Response to neoadjuvant chemoradiotherapy							
Response	NA	NA	NA	NA	35 (43.8%)	NA	45 (52.9%)
Non-response	NA	NA	NA	NA	45 (56.2%)	NA	40 (47.1%)

NA, Not available.

based clusters were highly correlated with TIME. In addition, the current TRPCRS was correlated with immune checkpoints, including PD-1, PD-L1, and CTLA4. Additionally, the results showed that patients with high-TRPC scores had lower TIDE but higher MSI expression than those with low-TRPC scores ($P< 0.05$), suggesting that the former could benefit from ICIs. These findings were validated by an external IMvigor 210 cohort (29), in which all patients received atezolizumab. These findings demonstrated that the novel TRPC score was considered as a promising biomarker for TIME and an alternative index for ICIs. Nonetheless, the correlation between TRPC and immunotherapy is still inclusive, which needs further validation, and the underlying mechanism needs to be further explored.

Although neoadjuvant treatment followed by radical surgery is the standard treatment for locally advanced rectal cancer (LARC) (18), the pathological complete response rate and survival benefit remain unsatisfactory and questionable (5). Hence, a widely recognized biomarker is the key to selecting a potential beneficiary. In the present study, the current TRPCRS was associated with neoadjuvant treatment response in the GSE45404 cohort, and patients with low-TRPC scores were more sensitive to neoadjuvant treatment than those with high-

TRPC scores and higher TRPC activity. In addition, the novel TRPCRS was associated with DFS in the GSE87211 cohort. Consequently, the current TRPCRS could be considered as an index of response to neoadjuvant treatment for patients with LARC, and neoadjuvant chemoradiotherapy should be strongly recommended for patients with low-TRPC scores.

More findings were recorded for patients with high-TRPC scores but tolerant to conventional NCRT in the present study. Initially, neutrophils were significantly enriched in the non-response group than in the response group ($P< 0.05$). Evidence showed that enrichment of neutrophils is one of the important characteristics of neutrophil extracellular trap (NET) (55), which might be a partial reason for chemoradiotherapy resistance, as previously reported (56–58). Previous studies showed that NET formation was positively regulated by MAPK signaling pathway (59, 60); however, the related mechanism remains unclear. In the present study, MAPK signaling pathway was positively correlated with TRPC activity ($P< 0.05$), which was positively correlated with TRPC score ($P< 0.05$). Hence, neutrophil enrichment mediated by activation of MAPK signaling pathway might be a potential mechanism for NCRT resistance, in which TRPC might play an important role. In future, it is a big "if" that combination with MAPK inhibitor and conventional chemoradiotherapy could improve the treatment response. Moreover, considering that patients with high-TRPC scores were more sensitive to ICIs than those with low-TRPC scores, neoadjuvant ICIs might be an alternative for those with high-TRPC scores and resistant to conventional chemoradiotherapy.

The current TRPCRS has several limitations. (1) Data from TCGA training cohort, meta-GEO, and FJCH validation cohorts were retrospectively collected. Therefore, the TRPC score should be validated by prospective cohorts. (2) A model consisting of TRPC score to predict the prognosis might have an intrinsic disadvantage, regardless of the importance of TRPCGs. (3) All eight genes were TRPC-related genes but not TRPCR. (4) Since all patients from FJCH had dMMR, corresponding analysis could not be conducted. (5) Mechanisms, such as MAPK signaling pathway, require *in vitro* and *in vivo* validation. (6) The clinical value of the current TRPCRS in ICIs and neoadjuvant treatment management needs further validation.

Conclusion

In conclusion, a novel risk score was developed using eight TRPCG with excellent discrimination and calibration for CRC prognosis. The current TRPCRS could be considered as a promising biomarker for ICIs and neoadjuvant treatment in CRC management. NCRT is recommended for patients with LARC with low-TRPC scores. In addition, combination of MAPK inhibitors and neoadjuvant immunotherapy could be an alternative treatment for patients with high-TRPC scores. Hence, TRPC might participate in the treatment response and TIME remodeling in CRC management, but it requires further *in vitro* and *in vivo* validation.

Data availability statement

The datasets presented in this study can be found in online repositories. The names of the repository/repositories and accession number(s) can be found in the article/Supplementary Materials.

Ethics statement

The studies involving human participants were reviewed and approved by The Ethics Committee of Fujian Cancer Hospital. The patients/participants provided their written informed consent to participate in this study.

Author contributions

LW, XtC, HjZ, LH, JcW, LdS, GC, and JxW contributed to conception and design. XtC and HjZ conducted data collection and analyzed the data. LW, LH, and JcW interpreted the data. LW, XtC, and LS drafted the manuscript. HjZ and JcW conducted the qRT-PCR experiment and proofread the experimental data. LdS, GC, and JxW contributed critical revision of the manuscript. All authors read and approved the final manuscript.

Funding

This research was funded by the Science and Technology Program of Fujian Province, China (No.2019L3018 and 2019YZ016006), the Fujian Province Natural Science Foundation (2021J01438), the Fujian Provincial Clinical Research Center for Cancer Radiotherapy and Immunotherapy (2020Y2012), Fujian Provincial Health and Family Planning Research Talent Training Program (2020GGB009), the National Clinical Key Specialty Construction Program, and Fujian Province Gastrointestinal, Respiratory and Genitourinary Malignant Tumor Radiotherapy Radiation and Treatment Clinical Medical Research Center (2021Y2014).

Acknowledgments

We thank the TCGA and GEO database for providing valuable and public datasets. The authors wish to thank Bullet Edits Limited for the linguistic editing and proofreading of the manuscript.

Conflict of interest

The authors declare that the research was conducted in the absence of any commercial or financial relationships that could be construed as a potential conflict of interest.

The reviewer S.Y declared a shared parent affiliation with the authors H.Z, J.W, G.C to the handling editor at the time of review.

Publisher's note

Supplementary material

The Supplementary Material for this article can be found online at: https://www.frontiersin.org/articles/10.3389/fimmu.2022.1014834/full#supplementary-material

References

1. Sung H, Ferlay J, Siegel RL, Laversanne M, Soerjomataram I, Jemal A, et al. Global cancer statistics 2020: GLOBOCAN estimates of incidence and mortality worldwide for 36 cancers in 185 countries. *CA Cancer J Clin* (2021) 71(3):209–49. doi: 10.3322/caac.21660

2. Siegel RL, Miller KD, Fuchs HE, Jemal A. Cancer statistic. *CA Cancer J Clin* (2022) 72(1):7–33. doi: 10.3322/caac.21708

3. Jung G, Hernandez-Illan E, Moreira L, Balaguer F, Goel A. Epigenetics of colorectal cancer: biomarker and therapeutic potential. *Nat Rev Gastroenterol Hepatol* (2020) 17(2):111–30. doi: 10.1038/s41575-019-0230-y

4. Keller DS, Berho M, Perez RO, Wexner SD, Chand M. The multidisciplinary management of rectal cancer. *Nat Rev Gastroenterol Hepatol* (2020) 17(7):414–29. doi: 10.1038/s41575-020-0275-y

5. Ciardiello F, Ciardiello D, Martini G, Napolitano S, Tabernero J, Cervantes A. Clinical management of metastatic colorectal cancer in the era of precision medicine. *CA Cancer J Clin* (2022) 72:372–401. doi: 10.3322/caac.21728

6. Cosens DJ, Manning A. Abnormal electroretinogram from a drosophila mutant. *Nature* (1969) 224(5216):285–7. doi: 10.1038/224285a0

7. Nilius B, Owsianik G. The transient receptor potential family of ion channels. *Genome Biol* (2011) 12(3):218. doi: 10.1186/gb-2011-12-3-218

8. Billeter AT, Hellmann JL, Bhatnagar A. Transient receptor potential ion channels: powerful regulators of cell function. *Ann Surg* (2014) 259(2):229–35. doi: 10.1097/SLA.0b013e3182a6359c

9. Earley S, Santana LF, Lederer WJ. The physiological sensor channels TRP and piezo: Nobel prize in physiology or medicine 2021. *Physiol Rev* (2022) 102(2):1153–8. doi: 10.1152/physrev.00057.2021

10. Vasincu A, Rusu RN, Ababei DC, Larion M, Bild W, Stanciu GD, et al. Endocannabinoid modulation in neurodegenerative diseases: In pursuit of certainty. *Biol (Basel)* (2022) 11(3). doi: 10.3390/biology11030440

11. Ding K, Gui Y, Hou X, Ye L, Wang L. Transient receptor potential channels, natriuretic peptides, and angiotensin receptor-neprilysin inhibitors in patients with heart failure. *Front Cardiovasc Med* (2022) 9:904881. doi: 10.3389/fcvm.2022.904881

12. Liu D, Zhu Z, Tepel M. The role of transient receptor potential channels in metabolic syndrome. *Hypertens Res* (2008) 31(11):1989–95. doi: 10.1291/hypres.31.1989

13. Prevarskaya N, Zhang L, Barritt G. TRP channels in cancer. *Biochim Biophys Acta* (2007) 8:937–46. doi: 10.1016/j.bbadis.2007.05.006

14. Gkika D, Prevarskaya N. Molecular mechanisms of TRP regulation in tumor growth and metastasis. *Biochim Biophys Acta* (2009) 1793(6):953–8. doi: 10.1016/j.bbamcr.2008.11.010

15. Bernardini M, Fiorio Pla A, Prevarskaya N, Gkika D. Human transient receptor potential (TRP) channel expression profiling in carcinogenesis. *Int J Dev Biol* (2015) 59(7-9):399–406. doi: 10.1387/ijdb.150232dg

16. Stoklosa P, Borgstrom A, Kappel S, Peinelt C. TRP channels in digestive tract cancers. *Int J Mol Sci* (2020) 21(5). doi: 10.3390/ijms21051877

17. Rizopoulos T, Assimakopoulou M. Transient receptor potential (TRP) channels in human colorectal cancer: evidence and perspectives. *Histol Histopathol* (2021) 36(5):515–26. doi: 10.14670/HH-18-308

18. Guida AM, Sensi B, Formica V, D'Angelillo RM, Roselli M, Del Vecchio Blanco G, et al. Total neoadjuvant therapy for the treatment of locally advanced rectal cancer: a systematic minireview. *Biol Direct* (2022) 17(1):16. doi: 10.1186/s13062-022-00329-7

19. Zhang X, Wu T, Cai X, Dong J, Xia C, Zhou Y, et al. Neoadjuvant immunotherapy for MSI-H/dMMR locally advanced colorectal cancer: New strategies and unveiled opportunities. *Front Immunol* (2022) 13:795972. doi: 10.3389/fimmu.2022.795972

20. Santoni G, Morelli MB, Amantini C, Santoni M, Nabissi M, Marinelli O, et al. "Immuno-transient receptor potential ion channels": The role in monocyte- and macrophage-mediated inflammatory responses. *Front Immunol* (2018), 9. doi: 10.3389/fimmu.2018.01273

21. Nguyen TN, Siddiqui G, Veldhuis NA, Poole DP. Diverse roles of TRPV4 in macrophages: A need for unbiased profiling. *Front Immunol* (2021) 12:828115. doi: 10.3389/fimmu.2021.828115

22. Tripathi MK, Deane NG, Zhu J, An H, Mima S, Wang X, et al. Nuclear factor of activated T-cell activity is associated with metastatic capacity in colon cancer. *Cancer Res* (2014) 74(23):6947–57. doi: 10.1158/0008-5472.CAN-14-1592

23. Smith JJ, Deane NG, Wu F, Merchant NB, Zhang B, Jiang A, et al. Experimentally derived metastasis gene expression profile predicts recurrence and death in patients with colon cancer. *Gastroenterology* (2010) 138(3):958–68. doi: 10.1053/j.gastro.2009.11.005

24. Lee DD, Seung HS. Learning the parts of objects by non-negative matrix factorization. *Nature* (1999) 401(6755):788–91. doi: 10.1038/44565

25. Tibshirani R. The lasso method for variable selection in the cox model. *Stat Med* (1997) 16(4):385–95. doi: 10.1002/(sici)1097-0258(19970228)16:4<385::aid-sim380>3.0.co;2-3

26. Freeman TJ, Smith JJ, Chen X, Washington MK, Roland JT , Means AL, et al. Smad4-mediated signaling inhibits intestinal neoplasia by inhibiting expression of beta-catenin. *Gastroenterology* (2012) 142562–571(3):e562. doi: 10.1053/j.gastro.2011.11.026

27. Yu G, Wang L, Han Y, He Q. clusterProfiler: an r package for comparing biological themes among gene clusters. *Omics: J Integr Biol* (2012) 16(5):284–7. doi: 10.1089/omi.2011.0118

28. Rooney M, Shukla S, Wu C, Getz G, Hacohen N. Molecular and genetic properties of tumors associated with local immune cytolytic activity. *Cell* (2015) 160:48–61. doi: 10.1016/j.cell.2014.12.033

29. Mariathasan S, Turley SJ, Nickles D, Castiglioni A, Yuen K, Wang Y, et al. TGFbeta attenuates tumour response to PD-L1 blockade by contributing to exclusion of T cells. *Nature* (2018) 554(7693):544–8. doi: 10.1038/nature25501

30. Agostini M, Zangrando A, Pastrello C, D'Angelo E, Romano G, Giovannoni R, et al. A functional biological network centered on XRCC3: a new possible marker of chemoradiotherapy resistance in rectal cancer patients. *Cancer Biol Ther* (2015) 16(8):1160–71. doi: 10.1080/15384047.2015.1046652

31. Hu Y, Gaedcke J, Emons G, Beissbarth T, Grade M, Jo P, et al. Colorectal cancer susceptibility loci as predictive markers of rectal cancer prognosis after surgery. *Genes Chromosomes Cancer* (2018) 57(3):140–9. doi: 10.1002/gcc.22512

32. Yang C, Huang S, Cao F , Zheng Y. A lipid metabolism-related genes prognosis biomarker associated with the tumor immune microenvironment in colorectal carcinoma. *BMC Cancer* (2021) 21 1182(1). doi: 10.1186/s12885-021-08902-5

33. Liu Y, Cheng L, Li C, Zhang C, Wang L, Zhang J. Identification of tumor microenvironment-related prognostic genes in colorectal cancer based on bioinformatic methods. *Sci Rep* (2021) 11(1):15040. doi: 10.1038/s41598-021-94541-6

34. Cao L, Chen E, Zhang H, Ba Y, Yan B, Li T, et al. Construction of a novel methylation-related prognostic model for colorectal cancer based on microsatellite status. *J Cell Biochem* (2021) 122(12):1781–90. doi: 10.1002/jcb.30131

35. Sobradillo D, Hernandez-Morales M, Ubierna D, Moyer MP, Nunez L, Villalobos C. A reciprocal shift in transient receptor potential channel 1 (TRPC1) and stromal interaction molecule 2 (STIM2) contributes to Ca2+ remodeling and cancer hallmarks in colorectal carcinoma cells. *J Biol Chem* (2014) 289(42):28765–82. doi: 10.1074/jbc.M114.581678

36. Arbabian A, Iftinca M, Altier C, Singh PP, Isambert H, Coscoy S. Mutations in calmodulin-binding domains of TRPV4/6 channels confer invasive properties to colon adenocarcinoma cells. *Channels (Austin)* (2020) 14(1):101–9. doi: 10.1080/19336950.2020.1740506

37. Khattar V, Wang L, Peng JB. Calcium selective channel TRPV6: Structure, function, and implications in health and disease. *Gene* (2022) 817:146192. doi: 10.1016/j.gene.2022.146192

38. Borrelli F, Pagano E, Romano B, Panzera S, Maiello F, Coppola D, et al. Colon carcinogenesis is inhibited by the TRPM8 antagonist cannabigerol, a cannabis-derived non-psychotropic cannabinoid. *Carcinogenesis* (2014) 35:2787–97. doi: 10.1093/carcin/bgu205

39. Sozucan Y, Kalender ME, Sari I, Suner A, Oztuzcu S, Arman K, et al. TRP genes family expression in colorectal cancer. *Exp Oncol* (2015) 37(3):208–12.

40. Liu X, Zhang P, Xie C, Sham KWY, Ng SSM, Chen Y, et al. Activation of PTEN by inhibition of TRPV4 suppresses colon cancer development. *Cell Death Dis* (2019) 10(6):460. doi: 10.1038/s41419-019-1700-4

41. Xie B, Zhao R, Bai B, Wu Y, Xu Y, Lu S, et al. Identification of key tumorigenesis–related genes and their microRNAs in colon cancer. *Oncol Rep* (2018) 40:3551–60. doi: 10.3892/or.2018.6726

42. Song G, Xu S, Zhang H, Wang Y, Xiao C, Jiang T, et al. TIMP1 is a prognostic marker for the progression and metastasis of colon cancer through FAK-PI3K/AKT and MAPK pathway. *J Exp Clin Cancer Res* (2016) 35(1):148. doi: 10.1186/s13046-016-0427-7

43. Nordgaard C, Doll S, Matos A, Hoeberg M, Kazi JU, Friis S, et al. Metallopeptidase inhibitor 1 (TIMP-1) promotes receptor tyrosine kinase c-kit signaling in colorectal cancer. *Mol Oncol* (2019) 13(12):2646–62. doi: 10.1002/1878-0261.12575

44. Al-Greene NT, Means AL, Lu P, Jiang A, Schmidt CR, Chakravarthy AB, et al. Four jointed box 1 promotes angiogenesis and is associated with poor patient survival in colorectal carcinoma. *PloS One* (2013) 8(7):e69660. doi: 10.1371/journal.pone.0069660

45. Maryan N, Statkiewicz M, Mikula M, Goryca K, Paziewska A, Strzalkowska A, et al. Regulation of the expression of claudin 23 by the enhancer of zeste 2 polycomb group protein in colorectal cancer. *Mol Med Rep* (2015) 12(1):728–36. doi: 10.3892/mmr.2015.3378

46. Alonso-Molero J, Gonzalez-Donquiles C, Fernandez-Villa T, de Souza-Teixeira F, Vilorio-Marques L, Molina AJ, et al. Alterations in PGC1alpha expression levels are involved in colorectal cancer risk: a qualitative systematic review. *BMC Cancer* (2017) 17(1):731. doi: 10.1186/s12885-017-3725-3

47. Yun SH, Roh MS, Jeong JS, Park JI. Peroxisome proliferator-activated receptor gamma coactivator-1alpha is a predictor of lymph node metastasis and poor prognosis in human colorectal cancer. *Ann Diagn Pathol* (2018) 33:11–6. doi: 10.1016/j.anndiagpath.2017.11.007

48. Zhou G, Peng K, Song Y, Yang W, Shu W, Yu T, et al. CD177+ neutrophils suppress epithelial cell tumourigenesis in colitis-associated cancer and predict good prognosis in colorectal cancer. *Carcinogenesis* (2018) 39(2):272–82. doi: 10.1093/carcin/bgx142

49. Diaz LAJr., Shiu KK, Kim TW, Jensen BV, Jensen LH, Punt C, et al. Pembrolizumab versus chemotherapy for microsatellite instability-high or mismatch repair-deficient metastatic colorectal cancer (KEYNOTE-177): final analysis of a randomised, open-label, phase 3 study. *Lancet Oncol* (2022) 23 (5):659–70. doi: 10.1016/S1470-2045(22)00197-8

50. Huyghe N, Benidovskaya E, Stevens P, Van den Eynde M. Biomarkers of response and resistance to immunotherapy in microsatellite stable colorectal cancer: Toward a new personalized medicine. *Cancers (Basel)* (2022) 14(9). doi: 10.3390/cancers14092241

51. Zhang X, Yang Z, An Y, Liu Y, Wei Q, Xu F, et al. Clinical benefits of PD-1/PD-L1 inhibitors in patients with metastatic colorectal cancer: a systematic review and meta-analysis. *World J Surg Oncol* (2022) 20(1):93. doi: 10.1186/s12957-022-02549-7

52. Boland CR, Goel A. Microsatellite instability in colorectal cancer. *Gastroenterology* (2010) 138 2073–2087(6):e2073. doi: 10.1053/j.gastro.2009.12.064

53. Llosa NJ, Luber B, Tam AJ, Smith KN, Siegel N, Awan AH, et al. Intratumoral adaptive immunosuppression and type 17 immunity in mismatch repair proficient colorectal tumors. *Clin Cancer Res* (2019) 25(17):5250–9. doi: 10.1158/1078-0432.CCR-19-0114

54. Wang F, Zhao Q, Wang YN, Jin Y, He MM, Liu ZX, et al. Evaluation of POLE and POLD1 mutations as biomarkers for immunotherapy outcomes across multiple cancer types. *JAMA Oncol* (2019) 5(10):1504–6. doi: 10.1001/jamaoncol.2019.2963

55. Cristinziano L, Modestino L, Antonelli A, Marone G, Simon HU, Varricchi G, et al. Neutrophil extracellular traps in cancer. *Semin Cancer Biol* (2022) 79:91–104. doi: 10.1016/j.semcancer.2021.07.011

56. Takeshima T, Pop LM, Laine A, Iyengar P, Vitetta ES, Hannan R, et al. Key role for neutrophils in radiation-induced antitumor immune responses. *Proc Natl Acad Sci U.S.A.* (2016) 113(40):11300–5. doi: 10.1073/pnas.1613187113

57. Wisdom AJ, Hong CS, Lin AJ, Xiang Y, Cooper DE, Zhang J, et al. Neutrophils promote tumor resistance to radiation therapy. *Proc Natl Acad Sci U.S.A.* (2019) 116(37):18584–9. doi: 10.1073/pnas.1901562116

58. Shinde-Jadhav S, Mansure JJ, Rayes RF, Marcq G, Ayoub M , Skowronski R, et al. Role of neutrophil extracellular traps in radiation resistance of invasive bladder cancer. *Nat Commun* (2021) 12(1) 2776. doi: 10.1038/s41467-021-23086-z

59. Arumugam S, Girish Subbiah K, Kemparaju K, Thirunavukkarasu C. Neutrophil extracellular traps in acrolein promoted hepatic ischemia reperfusion injury: Therapeutic potential of NOX2 and p38MAPK inhibitors. *J Cell Physiol* (2018) 233(4):3244–61. doi: 10.1002/jcp.26167

60. Ma F, Chang X, Wang G, Zhou H, Ma Z , Lin H, et al. Streptococcus suis serotype 2 stimulates neutrophil extracellular traps formation *via* activation of p38 MAPK and ERK1/2. *Front Immunol* (2018) 92854:2854. doi: 10.3389/fimmu.2018.02854

frontiers | Frontiers in Immunology

TYPE Review
PUBLISHED 20 October 2022
DOI 10.3389/fimmu.2022.1049043

OPEN ACCESS

EDITED BY
Fei Yu,
Tongji University School of Medicine, China

REVIEWED BY
Tomomi W. Nobashi,
Kyoto University, Japan
Guozhu Hou,
Chinese Academy of Medical Sciences and Peking Union Medical College, China

*CORRESPONDENCE
Meng Liu
louisa_liu@bjmu.edu.cn

†These authors have contributed equally to this work and share first authorship

SPECIALTY SECTION
This article was submitted to Cancer Immunity and Immunotherapy, a section of the journal Frontiers in Immunology

RECEIVED 20 September 2022
ACCEPTED 10 October 2022
PUBLISHED 20 October 2022

CITATION
Gao Y, Wu C, Chen X, Ma L, Zhang X, Chen J, Liao X and Liu M (2022) PET/CT molecular imaging in the era of immune-checkpoint inhibitors therapy.
Front. Immunol. 13:1049043.
doi: 10.3389/fimmu.2022.1049043

PET/CT molecular imaging in the era of immune-checkpoint inhibitors therapy

Yuan Gao†, Caixia Wu†, Xueqi Chen, Linlin Ma, Xi Zhang, Jinzhi Chen, Xuhe Liao and Meng Liu*

Department of Nuclear Medicine, Peking University First Hospital, Beijing, China

Cancer immunotherapy, especially immune-checkpoint inhibitors (ICIs), has paved a new way for the treatment of many types of malignancies, particularly advanced-stage cancers. Accumulating evidence suggests that as a molecular imaging modality, positron emission tomography/computed tomography (PET/CT) can play a vital role in the management of ICIs therapy by using different molecular probes and metabolic parameters. In this review, we will provide a comprehensive overview of the clinical data to support the importance of ^{18}F-fluorodeoxyglucose PET/CT (^{18}F-FDG PET/CT) imaging in the treatment of ICIs, including the evaluation of the tumor microenvironment, discovery of immune-related adverse events, evaluation of therapeutic efficacy, and prediction of therapeutic prognosis. We also discuss perspectives on the development direction of ^{18}F-FDG PET/CT imaging, with a particular emphasis on possible challenges in the future. In addition, we summarize the researches on novel PET molecular probes that are expected to potentially promote the precise application of ICIs.

KEYWORDS

positron emission tomography/computed tomography (PET/CT), molecular imaging, immune-checkpoint inhibitors (ICIs), tumor microenvironment (TME), metabolic parameter, molecular probe

Introduction

Cancer immunotherapy has paved a new way for the treatment of many types of malignancies, particularly advanced-stage cancers, by intervening in the abnormal immune processes, reshaping the tumor microenvironment (TME), and restoring immune surveillance (1). Immune-checkpoint inhibitors (ICIs), such as the blocking antibodies of programmed cell death protein-1 (PD-1), programmed death-ligand 1 (PD-L1), and cytotoxic T lymphocyte-associated protein 4 (CTLA-4), have brought considerable clinical benefits to cancer patients. However, only a subset of patients can benefit from ICIs therapies, and some might even experience severe immune-related

adverse events (irAEs) and detrimental hyperprogressive disease (2). Emerging preclinical and clinical evidence indicates that the reciprocity between ICIs and TME may play a complex and important influence on ICIs therapy, but the specific mechanism is still unclear. How to characterize TME noninvasively and effectively, so as to deeply elucidate its potential mechanisms in immunotherapy and precisely guide the use of ICIs, is continually attracting research interest worldwide.

It is well-known that positron emission tomography (PET)/computed tomography (CT) can reflect the biological information of the living body noninvasively and dynamically by using different kinds of imaging agents. Fluorine-18 fluorodeoxyglucose (^{18}F-FDG), the most commonly used PET/CT imaging agent, has been increasingly applied in the immunotherapeutic management. It can reflect the level of glucose accumulation in both primary tumor tissues and metastatic lesions by tracking glucose uptake through a single scan. The metabolic parameters obtained from ^{18}F-FDG PET/CT arguably provide useful indications of the tumor burden (3). Accumulating evidence suggests that ^{18}F-FDG PET/CT imaging can play a vital role in ICIs therapy, including TME characterization, irAEs assessment, efficacy evaluation, prognosis prediction, and so on.

In this review, we focus on the characteristics of TME associated with immunotherapy, and provide an overview of the clinical data associated with the application of ^{18}F-FDG PET/CT imaging in the treatment of ICIs. Furthermore, we discuss perspectives on the development direction of ^{18}F-FDG PET/CT imaging, with a particular emphasis on possible challenges in the future. We also summarize the researches on novel PET/CT molecular imaging, which may potentially promote the precise application of ICIs.

Characteristics and classifications of TME

Compared with traditional treatments, such as radiotherapy and chemotherapy, ICIs treatment is more closely related to TME. The efficacy of ICIs may be influenced by various mechanisms related to the tumor or the host, among which TME is being widely investigated as a critical factor. The characteristics of TME vary in different individuals and cancer types, which will affect the immune response to ICIs treatment.

Compositions and metabolism of TME

TME is composed of tumor cells, immune cells, stromal cells, extracellular matrix, and exosomes (4), thus forming a microenvironment with the characteristics of inflammation, hypoxia, acidity, and immunosuppression. Different types of cells in TME have their preferred metabolic phenotypes (Figure 1).

Tumor cells generally experience metabolic reprogramming, especially glucose metabolism, to adapt to immunosuppressive TME. Even under aerobic conditions, tumor cells are typically characterized by glycolysis, resulting in high rates of glucose intake with high lactate excretion, which is known as the Warburg effect (5). There are fundamental differences between the metabolic programs of cancer cells and immune cells, as well as between different immune cells (6).

Immune cells can be divided into immune-activating cells and immunosuppressive cells. The characteristics of TME might inhibit antitumor immune cells and lead to their exhaustion or senescence (7), but tumor-promoting immune cells mostly show tolerance (8). Immune-activating cells include $CD8^+$ effector T (Teff) cells, $CD8^+$ memory T (Tmem) cells, $CD4^+$ T helper 1 (Th 1) cells, dendritic cells (DCs), natural killer (NK) cells, inflammatory tumor-associated macrophages (M1-TAM), B cells, and neutrophils. Immunosuppressive cells include regulatory T (Treg) cells, myeloid-derived suppressor cells (MDSCs), and immunosuppressive macrophages (M2-TAM), which subvert antitumor immunity by secreting cytokines or interfering with metabolism (5).

Stromal cells include cancer-associated fibroblasts (CAFs), endothelial cells, and pericytes. Like immune cells, stromal cells could interact with tumor cells, modulate their metabolic behavior, and contribute to migration, invasion, and evasion of immune surveillance (9). CAFs can carry out aerobic glycolysis and secrete lactate and pyruvate as fuels for neighboring tumor cells. A metabolic cross-talk exists between tumor cells and CAFs, referred to as a reverse-Warburg effect. CAFs are also characterized by increased synthesis and secretion of glutamine, which is consumed by cancer cells, thus allowing them to sustain nucleotide generation and oxidative phosphorylation (OXPHOS) to obtain high proliferation (10).

Classifications of TME associated with ICIs therapy

With the continuous understanding of the dynamic interaction (promote or hinder) between the status of TME and the treatment with ICIs, several TME classifications based on immunotherapeutic rationale have been proposed. These types are associated with therapy response and might be helpful in selecting the appropriate immunotherapy strategy and suitable patients.

Tumor immune microenvironment (TIME) refers to the immunological characteristics of TME, mainly including the cell types, infiltration degrees, and molecular expression levels of immune cells. Based on the degree and location of tumor-infiltrating lymphocytes (TILs) in TIME, tumors can be classified into “cold” or “hot” ones, or more precisely, divided into three types of immune-inflamed, immune-excluded, and immune-desert (11). In addition, PD-L1 expression and TILs

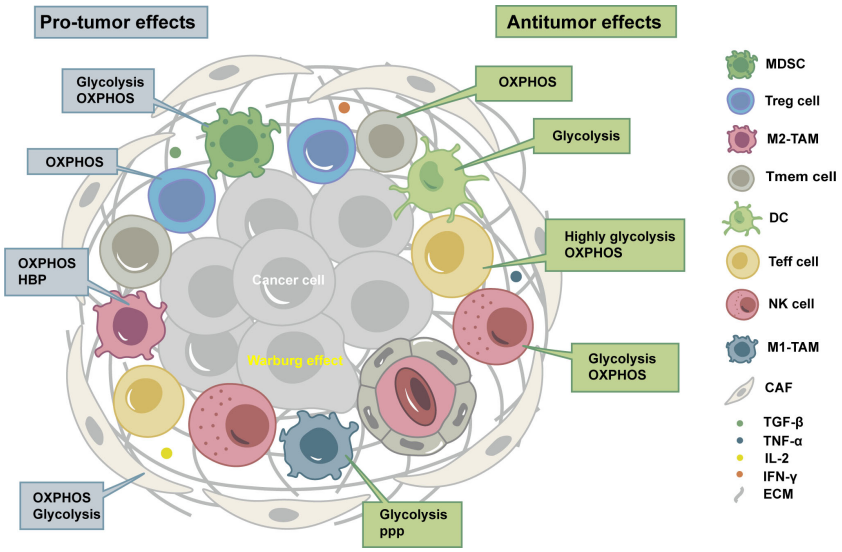

FIGURE 1
Tumor microenvironment (TME) is composed of tumor cells, immune cells, stromal cells, extracellular matrix, and exosomes, thus forming a microenvironment with the characteristics of inflammation, hypoxia, acidity, and immunosuppression. Different types of cells in TME have their preferred metabolic phenotypes. OXPHOS, oxidative phosphorylation; HBP, hexosamine biosynthesis pathway; PPP, pentose phosphate pathway; MDSC, myeloid-derived suppressor cell; Treg cell, regulatory T cell; M2-TAM, immunosuppressive macrophages; Tmem cell, $CD8^+$ memory T cells; DC, dendritic cell; Teff cell, $CD8^+$ effector T cells; NK cell, natural killer cell; M1-TAM, inflammatory tumor-associated macrophages; CAF, cancer-associated fibroblast; TGF-β, transforming growth factor-β; TNF-α, tumor necrosis factor-α; IL-2, Interleukin-2; IFN-γ, Interferon-γ; ECM, extracellular matrix.

infiltration are essential features of TIME related to ICIs (12, 13). Hence, TIME can be divided into four tumor immune microenvironment types (TIMTs) according to these two characteristics, i.e., PD-L1−/TIL−, PD-L1+/TIL+, PD-L1−/TIL+, and PD-L1+/TIL− (14).

Considering that the metabolic and immune characteristics of TME are important theoretical bases for tumor immunotherapy, Siska et al. recommended the metabolic-tumor-stroma score (MeTS) to describe the characteristics of tumor metabolism and cell heterogeneity (15): (1) OXPHOS metabolic type and high T cell infiltration; (2) reverse Warburg type; (3) mixed type; and (4) Warburg type and low T cell infiltration.

Application of ^{18}F-FDG PET/CT imaging in ICIs treatment

Due to the Warburg effect, tumor cells are usually characterized by high glucose metabolism, i.e., increased FDG uptake is often induced in the case of over-expression of glucose transporters (GLUT), such as GLUT1 and GLUT3. A set of studies have shown that GLUT1 expression is correlated with tumor size and hypoxia of TME, and the latter activates hypoxia-inducible factor 1-alpha (HIF-1α) to trigger the Warburg effect and upregulate GLUT expression (16). It has also been elucidated that HIF-1α could directly bind to the hypoxia response element in the PD-L1 proximal promoter and control its expression under hypoxic conditions (17). Besides, activation of some immune cells, including $CD4^+$ and $CD8^+$ T cells, is accompanied by increased metabolism, such as upregulated aerobic glycolysis, tricarboxylic acid (TCA) cycle, and OXPHOS (6). The above mechanisms may provide a theoretical basis for the role of ^{18}F-FDG PET/CT imaging in ICIs therapy, including characterization of TIME, assessment of irAEs, evaluation of therapeutic efficacy, and prediction of prognosis (Figure 2).

Characterization of TIME

Delineation of TIME characteristics can help treatment formulation, efficacy evaluation, and prognosis prediction (18). Due to the complexity of TIME components and their dynamic changes during the treatment process of ICIs, traditional methods such as biopsy have limitations in reflecting TIME. As a non-invasive and functional whole-body imaging modality, ^{18}F-FDG PET/CT imaging has some potential advantages in characterizing the overall glucose metabolism of tumor cells, activated immune cells, and stromal cells in the TME of the primary lesions.

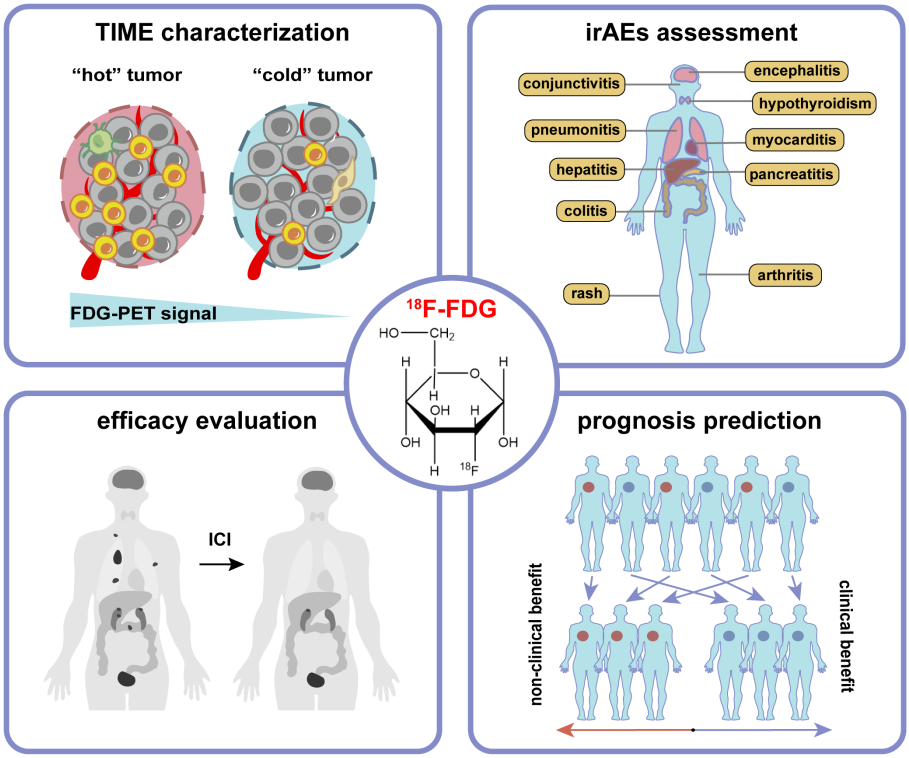

FIGURE 2
The application of ^{18}F-FDG PET/CT imaging in tumor immunotherapy includes characterization of tumor immune microenvironment (TIME), assessment of immune-related adverse events (irAEs), evaluation of therapeutic efficacy, and prediction of prognosis.

The majority of researches on the application of ^{18}F-FDG PET/CT imaging on TIME characterization focused on non-small-cell lung cancer (NSCLC) (Table 1). Zhao et al. carried out two studies with the largest sample sizes (419 cases and 428 cases) to investigate the relationship between PD-L1 expression and ^{18}F-FDG uptake, using 22C3 and SP142 assays, respectively (19, 20). They both showed that maximum standardized uptake value (SUVmax) was significantly associated with PD-L1 expression in NSCLC. A meta-analysis across seven studies (473 patients) showed that the predictive sensitivity of the SUVmax for the expression of PD-L1 in NSCLC patients was 75%, and the specificity was 73% (41). Other metabolic parameters, such as mean standardized uptake value (SUVmean) and the ratio of metabolic to morphological lesion volumes (MMVR), have been reported to be correlated with PD-1 or PD-L1 expression (26, 27). ^{18}F-FDG PET/CT radiomics have also been used to explore predictive models based on images and clinical information for PD-L1 expression (28–30). Additionally, Mitchell et al. found that high SUVmax was associated with reduced CD57$^+$ cell density and increased T cell exhaustion gene signature (21). Wang et al. revealed that high SUVmax was associated with high infiltration of CD8$^+$ T cells, M2 macrophages, and Foxp3$^+$ Treg cells (22).

In terms of TIMTs, Zhou et al. used dual-phase ^{18}F-FDG PET/CT imaging to reflect metabolic dynamics in NSCLC and constructed a model combined metabolic signature (Meta-Sig) and clinical factors to predict PD-L1$^+$/TIL$^+$ tumors (AUC: 0.869, sensitivity: 77.27%, specificity: 82.61%) (42). Wu et al. analyzed the correlation between SUVmax and TIMT classification in patients with cell clear renal cell carcinoma (ccRCC) and suggested that SUVmax might be used as an indicator for TIMTs and thus help guide the treatment with ICIs (32).

In addition, the correlation between ^{18}F-FDG PET/CT imaging and TIME in breast cancer, gastric cancer, colorectal cancer, bladder cancer, nasopharyngeal cancer, and oral squamous cell carcinoma has also been observed (Table 1).

Assessment of irAEs

The perturbation of ICIs on the balance of the immune system can lead to a loss of self-tolerance and excessive immune activation of normal tissues, resulting in irAEs (43). The irAEs can affect nearly all organ systems, such as the neurologic, pulmonary, cardiovascular, gastrointestinal, endocrine, genitourinary, integumentary, skeletal and joint systems, and

TABLE 1 Tumor microenvironment evaluation by ^{18}F-FDG PET/CT imaging.

Histology	Parameters	Conclusions	References
NSCLC	SUVmax	positively associated with PD-L1 expression	(19–25)
		positively associated with CD8$^+$ T cells, CD163$^+$ TAMs and Foxp3+ Treg cells; negatively associated with CD57$^+$ cells	(21, 22, 26)
	SUVmean	positively associated with PD-1 expression	(26)
	MMVR	negatively correlated with PD-L1 expression in TCs	(27)
	radiomics	models based on radiomics and/or clinicopathological characteristics showed good accuracy in predicting PD-L1 expression level	(28–30)
		showed good performance in predicting PD-L1$^+$/TIL$^+$ tumors	(31)
ccRCC	SUVmax	positively associated with PD-L1$^+$/TIL$^+$ and PD-L1$^-$/TIL$^+$ tumors	(32)
breast cancer	SUVmax	positively associated with TIL levels	(33–35)
		positively associated with PD-L1 expression	(33)
gastric cancer	SUVmax	positively correlated with CD3$^+$ and Foxp3$^+$ T cell counts	(36)
colorectal cancer	SUVmax, MTV, TLG	positively associated with PD-L1 expression	(37)
bladder cancer	SUVmax	positively associated with PD-L1 and PD-1 expression	(38)
nasopharyngeal carcinoma	SUVmax	negatively correlated with PD-L1 expression in TIICs and positively associated with PD-L1 expression in TCs	(39)
oral squamous cell carcinoma	SUVmax	negatively correlated with cold tumors (low tumoral PD-L1 and low stromal CD8$^+$TILs)	(40)

NSCLC, non-small cell lung carcinoma; ccRCC, clear cell renal cell carcinoma; TCs, tumor cells; TIICs, tumor-infiltrating immune cells; TME, tumor microenvironment; TIMT, tumor immune microenvironment type; TIL, tumor-infiltrating lymphocyte; PD-L1, programmed death-ligand 1; PD-1, programmed cell death protein-1; SUVmax, maximum standardized uptake value; SUVmean, mean standardized uptake value; MTV, metabolic tumor volume; TLG, total lesion glycolysis; MMVR, ratio of metabolic to morphological lesion volumes.

so on (44, 45). The irAEs resulting from different ICIs may vary. A systematic review found that deaths from CTLA-4 inhibitors were mainly caused by the irAEs of colitis (70%), and deaths from PD-1/PD-L1 inhibitors were mainly pneumonia (35%), hepatitis (22%), and neurotoxicity (15%) (46). For different types of tumors, the most commonly affected sites of irAEs are also different. For example, patients with NSCLC mainly show endocrine system and skin irAEs, and patients with melanoma mostly involve the skin and liver, while irAEs occur in patients with RCC are more common in the skin and gastrointestinal tract (47).

A number of current reports support that some irAEs seem to be associated with improved tumor response and better survival (48). This association may stay robust in certain cancer types (NSCLC, melanoma, RCC, and advanced urothelial cancer) and organ-specific irAEs (the skin and endocrine system) (49–52). But some reports pointed out that grade 3-5 irAEs (severe irAEs) are not associated with increased overall survival (OS) and progression-free survival (PFS) in NSCLC patients (53, 54). Oncologists should weigh the risk of irAEs against the benefit of ICIs before immunotherapy and take appropriate management once irAEs occur.

Therefore, it is necessary to judge the appearances of irAEs timely by noninvasive imaging methods. CT or magnetic resonance imaging (MRI) has been widely used to detect irAEs, especially in the lung, pancreas, liver, and nervous system (55). However, the utility of ^{18}F-FDG PET/CT imaging in irAEs screening and monitoring is largely under-recognized currently (2).

^{18}F-FDG PET/CT imaging may be a sensitive method to identify the development and severity of irAEs, which usually present as a new non-neoplastic lesion with increased FDG accumulation after ICI treatment (56). For instance, elevated thyroid SUVmax commonly suggests ICI-related thyroiditis (57), while a diffuse increase of FDG uptake in the pancreas is a characteristic manifestation of ICI-related pancreatitis (58). A study on patients with metastatic melanoma treated with ICIs found that novel quantitative imaging biomarkers, i.e. the SUV percentiles ($SUV_{X\%}$) of ^{18}F-FDG uptake within the target organs, could be predictive of irAEs in the bowel, stomach, and thyroid (56). This study also demonstrated that some irAEs could be detected on ^{18}F-FDG PET/CT imaging before the onset of clinical symptoms, which showed increased ^{18}F-FDG uptake in the affected organs. The typical ^{18}F-FDG PET/CT manifestations of irAEs can be seen in Figure 3.

Evaluation of therapeutic efficacy

ICIs treatment can achieve antitumor effects by eliminating immunosuppression and reinvigorating Tmem cells, which are good for the patient's long-term survival. However, ICIs can also lead to atypical response patterns, including pseudoprogression, hyperprogression, and mixed response.

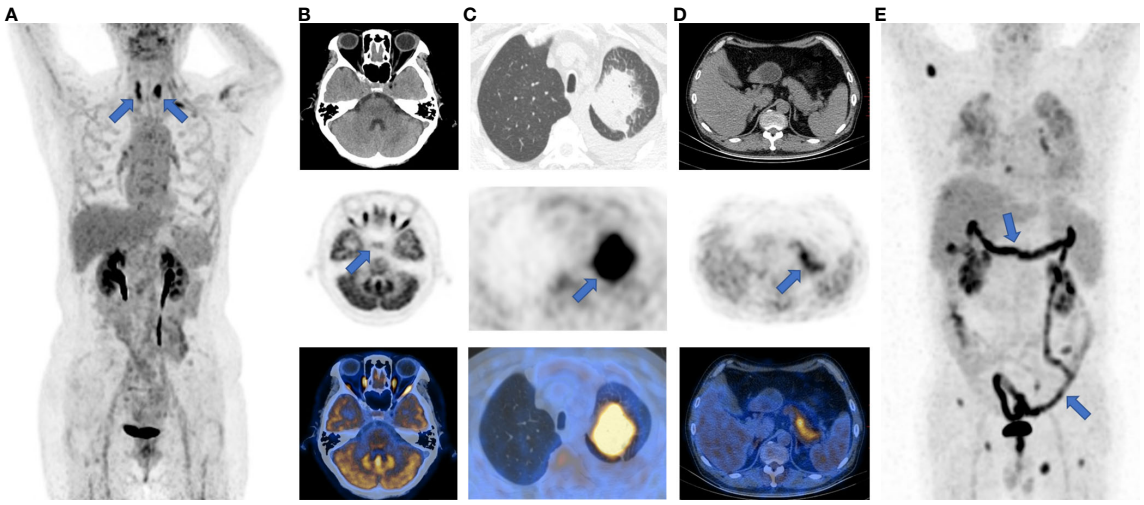

FIGURE 3
Typical images of irAEs in patients with ICI treatment. **(A)**, thyroiditis; **(B)**, hypophysitis; **(C)**, pneumonia; **(D)**, pancreatitis; **(E)**, enteritis. The sites of irAEs were marked with blue arrows on maximum intensity projection (MIP) and PET images.

In order to standardize the imaging evaluation of tumor treatment efficacy, a series of tumor treatment response evaluation criteria have been proposed. The CT-based evaluation criteria, i.e. Response Evaluation Criteria in Solid Tumors version 1.1 (RECIST 1.1) (59), were initially used directly. The typical cases evaluated by RECIST 1.1 were displayed in Figure 4. RECIST 1.1 was later adjusted for better ICI response evaluation. The modified RECIST 1.1 for immune-based therapeutics, i.e. iRECIST, classify the initial discovery of the suspected progression as initially unconfirmed progressive disease (iUPD) (60). Immune-modified RECIST (imRECIST) includes the measurable new lesions in the total tumor burden (61).

Meanwhile, the ^{18}F-FDG PET (PET/CT)-based evaluation criteria have also been successively proposed (Table 2). The European Organization for Research and Treatment of Cancer 1999 criteria (EORTC) is the first metabolism criterion using SUVmax changes to determine antitumor treatment response (62). In 2009, Wahl et al. proposed the PET Response Criteria in Solid Tumors (PERCIST) (63), which has also been modified further. Immune PERCIST (iPERCIST) introduced the concept of unconfirmed progressive metabolic disease (UPMD) (64). Since immunotherapy may induce new inflammatory lesions that are detectable on ^{18}F-FDG PET/CT, immunotherapy-modified response classification (imPERCIST5) was introduced. According to imPERCIST5, progressive metabolic disease (PMD) was defined only by an increase of the sum of peak standardized uptake values normalized for body lean body mass (SULpeak) by 30% (65). In 2018, Anwar et al. proposed PET Response Evaluation Criteria for Immunotherapy (PERCIMT) to evaluate clinical benefit based on the number and size of new lesions (66). According to PERCIMT, 4 or more new lesions (regardless of size), or 3 or more new lesions (diameter > 1 cm), or 2 or more new lesions (diameter > 1.5 cm), are all defined as no-clinical benefit, while the other cases are considered clinically benefited.

The comparative studies of different response evaluation criteria are shown in Table 3. In short, the continuous adjustment of immunotherapy response evaluation criteria aims to guide immunotherapy management more precisely and effectively.

Prediction of prognosis

Since only a certain proportion of patients can benefit from ICIs therapy, how to conduct pretreatment assessments and identify eligible patients has important clinical significance. Up to now, some potentially prognostic biomarkers have been explored, including tumor PD-L1 expression, tumor mutation burden (TMB), microsatellite instability (MSI), gene expression profiles, gastrointestinal microbiome, and so on (73). Nevertheless, the values of these biomarkers remain controversial, and some biomarkers (such as TMB and MSI) require complex, expensive, and time-consuming analyses. Despite imperfection, PD-L1 expression is still the most commonly used biomarker in clinic, especially for NSCLC patients (74).

There have been a variety of studies committed to discovering the prognostic value of ^{18}F-FDG PET/CT imaging on ICI treatment, but the results are inconsistent. The researches mainly focus on patients with NSCLC and melanoma, and the

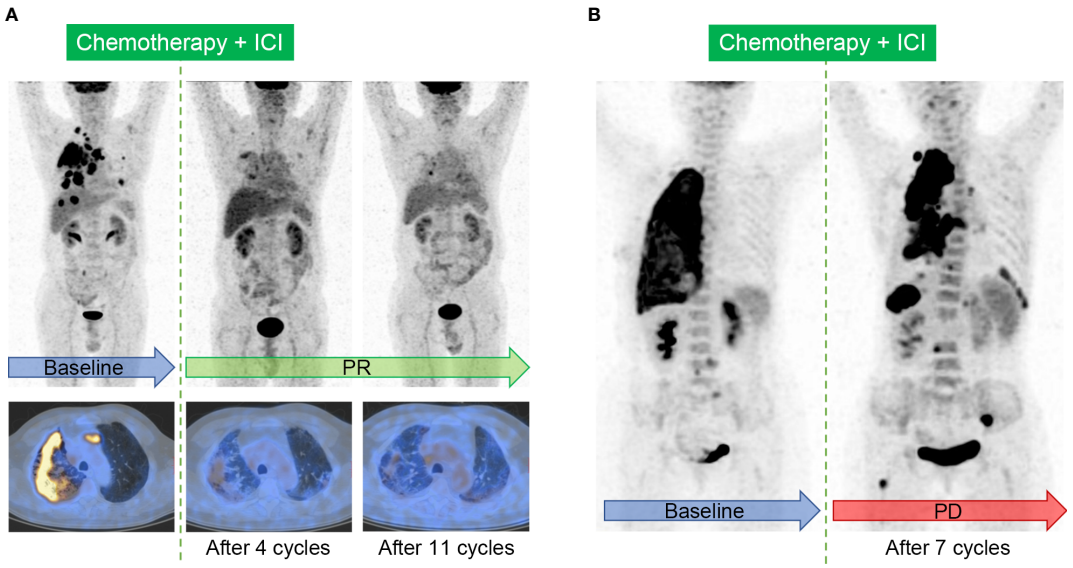

FIGURE 4
Typical cases evaluated by Response Evaluation Criteria in Solid Tumors (RECIST) 1.1 in patients with ICI treatment. **(A)**, Immunotherapy response in a 64-year-old male patient with right lung adenocarcinoma. The baseline image shows intensive FDG uptake in the primary tumor, accompanied with multifocal intrapulmonary metastasis, lymphadenopathy, and the involvement of pleura. Follow-up images after 4 cycles and sequential 11 cycles of the combination of chemotherapy and ICI show partial response (PR). **(B)**, Immunotherapy response in a 60-year-old female patient with right lung adenocarcinoma. Image after 7 cycles of the combination of chemotherapy and ICI shows the enlargement and increased metabolism in the primary tumor, and the onset of multiple new lesions in the lung, pleura, lymph nodes, liver, and bone, indicating progressive disease (PD).

metabolic parameters include SUVmax, SUVmean, metabolic tumor volume (MTV), total MTV (tMTV), total lesion glycolysis (TLG), and so on (Table 4). Although SUVmax is the most commonly used metabolic parameter, its prognostic value may be controversial (81, 87). Some researchers have also advocated that SUVmean may be suggestive (83). Other studies support the prognostic value of MTV and TLG for immunotherapy, indicating that high MTV and TLG are associated with poor

TABLE 2 Metabolism evaluation criteria for immunotherapy response.

Criterion	CMR	PMR	SMD	PMD
EORTC (1999) (62)	complete resolution of ^{18}F-FDG uptake within the tumor volume	SUV is reduced by at least 15% ~25% after 1 cycle of chemotherapy, and > 25% after more than one treatment cycle	not CMR, PMR, or PMD	SUV increase > 25%, visible increase in the extent of tumor ^{18}F-FDG uptake (> 20% in the longest dimension), or appearance of new ^{18}F-FDG uptake in metastatic lesions
PERCIST (2009) (63)	^{18}F-FDG uptake completely disappeared	SULpeak decrease by ≥30% in the target lesions, and absolute drop in SUL by at least 0.8 SUL units	not CMR, PMR, or PMD	SULpeak in the target lesions increase ≥ 30%, with ≥ 0.8 SUL unit increase; 75% increase in TLG; new ^{18}F-FDG-avid lesions that are typical of cancer and not related to treatment effect or infection
iPERCIST (2019) (64)	^{18}F-FDG uptake completely disappeared	SULpeak decrease by ≥30% in the target lesions	not CMR, PMR, or PMD	SULpeak increase ≥ 30% or new ^{18}F-FDG-avid lesions (UPMD) UPMD needs to be confirmed CPMD by a second PET after 4-8 weeks; if UPMD is followed by PMR or SMD, the bar is reset
imPERCIST5 (2019) (65)	^{18}F-FDG uptake completely disappeared	SULpeak decrease by ≥30% in the target lesions, and absolute drop in SUL by at least 0.8 SUL units	not CMR, PMR, or PMD	SULpeak in the target lesions increase ≥ 30%, with ≥ 0.8 SUL unit increase in tumor SUVpeak; New lesions were included in the sum of SULpeak if they showed higher uptake than existing target lesions or if fewer than 5 target lesions were detected on the baseline scan

EORTC, European Organization for Research and Treatment of Cancer 1999 criteria; PERCIST, PET Response Criteria in Solid Tumors; imPERCIST5, immunotherapy-modified PERCIST, 5-lesion analysis; iPERCIST, immune PERCIST; CMR, complete metabolic response; PMR, partial metabolic response; SMD, stable metabolic disease; PMD, progressive metabolic disease; UPMD, unconfirmed progressive metabolic disease; CPMD, confirmed progressive metabolic disease; SUV, standard uptake value; SULpeak, peak standardized uptake values normalized for body lean body mass; SUL, standardized uptake value of lean body mass; TLG, total lesion glycolysis; SUVpeak, peak standardized uptake value.

TABLE 3 Comparative studies on evaluation criteria of immunotherapy response.

Author/ Year	Study/ number	Histology	ICI Treatment	Criteria	Conclusion
Sachpekidis et al. (67). (2018)	prospective 41 patients	melanoma	ipilimumab	EORCT PERCIMT	The sensitivity of PERCIMT was significantly higher than EORTC, but the specificity was not significantly different.
Sachpekidis et al. (68). (2019)	prospective 16 patients	melanoma	ipilimumab	EORTC PERCIMT	PERCIMT shows more correct classification (15/16 patients) than EORTC (13/16 patients).
Goldfarb et al. (64). (2019)	retrospective 28 patients	NSCLC	nivolumab	iRECIST iPERCIST	iPERCIST can reclassify 39% of patients assessed by iRECIST.
Beer et al. (69). (2019)	prospective 42 patients	NSCLC	nivolumab, pembrolizumab or durvalumab	RECIST 1.1 iRECIST PERCIST	The three criteria are only moderately consistent, but there is no significant difference in the ability to assess PFS and OS after 12 months
Castello et al. (70). (2020)	prospective 35 patients	NSCLC	nivolumab or pembrolizumab	RECIST 1.1 imRECIST EORTC PERCIST imPERCIST PERCIMT	Fair agreement between imRECIST and EORTC, and PERCIST, and moderate for imRECIST and PERCIMT were detected. All criteria are significantly related to PFS, but only PERCIMT and imPERCIST are related to OS.
Dimitriou et al. (71). (2021)	retrospective 104 patients	melanoma	anti-PD-1 with or without anti-CTLA-4 treatment	RECIST EORTC	EORTC is better than RECIST in predicting progress, effectively assessing residual lesions on CT, and predicting long-term benefits.
Kitajima et al. (72). (2022)	retrospective 27 patients	melanoma	nivolumab or pembrolizumab	EORTC, PERCIST, imPERCIST	All the three FDG-PET criteria showed accuracy for response evaluation of ICI therapy and prediction of malignant melanoma patient prognosis.

RECIST, Response Evaluation Criteria in Solid Tumor; iRECIST, a modified RECIST 1.1 for immune-based therapeutics; EORTC, European Organization for Research and Treatment of Cancer 1999 criteria; PERCIMT, PET Response Evaluation Criteria for Immunotherapy; PERCIST, PET Response Criteria in Solid Tumors; iPERCIST, immune PERCIST; imPERCIST, immunotherapy-modified PERCIST; PFS, progression-free survival; OS, overall survival; NSCLC, non-small-cell lung cancer; PD-L1, programmed death-ligand 1; PD-1, programmed cell death protein-1; CTLA-4, cytotoxic T lymphocyte-associated protein 4.

prognosis (78, 80). However, the multivariate analysis of a prospective study on nivolumab found no significant correlation between TLG and OS (88). In addition, tMTV provides a good indication of the total cancer burden (3). Seban et al. demonstrated that tMTV > 75 cm^3 was associated with shorter OS and the absence of clinical disease benefit. They proposed a metabolic scoring system based on the derived neutrophil-to-lymphocyte ratio (dNLR) and tMTV, which stratified patients into three groups with different prognosis: poor prognosis (dNLR>3 and tMTV>75 cm^3), moderate prognosis (dNLR>3 or tMTV>75 cm^3) and good prognosis (dNLR ≤ 3 and tMTV ≤ 75 cm^3) (77). However, Vekens et al. discovered that tMTV and TLG did not have a predictive effect (87).

The main reasons for the inconsistent results may lie in the heterogeneity of patients included and the difference of treatment schemes in the study cohorts. The discrepancies between adopted end-point events and treatment response evaluation criteria may be other confounding issues. Further researches should be carried out to establish an ideal and universal method from the metabolism perspective for predicting the prognosis of pan-cancer, which would be validated in a large dataset.

In recent years, the rapid development of artificial intelligence has further promoted the application of ^{18}F-FDG PET/CT radiomics, which extracts a large number of quantitative features from PET/CT images through automated and high-throughput methods, in the prognosis evaluation after surgery, chemoradiotherapy, targeted therapy or immunotherapy. Mu et al. (91) constructed a deep learning model based on PET/CT images, namely the EGFR-deep learning score (EGFR-DLS), to provide non-invasive decision support for targeted therapy or immunotherapy for patients with NSCLC. Moreover, Mu et al. (92) established a nomogram including multi-parameter PET/CT radiomic features, Eastern Cooperative Oncology Group (ECOG) score, and distant metastasis to predict the prognosis of patients with stage IIIB-IV NSCLC receiving ICIs therapy.

Challenges and perspectives

With unprecedented advances in ICIs in cancer treatment, the value of ^{18}F-FDG PET/CT has been especially emphasized. Nevertheless, several challenges associated with ^{18}F-FDG PET/CT imaging need to be addressed to broaden its application in ICIs treatment. One major shortcoming is the lack of recognized

TABLE 4 Prognosis predictive role of ^{18}F-FDG PET/CT in immunotherapy.

Author/ Year	Study/ number	Histology	ICI treatment	Conclusion
Seban et al. (75) (2019)	retrospective, 55 patients	melanoma	anti-PD-1 IgG	Higher tMTV and BLR correlated with shorter survival
Ito et al. (76) (2019)	retrospective, 142 patients	melanoma	ipilimumab	wMTV was negatively correlated with OS
Seban et al. (77). (2020)	retrospective, 80 patients	NSCLC	anti-PD-1/PD-L1	tMTV > 75 cm^3 was associated with shorter OS and absence of disease clinical benefit
Hashimoto et al. (78). (2020)	retrospective, 85 patients	NSCLC	pembrolizumab or nivolumab	TLG and MTV were negatively correlated with PFS and OS
Castello et al. (79). (2020)	prospective, 50 patients	NSCLC	nivolumab or pembrolizumab	High TLG and MTV were significantly associated with hyperprogression and MTV remained a negatively independent predictor for OS
Yamaguchi et al. (80). (2020)	retrospective, 48 patients	NSCLC	pembrolizumab	Higher MTV correlated with worse outcomes for patients with PD-L1 expression ≥50%
Polverari et al. (81). (2020)	retrospective, 57 patients	NSCLC	pembrolizumab	Patients with higher MTV and TLG values were more likely to have disease progression and poor response to immunotherapy.
Chardin et al. (82) (2020)	prospective, 75 patients	NSCLC	pembrolizumab or nivolumab	MTV and TLG were negatively correlated with OS and could reliably predict early treatment discontinuation
Seban et al. (83). (2020)	retrospective, 63 patients	NSCLC	pembrolizumab	Both high tMTV and high SUVmean were independent predictors for decreased PFS, and tMTV was also negatively correlated with OS.
Wong et al. (84). (2020)	retrospective, 90 patients	melanoma	ipilimumab, pembrolizumab or nivolumab	High pre-treatment SLR was associated with short PFS and OS
Seban et al. (85). (2020)	retrospective, 56 patients	melanoma	ipilimumab and/ or pembrolizumab	In patients with mucosal melanoma, increased tumor SUVmax was correlated with shorter OS, while in patients with cutaneous melanoma, increased tMTV and BLR were independently correlated with shorter OS, PFS, and lower response
Dall' Olio et al. (86). (2021)	retrospective, 34 patients	NSCLC	pembrolizumab	tMTV ≥ 75cm^3 could be a prognostic predictor of inferior outcomes in patients with PD-L1 expression ≥ 50%
Vekens et al. (87). (2021)	retrospective, 30 patients	NSCLC	pembrolizumab	SUVmax was positively related to PFS. Clinical response and survival were independent of tMTV and TLG. Reduction of tMTV and TLG after 8 to 9 weeks of treatment was a better predictor of prolonged survival than RECIST 1.1.
Bauckneht et al. (88) (2021)	prospective, 45 patients	NSCLC	nivolumab	MTV was negatively related to OS
Awada et al. (89) (2021)	retrospective, 183 patients	melanoma	pembrolizumab	Elevated tMTV was associated with worse PFS and OS.
Gulturk et al. (90). (2021)	retrospective, 32 patients	RCC	nivolumab	Pre-treatment SUVmax was negatively related to PFS

SUVmax, maximum standardized uptake value; SUVmean, mean standardized uptake value; MTV, metabolic tumor volume; TLG, total lesion glycolysis; tMTV, total metabolic tumor volume; SLR, spleen-to-liver SUVmax ratio; BLR, bone marrow-to-liver SUVmax ratio; wMTV, whole-body metabolic tumor volume; PD-L1, programmed death-ligand 1; PD-1, programmed cell death protein-1; NSCLC, non-small-cell lung cancer; RCC, renal cell carcinoma; RECIST 1.1, Response Evaluation Criteria in Solid Tumors version 1.1; OS, overall survival; PFS, progression-free survival.

guidelines to instruct the application of ^{18}F-FDG PET/CT imaging in immunotherapy. On the other hand, although glucose metabolism parameters, such as SUVmax, have been shown to be significantly related to the immune characteristics of TME or prognosis, related studies were mostly retrospective, single-center and small-sample size, and there are controversies between the results of different studies. So, further prospective and large-sample cohort studies are still needed. Moreover,

current studies mainly focus on NSCLC and melanoma. With the extensive development of ICIs treatment and the accumulation of cases, researches concentrating on other cancers can be investigated. Besides, there remains a challenging area of investigations on biological mechanisms of the association between TME and ^{18}F-FDG PET/CT imaging, and basic and translational studies are encouraged to unravel the unknowns.

New PET molecular probe imaging for ICIs treatment

In addition to ^{18}F-FDG, researchers are also committed to developing a series of new PET molecular probes targeting the compositions of TME, some of which have entered preclinical or clinical applications (Figure 5). The principles of these designs are mostly based on the specific binding of radiolabeled antibodies, peptides, or small molecules with the corresponding targets. The emergence of new molecular imaging agents is expected to provide more accurate means to obtain dynamic information about TME for promoting individualized treatment.

PD-1/PD-L1 targeting

PD-L1 or PD-1 expression is reported to be related with prognosis after immunotherapy, and the detection of the two biomarkers mainly depends on immunohistochemistry (IHC) of biopsy or surgery materials. However, this invasive and snap-shot approach has some limitations, including the inability to reflect the heterogeneity and spatio-temporal dynamic expression of PD-L1 or PD-1 in tumor tissues, different antibody detection platforms and different thresholds leading to different results, and difficulties in obtaining histological specimens for some patients. Targeted molecular imaging can detect PD-L1 or PD-1 expression noninvasively and dynamically *in vivo* to compensate for the above shortcomings.

PD-1 imaging agents used in clinical trials include ^{89}Zr-pembrolizumab, ^{64}Cu-pembrolizumab, and ^{89}Zr-nivolumab. The first-in-humans study of ^{89}Zr-pembrolizumab in patients with advanced-stage NSCLC confirmed its safety and feasibility for immunotherapy. The findings indicated that patients with higher tumor uptake for ^{89}Zr-pembrolizumab showed a tendency for better response to pembrolizumab (93). A later study showed that ^{89}Zr-pembrolizumab uptake was positively associated with PFS and OS in melanoma and NSCLC patients (94).

PD-L1 targeting imaging agents mainly include ^{89}Zr-atezolizumab, ^{89}Zr-durvalumab, and ^{18}F-BMS-986192, all of which have been in clinical trials (95). Researchers uncovered that ^{89}Zr-atezolizumab uptake performed better than IHC or RNA sequencing-based predictive biomarkers in evaluating clinical responses for ICIs (96). ^{89}Zr-atezolizumab is also reported to be helpful in identifying RCC patients who may benefit from anti-PD-1/PD-L1 therapy (97). Meanwhile, a number of preclinical studies on PD-L1-targeting molecular

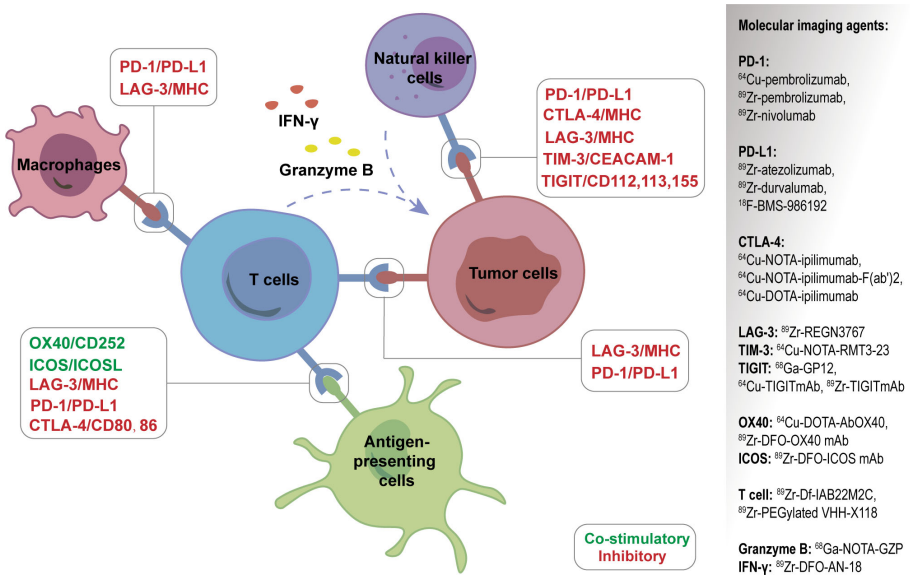

FIGURE 5
A series of new PET molecular probes targeting the compositions of tumor microenvironment (TME).

probes (including antibodies, peptides, and small molecules) using nuclear medicine, MRI, or optical imaging, have been documented (98, 99).

CTLA-4 targeting

CTLA-4 is another well-known immunosuppressive checkpoint. It is expressed on T cells and binds with CD80/86 ligands on DCs with a high affinity to prevent uncontrolled expansion of activated T cells. Accordingly, the blockade of CTLA-4 with antibodies has been used in clinic as a promising option for cancer patients. CTLA-4 targeting imaging agents include ^{64}Cu-NOTA-ipilimumab-F(ab')2, ^{64}Cu-NOTA-ipilimumab, and ^{64}Cu-DOTA-ipilimumab (100, 101), and all of them have not yet entered clinical trials.

Other immune checkpoints targeting

Apart from PD-1, PD-L1, and CTLA-4, several novel immune checkpoint molecules, both the inhibitory and stimulatory ones, have been discovered over the past decade (43). The former molecules include lymphocyte activation gene-3 (LAG-3), T cell immunoglobulin and mucin-domain containing-3 (TIM-3), T cell immunoglobulin and ITIM domain (TIGIT), sialic acid-binding immunoglobulin-like lectin 15 (Siglec-15), and V-domain Ig suppressor of T cell activation (VISTA), which express on a variety of immune cells and exhibit inhibitory roles in the context of malignancy.

The positive immune regulators, such as glucocorticoid-induced TNFR-related gene (GITR) and tumor necrosis factor receptor superfamily member 4 (OX40), are co-stimulatory molecules expressed on T cells. In addition, inducible T-cell co-stimulator (ICOS) is an indicator of T-cell-mediated immune response, and some animal experiments showed that ^{89}Zr-DFO-ICOS mAb targeting ICOS could monitor immunotherapy response (102, 103). With the discovery of new immune checkpoints, molecular probes targeting these targets are emerging.

T cell targeting

CD8$^+$ TILs are an important feature reflecting TIME and significantly impact the tumorigenesis and development of tumors. Responders showed higher numbers of pre-existing CD8$^+$ Teff cells within the tumor and at tumor margins prior to ICIs therapy (104). Therefore, targeted imaging of CD8$^+$ T cells is of great significance for immunotherapy.

^{89}Zr-Df-IAB22M2C, a new molecular probe targeting CD8$^+$ TILs, is used to assess CD8$^+$ TILs in tumors accurately. The first human trial of ^{89}Zr-Df-IAB22M2C has proven its safety and validity in patients with solid malignancies (105). ^{89}Zr-PEGylated VHH-X118 has also been confirmed to have the potential for CD8$^+$ TIL targeting imaging (106). Iravani et al. demonstrated that ^{18}F-FDG and other new imaging agents, such as those targeting CD8$^+$ TILs or T cell function, can be used for PET/CT imaging to guide ICI treatment in the future (107). However, due to the complexity of lymphocyte subsets, CD8$^+$ TILs imaging agents can only reflect part of the overall immune effect (108). Another problem with T cell targeting imaging is to determine the optimal timing of evaluation to reasonably reflect the activation degree of T cells.

Secretory substance targeting

Secretory substances exist in the extracellular environment and participate in information transmission and effect exertion. Imaging targeting such substances, such as granzyme B and interferon-gamma (IFN-γ), has potential advantages in showing the immune treatment response. With regards to granzyme B targeted imaging, ^{18}F-Ara-Gand and ^{68}Ga-NOTA-GZP can reflect the activation of CD8$^+$ T cells and help to distinguish between pseudoprogression and true progression (107). Another study showed that the detection of granzyme B with ^{68}Ga-NOTA-GZP helps differentiate the responders from non-responders to immunotherapy (109). ^{89}Zr-DFO-AN-18, a novel probe targeting IFN-γ, has been indicated to monitor the response to immunotherapy in mouse mammary tumors (110).

Conclusion

In summary, an in-depth understanding of the underlying mechanisms of cancer immunotherapy is an important cornerstone for expanding the benefits of ICIs treatment to a larger cancer population. Hence, diagnostic approaches, especially PET/CT molecular imaging, should be vigorously developed to identify patients who might benefit from ICIs treatment. Concurrently, under the guidance of PET/CT molecular imaging, clinicians can shift the paradigm to improve the outcome of cancer patients, and even facilitate the development of novel therapeutic strategies to enhance therapeutic effectiveness. It is believed that with the extensive availability of standardized protocols, various affordable imaging agents, and user-friendly analysis platforms, PET/CT imaging will play a more important role in the era of immuno-oncology.

Author contributions

Conceptualization, ML. Methodology, ML, YG, and CW. Material preparation, YG, CW, XC, LM, XZ, JC, and XL. Writing-original draft preparation, YG and CW. Writing-review and editing, ML and XC. Funding acquisition, ML. Supervision, ML. All authors contributed to the article and approved the submitted version.

Funding

This study was supported by grants from the National Natural Science Foundation of China (82172052), Beijing Natural Science Foundation (Z210007), and National High-Level Hospital Clinical Research Funding (Interdepartmental Clinical Research Project of Peking University First Hospital) (2022CR34).

Conflict of interest

The authors declare that the research was conducted in the absence of any commercial or financial relationships that could be construed as a potential conflict of interest.

Publisher's note

References

1. Zhang Y, Zhang Z. The history and advances in cancer immunotherapy: understanding the characteristics of tumor-infiltrating immune cells and their therapeutic implications. *Cell Mol Immunol* (2020) 17:807–21. doi: 10.1038/s41423-020-0488-6

2. Iravani A, Hicks RJ. Imaging the cancer immune environment and its response to pharmacologic intervention, part 1: The role of (18)F-FDG PET/CT. *J Nucl Med* (2020) 61:943–50. doi: 10.2967/jnumed.119.234278

3. Dall'Olio FG, Marabelle A, Caramella C, Garcia C, Aldea M, Chaput N, et al. Tumour burden and efficacy of immune-checkpoint inhibitors. *Nat Rev Clin Oncol* (2022) 19:75–90. doi: 10.1038/s41571-021-00564-3

4. Park K, Veena MS, Shin DS. Key players of the immunosuppressive tumor microenvironment and emerging therapeutic strategies. *Front Cell Dev Biol* (2022) 10:830208. doi: 10.3389/fcell.2022.830208

5. Elia I, Haigis MC. Metabolites and the tumour microenvironment: from cellular mechanisms to systemic metabolism. *Nat Metab* (2021) 3:21–32. doi: 10.1038/s42255-020-00317-z

6. Leone RD, Powell JD. Metabolism of immune cells in cancer. *Nat Rev Cancer* (2020) 20:516–31. doi: 10.1038/s41568-020-0273-y

7. Cascone T, McKenzie JA, Mbofung RM, Punt S, Wang Z, Xu C, et al. Increased tumor glycolysis characterizes immune resistance to adoptive T cell therapy. *Cell Metab* (2018) 27:977–987.e4. doi: 10.1016/j.cmet.2018.02.024

8. Angelin A, Gil-de-Gómez L, Dahiya S, Jiao J, Guo L, Levine MH, et al. Foxp3 reprograms T cell metabolism to function in low-glucose, high-lactate environments. *Cell Metab* (2017) 25:1282–1293.e7. doi: 10.1016/j.cmet.2016.12.018

9. Bussard KM, Mutkus L, Stumpf K, Gomez-Manzano C, Marini FC. Tumor-associated stromal cells as key contributors to the tumor microenvironment. *Breast Cancer Res* (2016) 18:84. doi: 10.1186/s13058-016-0740-2

10. Pavlides S, Whitaker-Menezes D, Castello-Cros R, Flomenberg N, Witkiewicz AK, Frank PG, et al. The reverse warburg effect: aerobic glycolysis in cancer associated fibroblasts and the tumor stroma. *Cell Cycle* (2009) 8:3984–4001. doi: 10.4161/cc.8.23.10238

11. Chen DS, Mellman I. Elements of cancer immunity and the cancer-immune set point. *Nature* (2017) 541:321–30. doi: 10.1038/nature21349

12. Hamada T, Soong TR, Masugi Y, Kosumi K, Nowak JA, da Silva A, et al. TIME (Tumor immunity in the MicroEnvironment) classification based on tumor CD274 (PD-L1) expression status and tumor-infiltrating lymphocytes in colorectal carcinomas. *Oncoimmunology* (2018) 7:e1442999. doi: 10.1080/2162402x.2018.1442999

13. Taube JM, Anders RA, Young GD, Xu H, Sharma R, McMiller TL, et al. Colocalization of inflammatory response with B7-h1 expression in human melanocytic lesions supports an adaptive resistance mechanism of immune escape. *Sci Transl Med* (2012) 4:127ra37. doi: 10.1126/scitranslmed.3003689

14. Kim TK, Vandsemb EN, Herbst RS, Chen L. Adaptive immune resistance at the tumour site: mechanisms and therapeutic opportunities. *Nat Rev Drug Discovery* (2022) 21:529–40. doi: 10.1038/s41573-022-00493-5

15. Siska PJ, Singer K, Evert K, Renner K, Kreutz M. The immunological warburg effect: Can a metabolic-tumor-stroma score (MeTS) guide cancer immunotherapy? *Immunol Rev* (2020) 295:187–202. doi: 10.1111/imr.12846

16. Xie H, Simon MC. Oxygen availability and metabolic reprogramming in cancer. *J Biol Chem* (2017) 292:16825–32. doi: 10.1074/jbc.R117.799973

17. Noman MZ, Desantis G, Janji B, Hasmim M, Karray S, Dessen P, et al. PD-L1 is a novel direct target of HIF-1α, and its blockade under hypoxia enhanced MDSC-mediated T cell activation. *J Exp Med* (2014) 211:781–90. doi: 10.1084/jem.20131916

18. Riera-Domingo C, Audigé A, Granja S, Cheng WC, Ho PC, Baltazar F, et al. Immunity, hypoxia, and metabolism-the ménage à trois of cancer: Implications for immunotherapy. *Physiol Rev* (2020) 100:1–102. doi: 10.1152/physrev.00018.2019

19. Zhao L, Liu J, Wang H, Shi J. Association between (18)F-FDG metabolic activity and programmed death ligand-1 (PD-L1) expression using 22C3 immunohistochemistry assays in non-small cell lung cancer (NSCLC) resection specimens. *Br J Radiol* (2021) 94:20200397. doi: 10.1259/bjr.20200397

20. Zhao L, Liu J, Shi J, Wang H. Relationship between SP142 PD-L1 expression and (18)F-FDG uptake in non-Small-Cell lung cancer. *Contrast Media Mol Imaging* (2020) 2020:2010924. doi: 10.1155/2020/2010924

21. Mitchell KG, Amini B, Wang Y, Carter BW, Godoy MCB, Parra ER, et al. (18)F-fluorodeoxyglucose positron emission tomography correlates with tumor immunometabolic phenotypes in resected lung cancer. *Cancer Immunol Immunother* (2020) 69:1519–34. doi: 10.1007/s00262-020-02560-5

22. Wang Y, Zhao N, Wu Z, Pan N, Shen X, Liu T, et al. New insight on the correlation of metabolic status on (18)F-FDG PET/CT with immune marker expression in patients with non-small cell lung cancer. *Eur J Nucl Med Mol Imaging* (2020) 47:1127–36. doi: 10.1007/s00259-019-04500-7

23. Miyazawa T, Otsubo K, Sakai H, Kimura H, Chosokabe M, Morikawa K, et al. Combining PD-L1 expression and standardized uptake values in FDG-PET/CT can predict prognosis in patients with resectable non-Small-Cell lung cancer. *Cancer Control* (2021) 28:10732748211038314. doi: 10.1177/10732748211038314

24. Wu X, Huang Y, Zhao Q, Wang L, Song X, Li Y, et al. PD-L1 expression correlation with metabolic parameters of FDG PET/CT and clinicopathological characteristics in non-small cell lung cancer. *EJNMMI Res* (2020) 10:51. doi: 10.1186/s13550-020-00639-9

25. Wang L, Ruan M, Lei B, Yan H, Sun X, Chang C, et al. The potential of (18)F-FDG PET/CT in predicting PDL1 expression status in pulmonary lesions of untreated stage IIIB-IV non-small-cell lung cancer. *Lung Cancer* (2020) 150:44–52. doi: 10.1016/j.lungcan.2020.10.004

26. Lopci E, Toschi L, Grizzi F, Rahal D, Olivari L, Castino GF, et al. Correlation of metabolic information on FDG-PET with tissue expression of immune markers in patients with non-small cell lung cancer (NSCLC) who are candidates for upfront surgery. *Eur J Nucl Med Mol Imaging* (2016) 43:1954–61. doi: 10.1007/s00259-016-3425-2

27. Jreige M, Letovanec I, Chaba K, Renaud S, Rusakiewicz S, Cristina V, et al. (18)F-FDG PET metabolic-to-morphological volume ratio predicts PD-L1 tumour expression and response to PD-1 blockade in non-small-cell lung cancer. *Eur J Nucl Med Mol Imaging* (2019) 46:1859–68. doi: 10.1007/s00259-019-04348-x

28. Li J, Ge S, Sang S, Hu C, Deng S. Evaluation of PD-L1 expression level in patients with non-small cell lung cancer by (18)F-FDG PET/CT radiomics and clinicopathological characteristics. *Front Oncol* (2021) 11:789014. doi: 10.3389/fonc.2021.789014

29. Mu W, Jiang L, Shi Y, Tunali I, Gray JE, Katsoulakis E, et al. Non-invasive measurement of PD-L1 status and prediction of immunotherapy response using deep learning of PET/CT images. *J Immunother Cancer* (2021) 9(6):e002118. doi: 10.1136/jitc-2020-002118

30. Monaco L, De Bernardi E, Bono F, Cortinovis D, Crivellaro C, Elisei F, et al. The "digital biopsy" in non-small cell lung cancer (NSCLC): a pilot study to predict the PD-L1 status from radiomics features of [18F]FDG PET/CT. *Eur J Nucl Med Mol Imaging* (2022) 49(10):3401–11. doi: 10.1007/s00259-022-05783-z

31. Zhou J, Zou S, Kuang D, Yan J, Zhao J, Zhu X. A novel approach using FDG-PET/CT-Based radiomics to assess tumor immune phenotypes in patients with non-small cell lung cancer. *Front Oncol* (2021) 11:769272. doi: 10.3389/fonc.2021.769272

32. Wu C, Cui Y, Liu J, Ma L, Xiong Y, Gong Y, et al. Noninvasive evaluation of tumor immune microenvironment in patients with clear cell renal cell carcinoma using metabolic parameter from preoperative 2-[(18)F]FDG PET/CT. *Eur J Nucl Med Mol Imaging* (2021) 48:4054–66. doi: 10.1007/s00259-021-05399-9

33. Hirakata T, Fujii T, Kurozumi S, Katayama A, Honda C, Yanai K, et al. FDG uptake reflects breast cancer immunological features: the PD-L1 expression and degree of TILs in primary breast cancer. *Breast Cancer Res Treat* (2020) 181:331–8. doi: 10.1007/s10549-020-05619-0

34. Park S, Min EK, Bae SJ, Cha C, Kim D, Lee J, et al. Relationship of the standard uptake value of (18)F-FDG-PET-CT with tumor-infiltrating lymphocytes in breast tumors measuring ≥ 1 cm. *Sci Rep* (2021) 11:12046. doi: 10.1038/s41598-021-91404-y

35. Sasada S, Shiroma N, Goda N, Kajitani K, Emi A, Masumoto N, et al. The relationship between ring-type dedicated breast PET and immune microenvironment in early breast cancer. *Breast Cancer Res Treat* (2019) 177:651–7. doi: 10.1007/s10549-019-05339-0

36. Lee S, Choi S, Kim SY, Yun MJ, Kim HI. Potential utility of FDG PET-CT as a non-invasive tool for monitoring local immune responses. *J Gastric Cancer* (2017) 17:384–93. doi: 10.5230/jgc.2017.17.e43

37. Jiang H, Zhang R, Jiang H, Zhang M, Guo W, Zhang J, et al. Retrospective analysis of the prognostic value of PD-L1 expression and (18)F-FDG PET/CT metabolic parameters in colorectal cancer. *J Cancer* (2020) 11:2864–73. doi: 10.7150/jca.38689

38. Chen R, Zhou X, Liu J, Huang G. Relationship between the expression of PD-1/PD-L1 and (18)F-FDG uptake in bladder cancer. *Eur J Nucl Med Mol Imaging* (2019) 46:848–54. doi: 10.1007/s00259-018-4208-8

39. Zhao L, Zhuang Y, Fu K, Chen P, Wang Y, Zhuo J, et al. Usefulness of [(18)F]fluorodeoxyglucose PET/CT for evaluating the PD-L1 status in nasopharyngeal carcinoma. *Eur J Nucl Med Mol Imaging* (2020) 47:1065–74. doi: 10.1007/s00259-019-04654-4

40. Togo M, Yokobori T, Shimizu K, Handa T, Kaira K, Sano T, et al. Diagnostic value of (18)F-FDG-PET to predict the tumour immune status defined by tumoural PD-L1 and CD8(+)tumour-infiltrating lymphocytes in oral squamous cell carcinoma. *Br J Cancer* (2020) 122:1686–94. doi: 10.1038/s41416-020-0820-z

41. Seol HY, Kim YS, Kim SJ. Diagnostic test accuracy of (18)F-FDG PET/CT for prediction of programmed death ligand 1 (PD-L1) expression in solid tumours: a meta-analysis. *Clin Radiol* (2021) 76:863.e19–863.e25. doi: 10.1016/j.crad.2021.06.012

42. Zhou J, Zou S, Cheng S, Kuang D, Li D, Chen L, et al. Correlation between dual-Time-Point FDG PET and tumor microenvironment immune types in non-small cell lung cancer. *Front Oncol* (2021) 11:559623. doi: 10.3389/fonc.2021.559623

43. Morad G, Helmink BA, Sharma P, Wargo JA. Hallmarks of response, resistance, and toxicity to immune checkpoint blockade. *Cell* (2021) 184:5309–37. doi: 10.1016/j.cell.2021.09.020

44. Darnell EP, Mooradian MJ, Baruch EN, Yilmaz M, Reynolds KL. Immune-related adverse events (irAEs): Diagnosis, management, and clinical pearls. *Curr Oncol Rep* (2020) 22:39. doi: 10.1007/s11912-020-0897-9

45. Nobashi T, Mittra E. PD-1 blockade-induced inflammatory arthritis. *Radiology* (2018) 289:616. doi: 10.1148/radiol.2018181532

46. Wang DY, Salem JE, Cohen JV, Chandra S, Menzer C, Ye F, et al. Fatal toxic effects associated with immune checkpoint inhibitors: A systematic review and meta-analysis. *JAMA Oncol* (2018) 4:1721–8. doi: 10.1001/jamaoncol.2018.3923

47. Das S, Johnson DB. Immune-related adverse events and anti-tumor efficacy of immune checkpoint inhibitors. *J Immunother Cancer* (2019) 7:306. doi: 10.1186/s40425-019-0805-8

48. Fan Y, Xie W, Huang H, Wang Y, Li G, Geng Y, et al. Association of immune related adverse events with efficacy of immune checkpoint inhibitors and overall survival in cancers: A systemic review and meta-analysis. *Front Oncol* (2021) 11:633032. doi: 10.3389/fonc.2021.633032

49. Haratani K, Hayashi H, Chiba Y, Kudo K, Yonesaka K, Kato R, et al. Association of immune-related adverse events with nivolumab efficacy in non-Small-Cell lung cancer. *JAMA Oncol* (2018) 4:374–8. doi: 10.1001/jamaoncol.2017.2925

50. Paderi A, Giorgione R, Giommoni E, Mela MM, Rossi V, Doni L, et al. Association between immune related adverse events and outcome in patients with metastatic renal cell carcinoma treated with immune checkpoint inhibitors. *Cancers (Basel)* (2021) 13(4):860. doi: 10.3390/cancers13040860

51. Kijima T, Fukushima H, Kusuhara S, Tanaka H, Yoshida S, Yokoyama M, et al. Association between the occurrence and spectrum of immune-related adverse events and efficacy of pembrolizumab in Asian patients with advanced urothelial cancer: Multicenter retrospective analyses and systematic literature review. *Clin Genitourin Cancer* (2021) 19:208–216.e1. doi: 10.1016/j.clgc.2020.07.003

52. Nobashi T, Baratto L, Reddy SA, Srinivas S, Toriihara A, Hatami N, et al. Predicting response to immunotherapy by evaluating tumors, lymphoid cell-rich organs, and immune-related adverse events using FDG-PET/CT. *Clin Nucl Med* (2019) 44:e272–9. doi: 10.1097/rlu.0000000000002453

53. Wang D, Chen C, Gu Y, Lu W, Zhan P, Liu H, et al. Immune-related adverse events predict the efficacy of immune checkpoint inhibitors in lung cancer patients: A meta-analysis. *Front Oncol* (2021) 11:631949. doi: 10.3389/fonc.2021.631949

54. Morimoto K, Yamada T, Takumi C, Ogura Y, Takeda T, Onoi K, et al. Immune-related adverse events are associated with clinical benefit in patients with non-Small-Cell lung cancer treated with immunotherapy plus chemotherapy: A retrospective study. *Front Oncol* (2021) 11:630136. doi: 10.3389/fonc.2021.630136

55. Tang YZ, Szabados B, Leung C, Sahdev A. Adverse effects and radiological manifestations of new immunotherapy agents. *Br J Radiol* (2019) 92:20180164. doi: 10.1259/bjr.20180164

56. Hribernik N, Huff DT, Studen A, Zevnik K, Klaneček Ž, Emamekhoo H, et al. Quantitative imaging biomarkers of immune-related adverse events in immune-checkpoint blockade-treated metastatic melanoma patients: a pilot study. *Eur J Nucl Med Mol Imaging* (2022) 49:1857–69. doi: 10.1007/s00259-021-05650-3

57. Eshghi N, Garland LL, Nia E, Betancourt R, Krupinski E, Kuo PH. (18)F-FDG PET/CT can predict development of thyroiditis due to immunotherapy for lung cancer. *J Nucl Med Technol* (2018) 46:260–4. doi: 10.2967/jnmt.117.204933

58. Das JP, Postow MA, Friedman CF, Do RK, Halpenny DF. Imaging findings of immune checkpoint inhibitor associated pancreatitis. *Eur J Radiol* (2020) 131:109250. doi: 10.1016/j.ejrad.2020.109250

59. Eisenhauer EA, Therasse P, Bogaerts J, Schwartz LH, Sargent D, Ford R, et al. New response evaluation criteria in solid tumours: revised RECIST guideline (version 1.1). *Eur J Cancer* (2009) 45:228–47. doi: 10.1016/j.ejca.2008.10.026

60. Seymour L, Bogaerts J, Perrone A, Ford R, Schwartz LH, Mandrekar S, et al. iRECIST: guidelines for response criteria for use in trials testing immunotherapeutics. *Lancet Oncol* (2017) 18:e143–52. doi: 10.1016/s1470-2045(17)30074-8

61. Hodi FS, Ballinger M, Lyons B, Soria JC, Nishino M, Tabernero J, et al. Immune-modified response evaluation criteria in solid tumors (imRECIST): Refining guidelines to assess the clinical benefit of cancer immunotherapy. *J Clin Oncol* (2018) 36:850–8. doi: 10.1200/jco.2017.75.1644

62. Young H, Baum R, Cremerius U, Herholz K, Hoekstra O, Lammertsma AA, et al. Measurement of clinical and subclinical tumour response using [18F]-fluorodeoxyglucose and positron emission tomography: review and 1999 EORTC recommendations. European organization for research and treatment of cancer (EORTC) PET study group. *Eur J Cancer* (1999) 35:1773–82. doi: 10.1016/s0959-8049(99)00229-4

63. Wahl RL, Jacene H, Kasamon Y, Lodge MA. From RECIST to PERCIST: Evolving considerations for PET response criteria in solid tumors. *J Nucl Med* (2009) 50 Suppl 1:122s–50s. doi: 10.2967/jnumed.108.057307

64. Goldfarb L, Duchemann B, Chouahnia K, Zelek L, Soussan M. Monitoring anti-PD-1-based immunotherapy in non-small cell lung cancer with FDG PET: introduction of iPERCIST. *EJNMMI Res* (2019) 9:8. doi: 10.1186/s13550-019-0473-1

65. Ito K, Teng R, Schöder H, Humm JL, Ni A, Michaud L, et al. (18)F-FDG PET/CT for monitoring of ipilimumab therapy in patients with metastatic melanoma. *J Nucl Med* (2019) 60:335–41. doi: 10.2967/jnumed.118.213652

66. Anwar H, Sachpekidis C, Winkler J, Kopp-Schneider A, Haberkorn U, Hassel JC, et al. Absolute number of new lesions on (18)F-FDG PET/CT is more predictive of clinical response than SUV changes in metastatic melanoma patients

receiving ipilimumab. *Eur J Nucl Med Mol Imaging* (2018) 45:376–83. doi: 10.1007/s00259-017-3870-6

67. Sachpekidis C, Anwar H, Winkler J, Kopp-Schneider A, Larribere L, Haberkorn U, et al. The role of interim (18)F-FDG PET/CT in prediction of response to ipilimumab treatment in metastatic melanoma. *Eur J Nucl Med Mol Imaging* (2018) 45:1289–96. doi: 10.1007/s00259-018-3972-9

68. Sachpekidis C, Kopp-Schneider A, Hakim-Meibodi L, Dimitrakopoulou-Strauss A, Hassel JC. ^{18}F-FDG PET/CT longitudinal studies in patients with advanced metastatic melanoma for response evaluation of combination treatment with vemurafenib and ipilimumab. *Melanoma Res* (2019) 29:178–86. doi: 10.1097/cmr.0000000000000541

69. Beer L, Hochmair M, Haug AR, Schwabel B, Kifjak D, Wadsak W, et al. Comparison of RECIST, iRECIST, and PERCIST for the evaluation of response to PD-1/PD-L1 blockade therapy in patients with non-small cell lung cancer. *Clin Nucl Med* (2019) 44:535–43. doi: 10.1097/rlu.0000000000002603

70. Castello A, Rossi S, Toschi L, Lopci E. Comparison of metabolic and morphological response criteria for early prediction of response and survival in NSCLC patients treated with anti-PD-1/PD-L1. *Front Oncol* (2020) 10:1090. doi: 10.3389/fonc.2020.01090

71. Dimitriou F, Lo SN, Tan AC, Emmett L, Kapoor R, Carlino MS, et al. FDG-PET to predict long-term outcome from anti-PD-1 therapy in metastatic melanoma. *Ann Oncol* (2021) 33(1):99–106. doi: 10.1016/j.annonc.2021.10.003

72. Kitajima K, Watabe T, Nakajo M, Ishibashi M, Daisaki H, Soeda F, et al. Tumor response evaluation in patients with malignant melanoma undergoing immune checkpoint inhibitor therapy and prognosis prediction using (18)F-FDG PET/CT: multicenter study for comparison of EORTC, PERCIST, and imPERCIST. *Jpn J Radiol* (2022) 40:75–85. doi: 10.1007/s11604-021-01174-w

73. Zhu J, Armstrong AJ, Friedlander TW, Kim W, Pal SK, George DJ, et al. Biomarkers of immunotherapy in urothelial and renal cell carcinoma: PD-L1, tumor mutational burden, and beyond. *J Immunother Cancer* (2018) 6:4. doi: 10.1186/s40425-018-0314-1

74. Brody R, Zhang Y, Ballas M, Siddiqui MK, Gupta P, Barker C, et al. PD-L1 expression in advanced NSCLC: Insights into risk stratification and treatment selection from a systematic literature review. *Lung Cancer* (2017) 112:200–15. doi: 10.1016/j.lungcan.2017.08.005

75. Seban RD, Nemer JS, Marabelle A, Yeh R, Deutsch E, Ammari S, et al. Prognostic and theranostic ^{18}F-FDG PET biomarkers for anti-PD1 immunotherapy in metastatic melanoma: association with outcome and transcriptomics. *Eur J Nucl Med Mol Imaging* (2019) 46:2298–310. doi: 10.1007/s00259-019-04411-7

76. Ito K, Schöder H, Teng R, Humm JL, Ni A, Wolchok JD, et al. Prognostic value of baseline metabolic tumor volume measured on (18)F-fluorodeoxyglucose positron emission tomography/computed tomography in melanoma patients treated with ipilimumab therapy. *Eur J Nucl Med Mol Imaging* (2019) 46:930–9. doi: 10.1007/s00259-018-4211-0

77. Seban RD, Mezquita L, Berenbaum A, Dercle L, Botticella A, Le Pechoux C, et al. Baseline metabolic tumor burden on FDG PET/CT scans predicts outcome in advanced NSCLC patients treated with immune checkpoint inhibitors. *Eur J Nucl Med Mol Imaging* (2020) 47:1147–57. doi: 10.1007/s00259-019-04615-x

78. Hashimoto K, Kaira K, Yamaguchi O, Mouri A, Shiono A, Miura Y, et al. Potential of FDG-PET as prognostic significance after anti-PD-1 antibody against patients with previously treated non-small cell lung cancer. *J Clin Med* (2020) 9 (3):725. doi: 10.3390/jcm9030725

79. Castello A, Rossi S, Mazziotti E, Toschi L, Lopci E. Hyperprogressive disease in patients with non-small cell lung cancer treated with checkpoint inhibitors: The role of (18)F-FDG PET/CT. *J Nucl Med* (2020) 61:821–6. doi: 10.2967/jnumed.119.237768

80. Yamaguchi O, Kaira K, Hashimoto K, Mouri A, Shiono A, Miura Y, et al. Tumor metabolic volume by (18)F-FDG-PET as a prognostic predictor of first-line pembrolizumab for NSCLC patients with PD-L1 ≥ 50. *Sci Rep* (2020) 10:14990. doi: 10.1038/s41598-020-71735-y

81. Polverari G, Ceci F, Bertaglia V, Reale ML, Rampado O, Gallio E, et al. (18) F-FDG pet parameters and radiomics features analysis in advanced nsclc treated with immunotherapy as predictors of therapy response and survival. *Cancers (Basel)* (2020) 12(5):1163. doi: 10.3390/cancers12051163

82. Chardin D, Paquet M, Schiappa R, Darcourt J, Bailleux C, Poudenx M, et al. Baseline metabolic tumor volume as a strong predictive and prognostic biomarker in patients with non-small cell lung cancer treated with PD1 inhibitors: a prospective study. *J Immunother Cancer* (2020) 8(2):e000645. doi: 10.1136/jitc-2020-000645

83. Seban RD, Assie JB, Giroux-Leprieur E, Massiani MA, Soussan M, Bonardel G, et al. FDG-PET biomarkers associated with long-term benefit from first-line immunotherapy in patients with advanced non-small cell lung cancer. *Ann Nucl Med* (2020) 34:968–74. doi: 10.1007/s12149-020-01539-7

84. Wong A, Callahan J, Keyaerts M, Neyns B, Mangana J, Aberle S, et al. (18)F-FDG PET/CT based spleen to liver ratio associates with clinical outcome to ipilimumab in patients with metastatic melanoma. *Cancer Imaging* (2020) 20:36. doi: 10.1186/s40644-020-00313-2

85. Seban RD, Moya-Plana A, Antonios L, Yeh R, Marabelle A, Deutsch E, et al. Prognostic ^{18}F-FDG PET biomarkers in metastatic mucosal and cutaneous melanoma treated with immune checkpoint inhibitors targeting PD-1 and CTLA-4. *Eur J Nucl Med Mol Imaging* (2020) 47:2301–12. doi: 10.1007/s00259-020-04757-3

86. Dall'Olio FG, Calabrò D, Conci N, Argalia G, Marchese PV, Fabbri F, et al. Baseline total metabolic tumour volume on 2-deoxy-2-[18F]fluoro-d-glucose positron emission tomography-computed tomography as a promising biomarker in patients with advanced non-small cell lung cancer treated with first-line pembrolizumab. *Eur J Cancer* (2021) 150:99–107. doi: 10.1016/j.ejca.2021.03.020

87. Vekens K, Everaert H, Neyns B, Ilsen B, Decoster L. The value of (18)F-FDG PET/CT in predicting the response to PD-1 blocking immunotherapy in advanced NSCLC patients with high-level PD-L1 expression. *Clin Lung Cancer* (2021) 22:432–40. doi: 10.1016/j.cllc.2021.03.001

88. Bauckneht M, Genova C, Rossi G, Rijavec E, Dal Bello MG, Ferrarazzo G, et al. The role of the immune metabolic prognostic index in patients with non-small cell lung cancer (NSCLC) in radiological progression during treatment with nivolumab. *Cancers (Basel)* (2021) 13(13):3117. doi: 10.3390/cancers13133117

89. Awada G, Jansen Y, Schwarze JK, Tijtgat J, Hellinckx L, Gondry O, et al. A comprehensive analysis of baseline clinical characteristics and biomarkers associated with outcome in advanced melanoma patients treated with pembrolizumab. *Cancers (Basel)* (2021) 13(2):168. doi: 10.3390/cancers13020168

90. Gulturk I, Yilmaz M, Yildiz Tacar S, Tural D. Prognostic importance of SUV-max values evaluated by ^{18}F-FDG-PET/CT before nivolumab treatment in patients with metastatic renal cell carcinoma. *Q J Nucl Med Mol Imaging* (2021). doi: 10.23736/s1824-4785.21.03395-1

91. Mu W, Jiang L, Zhang J, Shi Y, Gray JE, Tunali I, et al. Non-invasive decision support for NSCLC treatment using PET/CT radiomics. *Nat Commun* (2020) 11:5228. doi: 10.1038/s41467-020-19116-x

92. Mu W, Tunali I, Gray JE, Qi J, Schabath MB, Gillies RJ. Radiomics of (18)F-FDG PET/CT images predicts clinical benefit of advanced NSCLC patients to checkpoint blockade immunotherapy. *Eur J Nucl Med Mol Imaging* (2020) 47:1168–82. doi: 10.1007/s00259-019-04625-9

93. Niemeijer AN, Oprea-Lager DE, Huisman MC, Hoekstra OS, Boellaard R, de Wit-van der Veen BJ, et al. Study of (89)Zr-pembrolizumab PET/CT in patients with advanced-stage non-small cell lung cancer. *J Nucl Med* (2022) 63:362–7. doi: 10.2967/jnumed.121.261926

94. Kok IC, Hooiveld JS, van de Donk PP, Giesen D, van der Veen EL, Lub-de Hooge MN, et al. (89)Zr-pembrolizumab imaging as a non-invasive approach to assess clinical response to PD-1 blockade in cancer. *Ann Oncol* (2022) 33:80–8. doi: 10.1016/j.annonc.2021.10.213

95. Rakhshandehroo T, Smith BR, Glockner HJ, Rashidian M, Pandit-Taskar N. Molecular immune targeted imaging of tumor microenvironment. *Nanotheranostics* (2022) 6:286–305. doi: 10.7150/ntno.66556

96. Bensch F, van der Veen EL, Lub-de Hooge MN, Jorritsma-Smit A, Boellaard R, Kok IC, et al. (89)Zr-atezolizumab imaging as a non-invasive approach to assess clinical response to PD-L1 blockade in cancer. *Nat Med* (2018) 24:1852–8. doi: 10.1038/s41591-018-0255-8

97. Vento J, Mulgaonkar A, Woolford L, Nham K, Christie A, Bagrodia A, et al. PD-L1 detection using (89)Zr-atezolizumab immuno-PET in renal cell carcinoma tumorgrafts from a patient with favorable nivolumab response. *J Immunother Cancer* (2019) 7:144. doi: 10.1186/s40425-019-0607-z

98. Gao H, Wu Y, Shi J, Zhang X, Liu T, Hu B, et al. Nuclear imaging-guided PD-L1 blockade therapy increases effectiveness of cancer immunotherapy. *J Immunother Cancer* (2020) 8(2):e001156. doi: 10.1136/jitc-2020-001156

99. Du Y, Jin Y, Sun W, Fang J, Zheng J, Tian J. Advances in molecular imaging of immune checkpoint targets in malignancies: current and future prospect. *Eur Radiol* (2019) 29:4294–302. doi: 10.1007/s00330-018-5814-3

100. Ehlerding EB, Lee HJ, Jiang D, Ferreira CA, Zahm CD, Huang P, et al. Antibody and fragment-based PET imaging of CTLA-4+ T-cells in humanized mouse models. *Am J Cancer Res* (2019) 9:53–63.

101. Ehlerding EB, England CG, Majewski RL, Valdovinos HF, Jiang D, Liu G, et al. ImmunoPET imaging of CTLA-4 expression in mouse models of non-small cell lung cancer. *Mol Pharm* (2017) 14:1782–9. doi: 10.1021/acs.molpharmaceut.7b00056

102. Xiao Z, Mayer AT, Nobashi TW, Gambhir SS. ICOS is an indicator of T-cell-Mediated response to cancer immunotherapy. *Cancer Res* (2020) 80:3023–32. doi: 10.1158/0008-5472.Can-19-3265

103. Simonetta F, Alam IS, Lohmeyer JK, Sahaf B, Good Z, Chen W, et al. Molecular imaging of chimeric antigen receptor T cells by ICOS-ImmunoPET. *Clin Cancer Res* (2021) 27:1058–68. doi: 10.1158/1078-0432.Ccr-20-2770

104. Tumeh PC, Harview CL, Yearley JH, Shintaku IP, Taylor EJ, Robert L, et al. PD-1 blockade induces responses by inhibiting adaptive immune resistance. *Nature* (2014) 515:568–71. doi: 10.1038/nature13954

105. Pandit-Taskar N, Postow MA, Hellmann MD, Harding JJ, Barker CA, O'Donoghue JA, et al. First-in-Humans imaging with (89)Zr-Df-IAB22M2C anti-CD8 minibody in patients with solid malignancies: Preliminary pharmacokinetics, biodistribution, and lesion targeting. *J Nucl Med* (2020) 61:512–9. doi: 10.2967/jnumed.119.229781

106. Rashidian M, Ingram JR, Dougan M, Dongre A, Whang KA, LeGall C, et al. Predicting the response to CTLA-4 blockade by longitudinal noninvasive monitoring of CD8 T cells. *J Exp Med* (2017) 214:2243–55. doi: 10.1084/jem.20161950

107. Iravani A, Hicks RJ. Imaging the cancer immune environment and its response to pharmacologic intervention, part 2: The role of novel PET agents. *J Nucl Med* (2020) 61:1553–9. doi: 10.2967/jnumed.120.248823

108. van de Donk PP, Kist de Ruijter L, Lub-de Hooge MN, Brouwers AH, van der Wekken AJ, Oosting SF, et al. Molecular imaging biomarkers for immune checkpoint inhibitor therapy. *Theranostics* (2020) 10:1708–18. doi: 10.7150/thno.38339

109. Larimer BM, Wehrenberg-Klee E, Dubois F, Mehta A, Kalomeris T, Flaherty K, et al. Granzyme b PET imaging as a predictive biomarker of immunotherapy response. *Cancer Res* (2017) 77:2318–27. doi: 10.1158/0008-5472.Can-16-3346

110. Gibson HM, McKnight BN, Malysa A, Dyson G, Wiesend WN, McCarthy CE, et al. IFNγ PET imaging as a predictive tool for monitoring response to tumor immunotherapy. *Cancer Res* (2018) 78:5706–17. doi: 10.1158/0008-5472.Can-18-0253

frontiers | Frontiers in Immunology

TYPE Original Research
PUBLISHED 24 November 2022
DOI 10.3389/fimmu.2022.1050721

OPEN ACCESS

EDITED BY
Haojun Chen,
First Affiliated Hospital of Xiamen University, China

REVIEWED BY
Guichao Li,
Fudan University, China
Yimin Li,
First Affiliated Hospital of Xiamen University, China
Zhigang Liu,
The Fifth Affiliated Hospital of Sun Yat-sen University, China
Ji Zhu,
Fudan University, China

*CORRESPONDENCE
Jinluan Li
lijinluan@pku.org.cn
Junxin Wu
junxinwufj@aliyun.com

†These authors have contributed equally to this work and share first authorship

SPECIALTY SECTION
This article was submitted to Cancer Immunity and Immunotherapy, a section of the journal Frontiers in Immunology

RECEIVED 22 September 2022
ACCEPTED 26 October 2022
PUBLISHED 24 November 2022

CITATION
Zhou H, Chen Y, Xiao Y, Wu Q, Li H, Li Y, Su G, Ke L, Wu J and Li J (2022) Evaluation of the ability of fatty acid metabolism signature to predict response to neoadjuvant chemoradiotherapy and prognosis of patients with locally advanced rectal cancer. *Front. Immunol.* 13:1050721. doi: 10.3389/fimmu.2022.1050721

Evaluation of the ability of fatty acid metabolism signature to predict response to neoadjuvant chemoradiotherapy and prognosis of patients with locally advanced rectal cancer

Han Zhou[1†], Yanping Chen[2†], Yu Xiao[1†], Qian Wu[1], Hui Li[1], Yi Li[1], Guangjian Su[3], Longfeng Ke[2], Junxin Wu[1*] and Jinluan Li[1*]

[1]Department of Radiation Oncology, Clinical Oncology School of Fujian Medical University, Fujian Cancer Hospital, Fuzhou, China, [2]Department of Clinical Pathology, Clinical Oncology School of Fujian Medical University, Fujian Cancer Hospital, Fuzhou, China, [3]Department of Clinical Laboratory, Clinical Oncology School of Fujian Medical University, Fujian Cancer Hospital, Fuzhou, China

Neoadjuvant chemoradiotherapy (nCRT) is widely used to treat patients with locally advanced rectal cancer (LARC), and treatment responses vary. Fatty acid metabolism (FAM) is closely associated with carcinogenesis and cancer progression. In this study, we investigated the vital role of FAM on the gut microbiome and metabolism in the context of cancer. We screened 34 disease-free survival (DFS)-related, FAM-related, and radiosensitivity-related genes based on the Gene Expression Omnibus database. Subsequently, we developed a five-gene FAM-related signature using the least absolute shrinkage and selection operator Cox regression model. The FAM-related signature was also validated in external validation from Fujian Cancer Hospital for predicting nCRT response, DFS, and overall survival (OS). Notably, patients with a low-risk score were associated with pathological complete response and better DFS and OS outcomes. A comprehensive evaluation of the tumor microenvironment based on the FAM-related signature revealed that patients with high-risk scores were closely associated with activating type I interferon response and inflammation-promoting functions. In conclusion, our findings indicate the potential ability of FAM to predict nCRT response and the prognosis of DFS and OS in patients with LARC.

KEYWORDS

fatty acid metabolism, gut microbiome, metabolite, neoadjuvant chemoradiotherapy response, rectal cancer

Introduction

Colorectal cancer (CRC) is one of the three most common cancers and the second leading cause of cancer-related deaths worldwide (1). Rectal cancer accounts for approximately 30% of all newly diagnosed CRC cases (2). Neoadjuvant chemoradiotherapy (nCRT) followed by total mesorectal excision is the standard treatment modality for patients with locally advanced rectal cancer (LARC) (T3, T4, or N+) (3). nCRT has been confirmed to be associated with better survival outcomes, especially in improving disease-free survival (DFS) rates (4, 5). Patients with pathological complete response (pCR) have been confirmed to have much better overall survival (OS) and DFS. However, treatment responses varied widely among patients. About 15%–30% of patients achieve pCR after nCRT (6, 7). Hence, it is crucial to identify potential biomarkers to predict treatment response and prognosis in patients with rectal cancer who undergo nCRT.

Microbiomes and metabolites have been recognized as indispensable cancer hallmarks (8, 9). The gut microbiome is known to be related to tumor development, especially in digestive system tumors (10, 11). Metabolic reprogramming also plays an important role in cancer development (12–14). In addition, gut microbiome dysbiosis and metabolic disorders are associated with the development of CRC (15). The gut microbiome and metabolites can be used to predict treatment response to radiotherapy, chemotherapy, and immunotherapy (16, 17). In addition, the gut microbiome and metabolites have been shown to be useful in predicting nCRT response in patients with LARC (18, 19). However, little is known about the mechanisms by which the gut microbiome and metabolites influence radiotherapy response in rectal cancer (20).

Fatty acid metabolism (FAM) has been the focus of related research because of its close relationship with carcinogenesis and cancer progression (21). Fatty acids (FAs) are a principal structural component of the human body. They are also vital secondary messengers and materials for energy production (22). FAM has been confirmed to be associated with sensitivity to chemotherapy, radiotherapy, and targeted therapy in cancers (19, 23). Given the important role of FAM, therapies targeting FAM are of great concern. Previous studies have shown the potential ability of FAM-related genes to guide prognosis in CRC (24, 25). However, evidence of FAM-related genes predicting treatment response in patients with rectal cancer is lacking. Therefore, further exploration of the relationship between FAM-related genes and clinicopathological characteristics in patients with rectal cancer treated with nCRT would be helpful in developing personalized regimens and management.

In this study, we first analyzed the potential function of the gut microbiome and its metabolites in rectal cancer patients with different nCRT responses. Additionally, we established a reliable signature for FAM-related genes. We fully evaluated its ability to predict survival outcomes and treatment responses in rectal cancer patients treated with nCRT based on the Gene Expression Omnibus (GEO) database. The findings of this study provide new insights that may be used to personalize the treatment of patients with rectal cancer who have undergone nCRT.

Abbreviations: ASV, amplicon sequence variants; AUC, area under the curve; DFS, disease-free survival; FAs, fatty acids; FAM, fatty acid metabolism; GEO, Gene Expression Omnibus; GO, Gene Ontology; KEGG, Kyoto Encyclopedia of Genes and Genomes; LARC, locally advanced rectal cancer; LASSO, least absolute shrinkage and selection operator; LDA, linear discriminant analysis; MSEA, metabolite set enrichment analysis; OS, overall survival; ROC, receiver operating characteristic; TRG, tumor regression grade; VIP, variable importance in projection.

Materials and methods

Study participants

The procedure used in this study is shown in Figure 1. This study was approved by the Ethics Committee of the Fujian Cancer Hospital (No. K2017-082-01). Between September 2020 and September 2021, 42 patients with newly diagnosed rectal cancer were administered nCRT before surgery at Fujian Cancer Hospital. The inclusion criteria were 1) pathologically confirmed rectal adenocarcinoma; 2) clinical T3, T4, and/or N+ without distant metastasis; 3) long-course nCRT comprising 50 Gy in 25 fractions and concurrent oral capecitabine chemotherapy; 4) surgery 6–8 weeks after nCRT; 5) Fujian Province resident for >10 years. The exclusion criteria were as follows: 1) patients with metabolic diseases; 2) incomplete clinical information; 3) treatment interruption or did not accept nCRT before surgery; 4) antibiotic or steroid therapy within 6 months before nCRT.

The histopathological responses to nCRT were classified according to the American Joint Committee on Cancer tumor regression grade (TRG) system, which is considered to be the most accurate (26). Patients with TRG grade 0 (no residual tumor cells) were classified as pCR, whereas patients with TRG grades 1–3 were classified as non-pCR. These specimens were examined by two experienced clinical pathologists.

16S rRNA gene sequencing and bioinformatics analysis

The V3–V4 region of the rRNA gene was amplified using primers 341F and 806R (27). The "DADA2" package was used to convert the paired-end FASTQ files. Raw data were processed using Quantitative Insights Into Microbial Ecology 2 (QIIME2, v. 2021.11). Representative amplicon sequence variant (ASV) sequences were classified into organisms using a naive Bayesian model and the RDP classifier (v. 2.2), according to the SILVA database (v. 132).

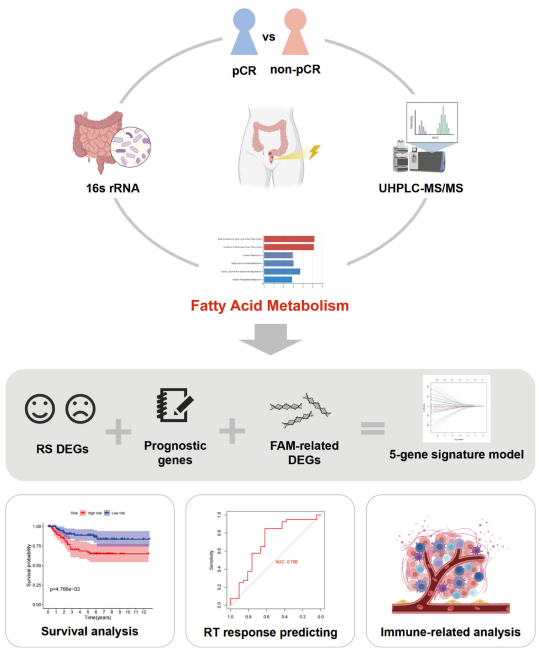

FIGURE 1
Workflow of this study. pCR, pathological complete response; UHPLC-MS/MS, ultra-high performance liquid chromatography–tandem mass spectrometry; RS, radiation sensitivity; FAM, fatty acid metabolism; RT, radiotherapy.

The abundance statistics for each taxon were visualized using Krona (v. 2.6). Venn analysis was performed using the R project "VennDiagram" package. The biomarker features were screened using linear discriminant analysis effect size (LEfSe) software (v. 1.0). Kyoto Encyclopedia of Genes and Genomes (KEGG) pathway analyses of ASVs were performed using the Phylogenetic Investigation of Communities by Reconstruction of Unobserved States 2 (PICRUSt2) Tool (v. 2.1.4). Wilcoxon rank sum tests were performed in the R package "vegan".

Ultra-high-performance liquid chromatography–tandem mass spectrometry analysis and statistical metabolism analyses

Ultra-high-performance liquid chromatography–tandem mass spectrometry (UHPLC-MS/MS) analyses were performed using a Vanquish UHPLC System (Thermo Fisher Scientific, Waltham, MA, USA) coupled with an Orbitrap Q Exactive™ HF-X mass spectrometer (Thermo Fisher Scientific). The peaks were then matched with the mzCloud (https://www.mzcloud.org/), mz Vault (Thermo Fisher Scientific), and Masslist databases (www.maldi-msi.org/mass) to obtain accurate qualitative and quantitative results.

A partial least-squares discriminant analysis (PLS-DA) was conducted with the "ropls" package in R. Variable importance in projection (VIP) based on PLS-DA was used to rank candidate metabolites ($p< 0.05$, t-test; VIP ≥ 1). Metabolite set enrichment analysis (MSEA) was used to evaluate pathway overrepresentation using the MetaboAnalyst module with the R package "MSEAp".

Date source

Gene expression and clinicopathological information were downloaded from the GEO database (https://www.ncbi.nlm.nih.gov/geo/). Two GEO cohorts (GSE56699 and GSE87211) were used in our study. The RNA sequencing data of two cohorts were corrected for batch effects by using the R package "sva". A total of 158 FAM-related genes were obtained from the Molecular Signatures Database (MSigDB) (http://www.broad.mit.edu/gsea/msigdb/, Supplementary Table 1). In addition, 82 frozen cancer samples of patients with LARC at Fujian Cancer Hospital (FJCH) between June 2016 to June 2021 were used for external validation. All the patients received nCRT and radical surgery. The clinical information of the GEO validation sets and FJCH set is detailed in Supplementary Table 2.

Single-sample gene set enrichment analysis

Single-sample gene set enrichment analysis (ssGSEA) was performed using the R package "GSVA" to calculate the pathway activity of "Hallmark_Fatty_Acid_Metabolism". The patients were then divided into high and low pathway activities based on the median of all patients' pathway activity.

Identification of differentially expressed genes

FAM-related differentially expressed genes (DEGs) of patients with high and low pathway activities were screened with an adjusted p-value of<0.05 by using the R package "limma". The same method was used to identify the radiosensitive (RS) DEGs between nCRT-sensitive and nCRT-resistant patients. Univariate Cox regression analysis was performed to select prognosis-related DEGs based on DFS by applying the Kaplan–Meier R package "survival" with a p-value of <0.05.

Development of the fatty acid metabolism-related signature

The intersection of FAM-related DEGs, RS DEGs, and prognosis-related DEGs yielded candidate FAM-related genes.

To avoid overfitting, the least absolute shrinkage and selection operator (LASSO) Cox regression algorithm was applied using the R package "glmnet". Finally, the risk score of FAM-related genes was calculated using the following formula:

$$Risk\ score = \sum_{i-1}^{n}(Coefficient_i \times Expression_i)$$

The patients were divided into high-risk and low-risk groups based on the median values. A heatmap of the model-related genes was generated for the two cohorts.

Assessment of fatty acid metabolism-related signature

FAM-related signatures were divided into two cohorts (GSE56699 and GSE87211). Patients in both cohorts were divided into high- and low-risk groups based on their FAM-related signature. Patients in both groups were then evaluated using the Kaplan–Meier survival analysis of DFS and OS by using the R package "survival". The time-dependent receiver operating characteristic (ROC) curve was calculated using the R package "timeROC" to evaluate the predictive accuracy of the FAM-score prognostic model.

Evaluation of fatty acid metabolism-related signature and clinicopathological features

Multivariate Cox regression analysis and Wilcoxon rank sum tests were performed to identify the relationship between risk scores and clinical features. The area under the curve (AUC) analysis was calculated by using the R package "pROC" to evaluate the accuracy of using risk scores in predicting nCRT response in patients with rectal cancer.

Function enrichment analysis of fatty acid metabolism-related signature

Gene Ontology (GO) function enrichment analysis and KEGG function enrichment analysis were performed based on DEGs between high-risk and low-risk patients.

Relationship between fatty acid metabolism-related signature with tumor microenvironment and immune-related analysis

The R package "GSVA" was applied to calculate the abundance of 28 immune-infiltrating tumor cell types in each patient. The Wilcoxon test was used to assess the differences between patients with high-risk and low-risk scores. The ESTIMATE algorithm was used to evaluate the immunity, tumor purity, and stromal scores of each patient. Furthermore, we analyzed the differential expression levels of immune checkpoints between high-risk score patients and low-risk score patients by applying the R package "limma".

Tissue samples and quantitative real-time polymerase chain reaction

Quantitative real-time polymerase chain reaction (qRT-PCR) was performed on 82 rectal cancer samples from FJCH. Total RNA was extracted from paraffin sections of tumor tissues using the E.Z.N.A. FFPE RNA Isolation Kit (R6954-01; Omega Bio-Tek, Doraville, GA, USA). The primer sequences are listed in Supplementary Table 3. Quantitative real-time PCR (qPCR) was used to determine RNA levels using SYBR Green (29139149001; Roche, Basel, Switzerland). RNA levels were normalized to those of β-actin. All the qRT-PCR analyses were performed in triplicates, and the average value was calculated by the Livak method.

Statistical analyses

R (version 3.6.1) was used to perform statistical analyses in this study. Bioinformatics analyses were performed using Omicsmart, which is a real-time interactive online data analysis platform (http://www.omicsmart.com). Pearson's χ^2 test and Student's t-test were used to compare normally distributed variables, whereas the Kruskal–Wallis test and Wilcoxon rank sum test were used to compare non-normally distributed variables. Statistical significance was set at $p< 0.05$.

Results

Relationship between baseline gut microbiome and neoadjuvant chemoradiotherapy response in patients with rectal cancer

Data from 14 patients were analyzed according to the inclusion and exclusion criteria. Detailed clinicopathological characteristics of the 14 patients are shown in Supplementary Table 4. There were 134 species included in the pCR group and 155 species in the non-pCR group (Supplementary Figure 1B). We first determined community composition at the species level in the top 10 microbiomes of the pCR and non-pCR groups (Supplementary Figure 1A). To further identify the significantly different gut microbiomes in patients with rectal cancer with

different nCRT responses, we performed LEfSe with |log10 LDA| ≥ 2 (Figure 2A; Supplementary Table 5). The microbiome of the phylum Proteobacteria, including the class Betaproteobacteriales and the families Xanthobacteraceae and Burkholderiaceae, was enriched in the pCR group, which may be associated with treatment response.

Functional analysis was performed, and the results are shown in a streamgraph (Supplementary Figure 1C). We found that the functions of each patient were enriched in the metabolism-related pathways. Finally, the difference analysis between the pCR and non-pCR groups showed significant differences in linoleic acid metabolism, which is included in lipid and FAM ($p < 0.05$, Figure 2B).

Characteristic of baseline metabolites of patients with rectal cancer with different neoadjuvant chemoradiotherapy responses

PLS-DA significantly segregated the patients into the pCR and non-pCR groups (Supplementary Figure 1D). We then screened the metabolites by combining the VIP scores based on PLS-DA and the p-values based on the t-test for the pCR and non-pCR groups. We found 72 metabolites with different abundance in patients with different nCRT responses at baseline (Figure 2C; Supplementary Table 6). Further functional enrichment analysis showed that different metabolites were primarily enriched in FAM (Figure 2D). Finally, propanoate and glycerol lipid metabolism were significantly different in patients with different nCRT responses ($p < 0.05$, Supplementary Figure 1E). Based on the analysis of the baseline gut microbiome and metabolites, we hypothesized that FAM may influence the response to nCRT in patients with rectal cancer.

Identification of different expression genes and construction of fatty acid metabolism-related signatures

We first scored 72 patients in GSE56699, based on 158 FAM-related genes (FAM-related genes). Patients who received pCR after nCRT had a higher score based on FAM-related genes than those who did not achieve pCR after nCRT ($p < 0.05$, Figure 3A). Once again, the results showed the vital role of FAM in influencing the treatment response in patients with rectal cancer. Thus, we divided the patients into two groups based on the median FAM-related genes score.

We identified 2,734 DEGs between the two groups with different FAM-related gene scores (Supplementary Table 7). Additionally, 2,912 RS DEGs were identified in patients with different nCRT responses (Supplementary Table 8), and 1,032 prognosis-related genes based on DFS were identified in patients from the GSE56699 dataset (Supplementary Table 9). Finally, 34 genes at the intersection of three parts of DEGs were recognized as potential candidate genes (Figure 3B; Supplementary Table 10). With the use of LASSO regression analysis, five genes (*CYP1B1*, *DDC*, *ANO1*, *DAPL1*, and *RIOK3*) were screened based on their

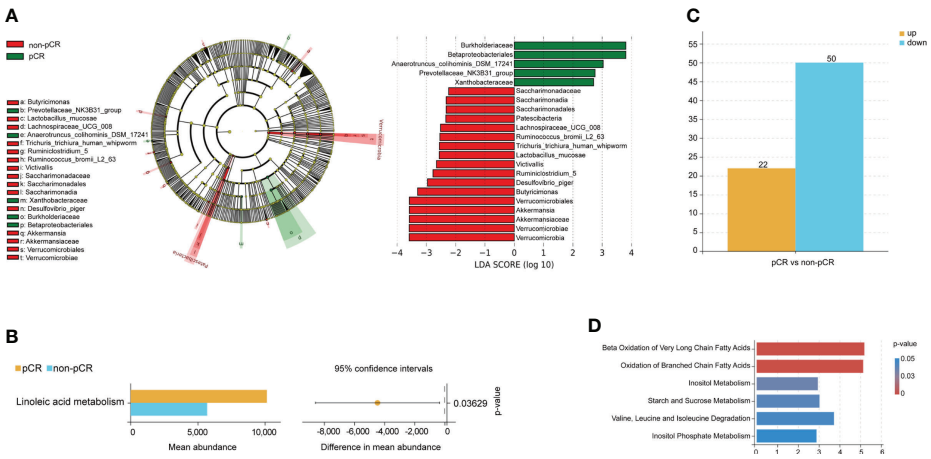

FIGURE 2
Gut microbiome and metabolism characteristics at the baseline associated with neoadjuvant chemoradiotherapy treatment response. **(A)** Differentially abundant taxa between pCR and non-pCR groups analyzed by LEfSe (Kruskal–Wallis test; $p < 0.05$; LDA > 2). **(B)** Differences in KEGG pathway analyses between pCR and non-pCR groups ($p < 0.05$). **(C)** The bar plots show upregulated and downregulated metabolites of patients with different nCRT responses. **(D)** MSEA of metabolites from each patient showed significantly enriched signaling pathways. nCRT, neoadjuvant chemoradiotherapy; pCR, pathological complete response; LEfSe, linear discriminant analysis (LDA) effect size; KEGG, Kyoto Encyclopedia of Genes and Genome; MSEA, metabolite set enrichment analysis.

10.3389/fimmu.2022.1050721

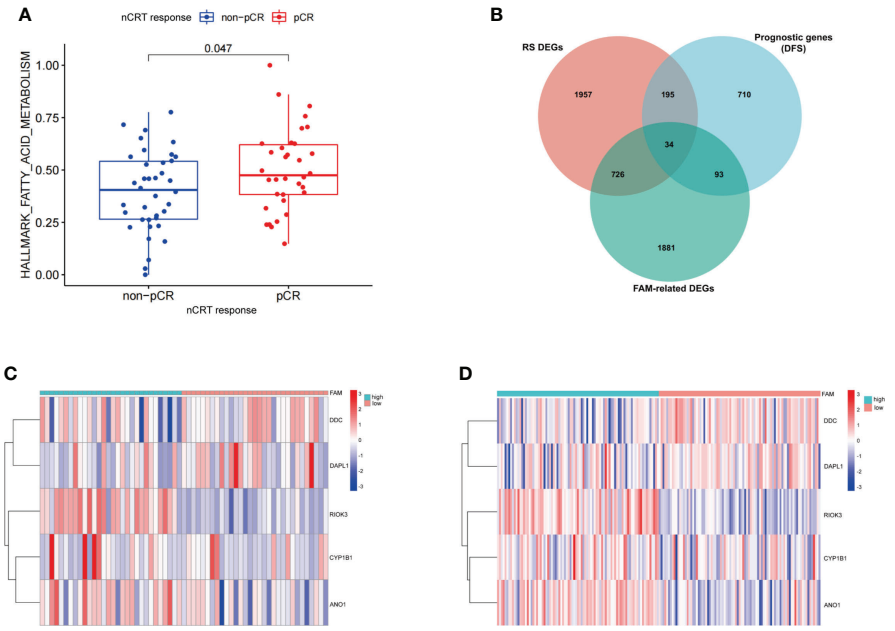

FIGURE 3
Construction of the FAM-related signature for patients with rectal cancer treated with neoadjuvant chemoradiotherapy. **(A)** The expression of FAM-related genes in relation to nCRT response. **(B)** Venn diagram identifying the intersection of genes among RS DEGs, FAM-related genes, and prognostic genes. **(C, D)** The expression levels of five FAM score-related genes in GEO database (GSE56699 and GSE87211). nCRT, neoadjuvant chemoradiotherapy; RS, radiation sensitivity; DEGs, differentially expressed genes; FAM, fatty acid metabolism; LASSO, least absolute shrinkage and selection operator.

minimum lambda values (Supplementary Figure 2, Supplementary Table 11). Among these five genes, two were protective genes (*DDC* and *DAPL1*) and three were risk-related genes (*CYP1B1*, *ANO1*, and *RIOK3*). Therefore, the FAM-related risk score was calculated using the following formula:

$$FAM\ \ risk\ \ score = Expression\ \ of\ \ CYP1B1 \times 0.2566 + Expression\ \ of\ \ DDC \times (-1.8227) + Expression\ \ of\ \ ANO1 \times 1.2239 + Expression\ \ of\ \ DAPL1 \times (-0.0843) + Expression\ \ of\ \ RIOK3 \times 7.5436$$

According to the FAM-related risk score, patients with a score lower than the median risk score were classified into the low-risk group, whereas those with a score higher than the median risk score were classified into the high-risk group. The expression levels of the five genes are described in the heatmap of the GSE56699 and GSE87211 datasets (Figures 3C, D). *DDC* and *DAPL1* showed lower expression levels than *CYP1B1*, *ANO1*, and *RIOK3* in patients in the high-risk group.

Prognostic analysis based on fatty acid metabolism-related signature

We evaluated the prognostic ability of FAM-related signatures in patients with rectal cancer from the training (GSE56699) and testing (GSE87211) datasets. All patients from the two datasets underwent nCRT. The distribution graph shows that the mortality rate of patients increased with an increase in the FAM-related risk score in the GSE56699 dataset (Figure 4A). The Kaplan–Meier survival curves revealed that patients in the low-risk group had significantly better DFS than those in the high-risk group ($p < 0.05$, Figure 4C). In addition, the AUC values of the 1-, 2-, and 3-year survival rates of the FAM-score prognostic model were 0.780, 0.910, and 0.942, respectively (Figure 4E). To further evaluate the prognostic ability of the FAM-score prognostic model, we calculated the FAM score in the test dataset (GSE87211). Similarly, patients with a low-risk score had a significantly favorable survival rate and DFS ($p < 0.05$, Figures 4B, D). The AUC values of the 1-, 2-, and 3-year survival rates in the test dataset were 0.736, 0.710, and 0.702, respectively (Figure 4F). Univariate and multivariate Cox regression analyses showed that the FAM score was an independent risk factor for DFS (both $p < 0.05$, Figure 4G).

In terms of OS, the same phenomenon was observed in both the training (GSE56699) and testing (GSE87211) datasets. The survival rates decreased with increasing risk scores (Supplementary Figures 3A, B). In the training cohort, OS was not significantly different between the high- and low-risk groups ($p = 0.2$, Supplementary Figure 3C). In the testing cohort, patients in the high-risk group had a worse OS than those in

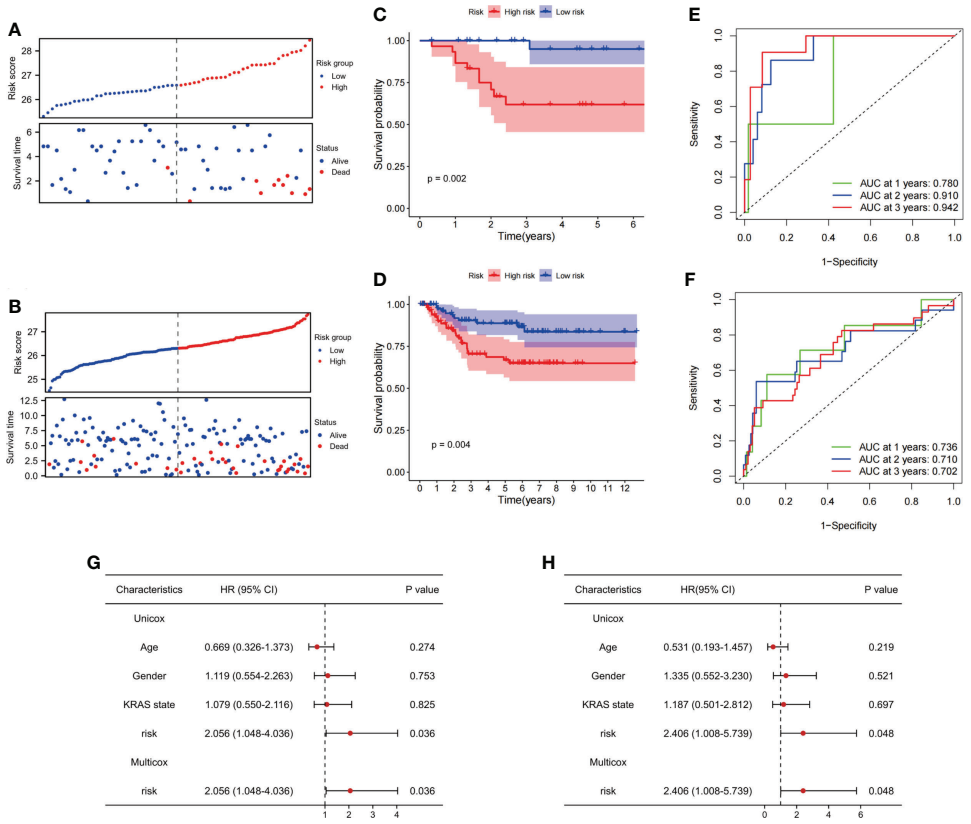

FIGURE 4
Evaluation of the ability of FAM-related signatures to predict prognosis in training and validation cohorts. **(A, B)** The association between DFS and FAM-related risk score in the training cohort (GSE56699) and the validation cohort (GSE87211). **(C, D)** Kaplan–Meier survival analyses of DFS between patients with high-risk scores and low-risk scores in the training and validation cohorts. **(E, F)** Time-dependent ROC curves used to evaluate the prognostic value of risk score in training and validation cohorts. **(G)** Univariate Cox analysis and multivariate Cox analysis of clinicopathological features and FAM-related signature in DFS. **(H)** Univariate Cox analysis and multivariate Cox analysis of clinicopathological features and FAM-related signature in OS. FAM, fatty acid metabolism; DFS, disease-free survival; ROC, receiver operating characteristic. OS, overall survival.

the low-risk group (p = 0.04, Supplementary Figure 3D). The AUC values of 1-, 2-, and 3-year overall survival rates in the training dataset were 0.933, 0.596, and 0.739, respectively, and in the testing dataset, they were 0.907, 0.868, and 0.864, respectively (Supplementary Figures 3E, F). Therefore, we considered that the FAM-score prognostic model has an excellent ability to predict DFS and OS in patients with rectal cancer who have undergone nCRT. Similarly, the FAM score was an independent risk factor for OS (p< 0.05, Figure 4H).

Association between clinicopathological features and fatty acid metabolism-related signature

FAM-related signatures were significantly associated with patient age (Supplementary Figure 4A). Patients who are less than 65 years of age had a higher FAM-related risk score than those older than 65 years (p = 0.039, Supplementary Figure 4B). In addition, patients who achieved pCR after nCRT had a lower risk score than nCRT-resistant patients (p = 0.002, Figure 5A). In predicting the nCRT responses of patients with rectal cancer, the FAM-related risk score showed promising predictive ability (AUC = 0.706, Figure 5B). Once more, our observations reflected the ability of the FAM score to predict nCRT response in patients with rectal cancer.

Comparison of fatty acid metabolism-related signature and previously published multi-gene signatures

The FAM-related signature showed the potential ability to predict DFS, OS, and even nCRT response in patients with rectal cancer. To further evaluate the predictive ability of the FAM-

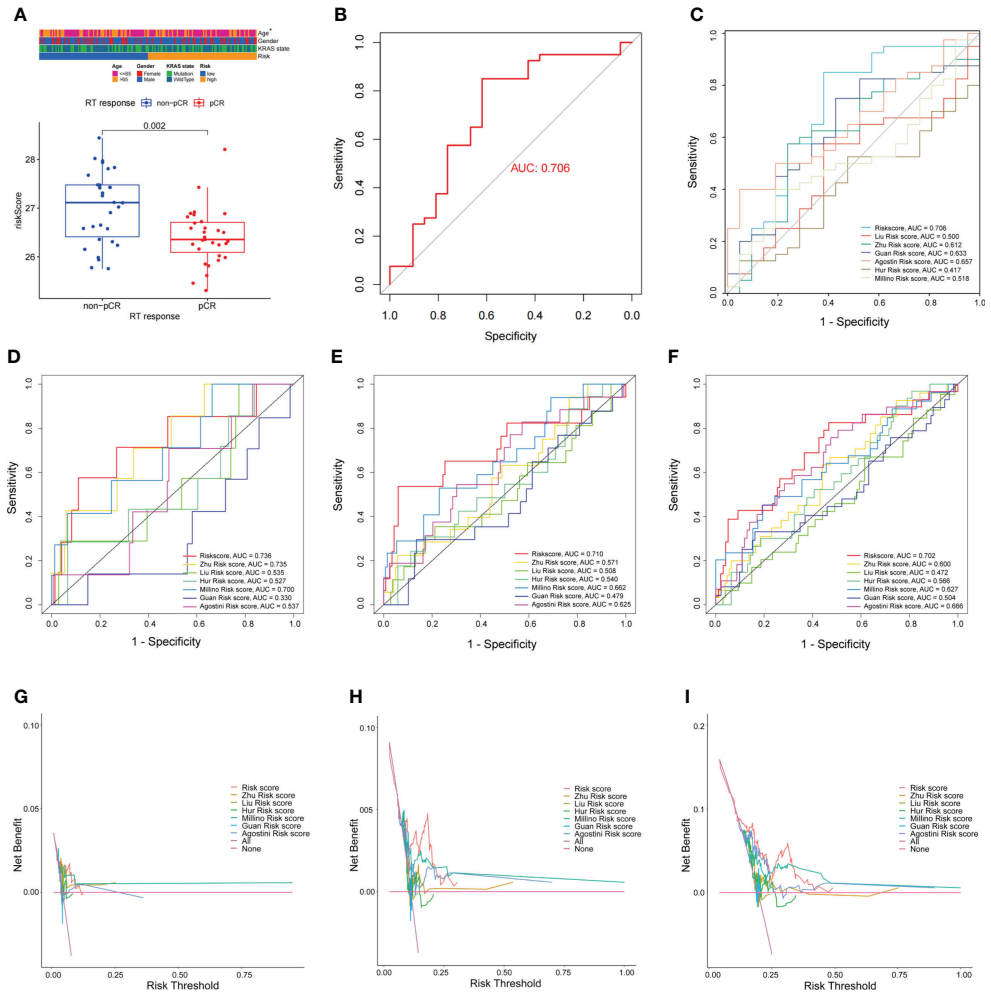

FIGURE 5
Comparison of FAM-related signature and previously published multi-gene models. **(A)** FAM-related risk score association with nCRT response. **(B)** ROC curves used to evaluate the ability of predicting nCRT response using FAM-related signature. **(C)** The ability of the FAM-score model to predict nCRT response of patients with rectal cancer treated with nCRT is better than previously published multi-gene models. **(D–F)** AUC values at 1-, 2-, and 3-years DFS of FAM-score model and previously published multi-gene models. **(G–I)** The DCA for FAM-score model compared with previously published multi-gene models. nCRT, neoadjuvant chemoradiotherapy; FAM, fatty acid metabolism; AUC, area under the curve; DCA, decision curve analysis.

related signature, we compared it with previously published multi-gene signatures. The FAM-related signature showed a better predictive ability for nCRT responses than the other previously published multi-gene signatures (Figure 5C). FAM-related signatures were more efficient in predicting the 1-, 2-, and 3-year DFS and OS of patients who received nCRT than other signatures (Figures 5D–F; Supplementary Figures 5A–C). Furthermore, the decision curve analysis (DCA) curves also suggested that the FAM-related signature outperformed the other signatures in predicting 1-, 2-, and 3-year DFS and OS (Figures 5G–I; Supplementary Figures 5D–F). Therefore, the FAM-related signature shows promising potential not only in predicting the prognosis of DFS and OS but also in predicting the nCRT response of patients with rectal cancer who underwent nCRT.

Function enrichment of differentially expressed genes between high- and low-risk groups

GO and KEGG enrichment analyses were used to reveal the biological processes and functions of the DEGs between the high- and low-risk groups based on FAM-related signatures. GO enrichment analysis revealed that the functions of DEGs were enriched in the biogenesis and targeting of proteins, including

the biogenesis of ribonucleoprotein complexes and calmodulin binding (Figure 6A). KEGG enrichment analysis revealed that the cAMP signaling pathway and neuroactive ligand–receptor interaction metabolic pathways were significantly enriched based on the DEGs between the two groups (Figure 6B).

The landscape and evaluation of immune checkpoints based on fatty acid metabolism-related risk score

To further reveal the relationship between FAM-related signatures and tumor features, we first evaluated the tumor microenvironment (TME) score, including the estimated score, immune score, and stromal score, of patients with rectal cancer who underwent nCRT (Figures 6C–E). Patients with high FAM scores were closely associated with higher estimated and immune scores (both $p < 0.05$). Interestingly, we found that the number of immune-related cells, including interdigitating dendritic cells (iDCs), macrophages, and NK cells, was much higher in patients with a high FAM score (Figure 6F). We next analyzed the immune checkpoints to determine why patients with high-risk scores had higher immune cell infiltration but showed a worse treatment response. We observed that patients with high-risk scores were associated with high-level expression of genes associated with immune checkpoints, including *BTLA*, *CD160*, *CD200*, *CD274* (PD-L1), *HHLA2*, *IDO2*, *LAG3*, and *LGALS9* ($p < 0.05$, Figure 6G). These results also showed that

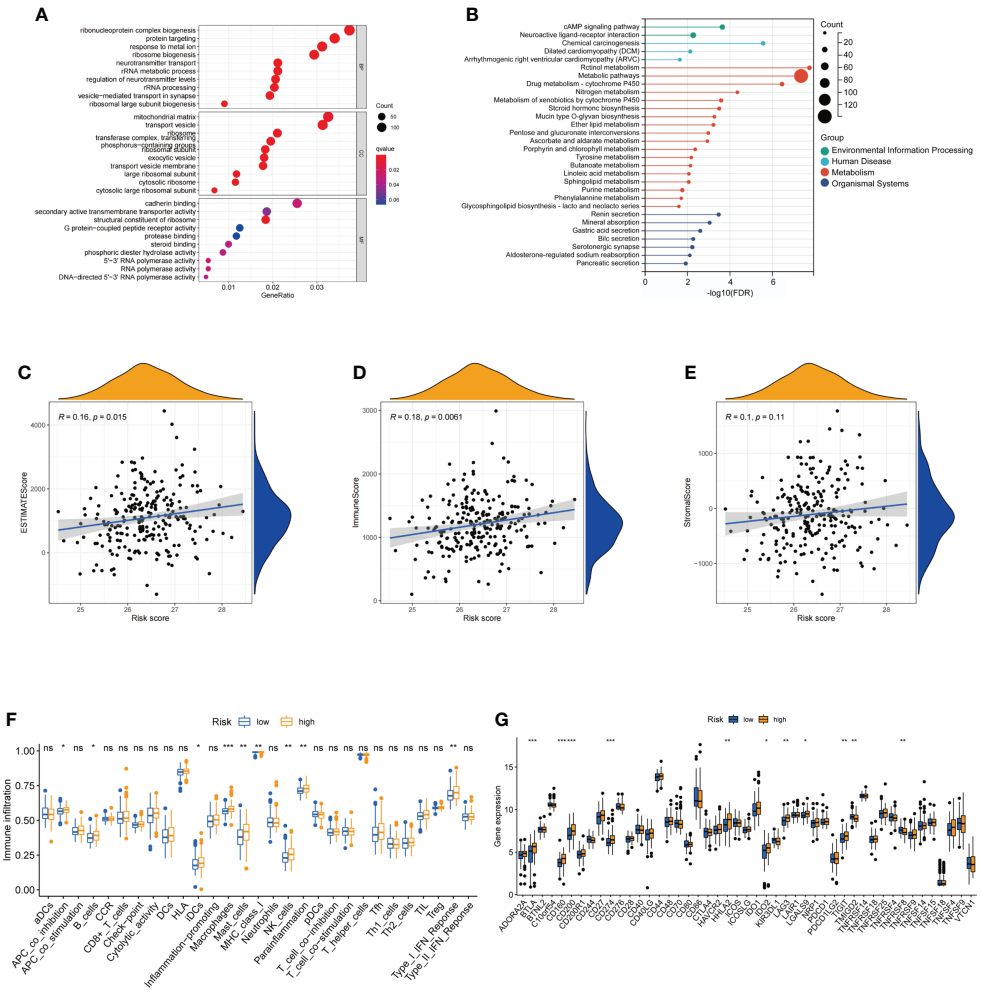

FIGURE 6
Functional analysis of differentially expressed genes and the immune landscape of fatty acid metabolism-related signatures. **(A, B)** The enriched GO and KEGG terms based on DEGs between low-risk and high-risk groups. **(C–E)** Correlation between estimate scores, immune scores, stromal scores, and risk scores. **(F)** The expression of immune checkpoints in low-risk and high-risk groups. **(G)** The ssGSEA score of immune cells and immune-related functions with low-risk and high-risk groups. GO, gene ontology; KEGG, Kyoto Encyclopedia of Genes and Genomes; DEGs, differentially expressed genes. ns: not significant; *: P< 0.05; **: P< 0.01; ***: P< 0.001.

patients with high-risk scores might respond better to therapies targeting the above checkpoints, especially PD-L1.

Validation of the fatty acid metabolism-related signature in the Fujian Cancer Hospital cohort

To confirm the ability of the FAM-related signature to predict DFS and OS, qPCR was used to examine the expression of five genes (*CYP1B1*, *DDC*, *ANO1*, *DAPL1*, and *RIOK3*) in 78 tumor tissues. The patients in our independent cohort were divided into high- and low-risk groups based on their FAM-related risk scores. Consistent with the training dataset, patients in the low-risk group had better DFS and OS rates (Figure 7A; Supplementary Figure 6A). The FAM-related signature also had the potential to predict DFS and OS based on ROC analysis (AUC values of 1-, 2-, and 3-year DFS rates were 0.813, 0.767, and 0.808, respectively; AUC values of 1-, 2-, and 3-year OS rates were 0.813, 0.735, and 0.762, respectively) (Figure 7B; Supplementary Figure 6B). Univariate and multivariate Cox regression analyses showed that the FAM score was an independent risk factor for DFS and OS (both $p< 0.05$, Figure 7C; Supplementary Figure 6C). In addition, patients with lower risk scores tend to achieve pCR in the FJCH cohort ($p = 0.021$, Figure 7D). The FAM-score model also showed a satisfactory ability to predict the response to nCRT (AUC = 0.718, Figure 7E).

Discussion

Metabolism is considered a hallmark of cancer and is closely associated with tumor occurrence and development (28, 29). FAM has also been linked to cancer development and treatment response (30, 31). To the best of our knowledge, this is the first report revealing the important role of FAM in locally advanced rectal cancer that applies gut microbiome, metabolome, and human transcriptome sequencing based on the GEO database in patients with rectal cancer treated with nCRT. In addition, the FAM-related signature composed of five genes showed excellent ability not only in predicting DFS and OS but also in predicting nCRT response in patients with rectal cancer treated with nCRT.

At the baseline of patients with rectal cancer who underwent nCRT, we observed that the gut microbiome from the phylum Proteobacteria, including the class Betaproteobacteriales and the families Burkholderiaceae and Xanthobacteraceae, was strongly associated with favorable nCRT response. Proteobacteria are a major constituent of the human gut microbiome and are associated with the synthesis of medium-chain fatty acids and long-chain fatty acids (32–34). *Anaerotruncuscolihominis_DSM_17241*, which is also enriched in the pCR group of Ruminococcaceae, produces butyric and acetic acids (35, 36). Functional enrichment analysis based on the significantly different gut microbiomes also confirmed that linoleic acid metabolism, a part of FAM, was significantly different between patients in the pCR and non-pCR groups. Linolenic acid is inversely associated with the development of CRC (37). In addition, functional enrichment based on metabolism analysis showed a vital role of FAM in our study. FA intake has been associated with the occurrence of CRC (37, 38). Furthermore, peroxidase damage to polyunsaturated fatty acids drives ferroptosis, which is strongly related to radiotherapy-induced cell death (39, 40). Recently, targeting FAM has become a potential method for radiation sensitization of cancers (23, 41).

A previous study reported an association between FAM-related genes and CRC (41). Nevertheless, no similar multi-gene signature that can predict prognosis and treatment response has been developed based on FAM-related genes in patients with rectal cancer treated with nCRT. According to our results, previous models for predicting the prognosis of rectal cancer did not perform the same ability in such patients. In the current study, a FAM-related signature was constructed using *CYP1B1*, *ANO1*, *RIOK3*, *DDC*, and *DAPL1*, with favorable AUC at 1-, 2-, and 3-year DFS and 1-, 2-, and 3-year OS. In addition, it showed a high AUC for predicting nCRT response in patients with rectal cancer treated with nCRT. Cytochrome P450 1B1 (*CYP1B1*), a member of the cytochrome P450 (*CYP*) family, is highly expressed in tumor tissues, including in CRC, but its expression is lower than in normal tissues (42). A previous study confirmed a significant relationship between *CYP1B1* expression and poor prognosis in patients with CRC, which is similar to our result (43). *CYP1B1* is considered to be an important modulator of FAM and a potential therapeutic target in cancer therapy because of its ability to activate procarcinogens (44, 45). Anoctamin 1 (*ANO1*) is upregulated in CRC and is associated with cancer development by activating the mitogen-activated protein kinase signaling pathway (46, 47). Furthermore, *Fusobacterium nucleatum* has been found to promote the expression of *ANO1* in CRC cells, which prevents CRC cell apoptosis caused by chemotherapy (48). Right open reading frame kinase 3 (*RIOK3*) has been reported to be involved in cancer invasion and metastasis (49, 50). In addition, the expression level of *RIOK3* increases with hypoxia, which is an important factor in preventing effective radiotherapy and immunotherapy of cancer (51, 52). L-DOPA decarboxylase (*DDC*) has been proposed in recent research to serve apoptotic and antiproliferative functions with phosphatidylinositol 3-kinase (PI3K) (53, 54). Moreover, high expression of *DDC* is closely associated with better prognosis in CRC (55). Death-associated protein like-1 (*DAPL1*) has also been confirmed to be associated with cell death in previous studies (56, 57). In our study, *CYP1B1*, *ANO1*, and *RIOK3* were negatively associated with prognosis and nCRT response in rectal cancer.

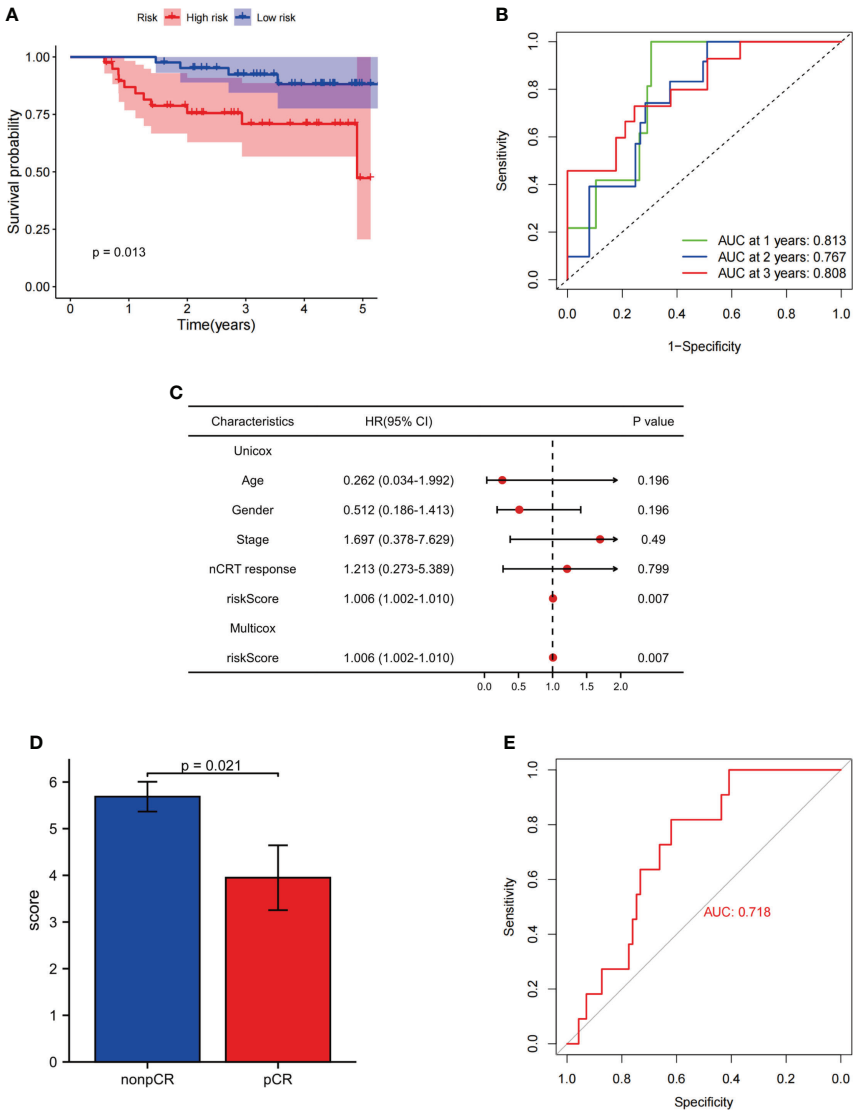

FIGURE 7
Evaluation of the ability of FAM-related signatures to predict prognosis and nCRT response in the FJCH set. **(A)** Kaplan–Meier survival analyses of DFS between patients with high-risk and low-risk scores in the independent cohort. **(B)** Time-dependent ROC curves used to evaluate the prognostic value of risk score. **(C)** Univariate Cox analysis and multivariate Cox analysis of clinicopathological features and FAM-related signature in DFS. **(D)** FAM-related risk score associated with nCRT response. **(E)** Evaluation of FAM-related signature to predict nCRT response. FAM, fatty acid metabolism; DFS, disease-free survival; OS, overall survival; ROC, receiver operating characteristic.

Nevertheless, *DDC* and *DAPL1* were positively associated with prognosis and treatment response in rectal cancer. This five-gene FAM-related model thus assists in predicting prognosis and guiding therapeutics in patients with rectal cancer treated with nCRT.

nCRT is undoubtedly an important treatment for LARC that can improve sphincter preservation and down-staging and decrease local recurrence. An increasing number of researches have shown that radioresistance is closely related to altered tumor metabolism (58, 59). Current evidence has confirmed the value of glycolytic metabolism in improving the sensitivity to radiation therapy for tumors (60), although the mechanism of fatty acid metabolism in improving the radiosensitivity of tumors is not clear. The extensive network of tumor metabolism is interconnected and plays an important role in affecting tumor radiosensitivity. Irradiation induces tumor cell death and can activate the immune response in the TME (61, 62). Interestingly, in this study, we observed that patients with high-risk scores had a higher abundance of immune cells and higher immune scores, which contradicted their higher immune cell infiltration and poor prognoses. However, further

exploration of immune checkpoints yielded an explanation. We found that immune checkpoints showed higher expression levels of *CD274* (PD-L1) in patients with high-risk scores. Overexpressed PD-L1 in cancer cells binds to PD-1 on tumor-infiltrating lymphocytes with impaired T-cell activation (62, 63). In addition, some types of cells in the TME, including dendritic cells, also express PD-L1, which orchestrates the immunosuppressive microenvironment that supports tumor growth (64). Therefore, immune-related cells cannot act efficiently because of PD-L1 overexpression, although there is a higher abundance of immune cells. In addition, high expression levels of PD-L1 are associated with a poor prognosis of rectal cancer (65, 66). Currently, the PD-1/PD-L1 axis is considered an immunotherapeutic target for cancers (67). With intense research on immunotherapy, a combination of conventional cancer treatment methods with PD-L1 may benefit patients with rectal cancer (68). Thus, the overexpression of PD-L1 may provide a new therapeutic strategy for rectal cancer patients treated with nCRT.

Despite these promising results, some limitations remain. First, the FAM-related signature was constructed based on the GEO database and examined in an independent cohort; however, multicenter, large-scale prospective research is still needed to confirm the ability of FAM-related signatures to predict prognosis and nCRT response in patients treated with nCRT. Furthermore, this was a retrospective study, and clinical data were in some cases incomplete or unavailable, which caused a selection bias and incomplete analysis. The potential mechanism by which FAM impacts prognosis and treatment response in patients with rectal cancer needs to be explored. In the future, the results of the present study, including the microbiome, metabolism, and high-throughput sequencing, must be validated both *in vitro* and *in vivo*.

Conclusion

In conclusion, FAM is an important link between the gut microbiome and treatment response. A novel FAM-related signature was constructed that has an excellent ability to predict prognosis in patients with rectal cancer treated with nCRT. In addition, the FAM-related risk score can also be recognized as a potential biomarker of nCRT response in such patients. Finally, the findings of this study provide innovative insights into the individualized management of patients with rectal cancer treated with nCRT.

Data availability statement

The datasets presented in this study can be found in online repositories. The names of the repository/repositories and accession number(s) can be found below: NCBI under accession number PRJNA818503.

Ethics statement

The studies involving human participants were reviewed and approved by The Ethics Committee of Fujian Cancer Hospital. The patients/participants provided their written informed consent to participate in this study.

Author contributions

JL, JW, and HZ conceived and designed the study. YL, HL, and QW collected the samples. YX and YC recorded patient information. LK and GS performed bioinformatics analyses of the sequencing data. This manuscript was prepared by JL, JW, and HZ. All authors have contributed to the manuscript and approved the submitted version.

Funding

This work was supported by a grant (no. 2021J01433) from the Natural Foundation of Fujian Province, Fujian Research and Training Grants for Young and Middle-aged Leaders in Healthcare, National Clinical Key Specialty Construction Program, 2021, and Startup Fund for scientific research, Fujian Medical University (grant number 2020QH2043).

Acknowledgments

We thank the researchers and study participants for their contributions. We thank the TCGA and GEO databases for providing valuable and public datasets.

Conflict of interest

The authors declare that the research was conducted in the absence of any commercial or financial relationships that could be construed as a potential conflict of interest.

Publisher's note

Supplementary material

The Supplementary Material for this article can be found online at: https://www.frontiersin.org/articles/10.3389/fimmu.2022.1050721/full#supplementary-material

References

1. Sung H, Ferlay J, Siegel RL, Laversanne M, Soerjomataram I, Jemal A, et al. Global cancer statistics 2020: GLOBOCAN estimates of incidence and mortality worldwide for 36 cancers in 185 countries. *CA: Cancer J For Clin* (2021) 71(3):209–49. doi: 10.3322/caac.21660

2. Siegel RL, Miller KD, Goding Sauer A, Fedewa SA, Butterly LF, Anderson JC, et al. Colorectal cancer statistics, 2020. *CA: Cancer J For Clin* (2020) 70(3):145–64. doi: 10.3322/caac.21601

3. Benson AB, Venook AP, Al-Hawary MM, Arain MA, Chen Y-J, Ciombor KK, et al. NCCN guidelines insights: Rectal cancer, version 6.2020. *J Natl Compr Cancer Network: JNCCN* (2020) 18(7):806–15. doi: 10.6004/jnccn.2020.0032

4. Ding M, Zhang J, Hu H, Cai Y, Ling J, Wu Z, et al. mFOLFOXIRI versus mFOLFOX6 as neoadjuvant chemotherapy in locally advanced rectal cancer: A propensity score matching analysis. *Clin Colorectal Cancer* (2022) 21(1):e12–20. doi: 10.1016/j.clcc.2021.11.009

5. Des Guetz G, Landre T, Bollet MA, Mathonnet M, Quéro L. Is there a benefit of oxaliplatin in combination with neoadjuvant chemoradiotherapy for locally advanced rectal cancer? An updated meta-analysis. *Cancers* (2021) 13(23):6035–45. doi: 10.3390/cancers13236035

6. Zhu J, Liu A, Sun X, Liu L, Zhu Y, Zhang T, et al. Multicenter, randomized, phase III trial of neoadjuvant chemoradiation with capecitabine and irinotecan guided by status in patients with locally advanced rectal cancer. *J Clin Oncol* (2020) 38(36):4231–9. doi: 10.1200/JCO.20.01932

7. Fokas E, Allgäuer M, Polat B, Klautke G, Grabenbauer GG, Fietkau R, et al. Randomized phase II trial of chemoradiotherapy plus induction or consolidation chemotherapy as total neoadjuvant therapy for locally advanced rectal cancer: CAO/ARO/AIO-12. *J Clin Oncol* (2019) 37(34):3212–22. doi: 10.1200/JCO.19.00308

8. Warburg O, Wind F, Negelein E. THE METABOLISM OF TUMORS IN THE BODY. *J Gen Physiol* (1927) 8(6):519–30. doi: 10.1085/jgp.8.6.519

9. Hanahan D. Hallmarks of cancer: New dimensions. *Cancer Discov* (2022) 12 (1):31–46. doi: 10.1158/2159-8290.CD-21-1059

10. Peek RM, Blaser MJ. Helicobacter pylori and gastrointestinal tract adenocarcinomas. *Nat Rev Cancer* (2002) 2(1):28–37. doi: 10.1038/nrc703

11. Mima K, Sukawa Y, Nishihara R, Qian ZR, Yamauchi M, Inamura K, et al. Fusobacterium nucleatum and T cells in colorectal carcinoma. *JAMA Oncol* (2015) 1(5):653–61. doi: 10.1001/jamaoncol.2015.1377

12. Park JH, Pyun WY, Park HW. Cancer metabolism: Phenotype, signaling and therapeutic targets. *Cells* (2020) 9(10):2308–38. doi: 10.3390/cells9102308

13. Hanahan D, Weinberg RA. Hallmarks of cancer: the next generation. *Cell* (2011) 144(5):646–74. doi: 10.1016/j.cell.2011.02.013

14. Pavlova NN, Thompson CB. The emerging hallmarks of cancer metabolism. *Cell Metab* (2016) 23(1):27–47. doi: 10.1016/j.cmet.2015.12.006

15. Chen F, Dai X, Zhou C-C, Li K-X, Zhang Y-J, Lou X-Y, et al. Integrated analysis of the faecal metagenome and serum metabolome reveals the role of gut microbiome-associated metabolites in the detection of colorectal cancer and adenoma. *Gut* (2022) 71(7):1315–25. doi: 10.1136/gutjnl-2020-323476

16. Chan SL. Microbiome and cancer treatment: Are we ready to apply in clinics? *Prog Mol Biol Transl Sci* (2020) 171:301–8. doi: 10.1016/bs.pmbts.2020.04.004

17. Helmink BA, Khan MAW, Hermann A, Gopalakrishnan V, Wargo JA. The microbiome, cancer, and cancer therapy. *Nat Med* (2019) 25(3):377–88. doi: 10.1038/s41591-019-0377-7

18. Yi Y, Shen L, Shi W, Xia F, Zhang H, Wang Y, et al. Gut microbiome components predict response to neoadjuvant chemoradiotherapy in patients with locally advanced rectal cancer: A prospective, longitudinal study. *Clin Cancer Res* (2021) 27(5):1329–40. doi: 10.1158/1078-0432.CCR-20-3445

19. Jang B-S, Chang JH, Chie EK, Kim K, Park JW, Kim MJ, et al. Gut microbiome composition is associated with a pathologic response after preoperative chemoradiation in patients with rectal cancer. *Int J Radiat Oncol Biol Phys* (2020) 107(4):736–46. doi: 10.1016/j.ijrobp.2020.04.015

20. Roy S, Trinchieri G. Microbiota: a key orchestrator of cancer therapy. *Nat Rev Cancer* (2017) 17(5):271–85. doi: 10.1038/nrc.2017.13

21. Beloribi-Djefaflia S, Vasseur S, Guillaumond F. Lipid metabolic reprogramming in cancer cells. *Oncogenesis* (2016) 5:e189. doi: 10.1038/oncsis.2015.49

22. Koundouros N, Poulogiannis G. Reprogramming of fatty acid metabolism in cancer. *Br J Cancer* (2020) 122(1):4–22. doi: 10.1038/s41416-019-0650-z

23. Tan Z, Xiao L, Tang M, Bai F, Li J, Li L, et al. Targeting CPT1A-mediated fatty acid oxidation sensitizes nasopharyngeal carcinoma to radiation therapy. *Theranostics* (2018) 8(9):2329–47. doi: 10.7150/thno.21451

24. Ding C, Shan Z, Li M, Chen H, Li X, Jin Z. Characterization of the fatty acid metabolism in colorectal cancer to guide clinical therapy. *Mol Ther Oncolytics* (2021) 20:532–44. doi: 10.1016/j.omto.2021.02.010

25. Peng Y, Xu C, Wen J, Zhang Y, Wang M, Liu X, et al. Fatty acid metabolism-related lncRNAs are potential biomarkers for predicting the overall survival of patients with colorectal cancer. *Front In Oncol* (2021) 11:704038. doi: 10.3389/fonc.2021.704038

26. Trakarnsanga A, Gönen M, Shia J, Nash GM, Temple LK, Guillem JG, et al. Comparison of tumor regression grade systems for locally advanced rectal cancer after multimodality treatment. *J Natl Cancer Inst* (2014) 106(10):248–53. doi: 10.1093/jnci/dju248

27. Guo M, Wu F, Hao G, Qi Q, Li R, Li N, et al. Improves immunity and disease resistance in rabbits. *Front In Immunol* (2017) 8:354. doi: 10.3389/fimmu.2017.00354

28. Vander Heiden MG, DeBerardinis RJ. Understanding the intersections between metabolism and cancer biology. *Cell* (2017) 168(4):657–69. doi: 10.1016/j.cell.2016.12.039

29. Kroemer G, Pouyssegur J. Tumor cell metabolism: cancer's achilles' heel. *Cancer Cell* (2008) 13(6):472–82. doi: 10.1016/j.ccr.2008.05.005

30. Bian X, Liu R, Meng Y, Xing D, Xu D, Lu Z. Lipid metabolism and cancer. *J Exp Med* (2021) 218(1):1606–22. doi: 10.1084/jem.20201606

31. Currie E, Schulze A, Zechner R, Walther TC, Farese RV. Cellular fatty acid metabolism and cancer. *Cell Metab* (2013) 18(2):153–61. doi: 10.1016/j.cmet.2013.05.017

32. Zhou S, Wang Y, Jacoby JJ, Jiang Y, Zhang Y, Yu LL. Effects of medium- and long-chain triacylglycerols on lipid metabolism and gut microbiota composition in C57BL/6J mice. *J Agric Food Chem* (2017) 65(31):6599–607. doi: 10.1021/acs.jafc.7b01803

33. Patrone V, Minuti A, Lizier M, Miragoli F, Lucchini F, Trevisi E, et al. Differential effects of coconut versus soy oil on gut microbiota composition and predicted metabolic function in adult mice. *BMC Genomics* (2018) 19(1):808. doi: 10.1186/s12864-018-5202-z

34. Huang EY, Leone VA, Devkota S, Wang Y, Brady MJ, Chang EB. Composition of dietary fat source shapes gut microbiota architecture and alters host inflammatory mediators in mouse adipose tissue. *JPEN J Parenter Enteral Nutr* (2013) 37(6):746–54. doi: 10.1177/0148607113486931

35. Peng Z, Cheng S, Kou Y, Wang Z, Jin R, Hu H, et al. The gut microbiome is associated with clinical response to anti-PD-1/PD-L1 immunotherapy in gastrointestinal cancer. *Cancer Immunol Res* (2020) 8(10):1251–61. doi: 10.1158/2326-6066.CIR-19-1014

36. Lawson PA, Song Y, Liu C, Molitoris DR, Vaisanen M-L, Collins MD, et al. Anaerotruncus colihominis gen. nov., sp. nov., from human faeces. *Int J Syst Evol Microbiol* (2004) 54(Pt 2):413–7. doi: 10.1099/ijs.0.02653-0

37. Butler LM, Yuan J-M, Huang JY, Su J, Wang R, Koh W-P, et al. Plasma fatty acids and risk of colon and rectal cancers in the Singapore Chinese health study. *NPJ Precis Oncol* (2017) 1(1):38. doi: 10.1038/s41698-017-0040-z

38. Shin A, Cho S, Sandin S, Lof M, Oh MY, Weiderpass E. Omega-3 and -6 fatty acid intake and colorectal cancer risk in Swedish women's lifestyle and health cohort. *Cancer Res Treat* (2020) 52(3):848–54. doi: 10.4143/crt.2019.550

39. Lang X, Green MD, Wang W, Yu J, Choi JE, Jiang L, et al. Radiotherapy and immunotherapy promote tumoral lipid oxidation and ferroptosis *via* synergistic repression of SLC7A11. *Cancer Discov* (2019) 9(12):1673–85. doi: 10.1158/2159-8290.CD-19-0338

40. Lei G, Zhang Y, Koppula P, Liu X, Zhang J, Lin SH, et al. The role of ferroptosis in ionizing radiation-induced cell death and tumor suppression. *Cell Res* (2020) 30(2):146–62. doi: 10.1038/s41422-019-0263-3

41. Han S, Wei R, Zhang X, Jiang N, Fan M, Huang JH, et al. CPT1A/2-mediated FAO enhancement-a metabolic target in radioresistant breast cancer. *Front In Oncol* (2019) 9:1201. doi: 10.3389/fonc.2019.01201

42. Murray GI, Taylor MC, McFadyen MC, McKay JA, Greenlee WF, Burke MD, et al. Tumor-specific expression of cytochrome P450 CYP1B1. *Cancer Res* (1997) 57(14):3026–31.

43. Liu X, Wang F, Wu J, Zhang T, Liu F, Mao Y, et al. Expression of CYP1B1 and B7-H3 significantly correlates with poor prognosis in colorectal cancer patients. *Int J Clin Exp Pathol* (2018) 11(5):2654–64.

44. Li F, Zhu W, Gonzalez FJ. Potential role of CYP1B1 in the development and treatment of metabolic diseases. *Pharmacol Ther* (2017) 178:18–30. doi: 10.1016/j.pharmthera.2017.03.007

45. Shimada T, Hayes CL, Yamazaki H, Amin S, Hecht SS, Guengerich FP, et al. Activation of chemically diverse procarcinogens by human cytochrome p-450 1B1. *Cancer Res* (1996) 56(13):2979–84.

46. Mokutani Y, Uemura M, Munakata K, Okuzaki D, Haraguchi N, Takahashi H, et al. Down-regulation of microRNA-132 is associated with poor prognosis of colorectal cancer. *Ann Surg Oncol* (2016) 23(Suppl 5):599–608. doi: 10.1245/s10434-016-5133-3

47. Duvvuri U, Shiwarski DJ, Xiao D, Bertrand C, Huang X, Edinger RS, et al. TMEM16A induces MAPK and contributes directly to tumorigenesis and cancer progression. *Cancer Res* (2012) 72(13):3270–81. doi: 10.1158/0008-5472.CAN-12-0475-T

48. Lu P, Xu M, Xiong Z, Zhou F, Wang L. Prevents apoptosis in colorectal cancer cells *via* the ANO1 pathway. *Cancer Manage Res* (2019) 11:9057–66. doi: 10.2147/CMAR.S185766

49. Rzymski T, Milani M, Pike L, Buffa F, Mellor HR, Winchester L, et al. Regulation of autophagy by ATF4 in response to severe hypoxia. *Oncogene* (2010) 29(31):4424–35. doi: 10.1038/onc.2010.191

50. Kimmelman AC, Hezel AF, Aguirre AJ, Zheng H, Paik J-H, Ying H, et al. Genomic alterations link rho family of GTPases to the highly invasive phenotype of pancreas cancer. *Proc Natl Acad Sci United States America* (2008) 105(49):19372–7. doi: 10.1073/pnas.0809966105

51. Singleton DC, Rouhi P, Zois CE, Haider S, Li JL, Kessler BM, et al. Hypoxic regulation of RIOK3 is a major mechanism for cancer cell invasion and metastasis. *Oncogene* (2015) 34(36):4713–22. doi: 10.1038/onc.2014.396

52. Graham K, Unger E. Overcoming tumor hypoxia as a barrier to radiotherapy, chemotherapy and immunotherapy in cancer treatment. *Int J Nanomed* (2018) 13:6049–58. doi: 10.2147/IJN.S140462

53. Vassiliou AG, Siaterli M-Z, Frakolaki E, Gkogkosi P, Paspaltsis I, Sklaviadis T, et al. L-dopa decarboxylase interaction with the major signaling regulator PI3K in tissues and cells of neural and peripheral origin. *Biochimie* (2019) 160:76–87. doi: 10.1016/j.biochi.2019.02.009

54. Artemaki PI, Papatsirou M, Boti MA, Adamopoulos PG, Christodoulou S, Vassilacopoulou D, et al. Revised exon structure of l-DOPA decarboxylase () reveals novel splice variants associated with colorectal cancer progression. *Int J Mol Sci* (2020) 21(22):8568–96. doi: 10.3390/ijms21228568

55. Kontos CK, Papadopoulos IN, Fragoulis EG, Scorilas A. Quantitative expression analysis and prognostic significance of l-DOPA decarboxylase in colorectal adenocarcinoma. *Br J Cancer* (2010) 102(9):1384–90. doi: 10.1038/sj.bjc.6605654

56. Chakrabarti S, Multani S, Dabholkar J, Saranath D. Whole genome expression profiling in chewing-tobacco-associated oral cancers: A pilot study. *Med Oncol* (2015) 32(3):60. doi: 10.1007/s12032-015-0483-4

57. Feng YY, Yang Y, Wang YY, Bai XX, Hai P, Zhao R. [Hypomethylation of DAPL1 associated with prognosis of lung cancer patients with EGFR Del19 mutation]. *Zhonghua Zhong Liu Za Zhi* (2021) 43(12):1264–8. doi: 10.3760/cma.j.cn112152-20190923-00618

58. Pitroda SP, Wakim BT, Sood RF, Beveridge MG, Beckett MA, MacDermed DM, et al. STAT1-dependent expression of energy metabolic pathways links tumour growth and radioresistance to the warburg effect. *BMC Med* (2009) 7:68. doi: 10.1186/1741-7015-7-68

59. Shimura T, Noma N, Sano Y, Ochiai Y, Oikawa T, Fukumoto M, et al. AKT-mediated enhanced aerobic glycolysis causes acquired radioresistance by human tumor cells. *Radiother Oncol* (2014) 112(2):302–7. doi: 10.1016/j.radonc.2014.07.015

60. Sattler UGA, Meyer SS, Quennet V, Hoerner C, Knoerzer H, Fabian C, et al. Glycolytic metabolism and tumour response to fractionated irradiation. *Radiother Oncol* (2010) 94(1):102–9. doi: 10.1016/j.radonc.2009.11.007

61. Lauber K, Ernst A, Orth M, Herrmann M, Belka C. Dying cell clearance and its impact on the outcome of tumor radiotherapy. *Front In Oncol* (2012) 2:116. doi: 10.3389/fonc.2012.00116

62. Barker HE, Paget JTE, Khan AA, Harrington KJ. The tumour microenvironment after radiotherapy: mechanisms of resistance and recurrence. *Nat Rev Cancer* (2015) 15(7):409–25. doi: 10.1038/nrc3958

63. Yi M, Yu S, Qin S, Liu Q, Xu H, Zhao W, et al. Gut microbiome modulates efficacy of immune checkpoint inhibitors. *J Hematol Oncol* (2018) 11(1):47. doi: 10.1186/s13045-018-0592-6

64. Jiang X, Wang J, Deng X, Xiong F, Ge J, Xiang B, et al. Role of the tumor microenvironment in PD-L1/PD-1-mediated tumor immune escape. *Mol Cancer* (2019) 18(1):10. doi: 10.1186/s12943-018-0928-4

65. Ji D, Yi H, Zhang D, Zhan T, Li Z, Li M, et al. Somatic mutations and immune alternation in rectal cancer following neoadjuvant chemoradiotherapy. *Cancer Immunol Res* (2018) 6(11):1401–16. doi: 10.1158/2326-6066.CIR-17-0630

66. Saigusa S, Toiyama Y, Tanaka K, Inoue Y, Mori K, Ide S, et al. Implication of programmed cell death ligand 1 expression in tumor recurrence and prognosis in rectal cancer with neoadjuvant chemoradiotherapy. *Int J Clin Oncol* (2016) 21(5):946–52. doi: 10.1007/s10147-016-0962-4

67. Brahmer JR, Tykodi SS, Chow LQM, Hwu W-J, Topalian SL, Hwu P, et al. Safety and activity of anti-PD-L1 antibody in patients with advanced cancer. *N Engl J Med* (2012) 366(26):2455–65. doi: 10.1056/NEJMoa1200694

68. Galluzzi L, Buqué A, Kepp O, Zitvogel L, Kroemer G. Immunological effects of conventional chemotherapy and targeted anticancer agents. *Cancer Cell* (2015) 28(6):690–714. doi: 10.1016/j.ccell.2015.10.012

frontiers | Frontiers in Immunology

TYPE Review
PUBLISHED 01 December 2022
DOI 10.3389/fimmu.2022.1074477

OPEN ACCESS

EDITED BY
Haojun Chen,
First Affiliated Hospital of Xiamen University, China

REVIEWED BY
Chentian Shen,
Shanghai Sixth People's Hospital, China
Zhongmin Tang,
University of Wisconsin-Madison, United States
Weiyu Chen,
Zhejiang University, China

*CORRESPONDENCE
Min Cao
drcaomin@126.com

†These authors have contributed equally to this work

SPECIALTY SECTION
This article was submitted to Cancer Immunity and Immunotherapy, a section of the journal Frontiers in Immunology

RECEIVED 19 October 2022
ACCEPTED 15 November 2022
PUBLISHED 01 December 2022

CITATION
Zhu S, Wang Y, Tang J and Cao M (2022) Radiotherapy induced immunogenic cell death by remodeling tumor immune microenvironment. *Front. Immunol.* 13:1074477. doi: 10.3389/fimmu.2022.1074477

Radiotherapy induced immunogenic cell death by remodeling tumor immune microenvironment

Songxin Zhu†, Yuming Wang†, Jun Tang† and Min Cao*

Department of Thoracic Surgery, Renji Hospital, School of Medicine, Shanghai Jiao Tong University, Shanghai, China

Emerging evidence indicates that the induction of radiotherapy(RT) on the immunogenic cell death (ICD) is not only dependent on its direct cytotoxic effect, changes in the tumor immune microenvironment also play an important role in it. Tumor immune microenvironment (TIME) refers to the immune microenvironment that tumor cells exist, including tumor cells, inflammatory cells, immune cells, various signaling molecules and extracellular matrix. TIME has a barrier effect on the anti-tumor function of immune cells, which can inhibit all stages of anti-tumor immune response. The remodeling of TIME caused by RT may affect the degree of immunogenicity, and make it change from immunosuppressive phenotype to immunostimulatory phenotype. It is of great significance to reveal the causes of immune escape of tumor cells, especially for the treatment of drug-resistant tumor. In this review, we focus on the effect of RT on the TIME, the mechanism of RT in reversing the TIME to suppress intrinsic immunity, and the sensitization effect of the remodeling of TIME caused by RT on the effectiveness of immunotherapy.

KEYWORDS

radiotherapy (RT), tumor immune microenvironment (TIME), immunogenic cell death (ICD), immune-checkpoint blockade (ICB), tumor

Introduction

Characteristics of tumor include sustained proliferation, resistance to cell death, angiogenesis, invasion and metastasis, as well as suppression of inflammation and immunity (1). Among them, immunosuppression, an important feature of the tumor immune microenvironment (TIME), is considered to be an important reason of tumor progression and metastasis and has become a therapeutic target for numerous tumor types. Radiotherapy (RT) with highly effective and non-specific in nature is one of the commonly used therapies in the treatment of malignant tumors. RT is regarded as the most effective cytotoxic therapy for treating patients with solid tumors and is used as first-line treatment in

approximately 60% of newly diagnosed patients (2, 3). Firstly, RT directly or indirectly induces DNA damage and endoplasmic reticulum (ER) stress, leading to tumor cell death, which is thought to target cancer cells. In addition, non-targeted and systemic effects of RT have also been identified (4). There is growing body of evidence that RT can remodel TIME to alter the original immunosuppressive state, exert anti-tumor effects, and exhibit enhanced immune responses and therapeutic effects when combined with immunotherapy (5–7). This article partly reviewed the impact of TIME on immunosuppression and the effects of RT on TIME, elaborated the mechanisms of reversal of TIME on the suppression of intrinsic immunity, and the sensitizing effect of the remodeling of TIME on the effectiveness of immunotherapy.

TIME

TIME is the structural and functional niche where tumor cells arise and live, and includes not only tumor cells and extracellular matrix (ECM), but also fibroblasts, epithelial cells (ECs), immune or inflammatory cells, blood and lymphatic vessels, etc (8). TIME, mediated by the secretion of a large variety of factors by a diverse range of cells, forms a local milieu that favors tumor proliferation, infiltration and metastasis. Tumorigenesis is usually accompanied by the activation of innate and adaptive immunity, called functional cancer immunosurveillance, which gradually results in the accumulation of immune or inflammatory cells within the TIME. The immune response plays a dual role in the complex interaction between tumor and host (pro-/anti- tumor) and undergoes cancer immunoediting processes (elimination, equilibrium, and escape), culminating in the formation of an immunosuppressive microenvironment that promotes malignant tumor progression. Natural killer (NK) cells are key cells in innate immunity, relying on granzymes and perforin for direct cell killing without prior sensitization or MHC restriction. In the adaptive immune system, $CD4^+$ T cells and dendritic cells (DCs) are important mediators, while $CD8^+$ cytotoxic T lymphocytes (CTLs) play the ultimate tumor-killing role. $CD4^+$ T cells, mainly T helper cells, broadly play an important adjuvant function in the recognition and clearance of tumor cells, through promoting the proliferation and activation of CTLs, the formation of memory CTLs, and enhancing the antigen presentation of DCs (9, 10). Cytolytic $CD4^+$ T cells recognize antigenic peptides presented by MHC-II molecules mainly on antigen-presenting cells (APCs), and are relevant to antitumor immunity in cancer patients (11, 12). DCs are the most important APCs that initiate adaptive immune responses *via* activation of naive T cells (13). DCs cross-present MHC-I molecules to $CD8^+$ T cells to induce the production of cytotoxic effector $CD8^+$ T cells, known as CTLs (14). CTLs recognize MHC-I molecules expressed by tumor cells and specifically kill tumor cells through Granule exocytosis and Fas ligand (Fas-L)-mediated apoptosis induction (15). Moreover, CTLs release interferon-γ (IFN-γ) and tumor necrosis factor α (TNF-α) to induce cytotoxicity within tumor cells (16). Tumor-associated macrophages (TAMs) are abundant in TME and are major players in the inflammatory response. In addition to promoting tumor cell proliferation and angiogenesis, TAMs suppress adaptive immune responses (17). Cancer Associated Fibroblasts (CAFs), the plentiful stromal cells in the TME, are a major source of extracellular matrix fibrogenic components such as collagen, hyaluronic acid and fibronectin (18). CAFs actively contribute to cancer invasion by modulating distinct malignant processes (angiogenesis, chronic inflammation and ECM remodeling) and therapeutic resistance (19). CAFs control the functional fate of innate and adaptive immune cells in the TIME by secreting cytokines/chemokines and engaging in direct intercellular interactions (20). Moreover, CAFs play important metabolic effects. The secretion of alanine by CAFs supports malignant cell growth and may also have a positive effect on T cell function (21, 22).

TIME suppresses intrinsic immunity

Although the immune system can clear tumors through the cancer-immune cycle, tumors often evade the body's immune surveillance by shaping an inhibitory TIME. The complex interactions between the mediators of pro- and anti-tumor in TIME ultimately determine trends of anti-tumor immunity (23, 24). Among these, pro-tumor immune cells include regulatory T cells (Tregs), myeloid-derived suppressor cells (MDSCs), TAMs, CAFs, and tumor-associated neutrophils (TANs). In TIME, CAFs, TAMs and Tregs form an immune barrier to CTLs-mediated anti-tumor immune responses (15). In addition, pro-tumor immune cells and immunosuppressive factors (e.g., transforming growth factor β, interleukin-10) act synergistically to exert important immunosuppressive effects, including inhibition of differentiation and maturation of DCs, inhibition of NK cell toxicity, inhibition of antigen presentation, inactivation of the pro-apoptotic pathway, and disturbance of T cell receptor signaling (25) (Figure 1).

Immunosuppression of tumor cells

Cytokines, chemokines and metabolites from tumor cells have a significant impact on TIME, such as transforming growth factor-β (TGF-β) and interleukin (IL)-10. Tumor cells inhibit the function of NK cells, $CD8^+$ T cells and evade recognition and attack by the immune system. Most tumor cells express a large amount of stem cell factor, which induces mast cells to infiltrate the tumor site. Mast cells inactivate T cells and NK cells, as well as inhibit their anti-tumor activity (31). Colony stimulating factor 1 (CSF1) produced by tumor cells promotes

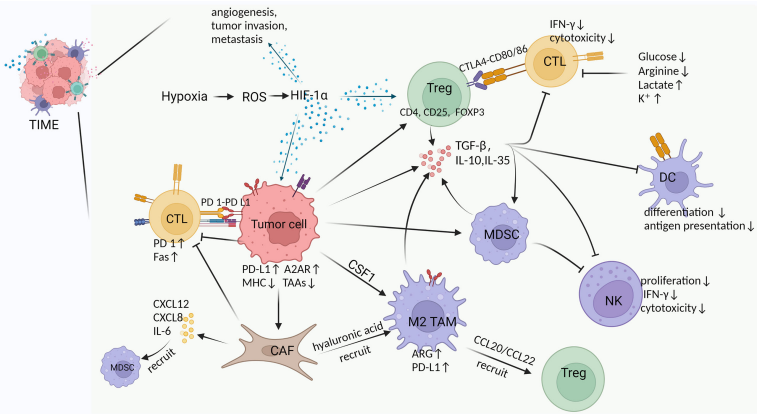

FIGURE 1
Cross-talk between various components in TIME. Hypoxia is an important feature of TIME in solid tumors, which exerts multiple effects by inducing HIF-1α, such as 1) promoting angiogenesis, tumor invasion and metastasis, 2) increasing Tregs abundance to suppress host immune response, and 3) upregulating PD-L1 and A2AR on tumor cells to evade immunity (26–30). Tumor cells induce and chemotactic immunosuppressive cells (Tregs, M2 TAMs, MDSCs, CAFs) to infiltrate in TIME by secreting TGF-β and CSF (31, 32). Moreover, tumor cells inherently upregulate PD-L1 and A2AR expression to suppress the immune function of CTLs, as well as downregulate MHC and tumor-associated antigens (TAAs) expression to reduce antigen presentation and immune activation (29, 30). Tregs produce multiple immunosuppressive cytokines and express CTLA4 to inhibit CTLs and DCs by binding CD80/86 (33). M2 TAMs in TIME suppress T cell function by upregulating ARG and PD-L1 expression while recruiting Tregs *via* CCL20/CCL22 (34–36). MDSCs produce inhibitory cytokines and inhibit the formation and cytotoxicity of NK cells by reducing NKG2D expression and IFN-γ secretion (37). CAFs secrete a large number of cytokines, chemokines and ECM, which exhibit immunosuppressive and tumor-supportive effects (31, 38, 39). For example, IL-6 from CAFs recruits MDSCs, CAFs reduce M1 macrophages while recruiting M2 TAMs *via* hyaluronic acid, upregulated expression of Fas and PD-1 suppresses and depletes T cells (40–42). Suppressive cytokines (e.g., TGF-β, IL-10, IL-35) can be produced by tumor cells and a variety of immunosuppressive cells in TIME to inhibit immune killing of CTLs, suppress the differentiation and antigen presentation of DCs, and restrain the proliferation and cytotoxicity of NK cells (43–46). In addition, glucose and arginine deficiency in TIME, as well as high lactate levels inhibit T cell function (47–51).

differentiation of TAMs and production of granulocyte-specific chemokines in CAFs (31). CSF1 receptor inhibitor and CXCR2 antagonist treatment inhibit the recruitment of MDSCs to TIME, exhibiting significant anti-tumor effects (32). TIME also modify certain inflammatory cell types so that they present a pro-tumor phenotype, in particular many chronic inflammation-associated inflammatory cells promoting tumor progression (52, 53). Hypoxia is a prevalent feature in solid tumor TIME and contributes to the suppression of immune killer cells and protection of tumor cells from immune attack (26, 27). Hypoxia-induced factor 1α (HIF-1α) is a key regulator of adaptive responses to hypoxia, involved in angiogenesis, tumor invasion and metastasis, and increases Tregs abundance by inducing FOXP3 (28). Moreover, HIF-1α also increases PD-L1 expression on tumor cells and suppresses immune cell responses by targeting PD-1 on activated T cells. Tumor cells reduce the expression of MHC or tumor antigens to avoid recognition and clearance by immune cells (29). Adenosine A2a receptor (A2AR) expressed on tumor cells inhibits the activation of immune cells and its expression is associated with cytokines such as HIF-1α. A2AR blockade reduces $CD4^+$ $FOXP3^+$ Tregs infiltration and enhances the anti-tumor response of $CD8^+$ T cells by attenuating hypoxic HIF-1α signaling (30).

Immunosuppression of Regulatory T cells

Tregs are an immunosuppressive subset of $CD4^+$ T cells characteristically expressing CD4, CD25, and FOXP3, and exhibit diversity and functional heterogeneity across tumor types. Hypoxia in TIME increases Tregs abundance by upregulating FOXP3 (28). Tregs, the important Tumor-Promoting Immune Cells, affect a variety of tumor-infiltrating immune cells by producing multiple immunosuppressive cytokines (such as TGF-β, IL-10 and IL-35) and exhibit a significant anti-tumor immune response (43). Tregs inhibit tumor killing by CTLs through TGF-β-dependent cell contact (54), inhibit the production of memory CTLs *via* cytotoxic-T-lymphocyte-associated protein-4 (CTLA-4) (33), and induction of CTLs death *via* granzyme B and perforin-dependent manner (55). In addition, Tregs inhibit IFN-γ secretion by $CD8^+$ T Cells and promote the polarization of M2 TAMs (suppressing immunity) (56). Tregs-expressed CTLA-4 binds to CD80/CD86 on DCs to downregulate co-stimulatory signaling and inhibit DCs function (57). Tregs restrain NK cell proliferation, IFN-γ production, degranulation and cytotoxicity (58). Tregs-produced TGF-β and IL-35 enhance the function of MDSCs (59).

Immunosuppression of tumor-associated macrophages

Macrophages account for >50% of tumor-infiltrating immune cells. According to function and cytokine secretion, macrophages are classified as classical activation (M1) with immunostimulatory function and alternative activation (M2) with immunosuppressive and tumor-supportive effects (60). Macrophages are referred to as TAMs in solid tumors, mainly M2, and there is a strong negative correlation between their presence and survival in a variety of solid tumors including breast, colon, bladder and lung cancers (61–64). TAMs are functionally heterogeneous and display remarkable plasticity, which allows macrophages to 'switching' into an 'M2' phenotype in TIME, associated with immunosuppressive, tumor angiogenic and metastatic consequences (44). In contrast to classical M1 macrophages, these M2 TAMs secrete large amounts of IL-10, and TGF-β, which exert anti-inflammatory effects (44). Hypoxia in TIME also increases arginase 1 (ARG1), VEGF, and macrophage-derived protein kinase signaling by activating mitogen-activated protein kinase signaling in TAMs (34, 65). ARG1 expression is upregulated in TAMs and tumor cells, inhibiting T cell activation by reducing arginine entry into tumor-infiltrating immune cells (34). M2 macrophages-derived CCL20/CCL22 is involved in the recruitment of Tregs (35). M2 TAMs also increases PD-L1 expression to attenuate the effect of CTLs (36).

Immunosuppression by myeloid-derived suppressor cells

MDSCs represent a heterogeneous population of immature myeloid cells with different transcriptional activity and differentiation states, including granulocytic or polymorphonuclear MDSCs (PMN-MDSCs) and monocytic MDSCs (M-MDSCs) (66). They prevent T cell-mediated adaptive immune responses and killing of tumor cells *via* the innate immune system mediated by NK cells or TAMs (67). Among them, PMN-MDSCs produce ROS and reduce T-cell responses to antigens (66). M-MDSCs produce nitric oxide or differentiate into immunosuppressive macrophages to suppress immune activation (68, 69). Similar to Tregs, the secretion of IL-10 and TGF-β by MDSCs impairs CTLs function and facilitates the induction of Tregs formation (45, 46). MDSCs also cause arginine deficiency by consuming nutrients in the TIME, which in turn causes Teff cell inactivation (46). In a xenograft mouse model, MDSCs inhibit NK cells formation and cytotoxicity by reducing natural killer group 2 member D (NKG2D) expression and IFN-γ secretion (37).

Immunosuppression of cancer-associated fibroblasts

CAFs generally exhibit immunosuppressive and tumor-supportive functions (70–72). CAFs secrete a large number of immunosuppressive cytokines and chemokines, such as CXCL12, CXCL8, IL-6, TNF, TGF-β, etc. (31). Among these, high levels of IL-6 recruit MDSCs, upregulate PD-L1 expression and induce tumor immunosuppression (40). CAFs inhibit the production of regulatory factors such as IFN-γ and TNF-α by T cells and block the migratory capacity of T cells (73). In addition, factors secreted by CAFs also reduce the migration of M1 macrophages and inhibit the pro-inflammatory function of M1 macrophages (41). Meanwhile, CAFs upregulate Fas and PD-1 expression on T cells and deplete $CD8^+$ T cells by binding PD-L2 and FasL (42). CAFs remodel the ECM and protect tumor cells from CTLs, for example, hyaluronic acid produced by CAFs recruits TAMs to the TIME (38, 74, 75). In short, CAF-derived cytokines/chemokines mediate immune escape, growth and metastasis of tumors (39). The SynCon FAP DNA vaccine reduces the number of FAP^+ CAFs by targeting Fibroblast activation protein (FAP), a major marker of CAFs, thereby inducing T cell activation and suppressing tumor metastasis (76, 77).

Immunosuppression of TGF-β

In preinvasive disease, TGF-β mainly acts as a tumor suppressor. Once the tumor has invaded, TGF-β promotes tumor progression through epithelial mesenchymal transition, angiogenesis, tumor metastasis, proliferation and immunosuppression of CAFs in TIME (16, 78–81). RT-mediated reactive oxygen species(ROS) production can activate TGF-β (82). TGF-β promotes immunosuppressive TIME through its effects on all immune subgroups (16). For example, TGF-β promotes stromal fibrosis and immune escape, which exclude T cells from infiltrating into tumor tissue, thereby mediating resistance to T cell-directed immunotherapy (64).

Immunosuppression of nutrient competition, metabolite and ion pooling

The high consumption of glucose and amino acids by tumor cells contributes to the achievement of tumor growth, metastasis and immune tolerance (83). Glucose deficiency leads to a decrease in glycolysis in immune cells, which hinders IFN-γ production and the function of CTLs (47). Arginine is exhausted by MDSCs and macrophages, resulting in arginine deficiency in TIME. The anti-tumor activity of T cells is inhibited due to protein biosynthesis-mediated cellular exhaustion (48, 49). Indoleamine 2,3-dioxygenase (IDO) is an important rate-limiting enzyme expressed in CAFs, macrophages, and tumor cells that catalyzes the production of kynurenine from tryptophan (84, 85). Tryptophan metabolites/enzymes suppress inflammatory responses by recruiting Tregs and inhibiting Teff cells proliferation (86, 87). High levels of

extracellular lactate inhibited the proliferation and cytokine production of human CTLs (88). Excess lactate led to an acidic environment that reduced arginine concentrations in TIME by inducing ARG1 expression in macrophages, which in turn inhibited $CD8^+$ T cell proliferation and function (50, 51). Intracellular lactate, a product of glycolysis, inhibits T-cell glycolysis by suppressing the mTORC1-mediated signaling pathway (89). The increase in extracellular fluid potassium ions caused by tumor necrosis leads to severe suppression of T cell effector function (90).

Immunosuppression of blood vessels

The immunosuppressive properties of TIME promote vascular destruction, which limits the infiltration of cytotoxic T lymphocytes into the tumor and exacerbates hypoxia (91). And there is a functional defect in the emerging vascular network in TIME that promotes hypoxia formation (92).

In summary, according to the immune characteristics in TIME, Tumor immunophenotype is usually classified as "cold" or "hot" tumors, which suggests individualized clinical treatment options. In "hot" or "inflamed" tumors, high expression of PD-L1, enrichment of Th1-type chemokines, and a large number of NK cells, $CD8^+$ T cells and APCs are found (93, 94). And it has been established that immune "hot" as a protective factor leads to better clinical outcomes when treated with anti-PD-1/PD-L1 (95). In contrast, "cold" tumors so-called "immune-desert" tumors, are characterized by a high number of Tregs and MDSCs, few NK cells, $CD8^+$ T cells, Th1 cells and DCs, but abundant immunosuppressive cytokines (93, 94).

Effects of RT on the TIME

RT is a form of local ablative physiotherapy, the principle of which was using high-energy radiation to treat localized tumors (96). In addition to damaging tumor cells through different pathways, RT also affects other components of the TIME, including immune cells, CAFs, etc. Besides, RT has both "Non-targeted" and abscopal effects on tumor cells. "Non-targeted" effects, also called bystander effects, are molecular signals from irradiated cells that affect adjacent non-irradiated tissues (97). An abscopal effect, explained by the regression of the tumor occurring at a site far from the radiation, is thought to be the result of a systemic immune response (98). Weichselbaum and colleagues experimentally confirmed that the host immune response was the primary cause of the RT response and not the intrinsic radio-sensitivity of the tumor cells (99). RT is involved in every process of the immune response, the recruitment and accumulation of T cells in tumors, the release and presentation of antigens, the initiation and activation of T lymphocytes, and the recognition and killing of tumor cells by T lymphocytes. The effect of RT on irradiated TIME is immunostimulatory or immunosuppressive, which is primarily influenced by the immune landscape of the tumor as well as the dose and fractionation of RT (100).

RT and tumor cells

RT achieves single- and double-stranded DNA damage, mis-repair and chromosomal aberrations through the induction of ROS and reactive nitrogen species (RNS) (92, 101). When RT-induced damage is limited, cells initiate damage repair mechanisms (including DNA damage response, the unfolded protein response and autophagy) to ensure the survival of irradiated cells and re-entry into the cell cycle (102). However, when damage cannot be resolved by repair mechanisms, the molecular mechanism of adaptation to stress switches from a cytoprotective to a cytostatic or cytotoxic mode, usually in one of these forms, ultimately leading to cellular senescence or regulated cell death (RCD) (103). Moreover, both protective repair mechanisms and senescence or RCD have an impact on the local microenvironment and organismal homeostasis, not only through the production of many different cytokines and chemokines, but also through the involvement of damage-associated molecular patterns (DAMPs), ions, and metabolites (103). RT-driven DNA damage response (DDR) can mediate immunostimulatory effects (104). For example, irradiated cancer cells express NK cell-activating ligands (NKALs) on the cell surface after DDR, which support antigen-independent NK cell activation by binding to specific receptors on NK cells (105). NF-κB is sensitive to intracellular alterations that occur after RT, including DNA damage and oxidative stress (102). RT-induced initiation of NF-κB signaling increased the release of cytokines including TNF and IL-1β (106). Tumor cells and CAFs have a proficient autophagic response and successful autophagic response to RT not only preserves cellular viability but also facilitates the maintenance of immunosuppression by TIME (102). However, apoptotic RCD resulting from failing DDR, UPR and autophagic responses transmits danger signals to TIME *via* membrane exposure and secreted factors in response to lethally irradiation (102). In addition, radiation also induces a variety of non-apoptotic cell death signals, for example, RT-driven mitotic catastrophe activates cGMP-AMP (cGAMP) synthase (cGAS)-stimulator of interferon genes (STING) signaling *via* TBK1 and IRF3, thereby facilitating the secretion of large amounts of type I IFN (107, 108). Necroptosis is a major pro-inflammatory RCD modality that may ultimately lead to increased tumor infiltration of myeloid cells and CTLs (103, 109). Genetic data suggested that necroptosis was the predominant RCD mechanism in non-small cell lung cancer (NSCLC) cells expressing high RIPK3 levels after ablative hypo-fractionated RT (110). In contrast, a study by Sandy Adjemian et al. showed that necroptosis was not the predominant form of

IR-induced death (111). The intrinsic radio-sensitivity of malignant cells exhibits intra- and inter-cancer variability, which depends not only on intrinsic cell characteristics (including efficient DDR, UPR and autophagic competence) but also on TIME factors (e.g. partial oxygen tension) (112–114). Depending on the radiation dose, high doses tend to trigger powerful cytotoxic effects and a strong immune response, while low doses tend to induce cellular senescence and acquire a senescence-associated secretory phenotype (SASP) mainly promoting immunosuppression (102, 115). Data suggest that when cells are irradiated with doses below 10 Gy, most DNA breaks can be repaired and the cells can resume their cell cycle, divide and remain viable. However, at doses higher than 10 Gy some DNA damage fail to repair, at which point mitotic catastrophe and many different forms of death occur (111).

Abscopal radiation-induced antitumor immune responses are rarely observed in clinical practice (116). Apparently, RT-induced antitumor immunity is dependent on RT-generated immune activation signals and immunosuppressive factors (4). One immunosuppressive component is TGF-β1, which promotes tumor progression, invasion and metastasis. Active TGF-β1 is produced in tumors after RT, particularly in endothelial cells undergoing low-dose ionizing-radiation (82, 117). TGF-β1 induces a phenotype of infiltrating inflammatory cells with immunosuppressive effects, e.g. TANs N2 with a protumor phenotype, TAMs M2 (118, 119). RT induces the expression of immunosuppressive molecules, such as PD-L1, through local cytokine-mediated extrinsic effects or P53-mediated intrinsic mechanisms (120, 121).

RT and lymphocytes

Various subtypes of T cells have different resistance to RT, and unlike Th cells and CTLs, Tregs cells are relatively radioresistant (122). B cells and their precursor cells are highly sensitive to radiation-induced DNA damage (123). However, focal radiation treatment of tumor sites at 12-18 Gy using a mouse model suggests that radiation alters B-cell activation, differentiation and clonogenicity, prompting B cells resistance to tumorigenesis (124). Irradiation induces B cells maturation and activation as well as increases the differentiation of tumor antigen-specific plasma cells (124). RT induces the expression of CD20, a common surface antigen on B cells, which is now used as a target for some therapeutic strategies, such as radio-immunotherapy (125).

RT and macrophages

Monocytes, the source of macrophages and DCs, show a high sensitivity to RT and oxidative damages that can lead to single- and double-strand DNA breaks (126). However, both macrophages and dendritic cells upregulate DNA damage repair mechanisms and display a relatively normal DNA repair damage response, leading to an increase in their radio-resistance (126). In TIME, a low-dose RT (LDRT) of 2 Gy induced the differentiation of iNOS$^+$M1 macrophages promoting a pro-immunogenic environment (127). In contrast, higher RT doses promoted tumor infiltration *via* pro-tumorigenic M2-TAMs polarization (128, 129). In addition, high-dose RT (>8 Gy) may promote anti-inflammatory activation of macrophages (130) and doses of 20 Gy activate the M2 TAMs with pathogenic properties *via* induction of the immunosuppressive molecules COX-2/PGE2 and NO (128, 131).

RT and DCs

Higher doses of irradiation (20 Gy) affect the function of DCs, leading to a reduction in the efficiency of antigen presentation and a reduced ability to induce T lymphocyte proliferation (126, 132). According to some reports, irradiated DCs secrete increased amounts of pro-inflammatory cytokines (including IL-1β and IL-12) and decreased amounts of anti-inflammatory cytokines such as IL-10 (133, 134). Fractionated RT along with anti-CTLA4 produced abscopal effects caused in part by an increased number of Batf3 DCs, which were abolished in Batf3-/- mice, confirming the important role of Batf3 DCs in RT-induced anti-tumor immunity (135–137).

RT and Natural Killer Cells

Mature NK cells have been reported to be relatively radioresistant, while their precursors are radiosensitive (138). It is generally accepted that the effect of RT on NK cells is influenced by the radiation dose, with low doses of RT activating NK cells and high doses leading to impaired NK function (139). Low doses of RT (0.075 Gy to 0.15 Gy) triggered increased expression of IFN-γ and TNF-α *in vitro*, and doses of 0.1 Gy to 0.2 Gy resulted in NK activation in an vivo rat model (139). RT induces an ATM-dependent DNA damage response in NK that promotes immune response and reduces exhaustion (140). Radiation increased the ability of NK cells to kill experimental cells such as MCA105 and K562cells (141, 142), and studies using human primary NK cells or the NK-92 cell line also confirmed increased NK cell-mediated cytotoxicity after radiation (143). In addition, RT also induces the migration of NK cells towards the tumor with the help of the chemokine CXCL16/CXCR6 (144). Clinical data from patients with cervical cancer showed increased cytotoxic activity of circulating NK cells post-RT, suggesting systemic activation of NK cells (145). Some studies have also shown a decrease in circulating NK cells but an increase in robust TIM3$^+$ NK cells after ablative RT (146). Conversely, several clinical studies have shown a decrease in NK cell activity post-RT (147–149).

RT and CAFs

CAFs are extremely radio-resistant, do not trigger apoptosis even at high doses of radiation (e.g. 30 Gy) and maintain a strong immunosuppressive effect on activated T cells (in a single dose of 18 Gy) (73). However, post-RT CAFs become senescent and produce a different combination of immunomodulatory molecules (73). In particular, senescent CAFs secrete high levels of TGF-β1, which mediates T-cell rejection and facilitates the establishment of immunosuppressive TIME (150, 151). RT was associated with increased radio-resistance of tumor cells, including in NSCLC, which may be due to the pro-tumor activity of CAFs (152). The pro-tumorigenic nature of radiated CAFs is achieved by direct tumor cell stimulation and suppression of immune cells, including macrophages, DCs, NK cells and T cells (41, 70, 73). Differently, *in vivo* models have shown that irradiation of CAF (iCAF) alters pro-cancer characteristics and reduces tumor engraftment and angiogenesis (153). In conclusion, CAFs are the main drivers of becoming established immunosuppressive TIME post-RT.

RT and vasculature, endothelial cells

There is evidence that single radiation doses of 5-10 Gy result in relatively mild vascular changes, while higher doses(>10 Gy) result in significant vascular damage, at which point reduced vascular flow due to endothelial cell death leads to hypoxia, reduced effector T cell recruitment and suppression of local immune responses in TIME (154). In addition, high doses of RT (HDRT) also exhibited pro-tumor effects by inducing HIF-1α/TGF-β signaling, increasing the number of CAFs and promoting fibrosis and remodeling of TIME (94).

RT and chemokines, cytokines, and other soluble factors

Increased expression of type I IFNs post-RT stimulates the expression of chemokines CXCL9 and CXCL10, which recruit CXCR3-expressing T cells to the TIME (94). In addition, type I IFNs promote Battf3-expressing DCs to present antigens to $CD8^+$ T cells and initiate anti-tumor immunity (155). IFN-γ promotes Th1 cells polarization and CTLs activation, but also upregulates PD-L1 expression in TIME (156, 157). HDRT induces the production of tumorigenic cytokines, such as HIF-1α/VEGF-A, which promotes the release of a large number of cytokines including IL-1, IL-6, IL-10, and TGF-β (94, 152). Among these, TGF-β exerts multiple immunosuppressive effects. TGF-β inhibits the expansion and cytotoxicity of $CD8^+$ T cells, suppresses the differentiation of $CD4^+$ T cells and induces Tregs transformation (94). In addition, RT-induced TGF-β signaling increases the number of CAFs whose release of CXCL12 binds to the ligands CXCR4 and CXCR7, exerting pleiotropic pro-tumor activity, including induction of tumor survival, metastasis and affecting immune cell infiltration, and function (158–162). RT-induced hypoxic TIME depletes glucose and essential amino acids, and metabolite accumulation occurs, such as lactate, adenosine, and kynurenine, which can blunt the function of CTLs while promoting the accumulation of Tregs (163).

Furthermore, while radiation initially induces an anti-tumor response, radiation also induces chronic inflammation and rebound immune suppression (64). During this phase, tumor-promoting macrophages are recruited to the tumor in a radiation dose-dependent manner, resulting in an immunosuppressive TIME that supports tumor regeneration or resistance. RT also induces HIF-1α which induces PD-L1 expression in tumor cells and TAMs, leading to resistance to RT and immunosuppression (164, 165). In addition, the inflammatory response induced by RT also induced upregulation of IDO, which increased TAMs and MDSCs in TIME, associated with tumor immunosuppression (166, 167). From this, it appears that radiation may have a temporary effect on the immune response to TIME, where there appears to be a window of anti-tumor response. The clinical data from the PACIFIC trial suggested that patients who started checkpoint suppression within 14 days of completing RT appeared to have better outcomes than those who started later (168).

Reversal of RT: From immunosuppression to immunostimulation

A growing number of studies have confirmed that radiation increases the amount of MHC on the cell surface, leading to the expression and release of immunostimulatory cytokines and danger signals, which in turn leads to the activation of innate and adaptive immune responses (92, 169). (Variations of multiple factors in TIME post-RT are summarized in Table 1.) RT acts in several aspects of the immune response, transforming the immunosuppressed state into an immune activated state, e.g. increased infiltration of immune cells in TIME, activation of innate and adaptive immunity, enhanced existing T cell responses, neoantigen-induced immune responses and diminished immunosuppression.

Increased immune cell infiltration in TIME

A single irradiation with 2 Gy increased the ability of tumor-specific $CD4^+$ and $CD8^+$ T cells to migrate into the tumor (127).

TABLE 1 Summary of alterations in immunomodulatory factors post-RT.

Factors		Immunomodulation	Effect of RT	Ref.
Immunocytes	$CD8^+$ T cells	Immunostimulation (tumor-specific cytotoxicity *via* MHC-I)	Increased infiltration and activation	(64, 135, 170–178)
	$CD4^+$ T cells	Immunostimulation (Enhancing CTLs responses or exerting cytolysis *via* binding MHC-II)	Increased infiltration and activation	(64, 179, 180)
	DCs	Immunostimulation (Uptake of TAAs, cross-presentation, and initiation of tumor-specific CTLs)	Increased infiltration and activation	(173, 177, 181–184)
	NK cells	Immunostimulation (Killing tumor cells directly without prior sensitization or MHC restriction)	Increased infiltration and cytotoxicity	(180, 185)
	Tregs	Immunosuppression (Inhibiting CTLs and NK cells, enhancing MDSCs and M2 TAMs)	Decreased infiltration	(173–177)
	M1 macrophages	Immunostimulation (Production of pro-inflammatory cytokines)	Increased polarization	(127, 180, 181, 186)
	MDSCs	Immunosuppression (Secretion of immunosuppressive cytokines, inhibition of T cells and NK cells)	Decreased infiltration	(170, 173, 176, 187)
Cytokines	Type I IFNs	Immunostimulation (Recruitment of $CD8^+$ T cells and $CD4^+$ T cells, activation of DCs)	Increased expression	(94, 155, 188–190)
	TGF-β	Immunosuppression (Inhibiting CTLs and NK cells, inducing Tregs, M2 TAMs, and N2 TANs)	Decreased expression	(180, 186)
Chemokines	CXCL9, CXCL10	Immunostimulation (Recruiting CXCR3-expressing T cells)	Increased expression	(94)
	CXCL16	Immunostimulation (Recruiting $CD8^+$ T cells)	Increased expression	(191)
	CXCL8	Immunostimulation (Inducing targeted migration of CD56dim NK cells)	Increased expression	(192)
Adhesion molecules	ICAM1, VCAM1	Immunostimulation (Recruitment and attachment of circulating leukocytes)	Increased expression	(92, 193, 194)
	E- selectin, P-selectin	Immunostimulation (Facilitating lymphocyte homing)	Increased expression	(195)
DAMPs	CRT	Immunostimulation (Prophagocytic signals for macrophages and DCs by binding to CD91 receptors)	Increased exposure	(196, 197)
	HMGB1	Immunostimulation (Activating T cells)	Increased release	(25, 174)
	ATP	Immunostimulation (Recruitment of monocytes and production of IL-1β)	Increased release	(198)
	Cytoplasmic DNA	Immunostimulation (Enhancing the expression of type I IFNs *via* cGAS-STING signaling)	Increased exposure	(188, 189, 199, 200)
Cell surface molecules and receptors	Fas	Immunostimulation (A specific death factor inducing apoptosis by binding to FasL)	Increased expression	(194, 201–203)
	MHC-I molecules	Immunostimulation (Transporting and displaying TAAs allowing $CD8^+$ T cells to identify)	Increased expression	(201, 204)
	Hsp70	Immunostimulation (Activating monocytes, macrophages and DCs)	Increased exposure	(205)
	NKG2D	Immunostimulation (enhancing cytotoxicity of T cells)	Increased expression ($CD4^+$ T cells)	(179, 206)
	NGK2D ligand	Immunostimulation (Sensitizing NK cell-mediated cytotoxicity)	Increased expression (tumor cells)	(207, 208)
	Neoantigen	Immunostimulation (Inducing neoantigen-specific $CD8^+$ T cells and $CD4^+$ T cells)	Increased expression	(203, 204, 209)
	CD47	Immunosuppression (An anti-phagocytic signal to promote immune evasion)	Decreased expression	(210)
	PD-L1	Immunosuppression (Inhibiting activation of T cells)	Increased expression	(120, 121, 176, 211)

LDRT-induced expression of inflammatory cytokines (IL-1β, TNF-α and type I and II IFN) and endothelial cell-activated adhesion molecules (ICAM1 and VCAM1) facilitates extravasation and activation of immune cells (92, 193). RT induced the expression of E- and P-selectin on the surface of vascular endothelial cells, facilitating lymphocyte homing (195). RT induced polarization of M1 macrophages and secretion of NO *via* iNOS activation, promoting normalization of blood vessels and facilitating adhesion and infiltration into the TIME (181). Cytoplasmic DNA produced by irradiated tumor cells is sensed by cGAS, which enhances the expression of type I IFNs through cGAS-STING signaling in host immune cells and tumor cells (188, 189). Increased

expression of type I IFNs after RT stimulates the expression of chemokines CXCL9 and CXCL10, which recruit CXCR3-expressing T cells to the TIME (94). Similarly, RT induced CXCL16 to interact with $CD8^+$ T cells to promote their recruitment activity (191). Tumor cells with senescent characteristics induce targeted migration of CD56dim NK cells by secreting CXCL8, which in turn initiates an innate anti-tumor immune response (192). In addition, radiation generates a pro-inflammatory microenvironment with remodeling of the vasculature, allowing T cells extravasation and tumor destruction (212). RT makes refractory "cold" tumors sensitive to immune checkpoint inhibitors by promoting the recruitment of anti-tumor T cells (213). One study showed that HDRT reshaped the immunosuppressive tumor microenvironment, leading to a significant increase in $CD8^+$ T cell tumor infiltration, while suppressing MDSCs, however, the number of $CD8^+$ T cells decreased when extended fractionated radiation was given (170). In studies on oral squamous cell carcinomas, metastatic renal cell carcinomas, and soft tissue sarcomas, neo-adjuvant RT increased the number of locally infiltrating immune cells in a variety of tumors, including $CD4^+$, $CD8^+$, and $CD20^+$ TILs (64, 171, 172). Recent experiments in both mouse models and patient tumors have found that LDRT induces predominantly infiltration of $CD4^+$ T cells with Th1 signatures in TIME (179). (Figure 2)

Innate and adaptive immune response activation

A series of studies have demonstrated that radiation induces innate and adaptive immune response activation, of which RT-induced ICD is a very important mechanism that alters intracellular immunogenicity through external stimulation (182, 214, 219). ICD is characterized by the translocation of the calreticulin (CRT), the release of high-mobility group box 1 (HMGB1) protein and the release of ATP following apoptosis (214). Among these, the ER-derived proteins CRT translocated from the ER to the cell surface are key to the ICD, which binds to CD91 receptors as prophagocytic signals for macrophages and DCs (196, 197). HMGB1 stimulates the TLR4/MyD88/TRIIF

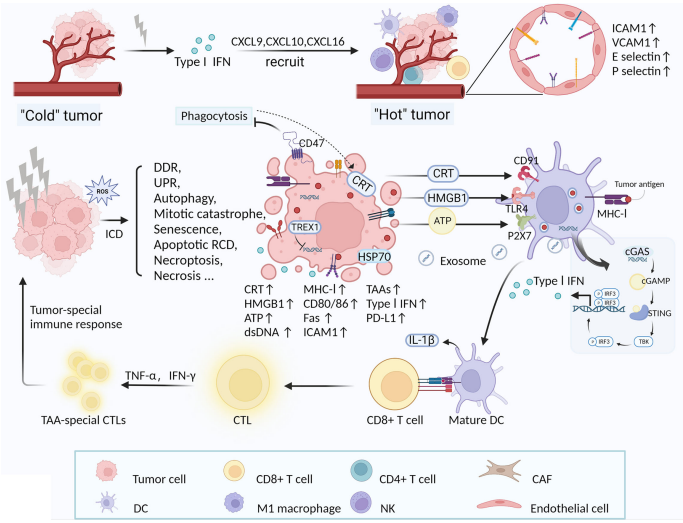

FIGURE 2
RT-induced increase in immune cells in TIME and tumor-special immune response activated by ICD. LDRT induces increased expression of a variety of molecules, including inflammatory cytokines (type I IFN), chemokines (CXCL9, CXCL10, CXCL16), adhesion molecules (ICAM1 and VCAM1) and E-/P-selectin, which facilitate the recruitment of multiple immune cells (DCs, NK cells, M1 macrophages, $CD8^+$ and $CD4^+$ T cells) (92, 94, 191, 193, 195). Concurrently, RT-induced vascular normalization also promotes immune cell infiltration in the TIME (181). Ultimately, RT transforms "cold" tumors (lymphocyte deficiency) into "hot" tumors sensitive to immunotherapy. RT directly or indirectly causes DNA damage in tumor cells and induces various forms of cellular responses and death, such as DDR, UPR, autophagy, mitotic catastrophe, senescence, apoptotic RCD, necroptosis, necrosis, etc (102, 103, 107, 108). Exposure and release of multiple DAMPs are critical for RT-induced ICD, including CRT (binding to CD91), HMGB1 (binding to TLR4), ATP (binding to P2Y2), and dsDNA (entering DCs) (25, 196–198, 214). DAMPs or danger signals recruit DCs and other APCs into irradiated TIME and to promote the maturation and activation of DCs. Mature DCs enhance uptake of tumor-associated antigens (TAAs) and subsequent cross-presentation with $CD8^+$ CTLs, thereby initiating a tumor-specific adaptive immune response (181–183). During the process, dsDNA from irradiated cells activates the cGAS-STING pathway signaling *via* TBK1 and IRF3 in host DCs and tumor cells, culminating in the production of type I IFN (188, 189, 199, 200). Type I IFN in TIME is thought to be crucial for the induction of anti-tumor immune responses by RT (165, 190). In addition, RT enhances the immunogenicity of tumor cells by modulating the expression of cell surface molecules and receptors, and enhances the existing immune response, such as MHC-I, stimulatory molecules (CD80, CD86), adhesion molecules (ICAM1), death receptors (Fas) (204, 207, 215–218). PD-L1 expression is increased on tumor cells post-RT, which is one of the important targets for ICB therapy (120, 121, 164, 165, 176).

pathway and activates T cells (25). In TIME, these factors act synergistically as DAMPs or danger signals to recruit DCs and other APCs into irradiated TIME and to promote the maturation and activation of DCs. Mature DCs enhance uptake of tumor-associated antigens (TAAs) and subsequent cross-presentation with $CD8^+$ CTLs, thereby initiating a tumor-specific adaptive immune response, activating T cells and forming memory phenotypes (181–183). The current study demonstrates that during RT-mediated ICD, tumor-derived dsDNA enters the cytoplasm of DCs and activates the cGAS-STING DNA-sensing pathway signaling a type-I IFN response in which TREX1 exerts an inhibitory effect by degrading DNA (199, 200). STING induces IFN-β transcription and type I IFN expression, which are required for DC activation, ultimately leading to cross-presentation of TAAs and initiation of tumor-specific CTLs (155, 190). In addition to host immune cells, DNA-sensing pathways in tumor cells were also activated, which increase type I IFN production (188, 189). Inflammatory pathways activated by STING ligands have adjuvant activity enhancing tumor-specific adaptive immune responses post-RT (220). ATP is involved in the recruitment of monocytes into tumors (via P2Y2 receptor) and in the production of IL-1β (via P2RX7 receptor and inflammasome NLRP3), which is required for the activation of T cells (198). Unlike Apoptotic cells, which are normally cleared *via* the anti-inflammatory pathway, necrotic cells are immunogenic due to loss of membrane integrity and sustained release of DAMPs, inducing strong immune and inflammatory responses (207, 221). For example, the apoptosis inhibitor zVAD-fmk effectively blocked programmed cell death and induced necrosis as a form of ICD, and its combination with radiation altered the infiltration of immune cells in TIME, i.e. increased DCs and $CD8^+$ T cells and decreased Tregs and MDSCs (173).(Figure 2)

Enhancement of existing T-cell responses

Preclinical studies have shown that SBRT can also enhance immunogenicity by modulating the expression of cell surface molecules and receptors to reinforce existing immune responses, such as MHC-I, stimulatory molecules (e.g. CD80, CD86), adhesion molecules (e.g. ICAM1), death receptors (e.g. Fas), NKG2D ligands, heat-shock proteins (e.g. HSP70), endoplasmic reticulum (ER)-derived calreticulin, etc. (204, 207, 215–218). Garnett et al. investigated the increase in five cell surface antigen proteins (including Fas, MHC-I, ICAM-1, CEA, or mucin-1) post-RT in 23 human carcinoma cell lines and the results suggested that 91% of human carcinoma cell lines showed dose-dependent increases in at least one antigen (201). Among other things, radiation increased Fas gene expression in tumor cells of CEA-expressing mice, thereby enhancing their sensitivity to CEA-specific CTL-mediated killing (201).

Several studies have confirmed that radiation increases the expression of tumor cell surface antigens, particularly MHC class I/II antigens, and that its expression upregulation is dose-dependent (222, 223). RT upregulates MHC-I molecules and generates unique MHC-I antigenic peptides that promote antigen-specific CTLs responses, one of the important mechanisms of RT induced immune sensitization (201, 204). RT has also been shown to enhance the susceptibility of tumor cells to immune-mediated cytotoxicity *via* the Fas/FasL pathway, a key mechanism for cell death mediated by NK cells and CTLs (202). Chakraborty et al. demonstrated that RT can upregulate Fas and ICAM-1 expression on MC38 mouse colon cancer cell lines in a dose-dependent manner (194). Hsp70 translocates from the cytoplasm to the extracellular matrix by binding to CD14, CD40, CD91, Lox1 and Toll-like receptors to activate monocytes, macrophages and DCs (205).

NKG2D is an essential costimulatory receptor expressed mainly on $CD8^+$ T cells and NK cells, contributing to enhanced cytotoxicity of T cells and prevention of Fas-mediated autophagy (224–226). In addition, $NKG2D^+$ $CD4^+$ T cells were found in cervical carcinoma while missing on $CD4^+$ T cells in the physiological state (179, 206). Tumors evade NKG2D through multiple mechanisms and soluble NKG2D ligands improve ICB effects, suggesting an significant anti-tumor function of the NKG2D pathway (227–230). RT was also found to upregulate NGK2D ligand expression on tumor cells, making them more sensitive to NK cell-mediated cytotoxicity (207, 208). Recently Fernanda G Herrera and colleagues found an increase of $NKG2D^+$ $CD4^+$ T cells in TIME post-LDRT and exhibited proliferative capacity (179). Furthermore, an elevated expression of NKG2D ligand RAE1 was observed in DCs, supporting a functional cross-talk between DCs and $CD4^+$ T cells *via* NGK2D pathway (179).

Neoantigen-induced immune responses

Silvia C Formenti et al. reported that RT in combination with CTLA-4 blockade induced anti-tumor responses in chemotherapy-refractory metastatic non-small cell lung cancer (NSCLC), where TCR-Seq analysis of responding patients suggested that $CD8^+$ T cells expanded rapidly *in vivo* due to the recognition of a new antigen encoded by a gene that was upregulated by radiation (209). RT upregulated the expression of genes containing immunogenic mutations in a mouse model of triple-negative breast cancer with poor immunogenicity and increased tumor cell surface death receptors Fas and DR5, with the result that neoantigen-specific $CD8^+$ T cells and $CD4^+$ T cells preferentially killed irradiated tumor cells as well as promoted epitope spreading (203). This suggests that exposure to RT-induced immunogenic mutations stimulates a systemic anti-tumor response. Factors released from dead cells may be the source of radiation-associated antigenic proteins

(RAAPs) (231). RT is able to modulate the peptide repertoire of irradiated cells, and in particular, radiation induces the expression of novel proteins that result in unique MHC-I antigenic peptides that enhance polyclonal antigen-specific CTLs responses (204).Whole-exome sequencing of NSCLC treated with PD-1 blockade confirmed treatment response was better when there was increased mutational burden, higher neoantigenic burden and mutations in the DNA repair pathway (232). This suggests that the response to immunotherapy after RT is associated with irradiation-induced neoantigens.

Decreased immunosuppression

Radiation also reduces the immunosuppressive properties to achieve remodeling of the TIME. TNF production by radiation-activated T cells leads to direct elimination of MDSCs locally and in the system (187). In contrast, found in experiments of RT combined with DNA vaccines, RT induced a decrease in Tregs, but not MDSCs (174). The transmembrane protein CD47 is overexpressed in most cancer cells and acts as an anti-phagocytic signal to promote immune evasion, with downregulation of expression in the presence of radiation exposure (210).

The effect of RT-induced reconfiguration of the TIME on the effectiveness of immunotherapy sensitization

Immunotherapies designed to activate the patient's immune system to kill cancer cells include chimeric antigen receptor T-cell therapy (CAR-T), immune-checkpoint blockade (ICB), and tumor vaccines. ICB is the most commonly used immunotherapy option. Immune checkpoints are a series of inhibitory pathways present in the immune system that are essential for the maintenance of self-tolerance and facilitate the regulation of duration and amplitude of physiological immune responses in order to mitigate additional tissue damage. Unfortunately, tumors use certain immune checkpoint pathways as the primary mechanism of immune resistance (211). CTLA-4 binds to its ligands B7-1 (CD80) and B7-2 (CD86) to generate inhibitory signals that suppress T cell activation and cytokine production and protect tumor cells from T cell attack (233). PD-1, mainly expressed in activated T cells, B cells and macrophages, binds to ligands (PD-L1 and PD-L2) to inhibit T cell activity, induce apoptosis of tumor-specific T cells and suppress Tregs apoptosis (234). PD-L1 is expressed on tumor cells, immune cells and epithelial cells, whereas PD-L2 is only induced on antigen-presenting cells (235). PD-L1 is overexpressed on tumor cells and is thought to be associated with immune escape. ICB alleviate the functional suppression of T cells and have been used to shift the balance of TIME from an immunosuppressed to an immune activated state, resulting in a sustained and durable anti-tumor response at multiple lesion sites (236). Anti-PD-1, anti-PD-L1 and anti-CTLA-4 are currently FDA-approved treatment options for a variety of cancer types (237). In addition, some emerging immune target studies have recently emerged, for example, lymphocyte activation gene 3 (LAG-3) overexpression in Tregs produces the immunosuppressive cytokines IL-10 and TGF-β, which inhibit the activity of effector T cells, and whose expression levels correlate with tumor progression and poor prognosis (238). Dual blockade of LAG-3 and PD-1 also increased the number of tumor-infiltrating $CD8^+$ T cells and reduced Tregs, thereby synergistically enhancing anti-tumor immunity (239). Dual blockade of PI3k-γ and CSF-1R promotes a shift in polarization state from M2 TAMs to M1 macrophages, reduces infiltration of MDSCs and enhances $CD8^+$ T cell activation in TIME (240). DC-based vaccines can activate T-cell responses by removing inhibition of antigen presentation (241).

As radiotherapy can produce anti-tumor immune response and a control mechanism of suppressive tumor immune response, thus the combination of RT and drugs targeting tumor immunosuppression enhances the anti-tumor immune response and improves the efficacy of single modality therapy (64). Currently, numerous preclinical and clinical studies reveal the synergistic effect of RT with ICB (155, 165, 179, 180, 209, 242–245), and part of the relevant clinical trials are summarized in Table 2. Jing Zeng and colleagues showed that the combination of PD-1 blockade and local RT led to long-term survival in mice with *in situ* brain tumors compared to single radiation or immunotherapy, and that immunological data showed increased infiltration of CTLs($CD8^+$/IFN-γ^+/TNF-α^+) and reduced infiltration of Tregs ($CD4^+$/FOXP3) in the combined treatment group (175). Single-cell RNA-sequencing revealed a significant increase in B cells germinal center formation after PD-1 blockade and radiotherapy (124). To take advantage of the enhanced radiation-induced endogenous anti-tumor immune response, increased PD-L1 expression on tumor cells or infiltrating immune cells must be counteracted by blocking the PD-1/PD-L1 pathway (211). In studies on NSCLC, PD-L1 expression was increased both *in vitro* and *in vivo* after conventionally fractionated radiation. Further studies showed that RT combined with anti-PD-L1 antibody enhanced anti-tumor immune responses by promoting $CD8^+$ T cell infiltration and reducing MDSCs and Tregs cell aggregation (176). Xiaoqiang Qi et al.'s study of the therapeutic effect of Minimally invasive radiofrequency ablation (RFA) combined with sunitinib in an HCC model showed that the combined treatment increased the frequency of $CD8^+$ T cells and DCs, reduced Tregs infiltration, and activated tumor-specific antigen (TSA) immune response, ultimately favoring inhibition of HCC growth (177). In addition, RFA caused the upregulation of PD-1 in tumor-infiltrating T cells by promoting hepatocyte growth factor (HGF) expression, which was inhibited by sunitinib treatment (177). The combination of anti-CTLA-4 antibody and fractionated RT regimens showed an enhanced antitumor response at the primary site *in situ* and an abscopal effect was observed (135). The frequency of $CD8^+$ T cells producing tumor-specific IFN-γ correlates with secondary tumor suppression (135). Ming-Cheng Chang et al. demonstrated that

TABLE 2 Landmark clinical trials of RT combined with immunotherapy for the treatment of cancers.

First Author	Patients	Cancer types	RT planning	Immunotherapy planning	Treatment schedule	Outcomes	Data source
Willemijn S M E Theelen (246)	92	Advanced Non-Small Cell Lung Cancer	8Gy×3	Pembrolizumab 200 mg/kg q3w	Pembrolizumab alone vs. pembrolizumab + SBRT	ORR 18% vs. 36%; p = 0.07 mPFS 1.9 vs 6.6; p = 0.19 mOS 7.6 vs. 15.9; p = 0.16	https://clinicaltrials.gov/ct2/show/NCT02492568
Willemijn S M E Theelen (247)	148	Metastatic non-small-cell lung cancer	8Gy×3, or 12.5Gy×4, or 3Gy×15	Pembrolizumab 200 mg/kg q3w	Pembrolizumab alone vs. pembrolizumab + SBRT	Best ARR 19.7% vs 41.7% (OR 2.96, p=0·0039) Best ACR 43.4% vs 65.3% (OR 2.51, p=0·0071) mPFS 4.4months vs 9.0 months (HR 0.67, p=0.0071) mOS 8.7months vs 19.2months (HR 0.67, p=0.0004)	https://clinicaltrials.gov/show/NCT02492568 https://clinicaltrials.gov/show/NCT02444741
Narek Shaverdian (248)	97	Stage IV advanced Non-Small Cell Lung Cancer	Previously received any RT	Pembrolizumab 2 mg/kg q3w or 10 mg/kg q3w or 10mg/kg q2w	Pembrolizumab with a history of RT vs pembrolizumab alone	mPFS 4.4 vs. 2.1; p = 0.019 mOS 10.7 vs. 5.3; p = 0.026	https://clinicaltrials.gov/ct2/show/NCT01295827
Yijun Hua (249)	25	recurrent nasopharyngeal carcinoma	2.2Gy×30	Toripalimab 240mg q3w	Toripalimab + RT	79.2% overall response, 95.8% disease control	https://clinicaltrials.gov/ct2/show/NCT03854838
Shankar Siva (250)	30	oligometastatic clear cell renal cell carcinoma	18-20Gy×1	Pembrolizumab 200mg q3w	Pembrolizumab+ RT	1- and 2-yr OS 90% and 74%, 1- and 2-yr PFS 60% and 45%	https://clinicaltrials.gov/ct2/show/NCT02855203
Alice Y Ho (251)	17	metastatic triple-negative breast cancer	600 cGy×5	Pembrolizumab 200mg q3w	Pembrolizumab+ RT	ORR 17.6%, CR 17.6%	https://clinicaltrials.gov/ct2/show/NCT02730130
Chad Tang (252)	31	Metastatic liver or lung Cancer	12.5Gy×4 or 6Gy×10	Ipilimumab 3 mg/kg q3w	Ipilimumab+ RT	10% PR, 13% SD	https://clinicaltrials.gov/ct2/show/NCT02239900
Hari Menon (253)	26	Metastatic Malignant Solid Neoplasm	7.3Gy (1.1-19.4Gy)	Pembrolizumab 200 mg/kg q3w, or Ipilimumab 3 mg/kg q3w	38 low-dose lesions vs 45 no-dose lesions	PR/CR 58% vs 18% (P = 0.0001) median change for longest diameter size -38.5% vs 8% (P < 0.0001)	https://clinicaltrials.gov/ct2/show/NCT02239900 https://clinicaltrials.gov/ct2/show/NCT02444741 https://clinicaltrials.gov/ct2/show/NCT02710253

ORR, overall response rate; mPFS, Median progression-free survival; mOS, median overall survival; ARR, out-of-field (abscopal) response rate; ACR, abscopal disease control rate; CR, complete responses; PR, partial response; SD, stable disease.

local RT stimulated DCs by inducing apoptosis and HMGB-1 release. RT combined with DNA vaccine increased the number of antigen-specific $CD8^+$ CTLs and enhanced antitumor efficacy and suggested that biweekly moderate radiation dose was a more optimal choice (174). Chemoradiotherapy-exposed TIMEs were highly enriched with newly infiltrated tumor-specific $CD8^+$ T cells and tissue-resident memory T cells, moreover, the authors found that chemoradiotherapy combined with dual CTLA-4 and PD-1 blockade achieved optimal anti-tumor effects (254). As recent studies have shown, LDRT combined with ICB improved the anti-tumor outcome of ICB by supporting M1 macrophages polarization, enhancing NK cells infiltration and reducing TGF-β levels. Moreover, Depletion of $CD4^+$ T cells and NK cells attenuated this anti-tumor effect, suggesting a key role of both cells in the anti-tumor immunity (180). Similarly, Preclinical and clinical studies supported LDRT induces predominantly infiltration of $CD4^+$ T cells with Th1 signatures in TIME (179).

It is currently believed that HDRT (>5 Gy per fraction) is of limited value in tumor immunomodulation due to the presence of inherent toxicity and immunosuppression, whereas more recent studies have elaborated that LDRT (<3Gy per fraction) stimulates innate and adaptive immune responses, as well as improves the sensitivity of primary and metastatic lesions to ICBs, which is expected to improve cancer treatment outcomes by combining ICB (7). Three recent preclinical studies (1 Gy in lung adenocarcinoma model, 2.5 Gy in melanoma tumors model, 0.5-2 Gy in ovarian cancer model) all elucidated that LDRT acts as a modifier of immune response, remodeling TIME, significantly increasing infiltration of effector immune cells including tumor-infiltrating myeloid cells, DCs, NK cells, $CD4^+$ and $CD8^+$ effector T cells, etc.,

and was superior to either treatment alone in combination with ICB (178–180). Currently, for "cold" tumors ICB is not effective (255, 256). The corresponding Phase I clinical studies(https://clinicaltrials.gov/ct2/show/NCT02710253, https://clinicaltrials.gov/ct2/show/NCT03728179) were conducted in patients with a variety of "immune desert" tumors, including but not limited to advanced melanoma, anaplastic thyroid carcinoma, and metastatic ovarian cancer, demonstrating the safety, feasibility, and significant therapeutic efficacy of RT in combination with ICB.

It is generally accepted that TGF-β signaling is a strong regulator of radiation response in normal and tumor tissues (257). A preclinical study showed that concurrent administration of TGF-β blockade and RT followed by a PD 1 inhibitor improved tumor control and prolonged survival in a mouse model of metastatic cancer (258). The combination of RT and TGF-β blockade thus offers a new direction for personalized cancer therapy. In recent years, multiple studies using radiosensitizer have revealed potent RT-induced antitumor immunity, while also providing new options for radio-immunotherapy. Experiments by Kaiyuan Ni et al. observed that intra-tumor injection of radiosensitizer repolarized M2 TAMs to M1 macrophages, reduced intra-tumor TGF-β and collagen density, as well as inactivated CAFs. When intravenous radiosensitizer was combined with ICB, the mouse model exhibited enhanced T cells infiltration and a robust abscopal effect (186). Radiosensitizer acting on the STING pathway significantly promoted the activation of DCs and enhanced systemic immune responses against primary and metastatic tumors (184). Recently developed biogenetic gold nanoparticles (Au@MC38), a radiosensitizer, intensified radiation-induced DNA damage and ROS production, exacerbated apoptosis and necrosis, enhanced ICD-mediated immune responses, and achieved a satisfactory survival benefit in combination with ICB (259). Recently, additional pathways have been identified that may be involved in the radio-immunotherapy process. For example, tumor-induced $CD45^{-}Ter119^{+}CD71^{+}$ erythroid progenitor cells (Ter cells) promote tumor progression by secreting artemin (ARTN), a neurotrophic peptide. Both topical RT and anti-PD-L1 treatment reduced Ter cell abundance and ARTN secretion in mice by an IFN- and $CD8^{+}$ T cell-dependent manner (260).

Regarding the fractionation and dose of RT, M Zahidunnabi Dewan et al. showed that fractionated but not single-dose RT induced local and systemic anti-tumor immune responses when in combination with anti-CTLA-4 antibody (135). Single radiation doses (>12 Gy) may attenuate immunogenicity through TREX1 induction, while hypo-fractionated regimens (i.e., 8 Gy × 3) may be more effective when used in combination with immunotherapy (188). Fractionated doses of 2.5 Gy×4 and 15 Gy×2 produced higher NK cytotoxicity than single doses (e.g. 30 Gy or 10 Gy) (185). Differently, a study by Byron C Burnette and colleagues suggested that local high single dose RT promotes type I IFN production, initiating a cascade of innate and adaptive immune attacks against tumors by enhancing the ability to prime trans-tumor infiltrating dendritic cells (TIDC) (189). Latest animal and clinical studies indicated that when tumor burden was high, it was necessary to combine high-dose RT, low-dose RT and ICB therapy to achieve optimal therapeutic effects, specifically, HDRT (12 Gy×3) to target primary tumors that had activated T cells, while LDRT (1 Gy×2) targeted metastatic lesions to modulate immunosuppressive stroma and sensitize ICB (180).Thus, fractions and doses can significantly alter the immune response to TIME radiation. Primarily, immune cells must be recruited into the tumor by RT and immune activation achieved, followed by additional immunotherapy in order to exert a stronger anti-tumor immune effect. However, more data are urgently needed to draw more consistent conclusions about RT activation of the immune response and the optimal dose and fractionation in combination therapies with immunotherapy. And there may not be a so-called optimal RT fraction and dose, but different fractions and doses may be the most effective way to utilize the immunogenic properties of radiation in multimodal tumor therapies (4). Regarding the timing of immunotherapy after RT, studies have shown that immune cells migrate into the TIME within two days after the last radiation and remain there for several days, suggesting that immunotherapy is best applied in the middle to end of the treatment cycle (96). Additional studies have also shown that the combination of anti-PD-1 Ab one week after the last irradiation did not improve the tumor effects of RT (165). Thus, hypo-fractionated RT may predominate and longer radiation pauses allow time for the immune system to activate and function (96).

Conclusion

RT remodels the suppressive TIME and mobilizes immune response, which creates the conditions for immunotherapy to work better and thus act locally and systematically against tumors. RT in combination with additional immunotherapy is a promising approach to induce specific anti-tumor immune responses. Accumulating clinical and preclinical data suggest that the immunogenic effects of radiotherapy may convert "cold" tumor into "hot" lesion with massive immune cell infiltration, thereby sensitizing unresponsive tumors to immunotherapy (213). There is a very delicate balance between activation of the immune system and RT-induced immunosuppression, depending on the specific radiation timing, fractionation, and dosing regimen. There is a need to initiate clinical trials and preclinical studies aimed at systematically evaluating the effects of different grading and treatment regimens to gain more insight into the optimal dose and schedule that may be able to induce synergy between immunotherapy and RT. As different immune cell types, with different states of differentiation, exhibit different radio-sensitivities, the selection of the most suitable radiotherapy regimen for combination with immunotherapy must carefully consider the radio-sensitivity of TIME and

circulating lymphocytes. In addition to this, which LDRT technology is preferable and which drug combinations benefit the most in radio-immunotherapy are critical issues to be explored more thoroughly in the future. Overall, although there is strong evidence from preclinical work that radiotherapy and immunotherapy are synergistic, clinical reports detailing the interaction of radiotherapy and immunotherapy are limited, and are currently under development.

Author contributions

SZ, YW, and JT wrote and edited the manuscript. MC designed the study and modified grammatical errors. All authors contributed to the article and approved the submission.

Conflict of interest

The authors declare that the research was conducted in the absence of any commercial or financial relationships that could be construed as a potential conflict of interest.

Publisher's note

References

1. Hanahan D, Weinberg RA. Hallmarks of cancer: The next generation. *Cell* (2011) 144(5):646–74. doi: 10.1016/j.cell.2011.02.013

2. Herrera FG, Bourhis J, Coukos G. Radiotherapy combination opportunities leveraging immunity for the next oncology practice. *CA Cancer J Clin* (2017) 67 (1):65–85. doi: 10.3322/caac.21358

3. Schaue D, McBride WH. Opportunities and challenges of radiotherapy for treating cancer. *Nat Rev Clin Oncol* (2015) 12(9):527–40. doi: 10.1038/nrclinonc.2015.120

4. Frey B, Ruckert M, Deloch L, Ruhle PF, Derer A, Fietkau R, et al. Immunomodulation by ionizing radiation-impact for design of radio-immunotherapies and for treatment of inflammatory diseases. *Immunol Rev* (2017) 280(1):231–48. doi: 10.1111/imr.12572

5. De Martino M, Daviaud C, Vanpouille-Box C. Radiotherapy: An immune response modifier for immuno-oncology. *Semin Immunol* (2021) 52:101474. doi: 10.1016/j.smim.2021.101474

6. Cytlak UM, Dyer DP, Honeychurch J, Williams KJ, Travis MA, Illidge TM. Immunomodulation by radiotherapy in tumour control and normal tissue toxicity. *Nat Rev Immunol* (2022) 22(2):124–38. doi: 10.1038/s41577-021-00568-1

7. Herrera FG, Romero P, Coukos G. Lighting up the tumor fire with low-dose irradiation. *Trends Immunol* (2022) 43(3):173–9. doi: 10.1016/j.it.2022.01.006

8. Wu T, Dai Y. Tumor microenvironment and therapeutic response. *Cancer Lett* (2017) 387:61–8. doi: 10.1016/j.canlet.2016.01.043

9. Bennett SR, Carbone FR, Karamalis F, Miller JF, Heath WR. Induction of a CD8+ cytotoxic T lymphocyte response by cross-priming requires cognate CD4+ T cell help. *J Exp Med* (1997) 186(1):65–70. doi: 10.1084/jem.186.1.65

10. Bourgeois C, Rocha B, Tanchot C. A role for CD40 expression on CD8+ T cells in the generation of CD8+ T cell memory. *Science* (2002) 297(5589):2060–3. doi: 10.1126/science.1072615

11. Kitano S, Tsuji T, Liu C, Hirschhorn-Cymerman D, Kyi C, Mu Z, et al. Enhancement of tumor-reactive cytotoxic CD4+ T cell responses after ipilimumab treatment in four advanced melanoma patients. *Cancer Immunol Res* (2013) 1 (4):235–44. doi: 10.1158/2326-6066.CIR-13-0068

12. Oh DY, Kwek SS, Raju SS, Li T, McCarthy E, Chow E, et al. Intratumoral CD4(+) T cells mediate anti-tumor cytotoxicity in human bladder cancer. *Cell* (2020) 181(7):1612–25 e13. doi: 10.1016/j.cell.2020.05.017

13. Fu C, Jiang A. Dendritic cells and CD8 T cell immunity in tumor microenvironment. *Front Immunol* (2018) 9:3059. doi: 10.3389/fimmu.2018.03059

14. Spranger S, Gajewski TF. Impact of oncogenic pathways on evasion of antitumour immune responses. *Nat Rev Cancer* (2018) 18(3):139–47. doi: 10.1038/nrc.2017.117

15. Farhood B, Najafi M, Mortezaee K. CD8(+) cytotoxic T lymphocytes in cancer immunotherapy: A review. *J Cell Physiol* (2019) 234(6):8509–21. doi: 10.1002/jcp.27782

16. Thomas DA, Massague J. TGF-beta directly targets cytotoxic T cell functions during tumor evasion of immune surveillance. *Cancer Cell* (2005) 8 (5):369–80. doi: 10.1016/j.ccr.2005.10.012

17. Solinas G, Germano G, Mantovani A, Allavena P. Tumor-associated macrophages (TAM) as major players of the cancer-related inflammation. *J Leukoc Biol* (2009) 86(5):1065–73. doi: 10.1189/jlb.0609385

18. Pereira BA, Vennin C, Papanicolaou M, Chambers CR, Herrmann D, Morton JP, et al. CAF subpopulations: A new reservoir of stromal targets in pancreatic cancer. *Trends Cancer* (2019) 5(11):724–41. doi: 10.1016/j.trecan.2019.09.010

19. Augsten M. Cancer-associated fibroblasts as another polarized cell type of the tumor microenvironment. *Front Oncol* (2014) 4:62. doi: 10.3389/fonc.2014.00062

20. Monteran L, Erez N. The dark side of fibroblasts: Cancer-associated fibroblasts as mediators of immunosuppression in the tumor microenvironment. *Front Immunol* (2019) 10:1835. doi: 10.3389/fimmu.2019.01835

21. Sousa CM, Biancur DE, Wang X, Halbrook CJ, Sherman MH, Zhang L, et al. Pancreatic stellate cells support tumour metabolism through autophagic alanine secretion. *Nature* (2016) 536(7617):479–83. doi: 10.1038/nature19084

22. Ron-Harel N, Ghergurovich JM, Notarangelo G, LaFleur MW, Tsubosaka Y, Sharpe AH, et al. T Cell activation depends on extracellular alanine. *Cell Rep* (2019) 28(12):3011–21.e4. doi: 10.1016/j.celrep.2019.08.034

23. Chen DS, Mellman I. Oncology meets immunology: the cancer-immunity cycle. *Immunity* (2013) 39(1):1–10. doi: 10.1016/j.immuni.2013.07.012

24. Locy H, de Mey S, de Mey W, De Ridder M, Thielemans K, Maenhout SK. Immunomodulation of the tumor microenvironment: Turn foe into friend. *Front Immunol* (2018) 9:2909. doi: 10.3389/fimmu.2018.02909

25. Shevtsov M, Sato H, Multhoff G, Shibata A. Novel approaches to improve the efficacy of immuno-radiotherapy. *Front Oncol* (2019) 9:156. doi: 10.3389/fonc.2019.00156

26. Joyce JA, Pollard JW. Microenvironmental regulation of metastasis. *Nat Rev Cancer* (2009) 9(4):239–52. doi: 10.1038/nrc2618

27. Palazon A, Martinez-Forero I, Teijeira A, Morales-Kastresana A, Alfaro C, Sanmamed MF, et al. The HIF-1alpha hypoxia response in tumor-infiltrating T lymphocytes induces functional CD137 (4-1BB) for immunotherapy. *Cancer Discov* (2012) 2(7):608–23. doi: 10.1158/2159-8290.CD-11-0314

28. Clambey ET, McNamee EN, Westrich JA, Glover LE, Campbell EL, Jedlicka P, et al. Hypoxia-inducible factor-1 alpha-dependent induction of FoxP3 drives regulatory T-cell abundance and function during inflammatory hypoxia of the mucosa. *Proc Natl Acad Sci USA* (2012) 109(41):E2784–93. doi: 10.1073/pnas.1202366109

29. Garcia-Lora A, Algarra I, Garrido F. MHC class I antigens, immune surveillance, and tumor immune escape. *J Cell Physiol* (2003) 195(3):346–55. doi: 10.1002/jcp.10290

30. Ma SR, Deng WW, Liu JF, Mao L, Yu GT, Bu LL, et al. Blockade of adenosine A2A receptor enhances CD8(+) T cells response and decreases regulatory T cells in head and neck squamous cell carcinoma. *Mol Cancer* (2017) 16(1):99. doi: 10.1186/s12943-017-0665-0

31. Zhang J, Shi Z, Xu X, Yu Z, Mi J. The influence of microenvironment on tumor immunotherapy. *FEBS J* (2019) 286(21):4160–75. doi: 10.1111/febs.15028

32. Kumar V, Donthireddy L, Marvel D, Condamine T, Wang F, Lavilla-Alonso S, et al. Cancer-associated fibroblasts neutralize the anti-tumor effect of CSF1 receptor blockade by inducing PMN-MDSC infiltration of tumors. *Cancer Cell* (2017) 32(5):654–68.e5. doi: 10.1016/j.ccell.2017.10.005

33. Kalia V, Penny LA, Yuzefpolskiy Y, Baumann FM, Sarkar S. Quiescence of memory CD8(+) T cells is mediated by regulatory T cells through inhibitory receptor CTLA-4. *Immunity* (2015) 42(6):1116–29. doi: 10.1016/j.immuni.2015.05.023

34. Carmona-Fontaine C, Deforet M, Akkari L, Thompson CB, Joyce JA, Xavier JB. Metabolic origins of spatial organization in the tumor microenvironment. *Proc Natl Acad Sci USA* (2017) 114(11):2934–9. doi: 10.1073/pnas.1700600114

35. Najafi M, Hashemi Goradel N, Farhood B, Salehi E, Nashtaei MS, Khanlarkhani N, et al. Macrophage polarity in cancer: A review. *J Cell Biochem* (2019) 120(3):2756–65. doi: 10.1002/jcb.27646

36. Bloch O, Crane CA, Kaur R, Safaee M, Rutkowski MJ, Parsa AT. Gliomas promote immunosuppression through induction of B7-H1 expression in tumor-associated macrophages. *Clin Cancer Res* (2013) 19(12):3165–75. doi: 10.1158/1078-0432.CCR-12-3314

37. Sadegh L, Chen PW, Brown JR, Han Z, Niederkorn JY. NKT cells act through third party bone marrow-derived cells to suppress NK cell activity in the liver and exacerbate hepatic melanoma metastases. *Int J Cancer* (2015) 137 (5):1085–94. doi: 10.1002/ijc.29480

38. Joyce JA, Fearon DT. T Cell exclusion, immune privilege, and the tumor microenvironment. *Science* (2015) 348(6230):74–80. doi: 10.1126/science.aaa6204

39. Cazet AS, Hui MN, Elsworth BL, Wu SZ, Roden D, Chan CL, et al. Targeting stromal remodeling and cancer stem cell plasticity overcomes chemoresistance in triple negative breast cancer. *Nat Commun* (2018) 9(1):2897. doi: 10.1038/s41467-018-05220-6

40. Liu H, Shen J, Lu K. IL-6 and PD-L1 blockade combination inhibits hepatocellular carcinoma cancer development in mouse model. *Biochem Biophys Res Commun* (2017) 486(2):239–44. doi: 10.1016/j.bbrc.2017.02.128

41. Berzaghi R, Ahktar MA, Islam A, Pedersen BD, Hellevik T, Martinez-Zubiaurre I. Fibroblast-mediated immunoregulation of macrophage function is maintained after irradiation. *Cancers (Basel)* (2019) 11(5):689. doi: 10.3390/cancers11050689

42. Lakins MA, Ghorani E, Munir H, Martins CP, Shields JD. Cancer-associated fibroblasts induce antigen-specific deletion of CD8 (+) T cells to protect tumour cells. *Nat Commun* (2018) 9(1):948. doi: 10.1038/s41467-018-03347-0

43. Wei X, Zhang J, Gu Q, Huang M, Zhang W, Guo J, et al. Reciprocal expression of IL-35 and IL-10 defines two distinct effector treg subsets that are required for maintenance of immune tolerance. *Cell Rep* (2017) 21(7):1853–69. doi: 10.1016/j.celrep.2017.10.090

44. Goswami KK, Bose A, Baral R. Macrophages in tumor: An inflammatory perspective. *Clin Immunol* (2021) 232:108875. doi: 10.1016/j.clim.2021.108875

45. Krishnamoorthy M, Gerhardt L, Maleki Vareki S. Immunosuppressive effects of myeloid-derived suppressor cells in cancer and immunotherapy. *Cells* (2021) 10(5):1170. doi: 10.3390/cells10051170

46. Novitskiy SV, Pickup MW, Gorska AE, Owens P, Chytil A, Aakre M, et al. TGF-beta receptor II loss promotes mammary carcinoma progression by Th17 dependent mechanisms. *Cancer Discov* (2011) 1(5):430–41. doi: 10.1158/2159-8290.CD-11-0100

47. Cham CM, Driessens G, O'Keefe JP, Gajewski TF. Glucose deprivation inhibits multiple key gene expression events and effector functions in CD8+ T cells. *Eur J Immunol* (2008) 38(9):2438–50. doi: 10.1002/eji.200838289

48. Fletcher M, Ramirez ME, Sierra RA, Raber P, Thevenot P, Al-Khami AA, et al. L-arginine depletion blunts antitumor T-cell responses by inducing myeloid-derived suppressor cells. *Cancer Res* (2015) 75(2):275–83. doi: 10.1158/0008-5472.CAN-14-1491

49. Rodriguez PC, Quiceno DG, Ochoa AC. L-arginine availability regulates T-lymphocyte cell-cycle progression. *Blood* (2007) 109(4):1568–73. doi: 10.1182/blood-2006-06-031856

50. Fischer K, Hoffmann P, Voelkl S, Meidenbauer N, Ammer J, Edinger M, et al. Inhibitory effect of tumor cell-derived lactic acid on human T cells. *Blood* (2007) 109(9):3812–9. doi: 10.1182/blood-2006-07-035972

51. Ohashi T, Akazawa T, Aoki M, Kuze B, Mizuta K, Ito Y, et al. Dichloroacetate improves immune dysfunction caused by tumor-secreted lactic acid and increases antitumor immunoreactivity. *Int J Cancer* (2013) 133(5):1107–18. doi: 10.1002/ijc.28114

52. Mantovani A, Allavena P, Sica A, Balkwill F. Cancer-related inflammation. *Nature* (2008) 454(7203):436–44. doi: 10.1038/nature07205

53. Medzhitov R. Origin and physiological roles of inflammation. *Nature* (2008) 454(7203):428–35. doi: 10.1038/nature07201

54. Budhu S, Schaer DA, Li Y, Toledo-Crow R, Panageas K, Yang X, et al. Blockade of surface-bound TGF-beta on regulatory T cells abrogates suppression of effector T cell function in the tumor microenvironment. *Sci Signal* (2017) 10(494): eaak9702. doi: 10.1126/scisignal.aak9702

55. Cao X, Cai SF, Fehniger TA, Song J, Collins LI, Piwnica-Worms DR, et al. Granzyme b and perforin are important for regulatory T cell-mediated suppression of tumor clearance. *Immunity* (2007) 27(4):635–46. doi: 10.1016/j.immuni.2007.08.014

56. Liu C, Chikina M, Deshpande R, Menk AV, Wang T, Tabib T, et al. Treg cells promote the SREBP1-dependent metabolic fitness of tumor-promoting macrophages *via* repression of CD8(+) T cell-derived interferon-gamma. *Immunity* (2019) 51(2):381–97.e6. doi: 10.1016/j.immuni.2019.06.017

57. Walker LS, Sansom DM. The emerging role of CTLA4 as a cell-extrinsic regulator of T cell responses. *Nat Rev Immunol* (2011) 11(12):852–63. doi: 10.1038/nri3108

58. Sarhan D, Hippen KL, Lemire A, Hying S, Luo X, Lenvik T, et al. Adaptive NK cells resist regulatory T-cell suppression driven by IL37. *Cancer Immunol Res* (2018) 6(7):766–75. doi: 10.1158/2326-6066.CIR-17-0498

59. Li C, Jiang P, Wei S, Xu X, Wang J. Regulatory T cells in tumor microenvironment: new mechanisms, potential therapeutic strategies and future prospects. *Mol Cancer* (2020) 19(1):116. doi: 10.1158/1557-3125.HIPPO19-B11

60. Cassetta L, Pollard JW. Targeting macrophages: therapeutic approaches in cancer. *Nat Rev Drug Discov* (2018) 17(12):887–904. doi: 10.1038/nrd.2018.169

61. Shankaran V, Ikeda H, Bruce AT, White JM, Swanson PE, Old LJ, et al. IFNgamma and lymphocytes prevent primary tumour development and shape tumour immunogenicity. *Nature* (2001) 410(6832):1107–11. doi: 10.1038/35074122

62. Steidl C, Lee T, Shah SP, Farinha P, Han G, Nayar T, et al. Tumor-associated macrophages and survival in classic hodgkin's lymphoma. *N Engl J Med* (2010) 362 (10):875–85. doi: 10.1056/NEJMoa0905680

63. Hanada T, Nakagawa M, Emoto A, Nomura T, Nasu N, Nomura Y. Prognostic value of tumor-associated macrophage count in human bladder cancer. *Int J Urol* (2000) 7(7):263–9. doi: 10.1046/j.1442-2042.2000.00190.x

64. Monjazeb AM, Schalper KA, Villarroel-Espindola F, Nguyen A, Shiao SL, Young K. Effects of radiation on the tumor microenvironment. *Semin Radiat Oncol* (2020) 30(2):145–57. doi: 10.1016/j.semradonc.2019.12.004

65. Kang FB, Wang L, Li D, Zhang YG, Sun DX. Hepatocellular carcinomas promote tumor-associated macrophage M2-polarization *via* increased B7-H3 expression. *Oncol Rep* (2015) 33(1):274–82. doi: 10.3892/or.2014.3587

66. Gabrilovich DI. Myeloid-derived suppressor cells. *Cancer Immunol Res* (2017) 5(1):3–8. doi: 10.1158/2326-6066.CIR-16-0297

67. Gabrilovich DI, Nagaraj S. Myeloid-derived suppressor cells as regulators of the immune system. *Nat Rev Immunol* (2009) 9(3):162–74. doi: 10.1038/nri2506

68. Veglia F, Perego M, Gabrilovich D. Myeloid-derived suppressor cells coming of age. *Nat Immunol* (2018) 19(2):108–19. doi: 10.1038/s41590-017-0022-x

69. Kwak T, Wang F, Deng H, Condamine T, Kumar V, Perego M, et al. Distinct populations of immune-suppressive macrophages differentiate from monocytic myeloid-derived suppressor cells in cancer. *Cell Rep* (2020) 33(13):108571. doi: 10.1016/j.celrep.2020.108571

70. Martinez-Zubiaurre I, Chalmers AJ, Hellevik T. Radiation-induced transformation of immunoregulatory networks in the tumor stroma. *Front Immunol* (2018) 9:1679. doi: 10.3389/fimmu.2018.01679

71. Kraman M, Bambrough PJ, Arnold JN, Roberts EW, Magiera L, Jones JO, et al. Suppression of antitumor immunity by stromal cells expressing fibroblast activation protein-alpha. *Science* (2010) 330(6005):827–30. doi: 10.1126/science.1195300

72. Ragunathan K, Upfold NLE, Oksenych V. Interaction between fibroblasts and immune cells following DNA damage induced by ionizing radiation. *Int J Mol Sci* (2020) 21(22):8635. doi: 10.3390/ijms21228635

73. Gorchs L, Hellevik T, Bruun JA, Camilio KA, Al-Saad S, Stuge TB, et al. Cancer-associated fibroblasts from lung tumors maintain their immunosuppressive abilities after high-dose irradiation. *Front Oncol* (2015) 5:87. doi: 10.3389/fonc.2015.00087

74. Pearce OMT, Delaine-Smith RM, Maniati E, Nichols S, Wang J, Bohm S, et al. Deconstruction of a metastatic tumor microenvironment reveals a common matrix response in human cancers. *Cancer Discov* (2018) 8(3):304–19. doi: 10.1158/2159-8290.CD-17-0284

75. Kobayashi N, Miyoshi S, Mikami T, Koyama H, Kitazawa M, Takeoka M, et al. Hyaluronan deficiency in tumor stroma impairs macrophage trafficking and

tumor neovascularization. *Cancer Res* (2010) 70(18):7073–83. doi: 10.1158/0008-5472.CAN-09-4687

76. Duperret EK, Trautz A, Ammons D, Perales-Puchalt A, Wise MC, Yan J, et al. Alteration of the tumor stroma using a consensus DNA vaccine targeting fibroblast activation protein (FAP) synergizes with antitumor vaccine therapy in mice. *Clin Cancer Res* (2018) 24(5):1190–201. doi: 10.1158/1078-0432.CCR-17-2033

77. Xia Q, Zhang FF, Geng F, Liu CL, Xu P, Lu ZZ, et al. Anti-tumor effects of DNA vaccine targeting human fibroblast activation protein alpha by producing specific immune responses and altering tumor microenvironment in the 4T1 murine breast cancer model. *Cancer Immunol Immunother* (2016) 65(5):613–24. doi: 10.1007/s00262-016-1827-4

78. David CJ, Huang YH, Chen M, Su J, Zou Y, Bardeesy N, et al. TGF-beta tumor suppression through a lethal EMT. *Cell* (2016) 164(5):1015–30. doi: 10.1016/j.cell.2016.01.009

79. Sounni NE, Dehne K, van Kempen L, Egeblad M, Affara NI, Cuevas I, et al. Stromal regulation of vessel stability by MMP14 and TGFbeta. *Dis Model Mech* (2010) 3(5-6):317–32. doi: 10.1242/dmm.003863

80. Friedl P, Alexander S. Cancer invasion and the microenvironment: plasticity and reciprocity. *Cell* (2011) 147(5):992–1009. doi: 10.1016/j.cell.2011.11.016

81. Calon A, Espinet E, Palomo-Ponce S, Tauriello DV, Iglesias M, Cespedes MV, et al. Dependency of colorectal cancer on a TGF-beta-driven program in stromal cells for metastasis initiation. *Cancer Cell* (2012) 22(5):571–84. doi: 10.1016/j.ccr.2012.08.013

82. Barcellos-Hoff MH, Derynck R, Tsang ML, Weatherbee JA. Transforming growth factor-beta activation in irradiated murine mammary gland. *J Clin Invest* (1994) 93(2):892–9. doi: 10.1172/JCI117045

83. Altman BJ, Stine ZE, Dang CV. From Krebs to clinic: Glutamine metabolism to cancer therapy. *Nat Rev Cancer* (2016) 16(11):749. doi: 10.1038/nrc.2016.71

84. Cheong JE, Sun L. Targeting the IDO1/TDO2-KYN-AhR pathway for cancer immunotherapy - challenges and opportunities. *Trends Pharmacol Sci* (2018) 39(3):307–25. doi: 10.1016/j.tips.2017.11.007

85. Moffett JR, Namboodiri MA. Tryptophan and the immune response. *Immunol Cell Biol* (2003) 81(4):247–65. doi: 10.1046/j.1440-1711.2003.t01-1-01177.x

86. Prendergast GC, Metz R, Muller AJ. IDO recruits tregs in melanoma. *Cell Cycle* (2009) 8(12):1818–9. doi: 10.4161/cc.8.12.8887

87. Romani L, Bistoni F, Perruccio K, Montagnoli C, Gaziano R, Bozza S, et al. Thymosin alpha1 activates dendritic cell tryptophan catabolism and establishes a regulatory environment for balance of inflammation and tolerance. *Blood* (2006) 108(7):2265–74. doi: 10.1182/blood-2006-02-004762

88. Mendler AN, Hu B, Prinz PU, Kreutz M, Gottfried E, Noessner E. Tumor lactic acidosis suppresses CTL function by inhibition of p38 and JNK/c-jun activation. *Int J Cancer* (2012) 131(3):633–40. doi: 10.1002/ijc.26410

89. Duvel K, Yecies JL, Menon S, Raman P, Lipovsky AI, Souza AL, et al. Activation of a metabolic gene regulatory network downstream of mTOR complex 1. *Mol Cell* (2010) 39(2):171–83. doi: 10.1016/j.molcel.2010.06.022

90. Eil R, Vodnala SK, Clever D, Klebanoff CA, Sukumar M, Pan JH, et al. Ionic immune suppression within the tumour microenvironment limits T cell effector function. *Nature* (2016) 537(7621):539–43. doi: 10.1038/nature19364

91. Wennerberg E, Vanpouille-Box C, Bornstein S, Yamazaki T, Demaria S, Galluzzi L. Immune recognition of irradiated cancer cells. *Immunol Rev* (2017) 280 (1):220–30. doi: 10.1111/imr.12568

92. Jarosz-Biej M, Smolarczyk R, Cichon T, Kulach N. Tumor microenvironment as a "Game changer" in cancer radiotherapy. *Int J Mol Sci* (2019) 20(13):3212. doi: 10.3390/ijms20133212

93. Junttila MR, de Sauvage FJ. Influence of tumour micro-environment heterogeneity on therapeutic response. *Nature* (2013) 501(7467):346–54. doi: 10.1038/nature12626

94. Portella L, Scala S. Ionizing radiation effects on the tumor microenvironment. *Semin Oncol* (2019) 46(3):254–60. doi: 10.1053/j.seminoncol.2019.07.003

95. Pan X, Zhang C, Wang J, Wang P, Gao Y, Shang S, et al. Epigenome signature as an immunophenotype indicator prompts durable clinical immunotherapy benefits in lung adenocarcinoma. *Brief Bioinform* (2022) 23(1): bbab481. doi: 10.1093/bib/bbab481

96. Derer A, Frey B, Fietkau R, Gaipl US. Immune-modulating properties of ionizing radiation: Rationale for the treatment of cancer by combination radiotherapy and immune checkpoint inhibitors. *Cancer Immunol Immunother* (2016) 65(7):779–86. doi: 10.1007/s00262-015-1771-8

97. Mukherjee S, Chakraborty A. Radiation-induced bystander phenomenon: insight and implications in radiotherapy. *Int J Radiat Biol* (2019) 95(3):243–63. doi: 10.1080/09553002.2019.1547440

98. Demaria S, Ng B, Devitt ML, Babb JS, Kawashima N, Liebes L, et al. Ionizing radiation inhibition of distant untreated tumors (abscopal effect) is immune mediated. *Int J Radiat Oncol Biol Phys* (2004) 58(3):862–70. doi: 10.1016/j.ijrobp.2003.09.012

99. Weichselbaum RR, Liang H, Deng L, Fu YX. Radiotherapy and immunotherapy: a beneficial liaison? *Nat Rev Clin Oncol* (2017) 14(6):365–79. doi: 10.1038/nrclinonc.2016.211

100. Romano E, Honeychurch J, Illidge TM. Radiotherapy-immunotherapy combination: How will we bridge the gap between pre-clinical promise and effective clinical delivery? *Cancers (Basel)* (2021) 13(3):457. doi: 10.3390/cancers13030457

101. Baumann M, Krause M, Overgaard J, Debus J, Bentzen SM, Daartz J, et al. Radiation oncology in the era of precision medicine. *Nat Rev Cancer* (2016) 16 (4):234–49. doi: 10.1038/nrc.2016.18

102. Rodriguez-Ruiz ME, Vitale I, Harrington KJ, Melero I, Galluzzi L. Immunological impact of cell death signaling driven by radiation on the tumor microenvironment. *Nat Immunol* (2020) 21(2):120–34. doi: 10.1038/s41590-019-0561-4

103. Galluzzi L, Vitale I, Aaronson SA, Abrams JM, Adam D, Agostinis P, et al. Molecular mechanisms of cell death: Recommendations of the nomenclature committee on cell death 2018. *Cell Death Differ* (2018) 25(3):486–541. doi: 10.1038/s41418-017-0012-4

104. Wilkins AC, Patin EC, Harrington KJ, Melcher AA. The immunological consequences of radiation-induced DNA damage. *J Pathol* (2019) 247(5):606–14. doi: 10.1002/path.5232

105. Lopez-Soto A, Gonzalez S, Smyth MJ, Galluzzi L. Control of metastasis by NK cells. *Cancer Cell* (2017) 32(2):135–54. doi: 10.1016/j.ccell.2017.06.009

106. Janus P, Szoltysek K, Zajac G, Stokowy T, Walaszczyk A, Widlak W, et al. Pro-inflammatory cytokine and high doses of ionizing radiation have similar effects on the expression of NF-kappaB-dependent genes. *Cell Signal* (2018) 46:23–31. doi: 10.1016/j.cellsig.2018.02.011

107. Mackenzie KJ, Carroll P, Martin CA, Murina O, Fluteau A, Simpson DJ, et al. cGAS surveillance of micronuclei links genome instability to innate immunity. *Nature* (2017) 548(7668):461–5. doi: 10.1038/nature23449

108. Harding SM, Benci JL, Irianto J, Discher DE, Minn AJ, Greenberg RA. Mitotic progression following DNA damage enables pattern recognition within micronuclei. *Nature* (2017) 548(7668):466–70. doi: 10.1038/nature23470

109. Snyder AG, Hubbard NW, Messmer MN, Kofman SB, Hagan CE, Orozco SL, et al. Intratumoral activation of the necroptotic pathway components RIPK1 and RIPK3 potentiates antitumor immunity. *Sci Immunol* (2019) 4(36):eaaw2004. doi: 10.1126/sciimmunol.aaw2004

110. Wang HH, Wu ZQ, Qian D, Zaorsky NG, Qiu MH, Cheng JJ, et al. Ablative hypofractionated radiation therapy enhances non-small cell lung cancer cell killing *via* preferential stimulation of necroptosis *In vitro* and in vivo. *Int J Radiat Oncol Biol Phys* (2018) 101(1):49–62. doi: 10.1016/j.ijrobp.2018.01.036

111. Adjemian S, Oltean T, Martens S, Wiernicki B, Goossens V, Vanden Berghe T, et al. Ionizing radiation results in a mixture of cellular outcomes including mitotic catastrophe, senescence, methuosis, and iron-dependent cell death. *Cell Death Dis* (2020) 11(11):1003. doi: 10.1038/s41419-020-03209-y

112. Yard BD, Adams DJ, Chie EK, Tamayo P, Battaglia JS, Gopal P, et al. A genetic basis for the variation in the vulnerability of cancer to DNA damage. *Nat Commun* (2016) 7:11428. doi: 10.1038/ncomms11428

113. Good JS, Harrington KJ. The hallmarks of cancer and the radiation oncologist: updating the 5Rs of radiobiology. *Clin Oncol (R Coll Radiol)* (2013) 25(10):569–77. doi: 10.1016/j.clon.2013.06.009

114. Hill RP. The changing paradigm of tumour response to irradiation. *Br J Radiol* (2017) 90(1069):20160474. doi: 10.1259/bjr.20160474

115. Faget DV, Ren Q, Stewart SA. Unmasking senescence: context-dependent effects of SASP in cancer. *Nat Rev Cancer* (2019) 19(8):439–53. doi: 10.1038/s41568-019-0156-2

116. McBride S, Sherman E, Tsai CJ, Baxi S, Aghalar J, Eng J, et al. Randomized phase II trial of nivolumab with stereotactic body radiotherapy versus nivolumab alone in metastatic head and neck squamous cell carcinoma. *J Clin Oncol* (2021) 39 (1):30–7. doi: 10.1200/JCO.20.00290

117. Rodel F, Frey B, Capalbo G, Gaipl U, Keilholz L, Voll R, et al. Discontinuous induction of X-linked inhibitor of apoptosis in EA.hy.926 endothelial cells is linked to NF-kappaB activation and mediates the anti-inflammatory properties of low-dose ionising-radiation. *Radiother Oncol* (2010) 97(2):346–51. doi: 10.1016/j.radonc.2010.01.013

118. Fridlender ZG, Sun J, Kim S, Kapoor V, Cheng G, Ling L, et al. Polarization of tumor-associated neutrophil phenotype by TGF-beta: "N1" versus "N2" TAN. *Cancer Cell* (2009) 16(3):183–94. doi: 10.1016/j.ccr.2009.06.017

119. Zhang F, Wang H, Wang X, Jiang G, Liu H, Zhang G, et al. TGF-beta induces M2-like macrophage polarization *via* SNAIL-mediated suppression of a

pro-inflammatory phenotype. *Oncotarget* (2016) 7(32):52294–306. doi: 10.18632/oncotarget.10561

120. Deng L, Liang H, Burnette B, Weicheslbaum RR, Fu YX. Radiation and anti-PD-L1 antibody combinatorial therapy induces T cell-mediated depletion of myeloid-derived suppressor cells and tumor regression. *Oncoimmunology* (2014) 3: e28499. doi: 10.4161/onci.28499

121. Cortez MA, Ivan C, Valdecanas D, Wang X, Peltier HJ, Ye Y, et al. PDL1 regulation by p53 *via* miR-34. *J Natl Cancer Inst* (2016) 108(1):djv303. doi: 10.1093/jnci/djv303

122. Liu S, Sun X, Luo J, Zhu H, Yang X, Guo Q, et al. Effects of radiation on T regulatory cells in normal states and cancer: Mechanisms and clinical implications. *Am J Cancer Res* (2015) 5(11):3276–85.

123. Nishii K, Gibbons DL, Titley I, Papworth D, Goodhead DT, Greaves M. Regulation of the apoptotic response to radiation damage in b cell development. *Cell Death Differ* (1998) 5(1):77–86. doi: 10.1038/sj.cdd.4400317

124. Kim SS, Shen S, Miyauchi S, Sanders PD, Franiak-Pietryga I, Mell L, et al. B cells improve overall survival in HPV-associated squamous cell carcinomas and are activated by radiation and PD-1 blockade. *Clin Cancer Res* (2020) 26(13):3345–59. doi: 10.1158/1078-0432.CCR-19-3211

125. Kunala S, Macklis RM. Ionizing radiation induces CD20 surface expression on human b cells. *Int J Cancer* (2001) 96(3):178–81. doi: 10.1002/ijc.1018

126. Bauer M, Goldstein M, Christmann M, Becker H, Heylmann D, Kaina B. Human monocytes are severely impaired in base and DNA double-strand break repair that renders them vulnerable to oxidative stress. *Proc Natl Acad Sci USA* (2011) 108(52):21105–10. doi: 10.1073/pnas.1111919109

127. Klug F, Prakash H, Huber PE, Seibel T, Bender N, Halama N, et al. Low-dose irradiation programs macrophage differentiation to an iNOS(+)/M1 phenotype that orchestrates effective T cell immunotherapy. *Cancer Cell* (2013) 24(5):589–602. doi: 10.1016/j.ccr.2013.09.014

128. Tsai CS, Chen FH, Wang CC, Huang HL, Jung SM, Wu CJ, et al. Macrophages from irradiated tumors express higher levels of iNOS, arginase-I and COX-2, and promote tumor growth. *Int J Radiat Oncol Biol Phys* (2007) 68 (2):499–507. doi: 10.1016/j.ijrobp.2007.01.041

129. Vitale I, Manic G, Coussens LM, Kroemer G, Galluzzi L. Macrophages and metabolism in the tumor microenvironment. *Cell Metab* (2019) 30(1):36–50. doi: 10.1016/j.cmet.2019.06.001

130. Meziani L, Deutsch E, Mondini M. Macrophages in radiation injury: a new therapeutic target. *Oncoimmunology* (2018) 7(10):e1494488. doi: 10.1080/2162402X.2018.1494488

131. Hellevik T, Martinez-Zubiaurre I. Radiotherapy and the tumor stroma: the importance of dose and fractionation. *Front Oncol* (2014) 4:1. doi: 10.3389/fonc.2014.00001

132. Cao MD, Chen ZD, Xing Y. Gamma irradiation of human dendritic cells influences proliferation and cytokine profile of T cells in autologous mixed lymphocyte reaction. *Cell Biol Int* (2004) 28(3):223–8. doi: 10.1016/j.cellbi.2003.12.006

133. Persa E, Szatmari T, Safrany G, Lumniczky K. *In vivo* irradiation of mice induces activation of dendritic cells. *Int J Mol Sci* (2018) 19(8):2391. doi: 10.3390/ijms19082391

134. Chun SH, Park GY, Han YK, Kim SD, Kim JS, Lee CG, et al. Effect of low dose radiation on differentiation of bone marrow cells into dendritic cells. *Dose Response* (2012) 11(3):374–84. doi: 10.2203/dose-response.12-041.Lee

135. Dewan MZ, Galloway AE, Kawashima N, Dewyngaert JK, Babb JS, Formenti SC, et al. Fractionated but not single-dose radiotherapy induces an immune-mediated abscopal effect when combined with anti-CTLA-4 antibody. *Clin Cancer Res* (2009) 15(17):5379–88. doi: 10.1158/1078-0432.CCR-09-0265

136. Desai P, Tahiliani V, Abboud G, Stanfield J, Salek-Ardakani S. Batf3-dependent dendritic cells promote optimal CD8 T cell responses against respiratory poxvirus infection. *J Virol* (2018) 92(16):e00495-18. doi: 10.1128/JVI.00495-18

137. Hildner K, Edelson BT, Purtha WE, Diamond M, Matsushita H, Kohyama M, et al. Batf3 deficiency reveals a critical role for CD8alpha+ dendritic cells in cytotoxic T cell immunity. *Science* (2008) 322(5904):1097–100. doi: 10.1126/science.1164206

138. Hochman PS, Cudkowicz G, Dausset J. Decline of natural killer cell activity in sublethally irradiated mice. *J Natl Cancer Inst* (1978) 61(1):265–8. doi: 10.1093/jnci/61.1.265

139. Chen J, Liu X, Zeng Z, Li J, Luo Y, Sun W, et al. Immunomodulation of NK cells by ionizing radiation. *Front Oncol* (2020) 10:874. doi: 10.3389/fonc.2020.00874

140. Alvarez M, Simonetta F, Baker J, Pierini A, Wenokur AS, Morrison AR, et al. Regulation of murine NK cell exhaustion through the activation of the DNA damage repair pathway. *JCI Insight* (2019) 5(14):e127729. doi: 10.1172/jci.insight.127729

141. Begovic M, Herberman R, Gorelik E. Increase in immunogenicity and sensitivity to natural cell-mediated cytotoxicity following *in vitro* exposure of MCA105 tumor cells to ultraviolet radiation. *Cancer Res* (1991) 51(19):5153–9.

142. Uchida A, Mizutani Y, Nagamuta M, Ikenaga M. Effects of X-ray irradiation on natural killer (NK) cell system. i. elevation of sensitivity of tumor cells and lytic function of NK cells. *Immunopharmacol Immunotoxicol* (1989) 11(2-3):507–19. doi: 10.3109/08923978909005381

143. Yang KL, Wang YS, Chang CC, Huang SC, Huang YC, Chi MS, et al. Reciprocal complementation of the tumoricidal effects of radiation and natural killer cells. *PloS One* (2013) 8(4):e61797. doi: 10.1371/journal.pone.0061797

144. Yoon MS, Pham CT, Phan MT, Shin DJ, Jang YY, Park MH, et al. Irradiation of breast cancer cells enhances CXCL16 ligand expression and induces the migration of natural killer cells expressing the CXCR6 receptor. *Cytotherapy* (2016) 18(12):1532–42. doi: 10.1016/j.jcyt.2016.08.006

145. Pinel MI, Esteves EB, Rumjanek VM. Increased natural killer cell activity in uterine cervix cancer patients undergoing radiation therapy. *Nat Immun* (1995) 14 (4):216–24.

146. McGee HM, Daly ME, Azghadi S, Stewart SL, Oesterich L, Schlom J, et al. Stereotactic ablative radiation therapy induces systemic differences in peripheral blood immunophenotype dependent on irradiated site. *Int J Radiat Oncol Biol Phys* (2018) 101(5):1259–70. doi: 10.1016/j.ijrobp.2018.04.038

147. Yamazaki H, Yoshioka Y, Inoue T, Tanaka E, Nishikubo M, Sato T, et al. Changes in natural killer cell activity by external radiotherapy and/or brachytherapy. *Oncol Rep* (2002) 9(2):359–63. doi: 10.3892/or.9.2.359

148. Mozaffari F, Lindemalm C, Choudhury A, Granstam-Bjorneklett H, Helander I, Lekander M, et al. NK-cell and T-cell functions in patients with breast cancer: Effects of surgery and adjuvant chemo- and radiotherapy. *Br J Cancer* (2007) 97(1):105–11. doi: 10.1038/sj.bjc.6603840

149. McGinnes K, Florence J, Penny R. The effect of radiotherapy on the natural killer (NK)-cell activity of cancer patients. *J Clin Immunol* (1987) 7(3):210–7. doi: 10.1007/BF00915726

150. Mariathasan S, Turley SJ, Nickles D, Castiglioni A, Yuen K, Wang Y, et al. TGFbeta attenuates tumour response to PD-L1 blockade by contributing to exclusion of T cells. *Nature* (2018) 554(7693):544–8. doi: 10.1038/nature25501

151. Tauriello DVF, Palomo-Ponce S, Stork D, Berenguer-Llergo A, Badia-Ramentol J, Iglesias M, et al. TGFbeta drives immune evasion in genetically reconstituted colon cancer metastasis. *Nature* (2018) 554(7693):538–43. doi: 10.1038/nature25492

152. Wennerberg E, Lhuillier C, Vanpouille-Box C, Pilones KA, Garcia-Martinez E, Rudqvist NP, et al. Barriers to radiation-induced *In situ* tumor vaccination. *Front Immunol* (2017) 8:229. doi: 10.3389/fimmu.2017.00229

153. Grinde MT, Vik J, Camilio KA, Martinez-Zubiaurre I, Hellevik T. Ionizing radiation abrogates the pro-tumorigenic capacity of cancer-associated fibroblasts co-implanted in xenografts. *Sci Rep* (2017) 7:46714. doi: 10.1038/srep46714

154. Park HJ, Griffin RJ, Hui S, Levitt SH, Song CW. Radiation-induced vascular damage in tumors: implications of vascular damage in ablative hypofractionated radiotherapy (SBRT and SRS). *Radiat Res* (2012) 177(3):311–27. doi: 10.1667/RR2773.1

155. Deng L, Liang H, Xu M, Yang X, Burnette B, Arina A, et al. STING-dependent cytosolic DNA sensing promotes radiation-induced type I interferon-dependent antitumor immunity in immunogenic tumors. *Immunity* (2014) 41 (5):843–52. doi: 10.1016/j.immuni.2014.10.019

156. Mandai M, Hamanishi J, Abiko K, Matsumura N, Baba T, Konishi I. Dual faces of IFNgamma in cancer progression: A role of PD-L1 induction in the determination of pro- and antitumor immunity. *Clin Cancer Res* (2016) 22 (10):2329–34. doi: 10.1158/1078-0432.CCR-16-0224

157. Spranger S, Spaapen RM, Zha Y, Williams J, Meng Y, Ha TT, et al. Up-regulation of PD-L1, IDO, and t(regs) in the melanoma tumor microenvironment is driven by CD8(+) T cells. *Sci Transl Med* (2013) 5(200):200ra116. doi: 10.1126/scitranslmed.3006504

158. Wang Z, Tang Y, Tan Y, Wei Q, Yu W. Cancer-associated fibroblasts in radiotherapy: challenges and new opportunities. *Cell Commun Signal* (2019) 17 (1):47. doi: 10.1186/s12964-019-0362-2

159. Ziani L, Chouaib S, Thiery J. Alteration of the antitumor immune response by cancer-associated fibroblasts. *Front Immunol* (2018) 9:414. doi: 10.3389/fimmu.2018.00414

160. Scala S. Molecular pathways: Targeting the CXCR4-CXCL12 axis–untapped potential in the tumor microenvironment. *Clin Cancer Res* (2015) 21 (19):4278–85. doi: 10.1158/1078-0432.CCR-14-0914

161. Guo F, Wang Y, Liu J, Mok SC, Xue F, Zhang W. CXCL12/CXCR4: A symbiotic bridge linking cancer cells and their stromal neighbors in oncogenic communication networks. *Oncogene* (2016) 35(7):816–26. doi: 10.1038/onc.2015.139

162. Orimo A, Gupta PB, Sgroi DC, Arenzana-Seisdedos F, Delaunay T, Naeem R, et al. Stromal fibroblasts present in invasive human breast carcinomas promote tumor growth and angiogenesis through elevated SDF-1/CXCL12 secretion. *Cell* (2005) 121(3):335–48. doi: 10.1016/j.cell.2005.02.034

163. Renner K, Singer K, Koehl GE, Geissler EK, Peter K, Siska PJ, et al. Metabolic hallmarks of tumor and immune cells in the tumor microenvironment. *Front Immunol* (2017) 8:248. doi: 10.3389/fimmu.2017.00248

164. Noman MZ, Desantis G, Janji B, Hasmim M, Karray S, Dessen P, et al. PD-L1 is a novel direct target of HIF-1alpha, and its blockade under hypoxia enhanced MDSC-mediated T cell activation. *J Exp Med* (2014) 211(5):781–90. doi: 10.1084/jem.20131916

165. Dovedi SJ, Adlard AL, Lipowska-Bhalla G, McKenna C, Jones S, Cheadle EJ, et al. Acquired resistance to fractionated radiotherapy can be overcome by concurrent PD-L1 blockade. *Cancer Res* (2014) 74(19):5458–68. doi: 10.1158/0008-5472.CAN-14-1258

166. Monjazeb AM, Kent MS, Grossenbacher SK, Mall C, Zamora AE, Mirsoian A, et al. Blocking indolamine-2,3-Dioxygenase rebound immune suppression boosts antitumor effects of radio-immunotherapy in murine models and spontaneous canine malignancies. *Clin Cancer Res* (2016) 22(17):4328–40. doi: 10.1158/1078-0432.CCR-15-3026

167. Li A, Barsoumian HB, Schoenhals JE, Caetano MS, Wang X, Menon H, et al. IDO1 inhibition overcomes radiation-induced "Rebound immune suppression" by reducing numbers of IDO1-expressing myeloid-derived suppressor cells in the tumor microenvironment. *Int J Radiat Oncol Biol Phys* (2019) 104(4):903–12. doi: 10.1016/j.ijrobp.2019.03.022

168. Antonia SJ, Villegas A, Daniel D, Vicente D, Murakami S, Hui R, et al. Durvalumab after chemoradiotherapy in stage III non-Small-Cell lung cancer. *N Engl J Med* (2017) 377(20):1919–29. doi: 10.1056/NEJMoa1709937

169. Ngwa W, Irabor OC, Schoenfeld JD, Hesser J, Demaria S, Formenti SC. Using immunotherapy to boost the abscopal effect. *Nat Rev Cancer* (2018) 18 (5):313–22. doi: 10.1038/nrc.2018.6

170. Filatenkov A, Baker J, Mueller AM, Kenkel J, Ahn GO, Dutt S, et al. Ablative tumor radiation can change the tumor immune cell microenvironment to induce durable complete remissions. *Clin Cancer Res* (2015) 21(16):3727–39. doi: 10.1158/1078-0432.CCR-14-2824

171. Suwa T, Saio M, Umemura N, Yamashita T, Toida M, Shibata T, et al. Preoperative radiotherapy contributes to induction of proliferative activity of CD8 + tumor-infiltrating T-cells in oral squamous cell carcinoma. *Oncol Rep* (2006) 15 (4):757–63. doi: 10.3892/or.15.4.757

172. Singh AK, Winslow TB, Kermany MH, Goritz V, Heit L, Miller A, et al. A pilot study of stereotactic body radiation therapy combined with cytoreductive nephrectomy for metastatic renal cell carcinoma. *Clin Cancer Res* (2017) 23 (17):5055–65. doi: 10.1158/1078-0432.CCR-16-2946

173. Werthmoller N, Frey B, Wunderlich R, Fietkau R, Gaipl US. Modulation of radiochemoimmunotherapy-induced B16 melanoma cell death by the pan-caspase inhibitor zVAD-fmk induces anti-tumor immunity in a HMGB1-, nucleotide- and T-cell-dependent manner. *Cell Death Dis* (2015) 6:e1761. doi: 10.1038/cddis.2015.129

174. Chang MC, Chen YL, Lin HW, Chiang YC, Chang CF, Hsieh SF, et al. Irradiation enhances abscopal anti-tumor effects of antigen-specific immunotherapy through regulating tumor microenvironment. *Mol Ther* (2018) 26(2):404–19. doi: 10.1016/j.ymthe.2017.11.011

175. Zeng J, See AP, Phallen J, Jackson CM, Belcaid Z, Ruzevick J, et al. Anti-PD-1 blockade and stereotactic radiation produce long-term survival in mice with intracranial gliomas. *Int J Radiat Oncol Biol Phys* (2013) 86(2):343–9. doi: 10.1016/j.ijrobp.2012.12.025

176. Gong X, Li X, Jiang T, Xie H, Zhu Z, Zhou F, et al. Combined radiotherapy and anti-PD-L1 antibody synergistically enhances antitumor effect in non-small cell lung cancer. *J Thorac Oncol* (2017) 12(7):1085–97. doi: 10.1016/j.jtho.2017.04.014

177. Qi X, Yang M, Ma L, Sauer M, Avella D, Kaifi JT, et al. Synergizing sunitinib and radiofrequency ablation to treat hepatocellular cancer by triggering the antitumor immune response. *J Immunother Cancer* (2020) 8(2):e001038. doi: 10.1136/jitc-2020-001038

178. Patel RB, Hernandez R, Carlson P, Grudzinski J, Bates AM, Jagodinsky JC, et al. Low-dose targeted radionuclide therapy renders immunologically cold tumors responsive to immune checkpoint blockade. *Sci Transl Med* (2021) 13 (602):eabb3631. doi: 10.1126/scitranslmed.abb3631

179. Herrera FG, Ronet C, Ochoa de Olza M, Barras D, Crespo I, Andreatta M, et al. Low-dose radiotherapy reverses tumor immune desertification and resistance to immunotherapy. *Cancer Discov* (2022) 12(1):108–33. doi: 10.1158/2159-8290.CD-21-0003

180. Barsoumian HB, Ramapriyan R, Younes AI, Caetano MS, Menon H, Comeaux NI, et al. Low-dose radiation treatment enhances systemic antitumor immune responses by overcoming the inhibitory stroma. *J Immunother Cancer* (2020) 8(2):e000537. doi: 10.1136/jitc-2020-000537

181. Marciscano AE, Haimovitz-Friedman A, Lee P, Tran PT, Tome WA, Guha C, et al. Immunomodulatory effects of stereotactic body radiation therapy: Preclinical insights and clinical opportunities. *Int J Radiat Oncol Biol Phys* (2021) 110(1):35–52. doi: 10.1016/j.ijrobp.2019.02.046

182. Golden EB, Pellicciotta I, Demaria S, Barcellos-Hoff MH, Formenti SC. The convergence of radiation and immunogenic cell death signaling pathways. *Front Oncol* (2012) 2:88. doi: 10.3389/fonc.2012.00088

183. Lee Y, Auh SL, Wang Y, Burnette B, Wang Y, Meng Y, et al. Therapeutic effects of ablative radiation on local tumor require CD8+ T cells: changing strategies for cancer treatment. *Blood* (2009) 114(3):589–95. doi: 10.1182/blood-2009-02-206870

184. Yan J, Wang G, Xie L, Tian H, Li J, Li B, et al. Engineering radiosensitizer-based metal-phenolic networks potentiate STING pathway activation for advanced radiotherapy. *Adv Mater* (2022) 34(10):e2105783. doi: 10.1002/adma.202105783

185. Hietanen T, Pitkanen M, Kapanen M, Kellokumpu-Lehtinen PL. Effects of single and fractionated irradiation on natural killer cell populations: Radiobiological characteristics of viability and cytotoxicity in vitro. *Anticancer Res* (2015) 35(10):5193–200.

186. Ni K, Xu Z, Culbert A, Luo T, Guo N, Yang K, et al. Synergistic checkpoint-blockade and radiotherapy-radiodynamic therapy *via* an immunomodulatory nanoscale metal-organic framework. *Nat BioMed Eng* (2022) 6(2):144–56. doi: 10.1038/s41551-022-00846-w

187. Kaminski JM, Shinohara E, Summers JB, Niermann KJ, Morimoto A, Brousal J. The controversial abscopal effect. *Cancer Treat Rev* (2005) 31(3):159–72. doi: 10.1016/j.ctrv.2005.03.004

188. Vanpouille-Box C, Alard A, Aryankalayil MJ, Sarfraz Y, Diamond JM, Schneider RJ, et al. DNA Exonuclease Trex1 regulates radiotherapy-induced tumour immunogenicity. *Nat Commun* (2017) 8:15618. doi: 10.1038/ncomms15618

189. Burnette BC, Liang H, Lee Y, Chlewicki L, Khodarev NN, Weichselbaum RR, et al. The efficacy of radiotherapy relies upon induction of type i interferon-dependent innate and adaptive immunity. *Cancer Res* (2011) 71(7):2488–96. doi: 10.1158/0008-5472.CAN-10-2820

190. Deng L, Liang H, Fu S, Weichselbaum RR, Fu YX. From DNA damage to nucleic acid sensing: A strategy to enhance radiation therapy. *Clin Cancer Res* (2016) 22(1):20–5. doi: 10.1158/1078-0432.CCR-14-3110

191. Matsumura S, Wang B, Kawashima N, Braunstein S, Badura M, Cameron TO, et al. Radiation-induced CXCL16 release by breast cancer cells attracts effector T cells. *J Immunol* (2008) 181(5):3099–107. doi: 10.4049/jimmunol.181.5.3099

192. Walle T, Kraske JA, Liao B, Lenoir B, Timke C, von Bohlen Und Halbach E, et al. Radiotherapy orchestrates natural killer cell dependent antitumor immune responses through CXCL8. *Sci Adv* (2022) 8(12):eabh4050. doi: 10.1126/sciadv.abh4050

193. Liao JK. Linking endothelial dysfunction with endothelial cell activation. *J Clin Invest* (2013) 123(2):540–1. doi: 10.1172/JCI66843

194. Chakraborty M, Abrams SI, Camphausen K, Liu K, Scott T, Coleman CN, et al. Irradiation of tumor cells up-regulates fas and enhances CTL lytic activity and CTL adoptive immunotherapy. *J Immunol* (2003) 170(12):6338–47. doi: 10.4049/jimmunol.170.12.6338

195. Gaugler MH, Squiban C, van der Meeren A, Bertho JM, Vandamme M, Mouthon MA. Late and persistent up-regulation of intercellular adhesion molecule-1 (ICAM-1) expression by ionizing radiation in human endothelial cells in vitro. *Int J Radiat Biol* (1997) 72(2):201–9. doi: 10.1080/095530097143428

196. Frey B, Rubner Y, Wunderlich R, Weiss EM, Pockley AG, Fietkau R, et al. Induction of abscopal anti-tumor immunity and immunogenic tumor cell death by ionizing irradiation - implications for cancer therapies. *Curr Med Chem* (2012) 19 (12):1751–64. doi: 10.2174/092986712800099811

197. Obeid M, Tesniere A, Ghiringhelli F, Fimia GM, Apetoh L, Perfettini JL, et al. Calreticulin exposure dictates the immunogenicity of cancer cell death. *Nat Med* (2007) 13(1):54–61. doi: 10.1038/nm1523

198. Ma Y, Pitt JM, Li Q, Yang H. The renaissance of anti-neoplastic immunity from tumor cell demise. *Immunol Rev* (2017) 280(1):194–206. doi: 10.1111/imr.12586

199. Diamond JM, Vanpouille-Box C, Spada S, Rudqvist NP, Chapman JR, Ueberheide BM, et al. Exosomes shuttle TREX1-sensitive IFN-stimulatory dsDNA from irradiated cancer cells to DCs. *Cancer Immunol Res* (2018) 6(8):910–20. doi: 10.1158/2326-6066.CIR-17-0581

200. Hemphill WO, Simpson SR, Liu M, Salsbury FRJr., Hollis T, Grayson JM, et al. TREX1 as a novel immunotherapeutic target. *Front Immunol* (2021) 12:660184. doi: 10.3389/fimmu.2021.660184

201. Garnett CT, Palena C, Chakraborty M, Tsang KY, Schlom J, Hodge JW. Sublethal irradiation of human tumor cells modulates phenotype resulting in

enhanced killing by cytotoxic T lymphocytes. *Cancer Res* (2004) 64(21):7985–94. doi: 10.1158/0008-5472.CAN-04-1525

202. Nagata S. Fas ligand-induced apoptosis. *Annu Rev Genet* (1999) 33:29–55. doi: 10.1146/annurev.genet.33.1.29

203. Lhuillier C, Rudqvist NP, Yamazaki T, Zhang T, Charpentier M, Galluzzi L, et al. Radiotherapy-exposed CD8+ and CD4+ neoantigens enhance tumor control. *J Clin Invest* (2021) 131(5):e138740. doi: 10.1172/JCI138740

204. Reits EA, Hodge JW, Herberts CA, Groothuis TA, Chakraborty M, Wansley EK, et al. Radiation modulates the peptide repertoire, enhances MHC class I expression, and induces successful antitumor immunotherapy. *J Exp Med* (2006) 203(5):1259–71. doi: 10.1084/jem.20052494

205. Hekim N, Cetin Z, Nikitaki Z, Cort A, Saygili EI. Radiation triggering immune response and inflammation. *Cancer Lett* (2015) 368(2):156–63. doi: 10.1016/j.canlet.2015.04.016

206. Garcia-Chagollan M, Jave-Suarez LF, Haramati J, Bueno-Topete MR, Aguilar-Lemarroy A, Estrada-Chavez C, et al. An approach to the immunophenotypic features of circulating CD4(+)NKG2D(+) T cells in invasive cervical carcinoma. *J BioMed Sci* (2015) 22:91. doi: 10.1186/s12929-015-0190-7

207. Tesniere A, Panaretakis T, Kepp O, Apetoh L, Ghiringhelli F, Zitvogel L, et al. Molecular characteristics of immunogenic cancer cell death. *Cell Death Differ* (2008) 15(1):3–12. doi: 10.1038/sj.cdd.4402269

208. Kim JY, Son YO, Park SW, Bae JH, Chung JS, Kim HH, et al. Increase of NKG2D ligands and sensitivity to NK cell-mediated cytotoxicity of tumor cells by heat shock and ionizing radiation. *Exp Mol Med* (2006) 38(5):474–84. doi: 10.1038/emm.2006.56

209. Formenti SC, Rudqvist NP, Golden E, Cooper B, Wennerberg E, Lhuillier C, et al. Radiotherapy induces responses of lung cancer to CTLA-4 blockade. *Nat Med* (2018) 24(12):1845–51. doi: 10.1038/s41591-018-0232-2

210. Vermeer DW, Spanos WC, Vermeer PD, Bruns AM, Lee KM, Lee JH. Radiation-induced loss of cell surface CD47 enhances immune-mediated clearance of human papillomavirus-positive cancer. *Int J Cancer* (2013) 133(1):120–9. doi: 10.1002/ijc.28015

211. Pardoll DM. The blockade of immune checkpoints in cancer immunotherapy. *Nat Rev Cancer* (2012) 12(4):252–64. doi: 10.1038/nrc3239

212. Ganss R, Ryschich E, Klar E, Arnold B, Hammerling GJ. Combination of T-cell therapy and trigger of inflammation induces remodeling of the vasculature and tumor eradication. *Cancer Res* (2002) 62(5):1462–70.

213. Demaria S, Coleman CN, Formenti SC. Radiotherapy: Changing the game in immunotherapy. *Trends Cancer* (2016) 2(6):286–94. doi: 10.1016/j.trecan.2016.05.002

214. Kroemer G, Galluzzi L, Kepp O, Zitvogel L. Immunogenic cell death in cancer therapy. *Annu Rev Immunol* (2013) 31:51–72. doi: 10.1146/annurev-immunol-032712-100008

215. Gameiro SR, Jammeh ML, Wattenberg MM, Tsang KY, Ferrone S, Hodge JW. Radiation-induced immunogenic modulation of tumor enhances antigen processing and calreticulin exposure, resulting in enhanced T-cell killing. *Oncotarget* (2014) 5(2):403–16. doi: 10.18632/oncotarget.1719

216. Gehrmann M, Radons J, Molls M, Multhoff G. The therapeutic implications of clinically applied modifiers of heat shock protein 70 (Hsp70) expression by tumor cells. *Cell Stress Chaperones* (2008) 13(1):1–10. doi: 10.1007/s12192-007-0006-0

217. Bottcher JP, Bonavita E, Chakravarty P, Blees H, Cabeza-Cabrerizo M, Sammicheli S, et al. NK cells stimulate recruitment of cDC1 into the tumor microenvironment promoting cancer immune control. *Cell* (2018) 172(5):1022–37 e14. doi: 10.1016/j.cell.2018.01.004

218. Molla M, Gironella M, Miquel R, Tovar V, Engel P, Biete A, et al. Relative roles of ICAM-1 and VCAM-1 in the pathogenesis of experimental radiation-induced intestinal inflammation. *Int J Radiat Oncol Biol Phys* (2003) 57(1):264–73. doi: 10.1016/S0360-3016(03)00523-6

219. Ahmed A, Tait SWG. Targeting immunogenic cell death in cancer. *Mol Oncol* (2020) 14(12):2994–3006. doi: 10.1002/1878-0261.12851

220. Baird JR, Friedman D, Cottam B, Dubensky TWJr., Kanne DB, Bambina S, et al. Radiotherapy combined with novel STING-targeting oligonucleotides results in regression of established tumors. *Cancer Res* (2016) 76(1):50–61. doi: 10.1158/0008-5472.CAN-14-3619

221. Munoz LE, Frey B, Pausch F, Baum W, Mueller RB, Brachvogel B, et al. The role of annexin A5 in the modulation of the immune response against dying and dead cells. *Curr Med Chem* (2007) 14(3):271–7. doi: 10.2174/092986707779941131

222. Chiriva-Internati M, Grizzi F, Pinkston J, Morrow KJ, D'Cunha N, Frezza EE, et al. Gamma-radiation upregulates MHC class I/II and ICAM-I molecules in multiple myeloma cell lines and primary tumors. *In Vitro Cell Dev Biol Anim* (2006) 42(3-4):89–95. doi: 10.1290/0508054.1

223. Ma ZF, Huang JR, Cui NP, Wen M, Chen BP, Li Z, et al. [Expressions of immunogenic molecules in low-dose radiotherapy-treated human renal clear cell carcinoma 786-0 cells]. *Zhonghua Yi Xue Za Zhi* (2013) 93(30):2385–7.

224. Maasho K, Opoku-Anane J, Marusina AI, Coligan JE, Borrego F. NKG2D is a costimulatory receptor for human naive CD8+ T cells. *J Immunol* (2005) 174(8):4480–4. doi: 10.4049/jimmunol.174.8.4480

225. Markiewicz MA, Carayannopoulos LN, Naidenko OV, Matsui K, Burack WR, Wise EL, et al. Costimulation through NKG2D enhances murine CD8+ CTL function: Similarities and differences between NKG2D and CD28 costimulation. *J Immunol* (2005) 175(5):2825–33. doi: 10.4049/jimmunol.175.5.2825

226. Groh V, Smythe K, Dai Z, Spies T. Fas-ligand-mediated paracrine T cell regulation by the receptor NKG2D in tumor immunity. *Nat Immunol* (2006) 7(7):755–62. doi: 10.1038/ni1350

227. Lazarova M, Steinle A. Impairment of NKG2D-mediated tumor immunity by TGF-beta. *Front Immunol* (2019) 10:2689. doi: 10.3389/fimmu.2019.02689

228. Groh V, Wu J, Yee C, Spies T. Tumour-derived soluble MIC ligands impair expression of NKG2D and T-cell activation. *Nature* (2002) 419(6908):734–8. doi: 10.1038/nature01112

229. Paczulla AM, Rothfelder K, Raffel S, Konantz M, Steinbacher J, Wang H, et al. Absence of NKG2D ligands defines leukaemia stem cells and mediates their immune evasion. *Nature* (2019) 572(7768):254–9. doi: 10.1038/s41586-019-1410-1

230. Zhang J, Larrocha PS, Zhang B, Wainwright D, Dhar P, Wu JD. Antibody targeting tumor-derived soluble NKG2D ligand sMIC provides dual co-stimulation of CD8 T cells and enables sMIC(+) tumors respond to PD1/PD-L1 blockade therapy. *J Immunother Cancer* (2019) 7(1):223. doi: 10.1186/s40425-019-0693-y

231. Ozpiskin OM, Zhang L, Li JJ. Immune targets in the tumor microenvironment treated by radiotherapy. *Theranostics* (2019) 9(5):1215–31. doi: 10.7150/thno.32648

232. Rizvi NA, Hellmann MD, Snyder A, Kvistborg P, Makarov V, Havel JJ, et al. Cancer immunology. mutational landscape determines sensitivity to PD-1 blockade in non-small cell lung cancer. *Science* (2015) 348(6230):124–8. doi: 10.1126/science.aaa1348

233. Sobhani N, Tardiel-Cyril DR, Davtyan A, Generali D, Roudi R, Li Y. CTLA-4 in regulatory T cells for cancer immunotherapy. *Cancers (Basel)* (2021) 13(6):1440. doi: 10.3390/cancers13061440

234. Han Y, Liu D, Li L. PD-1/PD-L1 pathway: Current researches in cancer. *Am J Cancer Res* (2020) 10(3):727–42.

235. Kim JM, Chen DS. Immune escape to PD-L1/PD-1 blockade: Seven steps to success (or failure). *Ann Oncol* (2016) 27(8):1492–504. doi: 10.1093/annonc/mdw217

236. Topalian SL, Drake CG, Pardoll DM. Immune checkpoint blockade: A common denominator approach to cancer therapy. *Cancer Cell* (2015) 27(4):450–61. doi: 10.1016/j.ccell.2015.03.001

237. Mehdizadeh S, Bayatipoor H, Pashangzadeh S, Jafarpour R, Shojaei Z, Motallebnezhad M. Immune checkpoints and cancer development: Therapeutic implications and future directions. *Pathol Res Pract* (2021) 223:153485. doi: 10.1016/j.prp.2021.153485

238. Chocarro L, Blanco E, Zuazo M, Arasanz H, Bocanegra A, Fernandez-Rubio L, et al. Understanding LAG-3 signaling. *Int J Mol Sci* (2021) 22(10):5282. doi: 10.3390/ijms22105282

239. Qin S, Xu L, Yi M, Yu S, Wu K, Luo S. Novel immune checkpoint targets: moving beyond PD-1 and CTLA-4. *Mol Cancer* (2019) 18(1):155. doi: 10.1186/s12943-019-1091-2

240. Li M, Li M, Yang Y, Liu Y, Xie H, Yu Q, et al. Remodeling tumor immune microenvironment *via* targeted blockade of PI3K-gamma and CSF-1/CSF-1R pathways in tumor associated macrophages for pancreatic cancer therapy. *J Control Release* (2020) 321:23–35. doi: 10.1016/j.jconrel.2020.02.011

241. Mastelic-Gavillet B, Balint K, Boudousquie C, Gannon PO, Kandalaft LE. Personalized dendritic cell vaccines-recent breakthroughs and encouraging clinical results. *Front Immunol* (2019) 10:766. doi: 10.3389/fimmu.2019.00766

242. Demaria S, Kawashima N, Yang AM, Devitt ML, Babb JS, Allison JP, et al. Immune-mediated inhibition of metastases after treatment with local radiation and CTLA-4 blockade in a mouse model of breast cancer. *Clin Cancer Res* (2005) 11(2 Pt 1):728–34. doi: 10.1158/1078-0432.728.11.2

243. Deng L, Liang H, Burnette B, Beckett M, Darga T, Weichselbaum RR, et al. Irradiation and anti-PD-L1 treatment synergistically promote antitumor immunity in mice. *J Clin Invest* (2014) 124(2):687–95. doi: 10.1172/JCI67313

244. Twyman-Saint Victor C, Rech AJ, Maity A, Rengan R, Pauken KE, Stelekati E, et al. Radiation and dual checkpoint blockade activate non-redundant immune mechanisms in cancer. *Nature* (2015) 520(7547):373–7. doi: 10.1038/nature14292

245. Postow MA, Callahan MK, Barker CA, Yamada Y, Yuan J, Kitano S, et al. Immunologic correlates of the abscopal effect in a patient with melanoma. *N Engl J Med* (2012) 366(10):925–31. doi: 10.1056/NEJMoa1112824

246. Theelen W, Peulen HMU, Lalezari F, van der Noort V, de Vries JF, Aerts J, et al. Effect of pembrolizumab after stereotactic body radiotherapy vs pembrolizumab alone on tumor response in patients with advanced non-small cell lung cancer: Results of the PEMBRO-RT phase 2 randomized clinical trial. *JAMA Oncol* (2019) 5(9):1276–82. doi: 10.1001/jamaoncol.2019.1478

247. Theelen WSME, Chen D, Verma V, Hobbs BP, Peulen HMU, Aerts JGJV, et al. Pembrolizumab with or without radiotherapy for metastatic non-small-cell lung cancer: A pooled analysis of two randomised trials [published correction appears in Lancet Respir Med. *Lancet Respir Med* (2021) 9(5):467–465. doi: 10.1016/S2213-2600(20)30391-X

248. Shaverdian N, Lisberg AE, Bornazyan K, Veruttipong D, Goldman JW, Formenti SC, et al. Previous radiotherapy and the clinical activity and toxicity of pembrolizumab in the treatment of non-small-cell lung cancer: A secondary analysis of the KEYNOTE-001 phase 1 trial. *Lancet Oncol* (2017) 18(7):895–903. doi: 10.1016/S1470-2045(17)30380-7

249. Hua Y, You R, Wang Z, Huang P, Lin M, Ouyang Y, et al. Toripalimab plus intensity-modulated radiotherapy for recurrent nasopharyngeal carcinoma: an open-label single-arm, phase II trial. *J Immunother Cancer* (2021) 9(11):e003290. doi: 10.1136/jitc-2021-003290

250. Siva S, Bressel M, Wood ST, Shaw MG, Loi S, Sandhu SK, et al. Stereotactic radiotherapy and short-course pembrolizumab for oligometastatic renal cell carcinoma-the RAPPORT trial. *Eur Urol* (2022) 81(4):364–72. doi: 10.1016/j.eururo.2021.12.006

251. Ho AY, Barker CA, Arnold BB, Powell SN, Hu ZI, Gucalp A, et al. A phase 2 clinical trialassessing theefficacy and safety of pembrolizumab and radiotherapy in patients with metastatic triple-negative breast cancer. *Cancer* (2020) 126(4):850–60. doi: 10.1002/cncr.32599

252. Tang C, Welsh JW, de Groot P, Massarelli E, Chang JY, Hess KR, et al. Ipilimumab with stereotactic ablative radiation therapy: Phase I results and immunologic correlates from peripheral T cells. *Clin Cancer Res* (2017) 23 (6):1388–96. doi: 10.1158/1078-0432.CCR-16-1432

253. Menon H, Chen D, Ramapriyan R, Verma V, Barsoumian HB, Cushman TR, et al. Influence of low-dose radiation on abscopal responses in patients receiving high-dose radiation and immunotherapy. *J Immunother Cancer* (2019) 7(1):237. doi: 10.1186/s40425-019-0718-6

254. Lauret Marie Joseph E, Kirilovsky A, Lecoester B, El Sissy C, Boullerot L, Rangan L, et al. Chemoradiation triggers antitumor Th1 and tissue resident memory-polarized immune responses to improve immune checkpoint inhibitors therapy. *J Immunother Cancer* (2021) 9(7):e002256. doi: 10.1136/jitc-2020-002256

255. Tumeh PC, Harview CL, Yearley JH, Shintaku IP, Taylor EJ, Robert L, et al. PD-1 blockade induces responses by inhibiting adaptive immune resistance. *Nature* (2014) 515(7528):568–71. doi: 10.1038/nature13954

256. Herbst RS, Soria JC, Kowanetz M, Fine GD, Hamid O, Gordon MS, et al. Predictive correlates of response to the anti-PD-L1 antibody MPDL3280A in cancer patients. *Nature* (2014) 515(7528):563–7. doi: 10.1038/nature14011

257. Wang J, Xu Z, Wang Z, Du G, Lun L. TGF-beta signaling in cancer radiotherapy. *Cytokine* (2021) 148:155709. doi: 10.1016/j.cyto.2021.155709

258. Vanpouille-Box C, Diamond JM, Pilones KA, Zavadil J, Babb JS, Formenti SC, et al. TGFbeta is a master regulator of radiation therapy-induced antitumor immunity. *Cancer Res* (2015) 75(11):2232–42. doi: 10.1158/0008-5472.CAN-14-3511

259. Qin X, Yang C, Xu H, Zhang R, Zhang D, Tu J, et al. Cell-derived biogenetic gold nanoparticles for sensitizing radiotherapy and boosting immune response against cancer. *Small* (2021) 17(50):e2103984. doi: 10.1002/smll.202103984

260. Hou Y, Liang HL, Yu X, Liu Z, Cao X, Rao E, et al. Radiotherapy and immunotherapy converge on elimination of tumor-promoting erythroid progenitor cells through adaptive immunity. *Sci Transl Med* (2021) 13(582): eabb0130. doi: 10.1126/scitranslmed.abb0130

frontiers | Frontiers in Immunology

TYPE Original Research
PUBLISHED 01 December 2022
DOI 10.3389/fimmu.2022.1063678

OPEN ACCESS

EDITED BY
Fei Yu,
Tongji University School of Medicine, China

REVIEWED BY
Lin Xie,
National Institutes for Quantum and Radiological Science and Technology, Japan
Zi (Sophia) Gu,
University of New South Wales, Australia

*CORRESPONDENCE
Ran Zhu
zhuran@suda.edu.cn
Wei Li
905623032@qq.com

†These authors have contributed equally to this work

SPECIALTY SECTION
This article was submitted to Cancer Immunity and Immunotherapy, a section of the journal Frontiers in Immunology

RECEIVED 07 October 2022
ACCEPTED 14 November 2022
PUBLISHED 01 December 2022

CITATION
Zhang C, Zhang Y, Liang M, Shi X, Jun Y, Fan L, Yang K, Wang F, Li W and Zhu R (2022) Near-infrared upconversion multimodal nanoparticles for targeted radionuclide therapy of breast cancer lymphatic metastases. *Front. Immunol.* 13:1063678. doi: 10.3389/fimmu.2022.1063678

Near-infrared upconversion multimodal nanoparticles for targeted radionuclide therapy of breast cancer lymphatic metastases

Chuan Zhang[1,2†], Yujuan Zhang[3†], Maolin Liang[1†], Xiumin Shi[1,2], Yan Jun[4], Longfei Fan[1], Kai Yang[1], Feng Wang[2], Wei Li[5*] and Ran Zhu[1*]

[1]State Key Laboratory of Radiation Medicine and Protection, School of Radiation Medicine and Protection, Collaborative Innovation Center of Radiation Medicine of Jiangsu Higher Education Institutions, Soochow University, Suzhou, Jiangsu, China, [2]Department of Nuclear Medicine, Nanjing First Hospital, Nanjing Medical University, Nanjing, China, [3]Department of Pathology, Experimental Center of Suzhou Medical College of Soochow University, Suzhou, Jiangsu, China, [4]The Affiliated Suzhou Hospital of Nanjing Medical University, Suzhou Municipal Hospital, Gusu School, Nanjing Medical University, Suzhou, Jiangsu, China, [5]Department of General Surgery, The Second Affiliated Hospital of Soochow University, Suzhou, Jiangsu, China

The theranostics of lymph node metastasis has always been one of the major obstacles to defeating breast cancer and an important decisive factor in the prognosis of patients. Herein, we design $NaGdF_4$:Yb,Tm@$NaLuF_4$ upconversion nanoparticles with PEG and anti-HER2 monoclonal antibody (trastuzumab, Herceptin) (NP-mAb), the delivery of NP-mAb through the lymphatic system allows for effective targeting and accumulation in lymphatic metastasis. Combination of radionuclides ^{68}Ga and ^{177}Lu could be chelated by the bisphosphate groups of NP-mAb. The obtained nanoprobe (NP-mAb) and nanonuclear drug (^{68}Ga-NP-mAb or ^{177}Lu-NP-mAb) exhibited excellent stability and show high accumulation and prolong retention in the lymph node metastasis after intratumoral injection into the foot pad by near-infrared fluorescence (NIRF), single-photon emission computed tomography (SPECT) and positron emission tomography (PET) imaging. Utilizing the β-rays released by ^{177}Lu, ^{177}Lu-NP-mAb could not only decrease the incidence of lymph node metastasis, but also significantly decrease the volumes of lymph node metastasis. Additionally, ^{177}Lu-NP-mAb induce no obvious toxicity to treated mice through blood routine, liver and kidney function assay. Therefore, nanoprobe and nanonuclear drug we designed could be acted as excellent theranostics agents for lymph node metastasis, providing potential alternatives diagnose and treatment option for lymph node metastasis.

KEYWORDS

breast cancer, lymph node metastasis, multimode imaging, radiotherapy, theranostic nanoplatform

Introduction

Tumor metastasis is an extremely severe step in the progression of tumors and approximately 90% of deaths in cancer patients are due to metastasis rather than the primary tumor (1). The lymphatic system is the preferred route for metastasis of most solid tumors *in vivo*, and draining lymph nodes are usually the earliest sites and the first station of metastasis (2, 3). Lymph node metastasis often indicates a poor prognosis, and is an important indicator of cancer progression (4, 5). The dissection and local radiotherapy of sentinel lymph nodes can significantly improve the prognosis of patients with lymph node metastasis, further emphasizing the development of effective theranostics strategies against lymph node metastasis (6–8). Recently, breast cancer has replaced lung cancer as the most common cancer worldwide (9). Similar to other solid tumors, lymph node metastasis plays a major role in promoting the invasion and metastasis of breast cancer. Therefore, reducing the occurrence of lymph node metastasis and removing tumor cells from the lymphatic system are the keys for combating breast cancer.

Current treatment methods for lymph node metastasis mainly include surgical resection, local radiotherapy and chemotherapy. Surgical resection as an invasive treatment have been widely used to perform regional or sentinel lymph node dissection. However, the efficiency of surgical resection usually depends on the diagnostic techniques of lymph nodes. Clinically, methylene blue dye, technetium colloid or fluorescent dye ICG are commonly used to locate and detect sentinel lymph nodes for guiding lymph node resection (10–13). However, these methods have certain limitations. It is difficult to detect the deep lymph nodes and distinguish the lymph node metastasis from normal lymph nodes. According to the literatures, local radiotherapy have been used for advanced patients with metastases to supraclavicular lymph nodes, reducing the risk of local recurrence and improving the overall survival (14, 15). However, the inevitable risks of exposure to radiation of the heart, lungs, and skin can lead to events such as acute radiation skin damage, lung damage, and increased incidence of heart disease (16–19). Similar to radiotherapy, chemotherapy is usually applied in the advanced patients with breast cancer. Recently, the neoadjuvant chemotherapy has been developed to reduce the size of the primary tumor and eliminate minor peripheral lesions before the surgery or radiotherapy, further improving the patient's prognosis and quality of life (20). Chemotherapeutic agents based on small molecules often result in poor lymphatic absorption in clinical applications, affecting the long-retention in lymph node metastasis (21, 22). More importantly, the systemic side effects of chemotherapy are very obvious (23). Therefore, it is an urgent need to develop new personalized theranostics treatment of lymph node metastasis in breast cancer.

Given its suitable size and surface properties, nanomaterials can freely enter the intercellular matrix (24). During the competitive absorption process between lymphatics and blood vessels, some nanomaterials will preferentially enter the lymphatic vessels from the interstitium (25–27). Therefore, interstitially administration (subcutaneous, intratumoral or peritumoral) of nanodrugs exhibit great potential to target the lymphatic system. The delivery of nanodrugs through the lymphatic system effectively targets and accumulates in lymph node metastasis, avoiding the rapid drug clearance caused by direct ingestion by the blood system and further reducing the risk of toxicity. Utilizing the nanomaterials as nano-drug carriers could optimize drug accumulation in solid tumor sites, achieving highly efficient and selective lymphatic system enrichment by subcutaneous administration (28–30). Although numerous papers have reported that nano-drug combined with small molecular drugs using the principle of lymphatic transport could show the draining lymph nodes and kill the cancer cells aggregated in the lymph node site, theranostic nanoplatform in combination with radioisotope therapy for lymphatic system has been rarely reported (31).

The passive targeting of nano-drugs based on the enhanced penetration and retention (EPR) effect is strongly influenced by tumor heterogeneity. For the metastatic tumor, nano-drugs without tumor targeting ability could induce the non-specific distribution and unnecessary side effects (32, 33). An effective way to overcome these passive targeting limitations is to introduce targeting ligands or antibodies on the surface of nanoparticles for improving the cancer cells uptake of nanodrugs through their active binding ability to receptors or antigens specifically expressed on the tumor cell surface (34–36). Human epidermal growth factor receptor 2 (HER2)-positive breast cancer is an aggressive type of breast cancer that tends to grow more rapidly and spread more easily. Anti-HER2 therapies such as Herceptin (trastuzumab), are highly effective in the clinic, significantly improving the prognosis of patients with HER2-positive breast cancer (37, 38). In addition, trastuzumab has been widely used in the development of various nanodrugs for the diagnosis and treatment of HER2-positive breast cancer (39, 40). Therefore, in this study, we developed rare-earth upconversion nanoprobe (NP-mAb) conjugated with trastuzumab. These NP-mAb could be efficiently labeled with diagnostic radioisotope ^{68}Ga (half-life: 68 min) and therapeutic radioisotope ^{177}Lu (half-life: 6.71 d) through simple chelation. The obtained nanonuclear drug (^{68}Ga-NP-mAb and ^{177}Lu-NP-mAb) and nanoprobe can be moved into the lymph node metastasis *via* the delivery of lymphatic system, which developed a new theranostic strategy for lymphatic targeting used for near-infrared fluorescence (NIRF), single-photon emission computed tomography (SPECT), positron emission tomography (PET) and targeted radionuclide therapy (TRT) of HER2-positive breast cancer lymph node metastasis tumor in mice (Scheme 1). TRT based on ^{177}Lu-NP-mAb could effectively inhibit the occurrence of lymph node metastasis and the growth of tumour in the footpad area and lymph node. Importantly,

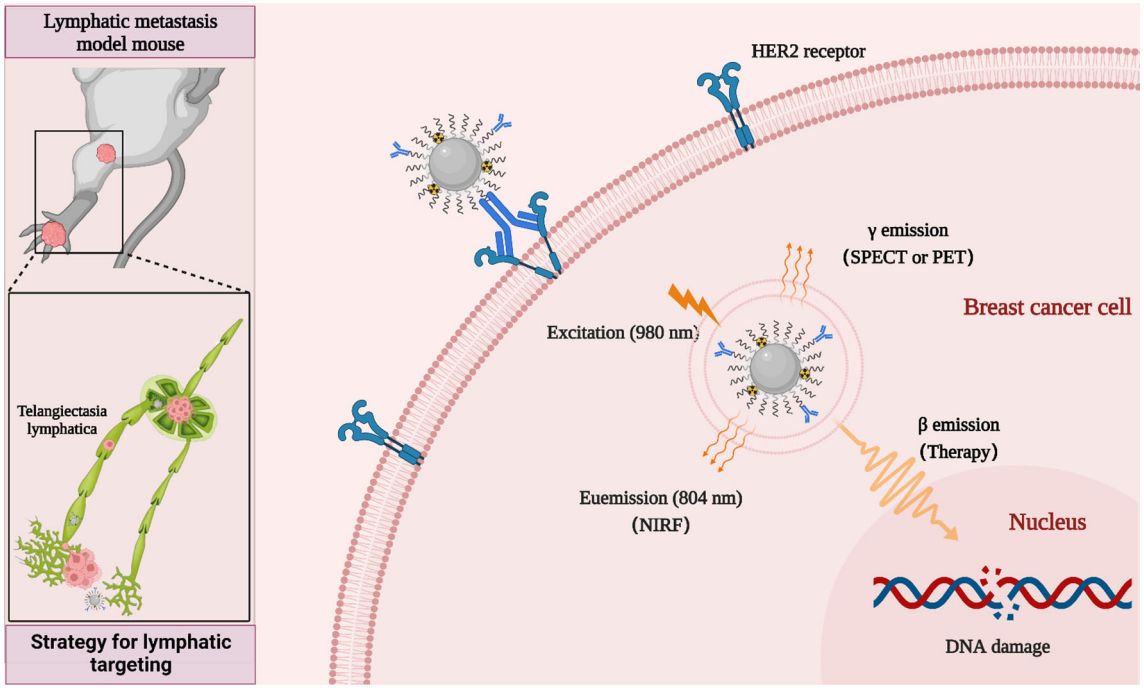

SCHEME 1
Schematic diagram of strategy for lymphatic targeting and theranostic nanoplatform.

such therapeutic strategy our developed even exhibited no obvious side effects on the blood system, liver and kidney function of mice. Therefore, our developed strategy will provide a new method for theranostic of lymphatic metastases.

Results and discussions

We began the study with the synthesis of rare-earth upconversion nanoparticles (UCNPs, $NaGdF_4$:Yb,Tm@$NaLuF_4$) *via* a liquid-solid-solution (LSS) solvothermal method (Figure 1A) (41–44). Then, UCNPs were chelated with bisphosphate-headed polyethylene glycol (PEG) ended with a maleimide group (dp-PEG-mal) to get water-soluble nanoparticles (i.e., NPs). To obtain the lock-and-key specific targeting ability toward HER2-positive breast cancer lymphatic metastasis, trastuzumab was conjugated with PEGylated NPs to obtain NP-mAb *via* a reaction between sulfhydryl residues of antibody and maleimide groups on the terminal PEG. Finally, positron-emitting ^{68}Ga and β-emitting ^{177}Lu radionuclides were labeled *via* chelating with bisphosphate groups to yield the final multimodal theranostic nanoparticles ^{68}Ga-NP-mAb and ^{177}Lu-NP-mAb, respectively. Transmission electron microscopy (TEM) characterization showed the spherical morphology of NPs (Figure 1B, left panel) and NP-mAb (Figure 1B, right panel) with an average size of 21.99 ± 2.88 nm and 22.5 ± 2.94 nm, respectively (Figure S1). Dynamic light scattering (DLS) analyses showed a narrow hydrodynamic size distribution of NPs with an average size of 50 nm, suggesting the hydrophobic UCNPs were successfully converted into hydrophilic UCNPs through the replacement of the oleic acid ligands-functionalized oil-dispersible UCNPs with hydrophilic PEG-coated UCNPs. A slight larger hydrodynamic size of 60 nm relative to PEGylated NPs was observed for NP-mAb (Figure 1C). Moreover, the zeta potential of the PEGylated NPs before and after antibody conjugation was changed from 4.81 to 12.63 mV (Figure 1D). These results strongly demonstrated that the monoclonal antibody molecules were successfully coupled on the surface of the NPs. Of note, antibody modification didn't influence the optical spectrum of NPs and NP-mAb with exhibiting a near-infrared emission centered at 804 nm under the excitation of 980-nm laser (Figure 1E). In addition, thin-layer paper chromatography assay indicated the radiolabeling yield of both ^{68}Ga-NP-mAb and ^{177}Lu-NP-mAb reached 95% with ideal radiolabeling stability as well as excellent stability for NP-mAb in PBS and 10% FBS (Figures 1F, G and Figures S2 and S3). Besides, the stability of NP-mAb in different solutions were investigated.

We next studied the cytotoxicity of NP-mAb to HER2-positive human breast carcinoma cell line SKBR3 cells and normal human liver cell line HL7702 cells by the CCK-8 assay. As shown in Figure 2A, after incubating with NP-mAb at various

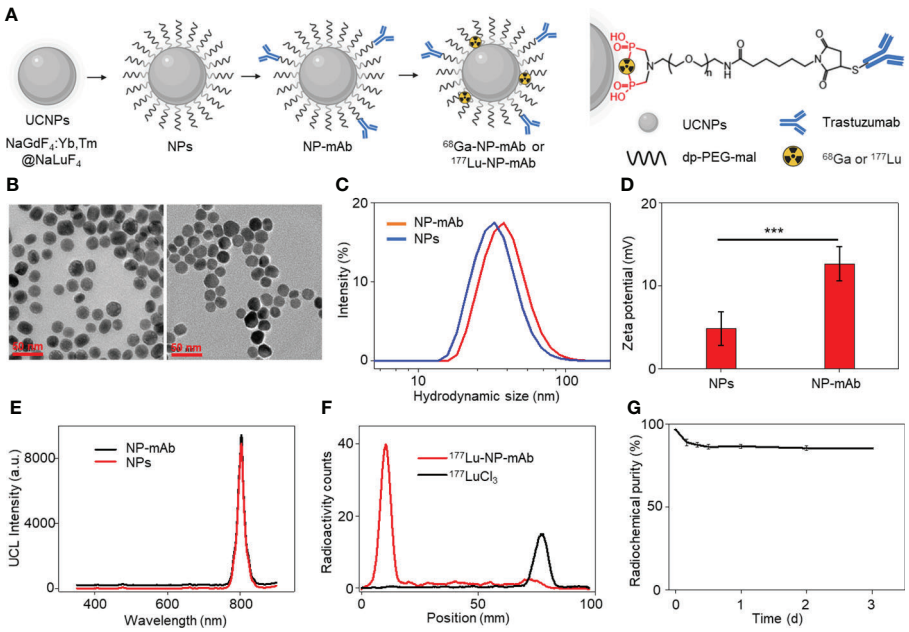

FIGURE 1
Synthesis and characterization of theranostic nanoplatform. **(A)** Schematic depicting the preparation of theranostic nanoplatform and structure diagram. **(B)** Transmission electron microscopy (TEM) image of NPs and NP-mAb nanoparticles. **(C)** Hydrodynamic size of NPs and NP-mAb in water determined by DLS. **(D)** Zeta potential of NPs and NP-mAb in water (***P< 0.001). **(E)** UV–vis spectra of NPs and NP-mAb under 980 nm light irradiation. **(F)** Radiochemical pure analysis of ^{177}Lu-NP-mAb and $^{177}LuCl_3$. **(G)** Radiolabeling stability of 177Lu-NP-mAb in PBS solution.

concentrations for 24 h, the nanoparticles showed minimized toxicity towards either SKBR3 cells or HL7702 cells, suggesting the suitable biocompatibility of NP-mAb for further *in vivo* study. To investigate the targeting capability of the NP-mAb, the cellular uptake study was conducted. SKBR3 cells with high HER2 expression were incubated with NPs and NP-mAb for 24 h, respectively, and the HER2 negative-expressed triple-negative human breast carcinoma cell line MDA-MB-231 cells were incubated with NP-mAb for 24 h. After incubation, the upconversion luminescence (UCL) signals of cells after different treatments were acquired under 980 nm laser irradiation (Figure 2B). The UCL signal of SKBR3 cells treated with NP-mAb presented a distinct signal, which was 4.28-fold and 7.1-fold higher than those of SKBR3 cells treated with NPs and MDA-MB-231 cells treated with NP-mAb, respectively (Figures 2B, C). These results proved that NP-mAb had better targeting efficiency towards HER2-positive SKBR3 cells, which was also verified by the UCL images of collected cell pellets after various treatments (Figure S4).

To investigate the cytotoxicity effect of ^{177}Lu-NP-mAb, SKBR3 cells were incubated with different concentrations of $^{177}LuCl_3$, ^{177}Lu-NPs, and ^{177}Lu-NP-mAb for 24 h, respectively. The cell viabilities were measured by CCK-8 assay. As shown in Figure 2D, the killing effect of ^{177}Lu-NP-mAb on SKBR3 cells was significantly higher than that of $^{177}LuCl_3$ and ^{177}Lu-NPs at all detected radioactive dosage attributing to the trastuzumab-mediated higher targeting efficiency of ^{177}Lu-NP-mAb relative to control groups. Meanwhile, the DNA damage of SKBR3 cells treated with ^{177}Lu-NP-mAb nanoparticles was also studied (Figure 2E). The γ-H2AX luminescence imaging showed that ^{177}Lu-NP-mAb induced significantly higher DNA damage than other control groups (Figure 2F).

As follows, NP-mAb and its radioactive counterpart ^{68}Ga-NP-mAb were used for *in vivo* imaging of lymphatic metastasis. HER2-positive SKBR3 breast cancer lymphatic metastasis model was established according to the literatures (45, 46). Mice model bearing SKBR3 lymphatic metastasis were intratumorally injected with NP-mAb or ^{68}Ga-NP-mAb (5 mCi ^{68}Ga/kg) in the foot pad, and imaged by a small animal upconversion luminescence *in vivo* imaging system (IVIS, Lumina XRMS, America) and a small animal positron emission tomography system (micro-PET, Siemens Inveon, Germany), respectively. As shown in Figure 3A, an obvious UCL signal was observed in the metastatic lymph node (red arrow) after 1 h injection of NP-mAb in the foot pad (yellow arrow), and the UCL signal was still evident at 5 h post-injection of nanoparticles. Time-dependent UCL signal changes in metastatic lymph node are shown in Figure 3B, indicating that NP-mAb can accumulate into the metastatic lymph node efficiently within 1 h post-injection of nanoparticles and enable a long-term longitudinal imaging window. Besides, for radioactive imaging, as displayed in Figure 3C, a significant radioactive signal was observed in

10.3389/fimmu.2022.1063678

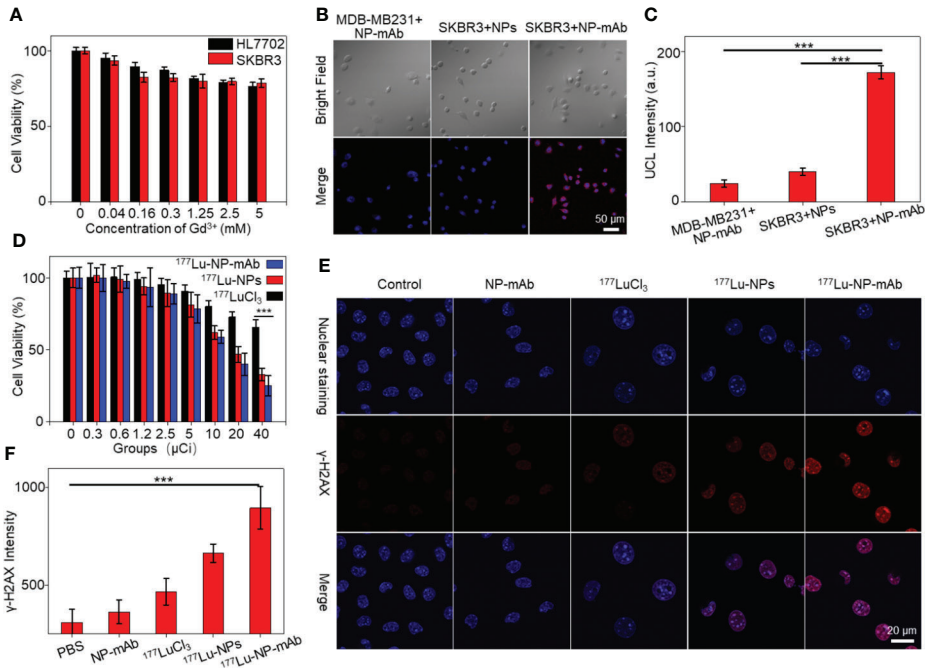

FIGURE 2
Cell experiments. **(A)** The cytotoxicity of NP-mAb at different concentrations. **(B)** Confocal imaging of the HER2 over-expressed cell line (SKBR3) and HER2 low-expressed cell line (MDA-MB-231) incubated with the NPs and NP-mAb, respectively (blue: Nuclear staining, red: UCL Channel, the embedded scale bars correspond to 50 μm). **(C)** UCL Intensity of confocal imaging in cell binding experiment (***P< 0.001). **(D)** Relative viabilities of SKBR3 cells treated with different doses of free ^{177}Lu, ^{177}Lu-NPs and ^{177}Lu-NP-mAb for 24 h. Asterisks indicate statistical significance (***P< 0.001). **(E)** γ-H2AX fluorescence images (blue: Nuclear staining, red: γ-H2AX) of SKBR3 cells with different treatments. **(F)** γ-H2AX Intensity of confocal imaging in DNA damage (***P< 0.001).

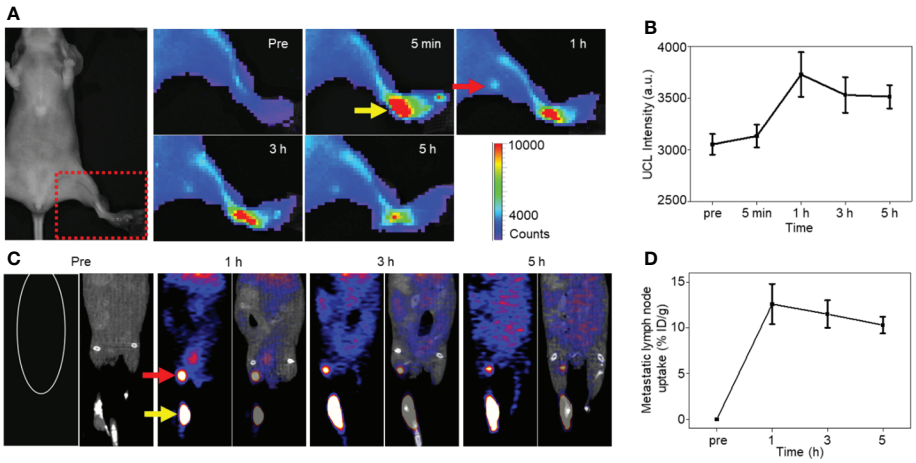

FIGURE 3
In vivo imaging experiments. **(A)** NIRF imaging of mice model bearing SKBR3 were obtained at different time points of NP-mAb injection (the red arrow indicates the site of metastatic lymph node, the yellow arrow indicates the injection site in foot pad). **(B)** Changes of upconversion luminescence signal in lymphatic metastasis after NP-mab injection. **(C)** PET imaging of mice model bearing SKBR3 were obtained at different time points of ^{68}Ga-NP-mAb injection (red arrow: lymphatic metastasis, yellow arrow: injection site in foot pad). **(D)** Changes of radioactive ingestion signal in lymphatic metastasis after ^{68}Ga-NP-mAb injection.

metastatic lymph node after 1 h injection of ^{68}Ga-NP-mAb in foot pad. Quantitative analyses showed similar result with UCL imaging and the highest uptake of the metastatic lymph node reached 12.6 ± 2.2% ID/g at 1 h post-injection of nanoparticles (Figure 3D). This further demonstrates that the nanoprobes can be transported through the lymphatic system and specifically gathered in the metastatic lymph node.

Before determining *in vivo* therapeutic effect of ^{177}Lu-NP-mAb, *in vivo* behavior of ^{177}Lu-NP-mAb in mice bearing SKBR3 lymphatic metastasis was investigated. Notably, except for β-ray emission for therapy, ^{177}Lu emits γ-ray emission (208 keV and 113 keV) with long radioactive half-time (6.7 day), enabling long-term monitoring the *in vivo* behavior of ^{177}Lu-NP-mAb in the metastatic lymph node by a small animal single-photon emission computed tomography imaging system (micro-SPECT, MILabs, Netherlands). As shown in Figure 4A, ^{177}Lu-NP-mAb-treated mice exhibited significant accumulation and prolonged retention of radionuclides in the lymphatic metastatic site (red arrow) with the uptake as high as 8.84 ± 1.68% ID/g even at 7 d post-injection of ^{177}Lu-NP-mAb shown in Figure 4B. Besides, *in vivo* biodistribution was also investigated at 24 h post injection of ^{177}Lu-NP-mAb in the footpad of mouse model (Figure 4C). We found that ^{177}Lu-NP-mAb exhibited an obvious accumulation (13.5 ± 6.38%ID/g) in lymphatic metastasis at 24 h except for the liver and spleen uptake. These results showed that the nanoprobe had good targeting performance in metastatic lymph nodes. In addition, there was a large amount of radioactive accumulation in the liver and spleen, which was related to the characteristics of nanoparticles and their easy uptake by the monocyte macrophage system (MPS).

Based on the excellent accumulation and retention of ^{177}Lu-NP-mAb in the metastatic lymph node, the therapeutic effect of ^{177}Lu-NP-mAb on primary and metastatic tumors was evaluated. The timeline of construction of tumor model, therapeutic treatment, and outcome analyses were shown in Figure 4D. After 2 weeks of inoculation of the tumor cells into nude mice, mice were injected with PBS, NP-mAb, $^{177}LuCl_3$, ^{177}Lu-NPs, or ^{177}Lu-NP-mAb in the footpad, respectively. After therapies, tumor volumes of both primary (yellow arrow, injection site in the foot pad) and metastatic lymphatic tumors (red arrow) were detected and calculated through small animal magnetic resonance imaging system (MRI, MRS3000, MR Solution, Britain) shown in Figure 4E. No obvious weight loss for all treatment groups (Figure 4F). According to the MRI data

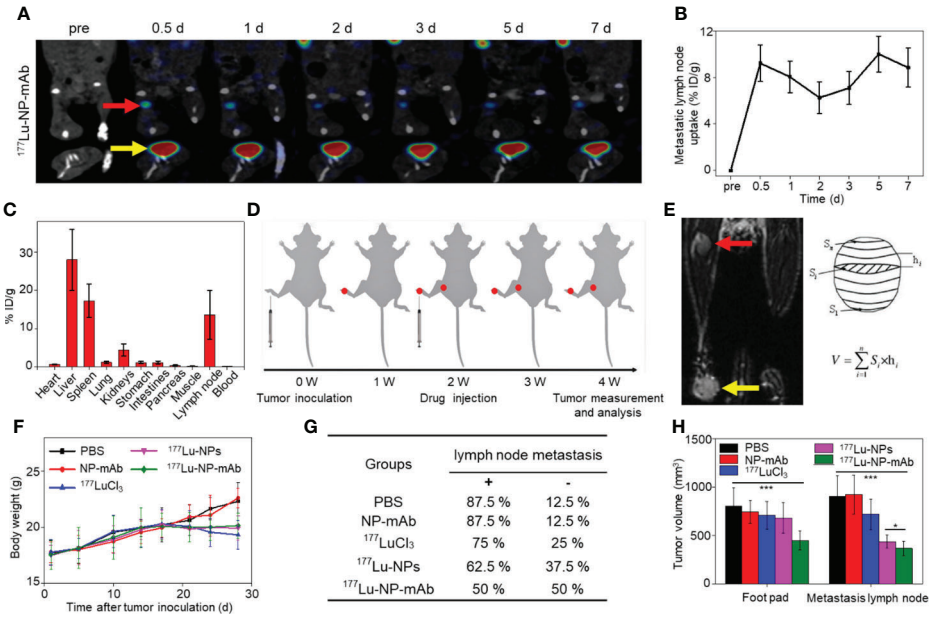

FIGURE 4
In vivo therapeutic efficacy by radiotherapy. **(A)** SPECT imaging of SKBR3 tumor bearing mice with ^{177}Lu-NP-mAb injected in the left foot pad at different time points (the red arrow indicates the site of metastatic lymph node, the yellow arrow indicates the injection site in foot pad). **(B)** Uptake curves of ^{177}Lu-NP-mAb in lymphatic metastasis at different time points. **(C)** *In vivo* biodistribution of ^{177}Lu-NP-mAb in major organs and tissues at 24 h after injected in the foot pad (error lines represent mean ± standard deviation, n = 3). **(D)** Schematic diagram of radioisotope therapy to suppress primary tumor and metastasis lymph nodes growth. **(E)** MRI imaging of lymphatic metastasis model mouse and Schematic diagram of tumor volume calculation method. **(F)** Changes in body weight of mice in each group during the therapeutic cycle. **(G)** Lymph node metastasis rate of different groups of mice (PBS, NP-mAb, $^{177}LuCl_3$, ^{177}Lu-NPs, and ^{177}Lu-NP-mAb, n = 8 for each group) after 2 weeks of radioisotope therapy (**+** indicates positive lymph node metastasis in mice, - indicates negative lymph node metastasis in mice). **(H)** The volume of primary tumor and metastatic lymph nodes in different groups of mice after 2 weeks of radioisotope therapy. Asterisks indicate statistical significance (***P< 0.001, *P< 0.05).

in Figure S5 and the analyses in Figure 4G, among all the treatment groups, the mice treated with ^{177}Lu-NP-mAb possessed the lowest risk of lymph node metastasis with metastatic occurrence probability decreased from 87.5% in PBS-treated group into 50% in ^{177}Lu-NP-mAb-treated group. Additionally, compared with PBS-treated group, the rate of lymph node metastasis was slightly decreased in the $^{177}LuCl_3$-treated group, which might be due to the antitumor effect of β-rays emitted by ^{177}Lu. In contrast, it was easier to understand that there was no change in the metastatic rate of lymph nodes in the NP-mAb treated group relative to PBS-treated group. We also collected the primary tumor and lymph node metastasis to record the volume of tumor using MRI (Figure S5). As shown in Figure 4H, the primary tumor volumes of mice treated with ^{177}Lu-NP-mAb was smaller than that of the other four groups, which might be related to the better distribution and intracellular uptake of ^{177}Lu-NP-mAb within the tumor. From the lymph node metastasis volume analysis, both ^{177}Lu-NPs and ^{177}Lu-NP-mAb could inhibit the tumor growth, suggesting that the nanoparticles could enter into the lymphatic system and accumulate in the lymph node. Moreover, the inhibitory effect of ^{177}Lu-NP-mAb group was better than that of the ^{177}Lu-NPs group (Average volume of lymph node metastasis: 360.76 ± 64.72 mm^3 to 448.53 ± 43.7 mm^3, $P<0.05$), demonstrating that the improved accumulation and retention of nanoparticles in lymph nodes by anti-HER2 antibody could enhance the therapeutic efficacy.

The potential side-effect of ^{177}Lu-NP-mAb was also investigated. The blood samples collected from mice after different treatments were used to evaluate the routine blood tests, liver and kidney function. As shown in Figure 5A, there was a slight decrease in blood indexes such as white blood cell count (WBC), red blood cell (RBC), platelet count (PLT) and hemoglobin (HGB) in ^{177}Lu-, ^{177}Lu-NPs- and ^{177}Lu-NP-mAb-treated groups, which was probably caused by radionuclides-induced bone marrow suppression. Further study showed that WBC, RBC, PLT and HGB have rapidly reduced to a certain extent at the first week after treatment with ^{177}Lu-NP-mAb, which kept stable at the next week (Figure S6). Such phenomenon are basically consistent with the changes of blood routine level in clinical radionuclide treatment, indicating that radionuclides-mediated bone marrow suppression mainly occurred during the first-week treatment and thus suggesting that prevention should be carried out before treatment to prevent the occurrence of bone marrow suppression. In addition, there are no obvious of liver and kidney toxicity among all the groups using liver function indexes including alanine aminotransferase (ALT), aspartate aminotransferase (AST), alkaline phosphatase (ALP), and gamma glutamyl transpeptidase (GGT) and renal function indexes blood urea (UREA) and creatinine (CREA) (Figures 5B, C). Therefore, ^{177}Lu-NP-mAb we designed could act as an excellent therapeutic agent for lymph node metastasis with minimal side-effects.

Besides, we also investigated the potential mechanism of radioisotope therapy in lymph node metastasis. Lymph nodes from mice with different treatments were collected for HE staining, TUNEL staining and CD44 immunohistochemistry (IHC) after 2 weeks post injection. HE staining and TUNEL staining of lymph nodes exhibited that^{177}Lu-NP-mAb induced most severe apoptosis compared with other control groups (Figure 5D). CD44 is widely expressed on the surface of breast tumor stem cells (47). CD44 IHC results of lymph node metastasis showed that CD44 expression level in the ^{177}Lu-NP-mAb-treated group was significantly decreased compared with the PBS-treated group, indicating that the tumor stem cells in lymph node metastasis decreased after treatment with ^{177}Lu-NP-mAb (Figure 5E). The flow cytometry of tumor cells collected from mice after different treatments also indicated the reduced CD44 expression in ^{177}Lu-NP-mAb-treated group (Figure S7A). In addition, epithelial cell adhesion molecule (EpCAM) expressed on the surface of most epithelial tumor cells, including breast cancer cells, is an important marker in circulating tumor cell detection (CTC). Flow cytometry results showed that the expression level of EpCAM in the ^{177}Lu-NP-mAb-treated group was significantly lower than that in PBS-treated group (Figure S7B). Therefore, ^{177}Lu-NP-mAb could significantly inhibit the lymph node metastasis and reduce the incidence of tumor metastasis.

Conclusion

In this work, we successfully designed a nanoprobe conjugated trastuzumab based on upconversion nanoparticles, further developed a nanonuclear drug labeled ^{68}Ga or ^{177}Lu, adopted a new imaging and theranostic strategy for lymphatic targeting, to realize the multimodal imaging and theranostics of lymph node metastasis. NIRF/PET/SPECT imaging showed that nanoprobe exhibited high accumulation and prolonged retention in lymph node metastasis. Importantly, the injected nanonuclear drug significantly reduced the occurrence of lymph node metastasis and inhibited the growth of lymph node metastasis. In addition, nanonuclear drug induced no obvious side-effect to treated mice though the blood routine, liver and kidney function assay. Therefore, this study not only provides a versatile nanoplatform for the applications of multimodal imaging and theranostics but also validates new strategy for lymphatic metastasis targeting by delivery of nanodrugs through the lymphatic system, which is meaningful to guide the exploration and advances of more effective theranostics strategies against tumors.

10.3389/fimmu.2022.1063678

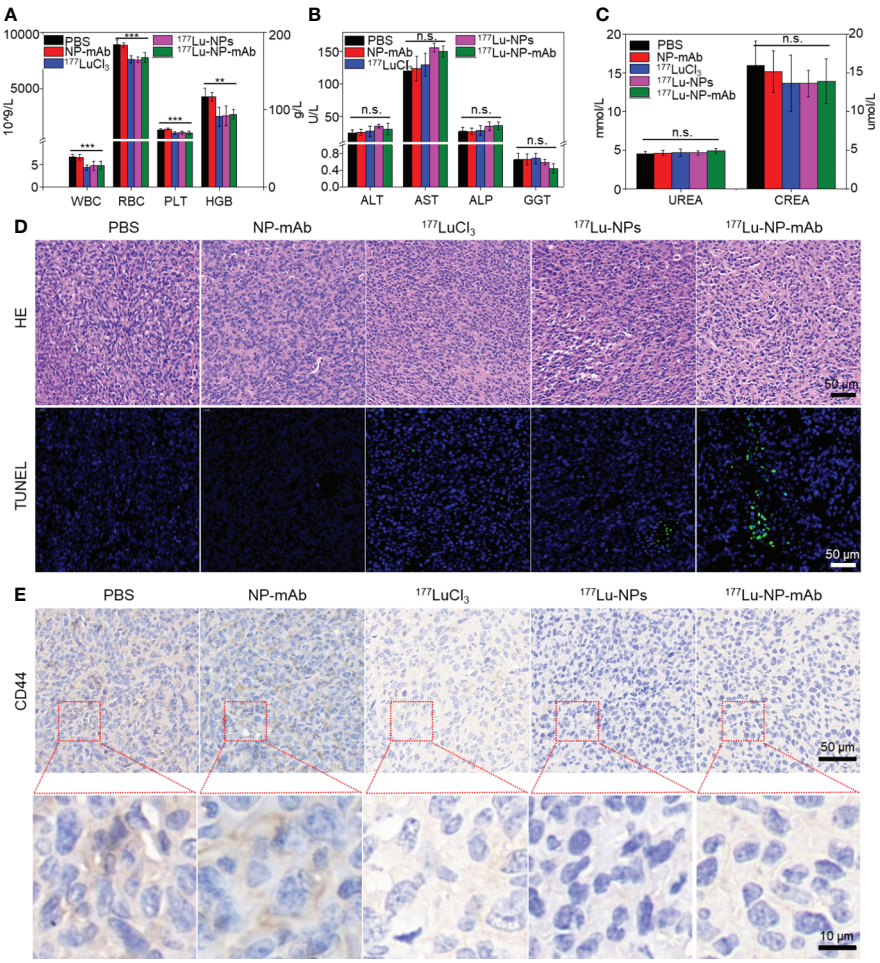

FIGURE 5
Histological evaluation and safety assay. **(A)** The blood routine tests of mice in different groups after 2 weeks post treatment. Asterisks indicate statistical significance (**P< 0.01, ***P< 0.001). **(B)** The liver function of mice in different groups after 2 weeks post treatment (n.s. indicates no significance). **(C)** The kidney function of mice in different groups after 2 weeks post treatment (n.s. indicates no significance). **(D)** Micrographs of H&E and TUNEL stained tumor slices from metastasis lymph nodes of mice with different groups at 2 weeks after treatment. Scale bar: 50 μm. **(E)** Micrographs of CD44 stained tumor slices from metastasis lymph nodes of mice with different groups at 2 weeks after treatment. Scale bar: 50/10 μm.

Materials and methods

Preparation of ^{68}Ga-NP-mAb and ^{177}Lu-NP-mAb

The detailed preparation of $NaGdF_4$:Yb,Tm@$NaLuF_4$ nanoparticles was provided in the Supporting Information. NP-mAb conjugation was prepared according to the previously reported methods (48). The ^{68}Ge/^{68}Ga generator (ITG, Germany) was eluted with 4 mL of 0.05 M HCl, and take the middle 2 ml of ^{68}Ga for labeling. ^{68}Ga solution (1 ml, 185-222 MBq) dissolved in 250 μL of 0.25 M sodium acetate (NaOAc) was added into the NP-mAb solution (1 mg/mL, 0.1 mL) and then stirred at room temperature for 30 min. The mixture was centrifuged at 3000 r/min for 5 min three times through 100 K ultrafiltration tube to remove the excess ^{68}Ga. The radiochemical purity of ^{68}Ga-NP-mAb was measured by paper chromatography (mobile phase: sodium citrate). $^{177}LuCl_3$-HCl solution (20 μL, 18.5–37MBq, ITM, Germany) dissolved in 20 μL of 0.25 M sodium acetate (NaOAc) was added into the NP-mAb solution (1 mg/mL, 0.05 mL) and then stirred at room temperature for 30 min. The mixture was centrifuged at 3000 r/min for 5 min three times through 100 K ultrafiltration tube to remove the excess ^{177}Lu. The radiochemical purity of ^{177}Lu-NP-mAb was measured by paper chromatography (mobile phase: EDTA). All radionuclide related work is carried out under perfect radiological protection.

In vitro experiments

The human breast cancer cell line SKBR3, MDA-MB-231 and human normal liver cell line HL-7702 were obtained from Cell Source Center, Chinese Academy of Science (Shanghai, China). SKBR3 cells were cultured and passaged in Dulbecco's Modified Eagle Medium (DMEM) supplemented with 10% fetal bovine serum (FBS), penicillin (100 U/mL), and streptomycin (0.1 mg/mL). MDA-MB-231 cells and HL-7702 cells were cultured and passaged in Roswell Park Memorial Institute 1640 Medium (RPMI-1640) supplemented with 10% fetal bovine serum (FBS), penicillin (100 U/mL), and streptomycin (0.1 mg/mL).

For *in vitro* potential toxicity assay, SKBR3 cells and HL-7702 cells were seeded in 96-well plates (5×10^3 cells/well) and cultured at 37°C overnight, respectively. The different concentrations of NP-mAb (0, 0.04, 0.16,0.31,1.25,2.5 and 5 mM) were added and cultured for 24 h. The cell culture medium was replaced by fresh medium in each well, and the cells were incubated for another 24 or 48 h. Cell viability was measured by the Cell Counting Kit-8 (CCK-8, Bimake, cat.no.B34304) assay.

For *in vitro* radioisotope therapy, SKBR3 cells were seeded in 96-well plates (5×10^3 cells/well) and cultured at 37°C overnight. The different concentrations of $^{177}LuCl_3$, ^{177}Lu-NPs and ^{177}Lu-NP-mAb (0, 0.3,0.6, 1.2,2.5,5,10,20 and 40 μCi) were added and then incubated for 24 h. The cell culture medium was replaced by fresh medium in each well, and the cells were incubated for another 24 h. Cell viability was measured by the CCK-8 assay.

For cell uptake experiments, SKBR3 cells and MDA-MB-231 cells were seeded onto a glass-bottom cell culture dish (Φ15 mm, NEST) at densities of 5×10^4 cells/well, respectively. After 12 h, SKBR3 cells were treated with NP-mAband NPs, respectively. MDA-MB-231 cells were treated with NP-mAb. After another 12 h of incubation, cells were stained with 4',6-diamidino-2-phenylindole (DAPI) and imaged by confocal microscopy (FV1200, OLYMPUS, Tokyo, Japan).

For γ-H2AX (Immunoway, cat.no.YT2154) staining studies, SKBR3 cells were seeded onto a glass-bottom cell culture dish (Φ15 mm, NEST) at densities of 5×10^4 cells/well. Cells were treated with PBS (control), NP-mAb, $^{177}LuCl_3$, ^{177}Lu-NPs and ^{177}Lu-NP-mAb, respectively. After 12 h of incubation, cells were stained with γ-H2AX and DAPI and then imaged by confocal microscopy (FV1200, OLYMPUS, Tokyo, Japan).

In vivo experiments

Female BALB/c nude mice (5-8 weeks) were purchased from Changzhou Cavens Company. All animal experiments were performed according to the experimental animal protocols of Soochow University, and the experiments were approved by the animal ethics committee of Soochow University.

To create the HER2-positive breast cancer lymphatic metastasis model, a single-cell suspension of 2×10^6 SKBR3 cells in 20 μL PBS was injected into the left footpad area of BALB/c nude mice. The popliteal lymph nodes could be palpated for enlargement and hardening after about 2 weeks, demonstrating that SKBR3 cells were successfully metastasized to the popliteal lymph nodes.

For *in vivo* NIRF imaging, mice bearing SKBR3 tumor were injected in the footpad with NP-mAb (120 μg/20 μl). NIRF imaging were acquired by IVIS at different time points before and after injection (Pre, 5 min, 1h, 3h, 5h). The imaging data were analyzed using Living Image®4.5 (PerkinElmer). For *in vivo* PET imaging, mice bearing SKBR3 tumor were injected into the footpad with ^{68}Ga-NP-mAb at radioactive dose of 100 μCi. Micro-PET was performed at different time points after injection (1h, 3h, 5h; n = 3). The imaging data were reconstructed and analyzed using Inveon Workplace (Siemens). The imaging data were reconstructed by 3-dimensional ordered subsets expectation maximum (3D OSEM) algorithm using Inveon Workplace (Siemens) without correction for attenuation or scatter. The CT data from the PET/CT examination were reconstructed in the coronal plane as 0.1-mm-thick sections. The following parameters were used for imaging: 80 kV, 100 mAs, 0.32 s per rotation. The imaging-derived percentage injected dose per gram (%ID/g) of lymphatic metastasis were calculated at Inveon Research WorkStation.

For *in vivo* SPECT imaging and bio-distribution studies, mice bearing SKBR3 tumor were injected into the footpad with ^{177}Lu- NP-mAb or ^{177}Lu- NPs at radioactive dose of 50 μCi. SPECT was performed using a general-purpose mouse collimator with 2.0 mm pinholes, and >1500 cps/MBq sensitivity with an U-SPECT+/CT imaging system (MILABS) at different time points after injection (Pre, 0.5d, 1d, 2d, 3d, 5d, and 7d; n = 3). Two 10-minute sets of data (frames) were acquired and combined. Pixel-based ordered subset expectation maximization (POSEM) reconstruction was used with 4 subsets, 6 iterations, and a 3D-Gaussian kernel (FWHM of 0.8 mm) filter. X-ray microCT was used for anatomic guidance and attenuation correction. The imaging data were reconstructed using the two-dimensional ordered subsets-expectation maximization algorithm. Volume rendered images were generated using professional PMOD software (MILabs).

Mice bearing SKBR3 lymphatic metastasis model were raised two weeks and then assigned into five groups including 1) PBS (control group), 2) NP-mAb treated group, 3) 177LuCl3 treated group (3.7 MBq per mouse), 4) ^{177}Lu-NPs treated group (3.7 MBq per mouse) and 5) ^{177}Lu- NP-mAb treated group (3.7 MBq per mouse corresponding to 50 ug of NP-mAb). These samples were injected in the left footpad area (n = 8), while the control group were

administrated with 0.02 mL of PBS (n = 8). After another two weeks, micro-MRI was used to measure the tumor volume in the foot pads and lymph node metastasis. The tumor volumes were calculated using the formula: ($V = \sum_{i=1}^{n} S_i \times h_i$) (49, 50). When the tumor volume reached 2 cm^3 or the weight loss exceeded 20%, the experiment was terminated and the animals were sacrificed.

Safety assessment

For immunofluorescence staining, the lymph node metastasis obtained from mice with different treatments including PBS, NP-mAb, 177LuCl3, ^{177}Lu- NPs and ^{177}Lu-NP-mAb were sliced and stained with anti-CD44 (abcam, Clone: EPR18668). Hematoxylin and eosin (H&E) staining and terminal deoxynucleotidyl transferase dUTP nick end labelling (TUNEL, Roche, cat.no.11684817910) assay also were carried out to evaluate morphologic changes and apoptosis of SKBR3 tumor cells. The mice were killed by cervical dislocation and the lymphatic metastases were surgically removed immediately. Then, the tissue samples of lymphatic metastases were fixed in 10% formalin before being stained and analyzed for pathological changes.

The blood routine, liver function and kidney function were investigated to evaluate the side effects of mice with different treatment. Blood routine assay including WBC, RBC, PLT and HGB were measured by XN-1000 F Automated Hematology Analyzer (KOBE, JAPAN). Liver and kidney functions including ALT, AST, ALP, GGT, UREA and CREA were measured by Clinical Chemistry Analyzer BS-420 (Mindray, China).

To study the antigen expression of SKBR3 cancer cells *in vivo*, immunocytochemistry was used to detect cell surface antigens. The lymph node metastasis obtained from mice with different treatments including PBS, NP-mAb, 177LuCl3, ^{177}Lu-NPs and ^{177}Lu- NP-mAb were homogenized in PBS (pH 7.4) containing 1% Fetal Bovine Serum (FBS) to acquire cell suspension. Afterwards, the SKBR3 cells were stained by anti-EpCAM (abcam, Clone: EPR20532-225) or anti-CD44 antibodies for flow cytometry assay.

Statistical analysis

All results are expressed as means ± SEM or SD as indicated. Significance between multiple groups was determined by one-way ANOVA analysis, t-test was used to compare the two groups of data. All statistical analyses were carried out using SPSS statistical software version 19.0 (IBM Corp., Armonk, NY, USA). $P<0.05$ was considered to indicate statistically significant differences.

Data availability statement

The original contributions presented in the study are included in the article/Supplementary Material. Further inquiries can be directed to the corresponding authors.

Ethics statement

The animal study was reviewed and approved by The animal ethics committee of Soochow University.

Author contributions

The manuscript was written through contributions of all authors. CZ, YZ and ML contributed equally. All authors contributed to the article and approved the submitted version.

Funding

This work was supported by the National Key Research Program of China (2018YFA0208800), National Natural Science Foundation of China (22076132, 21976128), the Natural Science Foundation of Jiangsu Province (BK20200100, BK20190830), Suzhou Administration of Science and Technology (SYS2020082), Key Talents Program for medical Application of nuclear Technology (XKTJ-HRC20210012) and the Project of State Key Laboratory of Radiation Medicine and Protection, Soochow University (GZK1201806).

Acknowledgments

We also would like to thank the members in the Zhu Lab at Soochow University and the members in the Wang Lab in Nanjing First Hospital, Nanjing Medical University. Thanks to the Jiangsu Province International Joint Laboratory For Regeneration Medicine.

Conflict of interest

The authors declare that the research was conducted in the absence of any commercial or financial relationships that could be construed as a potential conflict of interest.

Publisher's note

All claims expressed in this article are solely those of the authors and do not necessarily represent those

of their affiliated organizations, or those of the publisher, the editors and the reviewers. Any product that may be valuated in this article, or claim that may be made by its manufacturer, is not guaranteed or endorsed by the publisher.

Supplementary material

The Supplementary Material for this article can be found online at: https://www.frontiersin.org/articles/10.3389/fimmu.2022.1063678/full#supplementary-material

References

1. Steeg PS. Tumor metastasis: mechanistic insights and clinical challenges. *Nat Med* (2006) 12(8):895–904. doi: 10.1038/nm1469

2. Leong SPL, Tseng WW. Micrometastatic cancer cells in lymph nodes, bone marrow, and blood: Clinical significance and biologic implications. *CA: A Cancer J Clin* (2014) 64(3):195–206. doi: 10.3322/caac.21217

3. Xie Y, Bagby TR, Cohen MS, Forrest ML. Drug delivery to the lymphatic system: importance in future cancer diagnosis and therapies. *Expert Opin Drug Delivery* (2009) 6(8):785–92. doi: 10.1517/17425240903085128

4. Detmar M, Hirakawa S. The formation of lymphatic vessels and its importance in the setting of malignancy. *J Exp Med* (2002) 196(6):713–8. doi: 10.1084/jem.20021346

5. Nathanson SD. Insights into the mechanisms of lymph node metastasis. *Cancer* (2003) 98(2):413–23. doi: 10.1002/cncr.11464

6. Peters J, Foord S, Dieguez C, Salvador J, Hall R, Scanlon MF. Lack of effect of the TRH related dipeptide histidyl-proline diketopiperazine on TSH and PRL secretion in normal subjects, in patients with microprolactinomas and in primary hypothyroidism. *Clin Endocrinol (Oxf)* (1985) 23(3):289–93. doi: 10.1111/j.1365-2265.1985.tb00226.x

7. Giuliano AE, Hunt KK, Ballman KV, Beitsch PD, Whitworth PW, Blumencranz PW, et al. Axillary dissection vs no axillary dissection in women with invasive breast cancer and sentinel node metastasis: A randomized clinical trial. *JAMA* (2011) 305(6):569–75. doi: 10.1001/jama.2011.90

8. Donker M, van Tienhoven G, Straver ME, Meijnen P, van de Velde CJ, Mansel RE, et al. Radiotherapy or surgery of the axilla after a positive sentinel node in breast cancer (EORTC 10981-22023 AMAROS): a randomised, multicentre, open-label, phase 3 non-inferiority trial. *Lancet Oncol* (2014) 15(12):1303–10. doi: 10.1016/S1470-2045(14)70460-7

9. World Health Organization (WHO) and International Agency for Research on Cancer. *The global cancer observatory: Breast fact sheet* (2020). Available at: https://gco.iarc.fr/today/data/factsheets/cancers/20-Breast-fact-sheet.pdf.

10. Thongvitokomarn S, Polchai N. Indocyanine green fluorescence versus blue dye or radioisotope regarding detection rate of sentinel lymph node biopsy and nodes removed in breast cancer: A systematic review and meta-analysis. *Asian Pac J Cancer Prev* (2020) 21(5):1187–95. doi: 10.31557/APJCP.2020.21.5.1187

11. Ang CH, Tan MY, Teo C, Seah DW, Chen JC, Chan MYP, et al. Blue dye is sufficient for sentinel lymph node biopsy in breast cancer. *Br J Surg* (2014) 101 (4):383–9. doi: 10.1002/bjs.9390

12. Guo JJ, Yang HP, Wang S, Cao YM, Liu M, Xie F, et al. Comparison of sentinel lymph node biopsy guided by indocyanine green, blue dye, and their combination in breast cancer patients: a prospective cohort study. *World J Surg Oncol* (2017) 15:1477–7819. doi: 10.1186/s12957-017-1264-7

13. Zhou Y, Li Y, Mao F, Zhang J, Zhu Q, Shen S, et al. Preliminary study of contrast-enhanced ultrasound in combination with blue dye vs. indocyanine green fluorescence, in combination with blue dye for sentinel lymph node biopsy in breast cancer. *BMC Cancer* (2019) 19(1):939. doi: 10.1186/s12885-019-6165-4

14. Speers C, Pierce LJ. Postoperative radiotherapy after breast-conserving surgery for early-stage breast cancer: A review. *JAMA Oncol* (2016) 2(8):1075–82. doi: 10.1001/jamaoncol.2015.5805

15. Krug D, Baumann R, Budach W, Dunst J, Feyer P, Fietkau R, et al. Current controversies in radiotherapy for breast cancer. *Radiat Oncol* (2017) 12(1):25. doi: 10.1186/s13014-017-0766-3

16. Darby SC, Ewertz M, McGale P, Bennet AM, Blom-Goldman U, Bronnum D, et al. Risk of ischemic heart disease in women after radiotherapy for breast cancer. *New Engl J Med* (2013) 368(11):987–98. doi: 10.1056/NEJMoa1209825

17. Lettmaier S, Kreppner S, Lotter M, Walser M, Ott OJ, Fietkau R, et al. Radiation exposure of the heart, lung and skin by radiation therapy for breast cancer: A dosimetric comparison between partial breast irradiation using multicatheter brachytherapy and whole breast teletherapy. *Radiother Oncol* (2011) 100(2):189–94. doi: 10.1016/j.radonc.2010.07.011

18. Werner EM, Eggert MC, Bohnet S, Rades D. Prevalence and characteristics of pneumonitis following irradiation of breast cancer. *Anticancer Res* (2019) 39 (1791-7530):6355–8. doi: 10.21873/anticanres.13847

19. Taylor C, Correa C, Duane FK, Aznar MC, Anderson SJ, Bergh J, et al. Estimating the risks of breast cancer radiotherapy: Evidence from modern radiation doses to the lungs and heart and from previous randomized trials. *J Clin Oncol* (2017) 35(1527-7755):1641–9. doi: 10.1200/JCO.2016.72.0722

20. Mougalian SS, Soulos PR, Killelea BK, Lannin DR, Abu-Khalaf MM, DiGiovanna MP, et al. Use of neoadjuvant chemotherapy for patients with stage I to III breast cancer in the united states. *Cancer* (2015) 121(1097-0142):2544–52. doi: 10.1002/cncr.29348

21. Ryan GM, Kaminskas LM, Bulitta JB, McIntosh MP, Owen DJ, Porter CJH. PEGylated polylysine dendrimers increase lymphatic exposure to doxorubicin when compared to PEGylated liposomal and solution formulations of doxorubicin. *J Controlled Release* (2013) 172(1):128–36. doi: 10.1016/j.jconrel.2013.08.004

22. Kaminskas LM, Ascher DB, McLeod VM, Herold MJ, Le CP, Sloan EK, et al. PEGylation of interferon alpha2 improves lymphatic exposure after subcutaneous and intravenous administration and improves antitumour efficacy against lymphatic breast cancer metastases. *J Controlled Release* (2013) 168(2):200–8. doi: 10.1016/j.jconrel.2013.03.006

23. Love RR, Leventhal H, Easterling DV, Nerenz DR. Side effects and emotional distress during cancer chemotherapy. *Cancer* (1989) 63(3):604–12. doi: 10.1002/1097-0142(19890201)63:3<604::AID-CNCR2820630334>3.0.CO;2-2

24. Hawley AE, Davis SS, Illum L. Targeting of colloids to lymph nodes: influence of lymphatic physiology and colloidal characteristics. *Adv Drug Del Rev* (1995) 17(1):129–48. doi: 10.1016/0169-409X(95)00045-9

25. Swartz MA. The physiology of the lymphatic system. *Adv Drug Del Rev* (2001) 50(1):3–20. doi: 10.1016/S0169-409X(01)00150-8

26. Kaminskas LM, Kota J, McLeod VM, Kelly BD, Karellas P, Porter CJH. PEGylation of polylysine dendrimers improves absorption and lymphatic targeting following SC administration in rats. *J Controlled Release* (2009) 140(2):108–16. doi: 10.1016/j.jconrel.2009.08.005

27. Oussoren C, Zuidema J, Crommelin DJA, Storm G. Lymphatic uptake and biodistribution of liposomes after subcutaneous injection.: II. influence of liposomal size, lipid composition and lipid dose. *Biochim Biophys Acta (BBA) - Biomembranes* (1997) 1328(2):261–72. doi: 10.1016/S0005-2736(97)00122-3

28. Brannon-Peppas L, Blanchette JO. Nanoparticle and targeted systems for cancer therapy. *Adv Drug Del Rev* (2012) 64:206–12. doi: 10.1016/j.addr.2012.09.033

29. Alexis F, Pridgen EM, Langer R, Farokhzad OC. *Nanoparticle technologies for cancer therapy*. Berlin Heidelberg: Springer (2010) p. 55–86.

30. Li B, Yuan Z, He Y, Hung HC, Jiang S. Zwitterionic nanoconjugate enables safe and efficient lymphatic drug delivery. *Nano Lett* (2020) 20(6):4693–9. doi: 10.1021/acs.nanolett.0c01713

31. Cote B, Rao D, Alany RG, Kwon GS, Alani AWG. Lymphatic changes in cancer and drug delivery to the lymphatics in solid tumors. *Adv Drug Delivery Rev* (2019) 144(1872-8294):16–34. doi: 10.1016/j.addr.2019.08.009

32. Fang J, Nakamura H, Maeda H. The EPR effect: Unique features of tumor blood vessels for drug delivery, factors involved, and limitations and augmentation of the effect. *Adv Drug Del Rev* (2011) 63(3):136–51. doi: 10.1016/j.addr.2010.04.009

33. Maeda H. Macromolecular therapeutics in cancer treatment: The EPR effect and beyond. *J Controlled Release* (2012) 164(2):138–44. doi: 10.1016/j.jconrel.2012.04.038

34. Swain S, Sahu PK, Beg S, Babu SM. Nanoparticles for cancer targeting: Current and future directions. *Curr Drug Delivery* (2016) 13(8):1290–302. doi: 10.2174/1567201813666160713121122

35. Wang M, Thanou M. Targeting nanoparticles to cancer. *Pharmacol Res* (2010) 62(2):90–9. doi: 10.1016/j.phrs.2010.03.005

36. Bazak R, Houri M, El Achy S, Kamel S, Refaat T. Cancer active targeting by nanoparticles: a comprehensive review of literature. *J Cancer Res Clin Oncol* (2015) 141(5):769–84. doi: 10.1007/s00432-014-1767-3

37. Asif HM, Sultana S, Ahmed S, Akhtar N, Tariq M. HER-2 positive breast cancer - a mini-review. *Asian Pac J Cancer Prev* (2016) 17(4):1609–15. doi: 10.7314/APJCP.2016.17.4.1609

38. Harbeck N, Gnant M. Breast cancer. *Lancet* (2017) 389(10074):1134–50. doi: 10.1016/S0140-6736(16)31891-8

39. Chattopadhyay N, Cai Z, Pignol J-P, Keller B, Lechtman E, Bendayan R, et al. Design and characterization of HER-2-Targeted gold nanoparticles for enhanced X-radiation treatment of locally advanced breast cancer. *Mol Pharm* (2010) 7(6):2194–206. doi: 10.1021/mp100207t

40. Su C-Y, Chen M, Chen L-C, Ho Y-S, Ho H-O, Lin S-Y, et al. Bispecific antibodies (anti-mPEG/anti-HER2) for active tumor targeting of docetaxel (DTX)-loaded mPEGylated nanocarriers to enhance the chemotherapeutic efficacy of HER2-overexpressing tumors. *Drug Delivery* (2018) 25(1):1066–79. doi: 10.1080/10717544.2018.1466936

41. Ren F, Ding L, Liu H, Huang Q, Zhang H, Zhang L, et al. Ultra-small nanocluster mediated synthesis of Nd3+-doped core-shell nanocrystals with emission in the second near-infrared window for multimodal imaging of tumor vasculature. *Biomaterials* (2018) 175:30–43. doi: 10.1016/j.biomaterials.2018.05.021

42. Ren J, Jia G, Guo Y, Wang A, Xu S. Unraveling morphology and phase control of NaLnF4 upconverting nanocrystals. *J Phys Chem C* (2016) 120(2):1342–51. doi: 10.1021/acs.jpcc.5b11048

43. Wang X, Zhuang J, Peng Q, Li Y. A general strategy for nanocrystal synthesis. *Nature* (2005) 437(7055):121–4. doi: 10.1038/nature03968

44. Johnson NJ, Korinek A, Dong C, van Veggel FC. Self-focusing by ostwald ripening: a strategy for layer-by-layer epitaxial growth on upconverting nanocrystals. *J Am Chem Soc* (2012) 134(27):11068–71. doi: 10.1021/ja302717u

45. Li X, Dong Q, Yan Z, Lu W, Feng L, Xie C, et al. MPEG-DSPE polymeric micelle for translymphatic chemotherapy of lymph node metastasis. *Int J Pharm* (2015) 487(1-2):8–16. doi: 10.1016/j.ijpharm.2015.03.074

46. Long J, Luo G, Liu C, Cui X, Satoh K, Xiao Z, et al. Development of a unique mouse model for pancreatic cancer lymphatic metastasis. *Int J Oncol* (2012) 41(5):1662–8. doi: 10.3892/ijo.2012.1613

47. Al-Othman N, Alhendi A, Ihbaisha M, Barahmeh M, Alqaraleh M, Al-Momany BZ. Role of CD44 in breast cancer. *Breast Dis* (2020) 39(1):1–13. doi: 10.3233/BD-190409

48. Qiu S, Zeng J, Hou Y, Chen L, Ge J, Wen L, et al. Detection of lymph node metastasis with near-infrared upconversion luminescent nanoprobes. *Nanoscale* (2018) 10(46):21772–81. doi: 10.1039/C8NR05811C

49. Dempsey MF, Condon BR, Hadley DM. Measurement of tumor "size" in recurrent malignant glioma: 1D, 2D, or 3D? *AJNR Am J Neuroradiol* (2005) 26(4):770–6.

50. Hamoud Al-Tamimi MS, Sulong G, Shuaib IL. Alpha shape theory for 3D visualization and volumetric measurement of brain tumor progression using magnetic resonance images. *Magn Reson Imaging* (2015) 33(6):787–803. doi: 10.1016/j.mri.2015.03.008

frontiers | Frontiers in Immunology

TYPE Review
PUBLISHED 08 December 2022
DOI 10.3389/fimmu.2022.1067036

OPEN ACCESS

EDITED BY
Fei Yu,
Tongji University School of Medicine, China

REVIEWED BY
Ran Zhu,
Soochow University, China
Rohimah Mohamud,
Universiti Sains Malaysia (USM), Malaysia

*CORRESPONDENCE
Fan Xia
tcxiafan@hotmail.com
Zhen Zhang
zhen_zhang@fudan.edu.cn

†These authors have contributed equally to this work

SPECIALTY SECTION
This article was submitted to Cancer Immunity and Immunotherapy, a section of the journal Frontiers in Immunology

RECEIVED 11 October 2022
ACCEPTED 24 November 2022
PUBLISHED 08 December 2022

CITATION
Wang Y, Shen L, Wan J, Zhang H, Wu R, Wang J, Wang Y, Xu Y, Cai S, Zhang Z and Xia F (2022) Neoadjuvant chemoradiotherapy combined with immunotherapy for locally advanced rectal cancer: A new era for anal preservation. *Front. Immunol.* 13:1067036. doi: 10.3389/fimmu.2022.1067036

Neoadjuvant chemoradiotherapy combined with immunotherapy for locally advanced rectal cancer: A new era for anal preservation

Yaqi Wang[1,2,3,4], Lijun Shen[1,2,3,4], Juefeng Wan[1,2,3,4], Hui Zhang[1,2,3,4], Ruiyan Wu[1,2,3,4], Jingwen Wang[1,2,3,4], Yan Wang[1,2,3,4], Ye Xu[2,5], Sanjun Cai[2,5], Zhen Zhang[1,2,3,4*†] and Fan Xia[1,2,3,4*†]

[1]Department of Radiation Oncology, Fudan University Shanghai Cancer Center, Shanghai, China, [2]Department of Oncology, Shanghai Medical College, Fudan University, Shanghai, China, [3]Shanghai Clinical Research Center for Radiation Oncology, Shanghai, China, [4]Shanghai Key Laboratory of Radiation Oncology, Shanghai, China, [5]Department of Colorectal Surgery, Fudan University Shanghai Cancer Center, Shanghai, China

For locally advanced (T3-4/N+M0) rectal cancer (LARC), neoadjuvant chemoradiotherapy (nCRT) followed by total mesorectal excision (TME) is the standard treatment. It was demonstrated to decrease the local recurrence rate and increase the tumor response grade. However, the distant metastasis remains an unresolved issue. And the demand for anus preservation and better quality of life increases in recent years. Radiotherapy and immunotherapy can be supplement to each other and the combination of the two treatments has a good theoretical basis. Recently, multiple clinical trials are ongoing in terms of the combination of nCRT and immunotherapy in LARC. It was reported that these trials achieved promising short-term efficacy in both MSI-H and MSS rectal cancers, which could further improve the rate of clinical complete response (cCR) and pathological complete response (pCR), so that increase the possibility of 'Watch and Wait (W&W)' approach. However, the cCR and pCR is not always consistent, which occurs more frequent when nCRT is combined with immunotherapy. Thus, the efficacy evaluation after neoadjuvant therapy is an important issue for patient selection of W&W approach. Evaluating the cCR accurately needs the combination of multiple traditional examinations, new detective methods, such as PET-CT, ctDNA-MRD and various omics studies. And finding accurate biomarkers can help guide the risk stratification and treatment decisions. And large-scale clinical trials need to be performed in the future to demonstrate the surprising efficacy and to explore the long-term prognosis.

KEYWORDS

locally advanced rectal cancer, neoadjuvant chemoradiotherapy, immunotherapy, tumor response, anus preservation, research progress

Introduction

For locally advanced rectal cancer (LARC, T3-4/N+M0), the standard treatment is neoadjuvant chemoradiotherapy (nCRT) combined with total mesorectal excision (TME) followed by adjuvant chemotherapy. nCRT reduces local recurrence, promotes tumor downgrading, and improves the anus-preservation rate. Some patients can even achieve pathological complete response (pCR) (1), thus obtaining a better prognosis. Patients who achieve a clinical complete response (cCR) are also candidates for the nonoperative watch and wait (W&W) approach (2) to obtain better quality of life. However, given the increasing demand to achieve tumor regression and anus preservation in recent years, the traditional nCRT treatment model has encountered a bottleneck. Further improving tumor regression and long-term survival has become a challenge. In addition, reducing toxicity and improving quality of life also represent important issues. At present, significant efforts have been made to develop immunotherapy-based regimens. The use of nCRT combined with immunotherapy has also been studied recently in LARC patients, yielding gratifying short-term efficacy. The Immune-stimulating effect of nCRT could potentially overcome the resistance of microsatellite stable (MSS) colorectal cancer to immunotherapy and serve as a good paradigm for achieving synergistic optimization.

Current status of neoadjuvant chemoradiotherapy for locally advanced rectal cancer

For LARC patients, neoadjuvant radiotherapy includes long-course radiotherapy (LCRT, 50 Gy/25 Fx, 5-Fu or capecitabine sensitization) and short-course radiotherapy (SCRT, 25 Gy/5 Fx). nCRT can significantly reduce the local recurrence rate (<10%) and has become the standard treatment based on NCCN guidelines. The pCR rate for standard treatment is only 10-20%, and it did not improve the long-term prognosis.

To improve the efficacy of neoadjuvant therapy, researchers have attempted to increase the treatment intensity of nCRT. The CinClare study confirmed that the addition of irinotecan to nCRT could increase the pCR rate compared with the standard nCRT group (30.0% vs 15.0%) (3). Recently, researchers have tried to advance adjuvant chemotherapy ahead of surgery through the use of consolidation chemotherapy (4), induction chemotherapy (5), or even total neoadjuvant therapy (TNT) (6). Multiple clinical trials demonstrated that TNT could increase the complete response (CR, pCR + cCR) rate to greater than 30% and improve the anus-preservation rate. TNT also improved compliance with nCRT and controlled distant metastasis early, providing patients with sufficient systemic treatment to achieve long-term benefits.

However, given the increasing demand for anal preservation and good quality of life, the CR rate of TNT remains insufficient, especially for those with tumors in lower locations. To further improve efficacy, risk stratification, population selection, sensitivity testing and precision treatment are new directions worth exploring. New antitumor methods, such as immunotherapy (PD-1/PD-L1 monoclonal antibody), have gradually been introduced to the field of nCRT for LARC patients.

Theoretical basis of nCRT combined with immunotherapy

In recent years, immunotherapy has achieved great success in the treatment of a variety of malignant tumors and has become a new pillar of anticancer treatment. Microsatellite instability-high (MSI-H) patients have a higher tumor mutation burden (TMB) and increased tumor-infiltrating lymphocytes (TILs), which have naturally high sensitivity for immunotherapy (7, 8). The Keynote-177 study suggested that pembrolizumab monotherapy should be used as a new standard of first-line treatment for patients with metastatic dMMR/MSI-H colorectal cancer (9). However, dMMR/MSI-H tumors accounted for less than 5% of colorectal tumors, and greater than 95% of the tumors were classified as MSS tumors that are not very sensitive to immunotherapy alone. Therefore, improving the efficacy of MSS colorectal cancer is of great significance.

Preclinical studies have shown that radiotherapy promotes antitumor immunity. Radiotherapy induces the immunogenic death (ICD) of tumor cells; releases proinflammatory signals, such as neoantigens and damage-associated molecular patterns (DAMPs); and promotes the activation of antitumor T cells and the accumulation of TILs (10, 11). Radiotherapy can induce the upregulation of PD-L1 expression in tumor tissues and increase the sensitivity to immunotherapy. Radiotherapy combined with PD-L1 antibody can simultaneously regulate the tumor microenvironment, relieve its immunosuppressive effect, and enhance T-cell-derived antitumor cytokines (12, 13). Clinical studies of radiotherapy combined with immunotherapy have also observed the 'abscopal effect' (14, 15), which means that when a tumor at a certain location was treated with radiation, the tumor at another remote location also achieved a significant regression at the same time, probably because the radiation activates the systemic immune response. The above evidence shows that radiotherapy is expected to become one of the best types of therapy to combine with immunotherapy. Thus, through a mutual sensitization effect, the combination of nCRT and immunotherapy promotes synergism between local and systemic treatments, thereby achieving better tumor regression and long-term prognosis.

And the pathological files of the surgical specimens after nCRT and immunotherapy demonstrated the above changes, mainly including the following three features (16), i) Immune activation, as indicated by lymphoid infiltrates, tertiary lymphoid structures, and plasma cells; ii) Cell death, signified by foamy macrophages and cholesterol clefts; iii) The identification and histologic description of a tumor regression, including features of tissue repair, in particular proliferative fibrosis and neovascularization. And in terms of the LARC after nCRT plus immunotherapy in our cancer center, lymphocytic infiltration, cell necrosis and proliferative fibrosis and neovascularization are also found in post-surgery specimens.

Currently, the application of immunotherapy has gradually moved from posterior-line therapy to first-line therapy for metastatic cancers and has begun to be applied to adjuvant and neoadjuvant therapies for early-stage cancers. At the stage of neoadjuvant therapy, patients are generally in a better condition and are more susceptible to adverse treatment reactions. In terms of neoadjuvant therapy for colorectal cancer, the NICHE study and the PICC study confirmed that immunotherapy can increase the pCR rate of MSI-H/dMMR patients to greater than 60% (17, 18). At the 2022 ASCO Annual Meeting, it was reported that PD-1 monotherapy used in MSI-H/dMMR LARC achieved a cCR rate of 100% (14/14) (19). For MSS LARC patients, an increasing number of researchers are exploring the use of chemoradiotherapy combined with PD-1/PD-L1 inhibitors, and good results have been obtained.

Clinical trials of nCRT combined with immunotherapy

Currently, numerous clinical studies on nCRT combined with immunotherapy have reported preliminary results. Most of the studies were prospective stage I-II trials with small sample sizes. The enrolled patients were mainly classified as having MSS tumors. The primary endpoints included the main indicators of tumor regression, such as the pCR rate, cCR rate, TRG, and NAR score, as well as treatment safety (the incidence of adverse reactions). The study designs included both LCRT (conventional fractionated radiation, 50 Gy/25 Fx) and SCRT (hypofractionated radiation, 25 Gy/5 Fx), and the sequences of immunotherapy and nCRT varied greatly (sequential or concurrent). Major information of clinical trials with published data is summarized in Table 1 (LCRT-based trials) and Table 2 (SCRT-based trials). And for detailed information of all ongoing clinical trials, please refer to Supplementary Table 1 and Supplementary Table 2.

Long-course nCRT combined with immunotherapy

LCRT and immunotherapy are mainly combined through two modes: sequential or concurrent.

TABLE 1 Major clinical trials of the long course radiotherapy (LCRT) combined with immunotherapy for LARC.

Study	Phase	No.	Features	Study design	Results
Voltage-A	Ib	37	III 23%	LCRT → Nivo*5 → TME	pCR 30%
NSABP FR-2	II	45	III 89%	LCRT → Durva*4 → TME	mNAR 12.03 pCR 22.2% cCR 31.1%
PANDORA	II	55	T3-4 95% N+ 79%	LCRT → Nivo*3 → TME	pCR 32.7% MPR 25.5%
AVANA	II	100	III 94%	LCRT Avelumab*6 → TME	pCR 23% MPR 60%
R-IMMUNE	Ib	25	III 92%	LCRT Atezolizumab*4 → TME	pCR 24%
NRG -GI002	II	95	High risk+	FOLFOX*8 → LCRT Pembro*6 → TME	pCR 31.9% cCR 13.9%
PKUCH 04	II	25	76% N2 56% MRF+	CAPOX Camrelizumab *3 → LCRT → CAPOX*2 → TME	pCR 33.3% cCR 16% MPR 25%
Changhai	II	23	Super-low cT2 56.5% cN0 69.6%	LCRT Sintilimab*2 → CAPOX*6 Sintilimab*2 → TME	cCR 43.5% ncCR 26.1% Anal preservation 95.5% CR 52.2%
Beijing Friendship	II	12	cT3N0 cT1-3N+	LCRT Tislelizu*2 → Cape*1 Tislelizu*1 → TME	pCR 58.3%

10.3389/fimmu.2022.1067036

TABLE 2 Major clinical trials of the short course radiotherapy (SCRT) combined with immunotherapy for LARC.

Study	Phase	No.	Features	Study design	Results
Wuhan	II	26	High risk+	SCRT → CAPOX Camrelizumab *2 → TME	pCR 46%
Averectal	II	40	III 91%	SCRT → FOLFOX Avelumab *6 → TME	pCR 37.5% MPR 67.5%

The trials using sequential immunotherapy followed by nCRT mainly included VOLTAGE-A, NSABPFR-2, and PANDORA, all of which achieved better tumor responses than the standard nCRT regimen. The first results were reported by the VOLTAGE-A study in Japan (20). This study used traditional nCRT (50.4 Gy/25 Fx/capecitabine) followed by 5 courses of nivolumab monotherapy. The results showed that among the 37 MSS patients, 11 patients achieved pCR (30%), 3 patients achieved near-pCR (8%), and 1 patient achieved cCR and adopted the W&W approach. Only 3 patients experienced grade 3-4 toxicities. The American NSABPFR-2 trial (21) reported at the 2022 ASCO GI conference enrolled 45 patients with stage II-IV rectal cancer who received 4 courses of durvalumab monotherapy after nCRT followed by TME surgery. The primary endpoint was the neoadjuvant therapy (NAR) score. The results showed that the patient's mNAR score was 12.03, the pCR rate was 22.2%, the cCR rate was 31.1%, the R0 resection rate was 81.0%, and the anus-preservation rate was 71.4%. The main grade 3 toxicities included diarrhea, lymphopenia and low back pain. Only one patient had grade 4 adverse reactions (elevated amylase/lipase). Results from the Italian PANDORA study were reported at the 2022 ASCO Annual Meeting (22). The study used the Simon two-stage design. A total of 55 patients with LARC were enrolled. After nCRT (50.4 Gy/25 Fx/capecitabine), three courses of durvalumab monotherapy were administered. The results showed that 34.5% (19/55) of patients achieved pCR (TRG 0), 25.5% (14/55) of patients achieved near-pCR (TRG 1), and the Major Pathologic Response (MPR, less than 10% of the residual tumor compared with the baseline) rate was 60.0%. In addition, a low rate of grade 3-4 toxicities for nCRT or durvalumab was observed. The pCR rate of traditional nCRT was approximately 15-20%, and the overall CR rates (pCR + cCR) in these three studies all reached 30% or greater, suggesting that the combination of nCRT and immunotherapy achieved a good tumor response.

Trials of nCRT concurrent with immunotherapy included the ANAVA and R-IMMUE studies. The Italian ANAVA study reported at the 2021 ASCO Annual Meeting (23) enrolled 101 LARC patients. These patients were administered 6 courses of avelumab starting on the first day of nCRT. Among the 96 patients with final pathological results, 22 cases (23%) reached pCR, and 59 cases (61.5%) reached MPR. The rates of grade 3-4 nonimmune and immune-related toxicity were only 8% and 4%, respectively. The 2021 ESMO Annual Meeting reported the preliminary results of the Belgian R-IMMUNE study (24). Currently, the enrollment and treatment of phase Ib (6 cases) and the first stage (20 cases) of phase II (Simon two-stage design) have been completed. The enrolled patients were randomly divided into the standard nCRT group (45-50 Gy/5-Fu) and the nCRT-immunotherapy combination group (45-50 Gy/5-Fu + atezolizumab for 4 courses). The primary endpoint was the toxicity rate, and the secondary endpoint was the pCR rate. Preliminary results reported that 13% of patients experienced grade 3-4 toxicities (20/151 adverse events, including anastomotic fistula and infection in 10% of patients, urinary infection in 20%, renal function impairment in 5%, and immune-related thrombocytopenia in 5%; 34.6% (9/26) patients), and the pCR rate was 24% (6/25).

In addition, two additional studies implemented a TNT-like design. The 2021 ASCO-GI conference reported the results of the pembrolizumab cohort of the NRG-GI002 study (25). The control group received 8 courses of FOLFOX chemotherapy followed by nCRT concurrent with capecitabine, and the study group received 8 courses of FOLFOX chemotherapy followed by nCRT concurrent with capecitabine and pembrolizumab. The study endpoint was the NAR score. The results showed that the average NAR score of the control group and the pembrolizumab group were 14.08 and 11.53, respectively, and the difference was not statistically significant (P=0.26). The pCR values for the control group and the pembrolizumab group were 29.4% vs. 31.9% (P=0.75), respectively, and the cCR values were 13.6% vs. 13.9% (P=0.95), respectively. Although the statistical results showed that the tumor regression rates were similar in the two groups, the pCR+cCR rates in both groups were as high as approximately 44%. Thus, approximately half of patients achieved complete tumor remission, suggesting that the combination of the TNT pattern and immunotherapy is conducive to achieving the maximum degree of tumor regression. However, the addition of immunotherapy in this study failed to further improve tumor regression, which may be related to the low completion rate of pembrolizumab. Moreover, because lymphocytes are very sensitive to radiation, when radiotherapy is concurrently used with immunotherapy,

radiotherapy may kill locally accumulated or activated lymphocytes, thereby adversely affecting the immune response.

Another PKUCH04 study conducted in Beijing (26) included 25 high-risk LARC patients. These patients received 3 courses of CAPOX chemotherapy combined with camerelizumab followed by LCRT, 2 courses of CAPOX chemotherapy and finally TME surgery or the W&W strategy. Eventually, 21 patients underwent TME surgery, 7 patients achieved pCR (33.3%, 7/21), and 15 patients achieved MPR (71.4%, 15/21). The remaining 4 patients achieved cCR or near-cCR after neoadjuvant therapy and eventually chose the W&W strategy. The major grade 3-4 adverse reactions included lymphopenia in 24% of patients, diarrhea in 8%, and platelet reduction in 4%. No grade 4 adverse reactions occurred. The above two TNT-designed nCRT combined with immunotherapy achieved a CR rate of approximately 50% in LARC patients, significantly improving tumor regression compared with the traditional nCRT model.

Short-course radiotherapy combined with immunotherapy

SCRT and sequential chemotherapy are also commonly used modes of neoadjuvant treatment for LARC patients that can achieve pCR rates similar to those of LCRT. Studies have shown that the combination of hypofractionated SCRT and immunotherapy has more advantages. Hypofractionated SCRT has less of an effect on the peripheral blood lymphocytes of patients, thus promoting the antitumor effect of the immune system (27). Hypofractionated SCRT inhibits the recruitment of myeloid-derived suppressor cells (MDSCs) into tumors, reduces the expression of PD-L1 on the tumor surface and achieves a tumor growth inhibition rate that is superior to that of conventional fractionation (28). Moreover, abscopal effects in mice were also observed when hypofractionated radiotherapy was combined with immunotherapy (29).

A Chinese phase II study assessed SCRT (25 Gy/5 Fx) followed by 2 courses of XELOX plus carrelizumab and TME surgery (30). Among the 27 patients who underwent surgery (26 pMMR patients and 1 dMMR patient), the pCR rate was as high as 48% (13/27). The pCR rate in the pMMR subgroup was 46% (12/26), and the pCR rate in the dMMR subgroup was 100% (1/1). The R0 resection rate was 100%, the anal preservation rate was 89% (24/27), and the tumor downstaging rate was 70% (19/27). In this study, most patients had high risk factors for recurrence and metastasis (T4/N2/MRF+). This study achieved a very high pCR rate within only 2 months. This value even exceeded the pCR rate of the TNT model, which had the highest treatment intensity. These findings suggest that the combination of hypofractionated radiotherapy and immunotherapy may have a better effect, which was consistent with preclinical research. In addition, no serious adverse effects were observed, and grade 3 hematological toxicity could be alleviated after treatment in time. At present, a phase III multicenter clinical study is ongoing in the same cancer center.

The Averectal study conducted in Lebanon and Jordan recruited a total of 44 LARC patients who were treated with SCRT combined with 6 courses of mFOLFOX6 and avelumab (31). Except for 4 patients who were excluded from the analysis for various reasons, 15 of the remaining 40 patients achieved pCR (37.5%), and 12 patients achieved near-pCR (TRG 1, 30%). Thus, 67.5% of patients achieved very significant tumor regression. Additionally, the patients did not experience grade 3-4 immune-related toxicity, and the incidence of grade 3-4 surgery-related complications was only 5%. In addition, immunohistochemical staining of TILs was performed to calculate the immunoscore (IS). It was found that a higher IS was associated with a higher pCR rate.

In addition, another phase II trial named the TORCH study adopted the SCRT-based TNT model (32, 33) and reported surprising efficacy results for tumor regression at the 2022 ASCO Annual Meeting. This study included 130 patients who were randomly divided into the consolidation group and the induction group. Patients in the consolidation group first received SCRT followed by 6 courses of CAPOX and toripalimab. Patients in the induction group received 2 courses of CAPOX and toripalimab followed by SCRT and then 4 courses of CAPOX and toripalimab. Finally, the patients achieving cCR underwent TME surgery or adopted the W&W strategy. To date, 48 patients have completed neoadjuvant therapy. Twenty-four (24/48, 50.0%) achieved cCR, and 12 of them adopted the W&W strategy. Twenty-nine patients underwent TME surgery. The CR rate was 60.4% (29/48), the pCR rate was 60.7% (17/28), the MPR rate was 78.6% (22/28), and the anus-preservation rate was 88.9% (40/45). However, the follow-up period for W&W patients in the TORCH study was still relatively short, and the above data should be further updated after large sample size recruitment and long-term follow-up.

Radiotherapy combined with immunotherapy for early rectal cancer

Traditionally, direct surgery is recommended as the standard treatment for early-stage rectal cancer. However, in recent years, the need for organ function preservation has increased considerably. Early-stage tumors could achieve a higher CR rate through neoadjuvant therapy. Thus, neoadjuvant therapy has important clinical significance in patients with early-stage low rectal cancer. The 2022 ASCO Annual Meeting reported a phase II study from China (34), which enrolled 23 patients with T1-3aN0-1 ultralow rectal cancer who underwent 2 courses of

sintilimab during the same period of LCRT followed by 6 courses of sintilimab combined with capecitabine or CAPOX. Among the included patients, the baseline T2 rate was 56.5%, and the N0 rate was 69.6% (16/23). The cCR rate was 43.2% (10/23), the pCR rate was 20% (2/10), the CR (cCR + pCR) rate was 52.2% (12/23), and the anus-preservation rate was as high as 95.5% (21/22). The grade 3-4 toxicity rate was 17.4%. This study suggests that for early and mid-stage rectal cancer patients in whom anus preservation is difficult, nCRT combined with immunotherapy is expected to become a treatment option with high efficacy and low toxicity.

Opportunities and challenges of neoadjuvant chemoradiotherapy combined with immunotherapy

The combination of nCRT and immunotherapy in LARC has achieved an excellent pCR/cCR rate and an increased anal preservation rate, which indicates that a new era for anal preservation is coming. However, there are still many challenges remaining to be resolved, including the accuracy of efficacy evaluation, the sequences of radiation and chemotherapy/immunotherapy, biomarker analyses and the survival benefit, etc.

The new era of nCRT combined with immunotherapy

For LARC patients, the initial purpose of neoadjuvant chemoradiotherapy is to reduce local recurrence. However, the pCR rate is low, and distant metastasis has become the main failure mode of treatment. With the gradual optimization of neoadjuvant chemoradiotherapy regimens (such as enhancing the intensity of concurrent chemotherapy, increasing the cycles of interval chemotherapy, and even performing total neoadjuvant treatment (TNT)), the efficacy of tumor regression in patients gradually improved. Studies have shown that the TNT model can significantly increase the pCR rate to greater than 30%. More patients with cCR can adopt the nonsurgical W&W strategy, which increases the organ preservation rate and improves the quality of life. In addition, this strategy is expected to reduce distant metastasis and improve long-term survival. Therefore, neoadjuvant therapy for LARC has been transformed from the traditional era with the main purpose of controlling local recurrence to the new era with the goal of improving tumor regression, organ preservation, and long-term survival. The addition of immunotherapy has led to a more promising results in the new era. Although the results currently reported are mainly phase II small-sample studies, the results of studies with similar designs have good consistency.

In terms of LCRT-based clinical trials, except for the Voltage-A study (stage III 23%) and the Changhai study (ultralow cN0 69.6%), the vast majority of studies included greater than 85% of stage III patients. Most of the patients contained at least one feature of high risk of recurrence and metastasis (cN2/MRF+/EMVI+). In these patients, the CR rate of LCRT combined with immunotherapy can reach more than 30% (Voltage-A, NSABP FR-2, PANDORA). Thus, a CR rate similar to that of the TNT model can be achieved by only combining LCRT with PD-1 monoclonal antibody. On this basis, the combined immunotherapy-TNT model (NRG-GI002, PKUCH04, Changhai Hospital study) achieved a higher CR rate, and the pCR + cCR rates of the three studies were all 50% or greater. These findings represent a solid foundation for low rectal cancer patients to adopt the W&W strategy or reduce the scope of surgery to achieve organ preservation.

In terms of SCRT combined with immunotherapy, although a few clinical trials have published results, they all showed surprisingly high tumor regression efficacy with a pCR rate of 37.5-57.1%. The main model was SCRT followed by several cycles of chemotherapy and immunotherapy. The Wuhan study only performed two sequential cycles of CAPOX and carrelizumab and achieved an ultrahigh efficacy of 46%. The FUSCC TORCH study adopted the TNT model and performed SCRT combined with 6 cycles of CAPOX and toripalimab. The pCR rate is currently as high as 60.7%, and the CR rate is 60.4%. The above results show that hypofractionated radiotherapy combined with immunotherapy has a more powerful synergistic effect.

The challenge of evaluating the efficacy of nCRT combined with immunotherapy

Organ preservation has become one of the main goals of neoadjuvant therapy for rectal cancer, especially in patients with low rectal cancer. For patients with cCR after nCRT, the W&W strategy can be performed under close follow-up. If tumor regression is good, local resection of the lesion can also be performed through the anus, and the decision of supplementary TME is based on postoperative pathological characteristics. If significant residual tumor remains, radical surgery (TME) is recommended as soon as possible. Therefore, the evaluation of the efficacy of neoadjuvant therapy is very important and is an important basis for the selection of subsequent treatment strategies.

Currently, the main methods for assessing clinical response (including cCR) include digital anal examination (DRE), colonoscopy (for lesions or suspicious lesions with biopsy), pelvic MRI, transrectal ultrasonography (TRUS), and serum tumor marker levels (such as CEA). And the evaluation methods and criteria across different centers are not consistent (Table 3). Each of them has its strengths and weaknesses. Thus, the efficacy evaluation

TABLE 3 The different evaluation methods across different cancer centers.

Institutions	Country	Year	Evaluation Methods
Sao Paulo Hospital	Brazil	2014	DRE, Endoscopy, MRI, TRUS, PET-CT
Maastricht University Medical Center	Netherlands	2011	Endoscopy and biopsy, MRI
The OnCoRe Group	UK	2016	DRE, Endoscopy, MRI
MSKCC	USA	2015	DRE, Endoscopy, MRI
ESMO	Europe	2017	DRE, Endoscopy and biopsy, MRI, TRUS, CEA

needs the combination of the above methods. However, the consistency between the existing methods for the judgment of cCR after nCRT is not high with pCR. Smith FM et al. reported that pathological findings of 27% of cCR patients showed residual tumor cells (35). A considerable proportion of the rectal cancer tissue specimens with pCR did not meet the cCR criteria, mainly manifested as mucosal ulcer changes. The addition of immunotherapy may further increase the difference between imaging and pathological assessment results. For patients with effective immunotherapy, due to the increase in immune cell infiltration in the lesion, imaging studies may show that the lesion is stable or even enlarged, indicating false progression. Studies have shown that 14.8% of patients with metastatic CRC treated with PD-1 inhibitors had pseudoprogression (36). The presence of mixed signals of edema and fibrosis in the original tumor area after nCRT for rectal cancer may also interfere with the MR assessment of residual tumor. In addition, the uncertainty of imaging in the efficacy evaluation of immunotherapy also partially explains the small effect of the iRECIST criteria on the survival endpoint (37).

The preliminary results of studies on nCRT combined with immunotherapy for LARC showed that the CR rate was significantly increased. However, the transformation of this large tumor response improvement to the benefit of organ preservation depends on accurate evaluation methods and predictive indicators. In addition to traditional imaging methods, detection methods with higher sensitivity, such as PET/CT and ctDNA-MRD, and multidimensional assessments, such as radiomics, are urgently needed. The combination and optimization of traditional methods and new assessments will improve the judgment of tumor regression and facilitate the selection of subsequent treatment strategies.

The best sequence between radiation and chemotherapy/immunotherapy remains uncertain

The different sequences between radiation and chemotherapy/immunotherapy may lead to different effects. The use of radiation firstly can lead to the immunogenic cell death of tumor, release new tumor-associated antigens, promote the antigen-presenting function of dendritic cells and increase the infiltration of T lymphocytes, so radiation can promote the effect of sequential chemotherapy/immunotherapy. And the inductive use of chemotherapy/immunotherapy can also change the tumor microenvironment, promote the tumor angiogenesis and increase the oxygenic distribution, so that having a synergic effect with radiation.

The best sequence between radiation and chemotherapy/immunotherapy is uncertain. In terms of chemotherapy, both CAO/ARO/AIO-12 trial and OPRA trial compared the efficacy of inductive chemotherapy (chemotherapy before CRT) and consolidative chemotherapy (chemotherapy after CRT) and found that consolidative chemotherapy could obtain better pCR/cCR rates, so that leading to a higher anal preservation rate. In terms of the immunotherapy, animal experiments showed that radiation with concurrent immunotherapy achieved better tumor regression than radiation with sequential immunotherapy. And there is only one study (TORCH) conducted by China comparing the efficacy of induction immunotherapy and consolidative immunotherapy, which is recruiting now and didn't have the exact results of subgroup analyses yet. Furthermore, the tumor microenvironment analyses of biopsy tissues after treating with different sequences are needed to examine the pathological changes and investigate the underlying mechanisms.

Biomarker analysis helps screen for patients who will benefit from treatment

dMMR and MSI-H are recognized markers for predicting the efficacy of PD-1 inhibitors. However, greater than 95% of patients with rectal cancer have the pMMR/MSS type, which is not very sensitive to PD-1 inhibitors alone. Therefore, screening the population that may benefit from nCRT combined with immunotherapy is one of the key factors to improve efficacy. A small sample study from MSKCC found that the number of TILs was correlated with the efficacy of nCRT, suggesting that TILs may be involved in the tumor killing effect caused by nCRT (38). In a study conducted by Professor Galon's team in France, 249 rectal cancer biopsy specimens were analyzed. The quantitative IS of CD8+ T lymphocytes in the tumor center and infiltration

margin was correlated with the efficacy and prognosis of nCRT. None of the patients with high scores experienced tumor recurrence in the long-term follow-up, suggesting that this strategy can help to screen the population suitable for the W&W strategy (39).

Clinical trials of nCT combined with PD-1 inhibitors for LARC have also conducted biomarker analysis, including Voltage-A, NSABP FR-2, Averectal study, and Wuhan study. Voltage-A researchers used pretreatment tumor biopsy specimens for analysis. The results showed that the patients with greater than 1% of PD-L1-positive cells in the tumor microenvironment and the patients with CD8/eTreg>2.5 had a higher pCR rate. The 5 patients with both of the above features all achieved pCR, suggesting that the number and function of lymphocytes in the immune microenvironment were closely related to the efficacy of nCRT combined with immunotherapy. The Averectal study also analyzed baseline biopsy specimens and found that patients with high IS achieved a higher pCR rate. The Wuhan study showed that PD-L1 CPS ≥ 1 and TMB ≥ 10 were associated with a higher pCR rate.

In addition to commonly used immunotherapy-related biomarkers, such as MSI-H, PD-L1, immune score (or TIL quantitative analysis), and TMB, mutations in specific genes or pathways (such as POLE or POLD1 mutations, B2M or JAK1/2 mutations), the molecular structure and phenotype of various proteins in the microenvironment, the types and quantitative characteristics of metabolites, and the composition and function of the intestinal microbial population may all affect the immune response and the efficacy of immunotherapy. With the broadening of the concept of the immune microenvironment and the further refinement of various omics studies, future studies will focus more on the establishment of relevant models that accurately predict efficacy and tumor recurrence and metastasis and use biomarkers to guide patient stratification and treatment decisions.

The survival benefits of neoadjuvant immunotherapy remain to be confirmed

Regarding neoadjuvant therapy for LARC patients, in addition to the pCR rate/CR rate/organ preservation rate, recurrence-free survival (LRFS), disease progression-free survival (DFS), and overall survival (OS) are also important research endpoints. The existing nCRT model has greatly reduced the local recurrence rate to less than 10%. To control metastasis early and improve long-term survival, researchers have tried to move adjuvant chemotherapy forward and even perform the TNT model. The PRODIGE 23 study (40, 41) showed that compared with standard nCRT, 6 cycles of FOLFIRINOX chemotherapy before nCRT not only further increased the pCR rate (28% vs. 12%) but also significantly increased 3-y DFS% (76% vs. 69%) and 3-y DMFS% (79% vs. 72%). The RAPIDO study (42) showed that compared with standard nCRT, sequential 6 cycles of CAPOX or 9 cycles of FOLFOX chemotherapy after SCRT not only increased the pCR rate (28% vs. 14%) but also significantly reduced the disease-related treatment failure rate (DrTF, 23.7% vs. 30.4%) and distant metastasis rate (20.0% vs. 26.8%). The above results show that strengthening the intensity of neoadjuvant treatment and adopting the TNT model further promote tumor regression and have the potential to reduce metastasis and prolong long-term survival. The combination of nCRT and immunotherapy allows patients to receive systemic treatment earlier, which is expected to kill minimal disease earlier and reduce distant metastasis. Neoadjuvant immunotherapy can help the body obtain long-term immune memory by promoting the immune response and probably producing the smearing effect, finally achieving sustained tumor remission and long-term survival benefits. The above clinical trials have shown good short-term efficacy, but the follow-up time is insufficient. The tumor regression, toxicity and long-term survival caused by nCRT combined with immunotherapy deserve to be verified by phase III large-sample randomized controlled trials as soon as possible.

Summary

In the neoadjuvant treatment of LARC, the new model of nCRT combined with immunotherapy has shown good application potential and is expected to break through the bottleneck of the limited cCR/pCR rate of traditional nCRT and the low response rate of immunotherapy for MSS rectal cancer. An increasing number of studies have reported that radiotherapy combined with immunotherapy can significantly improve tumor regression and the CR rate and is safe and tolerable, thereby providing low rectal cancer patients with more opportunities to adopt the W&W strategy. In the future, we need more large-scale clinical trials to validate this new model and to explore how to improve the efficacy evaluation, select populations that would benefit based on various biomarkers, and explore the optimization model of the combination therapy. We look forward to converting the surprising short-term efficacy into improved survival time and quality of life for LARC patients.

Author contributions

FX selected the topic. Ji W, RW, and Yan W searched the registered clinical trials and prepared the Supplementary Tables. Yaq W reviewed all published articles and posters, and wrote the manuscript. Ju W and ZZ provided some revising suggestions on the Discussion section. JW, LS, HZ, and SC revised the manuscript. All of the authors critically read and approved the manuscript.

Funding

The study was supported by the National Natural Science Foundation of China (Grant No. 82003229) and the Project of Shanghai Leading Talent (Grant No. LJ097).

Conflict of interest

The authors declare that the research was conducted in the absence of any commercial or financial relationships that could be construed as a potential conflict of interest.

Publisher's note

All claims expressed in this article are solely those of the authors and do not necessarily represent those of their affiliated organizations, or those of the publisher, the editors and the reviewers. Any product that may be evaluated in this article, or claim that may be made by its manufacturer, is not guaranteed or endorsed by the publisher.

Supplementary material

The Supplementary Material for this article can be found online at: https://www.frontiersin.org/articles/10.3389/fimmu.2022.1067036/full#supplementary-material

SUPPLEMENTARY TABLE 1
The clinical trials of the long course radiotherapy combined with immunotherapy.

SUPPLEMENTARY TABLE 2
The clinical trials of the short course radiotherapy combined with immunotherapy.

References

1. Martin ST, Heneghan HM, Winter DC. Systematic review and meta-analysis of outcomes following pathological complete response to neoadjuvant chemoradiotherapy for rectal cancer. *Br J Surg* (2012) 99(7):918–28. doi: 10.1002/bjs.8702

2. van der Valk MJM, Hilling DE, Bastiaannet E, Meershoek-Klein Kranenbarg E, Beets GL, Figueiredo NL, et al. Long-term outcomes of clinical complete responders after neoadjuvant treatment for rectal cancer in the international watch & wait database (Iwwd): An international multicentre registry study. *Lancet* (2018) 391(10139):2537–45. doi: 10.1016/S0140-6736(18)31078-X

3. Zhu J, Liu A, Sun X, Liu L, Zhu Y, Zhang T, et al. Multicenter, randomized, phase iii trial of neoadjuvant chemoradiation with capecitabine and irinotecan guided by Ugt1a1 status in patients with locally advanced rectal cancer. *J Clin Oncol* (2020) 38(36):4231–9. doi: 10.1200/JCO.20.01932

4. Garcia-Aguilar J, Chow OS, Smith DD, Marcet JE, Cataldo PA, Varma MG, et al. Effect of adding Mfolfox6 after neoadjuvant chemoradiation in locally advanced rectal cancer: A multicentre, phase 2 trial. *Lancet Oncol* (2015) 16 (8):957–66. doi: 10.1016/S1470-2045(15)00004-2

5. Fernandez-Martos C, Pericay C, Aparicio J, Salud A, Safont M, Massuti B, et al. Phase ii, randomized study of concomitant chemoradiotherapy followed by surgery and adjuvant capecitabine plus oxaliplatin (Capox) compared with induction capox followed by concomitant chemoradiotherapy and surgery in magnetic resonance imaging-defined, locally advanced rectal cancer: Grupo cancer de recto 3 study. *J Clin Oncol* (2010) 28(5):859–65. doi: 10.1200/JCO.2009.25.8541

6. Cercek A, Roxburgh CSD, Strombom P, Smith JJ, Temple LKF, Nash GM, et al. Adoption of total neoadjuvant therapy for locally advanced rectal cancer. *JAMA Oncol* (2018) 4(6):e180071. doi: 10.1001/jamaoncol.2018.0071

7. Le DT, Durham JN, Smith KN, Wang H, Bartlett BR, Aulakh LK, et al. Mismatch repair deficiency predicts response of solid tumors to pd-1 blockade. *Science* (2017) 357(6349):409–13. doi: 10.1126/science.aan6733

8. Michael-Robinson JM, Biemer-Huttmann A, Purdie DM, Walsh MD, Simms LA, Biden KG, et al. Tumour infiltrating lymphocytes and apoptosis are independent features in colorectal cancer stratified according to microsatellite instability status. *Gut* (2001) 48(3):360–6. doi: 10.1136/gut.48.3.360

9. Andre T, Shiu KK, Kim TW, Jensen BV, Jensen LH, Punt C, et al. Pembrolizumab in microsatellite-Instability-High advanced colorectal cancer. *N Engl J Med* (2020) 383(23):2207–18. doi: 10.1056/NEJMoa2017699

10. Lugade AA, Moran JP, Gerber SA, Rose RC, Frelinger JG, Lord EM. Local radiation therapy of B16 melanoma tumors increases the generation of tumor antigen-specific effector cells that traffic to the tumor. *J Immunol* (2005) 174 (12):7516–23. doi: 10.4049/jimmunol.174.12.7516

11. Twyman-Saint Victor C, Rech AJ, Maity A, Rengan R, Pauken KE, Stelekati E, et al. Radiation and dual checkpoint blockade activate non-redundant immune mechanisms in cancer. *Nature* (2015) 520(7547):373–7. doi: 10.1038/nature14292

12. Dovedi SJ, Illidge TM. The antitumor immune response generated by fractionated radiation therapy may be limited by tumor cell adaptive resistance and can be circumvented by pd-L1 blockade. *Oncoimmunology* (2015) 4(7): e1016709. doi: 10.1080/2162402X.2015.1016709

13. Dovedi SJ, Adlard AL, Lipowska-Bhalla G, McKenna C, Jones S, Cheadle EJ, et al. Acquired resistance to fractionated radiotherapy can be overcome by concurrent pd-L1 blockade. *Cancer Res* (2014) 74(19):5458–68. doi: 10.1158/0008-5472.CAN-14-1258

14. Postow MA, Callahan MK, Barker CA, Yamada Y, Yuan J, Kitano S, et al. Immunologic correlates of the abscopal effect in a patient with melanoma. *N Engl J Med* (2012) 366(10):925–31. doi: 10.1056/NEJMoa1112824

15. Brix N, Tiefenthaller A, Anders H, Belka C, Lauber K. Abscopal, immunological effects of radiotherapy: Narrowing the gap between clinical and preclinical experiences. *Immunol Rev* (2017) 280(1):249–79. doi: 10.1111/imr.12573

16. Stein JE, Lipson EJ, Cottrell TR, Forde PM, Anders RA, Cimino-Mathews A, et al. Pan-tumor pathologic scoring of response to pd-(L)1 blockade. *Clin Cancer Res* (2020) 26(3):545–51. doi: 10.1158/1078-0432.CCR-19-2379

17. Chalabi M, Fanchi LF, Dijkstra KK, Van den Berg JG, Aalbers AG, Sikorska K, et al. Neoadjuvant immunotherapy leads to pathological responses in mmr-proficient and mmr-deficient early-stage colon cancers. *Nat Med* (2020) 26(4):566–76. doi: 10.1038/s41591-020-0805-8

18. Hu H, Kang L, Zhang J, Wu Z, Wang H, Huang M, et al. Neoadjuvant pd-1 blockade with toripalimab, with or without celecoxib, in mismatch repair-deficient or microsatellite instability-high, locally advanced, colorectal cancer (Picc): A single-centre, parallel-group, non-comparative, randomised, phase 2 trial. *Lancet Gastroenterol Hepatol* (2022) 7(1):38–48. doi: 10.1016/S2468-1253(21)00348-4

19. Cercek A, Lumish MA, Sinopoli JC. *Single agent pd-1 blockade as curative-intent treatment in mismatch repair deficient locally advanced rectal cancer*. Chicago: ASCO (2022). Available at: https://meetings.asco.org/abstracts-presentations/213772.

20. Bando H, Tsukada Y, Inamori K, Togashi Y, Koyama S, Kotani D, et al. Preoperative chemoradiotherapy plus nivolumab before surgery in patients with microsatellite stable and microsatellite instability-high locally advanced rectal cancer. *Clin Cancer Res* (2022) 28(6):1136–46. doi: 10.1158/1078-0432.CCR-21-3213

21. George TJ, Yothers G, Jacobs SA, Finley GG, Wade JL, Lima CMSPR. *Phase ii study of durvalumab following neoadjuvant chemort in operable rectal cancer: Nsabp fr-2*. San Francisco: ASCO GI (2022). doi: 10.1200/JCO.2022.40.4_suppl.099

22. Tamberi S, Grassi E, Zingaretti C, Papiani G. *Phase ii study of capecitabine plus concomitant radiation therapy followed by durvalumab (Medi4736) as preoperative treatment in rectal cancer: Pandora study final results*. Chicago:

ASCO (2022). Available at: https://meetings.asco.org/abstracts-presentations/208436.

23. Salvatore L, Bensi M, Corallo S, Bergamo F. *Phase ii study of preoperative chemoradiotherapy plus avelumab in patients with locally advanced rectal cancer: The avana study*. San Francisco: ASCO GI (2021). Available at: https://meetings.asco.org/abstracts-presentations/195969.

24. Carrasco J, Schröder D, Sinapi I, Cuyper AD, Beniuga G, Delmarcelle S, et al. *R-immune interim analysis: A phase Ib/Ii study to evaluate safety and efficacy of atezolizumab combined with radio-chemotherapy in a preoperative setting for patients with localized rectal cancer*. Paris: ESMO (2021). Available at: https://www.annalsofoncology.org/article/S0923-7534(21)03148-3/fulltext.

25. Rahma OE, Yothers G, Hong TS, Russell MM, You YN, Parker W, et al. Use of total neoadjuvant therapy for locally advanced rectal cancer: Initial results from the pembrolizumab arm of a phase 2 randomized clinical trial. *JAMA Oncol* (2021) 7(8):1225–30. doi: 10.1001/jamaoncol.2021.1683

26. WU A, Li Y, Ji D, Zhang L, Zhang X, Cai Y, et al. *Pkuch 04 trial: Total neoadjuvant chemoradiation combined with neoadjuvant pd-1 blockade for Pmmr/Mss locally advanced middle to low rectal cancer*. Chicago: ASCO (2022). Available at: https://meetings.asco.org/abstracts-presentations/208541.

27. Crocenzi T, Cottam B, Newell P, Wolf RF, Hansen PD, Hammill C, et al. A hypofractionated radiation regimen avoids the lymphopenia associated with neoadjuvant chemoradiation therapy of borderline resectable and locally advanced pancreatic adenocarcinoma. *J Immunother Cancer* (2016) 4:45. doi: 10.1186/s40425-016-0149-6

28. Lan J, Li R, Yin LM, Deng L, Gui J, Chen BQ, et al. Targeting myeloid-derived suppressor cells and programmed death ligand 1 confers therapeutic advantage of ablative hypofractionated radiation therapy compared with conventional fractionated radiation therapy. *Int J Radiat Oncol Biol Phys* (2018) 101(1):74–87. doi: 10.1016/j.ijrobp.2018.01.071

29. Dewan MZ, Galloway AE, Kawashima N, Dewyngaert JK, Babb JS, Formenti SC, et al. Fractionated but not single-dose radiotherapy induces an immune-mediated abscopal effect when combined with anti-Ctla-4 antibody. *Clin Cancer Res* (2009) 15(17):5379–88. doi: 10.1158/1078-0432.CCR-09-0265

30. Lin Z, Cai M, Zhang P, Li G, Liu T, Li X, et al. Phase ii, single-arm trial of preoperative short-course radiotherapy followed by chemotherapy and camrelizumab in locally advanced rectal cancer. *J Immunother Cancer* (2021) 9 (11): e003554. doi: 10.1136/jitc-2021-003554

31. Shamseddine A, Zeidan YH, El Husseini Z, Kreidieh M, Al Darazi M, Turfa R, et al. Efficacy and safety-in analysis of short-course radiation followed by mfolfox-6 plus avelumab for locally advanced rectal adenocarcinoma. *Radiat Oncol* (2020) 15(1):233. doi: 10.1186/s13014-020-01673-6

32. Wang Y, Shen L, Wan J, Zhang H, Wu R, Wang J, et al. Short-course radiotherapy combined with capox and toripalimab for the total neoadjuvant therapy of locally advanced rectal cancer: A randomized, prospective, multicentre, double-arm, phase ii trial (Torch). *BMC Cancer* (2022) 22(1):274. doi: 10.1186/s12885-022-09348-z

33. Wang Y, Xia F, Shen L, Wan J, Zhang H, Wu R, et al. *Short-course radiotherapy combined with capox and toripalimab for the total neoadjuvant therapy of locally advanced rectal cancer: Preliminary findings from a randomized, prospective, multicenter, double-arm, phase ii trial (Torch)*. Chicago: ASCO (2022). Available at: https://meetings.asco.org/abstracts-presentations/208603.

34. Zhou L, Yu G, Shen Y, Ding H, Zheng K, Wen R, et al. *The clinical efficacy and safety of neoadjuvant chemoradiation therapy with immunotherapy for the organ preservation of ultra low rectal cancer: A single arm and open label exploratory study*. Chicago: ASCO (2022). Available at: https://meetings.asco.org/abstracts-presentations/208587.

35. Smith FM, Wiland H, Mace A, Pai RK, Kalady MF. Clinical criteria underestimate complete pathological response in rectal cancer treated with neoadjuvant chemoradiotherapy. *Dis Colon Rectum* (2014) 57(3):311–5. doi: 10.1097/DCR.0b013e3182a84eba

36. Colle R, Radzik A, Cohen R, Pellat A, Lopez-Tabada D, Cachanado M, et al. Pseudoprogression in patients treated with immune checkpoint inhibitors for microsatellite instability-High/Mismatch repair-deficient metastatic colorectal cancer. *Eur J Cancer* (2021) 144:9–16. doi: 10.1016/j.ejca.2020.11.009

37. Park HJ, Kim GH, Kim KW, Lee CW, Yoon S, Chae YK, et al. Comparison of recist 1.1 and irecist in patients treated with immune checkpoint inhibitors: A systematic review and meta-analysis. *Cancers (Basel)* (2021) 13(1): 120. doi: 10.3390/cancers13010120

38. Kamran SC, Lennerz JK, Margolis CA, Liu D, Reardon B, Wankowicz SA, et al. Integrative molecular characterization of resistance to neoadjuvant chemoradiation in rectal cancer. *Clin Cancer Res* (2019) 25(18):5561–71. doi: 10.1158/1078-0432.CCR-19-0908

39. El Sissy C, Kirilovsky A, Van den Eynde M, Musina AM, Anitei MG, Romero A, et al. A diagnostic biopsy-adapted immunoscore predicts response to neoadjuvant treatment and selects patients with rectal cancer eligible for a watch-and-Wait strategy. *Clin Cancer Res* (2020) 26(19):5198–207. doi: 10.1158/1078-0432.CCR-20-0337

40. Kamrava M, Bernstein MB, Camphausen K, Hodge JW. Combining radiation, immunotherapy, and antiangiogenesis agents in the management of cancer: The three musketeers or just another quixotic combination? *Mol Biosyst* (2009) 5(11):1262–70. doi: 10.1039/b911313b

41. Conroy T, Bosset JF, Etienne PL, Rio E, Francois E, Mesgouez-Nebout N, et al. Neoadjuvant chemotherapy with folfirinox and preoperative chemoradiotherapy for patients with locally advanced rectal cancer (Unicancer-prodige 23): A multicentre, randomised, open-label, phase 3 trial. *Lancet Oncol* (2021) 22(5):702–15. doi: 10.1016/S1470-2045(21)00079-6

42. Bahadoer RR, Dijkstra EA, van Etten B, Marijnen CAM, Putter H, Kranenbarg EM, et al. Short-course radiotherapy followed by chemotherapy before total mesorectal excision (Tme) versus preoperative chemoradiotherapy, tme, and optional adjuvant chemotherapy in locally advanced rectal cancer (Rapido): A randomised, open-label, phase 3 trial. *Lancet Oncol* (2021) 22(1):29–42. doi: 10.1016/S1470-2045(20)30555-6

frontiers | Frontiers in Immunology

TYPE Review
PUBLISHED 12 January 2023
DOI 10.3389/fimmu.2022.1106644

OPEN ACCESS

EDITED BY
Kuangyu Shi,
University of Bern, Switzerland

REVIEWED BY
Ran Zhu,
Soochow University, China
Xiaotao Zhang,
The Affiliated Qingdao Central Hospital of Qingdao University, China

*CORRESPONDENCE
Xiangdong Sun
sunxd_81@126.com

†These authors have contributed equally to this work

SPECIALTY SECTION
This article was submitted to Cancer Immunity and Immunotherapy, a section of the journal Frontiers in Immunology

RECEIVED 24 November 2022
ACCEPTED 22 December 2022
PUBLISHED 12 January 2023

CITATION
Ji X, Jiang W, Wang J, Zhou B, Ding W, Liu S, Huang H, Chen G and Sun X (2023) Application of individualized multimodal radiotherapy combined with immunotherapy in metastatic tumors.
Front. Immunol. 13:1106644.
doi: 10.3389/fimmu.2022.1106644

Application of individualized multimodal radiotherapy combined with immunotherapy in metastatic tumors

Xiaoqin Ji†, Wanrong Jiang†, Jiasheng Wang, Bin Zhou, Wei Ding, Shuling Liu, Hua Huang, Guanhua Chen and Xiangdong Sun*

Department of Radiation Oncology, Affiliated Jinling Hospital, Medical School of Nanjing University, Nanjing, China

Radiotherapy is one of the mainstays of cancer treatment. More than half of cancer patients receive radiation therapy. In addition to the well-known direct tumoricidal effect, radiotherapy has immunomodulatory properties. When combined with immunotherapy, radiotherapy, especially high-dose radiotherapy (HDRT), exert superior systemic effects on distal and unirradiated tumors, which is called abscopal effect. However, these effects are not always effective for cancer patients. Therefore, many studies have focused on exploring the optimized radiotherapy regimens to further enhance the antitumor immunity of HDRT and reduce its immunosuppressive effect. Several studies have shown that low-dose radiotherapy (LDRT) can effectively reprogram the tumor microenvironment, thereby potentially overcoming the immunosuppressive stroma induced by HDRT. However, bridging the gap between preclinical commitment and effective clinical delivery is challenging. In this review, we summarized the existing studies supporting the combined use of HDRT and LDRT to synergistically enhance antitumor immunity, and provided ideas for the individualized clinical application of multimodal radiotherapy (HDRT+LDRT) combined with immunotherapy.

KEYWORDS

cancer, metastatic tumor, high-dose radiotherapy, low-dose radiotherapy, immunotherapy

Introduction

Radiotherapy has long been the cornerstone of cancer treatment for curative purposes as well as palliative relief of symptoms, thereby improving quality of life (1–4). In addition to inducing irreparable DNA damage with direct cytotoxic effects on cancer cells, there is growing evidence that radiotherapy can modulate the immune system, resulting in systemic antitumor immunity (5, 6). This systemic response is called abscopal effect, that is, radiation targeting one tumor lesion can induce *in situ* vaccination by killing tumor cells, and then lead to the regression of distant unirradiated tumors (7–9). Although radiotherapy alone rarely induces abscopal effects, the potential systemic antitumor ability provides a good basis for radiotherapy combined with immunotherapy.

Immunotherapy has been recognized as an effective oncologic therapy. In particular, immune checkpoint inhibitors (ICIs) have achieved surprising clinical efficacy in the treatment of advanced solid tumors (10–12). However, only a minority of patients with advanced cancers can experience persistent and stable benefit from ICIs alone (13). As a result, many clinical trials are exploring the synergistic effect of radiation therapy combined with immunotherapy to enhance antitumor immunity (14–18). The updated data of PACIFIC Trial demonstrated robust and sustained overall survival (OS) and durable progression free survival (PFS) benefit with durvalumab after chemoradiotherapy in patients with unresectable, stage III non-small-cell lung cancer (NSCLC) (19). These compelling clinical evidences provide a basis for further exploration of the best combination regimen.

The stereotactic body radiation therapy (SBRT, also known as stereotactic ablative radiotherapy [SABR]) is increasingly used to deliver highly targeted high doses with fewer fractions, because of the high rates of local tumor control with tolerable toxicity (20–22). In addition, high-dose radiotherapy (HDRT, such as SBRT) is more immunogenic than conventional radiotherapy. HDRT can mobilize innate and adaptive immunity against tumors (23–26). Therefore, scholars focused on the combination of HDRT with immunotherapy to enhance the antitumor immunity of patients. Several clinical studies have shown that SBRT combined with ICIs can significantly improve the response rates in metastatic tumors with well tolerated (27–29). Despite previous progression on anti-PD-1 therapy, SBRT has reinvigorated a systemic response (30). Nevertheless, in some cases, SBRT in conjunction with ICIs may not eliminate distant tumors, and benefit only a small fraction of patients (31, 32). HDRT can sometimes have inhibitory effects on antitumor immunity, such as recruiting immunosuppressive cells and increasing the secretion of immunoregulatory cytokines (33, 34). It is urgent to overcome the immune-suppressive barriers to increase the beneficiary population of immunotherapy.

Many studies have shown that low-dose radiotherapy (LDRT), i.e., lower than 2 Gy/fraction, can effectively reprogram the stroma from an immunosuppressive to immunostimulatory and synergize with immunotherapy (35–37). Interestingly, the mechanisms by which HDRT and LDRT regulate the antitumor immune system appear to be complementary (38). Therefore, the use of the multimodal radiotherapy regimen, such as HDRT and LDRT, can achieve optimal antitumor effects. We first proposed the concept of multimodal radiotherapy, that is, the combination of different radiotherapy modalities, such as SBRT combined with intensity modulated radiotherapy (IMRT), SBRT combined with LDRT, HDRT combined with LDRT, etc. Savage et al., compared a single-dose ablative fractionation of 24Gy with 22Gy followed by 4 fractions of 0.5Gy targeting the local tumor in C57BL/6 mice. They found that the addition of LDRT delayed local tumor progression and significantly improved survival. In addition, survival was significantly increased after whole-lung radiated by low dose (0.5Gyx4f), 12 days after completion of the primary tumor radiation (20Gyx3f) (39). Furthermore, some preclinical and clinical studies showed that the multimodal radiotherapy (HDRT and LDRT) combined with immunotherapy can enhance systemic anti-tumor immune responses (40–44). However, there are many problems about this novel combination therapy strategy. For example, the selection of immunotherapy agents, the sequence of multimodal radiotherapy combined with immunotherapy, the dose of radiation, the number of fractions, the site of high-dose irradiation, and the site of low-dose irradiation.

In this review, we discussed the optimal radiotherapy regimens for enhancing antitumor immunity. First, we investigated the modulation of radiation on the immune system, including immunoenhancing and immunosuppressive effects. Furthermore, we described the different mechanisms of HDRT and LDRT in immune regulation. Finally, we studied the rationale for combining multimodal radiotherapy (HDRT and LDRT) with immunotherapy to enhance antitumor immune responses.

The direct killing effect of radiation on tumor cells

Radiation therapy has been widely used to treat malignant tumors since the discovery of X-ray by Roentgen in 1895 (45). Approximately 60-70% of cancer patients require radiation therapy during treatment (7). In 1911, Regaud et al. proposed the concept of fractionated radiotherapy, in which a large doses can be divided into fractions over days or weeks (46). Nowadays, the conventional fractionated radiotherapy

regimen is usually 1.8-2 Gy daily, 5 fractions/week. Hypofractionated radiotherapy refers to increasing the single irradiation dose >2 Gy, which has the advantage of shortening the treatment time span of patients and avoiding accelerated tumor proliferation after radiotherapy. Over the past few decades, the field of radiation has undergone tremendous technological innovations that can significantly reduce radiation damage to healthy tissues with modern radiotherapy techniques such as helical tomotherapy, IMRT, proton radiotherapy, SBRT and FLASH radiotherapy (22, 47–52).

Irradiation can directly cause DNA damage, such as single-strand breaks (SSBs), double-strand breaks (DSBs), DNA cross-links, and DNA-protein cross-links, resulting in therapeutic effects on tumor cells, such as apoptosis, necrosis, senescence, and mitotic abnormalities (53, 54). Irradiation can indirectly induce damage to DNA molecular chain in cancer cells by ionizing water molecules to generate H^+ and OH^- (55). This indirect effect requires oxygen. Therefore, some hypoxic tumors are resistant to radiation, which is one of the reasons for tumor recurrence after radiotherapy. Hypoxia in hypoxic tumors causes less DNA damage than in well-oxygenated tumors at the same dose of radiation. In addition, hypoxia leads to activation of the hypoxia inducible factor (HIF) signaling pathway. Activation of HIF1 can affect the expression of hundreds of genes, including vascular endothelial growth factor (VEGF) and angiopoietin-1 (ANGPT1), which promote tumor survival (56). It also drives the expression of key enzymes in glycolysis, resulting in the accumulation of lactic acid, pyruvate, and the antioxidants glutathione and NADPH to limit DNA damage (57). Therefore, radiation alone is not enough to kill all cancer cells, and it is necessary to study combination therapy.

Effects of radiation on the immune system

Traditionally, it is believed that radiotherapy leads to the death of tumor cells through irreversible damage to DNA. Many studies have found that the local killing effects of radiotherapy can be enhanced or reduced by stimulating or inhibiting the immune response in two different ways (58–60). Radiotherapy is involved in the modulation of many immune processes, such as cancer antigens release and presentation, T lymphocytes priming and activation, T cells recruitment and accumulation into tumor, T lymphocytes recognition and killing of tumor cells (61). The regimens of radiotherapy and the biological characteristics of the tumor also affect changes in immune responses.

In situ tumor vaccine induced by radiation

Radiation results in the release of DNA DSBs from tumor cells into the cytoplasm (62). Cytosolic DNA is sensed by the cyclic GMP-AMP synthase stimulator (cGAS–STING) pathway of interferon genes. cGAS is a pattern recognition receptor that triggers the production of interferon I (IFN-I) through the downstream linker stimulator of interferon genes (STING) (63–65). IFN-I can stimulate dendritic cells (DCs) and T cell activation. This is critical for converting tumors into *in situ* vaccines (66). There is clinical evidence that IFN-I signaling is activated in spontaneously retreating tumors (67) and in metastases highly infiltrated by T cells (68, 69).

Radiation can induce immunogenic cell death (ICD), which can induce (local and/or systemic) release of tumor-associated antigens (TAAs), especially tumor neoantigens (TNAs) (70, 71). ICD is defined as a type of regulated cell death characterized by the release of damage-associated molecular patterns (DAMPs) after cells lose membrane integrity. DAMPs include calreticulin (CRT), the chromatin stabilization protein high-mobility group box 1 (HMGB1), adenosine triphosphate (ATP), and chaperons of the family of heat shock protein (e.g. HSP70) (72, 73). ICD leads to an adaptive immune response by favoring DC cross-presentation of tumor antigens to T cells. This can enhance anti-tumor immune responses and improve tumor control (72).

DAMPs and cytokines play important roles in radiation-induced ICD. First, calreticulin (CRT) is translocated from the endoplasmic reticulum to the cell surface and can act as an "eat-me" signal to antigen-presenting cells (APCs) (especially DCs and macrophages), *via* binding CD91 (a 2-macroglobulin receptor) (74, 75). This induces the subsequent release of cytokines, such as interleukin-6 (IL-6) and tumor necrosis factor alpha (TNF-α) (76). The CRT-CD91 interaction also mediates the recruitment of APCs to tumors, followed by DC phagocytosis of tumor cells and efficient presentation of tumor antigens to T cells. This ultimately leads to the activation of anti-tumor immune responses (77). Radiation can further enhance the endocytic activity of APCs by interfering with the CD47-signal regulatory protein α (SIRPα) phagocytic checkpoint pathway (78–81). CD47 is a marker of self-"don't eat me signal", and its loss on senescent or damaged cells leads to homeostatic phagocytosis (82). Importantly, CD47 is overexpressed in many tumors, and CD47 blockade has been identified as an attractive immunotherapeutic target (83, 84). Radiation induced loss of CD47 has been reported to enhance immune-mediated tumor clearance (78). Second, high-mobility group box 1 (HMGB1) is released from dying, necrotic, damaged tumor cells into the immune milieu and exerts robust immunomodulatory effects by binding to Toll-like receptor

(TLR)-4 and TLR-9 (85, 86). HMGB1 can promote DCs maturation and migration to lymph nodes for antigen cross-presentation to naive T cells (87). Third, the release of ATP, which binds to the purinergic receptor P2X7, acts as a "find me" signal for monocytes and DCs, leading to the activation of NLRP3/ASC/caspase-1 inflammasome, and ultimately induce the production of IL-18 and IL-1β (88). IL-1β promotes the activation of IFN-γ-producing tumor antigen-specific $CD8^+$ T cells (89). Fourth, HSP70 can be translocated from the cytoplasm to the extracellular matrix under conditions of radiation-induced cellular stress (90). HSP70 can activate monocytes, macrophages, and DCs by binding to CD14, CD40, CD91, Lox1 and Toll-like receptors (TLR2 and TLR4) (91). These results showed that the release of danger signals is critical for activating of antigen-presenting cells and for enhancing the immune response to tumor cells.

The cumulative effects of these molecular signals promote DCs phagocytosis of tumor cells, thereby facilitating DCs processing of tumor-derived antigens and subsequent DC-mediated cross-presentation to $CD8^+$ cytotoxic T lymphocytes to release or induce type I interferons. Overall, radiation can induce ICD, an important pathway for activating antitumor immunity, which can transform tumors into an "*in situ* vaccine".

Abscopal effect induced by radiation

In 1953, the abscopal effect was first described as the regression of unirradiated tumors in a patient receiving radiation therapy (92). Over past decades, the abscopal effect is of great interest among radiation oncologists, but it remains a rare and poorly understood phenomenon in the clinic. In the era of cancer immunotherapy, many studies have found that radiotherapy combined with immunotherapy can enhance the abscopal effect (93–95). The key mechanism of this abscopal effect is radiation-induced *in situ* vaccination through liberating TAAs (7, 96). These neoantigens are then taken up by APCs, which are involved in the cross-priming of naive $CD8^+$ T cells. Activated tumor-specific $CD8^+$ cytotoxic T cells can move to the primary tumor and the metastatic lesions, activate systemic immunogenicity, induce abscopal effects, and control the growth of irradiated and non-irradiated tumors (60, 97).

Reprogramming the tumor microenvironment through radiation

The tumor microenvironment (TME) is the internal environment on which tumor survival and development depends, and is associated with tumor growth, progression, and metastasis (98, 99). The dynamic changes in the TME lead to tumor cell variant selection. This results in the complexity of cancer heterogeneity and influences responses to different therapeutic strategies (100–102). TME can be segregated into four immune phenotypes based on tumor mutational burden and the presence of an inflammatory gene signature enriched for IFN-γ response genes (103). Chen et al. (61) classified TME into three types: an immune-inflamed, an immune-deserted and an immune-excluded. The TME of inflamed type, a "hot" phenotype with highly infiltration of $CD4^+$ and $CD8^+$ T cells, is accompanied by myeloid cells and monocytic cells. In addition, the immune cells are located in proximity to the tumor cells. Excellent responses to anti-PD-L1/PD-1 agents are most often in patients with inflamed tumors (104–106). On the contrary, the TME of deserted type refers to a "cold" phenotype lacking T lymphocytes infiltration in either the parenchyma or the stroma of the tumor. These deserted tumors rarely respond to therapeutic PD-L1/PD-1 antibodies (104). The TME of the immune-excluded type is an intermediate state characterized by the presence of abundant immune cells. However, the immune cells do not penetrate the tumor parenchyma, but instead remain in the stroma surrounding tumor cell nests (107, 108). Clinical responses are uncommon after anti-PD-L1/PD-1 treatment of these immune-excluded tumors. There is evidence of stroma-associated T cell activation and proliferation, but no infiltration (109). It is not clear how radiotherapy induces an immune-activating TME and radiotherapy leads to an immunosuppressive TME.

Immune-enhancing effects of radiation in TME

More and more evidences indicated that radiotherapy can enhance innate and adaptive immune responses to tumors, thereby enhancing tumor responsiveness to radiation (110–113). Radiation therapy can induce the *in situ* tumor vaccine, thereby promoting the activation and maturation of DCs. DCs take up TAAs from damaged tumor cells and move to draining lymph nodes, and then present TAAs to T cells. Activated T cells can move to tumors to kill tumor cells. In addition, radiotherapy can upregulate the NK pathway to mediate tumor cells killing.

The *in situ* vaccination effect of radiation contributes to the uptake, processing and presentation of TAAs by DCs (such as $CD11c^+CD11b^+$ APCs) (114, 115). DCs (specialized APCs) can cross-presenting extracellular antigens, especially cell-associated antigens, to $CD8^+$ T cells (116, 117). Many studies have shown that radiation can increase the levels of tumor-associated DCs, enhance the mobilization of these cells into draining lymph nodes, augment DCs maturation, and promote the ability of DCs (59, 60, 118). CD40 agonists are known to enhance DC function by increasing the surface expression of major histocompatibility complex (MHC) molecules and the production of proinflammatory cytokines (119). The cross-priming process

requires the cognate T-cell receptors (TCR) to recognize the peptide major histocompatibility complex (MHC), which requires the costimulatory molecules CD80/86-CD28/cytotoxic T lymphocyte-associated protein 4 (CTLA4) and CD40L-CD40. Radiation can upregulate MHC-I molecules on tumor cells, thereby enhancing TAA presentation (120). This enhances tumor cells recognized by cytotoxic T cells specific to tumor antigen, and lysis of tumor cells by cytotoxic T cells. Radiation induces an increase in MHC I antigen presentation through three different mechanisms: (1) a proteasome-dependent increase in cytosolic peptide levels; (2) activation of the mTOR pathway leads to increased translation of proteins; (3) an increased generation of radiation-specific peptides (120). In addition to these cell intrinsic mechanisms of MHC-I induction, radiation-induced IFN-γ induces MHC-I upregulation (121). Therefore, radiation can increase MHC-I levels in some tumors with low endogenous MHC-I, thereby increasing immune-mediated attack. Furthermore, radiation upregulates the NK pathway by activating natural killer group 2D (NKG2D) ligands, and increasing NK cell cytotoxicity, tumor infiltration, and the production of many cytokines (112, 122). In addition, radiation can upregulate Fas expression by tumor cells, resulting in increased cytotoxic T cell lysis through a Fas/FasL-dependent mechanism (123). Radiation can induce the expression of cytokines and chemokines, such as CXC-motif chemokine (CXCL) 9, CXCL10, CXCL11 and CXCL16, thereby promoting the recruitment of effector CD8 and T-helper 1 CD4 T cells (124, 125). Radiation induces increased expression of vascular cell adhesion molecule 1 (VCAM-1) and intercellular adhesion molecule 1 (ICAM1) in tumor vessels, thereby promoting tumor infiltration by T lymphocytes (7, 126). Many studies have indicated that the presence of tumor-infiltrating lymphocytes, especially effector T cells, before therapy is associated with better survival in cancer patients (127, 128). Anitei et al. found that the densities of $CD3^+$ T cells and cytotoxic $CD8^+$ T lymphocytes were significantly correlated with disease-free survival and overall survival in patients with rectal cancer treated with chemoradiotherapy (129). Therefore, radiation induces the release of chemokines that subsequently enrich the T−cell infiltrate, and enhance priming of infiltrating T cells, thereby providing a positive immunological outcome.

It is clearly that radiation can act on multiple tumor compartments to stimulate the tumor immune system. The antitumor immune-enhancing effects of radiotherapy were shown in Figure 1.

Immunosuppressive effects of radiation in the TME

In addition to modulating the TME to generate antitumor immune responses, radiation can lead to immunosuppression of the TME and induce the expression of molecules that prevent DCs from cross-presenting tumor antigens and/or T cells to kill tumor cells. It is necessary to study this topic, because the suppression of the immune microenvironment leads to worse prognosis, and it may also be a legitimate therapeutic target.

Many studies have shown that radiation can lead to the recruitment of regulatory T cells (Tregs), myeloid derived suppressor cells (MDSCs) and tumor associated macrophages (TAMs) in the tumor microenvironment (123, 130, 131). Tregs are a subset of $CD4^+$ T cells characterized by the expression of the transcription factor fork head box P3 (FOXP3). Tregs produce the cytokines transforming growth factor beta (TGF-β) and IL−10. This suppresses effector-T−cell activation and stimulates the suppressive functions of MDSCs (132). These results indicate that Tregs in tumors develop enhanced immunosuppressive properties after radiotherapy. Many studies indicate that the presence of highly suppressed Tregs in the circulation may represent a highly immunosuppressive environment induced by chemoradiotherapy, at least temporarily, in patients with glioblastoma and head and neck or cervical cancer (133–135). Therefore, targeting Tregs and/or their immunosuppressive effector molecules may be the key to reversing immunosuppression (136–138). After radiation therapy, the increased MDSCs can suppress the activation of both $CD4^+$ and $CD8^+$ T-cell responses in the TME *via* secretion of arginase-1 (ARG1) and nitric oxide synthase 2 (NOS2) (139, 140). In addition, MDSCs promote blood vessel formation and tumor regrowth (141, 142). Many studies in a variety of tumor models have shown that radiotherapy induces the recruitment of macrophages into tumor sites (123, 143). Radiation-induced recruitment of TAMs was dependent on increased expression of the chemokine CSF-1 (144). Although M1 macrophages can promote inflammation and antitumor immune responses, the M2 phenotype can promote tumor growth, angiogenesis, and metastasis after radiation (145, 146). Irradiated tumor cells release oxygen and nitrogen radicals that promote the polarization of macrophages from an inflammatory M1 phenotype into a tumor-supporting M2 phenotype. These M2 macrophages secrete the anti-inflammatory cytokines IL-10 and TGF-β, as well as the enzyme arginase-1, which lead to T cell suppression (147, 148). TGF-β can promote extracellular matrix production and angiogenesis, resulting in tumor cell proliferation, adhesion and metastasis (149, 150). TGF-β can impede anti-tumor immunity post-radiation by suppressing the effector functions of T-cells and natural killer cells, inhibiting DC maturation, promoting M2 macrophage polarity and the conversion of $CD4^+$ T-cells into immunosuppressive Tregs (151). Radiation can stimulate the upregulation of immune checkpoint inhibitory molecules, such as programmed cell death ligand 1 (PD-L1) on tumor cells and PD-1 or CTLA-4

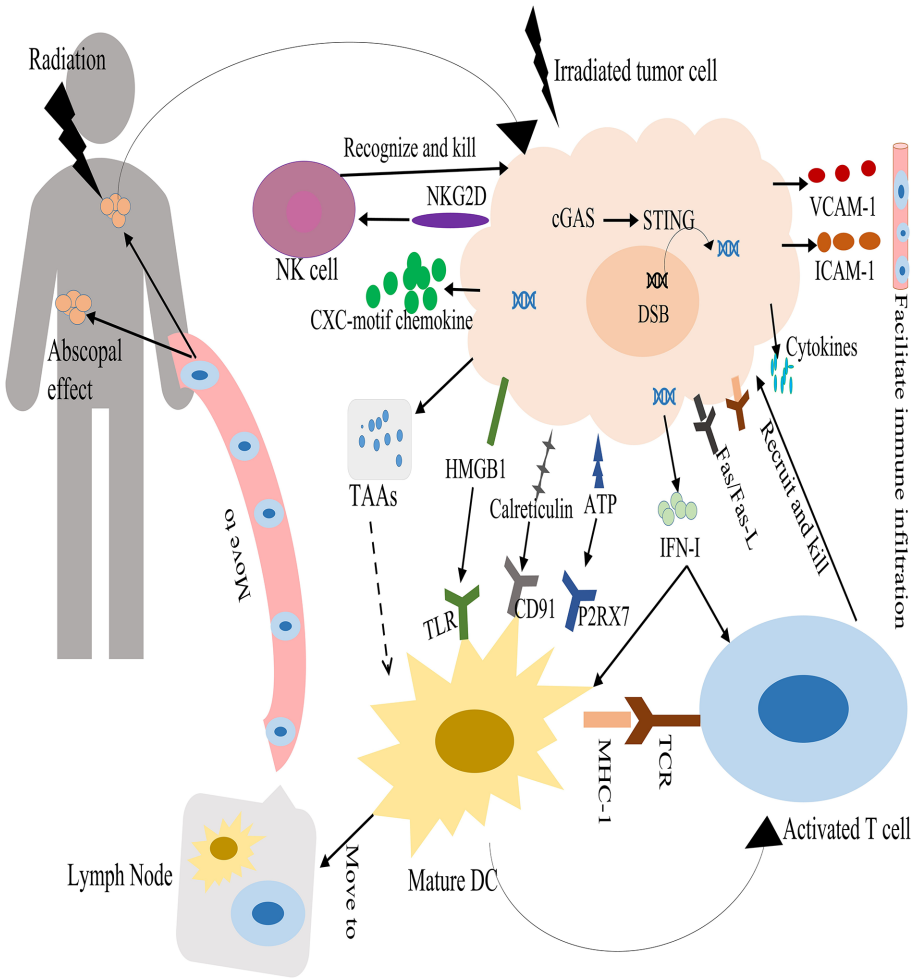

FIGURE 1
Antitumor immune enhancement of radiotherapy. Radiation therapy causes DNA DSBs in tumor cells and is sensed by the cGAS–STING pathway, resulting in the production of interferon I (IFN-I). In turn, IFN-I can stimulate dendritic cells (DCs) and T cell activation. Radiation therapy can induce immunogenic cell death. This releases danger-associated molecular patterns that promotes the activation and maturation of dendritic cells. DCs take up tumor-associated antigens (TAAs) from damaged tumor cells and travel to draining lymph nodes, and then present the TAAs on major histocompatibility complex class I (MHCI) to T cells through the T-cell receptor (TCR). Activated T cells move to the irradiated tumor and non-irradiated tumors through the blood circulation. Radiation can upregulate Fas and MHC-I molecules expression on tumors, and increase the release of cytokines and chemokines by tumor cells. This promotes the recruitment of activated T cells to kill tumor cells. In addition, radiation can upregulate the NK pathway to mediate tumor cells killing.

on cytotoxic T cells (CTLs). This can directly inhibit cytotoxic immune cell effector functions (152, 153). Therefore, when radiotherapy is combined with immune checkpoint inhibitors (such as anti-PD-1 antibody, anti-PD-L1 antibody and anti-CTLA4 antibody), T cell activity directed against tumor cells can be increased.

In summary, radiation can promote the recruitment and activation of DCs and cytotoxic T cells through a variety of mechanisms, but this may be counteracted by the migration of suppressive immune cells. This presents an opportunity to combine radiation with immunomodulatory agents to improve tumor control. The immunosuppressive effects of radiotherapy were shown in Figure 2.

The best combination of radiation therapy and immunotherapy

Radiation is increasingly used to control tumors locally, especially SBRT, with high rates of local control and significant benefits in terms of overall survival in many randomized trials (20, 154, 155). However, local tumor recurrence and distant tumor metastasis frequently occur when radiation therapy is used alone (156). Therefore, it is necessary to combine radiation therapy with other treatment options.

Immunotherapy has attracted great interest, and has become an established pillar of cancer therapeutics (99,

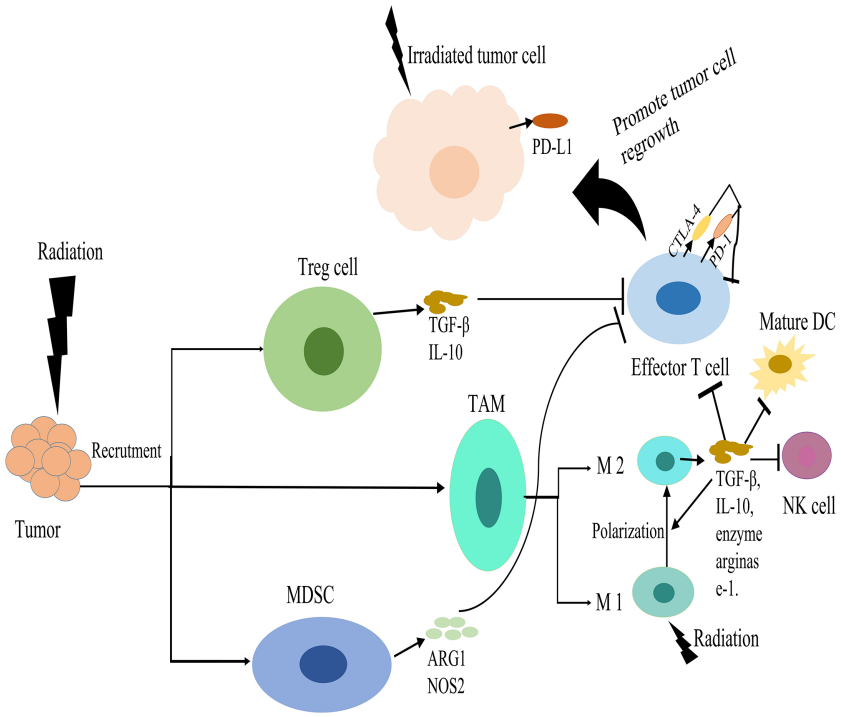

FIGURE 2
Immunosuppressive effects of radiotherapy. Radiation induces the recruitment of regulatory T cells (Tregs), myeloid derived suppressor cells (MDSCs) and tumor associated macrophages (TAMs) in the tumor microenvironment (TME). Tregs produce transforming growth factor beta (TGFβ) and IL-10, which suppress effector-T-cell activation. MDSCs can suppress the activation of T-cell responses *via* secretion of arginase-1 (ARG1) and nitric oxide synthase 2 (NOS2). Radiation can promote the polarization of macrophages from an inflammatory M1 phenotype into a tumor-supporting M2 phenotype. These M2 macrophages secrete IL-10 and TGFβ and the enzyme arginase-1, which suppress T cell. TGFβ can suppress the effector functions of T-cells and natural killer (NK) cells, inhibiting DC maturation, and promoting M2 macrophage polarity. Radiation stimulates upregulation of immune checkpoint inhibitory molecules, such as programmed cell death ligand 1 (PD-L1) on tumor cells and PD-1 or CTLA-4 on cytotoxic T cells, which down regulate T cell activation. These effects suppress the antitumor immunity and promote tumor cell regrowth.

157). Unfortunately, most immunotherapeutic strategies are not effective in inducing tumor regression when used alone, and a large number of patients do not respond or become refractory to immunotherapy (106, 158, 159). The overall response rate to anti-CTLA-4 antibody is around 15%, while the response rate to PD-1/PD-L1 antibodies was < 25% (160). There are serval reasons to prevent immunotherapy from reaching its full potential. First, the priming of tumor antigen-reactive T cells is insufficient. Second, the infiltration of antitumor effectors into the tumor was weak. Third, the tumor microenvironment is highly immunosuppressive. Fourth, cancer cells effectively evade recognition by immune effectors with impaired tumor-associated antigen presentation (101, 161, 162). It is a great clinical challenge to overcome immunotherapy resistance.

Many studies showed that radiotherapy and immunotherapy are complementary. Irradiated tumors exhibit distinct patterns of immunogenicity, thereby improving response to immunotherapy (93). In addition, tumors with immunotherapy are more sensitive to radiotherapy. This can promote the localized treatment of tumors. Many studies found that radiation with ICIs can successfully treat metastatic cancers. This not only induced a local response, but also significantly regressed distant lesions outside the irradiation field (163–167). Theelen et al. pointed out that the addition of radiotherapy to pembrolizumab immunotherapy significantly improved abscopal responses and survival in patients with metastatic non-small-cell lung cancer (NSCLC), compared with pembrolizumab alone (29). This indicates that radiotherapy can convert non-responders to ICIs into responders.

Although radiotherapy combined with immunotherapy can improve the immune response, not every combination of radiation and immunization has been validated in clinical trials (32, 168). To further improve the anti-tumor ability, we need to select the appropriate patient population, explore the optimal radiotherapy regimens (dose, fractionation and volume), immunotherapy regimens (such as CTLA-4 inhibitors and PD-1/PD-L1 inhibitors), the sequence of radiotherapy and immunotherapy, and reduce the immunosuppressive effects and toxicity of radiotherapy.

The appropriate radiotherapy regimens in combination with immunotherapy

Radiotherapy is a double-edged sword that is associated with immune activation and immune suppression. Therefore, it is necessary to study the optimal dose and fraction of radiotherapy to achieve optimal anti-tumor effects in combination with immunotherapy.

High-dose radiotherapy promotes tumor immunogenicity

Many studies have shown that HDRT (such as SBRT) in combination with ICIs is more likely to cause tumor cell necrosis, enhance anti-tumor immunity, and lead to significant tumor control (94, 169). HDRT has showed a more potent immunogenic effect against cancer cells than conventional radiotherapy (usually 1.8–2 Gy per day) (23, 25). The conventional radiotherapy usually lasts for several weeks. Therefore, lymphocytes can be rapidly cleared from the irradiated field, reducing tumor antigen-specific T cell populations through sustained site-specific cytotoxicity. HDRT takes advantages over traditional radiation therapy when combined with immunotherapy.

Exposed tumor to a radiation dose ranging from 5 and 12 Gy per fraction, the number of infiltrated $CD8^+$ cytotoxic T cells and NK cells were increased, while the number of Tregs was decreased. This is associated with the release of more anti-cancer cytokines, such as IFN-γ and TNF-α, and less immune suppressor cytokines, such as TGF-β and IL-10 (93, 170). Morisada et al. used hypo-fractioned radiation (8Gy*2f) or low-dose daily fractionated radiation (2Gy*10f) combined with anti-PD-1 antibody to treat mice bearing established syngeneic MOC1 oral carcinomas or MC38-CEA colon adenocarcinomas. They found that high-dose and low-dose fractionated radiation alone showed similar primary tumor control. However, anti-PD-1 antibody plus 8Gy*2f radiation rather than 2Gy*10f radiation, statistically significant enhanced $CD8^+$ cell dependent primary and abscopal tumors control by inducing expression of IFN and IFN-responsive genes on tumor cells (171). Lan et al. compared ablative hypo-fractionated radiotherapy (AHFRT, 23Gy/2f/9d) versus conventional fractionated radiotherapy (36Gy/9f/9d) in mice bearing tumors from Lewis lung carcinoma or melanoma B16F10 cells, under the same conditions with biological equivalent dose (BED). They showed that AHFRT combined with anti-PD-L1 antibody presented a superior efficacy in controlling tumor growth and augmenting systemic anti-cancer immunity. The mechanism is that AHFRT suppressed the recruitment of MDSCs into tumors by regulating the VEGF/VEGFR axis, reduced MDSC-associated PD-L1 expression and increased the cytotoxicity of $CD8^+$ T cells (25).

Many studies have shown that the abscopal effect was mainly observed in the combination of hypo-fractionated radiation regimens with ICIs. Dewan et al. used TSA and MCA38 cells to construct mouse tumor models. They found that fractionated radiation (8 Gy*3f or 6 Gy*5f) combined with anti-CTLA-4 antibody rather than single-dose radiation (20 Gy*1f) can induce an abscopal effect. In addition, 8 Gy*3f was more effective than 6 Gy*5f in eliciting systemic anti-tumor immunity combined with anti-CTLA-4 antibody (172). They further found that 20 Gy and 30 Gy single dose can attenuate cellular immunogenicity by inducing the DNA exonuclease Trex1 in various cancer cells, thereby degrading cytoplasmic DNA in irradiated cells (24). Cytosolic DNA stimulates secretion of IFN-β by cancer cells following activation of the DNA sensor cGAS and its downstream effector STING, which mediates optimal *in situ* vaccination (173). In fact, it was observed that the higher the dose per fraction, the more Trex1 was induced, resulting in significant DNA degradation. Therefore, the fractionated dose above the threshold (varies between 12 and 18 Gy in different cancer cells) for inducing Trex1 can result in downstream abrogation of IFN-β production, reducing DC recruitment and activation. Finally, it fails to induce systemic antitumor immune response (24). These results provide references for better selection of the radiotherapy regimens. However, these results also need to be validated clinically.

However, like conventional radiotherapy, HDRT can suppress tumor-reactive immunity by increasing the infiltration of Tregs and MDSCs, inducing an M2-like phenotype, and releasing TGF-β and IL-10 (143, 174). Lin et al. studied the effects of HDRT (8Gy/f) with and without anti-Gr-1 using syngeneic murine allograft prostate cancer models. They demonstrated that HDRT induced an early rise of MDSCs, followed by an increase of functionally active CD8 tumor-infiltrating lymphocytes. However, systemic depletion of MDSCs by anti-Gr-1 did not augment the antitumor immunity of HDRT because of the compensatory expansion of Treg-mediated immune suppression. This indicates that it is necessary to block MDSCs and Tregs for enhancing radiotherapy-induced antitumor immunity (33). Monjazeb et al. found that although HDRT induces an increase in $CD8^+$ T cells and $CD8^+/PD1^+/Ki67^+$ T-cells in the radiation field, HDRT may lead to a decrease in the ratio of M1/M2 macrophages in the tumor microenvironment (175). Furthermore, HDRT can inhibit the anti-tumor immune response by inducing tumor vascular damage. This can limit the infiltration of cytotoxic T lymphocytes into the tumor, and increase the hypoxic area (176, 177). Therefore, it is necessary to study the suppression of HDRT on the immune system, because it leads to poor prognosis, and it may be a reasonable therapeutic target.

In clinical practice, the combination of HDRT and immunotherapy is sometimes not superior to immunotherapy alone. Theelen et al. conducted a multicenter, randomized phase 2 study in advanced NSCLC patients who were treated with pembrolizumab either alone or after SBRT (8Gy*3f). They found that the overall response rate at 12 weeks was 18% in the pembrolizumab alone arm *vs* 36% in the pembrolizumab plus SBRT arm without statistical difference. In addition, no improvement in PFS or OS was achieved after the addition of SBRT (168). McBride et al. conducted another randomized clinical trial of nivolumab versus nivolumab plus SBRT (9 Gy*3f) in patients with metastatic or recurrent head and neck squamous cell carcinoma. The addition of SBRT to nivolumab did not statistically improve the objective response rate, OS or PFS, and there was no evidence of an abscopal effect in unselected patients (32). Therefore, ICIs and SBRT have synergistic local effects, but rare abscopal effects.

In conclusion, HDRT combined with immunotherapy does not always induce immune-enhancing antitumor effects and is only effective in a small subset of tumor patients. Tumor progression can still occur even if the complete remission is achieved. It is necessary to explore the best comprehensive treatment strategy.

Low-dose radiotherapy reverses tumor-suppressing immune system

Although HDRT in combination with ICIs shows promising efficacy for clinical application, the treatment outcome still needs to be further optimized. A recent theory proposed that LDRT can modulate the TME, perhaps revolutionizing tumor treatment efficacy. LDRT usually refers to doses below a threshold, that is, the amount of doses less than that can physically damage DNA or kill cancer cells directly (178). The most common LDRT doses are 0.5-2 Gy/fraction, with total doses up to 1-10 Gy (179, 180). According to previous reports, LDRT modulated the immune suppressive stroma by downregulating TGF-β, repolarizing macrophages to favor the M1 over the M2 phenotype, and significantly enhancing the infiltration of effector CD4 T cells and NK cells. LDRT improved the efficacy of anti-PD1 and anti-CTLA4 agents, thereby promoting the overall systemic antitumor response (41). We will describe the ways that LDRT modulates the immune system in detail.

First, LDRT promotes the differentiation of macrophages to an M1-like phenotype. M2 macrophages can suppress antitumor immunity, and promote a radioresistant phenotype by secreting immunosuppressive mediators, such as IL-10 and TGF-β (181). Therefore, transforming the type of macrophages is critical to improve the immune enhancing effect. Felix Klug et al. (179) demonstrated that LDRT (0.5-2 Gy) can effectively transform M2 macrophages to iNOS$^+$ M1 phenotypes, resulting in strong CD4$^+$ and CD8$^+$ T cells infiltration into human pancreatic carcinomas. After application of 0.5 Gy, the irradiated tumors contained the highest number of T cells, accompanied by an increase in CD4$^+$ FoxP3$^+$ T cells. In addition, LDRT can induce vascular normalization through crosstalk between macrophages and T cells. LDRT promoted T cell-mediated tumor eradication and prolonged survival (179). Prakash et al. irradiated advanced tumor-bearing Rip1-Tag5 mice with LDRT (2Gy*2f). They found profound changes in the inflammatory tumor microenvironment, characterized by induction of M1-related effecter cytokines as well as reduced cytokines of tumor-promoting and M2-related effecter cytokines (182). Furthermore, LDRT can program macrophages differentiation to an M1-like phenotype by ameliorating the hypoxia problem of tumors. Tumor hypoxia is known to be performed by angiogenesis-promoting HIF-1. This promotes angiogenesis, thereby interfering with tumor infiltration of CD8$^+$ T cells and retuning of M1 phenotypic macrophages across the inert endothelium. Finally, it results in immunosuppressive effects (183–185). Nadella et al. demonstrated that LDRT (2 Gy) can downregulate HIF-1 in irradiated tumors, thereby supporting the differentiation of naive macrophages toward the M1 phenotype (186). Therefore, solving the hypoxia problem of bulk tumors can enhance the immune efficacy. LDRT has also been clinically observed to promote the differentiation of M1-type macrophages (175). Monjazeb et al. conducted a multicenter phase 2 study of 20 patients with histologically confirmed metastatic microsatellite-stable colorectal adenocarcinoma who had received at least one line of chemotherapy. These patients were randomly assigned to repeated LDRT or HDRT with PD-L1/CTLA-4 inhibition. They found that LDRT has the potential to increase the ratio of M1/M2 macrophages (175).

Second, LDRT can promote anti-tumor cytotoxicity of NK cells. LDRT can augment the direct expansion and cytotoxicity of NK cells through the P38-MAPK pathway (187). In addition, Sonn et al. found that when purified NK cells were irradiated with 0.2 Gy, the toxicity of NK cells was enhanced, while cell proliferation and apoptosis were unaffected (188). Cheda et al. (189) compared BALB/c mice that received or did not receive LDRT (single dose of 0.1 or 0.2 Gy), which were then injected with sarcoma cells. They found that the number of pulmonary tumor colonies was significantly reduced, and the cytolytic function of NK cells was significantly stimulated in the irradiated mice compared with the control group. In addition, NK-inhibitory anti-asialo GM1 antibody can totally abolish the tumor suppressive effect of LDRT. These results indicate that LDRT suppresses the development of experimental tumor metastases by stimulating the cytolytic function of NK cells.

Third, LDRT enhances T-cell infiltration. Herrera et al. (190) reported that LDRT of murine tumors promoted T-cell infiltration and responded to combinatorial immunotherapy in

an IFN dependent manner. The mechanism is that LDRT induces $CD4^+$ cells with characteristics of exhausted effector cytotoxic cells. One subset expressed NKG2D and exhibited proliferative capacity, as well as a unique subset of activated DCs expressed the NKG2D ligand RAE1. Zhou et al. established an *in vivo* lung cancer model. They found that LDRT activated T cells and NK cells, and promoted splenocyte cytotoxicity and T cell infiltration in the tumor tissues (191). Hashimoto et al. found that low-dose total body irradiation (0.2 Gy) increased the proportion of $CD8^+$ cells in splenocytes, and even tumor-infiltrating lymphocytes were predominantly $CD8^+$. Low-dose total body irradiation (0.2 Gy) inhibited lung and lymph node metastasis in tumor-bearing rats (192). In addition, low-dose total body irradiation of 2 Gy represents a powerful tool to foster $CD4^+$ T cell-based cancer immunotherapies by favoring T helper 1 cells driven antitumoral immunity (193).

Fourth, LDRT can affect the function and activity of regulatory T cells (Tregs), thereby enhancing antitumor immunity. Tregs belong to a group of T lymphocytes that possess a negative immune regulatory function. The increased numbers of these cells in liver, breast, and ovarian cancer are closely related to the immune escape, occurrence, and development of tumor cells. Wang et al. found that LDRT (total 0.45 Gy) of the spleen can shrink tumors and increase the survival rate of rats with liver cancer. The mechanism by which LDRT enhances the immune effects may be that LDRT reduces the ratio of $CD4^+CD25^+$Treg/$CD4^+$ in the blood and $Foxp3^+$, IL-10, TGF-β and cytotoxic T lymphocyte-associated antigen 4(CTLA-4) expression (194). Liu et al. found that LDRT significantly reduced the percentage and absolute numbers of $CD4^+CD25^+Foxp3^+$ regulatory T cells in naive mice, whereas $CD4^+CD44^+/CD8^+CD44^+$ effector memory T cells were greatly increased in naive mice (195). These results indicate that LDRT is a potential approach to overcome the tumor immunosuppressive microenvironment.

Finally, LDRT enhances the efficacy of ICIs. Barsoumian et al. (41) established mouse tumor models and irradiated the tumors with different doses. They found that LDRT alone (1Gy*2f) can effectively prolong survival by controlling tumor growth. The anti-tumor efficacy was further significantly enhanced when combined with anti-PD1 and anti-CTLA-4 drugs. This may be because LDRT can significantly activate CD4 and CD8 T cells, and enhance NK cell infiltration and M1 macrophage polarization and reduce TGF-β cytokine. Nowosielska et al. (196) found that LDRT to the whole-body (0.1 or 1.0 Gy) combined with anti-CTLA-4 antibody and anti-PD-1 antibody and NVP-AUY922 significantly reduced tumorigenesis in mice, and inhibited the clonogenic potential of Lewis lung cancer cells *in vitro*. By using targeted radionuclide therapy to semi-selectively deliver radiation to mouse tumors, Patel et al. found that low-dose targeted radionuclide therapy enhances the response of immunologically "cold" tumors to ICIs. After the combination of targeted radionuclide therapy and ICIs, 45-66% of mice exhibited complete responses and tumor-specific T-cell memory, while only 0% with targeted radionuclide therapy or ICIs alone. The reason is that the combination therapy activates the production of proinflammatory cytokines in the TME, promotes tumor infiltration and clonal expansion of effector $CD8^+$ T cells, and reduces spontaneous metastasis (197). Furthermore, the addition of LDRT to PD-L1/CTLA-4 blockade was feasible and safe in clinical practice (175). In a phase I clinical study, Herrera et al. found that the adding LDRT (0.5 or 1 Gy per fraction) to the combination immunotherapy group showed a therapeutic effect for an overall disease control rate of 87.5% in patients with immune desert tumors. In addition, using a single-sample gene set enrichment analysis approach, they observed that responding tumors exhibited an increase in Th1, $CD8^+$ and T_{EM} signatures, whereas non-responding tumors exhibited an upregulation of M2 macrophage and neutrophil signatures (190). However, in some cases, LDRT combined with immunotherapy failed to induce effective antitumor immunity. Schoenfeld et al. (198) conducted an open-label, multicenter, randomised, phase 2 trial involving 90 patients with metastatic NSCLC resistant to PD(L)-1 therapy. Patients were randomly assigned to 3 arms, durvalumab plus tremelimumab alone, or in combination with LDRT (2 Gy/4f), or in combination with HDRT (24 Gy/3f). Radiotherapy was delivered at 1 week after initial durvalumab–tremelimumab administration. They found that neither HDRT nor LDRT increased the response to combined PD-L1 plus CTLA-4 inhibition.

The rationale for using LDRT is not necessarily to ablate or kill the tumors, but to activate the immune system to eliminate these lesions in concert with other therapeutic approaches. Clinically, LDRT has the following advantages over HDRT. First, the toxicity of LDRT is low. If radiotherapy is to be delivered simultaneously to several lesions within an organ, it is difficult to meet the dose limit to the organ at risk with SBRT, whereas dose limits will be easier to meet with LDRT. Therefore, LDRT is dosimetrically more feasible than SBRT in the treatment of large tumor volumes, or even a whole organ. Second, LDRT is safer for patients who have received radiation in the past. There is a minimal concern about exceeding normal tissue dose-constraints when re-radiation is performed by LDRT. Finally, LDRT is easier to be delivered. In clinical practice, LDRT can be performed through three-dimensional technology, while HDRT requires specialized imaging, respiratory gating, and even gold fiducials implantation.

In sum, LDRT provides an emerging approach to address limitations of radioimmunity mechanisms. It is necessary to further study this important method Immunomodulatory effects of LDRT in tumor microenvironment are shown in Figure 3.

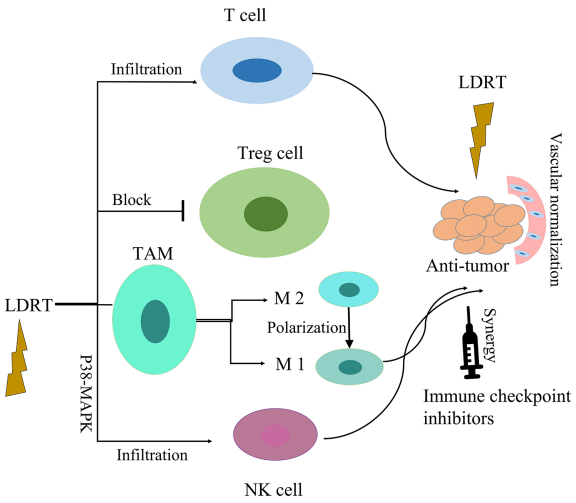

FIGURE 3
Immunomodulatory effects of LDRT in tumor microenvironment. LDRT modulates the tumor microenvironment by repolarizing macrophages to favor the M1 over the M2 phenotype, blocking regulatory T cells, and enhancing the infiltration of effector CD4 T cells and NK cells. Low-dose radiation can improve the efficacy of immune checkpoint inhibitors.

High-dose and low-dose radiotherapy synergistically enhance antitumor immune responses

HDRT and LDRT work differently on the immune system. We take full advantage of the advantages of HDRT and LDRT to enhance anti-tumor immune responses. HDRT can increase the release and presentation of tumor antigen, and stimulate immune cell activation. However, LDRT can modulate the TME to stimulate immune cell infiltration into the tumor stroma and the tumor bed of distant tumors. Next, we will introduce the preclinical and clinical studies of HDRT combined with LDRT, i.e., multimodal radiotherapy.

Studies showed that HDRT in combination with LDRT was superior to HDRT or LDRT alone in tumor control and activation of anti-tumor immunity (39, 199). Savage et al. (39) designed a novel radiation scheme (PAM-RT), a single high-dose radiation (22Gy) followed by post-ablation modulation with four daily low-dose fractions (0.5Gyx4f). They found that PAM-RT localized to the primary tumor in 3LL tumor-bearing mice can significantly delay tumor growth and increase survival. They treat metastatic breast cancer (4T1) mice with PAM-RT, where the primary tumor received high-dose irradiation (20 Gyx3f) and metastatic organs received low-dose irradiation (whole lung, 0.5 Gyx4f). Survival was significantly increased after whole-lung radiated by low dose compared with primary tumor ablative radiotherapy alone. The mechanism is that PAM-RT can promote remodeling of the TME in the primary tumor as well as the metastatic site by reducing Tregs, activating macrophages to an inflammatory phenotype, and promoting infiltration of $CD8^+$ CTLs into metastatic tumors. Liu et al. (199) used a combination of hypo-fractionated radiation therapy (8Gy×3f) targeted primary tumor with low-dose total body irradiation (0.1Gy) in a syngeneic mouse model of breast or colon carcinoma. They found that low-dose total body irradiation alone did not delay the growth of primary or secondary tumors. Hypo-fractionated radiation therapy led to a significant growth delay of the irradiated primary tumors, but did not have a systemic immune related response to secondary tumors. However, the combination of low-dose total body irradiation and hypo-fractionated radiation therapy significantly delayed the growth of both the primary and secondary tumors, and translated into the best OS with systemic antitumor response characteristics. The mechanism is that the combination therapy (HDRT and LDRT) induced infiltration of $CD8^+$ T cells, IFN-γ^+ $CD8^+$ T cells and DCs in unirradiated tumors, reduced granulocytic-myeloid-derived suppressor cells and M2 macrophages, and increased the percentage of antitumor eosinophil population. These results indicate that LDRT can serve as a potential therapeutic agent for patients with metastatic cancer. Their therapeutic potential is significantly enhanced when combined with HDRT.

Compared with the combination of ICIs with either LDRT or HDRT alone, the combination of LDRT and HDRT further enhanced the response to ICIs, resulting in an enhanced antitumor response (40–42, 197). Barsoumian et al. proposed the use of high dose and low dose radiation (RadScopal technique) with immune oncology agents (anti-TIGIT and anti-PD1 monoclonal antibodies) to against highly metastatic lung adenocarcinoma tumors in 129Sv/Ev mice. They found that the triple therapy can prolong the survival of treated mice, and halt the growth of primary and secondary tumors,and reduce the percentages of $TIGIT^+$ exhausted T-cells and $TIGIT^+$ regulatory T-cells (40). Yin et al. (42) compared HDRT/anti-PD1, HDRT/LDRT, or LDRT/anti-PD1 double treatments. They demonstrated that the enhancement of the abscopal response was achieved by triple therapy consisting of HDRT (8 Gy*3f) to treat the primary tumor, LDRT (2 Gy*1f) to treat the abscopal tumor, and anti-PD1 therapy. The enhanced abscopal effect was associated with increased infiltration of $CD8^+$ effector T cells and upregulated expression of T cell-attracting chemokines. The triple treatment also improved the tumor response in patients with metastatic NSCLC and was well tolerated. In addition, HDRT combined with LDRT and double agent checkpoint blockers can effectively control metastatic tumors by increasing $CD4^+$ effector T cells, enhancing NK cell activation, and increasing M1 macrophages in secondary tumors. Further clinical studies have shown that when the tumor burden was high, it was necessary to use HDRT to priming T cells at the primary tumor site, and LDRT to modulating the stroma of secondary (metastatic) tumors (41).

Surprisingly, the treatments combining HDRT with LDRT and immunotherapy have also achieved promising clinical results. Analyzing 26 cancer patients received LDRT (1-20 Gy in total), Menon et al. found that this was because of the scatter of HDRT or the intentional treatment at a second isocenter of LDRT. These patients underwent prospective clinical trials on the combination of radiotherapy and immunotherapy. They compared lesions that received LDRT with without radiation (< 1 Gy). 85% of lesions that received LDRT achieved PR/CR, while 18% of lesions that received no-dose (P=0.0001). This indicates that LDRT can increase systemic response rates of metastatic disease treated with HDRT and immunotherapy (43). They also conducted a phase II trial of ipilimumab with concurrent or sequential SBRT (50 Gy/4f or 60 Gy/10f) for metastatic lesions in the liver or lung. Some non-targeted lesions received LDRT (5–10 Gy) because they were anatomically close to another irradiated site. Further analysis showed that lesions that received LDRT were more likely to respond than those that did not (31% *vs* 5%, P=0.0091) (200). Patel et al. analyzed a phase II trial of HDRT (3–12.5 Gy/f up to 20–70 Gy total) with or without LDRT (1-10 Gy total; 0.5-2 Gy/f) for patients who had the metastatic disease that progressed on immunotherapy within 6 months. A total of 74 patients with NSCLC or melanoma were enrolled in the study. 39 patients received HDRT and 35 patients received the combination of HDRT and LDRT. There was no significant difference regarding disease control rate. However, the overall response rate for HDRT + LDRT *vs*. HDRT cohorts, lesions treated by LDRT was significantly improved rates of lesion-specific responses compared with nonirradiated lesions. This is because LDRT induced a remarkable increase of T- and NK cell infiltration into the irradiated lesions (180). These clinical studies indicate that HDRT and LDRT combined with immunotherapy can synergistically generate tumor-specific immune responses, thereby enhancing systemic antitumor effects.

In summary, multimodal radiotherapy, a combination of HDRT to stimulate T cell priming together with LDRT to modulate inhibitory tumor microenvironment, can enable immune cells to infiltrate into tumor bed and trigger antitumor responses. This provides a new treatment alternative for patients with advanced cancer after multiple lines of therapy, and brings immunotherapy into a new field of systemic disease control. Many clinical trials are investigating the efficacy and safety of different combinations of HDRT and LDRT in patients with advanced tumors (Table 1).

Challenges in clinical practice

Patient response to immunotherapy or immunotherapy combined with HDRT can be enhanced by delivering LDRT to certain tumor sites for the purpose of immunomodulating the TME, thereby promoting systemic propagation of anti-tumor immunity and the destruction of tumor by immune effector cells. However, it is necessary to further study clinical practices of high-dose and low-dose radiotherapy. For example, which tumor site should be treated with HDRT or LDRT? Whether HDRT and LDRT should be delivered to the same tumor site? What is the best sequence of HDRT and LDRT?

TABLE 1 Clinical trials of multimodal radiotherapy (HDRT and LDRT) in advanced tumors.

Trial number	Phase		Cancer type	Treatment strategy	Primary end points
NCT02710253	II	Single group	Hematopoietic and lymphoid cell neoplasm / Metastatic malignant solid neoplasm	SBRT(4f, 5f, or 10f) or EBRT(4f, 5f, or 10f) for any site of metastatic disease.	Disease control rate. Objective response. Incidence of adverse events.
NCT02416609	Not applicable	Single group	Advanced Pancreatic Cancer	In each cycle, Gem-based doublets will be administered concurrent with LDRT for a total of 4 cycles. If there is no progress, SBRT will be performed sequentially.	Progression free survival
NCT03085719	II	Not applicable	Head and neck cancer	Arm 1 is that HDRT (3f) is combined with pembrolizumab. Arm 2 is HDRT and LDRT in combination with pembrolizumab.	Overall response rate
NCT03812549	I	Single group	Stage IV NSCLC	SBRT (30Gy/3f) is first delivered to lung, in combination with LDRT starting from the 2nd day of SBRT, followed by sintilimab monotherapy starting within 7 days after the completion of radiotherapy. Sintilimab will be administered at 200mg every 3 weeks.	Safety and tolerability

Selection of irradiation sites for high and low dose radiotherapy

There are few literatures on the targeting volume selection in studies combing immunotherapy with multimodal radiotherapy (HDRT and LDRT). Based on existing reports and clinical experiences, we developed individualized strategies based on performance status of patients, clinical symptoms, extent of tumor burden, and the immune type of the tumor microenvironment (Figure 4). This individualized treatment regimen can not only control the tumor, but also improve the patient's quality of life.

Single site irradiation

For patients with only a single lesion, HDRT can be used to ablate the tumor for achieving the radical cure. This not only shrinks the tumor. but also promotes the release of antigens. Subsequent application of LDRT to modulate the tumor microenvironment can attenuate the immunosuppressive effects of SBRT, and increase immune effector cell infiltration, thereby synergistically enhancing the response to ICIs. However, it is necessary to study it in the future. At present, only a preclinical study has reported that HDRT followed by LDRT to the primary tumor can delay tumor growth and prolong survival in mice (39).

Multisite or all sites irradiation

Tumors are heterogeneous (201, 202). This indicates that tumor associated antigens (TAAs) present in some tumor sites may be different from those in other tumor sites, or may not be equally immunogenic. Targeting a single metastatic site in patients with multiple metastases cannot unmask TAAs in another site unless those TAAs are shared. Therefore, useful antitumor immune responses are not activated systemically.

Monjazeb et al. (175) did not observe objective responses outside the irradiation field. This indicates that irradiating 1-2 lesions in combination with the immune checkpoint blockade is not sufficient to mediate systemic antitumor immunity in patients with refractory colorectal cancer. In addition, in the multicenter, randomized phase 2 study, 76 patients with recurrent metastatic NSCLC were randomized to either pembrolizumab alone or pembrolizumab to a single tumor site after SBRT (3 doses of 8 Gy). The overall response rate of the added SBRT group was twice that of the control group. However, the results did not meet the criteria of a meaningful clinical benefit endpoint (168). Luke et al. conducted a phase I study enrolling patients with metastatic solid tumors who had progressed on standard treatment. 69 patients were treated with SBRT (total of 30-50Gy/3-5f) and at least one cycle of pembrolizumab. SBRT was delivered to two to four metastases, but not all metastases were irradiated. They found that multi-site SBRT can limit the progression of existing metastases, and enhance anti-tumor immune responses. This improves outcomes in metastatic patients treated with pembrolizumab

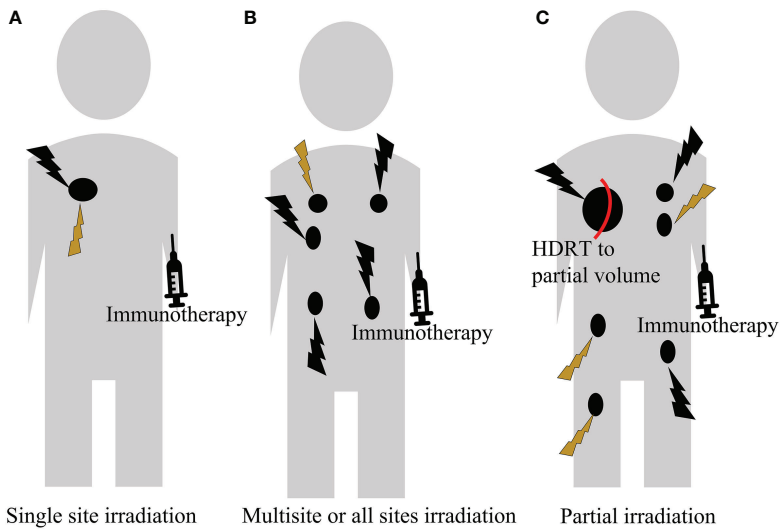

FIGURE 4
A personalized treatment regimen based on the patient's performance status, clinical symptom, extent of tumor burden, and the immune type of the tumor microenvironment. **(A)** For a single tumor, HDRT can initiate T cell priming, followed by LDRT to modulate the tumor microenvironment. **(B)** For oligometastatic disease, HDRT can be delivered to all lesions. If it is infeasible and intolerable, it can be supplemented with LDRT. **(C)** For extensive metastatic disease, partial volume HDRT can be delivered to one or a few lesions, followed by LDRT to other lesions.

(203). Iyengar et al. (21) found that the addition of SABR to all severe disease sites significantly improved PFS without increasing toxic effects. In addition, studies have reported that multisite SBRT followed by pembrolizumab was safely tolerated (27, 204). These clinical experiences indicate that irradiation of multiple sites or all metastatic lesions can maximize systemic synergy.

Patients classified as having oligo-metastases may be candidates for HDRT delivery to all lesions for immune priming and local control. In addition, direct delivery of SBRT to all tumor sites ensures tumor sterilization. However, irradiation of all lesions by HDRT may sometimes be infeasible and intolerable in clinical practice because of dose volume constraints in normal tissue surrounding the tumors. Therefore, some tumor lesions can be supplemented with low-dose irradiation.

In sum, multiple target irradiation tends to induce stronger antitumor immunity and generate more frequent abscopal responses than a single target. Therefore, it is necessary to further study this approach in clinical settings.

Partial irradiation

Systemic therapy is the standard of care in patients with non-oligometastatic cancers. However, the addition of SBRT can not only shrink the local tumor to induce an effect of *in situ* vaccination, but also relieve local symptoms, such as pain, obstruction and bleeding, etc. To enhance the systemic efficacy of immunotherapy, it is necessary to use HDRT to stimulate immune priming for the bulky or "cold" tumors. The partial irradiation may be considered in this case because of toxicity.

Preclinical experiments have shown that high-dose partial irradiation can delay tumor growth through immune activation. Markovsky et al. (205) treated 50% or 100% of tumors with radiation in a 67NR Murine Orthotopic Mammary Tumor Model and the less immunogenic Lewis Lung Carcinoma mouse model. They found that partial irradiation in immunocompetent mice resulted in a tumor response similar to full irradiation. This is because of the $CD8^+$ T cell-mediated immune stimulation mechanism. Furthermore, a significant abscopal effect was elicited after hemi-irradiation of the primary tumor with a single dose of 10Gy in the 67NR model. Yasmin-Karim et al. (206) found irradiating a field smaller than the entire tumor volume showed the same or better distal effect than irradiating the entire tumor volume field, and significantly reducing healthy tissue damage. This is due to higher infiltration of cytotoxic CD8+ T lymphocytes in treated and untreated tumors.

The partial irradiation combined with immunotherapy is clinically feasible. Luke et al. found that partial irradiation by SBRT was performed when the metastases were greater than 65 mL. They compared patients with at least one tumor partially irradiated to those with fully irradiated tumors, and found no statistically significant tumor control rate at 3 months (27). They further found no statistically significant difference in objective response rate, PFS, and OS between patients who received full and partial SBRT at multiple sites in the presence of pembrolizumab. Furthermore, a clinical response at the irradiated site can be induced without irradiating the entire metastases (203). Lemons et al. (207) reported that partially irradiated tumors exhibited similar control as completely irradiated tumors in patients with metastatic solid tumors treated with pembrolizumab and SBRT. These indicate that partial volume SBRT is enough to activate immune priming.

A novel partial irradiation technique, spatially fractionated radiation therapy (SFRT), can also induce an antitumor immune response. SFRT can deliver a high dose to a large irradiation field that is segmented into several small units with steep dose gradients, which lead to reduce the normal tissue toxicity (208–211). In the study of Johnsrud et al. (212), whole tumor irradiation or SFRT (a single dose of 20 Gy) alone or in combination with ICI were tested in mice using a triple negative breast tumor. In the group of SFRT, they observed the abscopal immune response in contralateral tumors with obviously increased infiltration of both antigen-presenting cells and activated T cells, followed by an increase in systemic IFNγ production and ultimately a delay in tumor growth. Further studies are needed to explore the new partial irradiation technique.

In addition to immunotherapy for those patients with extensive metastases, it is beneficial to apply partial volume HDRT to one or several lesions to induce immunogenic cell death. Then, applying LDRT to other lesions for tumor microenvironment modulation can enhance abscopal effects, thereby reducing tumor burden.

The optimal sequence of high and low dose radiotherapy

HDRT and LDRT combined with immune checkpoint blockades can improve local and systematic antitumor responses in advanced tumors. However, the optimal sequence of these therapies for optimal efficacy remains unclear.

For combination therapy, LDRT can be applied before or after HDRT. Many existing studies about the sequencing issue have different results. Savage et al. (39) divided C57BL/6 mice with palpable subcutaneous 3LL tumors into five treatment groups: no treatment, 24 Gy on day 1 or 5, four fractions of 1Gy followed by 20 Gy or 20 Gy followed by four fractions of 1Gy, four of which were treated with radiation therapy to the primary tumor. They found that 1Gyx4f after ablation radiation (20 Gy) showed the best tumor control and the longest survival. However, pre-treatment with low-dose radiotherapy resulted in

minimal tumor control compared with single-dose ablative radiotherapy. This is due to the rapid growth of 3LL tumors, and ablative radiation targeting the larger tumors on day 5. This can affect the efficacy of the priming radiation. Therefore, it is necessary to control rapidly growing tumors with high-dose radiotherapy first, and then modulate the immune microenvironment with low-dose radiotherapy. However, other scholars found that sequential administration of LDRT followed by HDRT achieved superior antitumor immunity than the start of HDRT before LDRT. Liu et al. (199) administered HDRT to the primary tumor at 48, 72, 96, and 120 h after low-dose total body irradiation (L-TBI) in mouse tumor models. Starting HDRT at 72 h after L-TBI can achieve the best overall survival and the maximum abscopal effect. In addition, they compared the time of L-TBI 3 days before or after HDRT, or simultaneously with HDRT. The results showed that HDRT 3 days after L-TBI exhibited the best therapeutic effect, for example, a significant inhibition of tumor growth and improved survival of the treated mice. They found that L-TBI followed by HDRT can induce an adaptive immune response and protect the immune system of the mice. Zhou et al. observed that LDRT pretreatment before HDRT was able to ameliorate the HDRT-induced immune impairment and enhance the antitumor immunity (191). Therefore, it is necessary to conduct large preclinical and clinical trials for the optimal sequencing of HDRT and LDRT.

However, the optimal timing of the addition of immunotherapy to HDRT and LDRT remains unclear. Some scholars pointed out that immunotherapy is more effective after radiotherapy than before. This is because radiotherapy can promote the release of TAAs and destroy any pre-existing immune tolerance in the tumor periphery. Wei et al. (213) demonstrated that the administration of αPD-1 antibody after local tumor irradiation could induce a potent abscopal response while the addition of αPD-1 before radiation abrogated the abscopal effect. This antitumor efficacy was associated with the expansion of polyfunctional intratumoral $CD8^+$ T cells, reduction of intratumoral dysfunctional $CD8^+$ T cells, and expansion of reprogrammable $CD8^+$ T cells. Many studies showed that the concurrent combination of anti-PD-L1 antibody and radiation achieved better tumor control than the sequential schedule (214, 215). Bestvina et al. conducted a randomized phase 1 trial comparing the combination of nivolumab and ipilimumab with sequential or concurrent multisite SBRT in patients with stage IV NSCLC. They found that the median PFS were 18.6 and 13.2 months for concurrent and sequential therapy, respectively. The concurrent treatment strategy was not more toxic than the sequential one (216). However, there are some different views. A phase 1 trial compared combined pembrolizumab with SBRT administered either prior to the first pembrolizumab cycle (arm A) or prior to the third pembrolizumab cycle (arm B). Their results indicated that ORR of arm B was significantly better than that of arm A (44.4% *vs* 0%) (217). This is because the administration of immunotherapy prior to SBRT stimulates antigen-presenting cells and effector T cells, thereby making these cells ready to respond to the tumor antigen efflux generated by SBRT (169). Therefore, it is necessary to further study the optimized sequence of high and low dose radiotherapy combined with immunotherapy according to the biological characteristics of tumors, the selection of immunotherapy drugs, and the effects of radiotherapy on the immune system.

Conclusion

In this paper, we introduced a multimodal radiotherapy regimen (HDRT combined with LDRT) to synergistically enhance the local and systemic antitumor immunity, and improve the response to immunotherapy, thereby achieving the best anti-tumor effects. HDRT induces *in situ* tumor vaccine and primes cytotoxic T cells. LDRT modulates the tumor microenvironment, which in turn promotes the infiltration and lethality of immunocompetent cells. This multimodal radiotherapy regimen can be applied to primary tumor and metastatic lesions, thereby improving the local and systemic antitumor immunity. It is even possible to irradiate the whole organ with LDRT to boost immunity for widespread organ metastases, such as the lungs or liver. In clinical practice, it is possible to individually implement multimodal radiotherapy coupled with immunotherapy according to the patient's performance status of patients, disease burden, and tumor immune microenvironment phenotypes. It is necessary to conduct a further study to solve those issues.

Author contributions

XS: Conceptualization. XJ, JW, SL, HH, WJ and GC searched the literature. XJ and WJ wrote the first draft. XS, WD and BZ wrote and edited overall. All authors contributed to the article and approved the submitted version.

Funding

The work was supported by grants from the Hospital Research Foundation of Jinling Hospital (YYQN2021084).

Conflict of interest

The authors declare that the research was conducted in the absence of any commercial or financial relationships that could be construed as a potential conflict of interest.

Publisher's note

References

1. Atun R, Jaffray DA, Barton MB, Bray F, Baumann M, Vikram B, et al. Expanding global access to radiotherapy. *Lancet Oncol* (2015) 16(10):1153–86. doi: 10.1016/S1470-2045(15)00222-3

2. Citrin DE. Recent developments in radiotherapy. *New Engl J Med* (2017) 377 (11):1065–75. doi: 10.1056/NEJMra1608986

3. Delaney G, Jacob S, Featherstone C, Barton M. The role of radiotherapy in cancer treatment: Estimating optimal utilization from a review of evidence-based clinical guidelines. *Cancer: Interdiscip Int J Am Cancer Soc* (2005) 104(6):1129–37. doi: 10.1002/cncr.21324

4. Caudell JJ, Torres-Roca JF, Gillies RJ, Enderling H, Kim S, Rishi A, et al. The future of personalised radiotherapy for head and neck cancer. *Lancet Oncol* (2017) 18(5):e266–e73. doi: 10.1016/S1470-2045(17)30252-8

5. Grassberger C, Ellsworth SG, Wilks MQ, Keane FK, Loeffler JS. Assessing the interactions between radiotherapy and antitumour immunity. *Nat Rev Clin Oncol* (2019) 16(12):729–45. doi: 10.1038/s41571-019-0238-9

6. Carvalho H, Villar RC. Radiotherapy and immune response: The systemic effects of a local treatment. *Clinics* (2018) 73:e557s. doi: 10.6061/clinics/2018/e557s

7. Herrera FG, Bourhis J, Coukos G. Radiotherapy combination opportunities leveraging immunity for the next oncology practice. *CA: Cancer J Clin* (2017) 67 (1):65–85. doi: 10.3322/caac.21358

8. Demaria S, Ng B, Devitt ML, Babb JS, Kawashima N, Liebes L, et al. Ionizing radiation inhibition of distant untreated tumors (Abscopal effect) is immune mediated. *Int J Radiat Oncol Biol Phys* (2004) 58(3):862–70. doi: 10.1016/j.ijrobp.2003.09.012

9. Janopaul-Naylor JR, Shen Y, Qian DC, Buchwald ZS. The abscopal effect: A review of pre-clinical and clinical advances. *Int J Mol Sci* (2021) 22(20):11061. doi: 10.3390/ijms222011061

10. Sharma P, Allison JP. The future of immune checkpoint therapy. *Science* (2015) 348(6230):56–61. doi: 10.1126/science.aaa8172

11. Brahmer JR, Tykodi SS, Chow LQ, Hwu W-J, Topalian SL, Hwu P, et al. Safety and activity of anti–Pd-L1 antibody in patients with advanced cancer. *New Engl J Med* (2012) 366(26):2455–65. doi: 10.1056/NEJMoa1200694

12. Reck M, Rodríguez-Abreu D, Robinson AG, Hui R, Csőszi T, Fülöp A, et al. Pembrolizumab versus chemotherapy for Pd-L1–positive non–Small-Cell lung cancer. *N Engl J Med* (2016) 375:1823–33. doi: 10.1056/NEJMoa1606774

13. Zhang Z, Liu X, Chen D, Yu J. Radiotherapy combined with immunotherapy: The dawn of cancer treatment. *Signal Transduction Targeted Ther* (2022) 7(1):1–34. doi: 10.1038/s41392-022-01102-y

14. Hui R, Özgüroğlu M, Villegas A, Daniel D, Vicente D, Murakami S, et al. Patient-reported outcomes with durvalumab after chemoradiotherapy in stage iii, unresectable non-Small-Cell lung cancer (Pacific): A randomised, controlled, phase 3 study. *Lancet Oncol* (2019) 20(12):1670–80. doi: 10.1016/S1470-2045(19)30519-4

15. Jabbour SK, Lee KH, Frost N, Breder V, Kowalski DM, Pollock T, et al. Pembrolizumab plus concurrent chemoradiation therapy in patients with unresectable, locally advanced, stage iii non–small cell lung cancer: The phase 2 keynote-799 nonrandomized trial. *JAMA Oncol* (2021) 7(9):1351–9. doi: 10.1001/jamaoncol.2021.2301

16. Antonia SJ, Villegas A, Daniel D, Vicente D, Murakami S, Hui R, et al. Durvalumab after chemoradiotherapy in stage iii non–Small-Cell lung cancer. *New Engl J Med* (2017) 377(20):1919–29. doi: 10.1056/NEJMoa1709937

17. Antonia SJ, Villegas A, Daniel D, Vicente D, Murakami S, Hui R, et al. Overall survival with durvalumab after chemoradiotherapy in stage iii nsclc. *New Engl J Med* (2018) 379(24):2342–50. doi: 10.1056/NEJMoa1809697

18. Kang J, Demaria S, Formenti S. Current clinical trials testing the combination of immunotherapy with radiotherapy. *J immunotherapy Cancer* (2016) 4(1):1–20. doi: 10.1186/s40425-016-0156-7

19. Spigel DR, Faivre-Finn C, Gray JE, Vicente D, Planchard D, Paz-Ares L, et al. Five-year survival outcomes from the pacific trial: Durvalumab after chemoradiotherapy in stage iii non–Small-Cell lung cancer. *J Clin Oncol* (2022) 40(12):1301. doi: 10.1200/JCO.21.01308

20. Gomez DR, Blumenschein GRJr., Lee JJ, Hernandez M, Ye R, Camidge DR, et al. Local consolidative therapy versus maintenance therapy or observation for patients with oligometastatic non-Small-Cell lung cancer without progression after first-line systemic therapy: A multicentre, randomised, controlled, phase 2 study. *Lancet Oncol* (2016) 17(12):1672–82. doi: 10.1016/S1470-2045(16)30532-0

21. Iyengar P, Wardak Z, Gerber DE, Tumati V, Ahn C, Hughes RS, et al. Consolidative radiotherapy for limited metastatic non–Small-Cell lung cancer: A phase 2 randomized clinical trial. *JAMA Oncol* (2018) 4(1):e173501–e. doi: 10.1001/jamaoncol.2017.3501

22. Ball D, Mai GT, Vinod S, Babington S, Ruben J, Kron T, et al. Stereotactic ablative radiotherapy versus standard radiotherapy in stage 1 non-Small-Cell lung cancer (Trog 09.02 chisel): A phase 3, open-label, randomised controlled trial. *Lancet Oncol* (2019) 20(4):494–503. doi: 10.1016/S1470-2045(18)30896-9

23. Formenti SC. Optimizing dose per fraction: A new chapter in the story of the abscopal effect? *Int J Radiat Oncology Biology Phys* (2017) 99(3):677–9. doi: 10.1016/j.ijrobp.2017.07.028

24. Vanpouille-Box C, Alard A, Aryankalayil MJ, Sarfraz Y, Diamond JM, Schneider RJ, et al. DNA Exonuclease Trex1 regulates radiotherapy-induced tumour immunogenicity. *Nat Commun* (2017) 8(1):1–15. doi: 10.1038/ncomms15618

25. Lan J, Li R, Yin L-M, Deng L, Gui J, Chen B-Q, et al. Targeting myeloid-derived suppressor cells and programmed death ligand 1 confers therapeutic advantage of ablative hypofractionated radiation therapy compared with conventional fractionated radiation therapy. *Int J Radiat Oncol Biol Phys* (2018) 101(1):74–87. doi: 10.1016/j.ijrobp.2018.01.071

26. Chen Y, Gao M, Huang Z, Yu J, Meng X. Sbrt combined with pd-1/Pd-L1 inhibitors in nsclc treatment: A focus on the mechanisms, advances, and future challenges. *J Hematol Oncol* (2020) 13(1):1–17. doi: 10.1186/s13045-020-00940-z

27. Luke JJ, Lemons JM, Karrison TG, Pitroda SP, Melotek JM, Zha Y, et al. Safety and clinical activity of pembrolizumab and multisite stereotactic body radiotherapy in patients with advanced solid tumors. *J Clin Oncol* (2018) 36 (16):1611. doi: 10.1200/JCO.2017.76.2229

28. Patel JD, Bestvina CM, Karrison T, Jelinek MJ, Juloori A, Pointer K, et al. Randomized phase I trial to evaluate c oncurrent or s equential I pilimumab, n ivolumab, and stereotactic body r adiotherapy in patients with stage iv non-small cell lung cancer (Cosinr study). *Am Soc Clin Oncol* (2020) 2020: 9616–9616. doi: 10.1200/JCO.2020.38.15_suppl.9616

29. Theelen WS, Chen D, Verma V, Hobbs BP, Peulen HM, Aerts JG, et al. Pembrolizumab with or without radiotherapy for metastatic non-Small-Cell lung cancer: A pooled analysis of two randomised trials. *Lancet Respir Med* (2021) 9 (5):467–75. doi: 10.1016/S2213-2600(20)30391-X

30. Maity A, Mick R, Huang AC, George SM, Farwell MD, Lukens JN, et al. A phase I trial of pembrolizumab with hypofractionated radiotherapy in patients with metastatic solid tumours. *Br J Cancer* (2018) 119(10):1200–7. doi: 10.1038/s41416-018-0281-9

31. Welsh J, Menon H, Chen D, Verma V, Tang C, Altan M, et al. Pembrolizumab with or without radiation therapy for metastatic non-small cell lung cancer: A randomized phase I/Ii trial. *J immunotherapy Cancer* (2020) 8(2): e001001. doi: 10.1136/jitc-2020-001001

32. McBride S, Sherman E, Tsai CJ, Baxi S, Aghalar J, Eng J, et al. Randomized phase ii trial of nivolumab with stereotactic body radiotherapy versus nivolumab alone in metastatic head and neck squamous cell carcinoma. *J Clin Oncol* (2021) 39 (1):30. doi: 10.1200/JCO.20.00290

33. Lin L, Kane N, Kobayashi N, Kono EA, Yamashiro JM, Nickols NG, et al. High-dose per fraction radiotherapy induces both antitumor immunity and immunosuppressive responses in prostate tumorshigh-dose radiation-induced immunity in prostate cancer. *Clin Cancer Res* (2021) 27(5):1505–15. doi: 10.1158/1078-0432.CCR-20-2293

34. Li A, Barsoumian HB, Schoenhals JE, Caetano MS, Wang X, Menon H, et al. Ido1 inhibition overcomes radiation-induced "Rebound immune suppression" by reducing numbers of Ido1-expressing myeloid-derived suppressor cells in the tumor microenvironment. *Int J Radiat Oncol Biol Phys* (2019) 104(4):903–12. doi: 10.1016/j.ijrobp.2019.03.022

35. Herrera FG, Romero P, Coukos G. Lighting up the tumor fire with low-dose irradiation. *Trends Immunol* (2022) 43(3):173–9. doi: 10.1016/j.it.2022.01.006

36. De Palma M, Coukos G, Hanahan D. A new twist on radiation oncology: Low-dose irradiation elicits immunostimulatory macrophages that unlock barriers to tumor immunotherapy. *Cancer Cell* (2013) 24(5):559–61. doi: 10.1016/j.ccr.2013.10.019

37. Lu K, He C, Guo N, Chan C, Ni K, Lan G, et al. Low-dose X-ray radiotherapy–radiodynamic therapy *Via* nanoscale metal–organic frameworks enhances checkpoint blockade immunotherapy. *Nat Biomed Eng* (2018) 2 (8):600–10. doi: 10.1038/s41551-018-0203-4

38. He K, Barsoumian HB, Bertolet G, Verma V, Leuschner C, Koay EJ, et al. Novel use of low-dose radiotherapy to modulate the tumor microenvironment of liver metastases. *Front Immunol* (2021) 12. doi: 10.3389/fimmu.2021.812210

39. Savage T, Pandey S, Guha C. Postablation modulation after single high-dose radiation therapy improves tumor control *Via* enhanced immunomodulationimmunologic consequences of radiation fractionation. *Clin Cancer Res* (2020) 26(4):910–21. doi: 10.1158/1078-0432.CCR-18-3518

40. Barsoumian HB, Sezen D, Menon H, Younes AI, Hu Y, He K, et al. High plus low dose radiation strategy in combination with tigit and Pd1 blockade to promote systemic antitumor responses. *Cancers* (2022) 14(1):221. doi: 10.3390/cancers14010221

41. Barsoumian HB, Ramapriyan R, Younes AI, Caetano MS, Menon H, Comeaux NI, et al. Low-dose radiation treatment enhances systemic antitumor immune responses by overcoming the inhibitory stroma. *J immunotherapy Cancer* (2020) 8(2):e000537. doi: 10.1136/jitc-2020-000537

42. Yin L, Xue J, Li R, Zhou L, Deng L, Chen L, et al. Effect of low-dose radiation therapy on abscopal responses to hypofractionated radiation therapy and anti-Pd1 in mice and patients with non-small cell lung cancer. *Int J Radiat Oncol Biol Phys* (2020) 108(1):212–24. doi: 10.1016/j.ijrobp.2020.05.002

43. Menon H, Chen D, Ramapriyan R, Verma V, Barsoumian HB, Cushman TR, et al. Influence of low-dose radiation on abscopal responses in patients receiving high-dose radiation and immunotherapy. *J immunotherapy Cancer* (2019) 7(1):1–9. doi: 10.1186/s40425-019-0718-6

44. Sezen D, Patel RR, Tang C, Onstad M, Nagarajan P, Patel SP, et al. Immunotherapy combined with high-and low-dose radiation to all sites leads to complete clearance of disease in a patient with metastatic vaginal melanoma. *Gynecologic Oncol* (2021) 161(3):645–52. doi: 10.1016/j.ygyno.2021.03.017

45. Lederman M. The early history of radiotherapy: 1895–1939. *Int J Radiat Oncol Biol Phys* (1981) 7(5):639–48. doi: 10.1016/0360-3016(81)90379-5

46. Regaud C, Nogier T. Sterilization rontgenienne totale et definitive, sans radiodermite, des testicules Du belier adulte: Conditions de sa realisation. *Compt Rend Soc Biol* (1911) 70:202–3.

47. Jeraj R, Mackie TR, Balog J, Olivera G, Pearson D, Kapatoes J, et al. Radiation characteristics of helical tomotherapy. *Med Phys* (2004) 31(2):396–404. doi: 10.1118/1.1639148

48. Welsh JS, Patel RR, Ritter MA, Harari PM, Mackie TR, Mehta MP. Helical tomotherapy: An innovative technology and approach to radiation therapy. *Technol Cancer Res Treat* (2002) 1(4):311–6. doi: 10.1177/153303460200100413

49. Bortfeld T. Imrt: A review and preview. *Phys Med Biol* (2006) 51(13):R363. doi: 10.1088/0031-9155/51/13/R21

50. Girdhani S, Sachs R, Hlatky L. Biological effects of proton radiation: What we know and don't know. *Radiat Res* (2013) 179(3):257–72. doi: 10.1667/RR2839.1

51. Pan HY, Jiang J, Hoffman KE, Tang C, Choi SL, Nguyen Q-N, et al. Comparative toxicities and cost of intensity-modulated radiotherapy, proton radiation, and stereotactic body radiotherapy among younger men with prostate cancer. *J Clin Oncol* (2018) 36(18):1823. doi: 10.1200/JCO.2017.75.5371

52. Bourhis J, Montay-Gruel P, Jorge PG, Bailat C, Petit B, Ollivier J, et al. Clinical translation of flash radiotherapy: Why and how? *Radiotherapy Oncol* (2019) 139:11–7. doi: 10.1016/j.radonc.2019.04.008

53. Bradley MO, Kohn KW. X-Ray induced DNA double strand break production and repair in mammalian cells as measured by neutral filter elution. *Nucleic Acids Res* (1979) 7(3):793–804. doi: 10.1093/nar/7.3.793

54. Toulany M. Targeting DNA double-strand break repair pathways to improve radiotherapy response. *Genes* (2019) 10(1):25. doi: 10.3390/genes10010025

55. Wang J-s, Wang H-j, Qian H-l. Biological effects of radiation on cancer cells. *Military Med Res* (2018) 5(1):1–10. doi: 10.1186/s40779-018-0167-4

56. Meijer TW, Kaanders JH, Span PN, Bussink J. Targeting hypoxia, hif-1, and tumor glucose metabolism to improve radiotherapy efficacy. *Clin Cancer Res* (2012) 18(20):5585–94. doi: 10.1158/1078-0432.CCR-12-0858

57. Wang Y, Liu Z-G, Yuan H, Deng W, Li J, Huang Y, et al. The reciprocity between radiotherapy and cancer immunotherapyradiosensitizing immunotherapy. *Clin Cancer Res* (2019) 25(6):1709–17. doi: 10.1158/1078-0432.CCR-18-2581

58. Victor T-S, Rech AJ, Maity A, Rengan R, Pauken KE, Stelekati E, et al. Radiation and dual checkpoint blockade activate non-redundant immune mechanisms in cancer. *Nature* (2015) 520(7547):373–7. doi: 10.1038/nature14292

59. Barker HE, Paget JT, Khan AA, Harrington KJ. The tumour microenvironment after radiotherapy: Mechanisms of resistance and recurrence. *Nat Rev Cancer* (2015) 15(7):409–25. doi: 10.1038/nrc3958

60. Weichselbaum RR, Liang H, Deng L, Fu Y-X. Radiotherapy and immunotherapy: A beneficial liaison? *Nat Rev Clin Oncol* (2017) 14(6):365–79. doi: 10.1038/nrclinonc.2016.211

61. Chen DS, Mellman I. Elements of cancer immunity and the cancer–immune set point. *Nature* (2017) 541(7637):321–30. doi: 10.1038/nature21349

62. Srinivas US, Tan BW, Vellayappan BA, Jeyasekharan AD. Ros and the DNA damage response in cancer. *Redox Biol* (2019) 25:101084. doi: 10.1016/j.redox.2018.101084

63. Jiang M, Chen P, Wang L, Li W, Chen B, Liu Y, et al. Cgas-sting, an important pathway in cancer immunotherapy. *J Hematol Oncol* (2020) 13(1):1–11. doi: 10.1186/s13045-020-00916-z

64. Chen Q, Sun L, Chen ZJ. Regulation and function of the cgas–sting pathway of cytosolic DNA sensing. *Nat Immunol* (2016) 17(10):1142–9. doi: 10.1038/ni.3558

65. Mackenzie KJ, Carroll P, Martin C-A, Murina O, Fluteau A, Simpson DJ, et al. Cgas surveillance of micronuclei links genome instability to innate immunity. *Nature* (2017) 548(7668):461–5. doi: 10.1038/nature23449

66. Deng L, Liang H, Xu M, Yang X, Burnette B, Arina A, et al. Sting-dependent cytosolic DNA sensing promotes radiation-induced type I interferon-dependent antitumor immunity in immunogenic tumors. *Immunity* (2014) 41(5):843–52. doi: 10.1016/j.immuni.2014.10.019

67. Wenzel J, Bekisch B, Uerlich M, Haller O, Bieber T, Tüting T. Type I interferon–associated recruitment of cytotoxic lymphocytes: A common mechanism in regressive melanocytic lesions. *Am J Clin Pathol* (2005) 124 (1):37–48. doi: 10.1309/4EJ9KL7CGDENVVLE

68. Harlin H, Meng Y, Peterson AC, Zha Y, Tretiakova M, Slingluff C, et al. Chemokine expression in melanoma metastases associated with Cd8+ T-cell recruitment. *Cancer Res* (2009) 69(7):3077–85. doi: 10.1158/0008-5472.CAN-08-2281

69. Woo S-R, Corrales L, Gajewski TF. The sting pathway and the T cell-inflamed tumor microenvironment. *Trends Immunol* (2015) 36(4):250–6. doi: 10.1016/j.it.2015.02.003

70. Golden EB, Marciscano AE, Formenti SC. Radiation therapy and the in situ vaccination approach. *Int J Radiat Oncol Biol Phys* (2020) 108(4):891–8. doi: 10.1016/j.ijrobp.2020.08.023

71. Mouw KW, Goldberg MS, Konstantinopoulos PA, D'Andrea AD. DNA Damage and repair biomarkers of immunotherapy responsedna repair biomarkers of immunotherapy response. *Cancer Discovery* (2017) 7(7):675–93. doi: 10.1158/2159-8290.CD-17-0226

72. Galluzzi L, Vitale I, Warren S, Adjemian S, Agostinis P, Martinez AB, et al. Consensus guidelines for the definition, detection and interpretation of immunogenic cell death. *J immunotherapy Cancer* (2020) 8(1):e000337. doi: 10.1136/jitc-2019-000337corr1

73. Ashrafizadeh M, Farhood B, Musa AE, Taeb S, Najafi M. Damage-associated molecular patterns in tumor radiotherapy. *Int Immunopharmacol* (2020) 86:106761. doi: 10.1016/j.intimp.2020.106761

74. Gardai SJ, McPhillips KA, Frasch SC, Janssen WJ, Starefeldt A, Murphy-Ullrich JE, et al. Cell-surface calreticulin initiates clearance of viable or apoptotic cells through trans-activation of lrp on the phagocyte. *Cell* (2005) 123(2):321–34. doi: 10.1016/j.cell.2005.08.032

75. Serrano-del Valle A, Anel A, Naval J, Marzo I. Immunogenic cell death and immunotherapy of multiple myeloma. *Front Cell Dev Biol* (2019) 7:50. doi: 10.3389/fcell.2019.00050

76. Obeid M, Panaretakis T, Joza N, Tufi R, Tesniere A, Van Endert P, et al. Calreticulin exposure is required for the immunogenicity of Γ-irradiation and uvc light-induced apoptosis. *Cell Death Differentiation* (2007) 14(10):1848–50. doi: 10.1038/sj.cdd.4402201

77. Wang Y-J, Fletcher R, Yu J, Zhang L. Immunogenic effects of chemotherapy-induced tumor cell death. *Genes Dis* (2018) 5(3):194–203. doi: 10.1016/j.gendis.2018.05.003

78. Vermeer DW, Spanos WC, Vermeer PD, Bruns AM, Lee KM, Lee JH. Radiation-induced loss of cell surface Cd47 enhances immune-mediated clearance of human papillomavirus-positive cancer. *Int J Cancer* (2013) 133(1):120–9. doi: 10.1002/ijc.28015

79. Matlung HL, Szilagyi K, Barclay NA, van den Berg TK. The Cd47-sirpα signaling axis as an innate immune checkpoint in cancer. *Immunol Rev* (2017) 276 (1):145–64. doi: 10.1111/imr.12527

80. Candas-Green D, Xie B, Huang J, Fan M, Wang A, Menaa C, et al. Dual blockade of Cd47 and Her2 eliminates radioresistant breast cancer cells. *Nat Commun* (2020) 11(1):1–15. doi: 10.1038/s41467-020-18245-7

81. Veillette A, Chen J. Sirpα–Cd47 immune checkpoint blockade in anticancer therapy. *Trends Immunol* (2018) 39(3):173–84. doi: 10.1016/j.it.2017.12.005

82. Chao MP, Weissman IL, Majeti R. The Cd47–sirpα pathway in cancer immune evasion and potential therapeutic implications. *Curr Opin Immunol* (2012) 24(2):225–32. doi: 10.1016/j.coi.2012.01.010

83. Huang C-Y, Ye Z-H, Huang M-Y, Lu J-J. Regulation of Cd47 expression in cancer cells. *Trans Oncol* (2020) 13(12):100862. doi: 10.1016/j.tranon.2020.100862

84. Feng R, Zhao H, Xu J, Shen C. Cd47: The next checkpoint target for cancer immunotherapy. *Crit Rev Oncology/Hematology* (2020) 152:103014. doi: 10.1016/j.critrevonc.2020.103014

85. Apetoh L, Ghiringhelli F, Tesniere A, Obeid M, Ortiz C, Criollo A, et al. Toll-like receptor 4–dependent contribution of the immune system to anticancer chemotherapy and radiotherapy. *Nat Med* (2007) 13(9):1050–9. doi: 10.1038/nm1622

86. Rapoport BL, Anderson R. Realizing the clinical potential of immunogenic cell death in cancer chemotherapy and radiotherapy. *Int J Mol Sci* (2019) 20(4):959. doi: 10.3390/ijms20040959

87. Wu C-Y, Yang L-H, Yang H-Y, Knoff J, Peng S, Lin Y-H, et al. Enhanced cancer radiotherapy through immunosuppressive stromal cell destruction in tumorscancer radiotherapy enhanced by stromal cell destruction. *Clin Cancer Res* (2014) 20(3):644–57. doi: 10.1158/1078-0432.CCR-13-1334

88. Golden EB, Apetoh L. Radiotherapy and immunogenic cell death. *Semin Radiat Oncol* (2015) 25(1):11–17. doi: 10.1016/j.semradonc.2014.07.005

89. Zitvogel L, Galluzzi L, Kepp O, Smyth MJ, Kroemer G. Type I interferons in anticancer immunity. *Nat Rev Immunol* (2015) 15(7):405–14. doi: 10.1038/nri3845

90. Pasi F, Paolini A, Nano R, Di Liberto R, Capelli E. Effects of single or combined treatments with radiation and chemotherapy on survival and danger signals expression in glioblastoma cell lines. *BioMed Res Int* (2014) 2014:453497. doi: 10.1155/2014/453497

91. Binder R, Vatner R, Srivastava P. The heat-shock protein receptors: Some answers and more questions. *Tissue Antigens* (2004) 64(4):442–51. doi: 10.1111/j.1399-0039.2004.00299.x

92. Mole R. Whole body irradiation–radiobiology or medicine? *Br J Radiol* (1953) 26(305):234–41. doi: 10.1259/0007-1285-26-305-234

93. Liu Y, Dong Y, Kong L, Shi F, Zhu H, Yu J. Abscopal effect of radiotherapy combined with immune checkpoint inhibitors. *J Hematol Oncol* (2018) 11(1):1–15. doi: 10.1186/s13045-018-0647-8

94. Ngwa W, Irabor OC, Schoenfeld JD, Hesser J, Demaria S, Formenti SC. Using immunotherapy to boost the abscopal effect. *Nat Rev Cancer* (2018) 18 (5):313–22. doi: 10.1038/nrc.2018.6

95. Reynders K, Illidge T, Siva S, Chang JY, De Ruysscher D. The abscopal effect of local radiotherapy: Using immunotherapy to make a rare event clinically relevant. *Cancer Treat Rev* (2015) 41(6):503–10. doi: 10.1016/j.ctrv.2015.03.011

96. Rodríguez-Ruiz ME, Vanpouille-Box C, Melero I, Formenti SC, Demaria S. Immunological mechanisms responsible for radiation-induced abscopal effect. *Trends Immunol* (2018) 39(8):644–55. doi: 10.1016/j.it.2018.06.001

97. Buchwald ZS, Wynne J, Nasti TH, Zhu S, Mourad WF, Yan W, et al. Radiation, immune checkpoint blockade and the abscopal effect: A critical review on timing, dose and fractionation. *Front Oncol* (2018) 8:612. doi: 10.3389/fonc.2018.00612

98. Hanahan D, Weinberg RA. Hallmarks of cancer: The next generation. *Cell* (2011) 144(5):646–74. doi: 10.1016/j.cell.2011.02.013

99. Donlon N, Power R, Hayes C, Reynolds J, Lysaght J. Radiotherapy, immunotherapy, and the tumour microenvironment: Turning an immunosuppressive milieu into a therapeutic opportunity. *Cancer Lett* (2021) 502:84–96. doi: 10.1016/j.canlet.2020.12.045

100. Riaz N, Havel JJ, Makarov V, Desrichard A, Urba WJ, Sims JS, et al. Tumor and microenvironment evolution during immunotherapy with nivolumab. *Cell* (2017) 171(4):934–49.e16. doi: 10.1016/j.cell.2017.09.028

101. Gajewski TF, Schreiber H, Fu Y-X. Innate and adaptive immune cells in the tumor microenvironment. *Nat Immunol* (2013) 14(10):1014–22. doi: 10.1038/ni.2703

102. Junttila MR, De Sauvage FJ. Influence of tumour micro-environment heterogeneity on therapeutic response. *Nature* (2013) 501(7467):346–54. doi: 10.1038/nature12626

103. O'Donnell JS, Teng MW, Smyth MJ. Cancer immunoediting and resistance to T cell-based immunotherapy. *Nat Rev Clin Oncol* (2019) 16(3):151–67. doi: 10.1038/s41571-018-0142-8

104. Herbst RS, Soria J-C, Kowanetz M, Fine GD, Hamid O, Gordon MS, et al. Predictive correlates of response to the anti-Pd-L1 antibody Mpdl3280a in cancer patients. *Nature* (2014) 515(7528):563–7. doi: 10.1038/nature14011

105. Rosenberg JE, Hoffman-Censits J, Powles T, van der Heijden MS, Balar AV, Necchi A, et al. Atezolizumab in patients with locally advanced and metastatic urothelial carcinoma who have progressed following treatment with platinum-based chemotherapy: A single-arm, multicentre, phase 2 trial. *Lancet* (2016) 387 (10031):1909–20. doi: 10.1016/S0140-6736(16)00561-4

106. Garon EB, Rizvi NA, Hui R, Leighl N, Balmanoukian AS, Eder JP, et al. Pembrolizumab for the treatment of non–Small-Cell lung cancer. *New Engl J Med* (2015) 372(21):2018–28. doi: 10.1056/NEJMoa1501824

107. Joyce JA, Fearon DT. T Cell exclusion, immune privilege, and the tumor microenvironment. *Science* (2015) 348(6230):74–80. doi: 10.1126/science.aaa6204

108. Vanpouille-Box C, Formenti SC. Dual transforming growth factor-B and programmed death-1 blockade: A strategy for immune-excluded tumors? *Trends Immunol* (2018) 39(6):435–7. doi: 10.1016/j.it.2018.03.002

109. Nikolos F, Hayashi K, Hoi XP, Alonzo ME, Mo Q, Kasabyan A, et al. Cell death-induced immunogenicity enhances chemoimmunotherapeutic response by converting immune-excluded into T-cell inflamed bladder tumors. *Nat Commun* (2022) 13(1):1–16. doi: 10.1038/s41467-022-29026-9

110. Frey B, Rubner Y, Wunderlich R, Weiss E-M, Pockley AG, Fietkau R, et al. Induction of abscopal anti-tumor immunity and immunogenic tumor cell death by ionizing irradiation-implications for cancer therapies. *Curr medicinal Chem* (2012) 19(12):1751–64. doi: 10.2174/092986712800099811

111. Formenti SC, Demaria S. Combining radiotherapy and cancer immunotherapy: A paradigm shift. *JNCI: J Natl Cancer Institute* (2013) 105 (4):256–65. doi: 10.1093/jnci/djs629

112. Park B, Yee C, Lee K-M. The effect of radiation on the immune response to cancers. *Int J Mol Sci* (2014) 15(1):927–43. doi: 10.3390/ijms15010927

113. Walle T, Martinez Monge R, Cerwenka A, Ajona D, Melero I, Lecanda F. Radiation effects on antitumor immune responses: Current perspectives and challenges. *Ther Adv Med Oncol* (2018) 10:1758834017742575. doi: 10.1177/1758834017742575

114. Rodriguez-Ruiz ME, Rodriguez I, Garasa S, Barbes B, Solorzano JL, Perez-Gracia JL, et al. Abscopal effects of radiotherapy are enhanced by combined immunostimulatory mabs and are dependent on Cd8 T cells and crossprimingradioimmunotherapy and abscopal effects. *Cancer Res* (2016) 76 (20):5994–6005. doi: 10.1158/0008-5472.CAN-16-0549

115. Taieb J, Chaput N, Ménard C, Apetoh L, Ullrich E, Bonmort M, et al. A novel dendritic cell subset involved in tumor immunosurveillance. *Nat Med* (2006) 12(2):214–9. doi: 10.1038/nm1356

116. Lee Y, Auh SL, Wang Y, Burnette B, Wang Y, Meng Y, et al. Therapeutic effects of ablative radiation on local tumor require Cd8+ T cells: Changing strategies for cancer treatment. *Blood J Am Soc Hematol* (2009) 114(3):589–95. doi: 10.1182/blood-2009-02-206870

117. Sharabi AB, Nirschl CJ, Kochel CM, Nirschl TR, Francica BJ, Velarde E, et al. Stereotactic radiation therapy augments antigen-specific Pd-1–mediated antitumor immune responses *Via* cross-presentation of tumor antigencross-presentation of tumor antigens augmented by radiotherapy. *Cancer Immunol Res* (2015) 3(4):345–55. doi: 10.1158/2326-6066.CIR-14-0196

118. Gupta A, Probst HC, Vuong V, Landshammer A, Muth S, Yagita H, et al. Radiotherapy promotes tumor-specific effector Cd8+ T cells *Via* dendritic cell activation. *J Immunol* (2012) 189(2):558–66. doi: 10.4049/jimmunol.1200563

119. Vonderheide RH, Glennie MJ. Agonistic Cd40 antibodies and cancer therapy. *Clin Cancer Res* (2013) 19(5):1035–43. doi: 10.1158/1078-0432.CCR-12-2064

120. Reits EA, Hodge JW, Herberts CA, Groothuis TA, Chakraborty M, K. Wansley E, et al. Radiation modulates the peptide repertoire, enhances mhc class I expression, and induces successful antitumor immunotherapy. *J Exp Med* (2006) 203(5):1259–71. doi: 10.1084/jem.20052494

121. Lugade AA, Sorensen EW, Gerber SA, Moran JP, Frelinger JG, Lord EM. Radiation-induced ifn-Γ production within the tumor microenvironment influences antitumor immunity. *J Immunol* (2008) 180(5):3132–9. doi: 10.4049/jimmunol.180.5.3132

122. Kim J-Y, Son Y-O, Park S-W, Bae J-H, Chung JS, Kim HH, et al. Increase of Nkg2d ligands and sensitivity to nk cell-mediated cytotoxicity of tumor cells by heat shock and ionizing radiation. *Exp Mol Med* (2006) 38(5):474–84. doi: 10.1038/emm.2006.56

123. Vatner RE, Formenti SC. Myeloid-derived cells in tumors: Effects of radiation. *Semin Radiat Oncol* (2015) 25(1):18–27. doi: 10.1016/j.semradonc.2014.07.008

124. Matsumura S, Wang B, Kawashima N, Braunstein S, Badura M, Cameron TO, et al. Radiation-induced Cxcl16 release by breast cancer cells attracts effector T cells. *J Immunol* (2008) 181(5):3099–107. doi: 10.4049/jimmunol.181.5.3099

125. Meng Y, Mauceri HJ, Khodarev NN, Darga TE, Pitroda SP, Beckett MA, et al. Ad. Egr-tnf and local ionizing radiation suppress metastases by interferon-B-Dependent activation of antigen-specific Cd8+ T cells. *Mol Ther* (2010) 18(5):912–20. doi: 10.1038/mt.2010.18

126. Lanitis E, Irving M, Coukos G. Targeting the tumor vasculature to enhance T cell activity. *Curr Opin Immunol* (2015) 33:55–63. doi: 10.1016/j.coi.2015.01.011

127. Fridman WH, Sautès-Fridman C, Galon J. The immune contexture in human tumours: Impact on clinical outcome. *Nat Rev Cancer* (2012) 12(4):298–306. doi: 10.1038/nrc3245

128. Dushyanthen S, Beavis PA, Savas P, Teo ZL, Zhou C, Mansour M, et al. Relevance of tumor-infiltrating lymphocytes in breast cancer. *BMC Med* (2015) 13 (1):1–13. doi: 10.1186/s12916-015-0431-3

129. Anitei M-G, Zeitoun G, Mlecnik B, Marliot F, Haicheur N, Todosi A-M, et al. Prognostic and predictive values of the immunoscore in patients with rectal cancer. *Clin Cancer Res* (2014) 20(7):1891–9. doi: 10.1158/1078-0432.CCR-13-2830

130. Kachikwu EL, Iwamoto KS, Liao Y-P, DeMarco JJ, Agazaryan N, Economou JS, et al. Radiation enhances regulatory T cell representation. *Int J Radiat Oncol Biol Phys* (2011) 81(4):1128–35. doi: 10.1016/j.ijrobp.2010.09.034

131. Brandmaier A, Formenti SC. The impact of radiation therapy on innate and adaptive tumor immunity. *Semin Radiat Oncol* (2020) 30(2):139–44. doi: 10.1016/j.semradonc.2019.12.005

132. Facciabene A, Motz GT, Coukos G. T-Regulatory cells: Key players in tumor immune escape and angiogenesis. *Cancer Res* (2012) 72(9):2162–71. doi: 10.1158/0008-5472.CAN-11-3687

133. Fadul CE, Fisher JL, Hampton TH, Lallana EC, Li Z, Gui J, et al. Immune response in patients with newly diagnosed glioblastoma multiforme treated with intranodal autologous tumor lysate-dendritic cell vaccination after radiation chemotherapy. *J immunotherapy (Hagerstown Md: 1997)* (2011) 34(4):382. doi: 10.1097/CJI.0b013e318215e300

134. Schuler PJ, Harasymczuk M, Schilling B, Saze Z, Strauss L, Lang S, et al. Effects of adjuvant chemoradiotherapy on the frequency and function of regulatory T cells in patients with head and neck Cancercd4+ Cd39+ treg and crt. *Clin Cancer Res* (2013) 19(23):6585–96. doi: 10.1158/1078-0432.CCR-13-0900

135. Qinfeng S, Depu W, Xiaofeng Y, Shah W, Hongwei C, Yili W. *In situ* observation of the effects of local irradiation on cytotoxic and regulatory T lymphocytes in cervical cancer tissue. *Radiat Res* (2013) 179(5):584–9. doi: 10.1667/RR3155.1

136. Ji D, Song C, Li Y, Xia J, Wu Y, Jia J, et al. Combination of radiotherapy and suppression of tregs enhances abscopal antitumor effect and inhibits metastasis in rectal cancer. *J immunotherapy Cancer* (2020) 8(2):e000826. doi: 10.1136/jitc-2020-000826

137. Zitvogel L, Kroemer G. Subversion of anticancer immunosurveillance by radiotherapy. *Nat Immunol* (2015) 16(10):1005–7. doi: 10.1038/ni.3236

138. de Streel G, Bertrand C, Chalon N, Liénart S, Bricard O, Lecomte S, et al. Selective inhibition of tgf-B1 produced by garp-expressing tregs overcomes resistance to pd-1/Pd-L1 blockade in cancer. *Nat Commun* (2020) 11(1):1–15. doi: 10.1038/s41467-020-17811-3

139. Kho VM, Mekers VE, Span PN, Bussink J, Adema GJ. Radiotherapy and Cgas/Sting signaling: Impact on mdscs in the tumor microenvironment. *Cell Immunol* (2021) 362:104298. doi: 10.1016/j.cellimm.2021.104298

140. Liang H, Deng L, Hou Y, Meng X, Huang X, Rao E, et al. Host sting-dependent mdsc mobilization drives extrinsic radiation resistance. *Nat Commun* (2017) 8(1):1–10. doi: 10.1038/s41467-017-01566-5

141. Ostrand-Rosenberg S. Myeloid-derived suppressor cells: More mechanisms for inhibiting antitumor immunity. *Cancer immunology immunotherapy* (2010) 59(10):1593–600. doi: 10.1007/s00262-010-0855-8

142. Nagaraj S, Gabrilovich DI. Myeloid-derived suppressor cells in human cancer. *Cancer J* (2010) 16(4):348–53. doi: 10.1097/PPO.0b013e3181eb3358

143. Seifert L, Werba G, Tiwari S, Ly NNG, Nguy S, Alothman S, et al. Radiation therapy induces macrophages to suppress T-cell responses against pancreatic tumors in mice. *Gastroenterology* (2016) 150(7):1659–72.e5. doi: 10.1053/j.gastro.2016.02.070

144. Xu J, Escamilla J, Mok S, David J, Priceman S, West B, et al. Csf1r signaling blockade stanches tumor-infiltrating myeloid cells and improves the efficacy of radiotherapy in prostate cancer. *Cancer Res* (2013) 73(9):2782–94. doi: 10.1158/0008-5472.CAN-12-3981

145. Mantovani A, Schioppa T, Porta C, Allavena P, Sica A. Role of tumor-associated macrophages in tumor progression and invasion. *Cancer Metastasis Rev* (2006) 25(3):315–22. doi: 10.1007/s10555-006-9001-7

146. Huang Y, Snuderl M, Jain RK. Polarization of tumor-associated macrophages: A novel strategy for vascular normalization and antitumor immunity. *Cancer Cell* (2011) 19(1):1–2. doi: 10.1016/j.ccr.2011.01.005

147. Allavena P, Sica A, Garlanda C, Mantovani A. The yin-yang of tumor-associated macrophages in neoplastic progression and immune surveillance. *Immunol Rev* (2008) 222(1):155–61. doi: 10.1111/j.1600-065X.2008.00607.x

148. Rodriguez PC, Quiceno DG, Zabaleta J, Ortiz B, Zea AH, Piazuelo MB, et al. Arginase I production in the tumor microenvironment by mature myeloid cells inhibits T-cell receptor expression and antigen-specific T-cell responses. *Cancer Res* (2004) 64(16):5839–49. doi: 10.1158/0008-5472.CAN-04-0465

149. Vanpouille-Box C, Diamond JM, Pilones KA, Zavadil J, Babb JS, Formenti SC, et al. Tgfβ is a master regulator of radiation therapy-induced antitumor immunity. *Cancer Res* (2015) 75(11):2232–42. doi: 10.1158/0008-5472.CAN-14-3511

150. Tuxhorn JA, McAlhany SJ, Yang F, Dang TD, Rowley DR. Inhibition of transforming growth factor-B activity decreases angiogenesis in a human prostate cancer-reactive stroma xenograft model. *Cancer Res* (2002) 62(21):6021–5.

151. Colton M, Cheadle EJ, Honeychurch J, Illidge TM. Reprogramming the tumour microenvironment by radiotherapy: Implications for radiotherapy and immunotherapy combinations. *Radiat Oncol* (2020) 15(1):1–11. doi: 10.1186/s13014-020-01678-1

152. Lim Y. Radiation-induced change of pd-1/Pd-L1 immune checkpoint in mouse colon cancer models. *Ann Oncol* (2019) 30:vii24. doi: 10.1093/annonc/mdz413.087

153. Illidge T, Lipowska-Bhalla G, Cheadle E, Honeychurch J, Poon E, Morrow M, et al. Radiation therapy induces an adaptive upregulation of pd-L1 on tumor cells which may limit the efficacy of the anti-tumor immune response but can be circumvented by anti-Pd-L1. *Int J Radiat Oncology Biology Phys* (2014) 90(1):S776. doi: 10.1016/j.ijrobp.2014.05.2247

154. Bezjak A, Paulus R, Gaspar LE, Timmerman RD, Straube WL, Ryan WF, et al. Safety and efficacy of a five-fraction stereotactic body radiotherapy schedule for centrally located non–Small-Cell lung cancer: Nrg Oncology/Rtog 0813 trial. *J Clin Oncol* (2019) 37(15):1316. doi: 10.1200/JCO.18.00622

155. Cheung P, Patel S, North SA, Sahgal A, Chu W, Soliman H, et al. Stereotactic radiotherapy for oligoprogression in metastatic renal cell cancer patients receiving tyrosine kinase inhibitor therapy: A phase 2 prospective multicenter study. *Eur Urol* (2021) 80(6):693–700. doi: 10.1016/j.eururo.2021.07.026

156. Pucar D, Hricak H, Shukla-Dave A, Kuroiwa K, Drobnjak M, Eastham J, et al. Clinically significant prostate cancer local recurrence after radiation therapy occurs at the site of primary tumor: Magnetic resonance imaging and step-section pathology evidence. *Int J Radiat Oncol Biol Phys* (2007) 69(1):62–9. doi: 10.1016/j.ijrobp.2007.03.065

157. Robert C. A decade of immune-checkpoint inhibitors in cancer therapy. *Nat Commun* (2020) 11(1):1–3. doi: 10.1038/s41467-020-17670-y

158. Brahmer JR, Pardoll DM. Immune checkpoint inhibitors: Making immunotherapy a reality for the treatment of lung cancer. *Cancer Immunol Res* (2013) 1(2):85–91. doi: 10.1158/2326-6066.CIR-13-0078

159. Fishman M. Challenges facing the development of cancer vaccines. *Cancer Vaccines* (2014) 1139:543–53. doi: 10.1007/978-1-4939-0345-0_39

160. Ribas A, Wolchok JD. Cancer immunotherapy using checkpoint blockade. *Science* (2018) 359(6382):1350–5. doi: 10.1126/science.aar4060

161. Sharma P, Hu-Lieskovan S, Wargo JA, Ribas A. Primary, adaptive, and acquired resistance to cancer immunotherapy. *Cell* (2017) 168(4):707–23. doi: 10.1016/j.cell.2017.01.017

162. Sharabi AB, Lim M, DeWeese TL, Drake CG. Radiation and checkpoint blockade immunotherapy: Radiosensitisation and potential mechanisms of synergy. *Lancet Oncol* (2015) 16(13):e498–509. doi: 10.1016/S1470-2045(15)00007-8

163. Hodge JW, Sharp HJ, Gameiro SR. Abscopal regression of antigen disparate tumors by antigen cascade after systemic tumor vaccination in combination with local tumor radiation. *Cancer Biotherapy Radiopharmaceuticals* (2012) 27(1):12–22. doi: 10.1089/cbr.2012.1202

164. Postow MA, Callahan MK, Barker CA, Yamada Y, Yuan J, Kitano S, et al. Immunologic correlates of the abscopal effect in a patient with melanoma. *New Engl J Med* (2012) 366(10):925–31. doi: 10.1056/NEJMoa1112824

165. Hiniker SM, Chen DS, Reddy S, Chang DT, Jones JC, Mollick JA, et al. A systemic complete response of metastatic melanoma to local radiation and immunotherapy. *Trans Oncol* (2012) 5(6):404–7. doi: 10.1593/tlo.12280

166. Golden EB, Demaria S, Schiff PB, Chachoua A, Formenti SC. An abscopal response to radiation and ipilimumab in a patient with metastatic non–small cell lung cancer. *Cancer Immunol Res* (2013) 1(6):365–72. doi: 10.1158/2326-6066.CIR-13-0115

167. Hiniker SM, Reddy SA, Maecker HT, Subrahmanyam PB, Rosenberg-Hasson Y, Swetter SM, et al. A prospective clinical trial combining radiation therapy with systemic immunotherapy in metastatic melanoma. *Int J Radiat Oncol Biol Phys* (2016) 96(3):578–88. doi: 10.1016/j.ijrobp.2016.07.005

168. Theelen WS, Peulen HM, Lalezari F, van der Noort V, De Vries JF, Aerts JG, et al. Effect of pembrolizumab after stereotactic body radiotherapy vs pembrolizumab alone on tumor response in patients with advanced non–small cell lung cancer: Results of the pembro-rt phase 2 randomized clinical trial. *JAMA Oncol* (2019) 5(9):1276–82. doi: 10.1001/jamaoncol.2019.1478

169. Bernstein MB, Krishnan S, Hodge JW, Chang JY. Immunotherapy and stereotactic ablative radiotherapy (Isabr): A curative approach? *Nat Rev Clin Oncol* (2016) 13(8):516–24. doi: 10.1038/nrclinonc.2016.30

170. Ashrafizadeh M, Farhood B, Musa AE, Taeb S, Rezaeyan A, Najafi M. Abscopal effect in radioimmunotherapy. *Int Immunopharmacol* (2020) 85:106663. doi: 10.1016/j.intimp.2020.106663

171. Morisada M, Clavijo PE, Moore E, Sun L, Chamberlin M, Van Waes C, et al. Pd-1 blockade reverses adaptive immune resistance induced by high-dose hypofractionated but not low-dose daily fractionated radiation. *Oncoimmunology* (2018) 7(3):e1395996. doi: 10.1080/2162402X.2017.1395996

172. Dewan MZ, Galloway AE, Kawashima N, Dewyngaert JK, Babb JS, Formenti SC, et al. Fractionated but not single-dose radiotherapy induces an immune-mediated abscopal effect when combined with anti–Ctla-4 antibodyfractionated radiation synergizes with immunotherapy. *Clin Cancer Res* (2009) 15(17):5379–88. doi: 10.1158/1078-0432.CCR-09-0265

173. Cai X, Chiu Y-H, Chen ZJ. The cgas-Cgamp-Sting pathway of cytosolic DNA sensing and signaling. *Mol Cell* (2014) 54(2):289–96. doi: 10.1016/j.molcel.2014.03.040

174. Muroyama Y, Nirschl TR, Kochel CM, Lopez-Bujanda Z, Theodros D, Mao W, et al. Stereotactic radiotherapy increases functionally suppressive regulatory T cells in the tumor microenvironmentexpansion of suppressive til-tregs after radiotherapy. *Cancer Immunol Res* (2017) 5(11):992–1004. doi: 10.1158/2326-6066.CIR-17-0040

175. Monjazeb AM, Giobbie-Hurder A, Lako A, Thrash EM, Brennick RC, Kao KZ, et al. A randomized trial of combined pd-L1 and ctla-4 inhibition with targeted low-dose or hypofractionated radiation for patients with metastatic colorectal cancerpd-L1/Ctla-4 inhibition with radiation for colorectal cancer. *Clin Cancer Res* (2021) 27(9):2470–80. doi: 10.1158/1078-0432.CCR-20-4632

176. Wang Y. Advances in hypofractionated irradiation-induced immunosuppression of tumor microenvironment. *Front Immunol* (2021) 11:612072. doi: 10.3389/fimmu.2020.612072

177. Begg K, Tavassoli M. Inside the hypoxic tumour: Reprogramming of the ddr and radioresistance. *Cell Death Discovery* (2020) 6(1):1–15. doi: 10.1038/s41420-020-00311-0

178. Mavragani IV, Laskaratou DA, Frey B, Candéias SM, Gaipl US, Lumniczky K, et al. Key mechanisms involved in ionizing radiation-induced systemic effects. a current review. *Toxicol Res* (2016) 5(1):12–33. doi: 10.1039/c5tx00222b

179. Klug F, Prakash H, Huber PE, Seibel T, Bender N, Halama N, et al. Low-dose irradiation programs macrophage differentiation to an Inos+/M1 phenotype that orchestrates effective T cell immunotherapy. *Cancer Cell* (2013) 24(5):589–602. doi: 10.1016/j.ccr.2013.09.014

180. Patel RR, He K, Barsoumian HB, Chang JY, Tang C, Verma V, et al. High-dose irradiation in combination with non-ablative low-dose radiation to treat metastatic disease after progression on immunotherapy: Results of a phase ii trial. *Radiotherapy Oncol* (2021) 162:60–7. doi: 10.1016/j.radonc.2021.06.037

181. Lin EY, Li J-F, Gnatovskiy L, Deng Y, Zhu L, Grzesik DA, et al. Macrophages regulate the angiogenic switch in a mouse model of breast cancer. *Cancer Res* (2006) 66(23):11238–46. doi: 10.1158/0008-5472.CAN-06-1278

182. Prakash H, Klug F, Nadella V, Mazumdar V, Schmitz-Winnenthal H, Umansky L. Low doses of gamma irradiation potentially modifies immunosuppressive tumor microenvironment by retuning tumor-associated macrophages: Lesson from insulinoma. *Carcinogenesis* (2016) 37(3):301–13. doi: 10.1093/carcin/bgw007

183. Lapeyre-Prost A, Terme M, Pernot S, Pointet A-L, Voron T, Tartour E, et al. Immunomodulatory activity of vegf in cancer. *Int Rev Cell Mol Biol* (2017) 330:295–342. doi: 10.1016/bs.ircmb.2016.09.007

184. Thomas AA, Fisher JL, Hampton TH, Christensen BC, Tsongalis GJ, Rahme GJ, et al. Immune modulation associated with vascular endothelial growth factor (Vegf) blockade in patients with glioblastoma. *Cancer Immunology Immunotherapy* (2017) 66(3):379–89. doi: 10.1007/s00262-016-1941-3

185. Voron T, Marcheteau E, Pernot S, Colussi O, Tartour E, Taieb J, et al. Control of the immune response by pro-angiogenic factors. *Front Oncol* (2014) 4:70. doi: 10.3389/fonc.2014.00070

186. Nadella V, Singh S, Jain A, Jain M, Vasquez KM, Sharma A, et al. Low dose radiation primed inos+ M1macrophages modulate angiogenic programming of tumor derived endothelium. *Mol carcinogenesis* (2018) 57(11):1664–71. doi: 10.1002/mc.22879

187. Yang G, Kong Q, Wang G, Jin H, Zhou L, Yu D, et al. Low-dose ionizing radiation induces direct activation of natural killer cells and provides a novel approach for adoptive cellular immunotherapy. *Cancer Biotherapy Radiopharmaceuticals* (2014) 29(10):428–34. doi: 10.1089/cbr.2014.1702

188. Sonn CH, Choi JR, Kim T-J, Yu Y-B, Kim K, Shin SC, et al. Augmentation of natural cytotoxicity by chronic low-dose ionizing radiation in murine natural killer cells primed by il-2. *J Radiat Res* (2012) 53(6):823–9. doi: 10.1093/jrr/rrs037

189. Cheda A, Wrembel-Wargocka J, Lisiak E, Nowosielska EM, Marciniak M, Janiak MK. Single low doses of X rays inhibit the development of experimental tumor metastases and trigger the activities of nk cells in mice. *Radiat Res* (2004) 161(3):335–40. doi: 10.1667/RR3123

190. Herrera FG, Ronet C, de Olza MO, Barras D, Crespo I, Andreatta M, et al. Low-dose radiotherapy reverses tumor immune desertification and resistance to immunotherapy. *Cancer Discovery* (2022) 12(1):108–33. doi: 10.1158/2159-8290.CD-21-0003

191. Zhou L, Zhang X, Li H, Niu C, Yu D, Yang G, et al. Validating the pivotal role of the immune system in low-dose radiation-induced tumor inhibition in Lewis lung cancer-bearing mice. *Cancer Med* (2018) 7(4):1338–48. doi: 10.1002/cam4.1344

192. Hashimoto S, Shirato H, Hosokawa M, Nishioka T, Kuramitsu Y, Matushita K, et al. The suppression of metastases and the change in host immune response after low-dose total-body irradiation in tumor-bearing rats. *Radiat Res* (1999) 151(6):717–24. doi: 10.2307/3580211

193. Sonanini D, Griessinger CM, Schörg BF, Knopf P, Dittmann K, Röcken M, et al. Low-dose total body irradiation facilitates antitumoral Th1 immune responses. *Theranostics* (2021) 11(16):7700. doi: 10.7150/thno.61459

194. Wang B, Li B, Dai Z, Ren S, Bai M, Wang Z, et al. Low-dose splenic radiation inhibits liver tumor development of rats through functional changes in Cd4+ Cd25+ treg cells. *Int J Biochem Cell Biol* (2014) 55:98–108. doi: 10.1016/j.biocel.2014.08.014

195. Liu R, Xiong S, Zhang L, Chu Y. Enhancement of antitumor immunity by low-dose total body irradiationis associated with selectively decreasing the proportion and number of T regulatorycells. *Cell Mol Immunol* (2010) 7(2):157–62. doi: 10.1038/cmi.2009.117

196. Nowosielska EM, Cheda A, Pociegiel M, Cheda L, Szymański P, Wiedlocha A. Effects of a unique combination of the whole-body low dose radiotherapy with inactivation of two immune checkpoints and/or a heat shock protein on the transplantable lung cancer in mice. *Int J Mol Sci* (2021) 22(12):6309. doi: 10.3390/ijms22126309

197. Patel RB, Hernandez R, Carlson P, Grudzinski J, Bates AM, Jagodinsky JC, et al. Low-dose targeted radionuclide therapy renders immunologically cold tumors responsive to immune checkpoint blockade. *Sci Trans Med* (2021) 13(602):eabb3631. doi: 10.1126/scitranslmed.abb3631

198. Schoenfeld JD, Giobbie-Hurder A, Ranasinghe S, Kao KZ, Lako A, Tsuji J, et al. Durvalumab plus tremelimumab alone or in combination with low-dose or hypofractionated radiotherapy in metastatic non-Small-Cell lung cancer refractory to previous pd (L)-1 therapy: An open-label, multicentre, randomised, phase 2 trial. *Lancet Oncol* (2022) 23(2):279–91. doi: 10.1016/S1470-2045(21)00658-6

199. Liu J, Zhou J, Wu M, Hu C, Yang J, Li D, et al. Low-dose total body irradiation can enhance systemic immune related response induced by hypo-fractionated radiation. *Front Immunol* (2019) 10:317. doi: 10.3389/fimmu.2019.00317

200. Welsh JW, Tang C, De Groot P, Naing A, Hess KR, Heymach JV, et al. Phase ii trial of ipilimumab with stereotactic radiation therapy for metastatic disease: Outcomes, toxicities, and low-dose radiation–related abscopal responsesipilimumab and sabr for lung or liver metastases. *Cancer Immunol Res* (2019) 7(12):1903–9. doi: 10.1158/2326-6066.CIR-18-0793

201. Easwaran H, Tsai H-C, Baylin SB. Cancer epigenetics: Tumor heterogeneity, plasticity of stem-like states, and drug resistance. *Mol Cell* (2014) 54(5):716–27. doi: 10.1016/j.molcel.2014.05.015

202. Marusyk A, Polyak K. Tumor heterogeneity: Causes and consequences. *Biochim Biophys Acta (BBA)-Reviews Cancer* (2010) 1805(1):105–17. doi: 10.1016/j.bbcan.2009.11.002

203. Luke JJ, Onderdonk BE, Bhave SR, Karrison T, Lemons JM, Chang P, et al. Improved survival associated with local tumor response following multisite radiotherapy and pembrolizumab: Secondary analysis of a phase I trialimmunoradiotherapy response in advanced solid malignancies. *Clin Cancer Res* (2020) 26(24):6437–44. doi: 10.1158/1078-0432.CCR-20-1790

204. Xiao A, Luke JJ, Partouche J, Karrison T, Chmura SJ, Al-Hallaq HA. Evaluation of dose distribution to organs-at-Risk in a prospective phase 1 trial of pembrolizumab and multisite stereotactic body radiation therapy (Sbrt). *Pract Radiat Oncol* (2022) 12(1):68–77. doi: 10.1016/j.prro.2021.09.005

205. Markovsky E, Budhu S, Samstein RM, Li H, Russell J, Zhang Z, et al. An antitumor immune response is evoked by partial-volume single-dose radiation in 2 murine models. *Int J Radiat Oncol Biol Phys* (2019) 103(3):697–708. doi: 10.1016/j.ijrobp.2018.10.009

206. Yasmin-Karim S, Ziberi B, Wirtz J, Bih N, Moreau M, Guthier R, et al. Boosting the abscopal effect using immunogenic biomaterials with varying radiation therapy field sizes. *Int J Radiat Oncol Biol Phys* (2022) 112(2):475–86. doi: 10.1016/j.ijrobp.2021.09.010

207. Lemons J, Luke J, Janisch L, Hseu R, Melotek J, Chmura S. The adscopal effect? control of partially irradiated versus completely irradiated tumors on a prospective trial of pembrolizumab and sbrt per nrg-Br001. *Int J Radiat Oncology Biology Phys* (2017) 99(2):S87. doi: 10.1016/j.ijrobp.2017.06.209

208. Schneider T, Fernandez-Palomo C, Bertho A, Fazzari J, Iturri L, Martin OA, et al. Combining flash and spatially fractionated radiation therapy: The best of both worlds. *Radiotherapy Oncol* (2022) 175:169–77. doi: 10.1016/j.radonc.2022.08.004

209. Griffin RJ, Ahmed MM, Amendola B, Belyakov O, Bentzen SM, Butterworth KT, et al. Understanding high-dose, ultra-high dose rate, and spatially fractionated radiation therapy. *Int J Radiat Oncol Biol Phys* (2020) 107(4):766–78. doi: 10.1016/j.ijrobp.2020.03.028

210. Prezado Y. Divide and conquer: Spatially fractionated radiation therapy. *Expert Rev Mol Med* (2022) 24:e3. doi: 10.1017/erm.2021.34

211. Yan W, Khan MK, Wu X, Simone CB, Fan J, Gressen E, et al. Spatially fractionated radiation therapy: History, present and the future. *Clin Trans Radiat Oncol* (2020) 20:30–8. doi: 10.1016/j.ctro.2019.10.004

212. Johnsrud AJ, Jenkins SV, Jamshidi-Parsian A, Quick CM, Galhardo EP, Dings RP, et al. Evidence for early stage anti-tumor immunity elicited by spatially fractionated radiotherapy-immunotherapy combinations. *Radiat Res* (2020) 194(6):688–97. doi: 10.1667/RADE-20-00065.1

213. Wei J, Montalvo-Ortiz W, Yu L, Krasco A, Ebstein S, Cortez C, et al. Sequence of Apd-1 relative to local tumor irradiation determines the induction of abscopal antitumor immune responses. *Sci Immunol* (2021) 6(58):eabg0117. doi: 10.1126/sciimmunol.abg0117

214. Dovedi SJ, Adlard AL, Lipowska-Bhalla G, McKenna C, Jones S, Cheadle EJ, et al. Acquired resistance to fractionated radiotherapy can be overcome by concurrent pd-L1 blockade. *Cancer Res* (2014) 74(19):5458–68. doi: 10.1158/0008-5472.CAN-14-1258

215. Dovedi S, Illidge T. The antitumor immune response generated by fractionated radiation therapy may be limited by tumor cell adaptive resistance and can be circumvented by pd-L1 blockade. *Oncoimmunology* (2015) 4(7):e1016709. doi: 10.1080/2162402X.2015.1016709

216. Bestvina CM, Pointer KB, Karrison T, Al-Hallaq H, Hoffman PC, Jelinek MJ, et al. A phase 1 trial of concurrent or sequential ipilimumab, nivolumab, and stereotactic body radiotherapy in patients with stage iv nsclc study. *J Thorac Oncol* (2022) 17(1):130–40. doi: 10.1016/j.jtho.2021.08.019

217. Sundahl N, Vandekerkhove G, Decaestecker K, Meireson A, De Visschere P, Fonteyne V, et al. Randomized phase 1 trial of pembrolizumab with sequential versus concomitant stereotactic body radiotherapy in metastatic urothelial carcinoma. *Eur Urol* (2019) 75(5):707–11. doi: 10.1016/j.eururo.2019.01.009

frontiers | Frontiers in Immunology

TYPE Review
PUBLISHED 31 January 2023
DOI 10.3389/fimmu.2023.1128774

OPEN ACCESS

EDITED BY
Haojun Chen,
First Affiliated Hospital of Xiamen University, China

REVIEWED BY
Tianlin Gao,
Qingdao University, China
Guangwei Liu,
Beijing Normal University, China

*CORRESPONDENCE
Fang Fang
fangfang7786@jlu.edu.cn
Hongguang Zhao
zhaohg@jlu.edu.cn

†These authors have contributed equally to this work and share first authorship

SPECIALTY SECTION
This article was submitted to Cancer Immunity and Immunotherapy, a section of the journal Frontiers in Immunology

RECEIVED 21 December 2022
ACCEPTED 17 January 2023
PUBLISHED 31 January 2023

CITATION
Yuan H, Gui R, Wang Z, Fang F and Zhao H (2023) Gut microbiota: A novel and potential target for radioimmunotherapy in colorectal cancer.
Front. Immunol. 14:1128774.
doi: 10.3389/fimmu.2023.1128774

Gut microbiota: A novel and potential target for radioimmunotherapy in colorectal cancer

Hanghang Yuan[1,2†], Ruirui Gui[1,2†], Zhicheng Wang[2], Fang Fang[2*] and Hongguang Zhao[1*]

[1]Department of Nuclear Medicine, The First Hospital of Jilin University, Changchun, China, [2]National Health Commission (NHC) Key laboratory of Radiobiology, School of Public Health, Jilin University, Changchun, China

Colorectal cancer (CRC) is one of the most common cancers, with a high mortality rate, and is a major burden on human health worldwide. Gut microbiota regulate human immunity and metabolism through producing numerous metabolites, which act as signaling molecules and substrates for metabolic reactions in various biological processes. The importance of host-gut microbiota interactions in immunometabolic mechanisms in CRC is increasingly recognized, and interest in modulating the microbiota to improve patient's response to therapy has been raising. However, the specific mechanisms by which gut microbiota interact with immunotherapy and radiotherapy remain incongruent. Here we review recent advances and discuss the feasibility of gut microbiota as a regulatory target to enhance the immunogenicity of CRC, improve the radiosensitivity of colorectal tumor cells and ameliorate complications such as radiotoxicity. Currently, great breakthroughs in the treatment of non-small cell lung cancer and others have been achieved by radioimmunotherapy, but radioimmunotherapy alone has not been effective in CRC patients. By summarizing the recent preclinical and clinical evidence and considering regulatory roles played by microflora in the gut, such as anti-tumor immunity, we discuss the potential of targeting gut microbiota to enhance the efficacy of radioimmunotherapy in CRC and expect this review can provide references and fresh ideas for the clinical application of this novel strategy.

KEYWORDS

colorectal cancer, radioimmunotherapy, gut microbiota, fecal microbiota transplantation, probiotics

1 Introduction

Colorectal cancer (CRC) is the third most common cancer in the world (1). Comprehensive data show that, globally, the incidence rate of CRC is 10%, and the mortality rate is 9.4%. The latest data shows that the average risk incidence rate and mortality of CRC among the middle-aged and elderly (50 years old and above) are declining, but it is worth noting that the incidence rate of CRC among young patients is increasing,

which is the second common cause of cancer related death in the world (2). With the development of medical science and technology, the traditional treatment methods of CRC, such as surgery, radiotherapy, chemotherapy and other technologies, are constantly improving. Their combinations, such as surgery combined with postoperative radiotherapy, surgery combined with chemotherapy, are also gradually applied to clinical practice. However, not all CRC patients respond positively to treatment. Some patients may even have treatment related adverse reactions, local recurrence and distant metastasis. Therefore, it is very important to study new treatment methods or improve existing combined treatment methods for prolonging the survival period and improving the quality of life of CRC patients.

In the past few decades, immunotherapy has become one of the new options for cancer treatment. This new therapy mainly kills tumor cells by regulating or directly manipulating the patient's own immune system. Compared with the traditional treatment of tumor, it has higher specificity, higher long-term survival rate and fewer side effects (3). For CRC, immunocheckpoint block (ICB) is the most common immunotherapy. However, "cold" CRC, which accounts for a large number of CRC patients, is not sensitive to ICB response. Studies have shown that the dMMR/MSI-H phenotype shows higher levels of ORR compared to the pMMR/MSS phenotype, which accounts for the majority. In addition, ICB increases the function of the immune system so that induce inflammatory side effects and induce immune-related adverse events (rash, colitis, diarrhea, hepatotoxicity, pneumonia, etc.) Therefore, how to improve the immunogenicity of "cold" CRC to improve the ability of the immune system to eradicate tumor cells is a recent research hotspot. What is exciting is that there is evidence that the organic combination of radiotherapy and immunotherapy can improve the sensitivity of CRC to immunotherapy, so as to enhance the ability of the immune system of CRC patients to kill tumor cells, resulting in an "1 + 1 > 2" effect.

It is worth mentioning that nowadays people generally believe that gut microbiota can support the overall health of human body by maintaining the integrity of intestinal structure and protecting the intestinal tract from pathogens. More and more studies have found that there is an unexpected association between gut microbiota and CRC. For CRC patients, it plays a role in the development, treatment and prognosis of cancer. More significantly, a growing number of studies have found a correlation between the gut microbiota and the treatment of CRC. In general, the gut microbiota tend to correlate with treatment efficacy and prognosis. For example, gut microbiota can influence the responsiveness to immunotherapy and the incidence of immune adverse events associated with immunotherapy in CRC. In the case of CRC radiotherapy, manipulation of the gut microbiota can also be used to promote sensitivity to radiotherapy and reduce radiation toxicity associated with radiotherapy.

In this review, we summarized several classical mechanisms of immunotherapy and radiotherapy in CRC, supplemented the latest research in the past few years, and discussed the feasibility and potential best combination strategy of radiotherapy and immunotherapy for CRC. More importantly, based on the important role of the gut microbiota in CRC immunotherapy and radiotherapy, we explored and reasonably speculated on the feasibility of the gut microbiota as a potential target and its roles in the combined radiotherapy, immunotherapy and radioimmunotherapy of CRC.

2 Gut microbiota—a potential therapeutic target for CRC

2.1 Microbiota landscope in CRC

Bacteria are an important component of the neoplastic microenvironment The bacterial-rich gut microbiota is known as the "forgotten organ" that affect many essential physiological processes in human body. The close relationship between alterations in the gut microbiota and CRC is widely recognized. Currently, the dominant flora in CRC progression remains undefined, but benefited from the development of microbiome profiling, including 16s rRNA and shotgun metagenomics, we have a more in-depth and comprehensive understanding of the taxonomic and functional characteristics of gut microbes and metabolites. A growing number of metagenomic and metataxonomic studies have revealed some potential anti-tumor probiotics and pro-carcinogenic microbiota.

Compared with healthy individuals, CRC patients have a lower abundance of protective probiotics and higher pro-cancer microbiota. A comprehensive analysis of the multinational microbiome using eight different cohorts of the CRC macrogenomic dataset found that: although the microbial species differed considerably in different groups, a subset of species with consistent alterations were identified, such as Alistipes onderdonkii, Parvimonas micra and Gemella morbillorum. A total of 48 bacterial species with elevated abundance were identified in CRC patients, including F. nucleatum, P. micra, Porphyromonas asaccharolytica, Desulfovibrio desulfuricans and Akkermansia muciniphila. Besides, protective species of butyrate-producing bacteria, such as Clostridium butyricum, Roseburia intestinalis and Butyrivibrio fibrisolvens, were reduced in patients with CRC compared to controls (4). Recent meta-analyses have ascertained cross-cohort microbial signatures associated with CRC, including enrichment for Clostridiaceae, Daniostoma, and Mycobacterium morganum (5, 6). Meta-analysis of 526 faecal shotgun metagenome datasets identified a microbial core of seven enriched bacteria in CRC, B. fragilis, a bacterium with enterotoxigenic capabilities associated with CRC, F. nucleatum, Parvimonas micra, Porphyromonas asaccharolytica, Prevotella intermedia, Alistipes finegoldii and Thermanaerovibrio acidaminovorans (7). Table 1 summarizes the microflora that are increased and decreased in CRC patients compared to healthy individuals.

In conclusion, based on previous studies, we have summarized a set of potential core microbiota markers for CRC, including cancer-promoting microbiota: Fusobacterium nucleatum, Parvimonas micra, Porphyromonas asaccharolytica, Bacteroides fragilis, Streptococcus gallolyticus and Cancer-inhibiting flora: Clostridium, Roseburia. These microflora may become future diagnostic biomarkers and therapeutic targets.

2.2 Mechanisms of microbiota for CRC progression

At homeostasis, interactions between host cells and microbiota facilitate important symbiotic functions and maintain the structural integrity of the gut. However, this symbiotic relationship can become maladapted in CRC, including deterioration of the epithelial cell barrier when microbial invasion triggers inflammation, disrupts the

TABLE 1 Taxonomy summary of the above mentioned intestinal flora changes in the development and progression of CRC.

Increased intestinal microbiota	Reduced intestinal microbiota
Prevotella intermedia (8)	Bacteroidetes (9)
Gemella morbillorum (10)	Coprobacter fastidosus (11)
Desulfovibrio (12)	Bifidobacterium (4)
Enterococcus faecalis (12)	Butyrivibrio fibrisolvens (4)
Dialister pneumosintes (10)	Clostridium butyricum (4)
Alistipes finegoldii (7)	Roseburia (13)
Fusobacterium nucleatum (13)	Eubacterium (13)
Parvimonas spp (13)	Dorea (13)
Porphyromonas asaccharolytica (13)	Coprococcus (13)
Ruminococcus torques (10)	Faecalibacterium (13)
Akkermansia muciniphila (14)	Talaromyces islandicus (4)
Veillonella parvula (15)	Sistotremastrum niveocremeum (4)
Peptostreptococcus (13)	Macrophomina phaseolina (4)
Streptococcus gallolyticus (16)	Aspergillus niger (4)
Thermanaerovibrio acidaminovorans (7)	
Filifactor alocis (10)	
Escherichia coli (8)	
Campylobacter (15)	
Enterotoxigenic Bacteroidetes (9)	

tumor immune microenvironment and generates pro-oncogenic metabolites and bacterial toxins. The following section will underline the mechanisms of intestinal flora in relation to precancerous lesions and clinical transformation of CRC (Figure 1).

2.2.1 Pro-inflammatory and immunomodulatory effects

Chronic inflammation is an important intrinsic factor that promotes carcinogenesis by inducing DNA damage, producing reactive oxygen and nitrogen species, regulating intestinal epithelial cell (IEC) polarization and the tumor microenvironment, activating transcriptional programs such as nuclear factor kappa-light-chain-enhancer of activated B cells (NF-κB) and STAT3 in IEC, and impeding anti-tumor immunity (17). Depending on IL-17 and the CEC IL-17R, enterotoxigenic Bacteroides fragilis (ETBF) colonization produces Bacteroides fragilis toxin to trigger strong selective distal colon NF-κB activation. The phenomenon reveals a STAT3- and Th17-dependent pathway of increased colonic tumor formation (18). Long XH et al. discovered in their constructed P. anaerobius-treated ApcMin/+ mice that P. anaerobius has a surface protein called putative cell wall binding repeat 2 (PCWBR2) which can bind α2/β1 integrin and activate the PI3K-Akt pathway in CRC tumor cells under the action of phospho-focal adhesion kinase. NF-κB in turn increased cytokine levels, such as IL-10 and IFN-γ, to stimulate the pro-inflammatory response (19). CRC patients have the higher abundance of Parvimonas micra compared with the healthy population. Colonization of P. micra upregulates genes involved in cell proliferation, stemness, angiogenesis and invasiveness/metastasis and enhances Th17 cell infiltration and Th17 secretion of cytokines (IL-17, IL-22 and IL-23) to promote CRC formation in mice (20).

2.2.2 Metabolites

The role of gut microbota metabolites on CRC is a double-edged sword. Multi-kingdom microbiota analyses found CRC patients have 26 additional metabolic pathways versus healthy people, including pathways involved in carbohydrate metabolism (e.g. butyrate, ascorbate and aldehyde metabolism) and D-arginine and D-ornithine metabolism; 23 reduced pathways including branched-chain amino acid (valine, leucine and isoleucine) and lipid metabolism (e.g. phospholipase D) pathways (4). Naoki Sugimura et al. found that L. gallinarum can produce metabolites such as L-tryptophan that induce apoptosis in CRC cells (21). β-Galactosidase is a key protein. By secreting it, Streptococcus thermophiles can promote CRC cell apoptosis and mediate the anticancer effects of Streptococcus thermophiles by disrupting energy homeostasis, activating oxidative phosphorylation and downregulating Hippo pathway kinases with galactose production. Meanwhile, β-Galactosidase also increases the intestinal abundance of known probiotics such as Bifidobacterium and Lactobacillus (22). Specific intestinal bacteria, such as E. faecalis, E. roseus, Bifidobacterium, E. fungalis, and Lactobacillus, could ferment dietary fiber into short-chain fatty acids (SCFA), which are enteroprotective and negatively associated with colorectal cancer. SCFA, including butyrate, propionate and acetate, prevent CRC through mechanisms like modulation of intestinal inflammation, the immune system and so on (23). In addition to inhibiting CRC, some metabolites produced by the gut microbiota also promote CRC. M. morganii can produce indolimine to induce increased intestinal permeability and may lead to abnormal DNA replication and abnormal IEC proliferation *in vivo* to exacerbate the CRC burden (24).

2.2.3 Bacterial toxins

Relying on METTL14-mediated N6-methyladenosine methylation, ETBF could downregulate miR-149-3p, which promotes proliferation of CRC cells (25). E. coli-produced colibactin can cause DNA damage and colibactin-producing E. coli (CoPEC) promotes the development of CRC in the mouse model with chronic inflammation induced by dextran sodium sulfate (DSS) and further enhances the pro-tumorigenic effect in the mouse model with IEC autophagy deficiency (26).

2.3 Therapeutic interventions for microbiota

Traditional strategies related to the prevention and treatment of CRC include probiotics, prebiotics, high-fiber dietary therapy, and fecal microbiota transplantation (FMT), which have been comprehensively reviewed (27). Still, these approaches are limited by their own drawbacks (e.g. low selectivity and specificity for specific sites of action and specific bacterial flora as well as safety issues in clinical translation). More useful therapeutic options targeting the intestinal flora are still expected (28). The above summary of the macrogenomic landscape of the CRC microbiota and the action mechanisms of the associated gut microbiota in CRC is valuable for the ensuing discussion of potential targets and clinical strategies for the diagnosis, treatment and prevention of CRC.

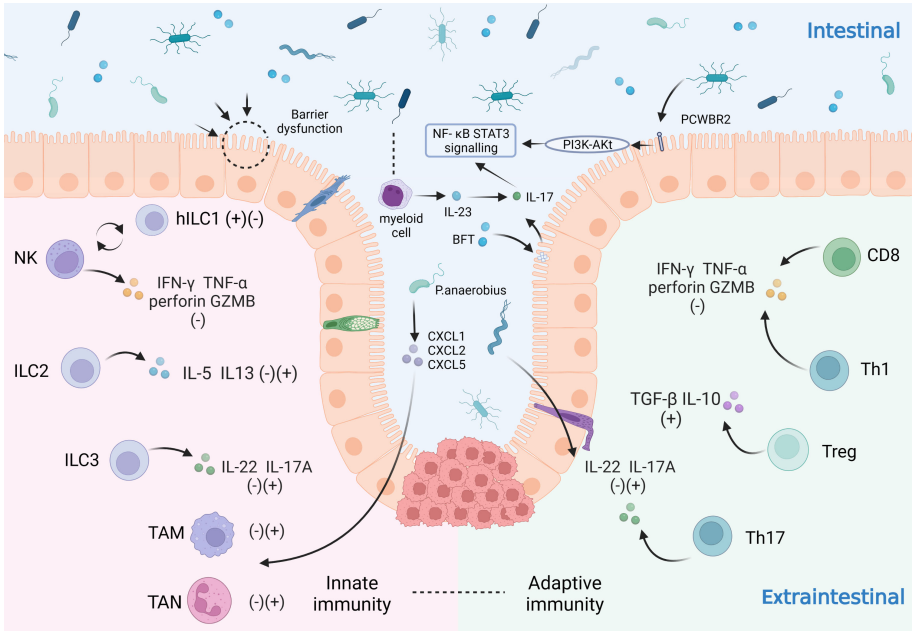

FIGURE 1
Influence of intestinal microbiota on the immune system in CRC patients. The immune system plays an important role in the development of CRC by virtue of its tumor-promoting and tumor-suppressing effects. The immune system can be categorized as the innate immune system and the adaptive immune system. In the innate immune system: NK cells secrete IFN-γ, TNF-α, perforin and GZMB to suppress tumors and can be converted to hILC1 under certain conditions; ILC2 secretes IL-5 and IL-3; ILC3 secretes IL-22 and IL-17A; tumor-associated neutrophils (TAN) and macrophages (TAM) also play a significant role; In the adaptive immune system: CD8+ T cells and Th1 cells secrete IFN-γ, TNF-α, perforin and GZMB; Treg cells secrete TGF-β and IL-10; Th17 cells secrete IL-22 and IL-17A. The innate and the adaptive immunity reinforce each other and play a pro-tumor or anti-tumor role together. The gut microbiota can influence on CRC cells through various mechanisms. For example: microbiota disrupt the gut barrier; some microbiota increase pro-inflammatory responses through PCWBR2 or activation of the NF-κB/STAT3 signaling pathway with lineage cells; others can act on domain CRC cells by regulating TAN, TAM through CXCL1/2/5.

Targeting the ETBF/miR-149-3p pathway presents a promising approach to treat patients with intestinal inflammation and CRC with a high amount of ETBF. IEC autophagy inhibits CoPEC from inducing CRC occurrence in ApcMin/+ mice model, suggesting that targeted induction of autophagy may be a promising strategy to inhibit the pro-tumorigenic effects of bacteria, which could be achieved by immunotherapy and radiotherapy (29). Cai F et al. suggested that polyunsaturated fatty acids (PUFAs) have the potential to sensitize HT29 cells, possibly due to an increase in intracellular lipid peroxidation products (30). Short-chain fatty acids directed modulation in human and mouse CRC models enhances response to chemotherapy and immunotherapy, and targeting SCFAs and PUFAs for abundance reconstruction may be a new approach to managing CRC (31).

So, targeting gut microbiota holds the promise of achieving precise microbial regulation, satisfactory therapeutic outcomes, minimizing the possibility of adverse reactions, identifying effective primary prevention strategies and further reducing CRC risk.

3 Strategies for gut microbiota to increase the efficiency of CRC immunotherapy

The intestine is the largest immune organ of the body. The unique intestinal immune system is the basis of the body's anti-tumor response; conversely, an imbalance in the intestinal immune system will facilitate the development of tumor. Meaningfully, the microbiota and the host have a mutually beneficial symbiosis. There is a close regulatory relationship between the microbiota and the host's immune system. In short, the microbiota can modulate both innate and adaptive immune functions in the body, thereby influencing oncogenesis and anti-tumor immune function.

3.1 The role of microbiota on the immune system

Innate immunity is a natural defense that produced in order to adapt to the environment. The main innate immune cells in the intestine are neutrophils, macrophages and innate lymphocytes (ILCs). TAN can be classified into an anti-tumorigenic "N1" phenotype and a pro-tumorigenic "N2" phenotype (32). The "N1" phenotype increases cytotoxicity through producing TNF-α, reactive oxygen species (ROS), etc. (32). Conversely, the "N2" phenotype promotes tumor development through the expression of arginase and various chemokines (33). The phenotype of TAN depends on the tumor microenvironment (TME). For example, TGF-β induces the "N2" phenotype, while the "N1" phenotype is induced by IFN-β (32). TAM can be classified as "M1", which exerts pro-inflammatory effects, and "M2", which exerts anti-inflammatory and tumor-promoting effects. It has been suggested that a high pan-macrophage density at the margins of tumor infiltration has a positive impact on the prognosis of CRC patients, while the opposite result is observed in the center (34). As the main intestinal

ILC cells, ILC1 and NK cells regulate the different steps of CRC development. It has been suggested that NK cell can transdifferentiate to a less cytotoxic ILC1-like phenotype in the presence of TGF-β, which is present in the TME of CRC (35). It has also been shown that high ILC1 levels may predict poor cancer prognosis (36).

Gut microbiota can regulate the innate immune system in various ways. Toll-like receptors (TLRs) bind to ligands to coordinate early host resistance to infection through signaling pathways such as NF-κB and mitogen-activated protein kinases (MAPK) (37). Specifically, TLR2 can form heterodimers with TLR1 and TLR6, which initiate MyD-88-dependent signaling pathways regulating cytokine transcription. Lactobacillus fermentum can identify TLR2/TLR1 and TLR2/TLR6 signaling (37). In intestinal injury associated with inflammatory bowel disease, TLR4 increases its sensitivity to LPS through the release of IFN-γ and TNF-α (38). Lactobacillus and Bifidobacterium suppress animal enteritis by reducing TNF-α by TLR4 (39). It has been shown that the promotion of IFN-γ release *via* TLR9 by S. amoebae may contribute to cytokine imbalance in UC (40). Abnormal TLR signaling activation in immune cells may also lead to the release of pro-inflammatory cytokines, resulting in acute or chronic intestinal inflammation (41).Additionally, TLRs, activated by microbiota, can also start adaptive immune responses.

Adaptive immunity is produced by lymphocytes through contacting with antigenic material and is specific and memory-based. Adaptive immunity in the gut occurs mainly in the lymphoid tissues associated with the gut (e.g. Pai's node, mesenteric lymph nodes), while T and B cells in the lamina propria also play an important role.

B cells can identify CRC antigens and produce specific antibodies in cooperation with helper T cells, thereby impeding CRC development and progression. CD8+ T cells are the immune cells that specifically target tumor cells. A study showed that IL-18 was highly expressed in 72% of tumor cells in CRC and can act as a trigger to prompt a series of immune responses from CD8+ T cells (42). Additionally, CD8+CD279+ cells could be a potential biomarker for predicting postoperative prognosis in CRC patients (43). CD4+ T cells can be divided into Th1 cells and regulatory T cells (Treg). Th1 cells are functionally similar to CD8+ T cells, while Treg cells exert immunosuppressive functions through IL-10, TGF-β. A study has shown that the density of combination of CD4+ and FOXP3+ cell is a precise prognostic marker. Furthermore, only one type, such as CD4+ or FOXP3+ cells, may be sufficient for a suitable TME to prevent recurrence (44). Th17 cells and IL-17 can influence the process of tumor through various mechanisms, including immune infiltration, promotion of cancer cell invasion and metastasis, etc. A study identified related genes (KRT23, ULBP2, ASRGL1, SERPINA1, SCIN, SLC28A2) that may affect the immune infiltration of Th17 cells in COAD patients and suggested that the effect of these genes on Th17 cells may be responsible for their dual product (45).

Gut microbiota can modulate adaptive immune function by stimulating the differentiation of T cell in the gut and by regulating T cell antigen recognition and tumor killing functions. Studies have shown that antigenic peptides derived from bacteria such as Akkermansia muciniphila can induce differentiation of Treg cells in the colon and improve intestinal inflammation (46). Short-chain fatty acids (SCFA) can increase Treg cells differentiation (47, 48), while SFB and S. fragilis induce differentiation of Th17 cells (46). In summary, as an important component of the CRC tumor microenvironment, the immune system interacts with the gut microbiota to control inflammation and anti-tumor immunity.

3.2 Potential for microbiota to improve ICB

ICB refers to suppressing tumor immune evasion and enhancing anti-tumor immunity by inhibiting the interaction between IC and tumor cells through IC inhibitors (ICI). Currently the immune checkpoint molecules PD-1 and CTLA-4 have been recognized as important targets for immunotherapy of CRC.

PD-1, a protein in the CD28 family on the surface of activated immune cells, binds to PD-L1 on the surface of tumor cells. It can block the PI3K pathway and thus inhibit T cell activation. CTLA-4 promotes tumor immune evasion by competitively binding to B7 ligands and inhibiting the function of Treg cells. At present, two PD-1 blocking antibodies, pembrolizumab and nivolumab, and the CTLA-4 receptor blocking antibody ipilimumab are approved by FDA for the treatment of dMMR/MSI-H CRC (49). Although ICBs offer a new direction for the treatment of cancers, the need to improve ICB efficacy and reduce immune-related adverse events (irAEs) continues to be a hot topic of research.

Recent studies have shown an association between higher levels of tumor mutational load (TMB) and improved survival for patients treated with ICB (50). Compared to the pMMR/MSS phenotype, The dMMR/MSI-H phenotype generally shows higher levels of TMB and immune cell infiltration (51). It has been shown that immunotherapy is effective in some cases of dMMR/MSI-H CRC, while many patients in the pMMR/MSS phenotype show resistance (52). For ICB, although dozens of clinical trials have demonstrated the effectiveness of ICB and it has received several FDA approvals, its response has been limited to patients with dMMR/MSI-H CRC (53). A recent meta-analysis showed that the MSS-H/dMMR subgroup had a higher ORR compared to the pMMR/MSS subgroup when treated with anti-PD-1/PD-L1 antibodies (54). However, the dMMR/MSI phenotype accounts for approximately 15-18% of CRC patients and 5% of metastatic CRC (mCRC) patients (55). This means that most CRC patients are the pMMR/MSS phenotype, and they often don't have satisfactory results after receiving ICB. Therefore, it is important to improve the efficacy of dMMR/MSI-H phenotype immunotherapy and explore new immunotherapies that benefit pMMR-MSI-L.

ICB may alter the composition of the patient's gut microbiota. A study analyzing patients with gastrointestinal cancers treated with anti-PD-1/PD-L1 therapy showed elevated relative abundance of Prevotella and Bacteroides in responders (56). In a mouse model of CRC, the ileal microbiome controlled the efficacy of PD-1 blockers in CRC (57). In addition, nonprotective E. faecalis can expresses sufficient SagA to enhance the anti-tumor effects of PD-L1 in mice (58). Cell lysates of Lactobacillus acidophilus combined with CTLA-4-blocking antibodies can enhance antitumor immunity in a mouse CRC model (59). Notably, because the composition of good or harmful microbiota may vary depending on the location of the tumor, further research is still needed in the field of immunotherapy for CRC. In addition, some studies have shown that irAEs are associated with reduced diversity and altered composition of the gut microbiota. A clinical study analyzed the microbiota of patients

with advanced non-small cell lung cancer treated with PD-1 antibodies. There were significant differences in microbiota composition in patients with diarrhea compared to non-diarrhea patients, as evidenced by non-diarrhea patients exhibiting higher abundance of Bacillus mimicus and lower abundance of thick-walled bacteria (60). This suggests that gut microbiota interventions may not only improve the efficacy of ICB, but may also be a starting point for the treatment and prevention of irAEs.

There are some perspectives on the mechanisms. On the one hand, the gut microbiota improves ICB efficacy through innate immunity. It has been demonstrated that microbiota can induce intra-tumoral monocyte production of IFN-1 to modulate TAM, which would ultimately improve ICB efficacy (61). It has also been found that an increase in bifidobacteria within the tumor will enhance NK cell function and thus enhance the therapeutic effect of PD-1 blockers (62). On the other hand, microbiota may also improve ICB efficacy through adaptive immunity. One study isolated a bacterial community of 11 types of bacteria from healthy human donor faeces. The bacterial community can induce CD8+ T cells in the gut and enhance the therapeutic efficacy of ICI in a tumor model (63). Other mouse models have also demonstrated that Lactobacillus acidophilus can improve anti-CTLA4 therapeutic efficacy in CRC by reducing Treg cells and "M2" TAM and by increasing CD8+ T cells (59). A phase I clinical trial found a relative increase in the abundance of enterococci in refractory metastatic melanoma following the use of PD-1 blockers and FMT, which led to intra-tumoral CD8+ T-cell infiltration and ultimately better tumor killing (64).

In addition to modulating the innate and adaptive immune system, microbiota can also enhance the immunogenicity of tumor cells to improve ICB efficacy. On the one hand, the gut microbiota metabolite inosine can directly enhance tumor intrinsic immunogenicity through UBA6 (65). On the other hand, microbiota can provide tumor cross-antigens and thus indirectly increase the immunogenicity of tumor cells (66). It is worth mentioning that metabolites of the gut microflora, such as inosine, short-chain fatty acids (SCFAs) (67, 68), arachidonic acid (66), bile acids and tryptophan are considered to be effective targets for improving the efficacy of ICB.

3.3 Strategies for improving ICB with gut microbiota

3.3.1 Fecal microbiota transplantation (FMT)

We know that patients with good gut microbiota status can improve the TME through microbiota, thereby enhancing the efficacy of ICB (69). FMT, which involves transplanting faecal microbes from patients who have responded to ICB into non-responders, holds promise for improving the efficacy of ICB and reducing irAEs. Previously, mice from the Jackson Laboratory (JAX) showed increased efficacy about anti-PD-1 immunotherapy, suggesting that the gut microbiota influence the efficacy of anti-PD-L1 therapy (70). A recent study found a stronger anti-tumor effect of PD-1 blockers in the faecal microbiome of cancer patients transplanted with a response to ICB compared to those transplanted with no response to ICB in mice that were germ-free or on antibiotics (71). Based on that, a number of clinical studies aiming at assessing the therapeutic potential of FMT-enhanced ICI are underway, mainly involving melanoma, prostate cancer, gastrointestinal tract cancer and lung cancer (72). However, there are fewer clinical studies on CRC.

In addition, one study demonstrated in CRC mice that FMT exerts an anti-inflammatory function by restoring the ratio and diversity of gut microbiota, which also suggests that " FMT + ICI" treatment may not only improve the efficacy of ICB treatment but may also reduce irAEs (73). However, before FMT is performed, donors are screened regularly to limit the spread of microorganisms that may cause infection. The safety of FMT also needs to be observed with long-term follow-up.

3.3.2 Probiotics

Prebiotics, probiotics and commensal bacteria have been studied in relation to anticancer treatment strategies such as chemotherapy and radiotherapy, but less research has been conducted on ICB. Excitingly, there is still considerable evidences that this therapy is beneficial in improving ICB efficacy and reducing immune-related adverse events.

A recent study, using a combination of anti-ePD-L1 and prebiotic Bilberry Anthocyanin to treat CRC in mice, suggested that prebiotics may improve ICB efficacy by restoring microflora diversity (74). Other studies in mice have also shown that probiotics such as Bifidobacterium and Mucorophilus in combination with ICB can enhance therapeutic efficacy (70). Similarly, administration of Lactobacillus rhamnosus GG enhances anti-PD-1 therapeutic efficacy by promoting CD8+ T cell function (75). Interestingly, another mouse model showed that administration of a probiotic (Bifidobacterium longum or Lactobacillus rhamnosus GG) reduced the frequency of IFN-γ(+)CD8+ T cells exhibiting an unfavourable antitumor response. Therefore, the mechanism of probiotics in ICB treatment still needs further research (76). In addition, there are also studies that show probiotics are associated with irAEs. One study found that administration of vancomycin may enhance the immunopathological response to ICB, which was associated with depletion of Lactobacillus. Further studies found that administration of the probiotic Lactobacillus reuteri completely eliminated ICB toxicity (77). It is important to note that although there are relevant data observed in mouse models, clinical evidence must be available to support the use of probiotics before they can be encouraged.

4 Microbiota and CRC radiotherapy

Currently, most early CRC can be cured by surgical resection, but advanced CRC are difficult to eliminate completely by surgery and require multimodal treatment including chemotherapy and radiotherapy as well as surgery. Especially, due to the proximity of the rectum to the pelvic organs, the absence of plasma serosa around the rectum and the technical difficulties in achieving wide surgical margins, radiotherapy has been established as the main treatment option for patients with advanced colorectal cancer in addition to surgery.

It is noteworthy that the results of a growing number of studies prove that the final outcome of radiotherapy is closely related to biological factors (78). There is a two-way interaction between

intestinal microbiota and radiotherapy. On the one hand, intestinal microbiota affects the antitumor clinical efficacy of radiotherapy, on the other hand, ionizing radiation changes the composition and function of intestinal microbiota, which in turn leads to the development of radiation enteropathy (79). Intestinal flora is of significant interest for its use in radiotherapy, as a protective agent and a biomarker in radiation exposure.

4.1 Mechanisms of microbiota in CRC radiotherapy

Next we focus on the two main mechanisms of ionizing radiation-induced dysbiosis of the intestinal flora. First, radiation can damage IEC, resulting in impaired intestinal barrier function, allowing bacteria to move deeper into the body and promoting the entry of bacterial metabolites into the bloodstream, which promotes inflammation (80). Second, radiation exposure can cause the formation of ROS, which are chemically active due to their unpaired electrons and can damage the DNA and other cellular structures of the intestinal microbiota, thereby triggering changes in the bacterial flora (81). In addition, the various microorganisms that make up the intestinal microbiota have different intrinsic radiosensitivities (82), so radiation exposure can alter the composition and relative proportions of the microbiota.

El Alam et al. (83) found that in patients treated with pelvic chemoradiotherapy, gut microbiome composition and relative abundance continually decreased in the overall. Although the diversity of the population's gut microbiota tended to return to baseline levels during the 12-week follow-up period, there are still significant changes in structure and composition, the most notable of which was the increase in the number of Bacteroidetes. Pooled results from other studies suggest that the inflammatory environment produced by radiotherapy leads to increased abundance of pathogenic pro-inflammatory bacteria (e.g. S. wadsworthensis and S. parvirubra) and mimics; decreased abundance of anti-inflammatory bacteria (e.g. E. faecalis and Prevotella histicola) and Phylum Firmicutes including Lachnospira pectinoschiza, Roseburia intestinalis, etc (84, 85). By sequencing the 16s rRNA gene in the mouse model, significant changes in gut microbial composition could be observed in the radiation background. Moreover, changes in the flora can lead to changes in their metabolites, such as lactic acid, which has a protective effect on the body (86). The foregoing studies imply the homeostasis dysregulation of intestinal flora and its metabolites after radiotherapy provides a potential target for improving the prognosis of CRC patients treated with radiotherapy.

Microbial colony metabolites may affect radiosensitization or radioresistance. ETBF has been proven to be enriched in CRC patients as a potential cancer-promoting colony, and it was found that Bacteroides fragilis toxin (BFT) and IL-17 produced by ETBF after colonization synergistically activate the STAT3 signaling pathway in IC (18). Park SY, et al. found that, JAK2/STAT3/CCND2 axis is a key mediator of radioresistance (87). Thus, we speculate that ETBF may enhance the radioresistance of CRC by generating BFT.

Based on these links, microbiota may be a modulating factor for ameliorating radiation adverse effects and radiation toxicity. Baseline gut microbiota diversity is a predictor of the extent of change in gut flora diversity during CRT. El Alam et al. (83) unexpectedly discovered that patients with high intestinal flora diversity at baseline had a greater decline in intestinal flora diversity from the start to the fifth week of CRT than patients with low intestinal flora abundance at baseline. This finding suggests that the optimal target group for CRT intervention may actually be patients with high baseline gut richness and diversity rather than the low. Interestingly, in the same year there was new evidence that patients with abundant microbial diversity had increased activation of CD4+ lymphocytes infiltrating cervical tumors as well as CD4 cell subpopulation expressing ki67 and CD69+ during radiotherapy (88). Considering that the combination of radiotherapy and immunotherapy can strengthen the anti-tumor immune microenvironment to the maximum extent and it has been demonstrated that intestinal flora can promote the efficacy of immunotherapy (70). We hypothesize that high abundance of gut microbiota may enhance the sensitivity of tumor cells to radiotherapy through immunomodulation. Given the similarities between cervical and colorectal cancer in terms of irradiation sites and modalities, we suspect that a similar effect might be achieved in radiotherapy for CRC.

4.2 Strategies associated with targeted colonies to improve the efficacy of radiotherapy

Results from experiments using an orthotopic syngeneic murine model of breast cancer treatment with focal irradiation as a mouse model indicated that treatment with an antibiotic (Abx) cocktail of ampicillin, imipenem, and cilastatin prior to radiotherapy reduced therapeutic efficacy, and a similar reduction was observed in a previous melanoma model. In contrast, the combination of radiotherapy and the fungal antibiotic enhances the clinical efficacy of RT and improves the immunosuppressive tumor microenvironment by increasing granzyme B-producing CD8 T cells (89). The results draw our attention to the potential of manipulating intestinal fungal flora through antibiotics to enhance antitumor immune responses to radiotherapy. Vancomycin, a glycopeptide antibiotic active against gram-positive bacteria, alters the composition of the intestinal microbiota when combined with radiotherapy in a preclinical model, and leads to increased antigen presentation of CD11c dendritic cells in tumor-draining lymph nodes of radiotherapy mice, which enhances the antitumor effect (90). Recently, the results of Yang K et al. showed that the vancomycin effect was abolished by butyrate, so that butyrate-producing bacteria, such as Lactobacillariophyceae and Rumenococcaceae, may be new therapeutic targets (91). At the meantime, we should also notice that inappropriate antibiotic use in ICI-treated patients may weaken treatment outcomes due to antibiotic-induced ecological dysregulation (92). Therefore, when selecting antibiotics, especially broad-spectrum antibiotics, it is critical to consider the potential risks of antibiotic therapy for cancer patients, including potential adverse effects on treatment efficacy and toxicity.

4.3 Radiation enteropathy and microbiota

Radiation changes microbiota and produces radiation toxicity. Pelvic irradiation is one of the methods of treatment for CRC. Although RT has a positive killing effect on cancer cells, radiation damage to normal organs

and tissues inevitably occurs during radiotherapy, especially for one of the most radiosensitive organs, the intestine. The intestinal damage caused by radiation is known as radiation enteropathy (RE), and radiological diarrhea (RID) is most common symptom. Frequent or persistent diarrhea has been reported in 51.9% of women treated with standard radiotherapy and 33.7% of women treated with intensity-modulated radiotherapy (93), which greatly reduces the patient's quality of life after surgery and is also likely to affect the efficacy of radiotherapy through delayed radiotherapy.

As RE has received increasing attention, the mechanisms by which RE occurs are being studied more and more clearly. There are considerable evidences that gut microbiota play an important role in the development of RE during pelvic irradiation and after treatment.

What is clear is that there are differences in the gut microbiota between those who develop diarrhea and those who do not in patients receiving radiotherapy. In experimental animals, germ-free mice are thought to exhibit less radiotoxicity than conventionally reared mice, suggesting that gut microbiota may influence radiation-induced intestinal toxicity (94). Similarly, in a mouse model of acute radiation-induced intestinal injury (RIII), acute RIII was found to occur with reduced diversity of gut microbiota, reduced abundance of beneficial bacteria and increased abundance of pathogens. Therefore, it is likely that the gut microbiota are potential biomarkers for the critical phase of RIII (95). In rectal cancer patients, Bifidobacterium, Clostridium and Synechococcus are enriched in patients without Diarrhea or Mild Diarrhea (96). In cervical cancer patients treated with pelvic radiotherapy, RE patients had significantly lower α-diversity but increased β-diversity of gut microbiota, with relatively high abundance of Aspergillus and Gammaproteobacteria and lower abundance of Aspergillus. Interestingly, Coprococc was found to be significantly enriched in patients who subsequently developed RE before receiving radiotherapy and had a graded associated microbial profile, suggesting that Gut microbial dysbiosis may be a potential biomarker for human RE (97). A recent systematic evaluation showed that in patients undergoing pelvic radiotherapy, the levels of thick-walled bacteria, Aspergillus and Actinobacteria, were higher in the gut of patients with diarrhea compared to those without diarrhea, while most posterior and anaphylactic bacteria were lower. And at the genus or class level, patients with diarrhea had the presence of Sutrobacter, Fine Golden Bacteria, Peptococcaceae (Clostridium), Prevotella 9, Faecalis, Desulfovibrio, Anaplasma, Verrobacter, Dictyostelium and Bacteroides, while intestinal dominant bacteria (e.g. Clostridium, Anaplasma, Brautia, Ruminococcaceae UCG-003, Faecalis Bacillus oscillatus, Prevotella and Roscoe) were reduced (98). In conclusion, there is an association between RE and dysbiosis of the gut microflora, more consistently: reduced diversity and abundance of microflora, increased abundance of pathogenic bacteria (e.g. Aspergillus, Clostridium) and reduced beneficial bacteria (E. faecalis, Bifidobacterium, etc.) (98).

4.3.1 Possible mechanisms between microbiota and RE

The relationship between microbiota and RE may be related to mechanisms such as inflammation, disruption of the epithelial barrier and intestinal permeability, and the release of immune molecules. One study proposes that, the gut microbiota are dysregulated following irradiation. This is likely to directly induce intestinal barrier dysfunction and inflammatory responses. The trial specifically cultured normal colonic epithelial cells with faecal bacteria from patients with severe RE and found that this increased intestinal permeability and stimulated cytokine and NF-κB activation (97). In another experiment, researchers found that irradiated microbiota stimulated increased secretion of IL-1β, which exacerbated radiation-induced intestinal tissue injury. Tissue injury improved after IL-1 was blocked, suggesting that IL-1β is involved in at least part of the microbiota-mediated radiation-induced intestinal injury (84). In addition, the metabolism of the gut microbiota is also disturbed to some extent after irradiation, especially lipid metabolism. It is well known that the lipid bilayer is the basis of the intestinal epithelial barrier and therefore disorders of lipid metabolism may also be an important factor in the development of RE.

However, studies on how the gut microbiota are involved in radiation-induced intestinal damage are still scarce, and it is necessary to clarify the mechanisms involved before applying microbial agents to improve RE. Next we will focus on strategies for reducing radiotoxicity through microbiota.

4.3.2 Strategies for reducing radiotoxicity through microbiota

Radiotherapy + FMT, probiotics, prebiotics, diet: Based on the potential role of gut microbiota in reducing radiotoxicity, several studies have begun to explore whether adverse effects caused by pelvic irradiation can be minimised by gut microbiota, with FMT and probiotics receiving the most attention.

An experimental study demonstrated that FMT attenuated acute radiation syndrome (ARS), and further studies found that FMT increased indole 3-propionic acid (IPA) levels in the faecal microbiota of irradiated mice, and that IPA ameliorated gastrointestinal toxicity after total abdominal irradiation without accelerating tumor growth (99). In a recent case report, investigators followed a patient who developed chronic hemorrhagic radiation proctitis after radiotherapy for cervical cancer. Significantly, after four courses of FMT treatment, the patient experienced relief of symptoms such as blood in the stool, abdominal pain and diarrhea, and significant changes in intestinal bacterial tests (100). In addition, a clinical study has shown that FMT can safely and effectively improve bowel function over time in CRE patients with chronic radiation enteritis (101). This further suggests the possibility of FMT in reducing the gastrointestinal toxicity of radiotherapy. It is worth noting that clinical studies on FMT and radiation enteritis induced by CRC radiotherapy, as well as studies on the mechanisms involved, are scarce, and the intestinal effects of FMT on the recipient are complex and unpredictable. Therefore, a large number of studies are still needed to demonstrate the feasibility and safety of FMT before it can be truly used in the clinic.

Probiotics such as Lactobacillus and Bifidobacterium have been shown to prevent gastrointestinal toxic reactions such as colitis and diarrhea. As microorganisms that play a beneficial role in cancer prevention and treatment, probiotics are thought to reduce the translocation of harmful bacteria as well as protect intestinal immune barrier function.

One experiment showed that the probiotic Lactobacillus rhamnosus GG has a radioprotective effect on the mouse intestine, possibly through the release of lipoteichoic acid, macrophage

activation and the migration of mesenchymal stem cells (102). Similarly, in the clinical setting, one study found that Lactobacillus rhamnosus GG reversed intestinal ecological dysregulation and diarrhea during cancer treatment (103). Interestingly, a meta-analysis noted that the widespread use of probiotic interventions for diarrhea secondary to cancer therapy did not show positive results (104). This suggests that research efforts should be focused on specific gastrointestinal toxicity as well as unique probiotic pairings. There is still a paucity of objective clinical evidence on the beneficial effects of probiotics on radiation gastrointestinal toxicity in CRC, and a lack of corresponding studies on how probiotics are formulated, administered and absorbed.

FLASH-Radiotherapy (FLASH RT): There are growing evidences that radiation can disrupt the gut microbiome and cause dysbiosis of the gut ecology, which in turn affects the effectiveness of radiotherapy as well as increasing radiotoxicity (79, 83). Significantly, recent studies have shown that FLASH irradiation can reduce changes in the gut microbiome compared to clinically conventional radiotherapy (CONV) (105). FLASH-RT is a new type of radiotherapy that will deliver a dose at an ultra-high dose rate (≥ 40 Gy/s) compared to CONV, which is thousands of times higher than CONV. FLASH-RT can significantly protect healthy tissue from radiation damage without altering tumor killing function. In 2019, the first patient with T cell cutaneous lymphoma underwent FLASH-RT and showed good results for both normal skin and tumor, demonstrating the clinical feasibility and safety of FLASH-RT (106).

A very important feature of FLASH-RT is the short exposure time, which may reduce the proportion of immune cells killed, thus allowing the immune system to exert more robust anti-tumor immunity as well as repairing normal tissue damage (107). On the immune cell side, it has been demonstrated that FLASH-RT promotes better recruitment of CD3+ T cells to the tumor core compared to CONVi, as well as higher levels of cytotoxic CD8α+ T cells in the TME (108). In terms of immune molecules, FLASH-RT can reduce TGF-β expression (109, 110), and low levels of TGF-β improve anti-tumor immune responses and inhibit Treg cells differentiation. In conclusion, FLASH-RT can improve antitumor immunity through immune molecules, but more studies are needed to confirm the role of the immune system in the FLASH-RT response.

Since the gut microbiota and the gut immune system are interdependent and influence each other, we speculate that it is likely that the gut microbiota also play a role when receiving FLASH-RT, which may eventually manifest itself through improved immune system function. It so happens that one study is consistent with our suspicions, and this study suggests that FLASH irradiation greatly reduces changes in the gut microflora compared to CONV irradiation (105). The ecological dysbiosis of the gut microflora is often an important manifestation of a dysregulated intestinal immune system, and a dysregulated immune system is a detrimental factor for both anti-tumor immunity and the protection of normal tissues.

However, further studies are still needed to confirm the role of the gut microbiota in modulating the effects of FLASH. It is worth mentioning that studies on FLASH and CRC are currently scarce and further studies are also still needed to confirm the feasibility and safety of FLASH in the treatment of CRC patients.

5 Potential association between microbiota and radioimmunotherapy for CRC

In addition to inducing DNA damage, local radiotherapy can also promote anti-tumor immunity. New insights in the field of cancer therapy suggest that radiotherapy carries out antitumor by enhancing immunogenicity, including increasing the sensitivity of cancer cells to killing by cytotoxic T cells (111), enhancing antigen processing and inducing the expression of unique radiation-associated peptides in cancer cells (112). Inducing irradiated cancer cells to release or express immunogenic molecules that enhance the anticancer immune response (113) and facilitating the regulation of TME for immune-mediated antitumor effects. CD8+ cytotoxic T lymphocytes (CTL) play an important role in these processes (114). Combination of radiotherapy with immunostimulatory anti-PD1 and anti-CD137 mAbs produces favorable effects on distant non-irradiated tumor lesions and the therapeutic activity is carried out by CD8 T cells (115).

cGAS is a kind of cytosolic dsDNA sensor, STING is a type of endoplasmic -reticulum-resident protein. When bound to dsDNA, the nucleotidyl transferase activity of cGAS is stimulated, triggering a signaling cascade reaction involving STING, which results in the production of type I IFN (116) to initiate the innate immune response and generate the subsequent adaptive anti-tumor immune response. DNA released from dying tumor cells may trigger IFN-α/β *via* STING, which in turn may act on both cross-triggered DC and CD8 T cells as necessary factors to favor CTL immune responses. Strategies aimed at local enhancement of IFN-α/β can make radiotherapy-induced tumor cell death more immunogenic (117). Thus, tumor cells killed by radiotherapy are immunogenic. cGAMP treatment and radiotherapy synergistically amplify the antitumor immune response, and the synergistic effect depends on the presence of STING in the host.

TAM are considered to be important immune cell components of the tumor microenvironment and are abundant myeloid cells in the stromal lumen of varied solid tumors (118). Radiotherapy activates the differentiation of M1 macrophages, promotes the influx of M1 macrophages into tumor cells and prevents the conversion to M2 type for the sake of ensuring the therapeutic effect. RT reprogrammed macrophages have a profound impact on tumor therapy. The conversion of the M2 to M1 phenotype promotes tumor therapy and acts as an implicit mediator of abscopal effects (119).

At the same time, however, it was found that RT-induced immunomodulatory effects are a double-edged sword. To some extent, radiotherapy also promotes immunosuppressive effects, as demonstrated by increased recruitment of MDSC, Treg and anti-inflammatory macrophages (M2 macrophages) (120). There is a balance between immunosuppression and immunostimulation. Without intervention, the function of CD8+ T cells is not sufficient to completely eradicate residual tumor cells under this balance, causing tumor recurrence and limiting the therapeutic effect of local radiotherapy. Many research results have demonstrated that the addition of immune checkpoint inhibitors can break this balance and optimize the superiority of CD8+ in anti-tumor (121).

Immunotherapy also promotes the abscopal effects of radiotherapy. Several cases have confirmed that radiotherapy

combined with anti-PD-1/PD-L1 is effective in controlling the development of tumors outside the radiation field. (Figure 2) Although it has been extensively studied, the specific mechanism of radiation-induced distant abscopal effect (RIAE) still needs further demonstration (114).

In CRC, although immunotherapy has shown some benefit in patients with the MSI-H/dMMR phenotype, the benefit is modest in the larger proportion of patients with MSS/pMMR phenotype. However, several recent studies have shown that radiotherapy combined with immunotherapy may improve the efficacy of immunotherapy as a viable and safe option for patients with MSS/pMMR phenotype. For example, a phase II clinical trial demonstrated that patients with MSS/pMMR rectal cancer treated with a combination of PD-1 inhibitors and nCRT demonstrated positive cCR rates and good tolerability (122). It is worth mentioning that the abscopal effect produced by radiotherapy combined with immunotherapy has also shown a through positive effect in the treatment of patients with colorectal cancer liver metastases (123).

Although positive and safe efficacy has been observed in a variety of solid tumors, clinical studies on radiotherapy-ablative combination therapy for CRC are still relatively few and the results of valuable studies are scarce, so further animal studies and clinical trials are needed to demonstrate the feasibility and safety of radiotherapy-ablative combination therapy for CRC patients, especially for MSS/pMMR phenotype who are not sensitive to immunotherapy and safety (Table 2).

5.1 Advantages of CRC radioimmunotherapy

For CRC patients, surgical treatment is ineffective in treating distant metastases and requires artificial fistulas, which are risky to metastases and recurrence. There is a consensus that combined radiotherapy and immunotherapy can improve the chance of distant septal effects, and its clinical effect on eliminating metastatic tumors in patients is remarkable, which improves the recurrence rate and quality of survival. Preclinical studies have shown that after isolated radiotherapy, IFN-γ produced by CD8+ T cells mediates the upregulation of PD-L1 on tumor cells and induces local antitumor response. Radiotherapy itself cannot maintain long-term antitumor immunity, while the immune limitation by radiotherapy can be alleviated by blocking the PD-1/PD-L1 axis (130). On the other hand, the presence of immunosuppressive cells such as Tregs, myeloid-derived suppressor cells (MDSC) and anti-inflammatory macrophages in TME will provoke resistance to anti-PD-1/PD-L1 therapy (131). Radiation therapy can kill cancer cells while triggering the release of pro-inflammatory mediators and increasing tumor-infiltrating immune cells, in other words, transforming immune "cold" tumors into "hot" ones, thus enhancing the efficacy of immunotherapy and improving the side effects and resistance of immunotherapy through the development of combination therapy regimens, and broadening the limits of immunotherapy.

5.2 Methods to enhance the efficacy of CRC radioimmunotherapy

Anti-PD-1/PD-L1 drugs are useful when cancer cells or Treg release large amounts of PD-1. Treg upregulation of PD-1 is in response to more infiltration and proliferation of NK cells and CTL. This may start a few hours after stereotactic body radiation therapy (SBRT). However, it has been reported that peak upregulation

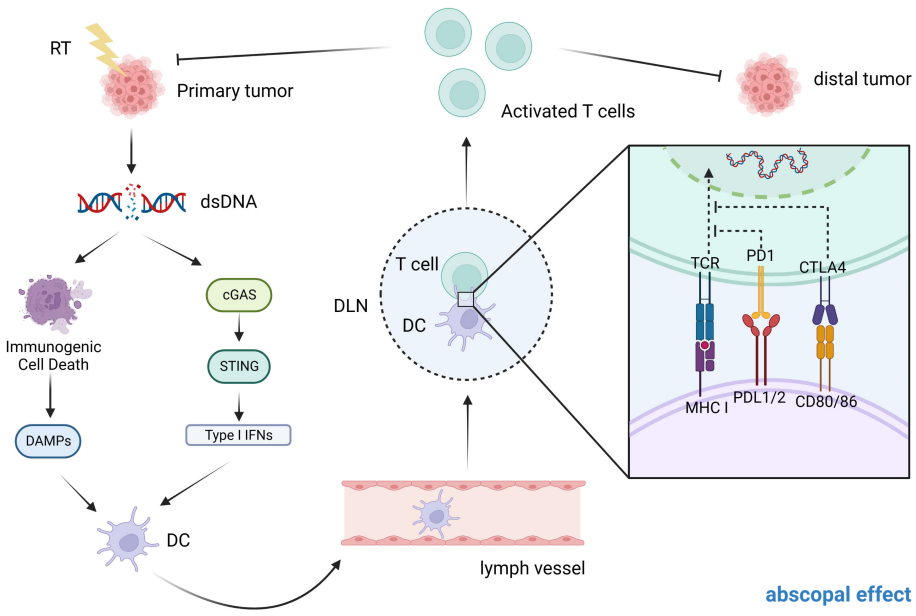

FIGURE 2
Possible mechanism of abscopal effect in CRC patients. After exposure to ionizing radiation, the primary tumor may undergo dsDNA breaks and this will cause a number of reactions. On the one hand, it can cause immunogenic cell death, which in turn releases DAMPs. On the other hand, dsDNA breaks activate the cGAS-STING signaling pathway, releasing type I IFN. Both of these results lead to the activation of DCs, which in turn activate CD8+ T cells (by presenting tumor antigens released from dying tumor cells) to mediate a specific anti-tumor immune response. In patients with metastatic tumors, when one tumor is irradiated, both of these modes can activate T cell activation and migration through the circulatory system to distant sites to induce the abscopal effect.

TABLE 2 Current clinical trials on combination therapy in CRC patients.

Clinicaltrials. gov. identifier	Type of trial	Status	immunology	radiotherapy	Primary outcome/ endpoint	Reference
NCT02888743	phase II	Active,not recruiting (2017/06-2022/11)	Durvalumab Tremelimumab	radiotherapy	Overall response rate	(124)
NCT04124601	phase II	Recruiting 2020/06- 2023/05)	Ipilimumab Nivolumab	Chemoradiotherapy	adverse events	(125)
NCT05215379	Phase II phase III	Recruiting (2022/10-2023/04)	xintilimab (injection)	neoadjuvant chemoradiation therapy	cCR	(122)
NCT04892498	phase II	Recruiting (2021/05-2023/08)	PD-1 inhibitor	Hypofractionated radiotherapy	PFS	(126)
NCT04304209	Phase II phase III	Recruiting (2019/10-2021/10)	Sintilimab	radiotherapy	pCR	(127)
NCT03503630	phase II	Active, not recruiting (2018/07-2024/01)	COMPOUND 2055269	radiotherapy	pCR	(128)
NCT04109755	phase II	Recruiting (2020/06-2022/06)	Pembrolizumab	SCRT	TRG	(128)
NCT03104439	phase II	Recruiting (2017/05-2024/07)	Nivolumab Ipilimumab	radiotherapy	CR PR SD	(129)
NCT03101475	phase II	Completed (2018/11-2022/02)	Durvalumab (MEDI4736) Tremelimumab	SBRT	iBOR	(129)
NCT02888743	phase II	Active, not recruiting (2017/06-202212)	Durvalumab Tremelimumab	radiotherapy	Overall response rate	(129)
NCT02437071	phase II	Active, not recruiting (2015/04-2023/04)	Pembrolizumab	radiotherapy	response rate	(129)

of PD-1 can occur a few days after tumor irradiation, after which PD-1 expression decreases. This response suggested that anti-pd-1 should be started as soon as possible during SBRT and continue for a few days (or possibly longer) after radiotherapy. Anti-CTLA-4 is useful both before and after SBRT; use of anti-CTLA-4 can reduce the effect of Treg on CTL, so that administration before radiotherapy increases immunogenicity, while administration after radiotherapy attenuates the depletion of antitumor immunity (132). The regulation of immune checkpoints such as PD-1, CTLA-4, TIM-3 and TIGIT is highly dependent on tumor type. Therefore, it is necessary to consider tumor genetic factors when selecting the optimal targets and to study their temporal response to SBRT.

Among the different radiotherapy techniques, SBRT is the best choice for inducing abscopal effects (133). Because it induces abscopal effects and has minimal stimulatory effects on tumor-promoting cells including M2 macrophages, Treg and MDSCs. Immune checkpoint inhibitors (ICI) have high efficacy in metastatic colorectal cancer (mCRC) with microsatellite instability (MSI), but are ineffective in microsatellite stable (MSS) tumors due to low tumor mutational load. Selective internal radiation therapy (SIRT) enhances neoantigen production, which triggers a systemic antitumor immune response (i.e. abscopal effect) (134).

The detailed mechanism of the distal effect induced by the combination treatment is not yet clear. Consequently, treatment protocols should be context-specific to maximize efficacy (114). Clinically, radiotherapy is being explored in combination with a plethora of immune-based therapies to optimize anti-tumor immunity (135). Enhanced type I IFN production, cGAS-STING signaling activation or the use of IR in combination with several other therapies can enhance anti-tumor immune responses (136).

As the study progressed, the combination of RT with anti-CTLA-4 and anti-PD-1/PD-L1 is used to achieve optimal therapeutic results. Researchers constructed three mouse models of metastatic tumors in melanoma, breast cancer and pancreatic cancer. The results showed

that anti-CTLA-4 initiated inhibition of Treg cells to expand the CD8/Treg ratio, and anti-PD-1/PD-L1 mainly increased the proportion of CD8+ TIL, but higher responses were obtained only with the involvement of RT, which diversified the T-cell receptor (TCR) of unirradiated tumor TIL (137).

Nanomedicine adjuvant technology introduces nanomedicines with optimized design to ameliorate the problem of low response rate and toxicity of cancer radioimmunotherapy, which are prepared by incorporating tumor antigens, immune or radioimodulators or biomarker-specific imaging agents into the corresponding optimized nanopreparations. This will help induce various biological effects such as generating *in situ* vaccination, promoting immunogenic cell death, overcoming radioresistance, reversing immunosuppression, and pre-stratifying patients and assessing treatment response or treatment-induced toxicity (138).

Since intestinal flora plays an important role in CRC tumor development and has some similar mechanisms and pathways of action as radiotherapy and immunotherapy. Thus, we will focus on the role of intestinal flora in the radiotherapy of CRC patients as follows.

5.3 Possibility of microbiota to improve the efficacy of radioimmunotherapy in CRC

The current cumulative evidence from CRC patients and animal studies has demonstrated a strong association between the gut microbiota and CRC. Enrichment of oncogenic flora not only elicits highly heterogeneous proliferation to form CRC, but also promotes tumor metastasis and drug resistance (139). Remarkably, gut microbiota can modulate both non-specific and specific immune functions in the body, which in turn affects tumor development as well as anti-tumor immune function. Bacteria can promote the transfer and cross-presentation of processed tumor antigen peptides in DC cells, reduce the frequency of CD4+CD25+ Treg cells and collectively promote T cell immunity (140). Bacterial constituents may also influence immunotherapy in CRC. For example, LPS is an outer membrane component of gram negative bacteria with abundant hydroxyl groups and some amide groups. Low doses of LPS are expected to be ideal stimulants for immune initiation (141). Furthermore, it has been demonstrated that there is a bi-directional interaction between the intestinal microbiota and radiotherapy. The gut microbiota can affect the anti-cancer clinical efficacy of radiotherapy, whilst ionizing radiation can alter the components and functions of the intestinal microbiota, which can lead to the development of radiation enteropathy. A potential mechanism for the abscopal effect-cGAS-STING signaling pathway can also be stimulated by the immunogenicity of microflora. Some reports suggest that bacterial DNA can activate the cGAS-STING pathway and upregulate type I interferon, which is a key cytokine for innate and adaptive immunity, resulting in an adjuvant anti-tumor immune response (142, 143). The above prompts us to speculate what role intestinal flora plays in radiotherapy, immunotherapy and radioimmunotherapy in CRC patients.

We speculate that there are two possible scenarios when gut microbiota are involved in combined radiation and immunotherapy and produce benefits: ① The gut microflora may be a bridge between radiotherapy and immunotherapy. Ionizing radiation causes changes in the environment in which the microbiota is located, which in turn promotes anti-tumor immunity and enhances the effects of immunotherapy. This suggests that the microbiota may act as a target for enhancing radioimmunotherapy. ② Although the gut microbiota is not a bridge, the outcome of microbiota therapy to enhance the efficacy of radiotherapy and immunotherapy is easy to guess due to the respective relevance of the microbiota to radiotherapy and immunotherapy. It may happen that modulation of the microbiota increases the efficacy of both radiotherapy and immunotherapy or only one of them. Furthermore, as the toxicities associated with radiation and immunotherapy are also important in the prognosis of CRC patients, modulating the microbiota is also expected to reduce the toxicities of both or either. In conclusion, the general principle is to improve both patient outcomes and prognosis, as well as to focus on prognostic quality of life.

Therapies for CRC targeting microbiota are constantly being updated and developed, including selective elimination of oncogenic microorganisms, lipopolysaccharide-promoted immunotherapy and targeted phage therapy (144). In addition to therapies targeting the intestinal microbiota itself, we observe that anti-tumor therapies mediated by bacteria as vectors have captured widespread attention because of their natural tumor-targeting ability and multiple immune-activating properties. For instance: due to its unique anaerobic properties, attenuated Salmonella typhimurium exhibits inherent tumor-specific colonization with little retention in normal organs and good biosafety (145). Today, the majority of CRC patients are of the pMMR/MSS phenotype who usually fail to receive satisfactory results after ICB therapy. It is a pity that the current general response rate to clinical immunotherapy is still low (20-30%) (146). Surprisingly, a recent study found a significant increase in PD-L1 expression in distal tumors treated with ^{131}I-VNP, which may be related to the production of ev (i.e. extracellular vesicles, which play an important role in various intercellular communication processes) and stimulation of increased interferon by tumor cells after effective IRT. This implies that the immune checkpoint inhibitor αPD-L1, when promptly administered, may improve the immune response rate and produce a better immunotherapeutic effect on the immune response rate of ^{131}I-VNP treatment. Moreover, the ^{131}I-labeled attenuated Salmonella vector can also utilize the strong cytophilic activity of bacteria to eliminate primary tumors, and the DNA fragments produced by bacteria and IRT activate the cGAS-STING pathway to produce a large number of anti-tumor cytokines, providing an anti-tumor immune response for innate immunity. Also, tumor-associated antigens produced by the bacterial vector itself and ^{131}I-VNP can significantly promote the maturation of DC cells, providing a basis for activating an adaptive anti-tumor immune response (147). Beyond the above strengths, compared with small nanomaterials, radiolabeled bacteria can be effectively retained at the tumor site for a long time, which can prevent tumor recurrence by inducing long-term immune memory effects, so as to achieve efficient IRT, reduce tumor recurrence rate and improve the quality of patient survival.

Besides, by studying the mechanism of gut microbiota in the development of CRC, we can also develop new anti-tumor targets and provide new ideas for new cancer treatment methods (148).

6 Summary and prospect

According to the above studies and discussions, we conjecture that based on the special role and close association of intestinal flora in the development of CRC, microbiota may act as a bridge to delicately connect radiotherapy and immunotherapy. Microbiota might act as an immunostimulant or immunomodulator to target the immune system of patients and thus influence the efficacy of immunotherapy, radiotherapy and their combination therapy. In particular, based on the fact that modulation of gut microbiota, such as FMT, possibly leads to a reduction in the incidence and severity of radiation enteritis and immune-related adverse events, gut microbiota may also be a common biological target for reducing the side effects of radioimmunotherapy, and how inhibition of this target to improve efficacy would also provide a positive direction for CRC patients to attain a longer survival and a higher quality of life after treatment. The above conjectures provide enlightening ideas for radioimmunotherapy mediated by bacterial pleiotropic immune activation functions. Novel interventions focusing on microbiota, such as bacterial engineering, next-generation probiotics, microbial-specific bactericidal antibiotics and fecal microbiota transplantation as monotherapies or add-on therapies, are promising for improving the efficacy of radioimmunotherapy.

Transforming conjecture into reality requires answering numerous outstanding questions, including the detailed mechanisms by which the microbiota modulates CRC and its associated therapies and requires insight into how the microbiota mediates the tumor microenvironment - either through direct effects on DNA damage and inflammation, or through other host-derived mechanisms. Fortunately, technological advances have provided us with revised tools to study the microbiota in the context of the growing number of physiological CRC model systems to decipher the challenging complexity of the colonic tumor microenvironment. We look forward to more breakthroughs in CRC genomics, metabolomics and immunology and hope that more experimental studies and clinical trials will follow to confirm these suspicions.

Author contributions

HY, RG, ZW, FF and HZ all contributed to the writing and editing of the manuscript. All authors contributed to the article and approved the submitted version.

Funding

This work was supported by the National Natural Science of Foundation of China (82102096); Science and technology Development Plan of Jilin (20210402026GH); Key Laboratory of Metrology and calibration technology (JLKG2021001C004).

Conflict of interest

The authors declare that the research was conducted in the absence of any commercial or financial relationships that could be construed as a potential conflict of interest.

Publisher's note

References

1. Siegel RL, Miller KD, Jemal A. Cancer statistics, 2019. *CA Cancer J Clin* (2019) 69 (1):7–34. doi: 10.3322/caac.21551

2. Siegel RL, Miller KD, Fuchs HE, Jemal A. Cancer statistics, 2022. *CA Cancer J Clin* (2022) 72(1):7–33. doi: 10.3322/caac.21708

3. Tan S, Li D, Zhu X. Cancer immunotherapy: Pros, cons and beyond. *BioMed Pharmacother* (2020) 124:109821. doi: 10.1016/j.biopha.2020.109821

4. Liu NN, Jiao N, Tan JC, Wang Z, Wu D, Wang AJ, et al. Multi-kingdom microbiota analyses identify bacterial-fungal interactions and biomarkers of colorectal cancer across cohorts. *Nat Microbiol* (2022) 7(2):238–50. doi: 10.1038/s41564-021-01030-7

5. Wirbel J, Pyl PT, Kartal E, Zych K, Kashani A, Milanese A, et al. Meta-analysis of fecal metagenomes reveals global microbial signatures that are specific for colorectal cancer. *Nat Med* (2019) 25(4):679–89. doi: 10.1038/s41591-019-0406-6

6. Thomas AM, Manghi P, Asnicar F, Pasolli E, Armanini F, Zolfo M, et al. Metagenomic analysis of colorectal cancer datasets identifies cross-cohort microbial diagnostic signatures and a link with choline degradation. *Nat Med* (2019) 25(4):667–78. doi: 10.1038/s41591-019-0405-7

7. Dai Z, Coker OO, Nakatsu G, Wu WKK, Zhao L, Chen Z, et al. Multi-cohort analysis of colorectal cancer metagenome identified altered bacteria across populations and universal bacterial markers. *Microbiome* (2018) 6(1):70. doi: 10.1186/s40168-018-0451-2

8. Avuthu N, Guda C. Meta-analysis of altered gut microbiota reveals microbial and metabolic biomarkers for colorectal cancer. *Microbiol Spectr* (2022) 10(4):e0001322. doi: 10.1128/spectrum.00013-22

9. Shuwen H, Yinhang W, Xingming Z, Jing Z, Jinxin L, Wei W, et al. Using whole-genome sequencing (Wgs) to plot colorectal cancer-related gut microbiota in a population with varied geography. *Gut Pathog* (2022) 14(1):50. doi: 10.1186/s13099-022-00524-x

10. Loftus M, Hassouneh SA, Yooseph S. Bacterial community structure alterations within the colorectal cancer gut microbiome. *BMC Microbiol* (2021) 21(1):98. doi: 10.1186/s12866-021-02153-x

11. Coker OO, Liu C, Wu WKK, Wong SH, Jia W, Sung JJY, et al. Altered gut metabolites and microbiota interactions are implicated in colorectal carcinogenesis and can be non-invasive diagnostic biomarkers. *Microbiome* (2022) 10(1):35. doi: 10.1186/s40168-021-01208-5

12. Balamurugan R, Rajendiran E, George S, Samuel GV, Ramakrishna BS. Real-time polymerase chain reaction quantification of specific butyrate-producing bacteria, desulfovibrio and enterococcus faecalis in the feces of patients with colorectal cancer. *J Gastroenterol Hepatol* (2008) 23(8 Pt 1):1298–303. doi: 10.1111/j.1440-1746.2008.05490.x

13. Gao R, Wu C, Zhu Y, Kong C, Zhu Y, Gao Y, et al. Integrated analysis of colorectal cancer reveals cross-cohort gut microbial signatures and associated serum metabolites. *Gastroenterology* (2022) 163(4):1024–37.e9. doi: 10.1053/j.gastro.2022.06.069

14. Osman MA, Neoh HM, Ab Mutalib NS, Chin SF, Mazlan L, Raja Ali RA, et al. Parvimonas micra, peptostreptococcus stomatis, fusobacterium nucleatum and akkermansia muciniphila as a four-bacteria biomarker panel of colorectal cancer. *Sci Rep* (2021) 11(1):2925. doi: 10.1038/s41598-021-82465-0

15. Du X, Li Q, Tang Z, Yan L, Zhang L, Zheng Q, et al. Alterations of the gut microbiome and fecal metabolome in colorectal cancer: Implication of intestinal

metabolism for tumorigenesis. *Front Physiol* (2022) 13:854545. doi: 10.3389/fphys.2022.854545

16. Quaglio AEV, Grillo TG, De Oliveira ECS, Di Stasi LC, Sassaki LY. Gut microbiota, inflammatory bowel disease and colorectal cancer. *World J Gastroenterol* (2022) 28 (30):4053–60. doi: 10.3748/wjg.v28.i30.4053

17. Tilg H, Adolph TE, Gerner RR, Moschen AR. The intestinal microbiota in colorectal cancer. *Cancer Cell* (2018) 33(6):954–64. doi: 10.1016/j.ccell.2018.03.004

18. Chung L, Orberg ET, Geis AL, Chan JL, Fu K, DeStefano Shields CE, et al. Bacteroides fragilis toxin coordinates a pro-carcinogenic inflammatory cascade *Via* targeting of colonic epithelial cells. *Cell Host Microbe* (2018) 23(3):421. doi: 10.1016/j.chom.2018.02.004

19. Long X, Wong CC, Tong L, Chu ESH, Ho Szeto C, Go MYY, et al. Peptostreptococcus anaerobius promotes colorectal carcinogenesis and modulates tumour immunity. *Nat Microbiol* (2019) 4(12):2319–30. doi: 10.1038/s41564-019-0541-3

20. Zhao L, Zhang X, Zhou Y, Fu K, Lau HC, Chun TW, et al. Parvimonas micra promotes colorectal tumorigenesis and is associated with prognosis of colorectal cancer patients. *Oncogene* (2022) 41(36):4200–10. doi: 10.1038/s41388-022-02395-7

21. Sugimura N, Li Q, Chu ESH, Lau HCH, Fong W, Liu W, et al. Lactobacillus gallinarum modulates the gut microbiota and produces anti-cancer metabolites to protect against colorectal tumourigenesis. *Gut* (2021) 71(10):2011–21. doi: 10.1136/gutjnl-2020-323951

22. Li Q, Hu W, Liu WX, Zhao LY, Huang D, Liu XD, et al. Streptococcus thermophilus inhibits colorectal tumorigenesis through secreting B-galactosidase. *Gastroenterology* (2021) 160(4):1179–93.e14. doi: 10.1053/j.gastro.2020.09.003

23. Gomes S, Teixeira-Guedes C, Silva E, Baltazar F, Preto A. Colon microbiota modulation by dairy-derived diet: New strategy for prevention and treatment of colorectal cancer. *Food Funct* (2022) 13(18):9183–94. doi: 10.1039/d2fo01720b

24. Cao Y, Oh J, Xue M, Huh WJ, Wang J, Gonzalez-Hernandez JA, et al. Commensal microbiota from patients with inflammatory bowel disease produce genotoxic metabolites. *Science* (2022) 378(6618):eabm3233. doi: 10.1126/science.abm3233

25. Cao Y, Wang Z, Yan Y, Ji L, He J, Xuan B, et al. Enterotoxigenic bacteroidesfragilis promotes intestinal inflammation and malignancy by inhibiting exosome-packaged mir-149-3p. *Gastroenterology* (2021) 161(5):1552–66.e12. doi: 10.1053/j.gastro.2021.08.003

26. Salesse L, Lucas C, Hoang MHT, Sauvanet P, Rezard A, Rosenstiel P, et al. Colibactin-producing escherichia coli induce the formation of invasive carcinomas in a chronic inflammation-associated mouse model. *Cancers (Basel)* (2021) 13(9):2060. doi: 10.3390/cancers13092060

27. Wang Y, Li H. Gut microbiota modulation: A tool for the management of colorectal cancer. *J Transl Med* (2022) 20(1):178. doi: 10.1186/s12967-022-03378-8

28. Sanders ME, Merenstein DJ, Reid G, Gibson GR, Rastall RA. Probiotics and prebiotics in intestinal health and disease: From biology to the clinic. *Nat Rev Gastroenterol Hepatol* (2019) 16(10):605–16. doi: 10.1038/s41575-019-0173-3

29. Lucas C, Salesse L, Hoang MHT, Bonnet M, Sauvanet P, Larabi A, et al. Autophagy of intestinal epithelial cells inhibits colorectal carcinogenesis induced by colibactin-producing escherichia coli in Apc(Min/+) mice. *Gastroenterology* (2020) 158(5):1373–88. doi: 10.1053/j.gastro.2019.12.026

30. Cai F, Sorg O, Granci V, Lecumberri E, Miralbell R, Dupertuis YM, et al. Interaction of Ω-3 polyunsaturated fatty acids with radiation therapy in two different colorectal cancer cell lines. *Clin Nutr* (2014) 33(1):164–70. doi: 10.1016/j.clnu.2013.04.005

31. Hou H, Chen D, Zhang K, Zhang W, Liu T, Wang S, et al. Gut microbiota-derived short-chain fatty acids and colorectal cancer: Ready for clinical translation? *Cancer Lett* (2022) 526:225–35. doi: 10.1016/j.canlet.2021.11.027

32. Mizuno R, Kawada K, Itatani Y, Ogawa R, Kiyasu Y, Sakai Y. The role of tumor-associated neutrophils in colorectal cancer. *Int J Mol Sci* (2019) 20(3):529. doi: 10.3390/ijms20030529

33. Germann M, Zangger N, Sauvain MO, Sempoux C, Bowler AD, Wirapati P, et al. Neutrophils suppress tumor-infiltrating T cells in colon cancer *Via* matrix metalloproteinase-mediated activation of tgfβ. *EMBO Mol Med* (2020) 12(1):e10681. doi: 10.15252/emmm.201910681

34. Yang Z, Zhang M, Peng R, Liu J, Wang F, Li Y, et al. The prognostic and clinicopathological value of tumor-associated macrophages in patients with colorectal cancer: A systematic review and meta-analysis. *Int J Colorectal Dis* (2020) 35(9):1651–61. doi: 10.1007/s00384-020-03686-9

35. Cuff AO, Sillito F, Dertschnig S, Hall A, Luong TV, Chakraverty R, et al. The obese liver environment mediates conversion of nk cells to a less cytotoxic Ilc1-like phenotype. *Front Immunol* (2019) 10:2180. doi: 10.3389/fimmu.2019.02180

36. Qi J, Crinier A, Escalière B, Ye Y, Wang Z, Zhang T, et al. Single-cell transcriptomic landscape reveals tumor specific innate lymphoid cells associated with colorectal cancer progression. *Cell Rep Med* (2021) 2(8):100353. doi: 10.1016/j.xcrm.2021.100353

37. Kaur H, Ali SA. Probiotics and gut microbiota: Mechanistic insights into gut immune homeostasis through tlr pathway regulation. *Food Funct* (2022) 13(14):7423–47. doi: 10.1039/d2fo00911k

38. Yue B, Luo X, Yu Z, Mani S, Wang Z, Dou W. Inflammatory bowel disease: A potential result from the collusion between gut microbiota and mucosal immune system. *Microorganisms* (2019) 7(10):440. doi: 10.3390/microorganisms7100440

39. Jakubczyk D, Leszczyńska K, Górska S. The effectiveness of probiotics in the treatment of inflammatory bowel disease (Ibd)-a critical review. *Nutrients* (2020) 12 (7):1973. doi: 10.3390/nu12071973

40. Aximujiang K, Kaheman K, Wushouer X, Wu G, Ahemaiti A, Yunusi K. Lactobacillus acidophilus and hkl suspension alleviates ulcerative colitis in rats by regulating gut microbiota, suppressing Tlr9, and promoting metabolism. *Front Pharmacol* (2022) 13:859628. doi: 10.3389/fphar.2022.859628

41. Duan T, Du Y, Xing C, Wang HY, Wang RF. Toll-like receptor signaling and its role in cell-mediated immunity. *Front Immunol* (2022) 13:812774. doi: 10.3389/fimmu.2022.812774

42. Mutala LB, Deleine C, Karakachoff M, Dansette D, Ducoin K, Oger R, et al. The caspase-1/Il-18 axis of the inflammasome in tumor cells: A modulator of the Th1/Tc1 response of tumor-infiltrating T lymphocytes in colorectal cancer. *Cancers (Basel)* (2021) 13(2):189. doi: 10.3390/cancers13020189

43. Hu Y, Zhao J, Shen Y, Zhang C, Xia Q, Zhang G, et al. Predictive value of tumor-infiltrating lymphocytes detected by flow cytometry in colorectal cancer. *Int Immunopharmacol* (2022) 113(Pt A):109286. doi: 10.1016/j.intimp.2022.109286

44. Nakagami Y, Hazama S, Suzuki N, Yoshida S, Tomochika S, Matsui H, et al. Cd4 and Foxp3 as predictive markers for the recurrence of T3/T4a stage ii colorectal cancer: Applying a novel discrete bayes decision rule. *BMC Cancer* (2022) 22(1):1071. doi: 10.1186/s12885-022-10181-7

45. Wang D, Yu W, Lian J, Wu Q, Liu S, Yang L, et al. Th17 cells inhibit Cd8(+) T cell migration by systematically downregulating Cxcr3 expression *Via* il-17a/Stat3 in advanced-stage colorectal cancer patients. *J Hematol Oncol* (2020) 13(1):68. doi: 10.1186/s13045-020-00897-z

46. Xing C, Du Y, Duan T, Nim K, Chu J, Wang HY, et al. Interaction between microbiota and immunity and its implication in colorectal cancer. *Front Immunol* (2022) 13:963819. doi: 10.3389/fimmu.2022.963819

47. Yoo JY, Groer M, Dutra SVO, Sarkar A, McSkimming DI. Gut microbiota and immune system interactions. *Microorganisms* (2020) 8(10):1587. doi: 10.3390/microorganisms8101587

48. Rogala AR, Oka A, Sartor RB. Strategies to dissect host-microbial immune interactions that determine mucosal homeostasis vs. *Intestinal Inflammation Gnotobiotic Mice. Front Immunol* (2020) 11:214. doi: 10.3389/fimmu.2020.00214

49. Korman AJ, Garrett-Thomson SC, Lonberg N. The foundations of immune checkpoint blockade and the ipilimumab approval decennial. *Nat Rev Drug Discovery* (2022) 21(7):509–28. doi: 10.1038/s41573-021-00345-8

50. Samstein RM, Lee CH, Shoushtari AN, Hellmann MD, Shen R, Janjigian YY, et al. Tumor mutational load predicts survival after immunotherapy across multiple cancer types. *Nat Genet* (2019) 51(2):202–6. doi: 10.1038/s41588-018-0312-8

51. Shia J. The diversity of tumours with microsatellite instability: Molecular mechanisms and impact upon microsatellite instability testing and mismatch repair protein immunohistochemistry. *Histopathology* (2021) 78(4):485–97. doi: 10.1111/his.14271

52. Shan J, Han D, Shen C, Lei Q, Zhang Y. Mechanism and strategies of immunotherapy resistance in colorectal cancer. *Front Immunol* (2022) 13:1016646. doi: 10.3389/fimmu.2022.1016646

53. Yuan J, Li J, Gao C, Jiang C, Xiang Z, Wu J. Immunotherapies catering to the unmet medical need of cold colorectal cancer. *Front Immunol* (2022) 13:1022190. doi: 10.3389/fimmu.2022.1022190

54. Li Y, Du Y, Xue C, Wu P, Du N, Zhu G, et al. Efficacy and safety of anti-Pd-1/Pd-L1 therapy in the treatment of advanced colorectal cancer: A meta-analysis. *BMC Gastroenterol* (2022) 22(1):431. doi: 10.1186/s12876-022-02511-7

55. Yao YC, Jin Y, Lei XF, Wang ZX, Zhang DS, Wang FH, et al. Impact of mismatch repair or microsatellite status on the prognosis and efficacy to chemotherapy in metastatic colorectal cancer patients: A bi-institutional, propensity score-matched study. *J Cancer* (2022) 13(9):2912–21. doi: 10.7150/jca.50285

56. Peng Z, Cheng S, Kou Y, Wang Z, Jin R, Hu H, et al. The gut microbiome is associated with clinical response to anti-Pd-1/Pd-L1 immunotherapy in gastrointestinal cancer. *Cancer Immunol Res* (2020) 8(10):1251–61. doi: 10.1158/2326-6066.Cir-19-1014

57. Roberti MP, Yonekura S, Duong CPM, Picard M, Ferrere G, Tidjani Alou M, et al. Chemotherapy-induced ileal crypt apoptosis and the ileal microbiome shape immunosurveillance and prognosis of proximal colon cancer. *Nat Med* (2020) 26 (6):919–31. doi: 10.1038/s41591-020-0882-8

58. Griffin ME, Espinosa J, Becker JL, Luo JD, Carroll TS, Jha JK, et al. Enterococcus peptidoglycan remodeling promotes checkpoint inhibitor cancer immunotherapy. *Science* (2021) 373(6558):1040–6. doi: 10.1126/science.abc9113

59. Zhuo Q, Yu B, Zhou J, Zhang J, Zhang R, Xie J, et al. Lysates of lactobacillus acidophilus combined with ctla-4-Blocking antibodies enhance antitumor immunity in a mouse colon cancer model. *Sci Rep* (2019) 9(1):20128. doi: 10.1038/s41598-019-56661-y

60. Sakai K, Sakurai T, De Velasco MA, Nagai T, Chikugo T, Ueshima K, et al. Intestinal microbiota and gene expression reveal similarity and dissimilarity between immune-mediated colitis and ulcerative colitis. *Front Oncol* (2021) 11:763468. doi: 10.3389/fonc.2021.763468

61. Lam KC, Araya RE, Huang A, Chen Q, Di Modica M, Rodrigues RR, et al. Microbiota triggers sting-type I ifn-dependent monocyte reprogramming of the tumor microenvironment. *Cell* (2021) 184(21):5338–56.e21. doi: 10.1016/j.cell.2021.09.019

62. Rizvi ZA, Dalal R, Sadhu S, Kumar Y, Kumar S, Gupta SK, et al. High-salt diet mediates interplay between nk cells and gut microbiota to induce potent tumor immunity. *Sci Adv* (2021) 7(37):eabg5016. doi: 10.1126/sciadv.abg5016

63. Tanoue T, Morita S, Plichta DR, Skelly AN, Suda W, Sugiura Y, et al. A defined commensal consortium elicits Cd8 T cells and anti-cancer immunity. *Nature* (2019) 565 (7741):600–5. doi: 10.1038/s41586-019-0878-z

64. Baruch EN, Youngster I, Ben-Betzalel G, Ortenberg R, Lahat A, Katz L, et al. Fecal microbiota transplant promotes response in immunotherapy-refractory melanoma patients. *Science* (2021) 371(6529):602–9. doi: 10.1126/science.abb5920

65. Zhang L, Jiang L, Yu L, Li Q, Tian X, He J, et al. Inhibition of Uba6 by inosine augments tumour immunogenicity and responses. *Nat Commun* (2022) 13(1):5413. doi: 10.1038/s41467-022-33116-z

66. Lu Y, Yuan X, Wang M, He Z, Li H, Wang J, et al. Gut microbiota influence immunotherapy responses: Mechanisms and therapeutic strategies. *J Hematol Oncol* (2022) 15(1):47. doi: 10.1186/s13045-022-01273-9

67. Nomura M, Nagatomo R, Doi K, Shimizu J, Baba K, Saito T, et al. Association of short-chain fatty acids in the gut microbiome with clinical response to treatment with nivolumab or pembrolizumab in patients with solid cancer tumors. *JAMA Netw Open* (2020) 3(4):e202895. doi: 10.1001/jamanetworkopen.2020.2895

68. Luu M, Riester Z, Baldrich A, Reichardt N, Yuille S, Busetti A, et al. Microbial short-chain fatty acids modulate Cd8(+) T cell responses and improve adoptive immunotherapy for cancer. *Nat Commun* (2021) 12(1):4077. doi: 10.1038/s41467-021-24331-1

69. Zhang J, Dai Z, Yan C, Zhang W, Wang D, Tang D0. A new biological triangle in cancer: Intestinal microbiota, immune checkpoint inhibitors and antibiotics. *Clin Transl Oncol* (2021) 23(12):2415–30. doi: 10.1007/s12094-021-02659-w

70. Sivan A, Corrales L, Hubert N, Williams JB, Aquino-Michaels K, Earley ZM, et al. Commensal bifidobacterium promotes antitumor immunity and facilitates anti-Pd-L1 efficacy. *Science* (2015) 350(6264):1084–9. doi: 10.1126/science.aac4255

71. Routy B, Le Chatelier E, Derosa L, Duong CPM, Alou MT, Daillère R, et al. Gut microbiome influences efficacy of pd-1-Based immunotherapy against epithelial tumors. *Science* (2018) 359(6371):91–7. doi: 10.1126/science.aan3706

72. Xu H, Cao C, Ren Y, Weng S, Liu L, Guo C, et al. Antitumor effects of fecal microbiota transplantation: Implications for microbiome modulation in cancer treatment. *Front Immunol* (2022) 13:949490. doi: 10.3389/fimmu.2022.949490

73. Wang Z, Hua W, Li C, Chang H, Liu R, Ni Y, et al. Protective role of fecal microbiota transplantation on colitis and colitis-associated colon cancer in mice is associated with treg cells. *Front Microbiol* (2019) 10:2498. doi: 10.3389/fmicb.2019.02498

74. Liu X, Wang L, Jing N, Jiang G, Liu Z. Biostimulating gut microbiome with bilberry anthocyanin combo to enhance anti-Pd-L1 efficiency against murine colon cancer. *Microorganisms* (2020) 8(2):175. doi: 10.3390/microorganisms8020175

75. Owens JA, Saeedi BJ, Naudin CR, Hunter-Chang S, Barbian ME, Eboka RU, et al. Lactobacillus rhamnosus gg orchestrates an antitumor immune response. *Cell Mol Gastroenterol Hepatol* (2021) 12(4):1311–27. doi: 10.1016/j.jcmgh.2021.06.001

76. Spencer CN, McQuade JL, Gopalakrishnan V, McCulloch JA, Vetizou M, Cogdill AP, et al. Dietary fiber and probiotics influence the gut microbiome and melanoma immunotherapy response. *Science* (2021) 374(6575):1632–40. doi: 10.1126/science.aaz7015

77. Wang T, Zheng N, Luo Q, Jiang L, He B, Yuan X, et al. Probiotics lactobacillus reuteri abrogates immune checkpoint blockade-associated colitis by inhibiting group 3 innate lymphoid cells. *Front Immunol* (2019) 10:1235. doi: 10.3389/fimmu.2019.01235

78. Buckley AM, Lynam-Lennon N, O'Neill H, O'Sullivan J. Targeting hallmarks of cancer to enhance radiosensitivity in gastrointestinal cancers. *Nat Rev Gastroenterol Hepatol* (2020) 17(5):298–313. doi: 10.1038/s41575-019-0247-2

79. Liu J, Liu C, Yue J. Radiotherapy and the gut microbiome: Facts and fiction. *Radiat Oncol* (2021) 16(1):9. doi: 10.1186/s13014-020-01735-9

80. Qu W, Zhang L, Ao J. Radiotherapy induces intestinal barrier dysfunction by inhibiting autophagy. *ACS Omega* (2020) 5(22):12955–63. doi: 10.1021/acsomega.0c00706

81. Fernandes A, Oliveira A, Soares R, Barata P. The effects of ionizing radiation on gut microbiota, a systematic review. *Nutrients* (2021) 13(9):3025. doi: 10.3390/nu13093025

82. Poonacha KNT, Villa TG, Notario V. The interplay among radiation therapy, antibiotics and the microbiota: Impact on cancer treatment outcomes. *Antibiotics (Basel)* (2022) 11(3):331. doi: 10.3390/antibiotics11030331

83. El Alam MB, Sims TT, Kouzy R, Biegert GWG, Jaoude J, Karpinets TV, et al. A prospective study of the adaptive changes in the gut microbiome during standard-of-Care chemoradiotherapy for gynecologic cancers. *PloS One* (2021) 16(3):e0247905. doi: 10.1371/journal.pone.0247905

84. Gerassy-Vainberg S, Blatt A, Danin-Poleg Y, Gershovich K, Sabo E, Nevelsky A, et al. Radiation induces proinflammatory dysbiosis: Transmission of inflammatory susceptibility by host cytokine induction. *Gut* (2018) 67(1):97–107. doi: 10.1136/gutjnl-2017-313789

85. Plastiras A, Sideris M, Gaya A, Haji A, Nunoo-Mensah J, Haq A, et al. Waiting time following neoadjuvant chemoradiotherapy for rectal cancer: Does it really matter. *Gastrointest Tumors* (2018) 4(3-4):96–103. doi: 10.1159/000484982

86. Sakamoto Y, Tsujiguchi T, Ito K, Yamanouchi K. Determination of gut bacterial metabolites in radiation exposed mice. *Radiat Prot Dosimetry* (2019) 184(3-4):493–5. doi: 10.1093/rpd/ncz094

87. Park SY, Lee CJ, Choi JH, Kim JH, Kim JW, Kim JY, et al. The Jak2/Stat3/Ccnd2 axis promotes colorectal cancer stem cell persistence and radioresistance. *J Exp Clin Cancer Res* (2019) 38(1):399. doi: 10.1186/s13046-019-1405-7

88. Sims TT, El Alam MB, Karpinets TV, Dorta-Estremera S, Hegde VL, Nookala S, et al. Gut microbiome diversity is an independent predictor of survival in cervical cancer patients receiving chemoradiation. *Commun Biol* (2021) 4(1):237. doi: 10.1038/s42003-021-01741-x

89. Shiao SL, Kershaw KM, Limon JJ, You S, Yoon J, Ko EY, et al. Commensal bacteria and fungi differentially regulate tumor responses to radiation therapy. *Cancer Cell* (2021) 39(9):1202–13.e6. doi: 10.1016/j.ccell.2021.07.002

90. Uribe-Herranz M, Rafail S, Beghi S, Gil-de-Gómez L, Verginadis I, Bittinger K, et al. Gut microbiota modulate dendritic cell antigen presentation and radiotherapy-induced antitumor immune response. *J Clin Invest* (2020) 130(1):466–79. doi: 10.1172/jci124332

91. Yang K, Hou Y, Zhang Y, Liang H, Sharma A, Zheng W, et al. Suppression of local type I interferon by gut microbiota-derived butyrate impairs antitumor effects of ionizing radiation. *J Exp Med* (2021) 218(3):e20201915. doi: 10.1084/jem.20201915

92. Elkrief A, Derosa L, Kroemer G, Zitvogel L, Routy B. The negative impact of antibiotics on outcomes in cancer patients treated with immunotherapy: A new independent prognostic factor? *Ann Oncol* (2019) 30(10):1572–9. doi: 10.1093/annonc/mdz206

93. Klopp AH, Yeung AR, Deshmukh S, Gil KM, Wenzel L, Westin SN, et al. Patient-reported toxicity during pelvic intensity-modulated radiation therapy: Nrg oncology-rtog 1203. *J Clin Oncol* (2018) 36(24):2538–44. doi: 10.1200/jco.2017.77.4273

94. Roy S, Trinchieri G. Microbiota: A key orchestrator of cancer therapy. *Nat Rev Cancer* (2017) 17(5):271–85. doi: 10.1038/nrc.2017.13

95. Zhao TS, Xie LW, Cai S, Xu JY, Zhou H, Tang LF, et al. Dysbiosis of gut microbiota is associated with the progression of radiation-induced intestinal injury and is alleviated by oral compound probiotics in mouse model. *Front Cell Infect Microbiol* (2021) 11:717636. doi: 10.3389/fcimb.2021.717636

96. Shi W, Shen L, Zou W, Wang J, Yang J, Wang Y, et al. The gut microbiome is associated with therapeutic responses and toxicities of neoadjuvant chemoradiotherapy in rectal cancer patients-a pilot study. *Front Cell Infect Microbiol* (2020) 10:562463. doi: 10.3389/fcimb.2020.562463

97. Wang Z, Wang Q, Wang X, Zhu L, Chen J, Zhang B, et al. Gut microbial dysbiosis is associated with development and progression of radiation enteritis during pelvic radiotherapy. *J Cell Mol Med* (2019) 23(5):3747–56. doi: 10.1111/jcmm.14289

98. Wang L, Wang X, Zhang G, Ma Y, Zhang Q, Li Z, et al. The impact of pelvic radiotherapy on the gut microbiome and its role in radiation-induced diarrhoea: A systematic review. *Radiat Oncol* (2021) 16(1):187. doi: 10.1186/s13014-021-01899-y

99. Xiao HW, Cui M, Li Y, Dong JL, Zhang SQ, Zhu CC, et al. Gut microbiota-derived indole 3-propionic acid protects against radiation toxicity *Via* retaining acyl-Coa-Binding protein. *Microbiome* (2020) 8(1):69. doi: 10.1186/s40168-020-00845-6

100. Zheng YM, He XX, Xia HH, Yuan Y, Xie WR, Cai JY, et al. Multi-donor multi-course faecal microbiota transplantation relieves the symptoms of chronic hemorrhagic radiation proctitis: A case report. *Med (Baltimore)* (2020) 99(39):e22298. doi: 10.1097/md.0000000000022298

101. Ding X, Li Q, Li P, Chen X, Xiang L, Bi L, et al. Fecal microbiota transplantation: A promising treatment for radiation enteritis? *Radiother Oncol* (2020) 143:12–8. doi: 10.1016/j.radonc.2020.01.011

102. Riehl TE, Alvarado D, Ee X, Zuckerman A, Foster L, Kapoor V, et al. Lactobacillus rhamnosus gg protects the intestinal epithelium from radiation injury through release of lipoteichoic acid, macrophage activation and the migration of mesenchymal stem cells. *Gut* (2019) 68(6):1003–13. doi: 10.1136/gutjnl-2018-316226

103. Banna GL, Torino F, Marletta F, Santagati M, Salemi R, Cannarozzo E, et al. Lactobacillus rhamnosus gg: An overview to explore the rationale of its use in cancer. *Front Pharmacol* (2017) 8:603. doi: 10.3389/fphar.2017.00603

104. Wardill HR, Van Sebille YZA, Ciorba MA, Bowen JM. Prophylactic probiotics for cancer therapy-induced diarrhoea: A meta-analysis. *Curr Opin Support Palliat Care* (2018) 12(2):187–97. doi: 10.1097/SPC.0000000000000338

105. Ruan JL, Lee C, Wouters S, Tullis IDC, Verslegers M, Mysara M, et al. Irradiation at ultra-high (Flash) dose rates reduces acute normal tissue toxicity in the mouse gastrointestinal system. *Int J Radiat Oncol Biol Phys* (2021) 111(5):1250–61. doi: 10.1016/j.ijrobp.2021.08.004

106. Bourhis J, Sozzi WJ, Jorge PG, Gaide O, Bailat C, Duclos F, et al. Treatment of a first patient with flash-radiotherapy. *Radiother Oncol* (2019) 139:18–22. doi: 10.1016/j.radonc.2019.06.019

107. Jin JY, Gu A, Wang W, Oleinick NL, Machtay M, Spring Kong FM. Ultra-high dose rate effect on circulating immune cells: A potential mechanism for flash effect? *Radiother Oncol* (2020) 149:55–62. doi: 10.1016/j.radonc.2020.04.054

108. Kim YE, Gwak SH, Hong BJ, Oh JM, Choi HS, Kim MS, et al. Effects of ultra-high doserate flash irradiation on the tumor microenvironment in Lewis lung carcinoma: Role of myosin light chain. *Int J Radiat Oncol Biol Phys* (2021) 109(5):1440–53. doi: 10.1016/j.ijrobp.2020.11.012

109. Cunningham S, McCauley S, Vairamani K, Speth J, Girdhani S, Abel E, et al. Flash proton pencil beam scanning irradiation minimizes radiation-induced leg contracture and skin toxicity in mice. *Cancers (Basel)* (2021) 13(5):1012. doi: 10.3390/cancers13051012

110. Buonanno M, Grilj V, Brenner DJ. Biological effects in normal cells exposed to flash dose rate protons. *Radiother Oncol* (2019) 139:51–5. doi: 10.1016/j.radonc.2019.02.009

111. Gameiro SR, Malamas AS, Bernstein MB, Tsang KY, Vassantachart A, Sahoo N, et al. Tumor cells surviving exposure to proton or photon radiation share a common immunogenic modulation signature, rendering them more sensitive to T cell-mediated killing. *Int J Radiat Oncol Biol Phys* (2016) 95(1):120–30. doi: 10.1016/j.ijrobp.2016.02.022

112. Gameiro SR, Jammeh ML, Wattenberg MM, Tsang KY, Ferrone S, Hodge JW. Radiation-induced immunogenic modulation of tumor enhances antigen processing and calreticulin exposure, resulting in enhanced T-cell killing. *Oncotarget* (2014) 5(2):403–16. doi: 10.18632/oncotarget.1719

113. Golden EB, Frances D, Pellicciotta I, Demaria S, Helen Barcellos-Hoff M, Formenti SC. Radiation fosters dose-dependent and chemotherapy-induced immunogenic cell death. *Oncoimmunology* (2014) 3:e28518. doi: 10.4161/onci.28518

114. Zhao X, Shao C. Radiotherapy-mediated immunomodulation and anti-tumor abscopal effect combining immune checkpoint blockade. *Cancers (Basel)* (2020) 12 (10):2762. doi: 10.3390/cancers12102762

115. Rodriguez-Ruiz ME, Rodriguez I, Garasa S, Barbes B, Solorzano JL, Perez-Gracia JL, et al. Abscopal effects of radiotherapy are enhanced by combined immunostimulatory mabs and are dependent on Cd8 T cells and crosspriming. *Cancer Res* (2016) 76 (20):5994–6005. doi: 10.1158/0008-5472.Can-16-0549

116. Sun L, Wu J, Du F, Chen X, Chen ZJ. Cyclic gmp-amp synthase is a cytosolic DNA sensor that activates the type I interferon pathway. *Science* (2013) 339(6121):786–91. doi: 10.1126/science.1232458

117. Deng L, Liang H, Xu M, Yang X, Burnette B, Arina A, et al. Sting-dependent cytosolic DNA sensing promotes radiation-induced type I interferon-dependent antitumor immunity in immunogenic tumors. *Immunity* (2014) 41(5):843–52. doi: 10.1016/j.immuni.2014.10.019

118. Jones KI, Tiersma J, Yuzhalin AE, Gordon-Weeks AN, Buzzelli J, Im JH, et al. Radiation combined with macrophage depletion promotes adaptive immunity and potentiates checkpoint blockade. *EMBO Mol Med* (2018) 10(12):e9342. doi: 10.15252/emmm.201809342

119. Ahn GO, Tseng D, Liao CH, Dorie MJ, Czechowicz A, Brown JM. Inhibition of mac-1 (Cd11b/Cd18) enhances tumor response to radiation by reducing myeloid cell recruitment. *Proc Natl Acad Sci U.S.A.* (2010) 107(18):8363–8. doi: 10.1073/pnas.0911378107

120. Kang C, Jeong SY, Song SY, Choi EK. The emerging role of myeloid-derived suppressor cells in radiotherapy. *Radiat Oncol J* (2020) 38(1):1–10. doi: 10.3857/roj.2019.00640

121. Deng L, Liang H, Burnette B, Beckett M, Darga T, Weichselbaum RR, et al. Irradiation and anti-Pd-L1 treatment synergistically promote antitumor immunity in mice. *J Clin Invest* (2014) 124(2):687–95. doi: 10.1172/jci67313

122. Zhou L, Yu G, Shen Y, Ding H, Zheng K, Wen R, et al. The clinical efficacy and safety of neoadjuvant chemoradiation therapy with immunotherapy for the organ preservation of ultra low rectal cancer: A single arm and open label exploratory study. *J Oncol* (2022) 40(16). doi: 10.1200/JCO.2022.40.16_suppl.e15603

123. Wang H, Li X, Peng R, Wang Y, Wang J. Stereotactic ablative radiotherapy for colorectal cancer liver metastasis. *Semin Cancer Biol* (2021) 71:21–32. doi: 10.1016/j.semcancer.2020.06.018

124. Monjazeb A, Giobbie-Hurder A, Lako A, Tesfaye AA, Stroiney A, Gentzler RD, et al. Analysis of colorectal cancer patients treated on etctn 10021: A multicenter randomized trial of combined pd-L1 and ctla-4 inhibition with targeted low-dose or hypofractionated radiation. *J Clin Oncol* (2019) 37(8_suppl):49. doi: 10.1200/JCO.2019.37.8_suppl.49

125. Laengle J, Kuehrer I, Pils D, Kabiljo J, Wöran K, Stift J, et al. Neoadjuvant chemoradiotherapy with sequential ipilimumab and nivolumab in rectal cancer (Chinorec): A prospective randomized, open-label, multicenter, phase ii clinical trial. *J ImmunoTherapy Cancer* (2020) 8(SUPPL 2):A51. doi: 10.1136/jitc-2020-ITOC7.100

126. Yang J, Zhou W, Ma Y, Su D, Kong Y, Xu M, et al. The response of pd-1 inhibitor combined with radiotherapy and gm-Csf(Prag) with or without il-2 in microsatellite stable metastatic colorectal cancer: Analysis of pooled data from two phase ii trials. *J Clin Oncol* (2022) 40(16). doi: 10.1200/JCO.2022.40.16_suppl.e15561

127. Xiao W, Lin JZ, Chen G, Wu XJ, Lu ZH, Wang Q, et al. Neoadjuvant chemoradiotherapy with or without pd-1 antibody sintilimab for Pmmr/Mss/Msi-l locally advanced rectal cancer: A randomized controlled study (Cohort b). *J Clin Oncol* (2022) 40(4 SUPPL). doi: 10.1200/JCO.2022.40.4_suppl.TPS210

128. Corrò C, Buchs NC, Tihy M, Durham-Faivre A, Bichard P, Frossard JL, et al. Study protocol of a phase ii study to evaluate safety and efficacy of neo-adjuvant pembrolizumab and radiotherapy in localized rectal cancer. *BMC Cancer* (2022) 22 (1):772. doi: 10.1186/s12885-022-09820-w

129. Wen X, Guo Z, Zhang X. Combined Pd-L1–targeted radionuclide therapy with immunotherapy in two models of colorectal cancer. *Nucl Med Biol* (2021) 96-97:S33. doi: 10.1016/S0969-8051(21)00316-4

130. Dovedi SJ, Adlard AL, Lipowska-Bhalla G, McKenna C, Jones S, Cheadle EJ, et al. Acquired resistance to fractionated radiotherapy can be overcome by concurrent pd-L1 blockade. *Cancer Res* (2014) 74(19):5458–68. doi: 10.1158/0008-5472.Can-14-1258

131. Lei Q, Wang D, Sun K, Wang L, Zhang Y. Resistance mechanisms of anti-Pd1/Pdl1 therapy in solid tumors. *Front Cell Dev Biol* (2020) 8:672. doi: 10.3389/fcell.2020.00672

132. Hettich M, Lahoti J, Prasad S, Niedermann G. Checkpoint antibodies but not T cell-recruiting diabodies effectively synergize with til-inducing Γ-irradiation. *Cancer Res* (2016) 76(16):4673–83. doi: 10.1158/0008-5472.Can-15-3451

133. Ashrafizadeh M, Farhood B, Eleojo Musa A, Taeb S, Rezaeyan A, Najafi M. Abscopal effect in radioimmunotherapy. *Int Immunopharmacol* (2020) 85:106663. doi: 10.1016/j.intimp.2020.106663

134. Randrian V, Pernot S, Le Malicot K, Catena V, Baumgaertner I, Tacher V, et al. Ffcd 1709-sirtci phase ii trial: Selective internal radiation therapy plus xelox, bevacizumab and atezolizumab in liver-dominant metastatic colorectal cancer. *Dig Liver Dis* (2022) 54 (7):857–63. doi: 10.1016/j.dld.2022.04.024

135. Gutiontov SI, Pitroda SP, Chmura SJ, Arina A, Weichselbaum RR. Cytoreduction and the optimization of immune checkpoint inhibition with radiation therapy. *Int J Radiat Oncol Biol Phys* (2020) 108(1):17–26. doi: 10.1016/j.ijrobp.2019.12.033

136. Storozynsky Q, Hitt MM. The impact of radiation-induced DNA damage on cgas-Sting-Mediated immune responses to cancer. *Int J Mol Sci* (2020) 21(22):8877. doi: 10.3390/ijms21228877

137. Twyman-Saint VC, Rech AJ, Maity A, Rengan R, Pauken KE, Stelekati E, et al. Radiation and dual checkpoint blockade activate non-redundant immune mechanisms in cancer. *Nature* (2015) 520(7547):373–7. doi: 10.1038/nature14292

138. Li H, Luo Q, Zhang H, Ma X, Gu Z, Gong Q, et al. Nanomedicine embraces cancer radio-immunotherapy: Mechanism, design, recent advances, and clinical translation. *Chem Soc Rev* (2022) 52:47–96. doi: 10.1039/d2cs00437b

139. Löwenmark T, Löfgren-Burström A, Zingmark C, Ljuslinder I, Dahlberg M, Edin S, et al. Tumour colonisation of parvimonas micra is associated with decreased survival in colorectal cancer patients. *Cancers (Basel)* (2022) 14(23). doi: 10.3390/cancers14235937

140. Song S, Vuai MS, Zhong M. The role of bacteria in cancer therapy - enemies in the past, but allies at present. *Infect Agent Cancer* (2018) 13:9. doi: 10.1186/s13027-018-0180-y

141. Qi Z, Pei P, Zhang Y, Chen H, Yang S, Liu T, et al. (131)I-Apd-L1 immobilized by bacterial cellulose for enhanced radio-immunotherapy of cancer. *J Control Release* (2022) 346:240–9. doi: 10.1016/j.jconrel.2022.04.029

142. Motwani M, Pesiridis S, Fitzgerald KA. DNA Sensing by the cgas-sting pathway in health and disease. *Nat Rev Genet* (2019) 20(11):657–74. doi: 10.1038/s41576-019-0151-1

143. Si W, Liang H, Bugno J, Xu Q, Ding X, Yang K, et al. Lactobacillus rhamnosus gg induces Cgas/Sting- dependent type I interferon and improves response to immune checkpoint blockade. *Gut* (2022) 71(3):521–33. doi: 10.1136/gutjnl-2020-323426

144. Song W, Tiruthani K, Wang Y, Shen L, Hu M, Dorosheva O, et al. Trapping of lipopolysaccharide to promote immunotherapy against colorectal cancer and attenuate liver metastasis. *Adv Mater* (2018) 30(52):e1805007. doi: 10.1002/adma.201805007

145. Yi X, Zhou H, Chao Y, Xiong S, Zhong J, Chai Z, et al. Bacteria-triggered tumor-specific thrombosis to enable potent photothermal immunotherapy of cancer. *Sci Adv* (2020) 6(33):eaba3546. doi: 10.1126/sciadv.aba3546

146. Fukumura D, Kloepper J, Amoozgar Z, Duda DG, Jain RK. Enhancing cancer immunotherapy using antiangiogenics: Opportunities and challenges. *Nat Rev Clin Oncol* (2018) 15(5):325–40. doi: 10.1038/nrclinonc.2018.29

147. Pei P, Zhang Y, Jiang Y, Shen W, Chen H, Yang S, et al. Pleiotropic immunomodulatory functions of radioactive inactivated bacterial vectors for enhanced cancer radio-immunotherapy. *ACS Nano* (2022) 16(7):11325–37. doi: 10.1021/acsnano.2c04982

148. Chen J, Zhang P, Zhao Y, Zhao J, Wu X, Zhang R, et al. Nitroreductase-instructed supramolecular assemblies for microbiome regulation to enhance colorectal cancer treatments. *Sci Adv* (2022) 8(45):eadd2789. doi: 10.1126/sciadv.add2789

frontiers | Frontiers in Immunology

TYPE Review
PUBLISHED 16 March 2023
DOI 10.3389/fimmu.2023.1148692

OPEN ACCESS

EDITED BY
Shaoli Song,
Fudan University, China

REVIEWED BY
Ana Vuletić,
Institute of Oncology and Radiology of Serbia, Serbia
Ende Zhao,
New York University, United States

*CORRESPONDENCE
Mohammad Krayem
mohammad.krayem@hubruxelles.be

SPECIALTY SECTION
This article was submitted to Cancer Immunity and Immunotherapy, a section of the journal Frontiers in Immunology

RECEIVED 20 January 2023
ACCEPTED 03 March 2023
PUBLISHED 16 March 2023

CITATION
Iliadi C, Verset L, Bouchart C, Martinive P, Van Gestel D and Krayem M (2023) The current understanding of the immune landscape relative to radiotherapy across tumor types.
Front. Immunol. 14:1148692.
doi: 10.3389/fimmu.2023.1148692

The current understanding of the immune landscape relative to radiotherapy across tumor types

Chrysanthi Iliadi[1,2], Laurine Verset[3], Christelle Bouchart[1], Philippe Martinive[1], Dirk Van Gestel[1] and Mohammad Krayem[1,2]*

[1]Department of Radiation Oncology, Institut Jules Bordet, Université Libre de Bruxelles (ULB), Hôpital Universitaire de Bruxelles (H.U.B), Brussels, Belgium, [2]Laboratory of Clinical and Experimental Oncology (LOCE), Institut Jules Bordet, Université Libre de Bruxelles (ULB), Hôpital Universitaire de Bruxelles (H.U.B), Brussels, Belgium, [3]Department of Pathology, Institut Jules Bordet, Université Libre de Bruxelles (ULB), Hôpital Universitaire de Bruxelles (H.U.B), Brussels, Belgium

Radiotherapy is part of the standard of care treatment for a great majority of cancer patients. As a result of radiation, both tumor cells and the environment around them are affected directly by radiation, which mainly primes but also might limit the immune response. Multiple immune factors play a role in cancer progression and response to radiotherapy, including the immune tumor microenvironment and systemic immunity referred to as the immune landscape. A heterogeneous tumor microenvironment and the varying patient characteristics complicate the dynamic relationship between radiotherapy and this immune landscape. In this review, we will present the current overview of the immunological landscape in relation to radiotherapy in order to provide insight and encourage research to further improve cancer treatment. An investigation into the impact of radiation therapy on the immune landscape showed in several cancers a common pattern of immunological responses after radiation. Radiation leads to an upsurge in infiltrating T lymphocytes and the expression of programmed death ligand 1 (PD-L1) which can hint at a benefit for the patient when combined with immunotherapy. In spite of this, lymphopenia in the tumor microenvironment of 'cold' tumors or caused by radiation is considered to be an important obstacle to the patient's survival. In several cancers, a rise in the immunosuppressive populations is seen after radiation, mainly pro-tumoral M2 macrophages and myeloid-derived suppressor cells (MDSCs). As a final point, we will highlight how the radiation parameters themselves can influence the immune system and, therefore, be exploited to the advantage of the patient.

KEYWORDS

radiotherapy, cancer, systemic immune response, immune tumor microenvironment, immune landscape, biomarker, immune cells

10.3389/fimmu.2023.1148692

Introduction

In recent years, sequencing of different tumors has revealed a vast heterogeneity across different cancer types but also between patients with the same diagnosis, highlighting the need for personalized medicine (1). The recent re-evaluation of the cancer hallmarks emphasized the essential role of the tumor microenvironment (TME) in tumor progression (2). The TME is a complex network of different cell populations and the interactions between them. The main cell neighborhoods of the TME are the tumor-, stromal-, vasculature- and immune cells. These cellular elements interact and create an evolving and dynamic environment that determines the response to different therapeutic regimens. Therefore, it is evident that an analysis of the multiple cell components in the TME can help design the most effective therapeutic strategy (3). The immune cells have a dual role in shaping the tumor by promoting or preventing its growth in a process named cancer immunoediting (4). In the framework of this process, the immune landscape, that is 1) the heterogeneous network of immune cells, 2) the immune components such as chemoattractants, and 3) other immunogenic factors such as tumor mutational burden (TMB), is widely studied (5). The balance of the different immune populations, the spatial localization, and the functional phenotype of the immune tumor microenvironment (iTME) establish the immune contexture (6). The immune landscape and contexture influence the response to treatment but are also contextually shaped by the therapeutic regimen itself.

Based on the immune landscape of solid tumors, several pan-cancer classifications were developed: the four consensus molecular subtypes - CMS (ie CMS1 - microsatellite instability immune, CMS2 - canonical, CMS3 - metabolic and CMS4 - mesenchymal) (7), the six immune transcriptomics subtypes – IS (ie wound healing, IFN-γ dominant, inflammatory, lymphocyte depleted, immunologically quiet and TGF-β dominant) (8) and most recently the four immune/fibrotic TME subtypes (ie IE/F – Immune Enriched/Fibrotic, IE, F, D-Desert) (9). As these strategies take into account the characteristics of the tumor microenvironment, they try to achieve more effective patient stratification than the traditional classification based on the histological characteristics of the tumor and the TNM staging system (10).

Radiotherapy (RT) is one of the standard therapeutic regimens that take advantage of the damaging effect of ionizing radiation on DNA, leading to proliferative cell death and direct killing of the tumor cells (11, 12). Indirectly, RT leads to contrasting results shaping the iTME either to an immunogenic or to an immunosuppressive phenotype (see Figure 1). Shifting the delicate balance towards the immunogenic phenotype, radiation-related killing of tumor cells leads to the release of neoantigens and damage-associated molecular patterns (DAMPs). These signals, in turn, lead to an increase in antigen presentation and therefore activation of the innate immune system, an increase of CD8+ cytotoxic T cell infiltration, and inhibition of immunosuppressive cells (13). Contrariwise, tipping the scale towards the immunosuppressive phenotype, the use of radiation results most of the time in the direct killing of T lymphocytes inside the radiation field, increments the myeloid-derived suppressor cells (MDSCs) and regulatory T cells (Tregs) infiltration, and activates cancer-associated fibroblasts (CAFs) (14) through the TGF-β pathway, therefore, promoting tumor growth (15–17). Interestingly, RT has not only a modulating effect on the iTME but also systemically alters the immune profile of the patient. As was shown in a meta-analysis study across different cancer types, RT resulted in a systemic reduction of CD3+ and CD4+ peripheral T cells one month after the last treatment (18). Moreover, the role of radiation in the immune status of the TME can be exploited in the form of *in-situ vaccination* depending on the dose and

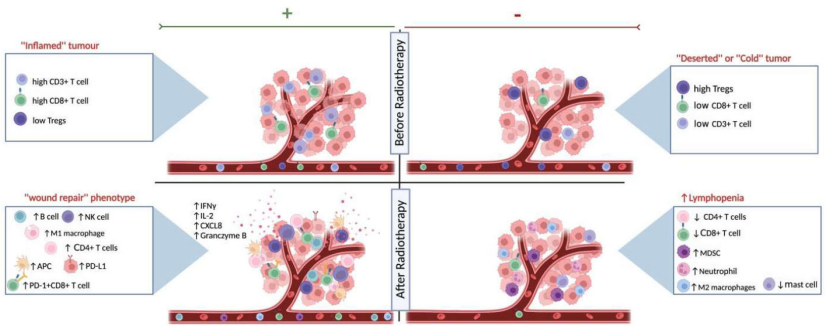

FIGURE 1
The effects of radiotherapy on the immune landscape. Schematic representation of the different states of systemic immune landscape and the tumor microenvironment before and after radiotherapy. As shown on the top left, the "inflamed immune" phenotype responds better to RT, as exhibited by higher immunoscores (CD3+ and CD8+ T cell densities), while the "deserted" or "cold" tumors on the top right respond less well to radiation therapy. The effects of RT on the immune landscape are influenced by the existing heterogeneous tumor microenvironment and the individual patient's immune response. On the one hand, after RT, there might be a shift towards the wound healing signature (bottom left) and patients with this immune-hot phenotype have increased survival after treatment and might also be eligible for combination therapy with immunotherapy. Radiation can also cause a lymphopenic systemic and iTME landscape (bottom right), resulting in a worse prognosis. Created with BioRender.com.

fractionation schedule of radiation, the pre-existing immune profile of the tissue and patient, and the radiosensitivity of the tumor itself (19, 20). The *in-situ* vaccination can lead to systemic effects with a few examples of abscopal effect (21).

This review will examine the complexity of the systemic and local immune environment in different types of cancer. Our discussion will focus on how radiation shapes the immune landscape. In addition, we will unravel the potential prognostic and predictive insight we can gain from the iTME and systemic immune profile of the patient to guide therapeutic decisions (see Table 1).

Methods

The Pubmed database was searched for literature articles and reviews published between January 1st, 2012 and October 31st, 2022 that investigate the effect of radiation therapy on the immune landscape of various malignancies. The search strategy included vocabulary related to radiotherapy (e.g., radiation, chemoradiation, fractionation) and to the immune system (e.g., immune cell, innate and adaptive immunity, infiltration, cytotoxicity). Additionally, each type of cancer was used as a keyword accompanied by the aforementioned terms to search for related information. Moreover, reference lists of selected reviews were screened to be redirected to the original study.

Results describing either prospective or retrospective settings were evaluated in full-text articles. Throughout this review, we make a distinction between the systemic immune landscape that includes changes in the peripheral blood mononuclear cells (PBMCs) and the immune landscape of the tumor microenvironment for which mainly formalin-fixed paraffin-embedded (FFPE) or fresh samples of the tumors are evaluated. The methods most commonly used for the analysis of the immune landscape are flow cytometry, immunohistochemistry or tissue microarrays, and transcriptomics analysis. To emphasize the importance of further investigation in pre-clinical models, we separated the data produced by such studies from data on human samples when available. Moreover, all treatment regimens were included, RT alone as well as CRT without restrictions on cytotoxic agents used. Finally, we included data describing the difference between treated and untreated specimens or samples before treatment (biopsies).

Finally, the records of the database ClinicalTrials.gov of the U.S. National Library of Medicine were searched to identify clinical trials that involved a combination of radiotherapy and immune checkpoint inhibitors for the following types of cancer. The search focused specifically on double-arm trials, which involve concurrent radiotherapy and immunotherapy in at least one experimental arm, as these trials can provide a more rigorous evaluation of treatment efficacy. By including a control group, the double-arm trial can help to establish whether any observed benefits are due to the combination of treatments, or whether they would have occurred with one of the treatments alone. Clinical trials classified as 'withdrawn' or 'unknown' were excluded. The results are presented in Table 2.

Immune landscape and radiotherapy

Parameters of the radiotherapy regimen that can influence the immune landscape

It is estimated that more than half of all cancer patients receive radiation therapy (11, 41). In a radiotherapy regimen, a variety of parameters can vary, such as the moment of treatment (neoadjuvant/preoperative or adjuvant treatment), the combination with other treatments like chemotherapy and/or immunotherapy, and the fractionation schedule, which altogether can result in a whole range of total doses at the end of treatment and treatment lengths.

As part of the modulation of the immune signature, fractionation plays an important role. A single dose of RT, compared to a multifractionated schedule, promotes a more immunogenic phenotype in prostate cancer cells *in vitro* (42). Moreover, in a murine orthotopic model of pancreatic cancer, RT recruited a greater number of T cells than fractionated RT (43). In particular, RT given as a single dose of 25Gy resulted in higher infiltration of cytotoxic T cells (CD8+) compared to the four times 10 Gy per fraction regimen. It is most interesting to note that there was no difference in tumor growth between the two groups, suggesting that different RT schedules had no effect on T-cell activity but only on infiltration.

Furthermore, changes in the immune landscape following fractionated RT can be affected by age and target volumes, especially when immune-related volumes are involved, such as blood vessels and bone marrow (44). As aging affects immune cells (25), it is only natural that the treatment's impact on the immune landscape will also be influenced by aging. In a small cohort of prostate cancer patients treated with RT was studied to determine if the changes in immune cell subsets were influenced by age. CD4+ effector cells and patient age exhibited a moderately positive correlation, but not in the exploratory cohort (44). So far no strong relationship between age and radiation effects on immunity has been demonstrated. More coherent results derive from the relationship between target volume and immune landscape after RT. Lymphopenia is a common side-effect of RT and smaller target volumes are likely to affect less the immune landscape than larger ones (45).

Treatment planning variables such as the interval between RT and surgery and of course the addition of chemotherapy can also influence the iTME. These parameters were explored in rectal cancer (46), where less cytotoxic T cells and T helper cells infiltrated tumors following a shorter radiotherapy-to-surgery interval compared to the longer waiting time after an equal radiation dose. In addition, in the same study, CRT led to a significant decrease in T regulatory cell infiltration, demonstrating the combination to work synergistically to reverse immune suppression.

It can be challenging to draw conclusions about the state of the tumor's immune status after radiotherapy, especially when we rely on biopsies, which are often not representative of the whole tumor mass. Moreover, the higher density of CD4+ and CD8+ T cells in surgical samples was correlated with the use of postoperative radiotherapy

10.3389/fimmu.2023.1148692

TABLE 1 Immune landscape elements associated with prediction and prognosis in patients that underwent radiotherapy.

Cancer Type	Sample type	Number of patients	Treatment	Methods	Response assessment	Immune landscape parameter	Reference number
Esophageal Cancer	PBMCs	297	CRT	FC	Better OS	Low Treg High CD4+CD8+	(22)
	Serum	63	RT	ELISA	Response *VS* Non-Response to treatment	Elevated levels of IL-2 and IFN-γ	(23)
	FFPE samples	81	CRT	IHC	Response to nCRT	High density of CD8+ T cells Foxp3+ T cells and PD-1+ T cells	(24)
	FFPE samples	31	CRT	IHC and qRT-PCR	–	Increase in CD8+ T cells after CRT	(25)
	FFPE samples	123	CRT	IHC	Worse OS	High CD8+ T cell inflitration	(26)
nasopharyngeal carcinoma	Tissue samples and peripheral blood	36	CRT	TCRβ sequencing	Longer DFS	Higher number of mucosa-resident ITCs	(27)
limited-stage small cell lung cancer (LS-SCLC)	PBMCs	98	CRT	FC	Higher PFS	Higher number of CD4+CD45RA+, CD8+CD38+	(28)
stage I NSCLC	PBMCs	19	SBRT	TCR sequencing	Poor MFS	Lower TCR diversity	(29)
Lung adenocarcinoma (LUAD)	mRNA data	423	RT	Functional genomics – differential expression analysis	Better response to RT	Low risk tumor-infiltrating B lymphocyte-specific genes (TILBSig)	(30)
hepatocellular carcinoma	Blood sample	164	SIRT	Blood count	Better OS	NLR < 7.2	(31)
locally advanced rectal cancer (LARC)	Biopsies	249	CRT	IHC	High DFS	High Immunoscore (CD3+ and CD8+ T cells in the tumor core and invasive margin)	(32)
Rectal Cancer	Biopsies and resection specimens	53	CRT	Functional genomics: gene expression profiling	Response to RT/CRT	"hot" iTME phenotype after treatment	(33)
rectal adenocarcinoma	FFPE recession samples, PBMCs or histologically normal rectal tissue	17	CRT	IHC	Response to CRT	Higher infiltration in CD8+ T cells	(34)
8 cancer types	Published literate	>10.328	Various	Meta-analysis	Poor OS	Low Immunoscore	(35)
Rectal Cancer	FFPE	166	CRT	IHC	Better DFS and OS	High Immunoscore (densities of CD3+ and CD8+ lymphocytes)	(36)
Pancreatic Cancer	PBMCs	66	CRT	ELISA or flow cytometry–based multiplex bead arrays	Greater mOS	above-median CXCL8 serum levels (>29.8 pg/ml) and	(37)
					Prolonged mOS	Above-median pretreatment NK cell numbers (NKhigh: CIBERSORT fraction, >4.5%)	
Pancreatic Cancer	FFPE tissue blocks	70	nCRT	mIHC/IF	longer RFS	low density of M2-type TAMs	(38)

RT, radiotherapy; CRT, chemoradiotherapy; SBRT, stereotactic body radiotherapy; SIRT, Selective internal radiation therapy; nCRT, NeoAdjuvant Therapy; OS, overall survival; mOS, median overall survival; PFS, progression free survival; DFS, disease free survival; FFPE, Formalin Fixated Paraffin Embedded Sample; PBMCs, Peripheral Blood Mononuclear Cells; mRNA, messenger ribonucleic acid; ELISA, Enzyme-Linked Immunosorbent Assay; IHC, Immunohistochemistry; FC, Flow Cytometry; MFS, Metastasis Free Survival; NLR, Neutrophil-to-Lymphocyte Ratio; mIHC/IF, Multiplex Immunohistochemistry/Immunofluorescence. "-" There is no correlation observed between the alteration in iTME and the parameters for evaluating response in patients.

TABLE 2 Clinical trials that strive to show therapeutic benefit of combining immunotherapy and radiotherapy.

Cancer Type	Immune Target	Antibody	RT Regimen	Experimental Arms	Primary Endpoint	Therapeutic Benefit or Clinical Trial Status *	Identifier or Reference
Head and Neck Cancer	PD-L1	Avelumab	69.96 Gy in 2.12 Gy/day over 6.5W	ICI + RT -cetuximab *VS* SOC	PFS	Active, not recruiting	NCT02999087
	PD-1 and CTLA-4	Nivolumab and Ipilimumab	56-66 Gy	Neoadjuvant/ Adjuvant ICI +CRT *VS* Surgical resection + Adjuvant CRT	DFS	Active, not recruiting	NCT03700905
Lung Cancer	PD-L1	Durvalumab	at least 60 Gy	CRT+ICI *VS* CRT +placebo	PFS	Median PFS was 16.8 months with ICI *VS* 5.6 months with placebo	NCT02125461 (39)
	PD-1	Pembrolizumab	50 Gy	CRT *VS* ICI and dose-painted radiotherapy	PFS	Recruiting	NCT03523702
	PD-L1	Atezolizumab	Radiotherapy up to 21 days	ICIs + RT *VS* ICIs	ORR	Recruiting	NCT03337698
	PD-1	Pembrolizumab	18 Gy in 3 X 6 Gy	ICI+ CRT *VS* ICI + CT	OS	Recruiting	NCT03774732
	PD-L1	Atezolizumab	61.2 GY	ICI + CRT + surgery *VS* CRT + surgery	pCR	Recruiting	NCT04989283
	PD-L1	Atezolizumab	3D-CRT or IMRT BID for 3W	CRT+IT *VS* CRT	OS	Recruiting	NCT03811002
	PD-L1	Durvalumab	15 Gy in 10 fractions	ICI with low-dose PCI *VS* ICI	Reduction of incidence of brain metastases	Recruiting	NCT04597671
	PD-1	Pembrolizumab	3 x 8 Gy	RT + ICI *VS* ICI	ORR	The ORR at 12 weeks was 18% in the control arm *vs* 36% in the experimental arm (P = .07)	(40) NCT02492568
Lung Cancer and Melanoma	PD-1 and CTLA-4	Nivolumab and Ipilimumab	1 x 18-22 Gy (18-22 Gy) or 5 x 6 Gy (30 Gy).	Stereotactic radiosurgery and ICI *VS* ICI	CNS-specific PFS	Recruiting	NCT05522660
Lung Cancer and Colorectal Cancer	PD-L1 and CTLA-4	Durvalumab and Tremelimumab	Not Specified	ICIs *VS* ICIs + big dose RT *VS* ICIs + low dose RT	ORR	Active, not recruiting	NCT02888743
Esophageal Cancer	PD-1/PD-L1	Not specified	50-66G/1.8-2.2Gy/ 25-30f	CRT *VS* CRT + ICI	OS in 1Y, 2Y, 3Y and 5Y	Recruiting	NCT04821778
	PD-1	Camrelizumab	50Gy/30f	ICI + CRT *VS* ICI + CT	ORR	Not yet recruiting	NCT05624099
	PD-1	Camrelizumab	50-50.4G, 1.8-2 Gy, 5d/w	ICI + CRT *VS* Placebo + CRT	PFS	Not yet recruiting	NCT04404491
	PD-L1	Durvalumab	50 Gy	CRT + ICI *VS* CRT	cPFS	Recruiting	NCT03777813
	PD-1	Camrelizumab	8 Gy/time, 3 -5 times	CRT + IT *VS* CT +IT	PFS	Not yet recruiting	NCT05183958
Cervical Cancer	PD-1	Serplulimab	80 Gy for small-volume tumors or 85 Gy for larger-volume tumors	IT + CRT *VS* CRT	PFS	Not yet recruiting	NCT05173272

(Continued)

TABLE 2 Continued

Cancer Type	Immune Target	Antibody	RT Regimen	Experimental Arms	Primary Endpoint	Therapeutic Benefit or Clinical Trial Status *	Identifier or Reference
Breast Cancer	PD-1	Pembrolizumab	Low-Dose or High-Dose RT	ICI *VS* ICI + Low-Dose RT *VS* ICI + High-Dose RT	TILs and pCR-LN	Recruiting	NCT04443348
	PD-1	Pembrolizumab	Focal hypo-fractionated RT 8 Gy x 3 fractions	RT *VS* RT+ICI *VS* RT+Ftl-3 ligand *VS* RT+Ftl-3+ ICI	Tolerability and pCR/cCR	Recruiting	NCT03804944
Ovarian Cancer	CD-40 and PD-L2	APX005M and Carboplatin	0.5 Gy/fr; days 1 and 15 q4 wks x 6 cycles. Maximum 24 wks of therapy; total dose 6 Gy.	SOC *VS* APX005M *VS* APX005M+RT	ORR	Not yet recruiting	NCT05201001
Prostate Cancer	PD-1 and CTLA-4	Nivolumab and Ipilimumab	8 Gray (Gy) x 3	RT + ICIs *VS* ICIs	ORR and PSA RR	Recruiting	NCT05655715
	PD-L1	Durvalumab	SBRT will be started one month after ICI in 3fr	RT + ICI *VS* RT	2-year PFS	Recruiting	NCT03795207
Pancreatic Cancer	PD-1	Pembrolizumab	50.4 Gy in 28fr over 28 days	nCRT+ICI *VS* nCRT	Number of TILS per hpf and DLT	Recruiting	NCT02305186
	PD-L1 (and TGF-β)	Bintrafusp alfa (M7824)	RT will be starting on Day 17 (+5 days)	ICIs + RT *VS* ICIs	DLT and Recommended Phase 2 Dose and BOR	Terminated (Study closed to accrual due to the worsening risk: benefit ratio for participants receiving bintrafusp alfa (M7824)	NCT04327986
Hepatocellular Carcinoma	PD-1	Sintilimab	30-54 Gy in 3-6fr over 1-2W	RT+ICI *VS* RT	24-week PFS	Recruiting	NCT04167293
Melanoma, Non-Hodgkin Lymphoma, Colorectal Cancer	CTLA-4	Ipilimumab	10 Gy x 3 fractions	ICI + RT *VS* ICI	DLT	0% Serious AE - Terminated (Planned Future Study)	NCT01769222
Advanced Malignancies	CD-137 (4-1BB), PD-L1 and CD137 (OX40)	Utomilumab, Avelumab, Ivuxolimab	Patients undergo RT on days -5 to -1/Dose Not Specified	ICIs *VS* ICIs+RT	Incidence of adverse events and Evaluation of CD8 immune biomarkers assessed in tumor and blood	Active, not recruiting	NCT03217747

RT, radiotherapy; CT, chemotherapy; CRT, chemoradiotherapy; SOC, Standard of Care; ICI, Immune Checkpoint Inhibitor; OS, overall survival; PFS, progression free survival; pCR-LN, Pathological Complete Response in the Lymph Nodes; ORR, Overall Response Rate; BOR, Best Overall Response; RR, Response Rate; DLT, Dose Limiting Toxicities; AE, Adverse Effects; TILS, Tumor Infiltrating Lymphocytes; PSA, Prostate-Specific Antigen; HPF, High Powered Field.

and good prognosis in a cohort of PDAC patients when large-section histopathology (LHS) slides were compared to small-section histopathology (SSH) slides that enclose less information on the TME. Therefore, the area that is covered during the analysis of immune staining can also be of great significance when it comes to evaluating prediction and/or progression.

It is crucial to thoroughly investigate the radiotherapy parameters that influence the iTME and systemic immune landscape, especially when combining radiation with immunotherapy for therapeutic purposes. For instance, a study involving lung cancer patients administered SBRT (3 doses of 8 Gy) in combination with pembrolizumab (anti-PD-1) demonstrated a doubling of the overall response rate (ORR) (40). Ongoing clinical trials are currently exploring the therapeutic benefits of this combination (see Table 2). A better understanding of how radiotherapy regimen parameters affect the synergy with immunotherapy could provide insights into the success or failure of such clinical trials (47).

Esophageal cancer

Esophageal (EC) and esophagogastric junction (EGJ) cancers are tumors that develop along the esophagus with the most

common types being squamous cell carcinoma (SCC) and adenocarcinoma (ADC) respectively. Their standard-of-care treatment for early-stage EC is endoscopic resection or surgical resection. Neoadjuvant chemoradiotherapy (nCRT) and surgery are recommended for more advanced stages (48) while immunotherapy with pembrolizumab can be as concurrent treatment as well. The results for immunotherapy are mixed as the anti-PD-1 reagent did not confer clinical benefit to patients with advanced PD-L1-positive gastroesophageal cancer (49). Therefore, much of the research in oesophageal cancer has been focused on understanding the immune landscape of the tumor in order to better stratify patients for immune checkpoint inhibitors (ICI) (50, 51).

Systemic immune landscape of EC and radiotherapy

A retrospective study using data from PBMCs of patients with non-operative EC that underwent chemoradiotherapy (CRT) showed that low density in Tregs and high concentration of double-positive (DP) CD4+ CD8+ T cells to be two independent predictive factors for response to CRT (22). Interestingly, the DP T cells represent a rarely studied subpopulation of immune cells that are found in cancer patients' blood and their role is not entirely clear as to whether they are immunosuppressive or cytotoxic (52). In metastatic colorectal cancer, this subpopulation has been found to favor immunosuppression and tumor growth (53) while in urological cancer it is correlated with differentiation of CD4+ naïve T cells to the pro-tumoral Th2 phenotype (54). In EC patients, high densities of DP T cells are associated with better outcomes, but further investigation is needed to uncover their precise role. Although Fei Lan et. all. Systemically observed a change after CRT, another group (55) observed no change in the density of CD4+, CD3+ and CD8+ T cells after only RT compared to only the chemotherapy group. These results might hint that the ablative effect on the PBMCs may be mainly attributed to the CRT combination and not to RT alone.

RT-induced immune reactions in patients with EC can be correlated with serum levels of two immunostimulatory cytokines, IL-2 and IFN-γ. These cytokines were found to be elevated during RT in responders compared to non-responders, in terms of better local control. Follow-up of these changes in PBMC immune populations or even better, in immunohistochemical profiles of primary tumors would be interesting (23).

Knowing that a radiation treatment results in severe lymphopenia in most EC patients, one always needs to consider that this systemic effect can also dampen the immune response in the tumor as well. Moreover, a high estimated dose of radiation to immune cells (EDRIC) was correlated with higher-grade lymphopenia also resulting in worse OS and PFS (56).

Another finding is the prognostic value of platelet to albumin ratio (PAR) which has been associated with worse overall survival (OS) and progression-free survival (PFS) among patients treated with RT for ESCC (57).

iTME of EC and radiotherapy

The dynamic changes that RT might impose on the tumor-infiltrating lymphocytes (TILs) have been explored retrospectively in FFPE samples of patients with EC treated with nCRT (24). In this study, Soeratram et al. classified the iTMEs according to the combined mean density of cytotoxic T cells (CD8+), T regulatory cells (FOXP3+), and immune-checkpoint molecule PD-1 positive cells into: "inflamed" (or "hot"), with most immune cells found in the tumor core (TC); "invasive margin" (or "excluded"), when most tumor-associated immune cells (TAICs) were found on the invasive margin (IM); and "desert" (or "cold"), consisting of samples with very low density in both compartments. In more than half of the nCRT recession samples (56%) the "inflamed" iTME was present, indicating a positive correlation between CRT and immune cell infiltration. Moreover, the most interesting studies are the ones that compare the pre-existing immune landscape on biopsies with the landscape after treatment in order to reveal dynamic changes. As such, based on pre-treatment biopsy and post-nCRT resection specimen pairs, an increase in the influx of CD8+ T cells was observed in the tumor epithelium, a finding which may aid treatment planning (24). This increase has also been found in a study by Kelly et al (25), when retrospectively comparing normal and malignant FFPE oesophageal epithelium post-nCRT samples with matched pre-treatment biopsies. The increase in lymphocyte infiltration like cytotoxic T cells and NK cells after CRT is commonly found in multiple studies on EC (58). It is important to further investigate the phenotype of these lymphocytes since on certain occasions there is an upregulation of immune checkpoint molecules as shown in ESCC patients treated with CRT where the increase in immune infiltration was parallel with an increase in one such molecule, the tyrosine-based inhibitory motif domain (TIGIT) (58). As for the two immune checkpoint therapeutic targets currently used in the clinic (59), there was an upregulation in programmed death-ligand 1 (PD-L1) expression after nCRT, yet the same trend was not evident for cytotoxic T-lymphocyte-associated protein 4 (CTLA-4). Based on complementary RNA data, nCRT increased IFNγ expression in tumor cells, perhaps as a result of the increased influx of cytotoxic T lymphocytes to balance the immune response by inducing tumor cells to express checkpoint molecules like PD-L1 and Indoleamine 2,3-Dioxygenase (IDO) (60). PD-L1 high expression on tumor cells was an independent prognostic factor for increased OS after RT (61). In another study (26) patients with esophageal adenocarcinoma (OAC) were divided based on their response to nCRT into poor, moderate, and good responders. Immunohistochemistry analysis was performed to quantify the expression of the following markers and subpopulations: CD3 (pan-T cell), CD4 (T helper cell), CD8 (62), FoxP3, and PD-L1 (expressed on cancer cells and antigen-presenting cells) (63, 64). Here, the tumor immune infiltrates, as seen by the CD3+ and CD8+ cells, were highly correlated with the cancer cell density. Surprisingly, only when the poor responders also displayed high levels of CD8+ T cells they had a poor OS, a trend that was not observed in the good/moderate responders. This result is contradictory to the consensus that high infiltration of cytotoxic T cells is favorable for the patient. A closer look at the phenotypic characteristics of these CD8+ T cells can shed more light on their specific function and on why their existence was negatively associated with OS.

In addition, the immune landscape can also be correlated with other aspects of the tumor microenvironment, and their

relationship with RT can be analyzed collectively. One of those characteristics is the tumor mutational burden (TMB) which refers to the total number of mutations in a tumor, is proportional to neoantigen production, and is used as a marker of immunogenicity (65). Researchers categorized EC patients into high TMB (TMB-H) and low TMB (TMB-L) based on the extent of TMB in their tumors (66). The patients were then further separated based on whether they got RT was their number of Tregs was quantified. Those not receiving RT had an increased influx of Tregs in the TMB-H group compared to the TMB-L group. However, RT patients from both groups showed no difference in immunosuppressive cell infiltration, which may indicate a balancing effect of the RT (66).

Higher TILs have been suggested by multiple studies to be a reliable prognostic factor for the progression of the disease. In ESCC patients treated with CRT, a higher TILs density in the stroma of biopsy samples during therapy was correlated with increased 5-year disease-free survival (DFS). These results might be used to predict the response of the patients to CRT avoiding unnecessary surgery. A more detailed investigation of the heterogeneous TIL compartment clarifying the different subpopulations would enhance the predictive validity of this model (67).

In conclusion, data from EC shows radiation to possibly have a positive effect on the recruitment of immune cells in the tumor and more specifically on CD8+ T cell infiltration. In addition, RT-dependent upregulation of immune checkpoint molecules such as PD-L1 is a promising indication for the combination of RT with immunotherapy.

Head and neck cancer

The term "head and neck cancer" refers to a group of cancers that are anatomically developed in the mouth, larynx, nose, sinuses, and throat, with squamous cell carcinoma (HNSCC) arising from epithelial cells lining the mucous membranes (68). In the case of HNSCC, radiation therapy is a standard treatment method that shows a better response in human papillomavirus (HPV) - positive patients than in HPV-negative ones (69). The virus-induced cancers display different biological and clinical characteristics but also dissimilar immune landscapes compared to their negative counterparts (70). A multicentre study analyzed the prognostic value of CD8+ and CD3+ T cells in correlation with HPV status in patients with HNSCC that underwent CRT treatment (71). This study concluded that the high density of cytotoxic T cells and HPV positivity are independent favorable factors for OS after CRT (71). This distinction of the virus status of HNSCC patients is therefore important to better exploit the unique characteristics of both subgroups and increase radiosensitivity.

Systemic immune landscape of HNSCC and radiotherapy

The combination of platinum-based chemotherapy and intensity-modulated radiotherapy (IMRT) in HPV-related oropharyngeal cancer shifted the balance into a systemic immunosuppressive state (72). After CRT an increased number of myeloid-derived suppressor cells (MDSC) and decreased numbers of CD8+ and CD4+ T cells were found while in the latter there was an upregulation in the expression of PD-1 immune-checkpoint molecule (72). These results partly come in agreement with the study of Sridharan et al. (73), which also showed an increase in circulating MDSC and in PD-1+ T cells. However, the systemic cytokine levels of CXCL10 and 16 respectively decreased and increased respectively in patients treated with radiation. CXCL10 is a cytokine believed to promote immunosuppression and tumor stemness (74, 75) while CXCL16 has a beneficial effect on cancer control since it promotes lymphocyte infiltration in the tumor (76). It is therefore clear that while an increase in immunosuppressive cell populations is observed, the cytokine profile changed to promote tumor regression.

J. Schuler and colleagues (77) compared the effect of CRT on the number of conventional CD4+ T cells (Tconv) and the subpopulation CD4+CD39+ Tregs that exercise their immunosuppressive action through the adenosine pathway (78). After CRT, the absolute number of CD4+ T cells and their percentage decreased, but within this Tconv population, CD4 +CD39+ Treg cells increased, indicating that these cells were relatively resistant to the CRT regimen used. Complementary to this, they found upregulation in CD39 expression, an ectonucleotidase involved in the adenosine pathway, which led to the conclusion that CRT might stimulate the suppressor functions of Tregs. The persistence of a highly immunosuppressive population of Tregs after CRT was observed at different time points which might explain the frequent recurrence of HNSCC (77).

iTME of HNSCC and radiotherapy in human samples

For nasopharyngeal carcinoma (NPC) the standard of care therapy is concurrent chemoradiotherapy (CCRT) which can have immunostimulatory effects and increase the patient's chances of survival (79). Chung et. al, focused on the Epstein-Barr viruspositive NPC, the most representative type of this cancer, and looked closely at the dynamic changes of the intratumorally T-cell clonotypes (ITCs) in search for predictive biomarkers for CCRT. They concluded that chemotherapy and RT combination drive the selection of ITCs to a remodeling of the unique TCRβ clonotypes. Surprisingly, CCRT does not lead to the expansion of the EBV-associated ITCs for an *in situ* vaccination effect as is widely believed to be the case (20, 27).

Most of the data available on head and neck cancer after RT are describing the systemic effect on the immune populations. This can always be seen as an indicator of the populations in the tumor contexture although we should be cautious when attempting to describe the iTME in head and neck cancer. Nevertheless, we can conclude that RT is increasing the number of immunosuppressive cell populations systemically like MSDCs and Tregs while also at the same time having a deleterious effect on CD8+ T cells. Intratumorally, an expansion in ITCs is observed therefore it would be very interesting to explore this further in relation to the systemic profile.

iTME of HNSCC and radiotherapy in preclinical models

As seen in patients, cells of the myeloid lineage show an expansion after RT (72). This has also been observed in a HNSCC murine model, where the density of CD11b+ infiltrated myeloid cells in the tumors increased after irradiation (80). Interestingly, when neutralizing antibodies against those bone marrow-derived infiltrates were used the tumors showed increased radiosensitivity and response to irradiation *in vivo* (81).

The interaction between the immune landscape and radiation in preclinical models of head and neck cancer is scarily known, but these studies remain important because they can provide insight into the driving pathways and sequence of events that shape the iTME.

Lung cancer

According to GLOBOCAN estimates for 2020 lung cancer is the primary cause of cancer-related mortality (82). From traditional approaches like surgery and RT to immunotherapy with ICIs, there are many ways to combat lung cancer and lung metastases. For all patients with advanced surgically treatable lung cancer, CRT is part of the treatment regimen and has been proven successful in controlling the disease (83). Moreover, immunotherapy has been shown to be helpful in treating non-small cell lung cancer patients who are PD-L1 positive (84). It is imperative that patients are divided into distinct groups in order to determine the most appropriate treatment approach for each, and the focus is once again on the tumor microenvironment and immune system (85).

Systemic immune landscape of lung cancer and radiotherapy

In a cohort of limited-stage small cell lung cancer patients (LS-SCLC), CRT resulted in an increase of all T cells (CD3+), cytotoxic T cells (CD3+CD8+), activated T effector cells (CD8+CD38+) and NKT cells (28). The same retrospective study also showed a reduction in the percentage of T helper cells (CD3+CD4+), naïve T cells (CD4+CD45RA+), B cells, NK cells, and T helper/T effector cell ratio in the patients. Of all these subpopulations of immune cells, the high densities of naïve T cells and activated effector T cell 3 months post-CRT were both independent predictor factors of good progression-free survival (PFS). Moreover, in line with results from the peripheral blood of Epstein-Barr virus-associated nasopharyngeal cancer patients referred to above (27), Wu et al. (29), also examined the systemic effect of irradiation on the T-cell receptor (TCR) repertoire in stage I non-small-cell lung cancer (NSCLC) and concluded that after RT the number of unique TCR clones was decreased. More interestingly, the higher the diversity of the TCR clones at baseline the more likely it was for the patient to respond well to stereotactic body radiation therapy (SBRT).

When examining lung cancer cases it is important to mention the transient or prolonged lymphopenia frequently observed after radiation and which depends on the thoracic volume that is targeted (86) and on the fractionation regimen (87). Lymphopenia can be used as a prognostic factor for disease progression (87) but also as a predictive marker since the neutrophil-to-lymphocyte ratio is negatively correlated with response to immunotherapy (88) and can help stratify the patients for alternative treatments after radiation.

iTME of lung cancer and radiotherapy in human samples

To study the dynamic changes in the immune contexture, Zhou et al. (89) analyzed paired tumor samples from NSCLC before and after SBRT. RT improved the TCR repertoire diversity, but also increased the PD-L1 expression in the TME. Moreover, there was an augmentation in the expression of immune-regulating factors such as C-X-C motif chemokines (CXCL10 and CXCL16), interferons (IFN I and II) and interferon receptors (IFN IR and IFN IIR) intratumorally. Drifting away from the TCR clonotypes and collectively looking at the TIL populations Shirasawa et al. (90), retrospectively accessed the impact of RT on the PD-L1 expression and CD8+ T cell infiltration in NSCLC patients. PD-L1 expression in cancer cells did not show a particular trend, however, the density of CD8+ T cells increased after CRT, which can be exploitable in the scope of ICI therapy. Of note, a meta-analysis for the gene signature was performed in patients with lung adenocarcinoma (LUAD) who were divided into groups: RR (radiotherapy resistant)-patients showing poor response to radiotherapy and RS (radiotherapy sensitive)-patients presenting with better prognosis after therapy (30). T cells, monocytic lineages, B lineages, fibroblasts, cytotoxic lymphocytes, CD8+ T cells, endothelial cells, and NK cells were enriched in the RS group, while neutrophils were enriched in the RR patients.

iTME of lung cancer and radiotherapy in pre-clinical models

Preclinical studies about the impact of radiotherapy on the immune landscape in lung cancer are more prevalent than clinical studies on human lung cancer. Zhang et al. (91) assessed the effect of irradiation on the immune contexture in a syngeneic murine model of Lewis Lung carcinoma. They graded the infiltrated MDSCs and cytotoxic CD8+ T cells in the tumors to find an increased recruitment of MDSCs-mediated immunosuppression. To further access the causal link between MSDS and cytotoxic T-cell infiltration, they depleted the polymorphonuclear (PMN) – MDSCs or inhibited the expression of arginase 1 (ARG1) on these cells. Both these actions led to a flux of CD8+ T cells inside the tumors. They concluded that PMN-MDSCs are upregulated after irradiation that they suppress the immune cells of the TME in an arginase-related manner. The systemic effect of irradiation was further examined in a primary lung tumor mouse model in which the B cell density increased while CD8+ cytotoxic T cells decreased showing a direct effect of irradiation on innate immunity (92). In a similar manner, the effects of low-dose fractionated RT on the iTME were studied in an orthotopic murine model (93). As seen before, radiation induced an expansion in the number of MDSCs, neutrophils and F4/80+ macrophages and more specifically the MHC-II_{hi} anti-tumoral M1 subpopulation, while on the other hand,

it significantly reduced the absolute number of CD8+ T cells in the spleen and lung. Further examination of the T cell compartment revealed expansion of Tregs (CS25+/CD127-) and PD-1+ T cells, suggesting a phenotypic shift towards immunosuppression that can be exploited for ICI therapy. Intratumorally, radiation recruits neutrophils as shown in a Lewis lung cancer adenocarcinoma murine model. The recruitment of tumor-associated neutrophils (TANs) leads to cytokine release and the subsequent CD8+ T cell infiltration. The increase in CD8+ T cell numbers in the TME is contradictory to the general trend of its systemic decrease after irradiation. This is a nice example of how a systemic effect does not necessarily translate in a similar manner intratumorally (94). To study the mechanism by which irradiation is affecting the immune cells in the tumor microenvironment, Wang et al. (95), performed *in vitro* experiments with NSCLC cell lines and CD8+ T cells from healthy donors. Contradictory to *in vivo* results that show an increase in PD-L1 expression in cancer cells, here they concluded that irradiation (IR) is augmenting CD8+ T cells immunity by suppressing PD-L1 expression in an IFNγ related manner.

Immunotherapy is frequently used in lung cancer, both alone and in combination with RT. Therefore, unraveling the immune landscape of the tumor could allow many patients to escape the adverse effects of the treatment. After radiation, there is an increase in the influx of MSDCs in the tumor but a balancing augmentation in the CD8+ T cells which comes in contradiction with the lymphopenia that is seen systemically.

Breast cancer

Breast cancer (BC), the most common cancer in women, is treated based on tumor staging, size, location, and the patient's health and preferences. Early-stage BC is usually treated with surgery and adjuvant RT and may also include CT or hormonal therapy. Advanced-stage BC focuses on controlling the disease and managing symptoms, with treatment options including CT, targeted therapy, hormonal therapy, or a combination (96, 97). The level of care provided for breast cancer is constantly changing, with emerging therapies and approaches, including immunotherapy, being researched, and evaluated through clinical trials. Likewise, research focusing on the immune landscape is underway to establish immune-based predictive biomarkers to improve patient stratification (98). As RT is primarily administered as an adjuvant treatment following surgery (96), efforts to identify biomarkers are shifting their focus toward the systemic immune landscape, rather than the iTME.

Systemic immune landscape of BC and radiotherapy

Radiation therapy is often associated with lymphopenia in breast cancer patients since the lung and heart, the two organs that contain blood in the thorax, are situated within the radiation field. This systemic state seems to be persistent even one year after RT (99). Therefore, it is crucial for clinicians to create dependable dosimetric models for use as a benchmark in dose prescription and treatment planning. Chen et al. investigated the connection between effective dose to the circulating immune cells (EDIC) and radiation-induced lymphopenia (RIL) in a group of breast cancer patients (100). The EDIC model calculates the dose based on the portion of blood flow to the lung, heart, and liver, as well as the body surface area exposed to radiation (101). As the EDIC value increased, the RIL rose correspondingly, suggesting that this model accurately reflects the dosimetric factor that directly affects lymphopenia. A more thorough examination of the subpopulations impacted by adjuvant RT revealed a decrease in T-cells and platelets, but not immunosuppressive myeloid subpopulations (CD13+CD56+ cells) (102). This comes into contradiction with the meta-analysis by Wang et al., which shows no significant difference in peripheral blood T cells after RT (18). However, it is important to highlight that the time point of the blood sampling after RT (immediately after or 48h later, etc) plays a role in the result recorded. A study looking at the T cell compartment in the blood found that adjuvant RT increased the memory and regulatory CD4+ T cells (103) which agrees with the increase in T helper cells during RT seen by Sage et al. (99). It is yet to be determined if these T helper cells are a representation of Tregs, and whether alternative therapeutic options could be employed to prevent immunosuppression. Given these discoveries, it is essential to conduct further research on peripheral blood immune populations to establish dependable biomarkers for monitoring disease progression and potential treatment combinations.

iTME of BC and radiotherapy in human samples and pre-clinical models

The reciprocal relationship between RT and iTME has not been extensively studied in breast cancer, as RT is not typically used as a NAT treatment for this type of cancer (104). However, the specific immune cells present in the iTME appear to be important for disease progression, as demonstrated by Schnellhardt et al. (105), who found that high densities of B and memory cells were associated with reduced DFS in early-stage BC. This led to the development of a prognostic score based on the cell densities of these subpopulations in the tumor core and stroma to determine different patient risk groups. Although patient data is limited, pre-clinical data can provide insight into the relationship between RT and iTME in breast cancer. *In vitro* studies have shown that RT of breast cancer cell lines (2 Gy or 5 Gy) resulted in an upregulation of the immune checkpoint molecules PD-L1 and PD-L2, which may have implications for combination with immunotherapy (106). The study of iTME in breast cancer aims to establish treatment combinations rather than biomarkers, as RT is mainly given in an adjuvant setting and thus the iTME is unlikely to affect treatment response.

Thus, radiotherapy is a frequently used supplementary treatment for breast cancer and has the potential to affect the immune system. The occurrence of low lymphocyte count induced by radiotherapy can contribute to the creation of immune tolerance. Additionally, radiotherapy may alter the composition of different subsets of the body's immune system, affecting T cells while having

no impact on myeloid suppressor cells. To better understand these changes and develop more effective radiotherapy regimens with or without concordant immunotherapy, further research is necessary.

Cervical cancer

Cervical cancer ranks second in incidence and mortality among women from countries with Human Development Index (HDI) (107) following breast cancer and is developed following an HPV viral infection (108). Research in the tumor microenvironment shows a highly heterogeneous profile that can be altered with the use of radiation.

Systemic immune landscape of cervical cancer and radiotherapy

Comparing the dynamic changes in the systemic immune contexture with the landscape of the TME can be very interesting to further understand the interactions taking place. In this scope, a retrospective study compared the effect of CRT in cervical cancer patients using blood samples and cervical brushing specimens at the same time points. CRT seemed to have a stronger effect on the tumor microenvironment since there was a significant decrease of the T helper cells intratumorally that was not seen in the periphery and more interestingly there was an increase in the activated T cells (CD69+ cells) only in the cervix (109).

iTME of cervical cancer and radiotherapy

Radiotherapy can have stimulatory effects on the iTME as was seen in a prospective analysis of tumor-associated macrophages (TAMs) of patients treated with radical RT (110). A RT-dependent increase in the number of TAMs in cervical cancer tissue and a parallel shift towards the M1-like or pro-tumoral phenotypic state of macrophages (increased expression of CCR7 and decreased expression of CD163) was observed. Extracellular vesicles (EVs) were found to be responsible for the reprogramming of TAMs and the increased phagocytic activity ex vivo, although further pre-clinical investigation is needed.

As far as lymphocytes are concerned, Li et al. (111). prospectively analyzed the dynamic changes in the iTME of patients with cervical cancer that were treated with CRT. The number of CD4+ and CD8+ T cells in the tumor decreased at the same time as PD-1 expression and TCR diversity declined. In accordance with these results, another study also showed significant reduced cytotoxic (CD8+) T cell and T regulatory cell infiltration after RT as seen in paired pre-RT biopsies and post-RT surgical specimens (112). Interestingly, they could not see a difference in the effect of RT on the PD-1 and PD-L1 expressing cells. Most notable was the data from Mori et al. (113), where they saw that the stromal CD8+ T cells increased only in the patients receiving RT alone while the combination of CRT caused a reduction in the same population. Although in contradiction with previous data that observed an increase in CD3+ T cells when using chemotherapy, this might suggest a systemic effect of chemotherapy that is mirrored in the iTME (114).

The data gathered from studies of cervical cancer suggest a highly heterogeneous environment, but there is a trend in which RT has an ablative effect on intratumorally T cells (115). This needs to be considered when the question of the implementation of immunotherapy arises since the cold iTME may present a greater risk of toxicity.

Ovarian cancer

Ovarian cancer is the most lethal female reproductive malignancy representing 1% of all new cancer cases and it is often characterized by late-stage diagnosis (116). Therapy usually consists of debulking surgery with neoadjuvant or adjuvant chemotherapy to reduce the tumor burden (117). Neoadjuvant chemotherapy has been shown to increase the infiltration of T regulatory cells (118) and stromal lymphocytes (119) which has implications for the use of immunotherapy. In recent years, new immunotherapeutic approaches such as ICIs, chimeric antigen receptor (CAR)- and TCR-engineered T cells are used therefore the immune landscape is brought to the forefront of ovarian cancer research (120). RT is rarely used in ovarian cancer, as these tumors spread through the peritoneal cavity, conventional radiation therapy targeting large volumes being too risky because of toxicity (121). To bypass this large-volume toxicity, researchers used low-dose radiation therapy (LDRT) in an *in vivo* orthotopic ovarian cancer model to reprogram the TME and enable immunotherapy to work more effectively (122). They observed an IFNγ-depended intra-tumoral influx of cytotoxic T cells, T helper cells and monocytes following low-dose radiation of 1Gy that can be combined with immunotherapy for a synergistic effect toward tumor regression. Most intriguing were the results of the following clinical study on patients with cold tumors where they also showcased an increase in T helper cells after radiation with subsequent tumor responsiveness to therapy. It would be interesting to see in the future more studies in larger cohorts to examine the combination of low-dose radiation therapy and immunotherapy in ovarian cancer.

Prostate cancer

Prostate cancer is the second most common cancer type in men above 50 years old (123). The biomarker that is used throughout prostate cancer follow-up is the prostate-specific antigen (PSA), and in recent years immunological parameters have been investigated for their prognostic and predictive validity (124).

Systemic immune landscape of prostate cancer and radiotherapy

Normofractionated RT was found to temporally decrease the density of T and B cells in a prospective immuno-modulating study (125). Moreover, the peripheral subsets of regulatory T cells and NK cells increased during treatment, which is in line with pre-clinical prostate cancer models (126, 127). Radiotherapy with charged particles such as carbon ions (CIR or carbon ion radiotherapy) was used in a

cohort of prostate cancer patients to ensure better dose distribution and greater relative biological effectiveness (RBE). Interestingly, among the immunomodulatory effects of CIR, they found a persistent increase in T helper cells during follow-up in parallel with an increase in CD19+ cells associated with a humoral activity. In addition, after CIR, the ratio of T helper to cytotoxic T cells (CD4+/CD8+) was higher in responders than in non-responders, indicating the immunological status to predict CIR outcome (128). Since CIR therapy has not been studied extensively yet, more research is needed to determine its effect on the immune landscape.

Photon radiotherapy can have an ablative effect, which can be avoided by using particle radiotherapy, such as CIR, however since there is further investigation is needed.

iTME of prostate cancer and radiotherapy

According to one of the first studies that looked at the effects of prostate SBRT on the immune landscape, radiation increases CD68 and CD163 macrophages while harming CD8+ T cells (126). The authors suggest further investigation with transcriptomic analysis in order to connect these alterations in the iTME with intratumoral cytokine profile. Moreover, macrophages showcase vast and complex plasticity in cases where they express mixed M1 and M2 surface markers (129). Therefore, the in depth transcriptomic analysis of the myeloid subpopulations will shed a light on their role in the iTME of prostate patients after RT.

iTME of prostate cancer and radiotherapy in a pre-clinical model

After SBRT, the iTME shifts towards a more immunosuppressive phenotype as evidenced by the increase in M2 macrophages and the decrease in cytotoxic T cells. An *in vivo* murine prostate cancer tumor model, presented after irradiation, an increase in Treg populations in the spleen and other organs (127). In particular, when TRAMP-C1 tumors were locally irradiated, this resulted in a greater percentage of CD4+CD25^{hi}Foxp3+ cells in the spleen while at the same time, all these cells expressed the exonuclease CD39. As a result, it appears that Tregs are not only escaping the harmful effects of this specific radiation dose regimen but are also retaining their immunosuppressive capacity.

Altogether, we can conclude that RT in prostate cancer is driving the TME toward immunosuppression. In one study by Fang Yu et al. (130), they tried to render the "cold" tumors "hot" by local injections of interleukin-12 in combination with RT to boost the immune system. They saw recruitment of Th1 and CD8+ T cells in the tumors after the combination therapy which resulted in a significant decrease in tumor size compared to the control group with RT alone. It would be interesting to investigate the effects on immune-checkpoint molecule expression in order to evaluate whether immunotherapy could be beneficial for these patients.

Pancreatic cancer

The most prevalent form of this cancer is the exocrine pancreatic ductal adenocarcinoma (PDAC) (131), which is among the most aggressive solid tumors due to the highly immunosuppressive TME and poor response to chemotherapy, radiotherapy and immunotherapy. This poor treatment response may in part be explained by the dense desmoplastic stroma and the abundance of immunosuppressive cells in the PDAC TME, which excludes antitumoral T cells, resulting in a *cold* tumor (132, 133). Radiation can, therefore, be beneficial in boosting the immune system's response to systemic therapies and in achieving tumor regression by altering the TME (134, 135).

Systemic immune landscape of pancreatic cancer and radiotherapy

In the context of pancreatic cancer, prognostic and predictive value may be conferred by systemic inflammatory markers. The survival rate of patients with locally advanced PDAC treated with SBRT was lower when the neutrophil-to-lymphocyte ratio (NLR) was high before treatment (136). Moreover, when localized pancreatic cancer is treated with anti-PD-1 antibodies, NLR is elevated due to lymphocyte depletion after SBRT and associated with worse survival (137). Low lymphocyte-to-monocyte ratio (LMR) after nCRT therapy followed by surgery was a poor predictor for prognosis in patients with borderline resectable pancreatic cancer (BRPC) (138). The poorer survival rate in BRPC and locally advanced unresectable pancreatic cancer (LAUPC) was confirmed to be associated with a high monocyte count but also a low γδ T cell count (139). γδ T cells are lymphocytes that are found in great numbers in the intestine and dermis (140). As this *unconventional* lymphocyte subset requires no cross-presentation of MHC, it has demonstrated enhanced effector capacity *in vitro*, which can explain why low numbers of it are associated with poor survival in humans (141). In addition, in a randomized controlled trial, serum levels of the pro-tumor CXCL8 cytokine were associated with a favorable prognosis in patients undergoing CRT for pancreatic cancer (37). As a result of RT-induced release of CXCL8 from tumor cells, NK infiltrates increased in PDAC tumors with cytotoxic gene signatures. It appears that CXCL8 plays a role in activating immune surveillance against tumors after RT, however, a detailed analysis of the systemic cytokine profile of patients is needed to draw more definitive conclusions. Additionally, since the NLR and LMR ratios have gained prominence as prognostic markers for pancreatic cancer (142, 143), multicenter studies with larger cohorts are recommended to implement these markers in regular clinical practice.

iTME of PDAC and radiotherapy in human samples

Radiation of the TME can induce immunogenic cell death since the increased antigen presentation stimulates an immune response against tumor cells. Hence, after nCRT an increased expression of DAMPs such as calreticulin, Hsp70, and MICA/B is observed. Moreover, there is an increase in the absolute number of T helper and cytotoxic cells (CD4+ and CD8+ respectively) and most importantly the Treg/TIL ratio is decreased and can be used as a predictor for longer survival (144).

Tumor samples that were treated with SBRT presented with increased immunogenic cell death (ICD) and PD-1+ T effector infiltrate compared with the untreated control group (145). A spatial analysis of this subpopulation revealed that these cells to be were outnumbered by surrounding immunosuppressive myeloid populations (monocytes, macrophages, and granulocytes), which could limit their function. Although the writers acknowledge that these cells are prone to exhaustion, they refer to the subpopulation of cytotoxic T cells expressing PD-1 as activated T cells to further support their claim that combining ICI therapy with RT will improve therapeutic outcomes in PDAC.

A detailed analysis of how radiation affects the immune landscape will shed light on the possibility of using CRT to downgrade PDAD tumors in a neoadjuvant setting (146, 147). In a study comparing nCRT to upfront surgery the number of T helper cells, B cells and Tregs decreased in the stroma but not in the tumor core (38). In addition, only M2-like macrophages in the tumor core were a reliable predictor of early disease recurrence after nCRT for PDAC. An interesting finding was that M2 TAM infiltration (CD206+ cells) decreased more in female PDAC patients after nCRT (148). The immune landscape and RT response in patients with PDAC may thus be affected by biological sex; however, conclusions cannot be drawn until further research on the subject is conducted.

iTME of PDAC and radiotherapy in pre-clinical models

With a murine pancreatic cancer model, Ye et al. evaluated the ability of SBRT to induce immunogenic cell death (149). They found SBRT with concurrent chemotherapy to increase antigen presentation and cytotoxic T-cell infiltration. The infiltrated cytotoxic T cells had an increased capacity for secreting IFNγ and elucidating an immune reaction. In another study, low-dose irradiation of pancreatic tumors in mice resulted in increased numbers of iNOS pro-inflammatory macrophages and subsequently the recruitment of T cells into the tumors (150). However, the data are conflicting since in an orthotopic pancreatic murine tumor model the proportion of M2 anti-inflammantory macrophages increased upon irradiation (151). Moreover, the shift towards an immunosuppressive milieu was further backed up by data showing fewer CD8 T cells and more T-helper 2 and T-regulatory cells present in the irradiated pancreata compared to controls. An additional study found that after low-dose irradiation of insulinomas, iNOS was upregulated in the peritoneal macrophages, whereas markers of M2 macrophages were downregulated, suggesting a skewing towards M1 macrophages after RT (152). Thus, in this subtype of pancreatic cancer, RT seems to be beneficial since it shifts the balance towards anti-tumoral effects. Further studies need to be performed to give a definite result.

In conclusion, PDAC TME is a complex network of interactions with different immune cell populations that can confer predictive validity as biomarkers. Consequently, some patients may benefit more from a combination of radiation and immunotherapy targeting these cells in order to achieve the best results.

Colorectal cancer

Colorectal cancer (CRC) is the third most common cancer type worldwide (153) and, due to lifestyle changes, it is becoming more common among individuals younger than 50 years old (154). Cancers of the colon (sigmoid, descending, transverse, and ascending) and rectum, which make up parts of the large intestine, are classified as colorectal cancers (155).

Colon cancer

iTME of colon cancer and radiotherapy in pre-clinical models and human samples

Radiation was found to increase the infiltration of immune cells into colon tumors in a murine model (156). More specifically, the number of macrophages ($CD11b^{high}$/F4-80+) increased on day 5 after hypofractionated radiotherapy while the number of APCs (MHCII +) and cytotoxic T cells increased significantly on day 8 compared to the non-irradiated controls. It is interesting to note that the infiltration of these cells only takes place during a very short period something that needs to be considered when designing treatment schedules. The importance of timing was also highlighted by Gerber et al. (157). Since they could distinguish the responsive tumors from the non-responsive ones as early as 4 days after irradiation. Most notably, in the tumors responding well, they could see an increase in the levels of IFN-γ and the infiltration of immune cells was increased to further boost the activity of the cytotoxic T cells. In a syngeneic colon cancer model, Joseph et al. (158) observed an expansion of CD8+ T cells after CRT and more specifically of tumor-specific CD3+ tissue-resident memory cells (T_{RM}). Dissecting the molecular mechanism behind this expansion and activation, the researchers identified the tumor-draining lymph node (TDLN) resident CD103+ dendritic cells to be the drivers of this priming (158). Based on other preclinical data, radiation enhances antigen-presenting cells' activity, as expected due to immunogenic cell death (ICD). A therapy targeting these cells can develop in the form of antibodies against checkpoint molecules such as CD47 (159, 160) that may synergize with radiation to promote tumor regression.

In human CRC biopsy samples, Schaue et al. focused on the effect of radiation on tumor-specific T-cell reactivity (161). After completing CRT, they found that tumor-specific T cells increased in the majority of patients. Moreover, the T cells expressing survivin, a tumor-specific antigen found in many cancers and believed to be immunogenic (162), did not decrease indicating that the treatment did not impair their ability to respond.

Rectal cancer

Although, rectal cancer (RC) and colon cancer are commonly lumped together under the umbrella term colorectal cancer, but in recent years, there has been growing evidence that they yield more differences than just the anatomical location. In particular, they

differ in embryonic origin, physiological function, anatomy, metastatic patterns, and first-line therapy, so it is important to separate the two when studying them (163). Rectal adenocarcinomas, the most prevalent form of rectal cancer, develop from malignant epithelial cells in the last 15cm of the colon, and for patients presenting with locally advanced rectal adenocarcinoma (LARC) neoadjuvant treatment that includes radiation is commonly prescribed (164). At the same time, total mesorectal excision surgery, which removes the entire rectum and the surrounding mesorectum with the pararectal lymph nodes, is the standard of care after neoadjuvant treatment, and negatively impacts the quality of life (QoL) of the patient (165). There is increasing interest in non-surgical strategies to decrease treatment-related toxicity after complete tumor remission due to neoadjuvant treatment (166). Therefore, patients that present with early-disease stages, responding better to nCRT, could be spared of the detrimental effects on the QoL of total mesorectal excision if they could be accurately stratified before surgery. As a result, patients could be categorized for a wait-and-watch approach to spare the organ and eventually achieve local control based on the immune landscape, both systemically and intratumorally.

Systemic immune landscape of rectal cancer and radiotherapy

The neutrophil, platelet, and lymphocyte count after CRT have been associated with prognosis in multiple cancer types. In rectal cancer, a high systemic inflammation index (SII) was associated with poor OS after CRT in patients with rectal cancer (167). The SII is a measure of the neutrophil to platelet count with the total lymphocytes and can accurately describe the systemic immune landscape (168).

iTME of rectal cancer and radiotherapy in human samples

Recently, immunological tissue-based biomarkers started to gain momentum with the most noticeable being the Immunoscore which measures the density of CD3+ and CD8+ TILs (169). To date, the Immunoscore has been confirmed to have a prognostic-only value after a meta-analysis of 10.000 colon cancer patients showing a high immunoscore (IS=4) to be correlated with the lowest risk of recurrence, the longest OS and the longest DFS (35, 170). As far as radiation is concerned, a biopsy-based immunoscore (ISb) was successfully used to predict response to neoadjuvant chemotherapy and selection for watch-and-wait therapy in patients with LARC (32). Moreover, the immunoscore was analyzed in pairs of biopsies and surgical samples of rectal cancer patients that received nCRT. After CRT Anitei et al. saw a significant increase in the infiltrating CD3+ and CD8+ cells that also correlated with tumor downstaging marking the immunoscore as a good potential biomarker for response to RT (36). Furthermore, an increase in the influx of CD3+ and CD8+ TILs was observed in post-treatment samples compared to the pre-treated counterparts suggesting an immunogenic effect of radiation (171). The most recent validation for immunoscore as a strong predictive biomarker comes from a study by Sinicrope et al. (172), where the higher DFS of patients with stage III colorectal cancer was predicted by their high immunoscore using Immunoscore® Colon CE-IVD test standardized assay indented for routine clinical practice (173). Given all of these, there is a strong correlation between immunoscore and response to treatment. However, functional evaluation of T cells is always required since high density does not necessarily indicates cytotoxic activity.

Another study by Mirjolet et al. analyzed the immune infiltration of cytotoxic T cells and Tregs in biopsies and surgical sample pairs of patients that received preoperative RT for LARC. The infiltration was assessed by calculation of the CD8+/FoxP3+ ratio in the epithelium and stromal compartment. A decrease in Treg populations was observed after the use of RT whereas the density of cytotoxic T cells remained unchanged leading to an overall increase in the ratio (174). To better support these data, another study also found an increase in the cytotoxic T-cell density in samples taken during RT compared to the pre-treatment samples (175). As observed in patients by Joseph et al. (158), CRT also polarizes the iTME towards an activated and memory Th1 transcriptomic signature. Interestingly, the same group saw a higher expression of PD-L1 by immune cells in CRT compared to RT alone, which could be exploited later with the use of ICI. The presence of T helper cells in the TME influences other cell populations such as cytotoxic T cells as was shown by mIHC of the different cell neighborhoods (46).

Following these data, Kamran et al. (34) evaluated transcriptomics data from pre- and post-CRT–matched tumor samples from a cohort of rectal cancer patients that included several non-responders (NR). As expected, CRT changed the immunological profile with an increase in the immune cell infiltration of naïve B cells, cytotoxic T cells, monocytes, pro-tumoral macrophages and resting mast cells. On the other hand, CRT seemed to negatively affect the memory B cells and activated mast cells that were abundant in the pre-CRT samples.

iTME of rectal cancer and radiotherapy in pre-clinical models

Irradiating *ex-vivo* non-treated human rectal cancer tissue and assessing phenotypically the macrophage populations with flow cytometry, Stary et al., observed polarization of the irradiated TAMs towards an M1-like phenotype which was functionally supported by *in vitro* data showing increased levels of phagocytosis after low-dose radiation. More interestingly, they observed an increase in the M1/M2 ratio in rectal cancer patients that underwent hyper-fractionated short-course RT compared to treatment-naïve specimens from patients of the same clinical TNM stage (176). In another study, Wilkins et al. analyzed the immune gene expression profiles (GEP) of sample pairs of pre-treatment biopsy and surgical excision after RT/CRT and there was an increase of the M2-like phenotypic marker CD163 in non-responders to RT. In addition, after RT, the good responders adopted an immune-hot phenotype with increased T-cell

infiltration, upregulation of inflammatory pathways and "wound repair" stroma phenotype (33).

It is challenging to study the immune landscape associated with gastrointestinal cancer because of its heterogeneous nature (see Figure 2) but we can observe a shift towards M2 polarization after RT and an increase in the influx of CD8+ T cells intratumorally in the same way as in other tumor types.

Anal cancer

Anal squamous cell carcinoma (ASCC) is a rare disease whose incidence is increasing in the western world (177) and is linked to human papillomavirus (HPV) (178). In a cohort of locally advanced anal carcinoma patients with HPV-positive and negative cases, the majority were treated with CRT or RT alone. After a follow-up period of 20 years CD3+, CD8+ and PD-1+ tumor-infiltrating lymphocytes were revealed as favorable prognostic markers after radiation (179). As we have seen in other types of cancer, this result is not uncommon. Worth noting, that CD4+ T cell numbers in either too low or too high density, which is considered a hormetic effect (180), also predicted more favorable outcomes for the patients. The authors hypothesized that the balance between the different subpopulations of CD4+ T cells (Th1, Th2, Th17, Treg) is the main reason why good prognosis can be associated with both low and high concentrations of T helper cells. As pro-inflammatory and pro-tumor immune cells share common markers, phenotypic characterization of these subpopulations is valuable for the understanding of TME. There is a need for further investigation of this phenomenon, but anal cancer immune landscape studies are limited following RT. Luckily, the pattern of favorable prognosis correlated with hot TME can be seen (and thus studied) in other cancers as well.

Liver cancer

Hepatocellular carcinoma

Hepatocellular carcinoma (HCC) is the most common form of liver cancer accounting for more than 80% of the cases and has a higher mortality rate. There is great heterogeneity in HCC which can be expanded into three different levels: interpatient heterogeneity where the differences can be seen from patient to patient, intertumoral heterogeneity from one tumor nodule to another and intratumoral heterogeneity between the different regions of the same tumor (181, 182). This vast heterogeneity can be seen in the iTME and influences the response to the various treatments (183). Craciun et al. showed that after selective internal

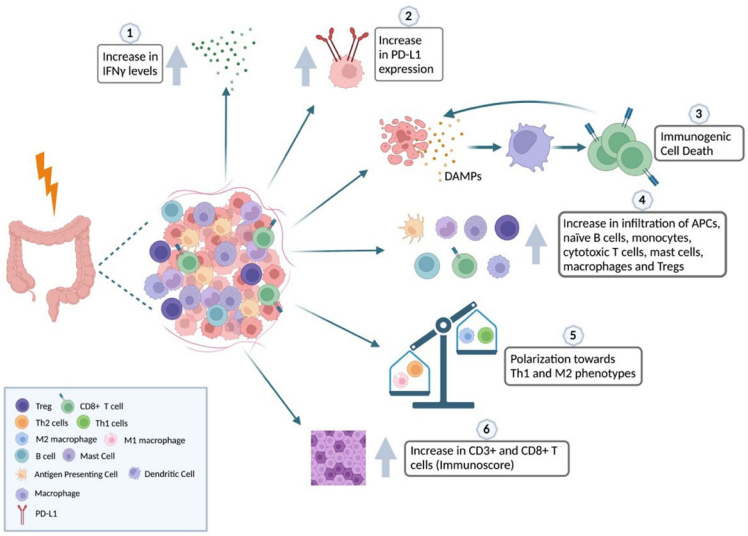

FIGURE 2
Impact of radiation in the iTME of colorectal cancer. The relationship between radiotherapy and the immune landscape of CRC is complex and context-dependent. Radiotherapy has the potential to harm normal tissues and stimulate the secretion of inflammatory cytokines like IFNγ (1). This, in turn, can recruit immune cells that hinder the immune response against the tumor. Additionally, radiotherapy can trigger the upregulation of immune checkpoint molecules that block immune cell activity (2). However, radiotherapy can also induce immunogenic cell death (ICD), a process where cancer cells release molecules that activate the immune system and promote an immune response against the tumor (3). ICD can increase the infiltration of immune cells, such as APCs, naïve B cells, monocytes, cytotoxic T cells, mast cells, macrophages, and Tregs, into the tumor microenvironment (4). Furthermore, radiotherapy can shift the balance of macrophages towards a pro-tumoral phenotype and T-helper cells towards the Th1 phenotype involved in cell-mediated immunity (5). Effective use of radiotherapy in CRC treatment depends on various factors, such as tumor stage and location, patient characteristics, and the timing and sequencing of radiotherapy with other treatments, including chemotherapy and immunotherapy. Using biomarkers, such as the Immunoscore based on the densities of CD3+ and CD8+ T cells, can help classify patients better, as it has been shown to increase after RT and correlates with tumor downstaging and potential response to therapy (6). Created with BioRender.com.

radiation therapy (SIRT) the infiltration of T helper and cytotoxic, and granzyme B expression was significantly increased in patients with HCC indicating a shift towards an immunostimulatory milieu (184).

Systemically, lymphopenia is a common side effect of radiation in the immune landscape and can be used as a biomarker. Also in HCC, the NLR is elevated after SIRT. An elevated NLR or low lymphocyte count is a poor prognosis factor for disease progression and should be considered for decision-making during and after treatment (31). A short fractionation regimen of RT could potentially spare the lymphocyte population from depleting and speed the recovery of the patient after therapy (185). This result was confirmed by another cohort of HCC where the elevated number of circulating lymphoid cell populations was correlated with better OS after irradiation (33).

Finally, to unravel the abscopal effect, the indirect shrinking of the tumors outside the irradiated field due to systemic immune modulatory properties of the radiotherapy, Hee Park et al. (186) used a murine model of HCC which revealed an increase in the number of tumor-specific T cells and IFN expression in splenocytes after RT. Moreover, a subsequent increase of dendritic cells in the tumor-draining lymph nodes and of cytotoxic T cells in the metastatic tumor site further supports the hypothesis of fimmu.2023.1148692the irradiation-induced activation of the immune system (187).

Intrahepatic cholangiocarcinoma

Primary liver cancer has two common subtypes: HCC developing from hepatocytes and intrahepatic cholangiocarcinoma (ICC) that arise from the small intrahepatic bile duct epithelium (188).

When looking at patients with ICC after hypofractionated proton therapy, strangely a longer OS was significantly correlated with a higher number of naïve (CD4+CD25+) and memory (CD4+CD127+) T cells in the blood at the beginning of hypofractionated proton therapy (189). For HCC patients, the same subpopulations of cells did not have any significance, since only the activated cytotoxic T cells (CD8+CD25+) mid-treatment were a strong prognostic factor for survival. In another study, the MDSC monocytic subtype of $CD14^{+}HLA\text{-}DR^{-/low}$ which is part of the immature myeloid cell lineage and is thought to be highly immunosuppressive significantly increased in the blood of HCC patients after radiation therapy (3D-CRT or IMRT) (190).

Further studies are required to clarify the effects of radiation on the immune landscape based on the limited results from the two subtypes of liver cancer. The radiation therapy for HCC, however, has the potential to increase the infiltration of TIL, as it does for other cancer types, which may be beneficial to patients.

Skin cancer

Skin cancer includes basal cell carcinoma (BCC) and squamous cell carcinoma (SCC), together with merkel cell cancer collectively named non-melanoma skin cancers (NMSC) and melanoma. A skin malignancy's type and stage at the time of diagnosis determines the treatment options. In terms of cosmetic and functional outcomes, radiotherapy may offer better tissue preservation in definitive, adjuvant and palliative settings than surgery. NMSCs are radioresponsive tumors and have local control rates of 90-95% after RT (191). Melanoma is less radiosensitive but interestingly immunotherapy is particularly effective and the combination with RT is believed to yield promising results (192, 193). It is possible to identify potential markers to guide future treatment plans by analyzing the immune landscape after RT for skin cancer (194). In this scope, Bazyar et al. (195) assessed the immunological changes using micro planar radiation therapy (MRT), a technique that spatially delivers high-dose beams (peaks) in certain tumor regions sparing other areas (valleys). The advantage of this technique is believed to be the greater protective effect on normal tissue and tumoral specificity. In their study, micro planar radiation therapy was compared to CRT in a radioresistant B16-F10 murine melanoma model yielding better tumor regression and survival. Most importantly, this effect was attributed to a higher influx of CD8+ T cells and a lower influx of intratumoral Tregs.

Perspectives

The heterogeneity of primary tumors among patients (interpatient heterogeneity) and even within the same patient (inter– and intra- tumoral heterogeneity) hinders oncology. It is imperative to overcome the bottleneck of heterogeneity along with a shift towards personalized treatment so medical decisions and interventions can be tailored to the individual. The study and elucidation of the iTME can help in both directions since on the one hand, the immune contexture can be common between different histological cancer types as analyzed in this review, and on the other hand, the immunological profile of the tumor can serve as a guide to treatment.

Several advantages of radiotherapy are offered to patients, such as tumor downstaging for better growth control and easier surgical removal, localized treatment with less toxicity in healthy organs than systemic chemotherapy and ICIs, as well as the recent option of organ preservation, which increases the quality of life for patients. Enhancing radiotherapy's effectiveness is therefore in the patient's best interests. Various factors can affect the response to radiotherapy, one of which is the immune landscape systemically and/or intratumorally. A wide range of factors influences the effect of radiotherapy on the immune landscape, including dose and fractionation, target volume, radiation fields, and histological type and grade. It is important to understand how radiotherapy changes the immune landscape, as well as how the existing immune landscape influences the patient's response, in order to develop therapeutic interventions that will improve the efficacy of radiotherapy and convert some ineffective responses into effective ones.

Author contributions

CI collected the data and drafted the manuscript. MK revised the manuscript. DG, PM, LV and CB provided additional revisions. All authors contributed to the article and approved the submitted version.

Funding

This work benefits from the support of "L'Association Jules Bordet". CI is a FRIA grantee of the Fonds de la Recherche Scientifique - FNRS under grant n° 1.E.002.23F.

Conflict of interest

The authors declare that the research was conducted in the absence of any commercial or financial relationships that could be construed as a potential conflict of interest.

Publisher's note

References

1. Vogelstein B, Papadopoulos N, Velculescu VE, Zhou S, Diaz LA, Kinzler KW. Cancer genome landscapes. *Science* (2013) 339:1546–58. doi: 10.1126/science.1235122

2. Hanahan D. Hallmarks of cancer: New dimensions. *Cancer Discovery* (2022) 12 (1):31–46. doi: 10.1158/2159-8290.CD-21-1059

3. Khalaf K, Hana D, Chou JTT, Singh C, Mackiewicz A, Kaczmarek M. Aspects of the tumor microenvironment involved in immune resistance and drug resistance. *Front Immunol* (2021) 12:1764. doi: 10.3389/fimmu.2021.656364

4. Dunn GP, Bruce AT, Ikeda H, Old LJ, Schreiber RD. Cancer immunoediting: from immunosurveillance to tumor escape. *Nat Immunol* (2002) 3(11):991–8. doi: 10.1038/ni1102-991

5. Pérez-Romero K, Rodríguez RM, Amedei A, Barceló-Coblijn G, Lopez DH. Immune landscape in tumor microenvironment: Implications for biomarker development and immunotherapy. *Int J Mol Sci* (2020) 21:5521. doi: 10.3390/ijms21155521

6. Bruni D, Angell HK, Galon J. The immune contexture and immunoscore in cancer prognosis and therapeutic efficacy. *Nat Rev Cancer* (2020) 20(11):662–80. doi: 10.1038/s41568-020-0285-7

7. Guinney J, Dienstmann R, Wang X, de Reyniès A, Schlicker A, Soneson C, et al. The consensus molecular subtypes of colorectal cancer. *Nat Med* (2015) 21(11):1350–6. doi: 10.1038/nm.3967

8. Thorsson V, Gibbs DL, Brown SD, Wolf D, Bortone DS, Ou Yang TH, et al. The immune landscape of cancer. *Immunity* (2018) 48(4):812–830.e14. doi: 10.1016/j.immuni.2018.03.023

9. Bagaev A, Kotlov N, Nomie K, Svekolkin V, Gafurov A, Isaeva O, et al. Conserved pan-cancer microenvironment subtypes predict response to immunotherapy. *Cancer Cell* (2021) 39(6):845–865.e7. doi: 10.1016/j.ccell.2021.04.014

10. Amin MBAmerican Joint Committee on Cancer, American Cancer Society. *AJCC cancer staging manual. Eight edition*. Mahul B, Amin ,MD, Edge SB, Gress DM, Meyer LR, editors. Chicago IL: American Joint Committee on Cancer, Springer (2017). p. 1024.

11. Lievens Y, Schutter HD, Stellamans K, Rosskamp M, Eycken LV. Radiotherapy access in Belgium: How far are we from evidence-based utilisation? *Eur J Cancer* (2017) 84:102–13. doi: 10.1016/j.ejca.2017.07.011

12. Lhuillier C, Rudqvist NP, Elemento O, Formenti SC, Demaria S. Radiation therapy and anti-tumor immunity: exposing immunogenic mutations to the immune system. *Genome Med* (2019) 11(1):1–10. doi: 10.1186/s13073-019-0653-7

13. Wei J, Montalvo-Ortiz W, Yu L, Krasco A, Ebstein S, Cortez C, et al. Sequence of αPD-1 relative to local tumor irradiation determines the induction of abscopal antitumor immune responses. *Sci Immunol* (2021) 6(58):eabg0117. doi: 10.1126/sciimmunol.abg0117.

14. Hellevik T, Berzaghi R, Lode K, Islam A, Martinez-Zubiaurre I. Immunobiology of cancer-associated fibroblasts in the context of radiotherapy. *J Transl Med* (2021) 19 (1):437. doi: 10.1186/s12967-021-03112-w

15. Bando H, Tsukada Y, Ito M, Yoshino T. Novel immunological approaches in the treatment of locally advanced rectal cancer. *Clin Colorectal Cancer* (2021) 21(1):3–9. doi: 10.1016/j.clcc.2021.10.001

16. Jarosz-Biej M, Smolarczyk R, Cichoń T, Kułach N. Tumor microenvironment as a "Game changer" in cancer radiotherapy. *Int J Mol Sci* (2019) 20(13):3212. doi: 10.3390/ijms20133212

17. Chiang CS, Fu SY, Wang SC, Yu CF, Chen FH, Lin CM, et al. Irradiation promotes an m2 macrophage phenotype in tumor hypoxia. *Front Oncol* (2012) 2:89. doi: 10.3389/fonc.2012.00089

18. Wang Q, Li S, Qiao S, Zheng Z, Duan X, Zhu X. Changes in T lymphocyte subsets in different tumors before and after radiotherapy: A meta-analysis. *Front Immunol* (2021) 12:648652. doi: 10.3389/fimmu.2021.648652

19. Formenti SC, Demaria S. Radiation therapy to convert the tumor into an *in situ* vaccine. *Int J Radiat Oncol Biol Phys* (2012) 84(4):879–80. doi: 10.1016/j.ijrobp.2012.06.020

20. Golden EB, Marciscano AE, Formenti SC. Radiation therapy and the *In situ* vaccination approach. *Int J Radiat Oncol Biol Phys* (2020) 108(4):891–8. doi: 10.1016/j.ijrobp.2020.08.023

21. Craig DJ, Nanavaty NS, Devanaboyina M, Stanbery L, Hamouda D, Edelman G, et al. The abscopal effect of radiation therapy. *Future Oncol* (2021) 17(13):1683–94. doi: 10.2217/fon-2020-0994

22. Lan F, Xu B, Li J. A low proportion of regulatory T cells before chemoradiotherapy predicts better overall survival in esophageal cancer. *Ann Palliat Med* (2021) 10(2):2195–202. doi: 10.21037/apm-21-196

23. Ma J, Jin L, Li YD, He C, Guo X, Liu R, et al. The intensity of radiotherapy-elicited immune response is associated with esophageal cancer clearance. *J Immunol Res* (2014) 2014:794249. doi: 10.1155/2014/794249

24. Soeratram TT, Creemers A, Meijer SL, de Boer OJ, Vos W, Hooijer GK. Tumor-immune landscape patterns before and after chemoradiation in resectable esophageal adenocarcinomas. *J Pathol* (2022) 256(3):282–96. doi: 10.1002/path.5832

25. Kelly RJ, Zaidi AH, Smith MA, Omstead AN, Kosovec JE, Matsui D, et al. The dynamic and transient immune microenvironment in locally advanced esophageal adenocarcinoma post chemoradiation. *Ann Surg* (2018) 268(6):992–9. doi: 10.1097/SLA.0000000000002410

26. Koemans WJ, van Dieren JM, van den Berg JG, Meijer GA, Snaebjornsson P, Chalabi M, et al. High CD8+ tumour-infiltrating lymphocyte density associates with unfavourable prognosis in oesophageal adenocarcinoma following poor response to neoadjuvant chemoradiotherapy. *Histopathology* (2021) 79(2):238–51. doi: 10.1111/his.14361

27. Chung YL, Wu ML. Clonal dynamics of tumor-infiltrating T-cell receptor beta-chain repertoires in the peripheral blood in response to concurrent chemoradiotherapy for Epstein-Barr virus-associated nasopharyngeal carcinoma. *Oncoimmunology* (2021) 10(1):1968172. doi: 10.1080/2162402X.2021.1968172

28. Chen Y, Jin Y, Hu X, Chen M. Effect of chemoradiotherapy on the proportion of circulating lymphocyte subsets in patients with limited-stage small cell lung cancer. *Cancer Immunol Immunother CII* (2021) 70(10):2867–76. doi: 10.1007/s00262-021-02902-x

29. Wu L, Zhu J, Rudqvist NP, Welsh J, Lee P, Liao Z, et al. T-Cell receptor profiling and prognosis after stereotactic body radiation therapy for stage I non-Small-Cell lung cancer. *Front Immunol* (2021) 12:719285. doi: 10.3389/fimmu.2021.719285

30. Han L, Shi H, Luo Y, Sun W, Li S, Zhang N, et al. Gene signature based on b cell predicts clinical outcome of radiotherapy and immunotherapy for patients with lung adenocarcinoma. *Cancer Med* (2020) 9(24):9581–94. doi: 10.1002/cam4.3561

31. Estrade F, Lescure C, Muzellec L, Pedrono M, Palard X, Pracht M, et al. Lymphocytes and neutrophil-to-Lymphocyte ratio variations after selective internal radiation treatment for HCC: A retrospective cohort study. *Cardiovasc Intervent Radiol* (2020) 43(8):1175–81. doi: 10.1007/s00270-020-02467-9

32. El Sissy C, Kirilovsky A, Van den Eynde M, Muşină AM, Anitei MG, Romero A, et al. A diagnostic biopsy-adapted immunoscore predicts response to neoadjuvant treatment and selects patients with rectal cancer eligible for a watch-and-Wait strategy.

Clin Cancer Res Off J Am Assoc Cancer Res (2020) 26(19):5198–207. doi: 10.1158/1078-0432.CCR-20-0337

33. Wilkins A, Fontana E, Nyamundanda G, Ragulan C, Patil Y, Mansfield D, et al. Differential and longitudinal immune gene patterns associated with reprogrammed microenvironment and viral mimicry in response to neoadjuvant radiotherapy in rectal cancer. *J Immunother Cancer* (2021) 9(3):e001717. doi: 10.1136/jitc-2020-001717

34. Kamran SC, Lennerz JK, Margolis CA, Liu D, Reardon B, Wankowicz SA, et al. Integrative molecular characterization of resistance to neoadjuvant chemoradiation in rectal cancer. *Clin Cancer Res* (2019) 25(18):5561–71. doi: 10.1158/1078-0432.CCR-19-0908

35. Zhang X, Yang J, Du L, Zhou Y, Li K. The prognostic value of immunoscore in patients with cancer: A pooled analysis of 10,328 patients. *Int J Biol Markers* (2020) 35 (3):3–13. doi: 10.1177/1724600820927409

36. Anitei MG, Zeitoun G, Mlecnik B, Marliot F, Haicheur N, Todosi AM, et al. Prognostic and predictive values of the immunoscore in patients with rectal cancer. *Clin Cancer Res* (2014) 20(7):1891–9. doi: 10.1158/1078-0432.CCR-13-2830

37. Walle T, Kraske JA, Liao B, Lenoir B, Timke C, von Bohlen Und Halbach E, et al. Radiotherapy orchestrates natural killer cell dependent antitumor immune responses through CXCL8. *Sci Adv* (2022) 8(12):eabh4050. doi: 10.1126/sciadv.abh4050

38. Okubo S, Suzuki T, Hioki M, Shimizu Y, Toyama H, Morinaga S, et al. The immunological impact of preoperative chemoradiotherapy on the tumor microenvironment of pancreatic cancer. *Cancer Sci* (2021) 112(7):2895–904. doi: 10.1111/cas.14914

39. Antonia SJ, Villegas A, Daniel D, Vicente D, Murakami S, Hui R, et al. Durvalumab after chemoradiotherapy in stage III non–Small-Cell lung cancer. *N Engl J Med* (2017) 377(20):1919–29. doi: 10.1056/NEJMoa1709937

40. Theelen WSME, Peulen HMU, Lalezari F, van der Noort V, de Vries JF, Aerts JGJV, et al. Effect of pembrolizumab after stereotactic body radiotherapy vs pembrolizumab alone on tumor response in patients with advanced non-small cell lung cancer: Results of the PEMBRO-RT phase 2 randomized clinical trial. *JAMA Oncol* (2019) 5(9):1276–82. doi: 10.1001/jamaoncol.2019.1478

41. Barton MB, Jacob S, Shafiq J, Wong K, Thompson SR, Hanna TP, et al. Estimating the demand for radiotherapy from the evidence: A review of changes from 2003 to 2012. *Radiother Oncol* (2014) 112(1):140–4. doi: 10.1016/j.radonc.2014.03.024

42. Eke I, Aryankalayil MJ, Bylicky MA, Sandfort V, Vanpouille-Box C, Nandagopal S, et al. Long-term expression changes of immune-related genes in prostate cancer after radiotherapy. *Cancer Immunol Immunother CII* (2022) 71(4):839–50. doi: 10.1007/s00262-021-03036-w

43. Lee YH, Yu CF, Yang YC, Hong JH, Chiang CS. Ablative radiotherapy reprograms the tumor microenvironment of a pancreatic tumor in favoring the immune checkpoint blockade therapy. *Int J Mol Sci* (2021) 22(4):2091. doi: 10.3390/ijms22042091

44. Hoffmann E, Paulsen F, Schaedle P, Zips D, Gani C, Rammensee HG, et al. Radiotherapy planning parameters correlate with changes in the peripheral immune status of patients undergoing curative radiotherapy for localized prostate cancer. *Cancer Immunol Immunother CII* (2022) 71(3):541–52. doi: 10.1007/s00262-021-03002-6

45. Sage EK, Schmid TE, Geinitz H, Gehrmann M, Sedelmayr M, Duma MN, et al. Effects of definitive and salvage radiotherapy on the distribution of lymphocyte subpopulations in prostate cancer patients. *Strahlenther Onkol Organ Dtsch Rontgengesellschaft Al.* (2017) 193(8):648–55. doi: 10.1007/s00066-017-1144-7

46. Graham Martínez C, Barella Y, Kus Öztürk S, Ansems M, Gorris MAJ, van Vliet S, et al. The immune microenvironment landscape shows treatment-specific differences in rectal cancer patients. *Front Immunol* (2022), 13:1011498. doi: 10.3389/fimmu.2022.1011498

47. Zhang Z, Liu X, Chen D, Yu J. Radiotherapy combined with immunotherapy: the dawn of cancer treatment. *Signal Transduct Target Ther* (2022) 7(1):1–34. doi: 10.1038/s41392-022-01102-y

48. Bosset JF, Gignoux M, Triboulet JP, Tiret E, Mantion G, Elias D, et al. Chemoradiotherapy followed by surgery compared with surgery alone in squamous-cell cancer of the esophagus. *N Engl J Med* (1997) 337(3):161–7. doi: 10.1056/NEJM199707173370304

49. Fuchs CS, Özgüroğlu M, Bang YJ, Di Bartolomeo M, Mandala M, Ryu MH, et al. Pembrolizumab versus paclitaxel for previously treated PD-L1-positive advanced gastric or gastroesophageal junction cancer: 2-year update of the randomized phase 3 KEYNOTE-061 trial. *Gastric Cancer Off J Int Gastric Cancer Assoc Jpn Gastric Cancer Assoc* (2022) 25(1):197–206. doi: 10.1007/s10120-021-01227-z

50. Huang TX, Fu L. The immune landscape of esophageal cancer. *Cancer Commun* (2019) 39:79. doi: 10.1186/s40880-019-0427-z

51. Greally M, Ilson DH. Neoadjuvant therapy for esophageal cancer: Who, when, and what? *Cancer* (2018) 124(22):4276–8. doi: 10.1002/cncr.31768.

52. Overgaard NH, Jung JW, Steptoe RJ, Wells JW. CD4+/CD8+ double-positive T cells: more than just a developmental stage? *J Leukoc Biol* (2015) 97(1):31–8. doi: 10.1189/jlb.1RU0814-382

53. Sarrabayrouse G, Corvaisier M, Ouisse LH, Bossard C, Le Mével B, Potiron L, et al. Tumor-reactive CD4+ CD8αβ+ CD103+ αβT cells: A prevalent tumor-reactive T-cell subset in metastatic colorectal cancers. *Int J Cancer* (2011) 128(12):2923–32. doi: 10.1002/ijc.25640

54. Bohner P, Chevalier MF, Cesson V, Rodrigues-Dias S-C, Dartiguenave F, Burruni R, et al. Double positive CD4+CD8+ T cells are enriched in urological cancers and favor T helper-2 polarization. *Front Immunol* (2019) 10:622. doi: 10.3389/fimmu.2019.00622

55. Gao Y, Kang M, Niu L, Xu L, Xie X, Chen D, et al. The effects of radiotherapy after thoracic and laparoscopic surgery on patients with esophageal cancer and on their prognoses. *Am J Transl Res* (2021) 13(6):6446–56.

56. Cai S, Fan Y, Guo Q, Sun Y, Zhao P, Tian Y, et al. Impact of radiation dose to circulating immune cells on tumor control and survival in esophageal cancer. *Cancer Biother Radiopharm* (2021). doi: 10.1089/cbr.2021.0250

57. Huang Z, Zheng Q, Yu Y, Zheng H, Wu Y, Wang Z, et al. Prognostic significance of platelet-to-albumin ratio in patients with esophageal squamous cell carcinoma receiving definitive radiotherapy. *Sci Rep* (2022) 12(1):3535. doi: 10.1038/s41598-022-07546-0

58. Zhao K, Jiang L, Si Y, Zhou S, Huang Z, Meng X. TIGIT blockade enhances tumor response to radiotherapy *via* a CD103 + dendritic cell-dependent mechanism. *Cancer Immunol Immunother* (2023) 72(1):193–209. doi: 10.1007/s00262-022-03227-z

59. Cancer Research Institute. Cancer immunotherapy timeline of progress . Available at: https://www.cancerresearch.org/en-us/immunotherapy/timeline-of-progress.

60. Rožman P, Švajger U. The tolerogenic role of IFN-γ. *Cytokine Growth Factor Rev* (2018) 41:40–53. doi: 10.1016/j.cytogfr.2018.04.001

61. Huang TC, Liang CW, Li YI, Guo JC, Lin CC, Chen YJ, et al. Prognostic value of PD-L1 expression on immune cells or tumor cells for locally advanced esophageal squamous cell carcinoma in patients treated with neoadjuvant chemoradiotherapy. *J Cancer Res Clin Oncol* (2022) 148(7):1803–11. doi: 10.1007/s00432-021-03772-7

62. Mohme M, Neidert MC. Tumor-specific T cell activation in malignant brain tumors. *Front Immunol* (2020) 11:205. doi: 10.3389/fimmu.2020.00205

63. Wang X, Teng F, Kong L, Yu J. PD-L1 expression in human cancers and its association with clinical outcomes. *OncoTargets Ther* (2016) 9:5023–39. doi: 10.2147/OTT.S105862

64. Weissferdt A, Fujimoto J, Kalhor N, Rodriguez J, Bassett R, Wistuba II, et al. Expression of PD-1 and PD-L1 in thymic epithelial neoplasms. *Mod Pathol* (2017) 30 (6):826–33. doi: 10.1038/modpathol.2017.6

65. Rizvi NA, Hellmann MD, Snyder A, Kvistborg P, Makarov V, Havel JJ, et al. Cancer immunology. mutational landscape determines sensitivity to PD-1 blockade in non-small cell lung cancer. *Science* (2015) 348(6230):124–8. doi: 10.1126/science.aaa1348

66. Yuan C, Xiang L, Cao K, Zhang J, Luo Y, Sun W, et al. The prognostic value of tumor mutational burden and immune cell infiltration in esophageal cancer patients with or without radiotherapy. *Aging* (2020) 12(5):4603–16. doi: 10.18632/aging.102917

67. Qian D, Wang Y, Zhao G, Cao F, Er P, Chen X, et al. Tumor remission and tumor-infiltrating lymphocytes during chemoradiation therapy: Predictive and prognostic markers in locally advanced esophageal squamous cell carcinoma. *Int J Radiat Oncol Biol Phys* (2019) 105(2):319–28. doi: 10.1016/j.ijrobp.2019.06.079

68. Marur S, Forastiere AA. Head and neck squamous cell carcinoma: Update on epidemiology, diagnosis, and treatment. *Mayo Clin Proc* (2016) 91(3):386–96. doi: 10.1016/j.mayocp.2015.12.017

69. Zhou C, Parsons JL. The radiobiology of HPV-positive and HPV-negative head and neck squamous cell carcinoma. *Expert Rev Mol Med* (2020) 22:e3. doi: 10.1017/erm.2020.4

70. Wong KCW, Johnson D, Hui EP, Lam RCT, Ma BBY, Chan ATC. Opportunities and challenges in combining immunotherapy and radiotherapy in head and neck cancers. *Cancer Treat Rev* (2022) 105:102361. doi: 10.1016/j.ctrv.2022.102361

71. Balermpas P, Rödel F, Rödel C, Krause M, Linge A, Lohaus F, et al. CD8+ tumour-infiltrating lymphocytes in relation to HPV status and clinical outcome in patients with head and neck cancer after postoperative chemoradiotherapy: A multicentre study of the German cancer consortium radiation oncology group (DKTK-ROG). *Int J Cancer* (2016) 138(1):171–81. doi: 10.1002/ijc.29683

72. Parikh F, Duluc D, Imai N, Clark A, Misiukiewicz K, Bonomi M, et al. Chemoradiotherapy-induced upregulation of PD-1 antagonizes immunity to HPV-related oropharyngeal cancer. *Cancer Res* (2014) 74(24):7205–16. doi: 10.1158/0008-5472.CAN-14-1913

73. Sridharan V, Margalit DN, Lynch SA, Severgnini M, Zhou J, Chau NG, et al. Definitive chemoradiation alters the immunologic landscape and immune checkpoints in head and neck cancer. *Br J Cancer* (2016) 115(2):252–60. doi: 10.1038/bjc.2016.166

74. Ouyang Y, Liu K, Hao M, Zheng R, Zhang C, Wu Y, et al. Radiofrequency ablation-increased CXCL10 is associated with earlier recurrence of hepatocellular carcinoma by promoting stemness. *Tumour Biol J Int Soc Oncodevelopmental Biol Med* (2016) 37(3):3697–704. doi: 10.1007/s13277-015-4035-5

75. Lunardi S, Lim SY, Muschel RJ, Brunner TB. IP-10/CXCL10 attracts regulatory T cells: Implication for pancreatic cancer. *OncoImmunology* (2015) 4(9):e1027473. doi: 10.1080/2162402X.2015.1027473

76. Hojo S, Koizumi K, Tsuneyama K, Arita Y, Cui Z, Shinohara K, et al. High-level expression of chemokine CXCL16 by tumor cells correlates with a good prognosis and increased tumor-infiltrating lymphocytes in colorectal cancer. *Cancer Res* (2007) 67 (10):4725–31. doi: 10.1158/0008-5472.CAN-06-3424

77. Schuler PJ, Harasymczuk M, Schilling B, Saze Z, Strauss L, Lang S, et al. Effects of adjuvant chemoradiotherapy on the frequency and function of regulatory T cells in patients with head and neck cancer. *Clin Cancer Res Off J Am Assoc Cancer Res* (2013) 19(23):6585–96. doi: 10.1158/1078-0432.CCR-13-0900

78. Dwyer KM, Hanidziar D, Putheti P, Hill PA, Pommey S, McRae JL, et al. Expression of CD39 by human peripheral blood CD4+CD25+ T cells denotes a regulatory memory phenotype. *Am J Transplant Off J Am Soc Transplant Am Soc Transpl Surg* (2010) 10(11):2410–20. doi: 10.1111/j.1600-6143.2010.03291.x

79. Chen YP, Ismaila N, Chua MLK, Colevas AD, Haddad R, Huang SH, et al. Chemotherapy in combination with radiotherapy for definitive-intent treatment of stage II-IVA nasopharyngeal carcinoma: CSCO and ASCO guideline. *J Clin Oncol Off J Am Soc Clin Oncol* (2021) 39(7):840–59. doi: 10.1200/JCO.20.03237

80. Ahn GO, Brown JM. Matrix metalloproteinase-9 is required for tumor vasculogenesis but not for angiogenesis: role of bone marrow-derived myelomonocytic cells. *Cancer Cell* (2008) 13(3):193–205. doi: 10.1016/j.ccr.2007.11.032

81. Ahn GO, Tseng D, Liao CH, Dorie MJ, Czechowicz A, Brown JM. Inhibition of mac-1 (CD11b/CD18) enhances tumor response to radiation by reducing myeloid cell recruitment. *Proc Natl Acad Sci U S A.* (2010) 107(18):8363–8. doi: 10.1073/pnas.0911378107

82. Sung H, Ferlay J, Siegel RL, Laversanne M, Soerjomataram I, Jemal A, et al. Global cancer statistics 2020: GLOBOCAN estimates of incidence and mortality worldwide for 36 cancers in 185 countries. *CA Cancer J Clin* (2021) 71(3):209–49. doi: 10.3322/caac.21660

83. Miller M, Hanna N. Advances in systemic therapy for non-small cell lung cancer. *BMJ* (2021) 375:n2363. doi: 10.1136/bmj.n2363

84. Brozos-Vázquez EM, Díaz-Peña R, García-González J, León-Mateos L, Mondelo-Macía P, Peña-Chilet M, et al. Immunotherapy in nonsmall-cell lung cancer: current status and future prospects for liquid biopsy. *Cancer Immunol Immunother CII* (2021) 70(5):1177–88. doi: 10.1007/s00262-020-02752-z

85. Nishino M, Ramaiya NH, Hatabu H, Hodi FS. Monitoring immune-checkpoint blockade: response evaluation and biomarker development. *Nat Rev Clin Oncol* (2017) 14(11):655–68. doi: 10.1038/nrclinonc.2017.88

86. Abravan A, Eide HA, Helland Å, Malinen E. Radiotherapy-related lymphopenia in patients with advanced non-small cell lung cancer receiving palliative radiotherapy. *Clin Transl Radiat Oncol* (2020) 22:15–21. doi: 10.1016/j.ctro.2020.02.005

87. Wang X, Lu J, Teng F, Yu J. Lymphopenia association with accelerated hyperfractionation and its effects on limited-stage small cell lung cancer patients' clinical outcomes. *Ann Transl Med* (2019) 7(16):385. doi: 10.21037/atm.2019.07.58

88. Karantanos T, Karanika S, Seth B, Gignac G. The absolute lymphocyte count can predict the overall survival of patients with non-small cell lung cancer on nivolumab: a clinical study. *Clin Transl Oncol* (2019) 21(2):206–12. doi: 10.1007/s12094-018-1908-2

89. Zhou P, Chen D, Zhu B, Chen W, Xie Q, Wang Y, et al. Stereotactic body radiotherapy is effective in modifying the tumor genome and tumor immune microenvironment in non-small cell lung cancer or lung metastatic carcinoma. *Front Immunol* (2020) 11:594212. doi: 10.3389/fimmu.2020.594212

90. Shirasawa M, Yoshida T, Matsumoto Y, Shinno Y, Okuma Y, Goto Y, et al. Impact of chemoradiotherapy on the immune-related tumour microenvironment and efficacy of anti-PD-(L)1 therapy for recurrences after chemoradiotherapy in patients with unresectable locally advanced non-small cell lung cancer. *Eur J Cancer Oxf Engl 1990.* (2020) 140:28–36. doi: 10.1016/j.ejca.2020.08.028

91. Zhang Md J, Zhang Md L, Yang Md Y, Liu Md Q, Ma Md H, Huang Md A, et al. Polymorphonuclear-MDSCs facilitate tumor regrowth after radiation by suppressing CD8+ T cells. *Int J Radiat Oncol Biol Phys* (2021) 109(5):1533–46. doi: 10.1016/j.ijrobp.2020.11.038

92. Pan S, Wang J, Wu A, Guo Z, Wang Z, Zheng L, et al. Radiation exposure-induced changes in the immune cells and immune factors of mice with or without primary lung tumor. *Dose-Response Publ Int Hormesis Soc* (2020) 18 (2):1559325820926744. doi: 10.1177/1559325820926744

93. Reijmen E, De Mey S, De Mey W, Gevaert T, De Ridder K, Locy H, et al. Fractionated radiation severely reduces the number of CD8+ T cells and mature antigen presenting cells within lung tumors. *Int J Radiat Oncol Biol Phys* (2021) 111 (1):272–83. doi: 10.1016/j.ijrobp.2021.04.009

94. Liu Q, Hao Y, Du R, Hu D, Xie J, Zhang J, et al. Radiotherapy programs neutrophils to an antitumor phenotype by inducing mesenchymal-epithelial transition. *Transl Lung Cancer Res* (2021) 10(3):1424–43. doi: 10.21037/tlcr-21-152

95. Wang CI, Chang YF, Sie ZL, Ho AS, Chang JS, Peng CL, et al. Irradiation suppresses IFNγ-mediated PD-L1 and MCL1 expression in EGFR-positive lung cancer to augment CD8+ T cells cytotoxicity. *Cells* (2021) 10(10):2515. doi: 10.3390/cells10102515

96. Cardoso F, Kyriakides S, Ohno S, Penault-Llorca F, Poortmans P, Rubio IT, et al. Early breast cancer: ESMO clinical practice guidelines for diagnosis, treatment and follow-up†. *Ann Oncol Off J Eur Soc Med Oncol* (2019) 30(8):1194–220. doi: 10.1093/annonc/mdz173

97. Gennari A, André F, Barrios CH, Cortés J, de Azambuja E, DeMichele A, et al. ESMO clinical practice guideline for the diagnosis, staging and treatment of patients with metastatic breast cancer. *Ann Oncol Off J Eur Soc Med Oncol* (2021) 32(12):1475–95. doi: 10.1016/j.annonc.2021.09.019

98. Ho AY, Wright JL, Blitzblau RC, Mutter RW, Duda DG, Norton L, et al. Optimizing radiation therapy to boost systemic immune responses in breast cancer: A critical review for breast radiation oncologists. *Int J Radiat Oncol Biol Phys* (2020) 108 (1):227–41. doi: 10.1016/j.ijrobp.2020.05.011

99. Sage EK, Schmid TE, Sedelmayr M, Gehrmann M, Geinitz H, Duma MN, et al. Comparative analysis of the effects of radiotherapy versus radiotherapy after adjuvant chemotherapy on the composition of lymphocyte subpopulations in breast cancer patients. *Radiother Oncol* (2016) 118(1):176–80. doi: 10.1016/j.radonc.2015.11.016

100. Chen F, Jin JY, Hui TSK, Jing H, Zhang H, Nong Y, et al. Radiation induced lymphopenia is associated with the effective dose to the circulating immune cells in breast cancer. *Front Oncol* (2022) 12:768956. doi: 10.3389/fonc.2022.768956

101. Xu C, Jin JY, Zhang M, Liu A, Wang J, Mohan R, et al. The impact of the effective dose to immune cells on lymphopenia and survival of esophageal cancer after chemoradiotherapy. *Radiother Oncol* (2020) 146:180–6. doi: 10.1016/j.radonc.2020.02.015

102. Lewin NL, Luetragoon T, Shamoun L, Oliva D, Andersson BÅ, Löfgren S, et al. The influence of adjuvant radiotherapy and single nucleotide polymorphisms on circulating immune response cell numbers and phenotypes of patients with breast cancer. *Anticancer Res* (2019) 39(9):4957–63. doi: 10.21873/anticanres.13684

103. Cattin S, Fellay B, Calderoni A, Christinat A, Negretti L, Biggiogero M, et al. Circulating immune cell populations related to primary breast cancer, surgical removal, and radiotherapy revealed by flow cytometry analysis. *Breast Cancer Res* (2021) 23 (1):64. doi: 10.1186/s13058-021-01441-8

104. Ahmed M, Jozsa F, Douek M. A systematic review of neo-adjuvant radiotherapy in the treatment of breast cancer. *Ecancermedicalscience* (2021) 15:1175. doi: 10.3332/ecancer.2021.1175

105. Schnellhardt S, Erber R, Büttner-Herold M, Rosahl MC, Ott OJ, Strnad V, et al. Tumour-infiltrating inflammatory cells in early breast cancer: An underrated prognostic and predictive factor? *Int J Mol Sci* (2020) 21(21):8238. doi: 10.3390/ijms21218238

106. Hader M, Savcigil DP, Rosin A, Ponfick P, Gekle S, Wadepohl M, et al. Differences of the immune phenotype of breast cancer cells after ex vivo hyperthermia by warm-water or microwave radiation in a closed-loop system alone or in combination with radiotherapy. *Cancers* (2020) 12(5):1082. doi: 10.3390/cancers12051082

107. Fidler MM, Soerjomataram I, Bray F. A global view on cancer incidence and national levels of the human development index. *Int J Cancer* (2016) 139(11):2436–46. doi: 10.1002/ijc.30382

108. Crosbie EJ, Einstein MH, Franceschi S, Kitchener HC. Human papillomavirus and cervical cancer. *Lancet* (2013) 382(9895):889–99. doi: 10.1016/S0140-6736(13)60022-7

109. Dorta-Estremera S, Colbert LE, Nookala SS, Yanamandra AV, Yang G, Delgado A, et al. Kinetics of intratumoral immune cell activation during chemoradiation for cervical cancer. *Int J Radiat Oncol* (2018) 102(3):593–600. doi: 10.1016/j.ijrobp.2018.06.404

110. Ren J, Li L, Yu B, Xu E, Sun N, Li X, et al. Extracellular vesicles mediated proinflammatory macrophage phenotype induced by radiotherapy in cervical cancer. *BMC Cancer* (2022) 22(1):88. doi: 10.1186/s12885-022-09194-z

111. Li R, Liu Y, Yin R, Yin L, Li K, Sun C, et al. The dynamic alternation of local and systemic tumor immune microenvironment during concurrent chemoradiotherapy of cervical cancer: A prospective clinical trial. *Int J Radiat Oncol Biol Phys* (2021) 110(5):1432–41. doi: 10.1016/j.ijrobp.2021.03.003

112. Someya M, Tsuchiya T, Fukushima Y, Hasegawa T, Takada Y, Hori M, et al. Association between cancer immunity and treatment results in uterine cervical cancer patients treated with radiotherapy. *Jpn J Clin Oncol* (2020) 50(11):1290–7. doi: 10.1093/jjco/hyaa149

113. Mori Y, Sato H, Kumazawa T, Permata TBM, Yoshimoto Y, Murata K, et al. Analysis of radiotherapy-induced alteration of CD8+ T cells and PD-L1 expression in patients with uterine cervical squamous cell carcinoma. *Oncol Lett* (2021) 21(6):446. doi: 10.3892/ol.2021.12707

114. Lippens L, Van Bockstal M, De Jaeghere EA, Tummers P, Makar A, De Geyter S, et al. Immunologic impact of chemoradiation in cervical cancer and how immune cell infiltration could lead toward personalized treatment. *Int J Cancer* (2020) 147 (2):554–64. doi: 10.1002/ijc.32893

115. van Luijk IF, Smith SM, Marte Ojeda MC, Oei AL, Kenter GG, Jordanova ES. A review of the effects of cervical cancer standard treatment on immune parameters in peripheral blood, tumor draining lymph nodes, and local tumor microenvironment. *J Clin Med* (2022) 11(9):2277. doi: 10.3390/jcm11092277

116. Stewart C, Ralyea C, Lockwood S. Ovarian cancer: An integrated review. *Semin Oncol Nurs.* (2019) 35(2):151–6. doi: 10.1016/j.soncn.2019.02.001

117. Chandra A, Pius C, Nabeel M, Nair M, Vishwanatha JK, Ahmad S, et al. Ovarian cancer: Current status and strategies for improving therapeutic outcomes. *Cancer Med* (2019) 8(16):7018–31. doi: 10.1002/cam4.2560

118. Pölcher M, Braun M, Friedrichs N, Rudlowski C, Bercht E, Fimmers R, et al. Foxp3+ cell infiltration and granzyme B+/Foxp3+ cell ratio are associated with outcome in neoadjuvant chemotherapy-treated ovarian carcinoma. *Cancer Immunol Immunother* (2010) 59(6):909–19. doi: 10.1007/s00262-010-0817-1

119. Mesnage SJL, Auguste A, Genestie C, Dunant A, Pain E, Drusch F, et al. Neoadjuvant chemotherapy (NACT) increases immune infiltration and programmed death-ligand 1 (PD-L1) expression in epithelial ovarian cancer (EOC). *Ann Oncol* (2017) 28(3):651–7. doi: 10.1093/annonc/mdw625

120. Yang C, Xia BR, Zhang ZC, Zhang YJ, Lou G, Jin WL. Immunotherapy for ovarian cancer: Adjuvant, combination, and neoadjuvant. *Front Immunol* (2020) 11:577869. doi: 10.3389/fimmu.2020.577869

121. Fyles AW, Dembo AJ, Bush RS, Levin W, Manchul LA, Pringle JF, et al. Analysis of complications in patients treated with abdomino-pelvic radiation therapy

for ovarian carcinoma. *Int J Radiat Oncol Biol Phys* (1992) 22(5):847–51. doi: 10.1016/0360-3016(92)90778-G

122. Herrera FG, Ronet C, Ochoa de Olza M, Barras D, Crespo I, Andreatta M, et al. Low-dose radiotherapy reverses tumor immune desertification and resistance to immunotherapy. *Cancer Discovery* (2022) 12(1):108–33. doi: 10.1158/2159-8290.CD-21-0003

123. Parker C, Castro E, Fizazi K, Heidenreich A, Ost P, Procopio G, et al. Prostate cancer: ESMO clinical practice guidelines for diagnosis, treatment and follow-up. *Ann Oncol Off J Eur Soc Med Oncol* (2020) 31(9):1119–34. doi: 10.1016/j.annonc.2020.06.011

124. Thompson IM, Ankerst DP, Chi C, Goodman PJ, Tangen CM, Lucia MS, et al. Assessing prostate cancer risk: results from the prostate cancer prevention trial. *J Natl Cancer Inst* (2006) 98(8):529–34. doi: 10.1093/jnci/djj131

125. Eckert F, Schaedle P, Zips D, Schmid-Horch B, Rammensee HG, Gani C, et al. Impact of curative radiotherapy on the immune status of patients with localized prostate cancer. *Oncoimmunology* (2018) 7(11):e1496881. doi: 10.1080/2162402X.2018.1496881

126. Kane N, Romero T, Diaz-Perez S, Rettig MB, Steinberg ML, Kishan AU, et al. Significant changes in macrophage and CD8 T cell densities in primary prostate tumors 2 weeks after SBRT. *Prostate Cancer Prostatic Dis* (2022). doi: 10.1038/s41391-022-00498-6

127. Kachikwu EL, Iwamoto KS, Liao YP, DeMarco JJ, Agazaryan N, Economou JS, et al. Radiation enhances regulatory T cell representation. *Int J Radiat Oncol Biol Phys* (2011) 81(4):1128–35. doi: 10.1016/j.ijrobp.2010.09.034

128. Yang ZR, Zhao N, Meng J, Shi ZL, Li BX, Wu XW, et al. Peripheral lymphocyte subset variation predicts prostate cancer carbon ion radiotherapy outcomes. *Oncotarget* (2016) 7(18):26422–35. doi: 10.18632/oncotarget.8389

129. Trombetta AC, Soldano S, Contini P, Tomatis V, Ruaro B, Paolino S, et al. A circulating cell population showing both M1 and M2 monocyte/macrophage surface markers characterizes systemic sclerosis patients with lung involvement. *Respir Res* (2018) 19(1):186. doi: 10.1186/s12931-018-0891-z

130. Yu CF, Chang CH, Wang CC, Hong JH, Chiang CS, Chen FH. Local interleukin-12 treatment enhances the efficacy of radiation therapy by overcoming radiation-induced immune suppression. *Int J Mol Sci* (2021) 22(18):10053. doi: 10.3390/ijms221810053

131. Cassidy J, Bissett D, Spence OBE RAJ, Payne M, Morris-stiff G.. Oxford handbook of oncology, 3 edn. Oxford medical handbooks. *Oxford: Oxford Academic* (2010). doi: 10.1093/med/9780199563135.001.1

132. Karamitopoulou E. Tumour microenvironment of pancreatic cancer: immune landscape is dictated by molecular and histopathological features. *Br J Cancer* (2019) 121(1):5–14. doi: 10.1038/s41416-019-0479-5

133. Muller M, Haghnejad V, Schaefer M, Gauchotte G, Caron B, Peyrin-Biroulet L, et al. The immune landscape of human pancreatic ductal carcinoma: Key players, clinical implications, and challenges. *Cancers* (2022) 14(4):995. doi: 10.3390/cancers14040995

134. Chuong M, Chang ET, Choi EY, Mahmood J, Lapidus RG, Davila E, et al. Exploring the concept of radiation "Booster shot" in combination with an anti-PD-L1 mAb to enhance anti-tumor immune effects in mouse pancreas tumors. *J Clin Oncol Res* (2017) 5(2):1058.

135. Bouchart C, Navez J, Closset J, Hendlisz A, Van Gestel D, Moretti L, et al. Novel strategies using modern radiotherapy to improve pancreatic cancer outcomes: toward a new standard? *Ther Adv Med Oncol* (2020) 12:1758835920936093. doi: 10.1177/1758835920936093

136. Alagappan M, Pollom EL, von Eyben R, Kozak MM, Aggarwal S, Poultsides GA, et al. Albumin and neutrophil-lymphocyte ratio (NLR) predict survival in patients with pancreatic adenocarcinoma treated with SBRT. *Am J Clin Oncol* (2018) 41(3):242–7. doi: 10.1097/COC.0000000000000263

137. Reddy AV, Hill CS, Sehgal S, Zheng L, He J, Laheru DA, et al. Post-radiation neutrophil-to-lymphocyte ratio is a prognostic marker in patients with localized pancreatic adenocarcinoma treated with anti-PD-1 antibody and stereotactic body radiation therapy. *Radiat Oncol J* (2022) 40(2):111–9. doi: 10.3857/roj.2021.01060

138. Kawai M, Hirono S, Okada KI, Miyazawa M, Shimizu A, Kitahata Y, et al. Low lymphocyte monocyte ratio after neoadjuvant therapy predicts poor survival after pancreatectomy in patients with borderline resectable pancreatic cancer. *Surgery* (2019) 165(6):1151–60. doi: 10.1016/j.surg.2018.12.015

139. Yoo C, Lee SS, Song KB, Jeong JH, Hyung J, Park DH, et al. Neoadjuvant modified FOLFIRINOX followed by postoperative gemcitabine in borderline resectable pancreatic adenocarcinoma: a phase 2 study for clinical and biomarker analysis. *Br J Cancer* (2020) 123(3):362–8. doi: 10.1038/s41416-020-0867-x

140. Silva-Santos B, Serre K, Norell H. γδ T cells in cancer. *Nat Rev Immunol* (2015) 15(11):683–91. doi: 10.1038/nri3904

141. Lo Presti E, Dieli F, Meraviglia S. Tumor-infiltrating γδ T lymphocytes: Pathogenic role, clinical significance, and differential programing in the tumor microenvironment. *Front Immunol* (2014) 5:607. doi: 10.3389/fimmu.2014.00607

142. Wolfe AR, Siedow M, Nalin A, DiCostanzo D, Miller ED, Diaz DA, et al. Increasing neutrophil-to-lymphocyte ratio following radiation is a poor prognostic factor and directly correlates with splenic radiation dose in pancreatic cancer. *Radiother Oncol J Eur Soc Ther Radiol Oncol* (2021) 158:207–14. doi: 10.1016/j.radonc.2021.02.035

143. Iwai N, Okuda T, Sakagami J, Harada T, Ohara T, Taniguchi M, et al. Neutrophil to lymphocyte ratio predicts prognosis in unresectable pancreatic cancer. *Sci Rep* (2020) 10(1):18758. doi: 10.1038/s41598-020-75745-8

144. Murakami T, Homma Y, Matsuyama R, Mori R, Miyake K, Tanaka Y, et al. Neoadjuvant chemoradiotherapy of pancreatic cancer induces a favorable immunogenic tumor microenvironment associated with increased major histocompatibility complex class I-related chain A/B expression. *J Surg Oncol* (2017) 116(3):416–26. doi: 10.1002/jso.24681

145. Mills BN, Qiu H, Drage MG, Chen C, Mathew JS, Garrett-Larsen J, et al. Modulation of the human pancreatic ductal adenocarcinoma immune microenvironment by stereotactic body radiotherapy. *Clin Cancer Res Off J Am Assoc Cancer Res* (2022) 28(1):150–62. doi: 10.1158/1078-0432.CCR-21-2495

146. Gillen S, Schuster T, Meyer Zum Büschenfelde C, Friess H, Kleeff J. Preoperative/neoadjuvant therapy in pancreatic cancer: a systematic review and meta-analysis of response and resection percentages. *PloS Med* (2010) 7(4):e1000267. doi: 10.1371/journal.pmed.1000267

147. Michelakos T, Cai L, Villani V, Sabbatino F, Kontos F, Fernández-Del Castillo C, et al. Tumor microenvironment immune response in pancreatic ductal adenocarcinoma patients treated with neoadjuvant therapy. *J Natl Cancer Inst* (2021) 113(2):182–91. doi: 10.1093/jnci/djaa073

148. Matsuki H, Hiroshima Y, Miyake K, Murakami T, Homma Y, Matsuyama R, et al. Reduction of gender-associated M2-like tumor-associated macrophages in the tumor microenvironment of patients with pancreatic cancer after neoadjuvant chemoradiotherapy. *J Hepato-Biliary-Pancreat Sci* (2021) 28(2):174–82. doi: 10.1002/jhbp.883

149. Ye J, Mills BN, Zhao T, Han BJ, Murphy JD, Patel AP, et al. Assessing the magnitude of immunogenic cell death following chemotherapy and irradiation reveals a new strategy to treat pancreatic cancer. *Cancer Immunol Res* (2020) 8(1):94–107. doi: 10.1158/2326-6066.CIR-19-0373

150. Klug F, Prakash H, Huber PE, Seibel T, Bender N, Halama N, et al. Low-dose irradiation programs macrophage differentiation to an iNOS+/M1 phenotype that orchestrates effective T cell immunotherapy. *Cancer Cell* (2013) 24(5):589–602. doi: 10.1016/j.ccr.2013.09.014

151. Seifert L, Werba G, Tiwari S, Giao Ly NN, Nguy S, Alothman S, et al. Radiation therapy induces macrophages to suppress T-cell responses against pancreatic tumors in mice. *Gastroenterology* (2016) 150(7):1659–1672.e5. doi: 10.1053/j.gastro.2016.02.070

152. Prakash H, Klug F, Nadella V, Mazumdar V, Schmitz-Winnenthal H, Umansky L. Low doses of gamma irradiation potentially modifies immunosuppressive tumor microenvironment by retuning tumor-associated macrophages: lesson from insulinoma. *Carcinogenesis* (2016) 37(3):301–13. doi: 10.1093/carcin/bgw007

153. Center MM, Jemal A, Smith RA, Ward E. Worldwide variations in colorectal cancer. *CA Cancer J Clin* (2009) 59(6):366–78. doi: 10.3322/caac.20038

154. Sinicrope FA. Increasing incidence of early-onset colorectal cancer. *N Engl J Med* (2022) 386(16):1547–58. doi: 10.1056/NEJMra2200869

155. Treanor D, Quirke P. Pathology of colorectal cancer. *Clin Oncol R Coll Radiol G B* (2007) 19(10):769–76. doi: 10.1016/j.clon.2007.08.012

156. Frey B, Rückert M, Weber J, Mayr X, Derer A, Lotter M, et al. Hypofractionated irradiation has immune stimulatory potential and induces a timely restricted infiltration of immune cells in colon cancer tumors. *Front Immunol* (2017) 8:231. doi: 10.3389/fimmu.2017.00231

157. Gerber SA, Lim JYH, Connolly KA, Sedlacek AL, Barlow ML, Murphy SP, et al. Radio-responsive tumors exhibit greater intratumoral immune activity than nonresponsive tumors. *Int J Cancer* (2014) 134(10):2383–92. doi: 10.1002/ijc.28558

158. Joseph ELM, Kirilovsky A, Lecoester B, Sissy CE, Boullerot L, Rangan L, et al. Chemoradiation triggers antitumor Th1 and tissue resident memory-polarized immune responses to improve immune checkpoint inhibitors therapy. *J Immunother Cancer* (2021) 9(7):e002256. doi: 10.1136/jitc-2020-002256

159. Tseng D, Volkmer JP, Willingham SB, Contreras-Trujillo H, Fathman JW, Fernhoff NB, et al. Anti-CD47 antibody-mediated phagocytosis of cancer by macrophages primes an effective antitumor T-cell response. *Proc Natl Acad Sci U S A.* (2013) 110(27):11103–8. doi: 10.1073/pnas.1305569110

160. Candas-Green D, Xie B, Huang J, Fan M, Wang A, Menaa C, et al. Dual blockade of CD47 and HER2 eliminates radioresistant breast cancer cells. *Nat Commun* (2020) 11(1):4591. doi: 10.1038/s41467-020-18245-7

161. Schaue D, Comin-Anduix B, Ribas A, Zhang L, Goodglick L, Sayre JW, et al. T-Cell responses to survivin in cancer patients undergoing radiation therapy. *Clin Cancer Res Off J Am Assoc Cancer Res* (2008) 14(15):4883–90. doi: 10.1158/1078-0432.CCR-07-4462

162. Ambrosini G, Adida C, Altieri DC. A novel anti-apoptosis gene, survivin, expressed in cancer and lymphoma. *Nat Med* (1997) 3(8):917–21. doi: 10.1038/nm0897-917

163. Tamas K, Walenkamp AME, de Vries EGE, van Vugt M a. TM, Beets-Tan RG, van Etten B, et al. Rectal and colon cancer: Not just a different anatomic site. *Cancer Treat Rev* (2015) 41(8):671–9. doi: 10.1016/j.ctrv.2015.06.007

164. Glynne-Jones R, Wyrwicz L, Tiret E, Brown G, Rödel C, Cervantes A, et al. Rectal cancer: ESMO clinical practice guidelines for diagnosis, treatment and follow-up. *Ann Oncol* (2017) 28:iv22–40. doi: 10.1093/annonc/mdx224

165. Ribi K, Marti WR, Bernhard J, Grieder F, Graf M, Gloor B, et al. Quality of life after total mesorectal excision and rectal replacement: Comparing side-to-End, colon J-

pouch and straight colorectal reconstruction in a randomized, phase III trial (SAKK 40/04). *Ann Surg Oncol* (2019) 26(11):3568–76. doi: 10.1245/s10434-019-07525-2

166. Garcia-Aguilar J, Patil S, Gollub MJ, Kim JK, Yuval JB, Thompson HM, et al. Organ preservation in patients with rectal adenocarcinoma treated with total neoadjuvant therapy. *J Clin Oncol Off J Am Soc Clin Oncol* (2022) 40(23):2546–56. doi: 10.1200/JCO.22.00032

167. Lin YE, Huang SY, Chang TH, Chou TW, Hung LC, Huang CC, et al. Prognostic significance of the preoperative hematological parameters in non-metastatic rectal cancer patients undergoing neoadjuvant chemoradiotherapy and radical surgery. *Therapeutic Radiol Oncol* (2022) 6:8. doi: 10.21037/tro-21-35

168. Wang Q, Zhu D. The prognostic value of systemic immune-inflammation index (SII) in patients after radical operation for carcinoma of stomach in gastric cancer. *J Gastrointest Oncol* (2019) 10(5):965–78. doi: 10.21037/jgo.2019.05.03

169. Galon J, Costes A, Sanchez-Cabo F, Kirilovsky A, Mlecnik B, Lagorce-Pagès C, et al. Type, density, and location of immune cells within human colorectal tumors predict clinical outcome. *Science* (2006) 313(5795):1960–4. doi: 10.1126/science.1129139

170. Lanzi A, Pagès F, Lagorce-Pagès C, Galon J. The consensus immunoscore: toward a new classification of colorectal cancer. *Oncoimmunology* (2020) 9(1):1789032. doi: 10.1080/2162402X.2020.1789032

171. Teng F, Mu D, Meng X, Kong L, Zhu H, Liu S, et al. Tumor infiltrating lymphocytes (TILs) before and after neoadjuvant chemoradiotherapy and its clinical utility for rectal cancer. *Am J Cancer Res* (2015) 5(6):2064–74.

172. Sinicrope FA, Shi Q, Hermitte F, Zemla TJ, Mlecnik B, Benson AB, et al. Contribution of immunoscore and molecular features to survival prediction in stage III colon cancer. *JNCI Cancer Spectr* (2020) 4:pkaa023. doi: 10.1093/jncics/pkaa023

173. Hermitte F. Biomarkers immune monitoring technology primer: Immunoscore® colon. *J Immunother Cancer* (2016) 4(1):57. doi: 10.1186/s40425-016-0161-x

174. Mirjolet C, Charon-Barra C, Ladoire S, Arbez-Gindre F, Bertaut A, Ghiringhelli F, et al. Tumor lymphocyte immune response to preoperative radiotherapy in locally advanced rectal cancer: The LYMPHOREC study. *OncoImmunology* (2018) 7(3):e1396402. doi: 10.1080/2162402X.2017.1396402

175. Jeon SH, Lim YJ, Koh J, Chang WI, Kim S, Kim K, et al. A radiomic signature model to predict the chemoradiation-induced alteration in tumor-infiltrating CD8+ cells in locally advanced rectal cancer. *Radiother Oncol J Eur Soc Ther Radiol Oncol* (2021) 162:124–31. doi: 10.1016/j.radonc.2021.07.004

176. Stary V, Wolf B, Unterleuthner D, List J, Talic M, Längle J, et al. Short-course radiotherapy promotes pro-inflammatory macrophages *via* extracellular vesicles in human rectal cancer. *J Immunother Cancer* (2020) 8(2):e000667. doi: 10.1136/jitc-2020-000667

177. Islami F, Ferlay J, Lortet-Tieulent J, Bray F, Jemal A. International trends in anal cancer incidence rates. *Int J Epidemiol* (2017) 46(3):924–38. doi: 10.1093/ije/dyw276

178. Shiels MS, Kreimer AR, Coghill AE, Darragh TM, Devesa SS. Anal cancer incidence in the united states, 1977–2011: Distinct patterns by histology and behavior. *Cancer Epidemiol biomark Prev Publ Am Assoc Cancer Res Cosponsored Am Soc Prev Oncol* (2015) 24(10):1548–56. doi: 10.1158/1055-9965.EPI-15-0044

179. Bruyere D, Monnien F, Colpart P, Roncarati P, Vuitton L, Hendrick E, et al. Treatment algorithm and prognostic factors for patients with stage I–III carcinoma of the anal canal: a 20-year multicenter study. *Mod Pathol* (2021) 34(1):116–30. doi: 10.1038/s41379-020-0637-6

180. Mattson MP. Hormesis defined. *Ageing Res Rev* (2008) 7(1):1–7. doi: 10.1016/j.arr.2007.08.007

181. Craig AJ, von Felden J, Garcia-Lezana T, Sarcognato S, Villanueva A. Tumour evolution in hepatocellular carcinoma. *Nat Rev Gastroenterol Hepatol* (2020) 17(3):139–52. doi: 10.1038/s41575-019-0229-4

182. Chung A, Nasralla D, Quaglia A. Understanding the immunoenvironment of primary liver cancer: A histopathology perspective. *J Hepatocell Carcinoma* (2022) 9:1149–69. doi: 10.2147/JHC.S382310

183. Guo Y, Yang J, Ren K, Tian X, Gao H, Tian X, et al. The heterogeneity of immune cell infiltration landscape and its immunotherapeutic implications in hepatocellular carcinoma. *Front Immunol* (2022) 13:861525. doi: 10.3389/fimmu.2022.861525

184. Craciun L, de Wind R, Demetter P, Lucidi V, Bohlok A, Michiels S, et al. Retrospective analysis of the immunogenic effects of intra-arterial locoregional therapies in hepatocellular carcinoma: a rationale for combining selective internal radiation therapy (SIRT) and immunotherapy. *BMC Cancer* (2020) 20:135. doi: 10.1186/s12885-020-6613-1

185. Sung W, Grassberger C, McNamara AL, Basler L, Ehrbar S, Tanadini-Lang S, et al. A tumor-immune interaction model for hepatocellular carcinoma based on measured lymphocyte counts in patients undergoing radiotherapy. *Radiother Oncol J Eur Soc Ther Radiol Oncol* (2020) 151:73–81. doi: 10.1016/j.radonc.2020.07.025

186. Ngwa W, Irabor OC, Schoenfeld JD, Hesser J, Demaria S, Formenti SC. Using immunotherapy to boost the abscopal effect. *Nat Rev Cancer* (2018) 18(5):313–22. doi: 10.1038/nrc.2018.6

187. Park JH, Kim HY, Lee A, Seo YK, Kim IH, Park ET, et al. Enlightening the immune mechanism of the abscopal effect in a murine HCC model and overcoming the late resistance with anti-PD-L1. *Int J Radiat Oncol Biol Phys* (2021) 110(2):510–20. doi: 10.1016/j.ijrobp.2020.12.031

188. Feng M, Pan Y, Kong R, Shu S. Therapy of primary liver cancer. *Innovation* (2020) 1(2):100032. doi: 10.1016/j.xinn.2020.100032

189. Grassberger C, Hong TS, Hato T, Yeap BY, Wo JY, Tracy M, et al. Differential association between circulating lymphocyte populations with outcome after radiation therapy in subtypes of liver cancer. *Int J Radiat Oncol Biol Phys* (2018) 101(5):1222–5. doi: 10.1016/j.ijrobp.2018.04.026

190. Wang D, An G, Xie S, Yao Y, Feng G. The clinical and prognostic significance of CD14+HLA-DR–/low myeloid-derived suppressor cells in hepatocellular carcinoma patients receiving radiotherapy. *Tumor Biol* (2016) 37(8):10427–33. doi: 10.1007/s13277-016-4916-2

191. Veness MJ, Delishaj D, Barnes EA, Bezugly A, Rembielak A. Current role of radiotherapy in non-melanoma skin cancer. *Clin Oncol* (2019) 31(11):749–58. doi: 10.1016/j.clon.2019.08.004

192. Wolchok JD, Chiarion-Sileni V, Gonzalez R, Rutkowski P, Grob JJ, Cowey CL, et al. Overall survival with combined nivolumab and ipilimumab in advanced melanoma. *N Engl J Med* (2017) 377(14):1345–56. doi: 10.1056/NEJMoa1709684

193. Ralli M, Botticelli A, Visconti IC, Angeletti D, Fiore M, Marchetti P, et al. Immunotherapy in the treatment of metastatic melanoma: Current knowledge and future directions. *J Immunol Res* (2020) 2020:9235638. doi: 10.1155/2020/9235638

194. Gambichler T, Schröter U, Höxtermann S, Susok L, Stockfleth E, Becker JC. Decline of programmed death-1-positive circulating T regulatory cells predicts more favourable clinical outcome of patients with melanoma under immune checkpoint blockade. *Br J Dermatol* (2020) 182(5):1214–20. doi: 10.1111/bjd.18379

195. Bazyar S, O'Brien ET, Benefield T, Roberts VR, Kumar RJ, Gupta GP, et al. Immune-mediated effects of microplanar radiotherapy with a small animal irradiator. *Cancers* (2021) 14(1):155. doi: 10.3390/cancers14010155

10.3389/fimmu.2023.1148692

Glossary

AAC	Anal Adenocarcinoma
APCs	Antigen Presenting Cells
ASCC	Anal Cell Carcinoma
BCC	Basal Cell Carcinoma
BC	Breast Cancer
CAFs	Cancer Associated Fibroblasts
CAR	Chimeric Antigen Receptor
CCRT	Concurrent Chemoradiotherapy
CIR	Carbon Ion Radiotherapy
CMS	Consensus Molecular Subtypes
CRC	Colorectal Cancer
CRT	Chemoradiotherapy
CTLA-4	Cytotoxic T-Lymphocyte Associated Protein 4
CTV	Clinical Target Volume
DAMPs	Damage-Associated Molecular Patterns
DFS	Disease Free Survival
EC	Esophageal Cancer
FC	Flow Cytometry
FFPE	Formalin Fixed Paraffin Embedded
HCC	Hepatocellular Carcinoma
HNSCC	Head and Neck Squamous Cell Carcinoma
HPV	Human Papillomavirus
ICC	Intrahepatic Cholangiocarcinoma
ICI	Immune Checkpoint Inhibitor
IDO	Indoleamine 2,3-dioxygenase
IE/F	Immune/Fibrotic TME Subtypes
IFN-γ	Interferon gamma
IHC	Immunohistochemistry
IM	Invasive Margin
IMRT	Intensity - Modulated Radiotherapy
IS	Immunoscore
ITCs	Intratumorly T cells Clonotypes
iTME	Immune Tumor Microenvironment
LARC	Locally Advanced Rectal Cancer
LMR	Lymphocyte-to-Monocyte Ratio
LS-SCLC	Limited Stage Small Cell Lung Cancer
LUAD	Lung Adenocarcinoma
MDSCs	Myeloid-Derived Suppressor Cells
MHC	Major Histocompatibility Complex
mIHC	Multiplex Immunohistochemistry
nCRT	Neoadjuvant Chemoradiotherapy
NK	Natural Killer Cells
NLR	Neutrophil-to-Lymphocyte Ratio
NPC	Nasopharyngeal Carcinoma
NSCLC	Non Small Cell Lung Cancer
OAC	Esophageal Adenocarcinoma
OS	Overall Survival
PBMCs	Peripheral Blood Mononuclear Cells
PD-L1	Programmed Death Ligand
PDAC	Pancreatic Ductal Adenocarcinoma
PFS	Progression Free Survival
PSA	Prostate Specific Antigen
QoL	Quality of Life
RT	Radiotherapy
SBRT	Stereotactic Body Radiotherapy
SCC	Squamous Cell Carcinoma
TAMs	Tumor Associated Macrophages
TANs	Tumor Associated Neutrophils
TCR	T Cell Receptor
TDLN	Tumor Draining Lymph Node
TGFβ	Tumor Growth Factor β
Th	T helper cells
TILs	Tumor Infiltrating Lymphocytes
TMB	Mutational Burden
TME	Tumor Microenvironment
TNM	TNM Classification of Malignant Tumors
RT	Radiotherapy
Tregs	Regulatory T cells
TS	Tumor Core

(Continued)

Continued

frontiers | Frontiers in Immunology

TYPE Original Research
PUBLISHED 06 June 2023
DOI 10.3389/fimmu.2023.1138920

OPEN ACCESS

EDITED BY
Fei Yu,
Tongji University School of Medicine, China

REVIEWED BY
Jean-Marc Barret,
GamaMabs Pharma, France
Linlin Guo,
The Ohio State University, United States
Magnus Dillon,
Institute of Cancer Research (ICR), United Kingdom

*CORRESPONDENCE
Randi G. Syljuåsen
randi.syljuasen@rr-research.no

RECEIVED 06 January 2023
ACCEPTED 15 May 2023
PUBLISHED 06 June 2023

CITATION
Eek Mariampillai A, Hauge S, Kongsrud K and Syljuåsen RG (2023) Immunogenic cell death after combined treatment with radiation and ATR inhibitors is dually regulated by apoptotic caspases. *Front. Immunol.* 14:1138920. doi: 10.3389/fimmu.2023.1138920

Immunogenic cell death after combined treatment with radiation and ATR inhibitors is dually regulated by apoptotic caspases

Adrian Eek Mariampillai[1,2], Sissel Hauge[1], Karoline Kongsrud[1] and Randi G. Syljuåsen[1]*

[1]Department of Radiation Biology, Institute for Cancer Research, Norwegian Radium Hospital, Oslo University Hospital, Oslo, Norway, [2]Institute of Clinical Medicine, Faculty of Medicine, University of Oslo, Oslo, Norway

Introduction: Inhibitors of the ATR kinase act as radiosensitizers through abrogating the G2 checkpoint and reducing DNA repair. Recent studies suggest that ATR inhibitors can also increase radiation-induced antitumor immunity, but the underlying immunomodulating mechanisms remain poorly understood. Moreover, it is poorly known how such immune effects relate to different death pathways such as caspase-dependent apoptosis. Here we address whether ATR inhibition in combination with irradiation may increase the presentation of hallmark factors of immunogenic cell death (ICD), and to what extent caspase activation regulates this response.

Methods: Human lung cancer and osteosarcoma cell lines (SW900, H1975, H460, U2OS) were treated with X-rays and ATR inhibitors (VE822; AZD6738) in the absence and presence of a pan-caspase inhibitor. The ICD hallmarks HMGB1 release, ATP secretion and calreticulin surface-presentation were assessed by immunoblotting of growth medium, the *CellTiter-Glo* assay and an optimized live-cell flow cytometry assay, respectively. To obtain accurate measurement of small differences in the calreticulin signal by flow cytometry, we included normalization to a barcoded control sample.

Results: Extracellular release of HMGB1 was increased in all the cell lines at 72 hours after the combined treatment with radiation and ATR inhibitors, relative to mock treatment or cells treated with radiation alone. The HMGB1 release correlated largely – but not strictly – with loss of plasma membrane integrity, and was suppressed by addition of the caspase inhibitor. However, one cell line showed HMGB1 release despite caspase inhibition, and in this cell line caspase inhibition induced pMLKL, a marker for necroptosis. ATP secretion occurred already at 48 hours after the co-treatment and did clearly not correlate with loss of plasma membrane integrity. Addition of pan-caspase inhibition further increased the ATP secretion. Surface-presentation of calreticulin was increased at 24-72 hours after irradiation, but not further increased by either ATR or caspase inhibition.

Conclusion: These results show that ATR inhibition can increase the presentation of two out of three ICD hallmark factors from irradiated human cancer cells. Moreover, caspase activation distinctly affects each of the hallmark factors, and therefore likely plays a dual role in tumor immunogenicity by promoting both immunostimulatory and -suppressive effects.

KEYWORDS

immunogenic cell death (ICD), radiation therapy (radiotherapy), ATR, caspase, CALR (calreticulin), ATP - adenosine triphosphate, HMGB1 (high mobility group box 1)

1 Introduction

Radiotherapy is a cornerstone of cancer treatment, but is often not sufficient for tumor ablation on its own. Hence, radiotherapy is typically combined with other treatment modalities. The serine/threonine protein kinase ATR, which regulates cell cycle checkpoints and DNA repair, is a promising target for such combination treatment. Cancer cells are often found to have a dysfunctional G1 checkpoint, rendering them more reliant on the G2 checkpoint (1, 2). Upon radiation-induced DNA damage, activated ATR is required for the S and G2 checkpoints and homologous recombination repair (3, 4). Inhibition of ATR activity will thus cause the cells to progress through mitosis with unrepaired DNA, resulting in more cell death *via* mitotic catastrophe (5). ATR inhibitors (ATRi) are thus acting as radiosensitizers (6, 7). Combined treatment with radiation and ATR inhibitors is currently tested in clinical trials (8, 9).

In addition to DNA damage and cell death, radiotherapy causes both immunogenic and immunosuppressive effects in the cancer microenvironment [reviewed in (10, 11)]. A major goal is to enhance and exploit the immunostimulatory properties of radiotherapy, in order to prime antitumor immunity and optimize combination with *e.g.* immune checkpoint blockade. However, the interaction between radiotherapy and the immune system is complex, and more knowledge is needed in order to fully understand its possibilities and limitations. Immunostimulatory effects of radiotherapy may *e.g.* be induced when irradiated cancer cells undergo immunogenic cell death (ICD) (12) [reviewed in (13, 14)]. ICD is defined as cell death with the potential to induce immune responses through presentation of damage-associated molecular patterns (DAMPs) (15, 16). The presentation of three such DAMPs have been established as major hallmarks for ICD, namely release of the non-histone nuclear protein high mobility group box-1 (HMGB1), secretion of adenosine 5'-triphosphate (ATP) and surface-presentation of the endoplasmic reticulum protein calreticulin (ecto-CALR) (17). When these DAMPs are presented on or from dying cancer cells, they act as adjuvants (or 'danger signals') (18), enabling dendritic cells of the immune system to recognize tumor-associated antigens (TAAs) as dangerous, and thus induce T cell responses towards the tumor cells (16).

Interestingly, recent preclinical studies suggest that ATR inhibition can increase the immunostimulatory effects of radiotherapy. This has been demonstrated in multiple murine models *in vivo*, where ATR inhibition combined with irradiation caused activation of $CD8^+$ T cells, dendritic cells and natural killer cells, induction of immunological memory and less regulatory T cell-mediated immunosuppression (11, 19–21). Nevertheless, the underlying molecular mechanisms are incompletely understood. ATR inhibition may cause downregulation of programmed cell death 1 ligand 1 (PD-L1) and leukocyte surface antigen 47 (CD47), thereby giving a partial suppression of the PD-1/PD-L1 and SIRPα/CD47 immune checkpoints (22). ATR inhibition can also promote efferocytosis, where apoptotic tumor cells are engulfed by phagocytes such as dendritic cells (23). Moreover, ATR inhibition can increase type I interferon (IFN) signaling *via* induction of cytosolic DNA or RNA in irradiated tumor cells (24–26). ATR thus appears to regulate multiple immunomodulating mechanisms after irradiation. However, to our knowledge, it is not known whether ATR inhibition also affects radiation-induced expression of the abovementioned hallmark factors of ICD.

ICD may be linked to specific cell death mechanisms such as apoptosis, which is executed by activated caspases [reviewed in (27)]. Caspase activation has been shown to promote chemotherapy-induced ATP secretion and calreticulin surface-presentation (28, 29). On the other hand, caspases are generally associated with immunosuppression, as a part of the intended immunological silence of apoptosis [reviewed in (27)]. Apoptotic caspases may therefore also inhibit treatment-induced antitumor immune responses. They can for instance inhibit the mentioned type I IFN response through mediating cleavage of the cytosolic DNA sensor cGAS or other components of the cGAS–STING–IFN pathway [reviewed in (30, 31)]. In line with this, we recently showed that the IFN response to treatment with irradiation and ATR inhibition is counteracted by caspase activation (26). Apoptotic caspases also suppress the release of HMGB1 from mouse melanoma cells after irradiation (32), and may also indirectly inactivate HMGB1 (33). Furthermore, combining irradiation with caspase inhibition gives enhanced antitumor immune responses and tumor regression in murine tumor models *in vivo* (34–36). Caspase inhibition may thus be a potential strategy to enhance the immunostimulatory effects of radiotherapy.

In this study, we hypothesized that irradiation combined with ATR inhibition increases the extent of immunogenic cell death, as ATR inhibition abrogates the radiation-induced G2 checkpoint and disables DNA repair. We also hypothesized that caspase activation contributes to regulate ICD in this setting, in concordance with the previously reported chemotherapy-induced ICD mentioned above (28, 29). The results show that ATR inhibition can increase radiation-induced presentation of HMGB1 and ATP – two of the three ICD hallmark factors. This suggests that the combination treatment with irradiation and ATR inhibition may contribute to priming of antitumor immunity. Furthermore, we show that caspase inhibition has distinct effects on each of the ICD factors, and that caspase activation therefore may promote both immunostimulatory and -suppressive effects after the combined treatment.

2 Results

2.1 Combined treatment with radiation and ATR inhibitors triggers extracellular release of HMGB1 from human cancer cells

In order to evaluate whether ATR inhibitors can increase the expression of ICD hallmark factors after irradiation, we first measured HMGB1 release by immunoblotting of growth medium harvested at 72 hours after treatment (Figures 1A, B). The human osteosarcoma cell line U2OS and the human non-small-cell lung cancer (NSCLC) cell lines H460, SW900 and H1975 were included in this analysis. We have previously observed increased IFN signaling in U2OS and the NSCLC cell lines at 72 hours after treatment with 5 Gy X-rays and the two ATR inhibitors VE822 and AZD6738 at concentrations of 250 nM and 1250 nM, respectively (26). We hence used the same radiation dose, ATR inhibitor concentrations and time-point as in the previous study. All cell lines showed similar kinetics of G2 checkpoint abrogation (26). They also showed increased amount of non-viable cells at 72 hours after the co-treatment with radiation and ATR inhibitors (Supplementary Figure S1A). We found that the co-treatment increased the presence of HMGB1 in the medium of samples from all the cell lines, relative to either the mock treatment or radiation treatment alone (Figure 1B). In addition, 5 Gy irradiation alone increased extracellular HMGB1 in two of the cell lines (H460 and H1975) and gave a non-significant increase in another (SW900) (Figure 1B). As the serum of the growth medium will contain bovine HMGB1, we included a medium control sample to our analysis, to verify that the signals were higher than the background HMGB1 level (Figure 1B). Of note, HMGB1 release was also increased by the co-treatment if cells were cultured in serum-free medium with the serum substitute B-27 (Supplementary Figure S1B). Timecourse analysis of U2OS cells showed that the release of HMGB1 did not occur much earlier than 72 hours after treatment, as it was not detected at 24-48 hours (Supplementary Figure S1C). This correlated with an increased amount of non-viable cells at 72 hours (Supplementary Figure S1D). Furthermore, a lower concentration of the ATR inhibitor VE822 (50 nM) did not yield detectable HMGB1 release (Supplementary Figure S1C).

The release of HMGB1 is believed to occur in a two-step process. First, the HMGB1 translocates from its primary location in the nucleus to the cytoplasm (37). From here, the HMGB1 can be actively secreted (38–40) or passively released [reviewed in (41)] over the cell membrane to the extracellular space. As the immunoblotting of HMGB1 only measured the extracellular HMGB1, we used immunofluorescence microscopy to assess nuclear *versus* cytoplasmic HMGB1 localization following the combined treatment. Whereas HMGB1 was detected only in the nucleus of non-treated U2OS cells, HMGB1 was localized both to the nucleus and to the cytoplasm after treatment with ATR inhibition and irradiation, thus confirming transport of HMGB1 from the nucleus to the cytoplasm (Figure 1C). We next wanted to assess whether the subsequent extracellular release of HMGB1 only occurred from cells with disintegrated cell membranes. To test this, we measured the levels of remaining intracellular HMGB1 in viable *versus* non-viable U2OS cells after treatment. The cell samples were viability-stained with Pacific Blue (PB), before formalin fixation, staining with an anti-HMGB1 antibody and flow cytometry analysis (Supplementary Figure S2A). A barcoded mock sample was added to all samples for accurate quantification of HMGB1 levels. The overall levels of intracellular HMGB1 in viable cells (PB^-) were not markedly reduced after any of the treatments (Figure 1D) and were generally higher than for non-viable cells (Supplementary Figure S2B; bottom histograms). We noted that irradiation alone caused a slight increase in intracellular HMGB1 (Figure 1D). This could likely be related to increased cell size, particularly at 24-48 hours after treatment when irradiated cells remain arrested at the G2 checkpoint. However, when examining the HMGB1 histograms from viable cells at 72 hours post treatment, a proportion of the viable cells (PB^-) from samples treated with ATR inhibition and irradiation showed low HMGB1 levels comparable to the bulk population of non-viable cells (Supplementary Figure S2B). *Vice versa*, a proportion of the non-viable cells (PB^+) showed high HMGB1 levels, comparable to the levels of the bulk population of viable cells (Supplementary Figure S2B, bottom). Taken together, these results suggest that HMGB1 release after treatment with ATR inhibition and irradiation occurs more frequently for non-viable than viable cells, but it is not strictly correlated with loss of membrane integrity.

2.2 Combined treatment with radiation and ATR inhibitors increases secretion of ATP

To measure ATP secreted to the growth medium, we treated cell samples and incubated them for 24-72 hours. As serum may contain ATPases that can perturb the ATP measurements, we replaced the growth medium with fresh, serum-free medium six hours prior to medium harvest (Figure 2A). *CellTiter-Glo* measurements of the harvested medium samples revealed an increase in ATP secretion at 48-72 hours after irradiation alone in H1975, SW900 and H460, but not in U2OS cells (Figures 2B–E). The co-treatment led to increased secretion in U2OS, H1975 and H460 cells, as there was a higher secretion after the co-treatment compared to after treatment with radiation or ATR inhibitor alone in all experiments (Figures 2B, C, E). Timecourse analysis showed that the co-treatment increased ATP secretion at 48 and 72 hours, but not at 24 hours after treatment

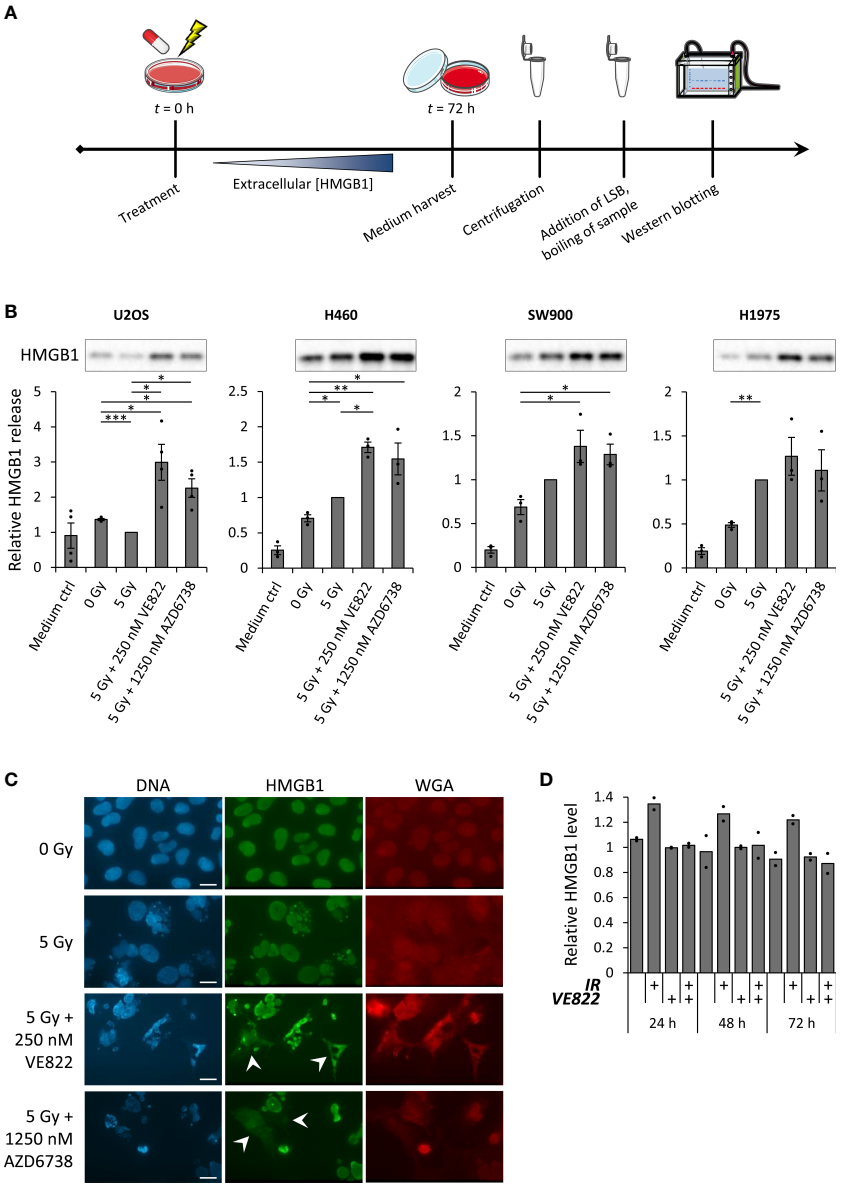

FIGURE 1
Combined treatment with radiation and ATR inhibitors translocate HMGB1 from the nucleus to the cytoplasm, and increase radiation-induced extracellular HMGB1 release. **(A)** Experimental set-up for measurement of HMGB1 release. Medium from treated cells was collected 72 hours post treatment to allow for accumulation of extracellular HMGB1. After harvest, the samples were centrifuged in order to exclude floating cells, before they were diluted in loading sample buffer (LSB) and analyzed by SDS-PAGE and western blotting. **(B)** Results from three or more experiments performed as in **(A)** for U2OS, H460, SW900 and H1975 cells. Bar charts show quantification of extracellular HMGB1. In each experiment the values are normalized to the values for the 5 Gy treatment. *p* values were calculated as described in the Materials and methods section (not included for medium controls). Immunoblots on top of the bar charts are from a representative experiment. **(C)** Micrographs of U2OS cells stained with antibody against HMGB1 (green), the nuclear stain Hoechst (blue) and cell membrane staining, fluorochrome-conjugated WGA (red) at 72 hours post treatment. White arrows indicate cells with cytoplasmic HMGB1 signal. Scale bar = 20 µm. **(D)** Relative levels of intracellular HMGB1 in viable U2OS cells at indicated time-point after treatment with ionizing radiation (5 Gy; IR) and/or the ATR inhibitor VE822 (250 nM), as measured by flow cytometry. Cells were stained with Pacific Blue (PB) before fixation to distinguish between viable (PB^-) and non-viable (PB^+) cells. (Viable cells were gated as in Supplementary Figure S2B). $n = 2$. $*p \leq 0.05$, $**p \leq 0.01$, $***p \leq 0.001$.

(Figures 2B, C). However, the ATP secretion was not increased after the co-treatment compared to after irradiation alone in SW900 cells (Figure 2D). Although ATP secretion was clearly most pronounced with the highest ATR inhibitor concentration of 250 nM VE822, a small increase in ATP secretion was also observed 72 hours after irradiation in combination with 50 nM VE822 (Figure 2B). Of note is that the results for H460 had to be normalized to the cell number of the dish at time of harvest, as the treatments severely impacted the cell growth relative to the rapidly dividing mock sample (Figure 2E). Altogether, these results show that ATP secretion is increased after irradiation alone in three of the cell lines, and increased relative to mock in all cell lines after the co-treatment. Interestingly, the ATP secretion is markedly increased already at 48 hours after the co-treatment.

10.3389/fimmu.2023.1138920

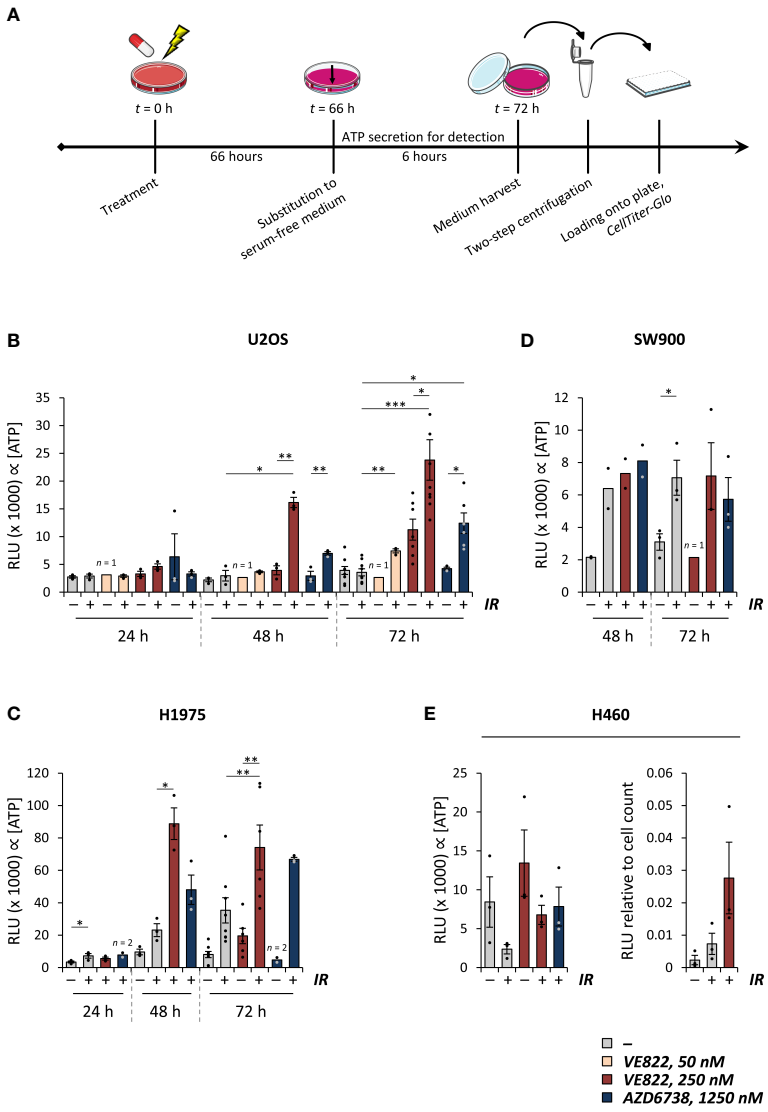

FIGURE 2
Combined treatment with radiation and ATR inhibitors increases ATP secretion. **(A)** Experimental set-up for measurement of ATP secretion, exemplified for the 72 hour time-point. Treated samples were incubated for 72 hours. Six hours prior to medium harvest, the medium was replaced with a reduced amount of serum-free medium. The media were collected from the samples, and centrifuged twice for cell exclusion, before the medium supernatants were analyzed by use of the *CellTiter-Glo* assay. Same set-up was employed for the other time-points, still with medium replacement for the last six hours. **(B-D)** Results from experiments performed as in **(A)** for U2OS **(B)**, H1975 **(C)** and SW900 cells **(D)** at indicated time-points after treatment with ionizing radiation (5 Gy; IR) and/or ATR inhibitors (VE822 or AZD6738 at indicated concentration). Bar charts show crude relative luminescence values (relative luminescence units; RLU), which is proportional to the extracellular concentration of ATP. *p* values were calculated for difference between co-treatments and irradiation alone or ATR inhibition alone. For statistical analysis between groups of different size, only data that paired up from the same experiments were included. **(E)** Results from experiments performed as in **(A)** in H460 cells, presented as for **(B-D)** (left). To correct for vast differences in cell count after treatment in this cell line, the relative luminescence values were normalized to cell counts at time of harvest (right). *$p \leq 0.05$, **$p \leq 0.01$, ***$p \leq 0.001$.

2.3 An optimized ecto-CALR detection protocol reveals increased ecto-CALR after irradiation, but no further increase after combined treatment with radiation and ATR inhibitors

Cells undergoing ICD may translocate calreticulin from the endoplasmic reticulum to the cell surface. Nevertheless, the increase in ecto-CALR might be small, making accurate detection important. We therefore optimized a live-cell flow cytometry-based detection protocol, in which we included a barcoding strategy to eliminate any variation that might occur due to differences in antibody staining between samples. First, a mock sample, consisting of non-treated cells, was stained with cell permeable Hoechst 33342 and distributed in equal portions to the samples with treated, non-stained cells. Thereafter, the barcoded samples were stained with anti-CALR and secondary antibodies, as well as the non-permeable DNA-stain propidium iodide for live/dead cell differentiation (Figure 3A). In this way, the Hoechst-stained mock sample served as an internal standard enabling normalization of the ecto-CALR

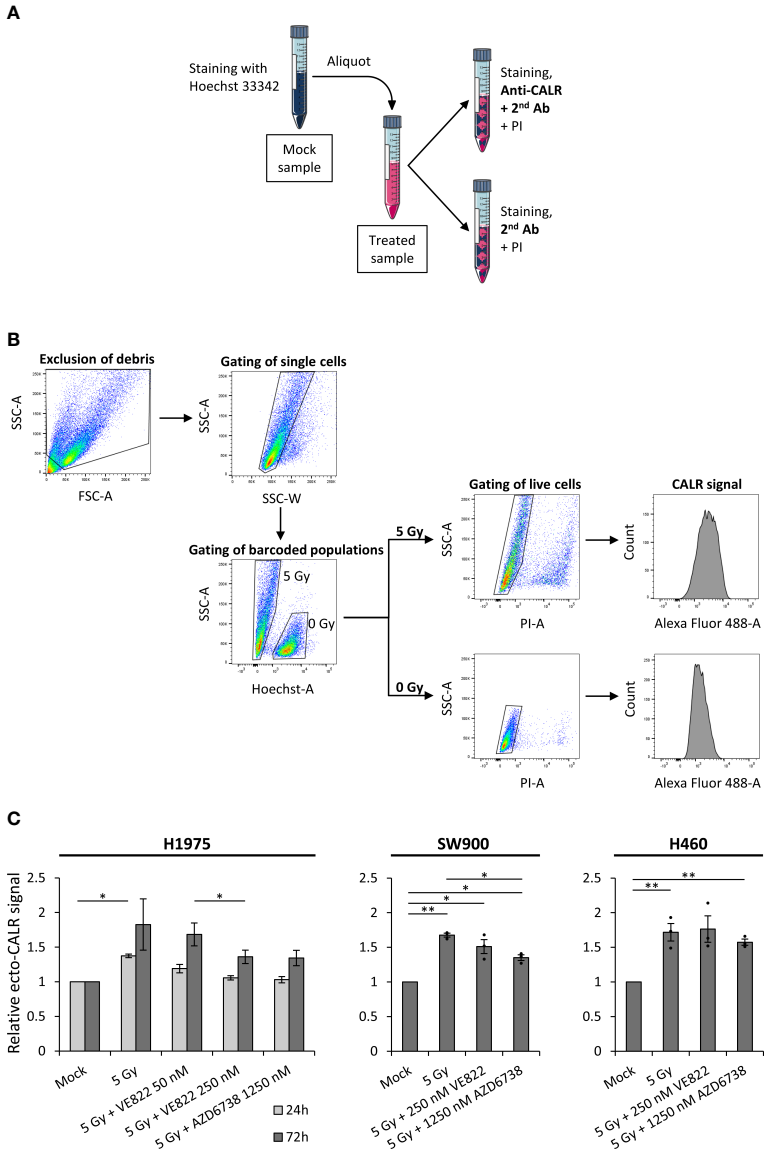

FIGURE 3
Surface-presentation of calreticulin is increased upon irradiation, but is not further increased by the addition of ATR inhibitors. **(A)** Procedure of Hoechst 33342-based barcoding, in which a live mock sample was stained with permeable Hoechst 33342, before it was divided equally to differently treated live-cell samples. Each of the barcoded samples were thereafter split into two aliquots; one for primary anti-calreticulin (anti-CALR) staining and one for secondary antibody control staining. The two aliquots were thereafter stained with propidium iodide (PI) for discrimination of live and dead cells. **(B)** The gating hierarchy employed for the flow cytometry analysis. Debris was excluded and cells were gated in a forward-scatter area (FSC-A) *versus* side-scatter area (SSC-A) plot. Cell singlets were gated in a side-scatter width (SSC-W) *versus* SSC-A plot. The barcoded populations were separated in a Hoechst-A *versus* SSC-A plot, in which the Hoechst 33342-stained mock population is shifted upwards the Hoechst-A axis. Live cells were gated in PI-A *versus* SSC-A plots, in which dead (PI^+) cells are shifted upwards the PI-A axis. Finally, histograms of the ecto-CALR signals (Alexa Fluor 488) are obtained from the live cells in both of the barcoded populations, and the median value of ecto-CALR signal is obtained from each histogram. Similar gating hierarchy and analysis was done for the secondary antibody control samples. (Demonstrated in H1975 cells). **(C)** Results from experiments performed as in **(A, B)** for H1975, SW900 and H460 cells after treatment with ionizing radiation and ATR inhibitors. Bar charts show ecto-CALR signals normalized to the barcoded mock population of each sample. Note that results from both a 24 hours time-point (light grey) and 72 hours time-point (dark grey) are shown for H1975, whereas results from the 72 hours time-point are shown for SW900 and H460. *$p \leq 0.05$, **$p \leq 0.01$.

signals from all treated samples to the ecto-CALR signal of a common mock sample. The mock and treated cell populations were separated by the Hoechst 33342 signal during data analysis (Figure 3B). All of the barcoded samples were split into secondary antibody controls as well, and we performed similar analysis for these secondary antibody controls. Hence, we could subtract the background signals of the secondary antibody controls from the ecto-CALR signals (Supplementary Figure S3). Importantly, the background signals of the secondary antibody controls were shifted upon the various treatments, and it was therefore crucial to include secondary antibody controls for all samples in the experiment.

Using this method, we found that irradiation alone (5 Gy) increased ecto-CALR presentation by a factor of ~1.5 at 24 hours post treatment and ~1.8 at 72 hours post treatment relative to mock

in H1975 (Figure 3C). No further increase was seen after the co-treatment with radiation and ATR inhibitors (Figure 3C). Rather, the co-treatment showed a trend towards reduction in radiation-induced ecto-CALR presentation in H1975. Similarly, we observed an increase in ecto-CALR at 72 hours post irradiation for SW900 and H460, but no further increase after the co-treatment (Figure 3C). U2OS cells were not included in this assay as the ecto-CALR signals were too low to be distinguished from the secondary antibody controls in this cell line (data not shown). We conclude that our optimized flow cytometry assay reveals a small increase in ecto-CALR after irradiation alone, but no further increase after co-treatment with irradiation and ATR inhibition.

2.4 Inhibition of apoptotic caspases differentially modulates the HMGB1 release, ATP secretion and ecto-CALR after combined treatment with radiation and ATR inhibition

We have previously shown that activated caspases suppress IFN-β secretion after the co-treatment with irradiation and ATR inhibition (26). To assess whether caspase activation also affects ICD after irradiation and ATR inhibition, we used the inhibitor Q-VD-OPh, which inhibits several caspases including the apoptotic caspases 3, 7, 8 and 9. In contrast to the effects on IFN-β secretion, we found that the caspase inhibitor strongly suppressed the HMGB1 release in H460 and U2OS cells, suggesting that the HMGB1 release is coupled to caspase activity and apoptosis (Figure 4A, B). In line with a specific role of apoptotic caspases in this process, the HMGB1 release was not much affected by two inhibitors of caspase-1 that did not suppress caspase-3 cleavage (Supplementary Figure S4A). Notably, Q-VD-OPh did not appear to inhibit HMGB1 release in H1975 cells, despite inhibition of caspase-3 cleavage (Figure 4A-C; Supplementary Figure S4B). However, in this cell line caspase inhibition caused increased phosphorylation of the pseudokinase mixed lineage kinase domain-like protein (pMLKL), a marker for necroptosis (Figure 4C). Necroptosis has previously been linked to HMGB1 release after caspase inhibition (32). The HMGB1 release after caspase inhibition in H1975 is thus likely caused by redirection of cell death towards necroptosis. On the other hand, the ATP secretion measured by the *CellTiter-Glo* assay was actually increased upon addition of Q-VD-OPh in U2OS and slightly increased in H1975 (Figure 4D), the two cell lines with highest increase in Figure 2. Caspase inhibition thus gave opposite effects on HMGB1 release and ATP secretion in U2OS cells. Caspase inhibition showed no major effects on the ecto-CALR signal in either H1975 or H460 cells (Figure 4E). (As mentioned above, U2OS was not included in the ecto-CALR measurements as the signal was too low). During flow cytometry analysis, we also quantified the percentage of live cells based on the exclusion of propidium iodide positive cells. As expected, the caspase inhibitor partly rescued the decrease in cell viability seen upon the co-treatment with irradiation and ATR inhibition (Supplementary Figure S4C). Altogether, these results show that treatment-induced caspase activation gives distinct effects on each of the ICD hallmark factors, as well as on IFN-β signaling, thus likely promoting both immunostimulatory and -suppressive effects.

3 Discussion

In this study, we have assessed presentation of three hallmark factors for immunogenic cell death – namely release of HMGB1, secretion of ATP and surface-presentation of CALR – in human cancer cell lines after treatment with radiation and ATR inhibitors. To our knowledge, this is the first study reporting whether ATR inhibition can increase the radiation-induced expression of these ICD factors. We found that the combined treatment with radiation and ATR inhibitors can increase the release of HMGB1 and secretion of ATP, but not surface-presentation of CALR, in several human cancer cell lines. Previous studies have shown that ATR inhibition affects multiple immunomodulating mechanisms after irradiation, including type I IFN responses, efferocytosis and immune checkpoints (22–26). Our new results suggest that increased HMGB1 release and ATP secretion may be added to this list of immunomodulating mechanisms that promote antitumor immunity after the combined treatment.

Moreover, our results show that activated caspases can modulate the ICD response after treatment with irradiation and ATR inhibition: Caspase inhibition can abolish the extracellular release of HMGB1, as shown for two cell lines, but increases the ATP secretion and does not alter the CALR surface presentation. We have previously reported that caspase inhibition strongly increases a type I IFN response after the combined treatment with radiation and ATR inhibitors (26). Caspase inhibition thus leads to distinct effects on each of these factors: It clearly exerts immunostimulatory effects on IFN signaling and also appears to promote immunostimulatory ICD through increased ATP secretion. Nevertheless, it contributes neither stimulatory nor suppressive through ecto-CALR presentation, and can exert immunosuppression through vastly reducing the HMGB1 release. An interesting issue for future studies is to determine which of these factors are most important for antitumor immunity, in order to evaluate the physiological potential of the caspase inhibition. Potentially, the strong increase in IFN secretion upon triple-treatment with irradiation, ATR inhibition and caspase inhibition may outweigh the concomitant loss of HMGB1 release, thus resulting in an overall increased antitumor immune response. Notably our finding of caspase-dependent HMGB1 release is consistent with results in *e.g.* apoptosis-mediated sepsis (42) and for macrophages treated with a proteasome inhibitor (43). Furthermore, our results suggest that caspase inhibition does not always abolish the HMGB1 release, as shown for H1975 cells where the caspase inhibition also caused phosphorylation of MLKL, a necroptosis marker. As mentioned above, the results in H1975 resemble the previous report of necroptosis and HMGB1 release after caspase inhibition and irradiation in mouse melanoma cells (32). Triple-treatment with caspase inhibition, irradiation and ATR inhibition can thus likely induce necroptosis-dependent HMGB1 release in some cases. Interestingly, our finding that ATP secretion

10.3389/fimmu.2023.1138920

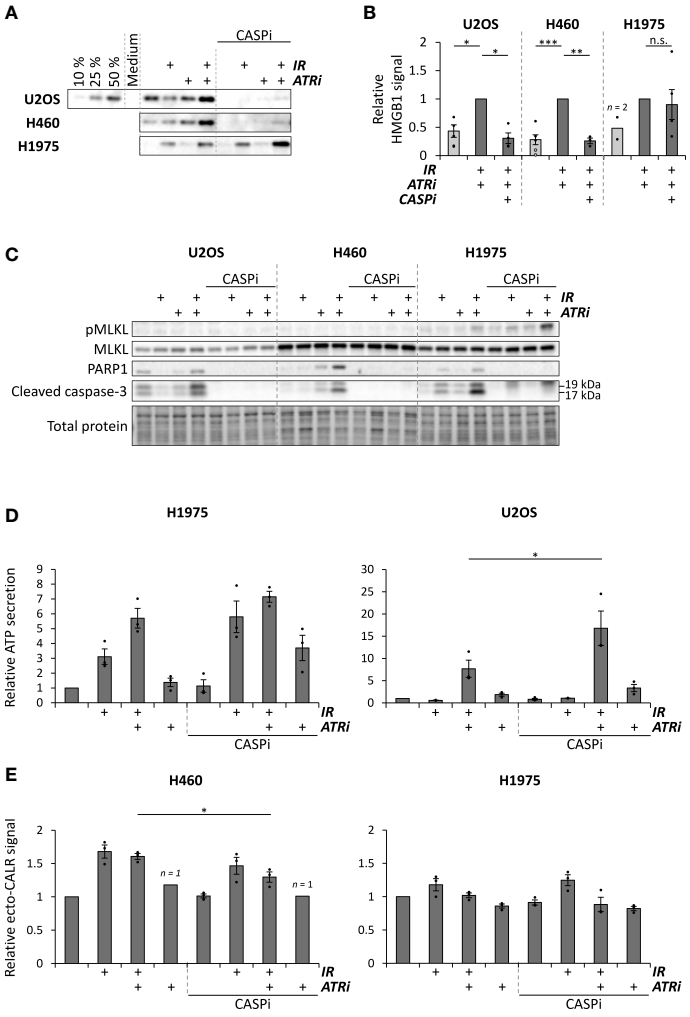

FIGURE 4
Caspase inhibition can suppress HMGB1 release, increases ATP secretion and does not alter ecto-CALR presentation after combined treatment with radiation and ATR inhibitors. **(A)** Representative immunoblots of extracellular HMGB1 in medium supernatants from U2OS, H460 and H1975 cells at 72 hours after treatments with 5 Gy radiation (IR) and/or 250 nM VE822 (ATRi) and 10 μM of the pan-caspase inhibitor Q-VD-OPh (CASPi). Gradient in the U2OS blot represents different volumes loaded from the co-treated sample. **(B)** Quantification of extracellular HMGB1 in independent experiments performed as for the immunoblots in **(A)**, from samples treated with 5 Gy or 6 Gy (IR; black and grey dots, respectively), 250 nM VE822 (ATRi) and 10 μM Q-VD-OPh (CASPi), normalized to the sample treated with IR + ATRi. (Please note that 1, 3, 2 and 3 data-points for the mock of U2OS and H1975 and the triple-treatment for U2OS and H460, respectively, were non-detectable and hence excluded from the quantification. Averages for these treatments were therefore even lower in reality). n.s. = non-significant. **(C)** Immunoblots of cleaved caspase-3, cleaved PARP1, phosphorylated MLKL and total MLKL in cell lysates corresponding to the supernatants used for the HMGB1 immunoblots in **(A)**. **(D)** ATP secretion in H1975 and U2OS cells with and without caspase inhibitor Q-VD-OPh (CASPi, 10 μM), normalized to the mock sample. ATP secretion was measured at 72 hours post treatment as in Figure 2A. **(E)** Results from the ecto-CALR flow cytometry assay in H460 and H1975 cells treated for 72 hours with and without 10 μM Q-VD-OPh (CASPi). Values are normalized to the barcoded mock signal (0 Gy), as in Figure 3. *$p \leq 0.05$, **$p \leq 0.01$, ***$p \leq 0.001$.

is increased by caspase inhibition is in contrast to previous studies showing caspase-dependent ATP secretion during chemotherapy-induced ICD (28). The co-treatment with irradiation and ATR inhibition thus likely activates an alternative, non-apoptotic mechanism of ATP secretion. Indeed, ATP secretion independent of the apoptosis mediators BAX and BAK has been reported in cells with intact plasma membrane (16). In line with this, the measured ATP in our experiments most likely reflects secretion from live cells, as it was high already at 48 hours after treatment and was increased when the viability was increased by caspase inhibition.

To accurately measure the surface-presentation of CALR, we included a unique barcoding strategy in our live-cell flow cytometry assay. Previous studies that have used flow cytometry to measure ecto-CALR have also included a dye to distinguish live from dead cells (*e.g.* (44, 45)), similar to the use of propidium iodide in our assay. However, we are not aware of any previous study that has included a similar barcoding strategy for ecto-CALR measurements. By including barcoding with the membrane-permeable Hoechst 33342 dye, the CALR signal of each sample can be normalized to the CALR signal of a common live-cell standard. As the Hoechst-stained cells are added to the samples prior to antibody staining, this procedure eliminates any potential variation due to *e.g.* differences in antibody concentration or cell numbers between the samples. Notably, the background signals of the secondary antibody controls

increased upon treatment with irradiation and/or ATR inhibition. As a similar increase in background signals was seen for non-stained cells (data not shown), this most likely reflects increased autofluorescence due to treatment-induced changes to the cell. This increase in background signals particularly becomes important when measuring the expression of low-abundance surface proteins, such as ecto-CALR. When measuring ecto-CALR it is thus necessary to accurately obtain the background signal for each treatment. In our optimized flow cytometry protocol, we measure the background signals in aliquots taken from every sample, which then also contains the Hoechst-stained mock cells. We thus obtain a highly accurate measurement of the background signals.

Previous studies have shown that radiation treatment alone can induce ICD, as measured by several DAMPs (12, 46). This is further substantiated in our study. We detected radiation-induced increases in both HMGB1 release, ATP secretion and ecto-CALR in several cell lines. Notably the responses appear to vary between cell lines, as HMGB1 release and ATP secretion were not detected after irradiation alone in U2OS cells. Interestingly, this difference between U2OS and the other cell lines was not likely caused by a corresponding difference in radioresistance. The amount of non-viable cells after irradiation was not markedly lower for U2OS than the other cell lines (Supplementary Figure S1), and previous studies have shown largely similar clonogenic survival for U2OS, H460 and H1975 after irradiation (47, 48). Treatment with ATR inhibitor alone also gave detectable increases in HMGB1 release and ATP secretion, but only for the highest concentration of VE822 (250 nM) at 72 hours post treatment, and not for AZD6738. The effects of the co-treatment could thus not be explained by the effects of ATR inhibition alone. Importantly, the combined treatment with irradiation and ATR inhibition caused increased HMGB1 release and ATP secretion compared to mock in all cell lines tested. The ultimate functional endpoint of ICD is the priming of tumor-specific T cell responses, mediated through recruitment of antigen-presenting cells to the tumor microenvironment. Although it has been reported that simultaneous presence of every ICD hallmark factor is crucial for ICD *per se* (49), it is reasonable to assume that it is the total immunogenicity of the microenvironment – contributed by the concoction of many different DAMPs – that governs the functional endpoint. Hence, lack of response for some of the hallmarks, such as ecto-CALR in this study, does not rule out the immunogenic potential, as long as there is adequate presence of other immunogenic factors.

The immunostimulatory effects of ATR inhibition in combination with irradiation may potentially be exploited to improve the efficacy of immune checkpoint blockade. Indeed, triple-treatment with radiotherapy, ATR inhibitor and anti-PD-L1 antibodies have been shown to increase antitumor immunity in preclinical mouse models. In a hepatocellular carcinoma model, the triple-treatment caused increased $CD8^+$ T cell infiltration, less regulatory T cells and increased immunological memory compared to after co-treatment with radiotherapy and anti-PD-L1 (21). Similarly, $CD8^+$ T cell infiltration was increased after triple-treatment of murine colorectal cancer models (50). Another study found that the activity of natural killer (NK) cells was boosted by immune checkpoint blockade (targeting either PD-1 or T cell immunoreceptor with Ig and ITIM domains (TIGIT)) in combination with ATR inhibition and radiotherapy in a murine oral squamous cell carcinoma model (51). Moreover, analogous to the combination studies with radiotherapy, long-lasting antitumor immunity was also observed in a murine colorectal model when ATR inhibition was combined with anti-PD-L1 antibodies and platinum-based chemotherapy (52). Promising preclinical results have led to several ongoing early-phase clinical trials with immune checkpoint blockade in combination with ATR inhibitors, and at least one of these studies addresses the triple-treatment with radiotherapy [reviewed in (11, 53)]. Of note is that even the co-treatment of radiotherapy and immune checkpoint blockade is far from fully developed. Both the optimal radiation dose and timing and sequence of treatment remain to be determined [reviewed in (54–56)]. The optimization of the triple-treatment is even more complex. Interestingly, it was recently shown that prolonged ATR inhibitor treatment can abolish the antitumor immune responses in two murine cancer models (colorectal CT26 and melanoma B16-F10). A short-term ATR inhibitor treatment and subsequent cessation was required to increase $CD8^+$ T cell responses to radiotherapy and immune checkpoint inhibitors (57).

In conclusion, our results substantiate the potential for ICD induction by radiotherapy, and show that irradiation in combination with ATR inhibition further increases this potential. Induction of ICD may thus likely contribute, at least to some extent, to the immunostimulatory properties of such combined treatment. Moreover, our results show distinct roles of caspase activation in the regulation of each ICD hallmark. Further studies revealing the exact immunomodulating mechanisms induced by irradiation and ATR inhibition may help to develop new biomarkers for treatment response and to optimize treatment schedules. Understanding these mechanisms will also likely help to further exploit the immunostimulatory properties of the combined treatment, *e.g. via* subsequent treatment with immune checkpoint blockade.

4 Methods and materials

4.1 Cell culturing and treatment

Human U2OS osteosarcoma and H460 NSCLC cells were grown in Dulbecco's modified Eagle's medium with GlutaMAX-I (Gibco by Life Technologies, ThermoFisher Scientific #61965059), and human H1975 and SW900 NSCLC cells were grown in Roswell Park Memorial Institute 1640 medium with GlutaMAX-I (Gibco by Life Technologies, ThermoFisher Scientific #61870044) in a humidified 5% CO_2 atmosphere at 37°C. Both media were supplemented with 10% foetal bovine serum (FBS, Biowest #S1810) and 1% penicillin–streptomycin solution (10,000 IU/ml; 10,000 µg/ml) (Pen Strep, Gibco by Life Technologies, ThermoFisher Scientific #15140122). Cell line identity was confirmed by short tandem repeat analysis, and the cultures were tested for *Mycoplasma* infection. The cells were treated with ATR inhibitors VE822 (berzosertib/VX970, Selleckchem #S7102) at 250

nM or 50 nM and AZD6738 (ceralasertib, Selleckchem #S7693) at 1250 nM, and the pan-caspase inhibitor Q-VD-OPh (quinoline-Val-Asp-difluorophenoxymethylketone, MedChemExpress #HY12305) at 10 μM, for 10-30 minutes before X-irradiation (160 kV Faxitron Corporation CP-160, dose rate 1 Gy/min). Caspase-1 inhibitors Ac-YVAD-cmk (acetyl-Tyr-Val-Ala-Asp-chloromethylketone) and VX-765 (belnacasan) (both from InvivoGen, #inh-yvad and #inh-vx765i-1, respectively) were employed at 60 and 120 μM.

4.2 Western blotting of released HMGB1 in growth medium supernatants

For measuring extracellular HMGB1, an equal number of cells were seeded in 6 cm dishes for all samples within an experiment. Cells were treated as indicated and incubated for 72 hours, before the growth medium supernatants were harvested. The medium was centrifuged at 12100 × *g* for 5 minutes for exclusion of cells and debris, and the resulting supernatants were diluted 1:2 in 5X loading buffer (Pierce Lane Marker Reducing Sample Buffer, ThermoFisher Scientific #39000) and boiled at 95°C for 10 minutes. The samples were loaded onto SDS polyacrylamide 4-15% gradient gels (Mini-Protean TGX, Bio-Rad #4561086) for electrophoresis, and blotted onto nitrocellulose membrane (Bio-Rad #1704270). The membrane was stained with Ponceau S (Sigma-Aldrich #P7170), and blocked in 5% non-fat skimmed milk (Sigma-Aldrich #70166) in phosphate-buffered saline with 0.1% Tween-20 (Bio-Rad #1610781) (PBST). The membrane was stained with anti-HMGB1 antibodies (Abcam, ab18256, 1:2000 in blocking solution) at 4°C over-night, and thereafter stained with horseradish-conjugated secondary antibodies (Jackson ImmunoResearch, #111-035-144, 1:10 000 in blocking solution) for minimum 30 minutes before addition of enhanced chemiluminescence (ECL) solution (SuperSignal West, ThermoFisher Scientific #34580/#34076/#34095) and processing (ChemiDoc MP, Bio-Rad). Quantification was performed in Image Lab 4.1 (Bio-Rad). For blotting of caspases in the corresponding cell lysates, cells were washed with PBS and stored at -80°C. The cells were lysed with whole-cell lysis buffer [20 mM NaCl, 2 mM $MgCl_2$, 50 mM Tris-HCl pH 7.5, 0.5% Triton X-100 (Sigma-Aldrich #T9284)] with protease and phosphatase inhibitor cocktails (cOmplete mini (EDTA-free) and PhosSTOP EASYpack, Roche, Sigma-Aldrich #5892791001 and #4906837001) and benzonase (100 IU/ml; Merck/Sigma-Aldrich #70664-3). The lysates were diluted based on protein concentration measurements (Micro BCA Protein Assay kit, ThermoFisher Scientific #23235), before 5X loading buffer was diluted 1:4 in each sample. The samples were boiled before SDS-PAGE (Criterion TGX Stain-Free gels, Bio-Rad #5678085) and immunoblotting as described above. *Primary antibodies*: Cleaved Caspase-3 (Asp175) (5A1E), 1:100, Cell Signaling Technology #9664. PARP1 (F2), 1:200, Santa Cruz Biotechnology #sc-8007. MLKL phospho-Ser358 (D6H3V), 1:1000, Cell Signaling Technology #91689. MLKL (D2I6N), 1:1000, Cell Signaling Technology #14993. γ-tubulin, 1:1000, Sigma-Aldrich #T6557. Quantification of HMGB1 blots were performed by use of loaded volume gradients (see *e.g.* 50%, 25%, 10% in Figure 4A).

4.3 Immunofluorescence microscopy analysis of HMGB1 release

Cells were seeded ($3{\cdot}10^5$ cells for treatments, $1{\cdot}10^5$ for mock) in 6 cm dishes containing glass coverslips, and incubated over-night. The samples were treated as indicated, and incubated for 72 hours. The coverslips were washed with phosphate-buffered saline (PBS) and the cells were fixated with a 10% formalin solution (Sigma-Aldrich #HT5011) for 10 minutes. The cells were washed three times in PBS, and stained with Alexa Fluor 594-conjugated wheat germ agglutinin (WGA) (1:1000, ThermoFisher Scientific #W11261) for 10 minutes. The cells were washed three times in PBS and permeabilized with 0.2% Triton X-100 (Sigma-Aldrich #T9284) in PBS for 5 minutes. The cells were washed and stained with anti-HMGB1 antibodies (Abcam, ab18256, 1:1000 in growth medium with 10% FBS) for 1 hour, followed by three washes in PBS and secondary antibody staining (Molecular Probes by Life Technologies (ThermoFisher Scientific #A-21206), Alexa Fluor 488, 1:1000 in growth medium with 10% FBS) for 30 minutes. The cells were washed, stained with 0.6 μg/ml permeable Hoechst 33342 (Invitrogen, ThermoFisher Scientific #H3570) in PBS for 5 minutes and eventually mounted onto object slides with mowiol solution (Mowiol 4-88, Sigma-Aldrich #81381).

4.4 Flow cytometric analysis of viability and intracellular HMGB1

Cells were harvested by trypsinization and centrifuged at approx. 400 × *g*. Resulting cell pellets were stained with Pacific Blue (0.0375 ng/μl final concentration, $V = 200$ μl), and incubated at 4°C for 15 minutes. The samples were washed with 3 ml PBS/1% FBS, and centrifuged as before. For the viability measurements presented in Supplementary Figure S1, the resulting cell pellets were thereafter fixated with 70% EtOH, and stored at -20°C. For intracellular staining of HMGB1, the cell pellets were fixated in 10% formalin solution (Sigma-Aldrich #HT5011) for 10 minutes at room temperature, before they were washed in PBS, resuspended in 70% EtOH and stored at -20°C. An aliquot of a barcode-stained (succinimidyl ester-conjugated Alexa Fluor 647, ThermoFisher Scientific #A20006) mock sample was added to all samples, similarly as before (*e.g.* (47)), allowing accurate quantification of HMGB1 levels. The samples were washed with PBS/2% FBS, and the cell pellets were stained with primary anti-HMGB1 antibodies (Abcam, ab18256, 1:500 in flow cytometry staining buffer [0.1% IGEPAL CA-630 (Sigma-Aldrich #I3021), 6.5 mM Na_2HPO_4, 1.5 mM KH_2PO_4, 2.7 mM KCl, 137 mM NaCl, 0.5 mM EDTA pH 7.5)] for 1 hour and secondary anti-rabbit Alexa Fluor 488 (Molecular Probes by Life Technologies (ThermoFisher Scientific #A-21206),

1:500 in flow cytometry staining buffer) for 30 minutes. The samples were thereafter analysed by flow cytometry (BD LSR II, BD Biosciences). Subsequent analyses were conducted with FlowJo v10.

4.5 *CellTiter-Glo* detection of secreted ATP in growth medium supernatants

Cells were treated with radiation and ATR inhibitors as described and incubated until 6 hours before harvest. The growth media were aspirated, before the dishes were washed with PBS, and then given 1 ml serum-free medium (with inhibitors at given dose, if used). The samples were incubated for the remaining 6 hours – of which ATP secretion would be detected – before the growth media were harvested. The medium supernatants were centrifuged at 12100 × *g* for 5 minutes, and the resulting supernatants were transferred to new tubes. The supernatants were centrifuged a second time at 12100 × *g* – to ensure exclusion of any floating cells – and the resulting supernatants were loaded onto a 96-well plate with clear bottoms and white walls (Corning Costar 3610, Sigma-Aldrich #CLS3610-48EA), together with samples for an ATP standard curve. The samples subsequently underwent the *CellTiter-Glo* procedure after the supplier's protocol (CellTiter-Glo Luminescent Cell Viability Assay, Promega #G7572), before spectrophotometric analysis.

4.6 Live-cell flow cytometric detection of surface-presented calreticulin

Cells were seeded and let adhere over-night, before the cells were treated as described, and incubated for 24 or 72 hours. The dishes were harvested – both growth medium supernatants and adhered cells – by use of TrypLE Express (Gibco by Life Technologies, ThermoFisher Scientific #12563029). First, the mock sample was centrifuged at approx. 400 × *g* (2000 rpm). The cell pellet was resuspended in 100 µl medium with 1 µg/ml Hoechst 33342 (Invitrogen, ThermoFisher Scientific #H3570) and incubated at room temperature for 30 minutes, for barcode staining. The barcode-stained sample was thereafter washed with PBS/1% FBS and resuspended in PBS/1% FBS. Meanwhile, the remaining samples were harvested. Equal aliquots of the barcode-stained mock samples were thereafter added to each of the remaining samples, before these were split in two for subsequent primary antibody staining and secondary antibody control staining. The samples were centrifuged at approx. 500 × *g*, and the cell pellets were resuspended in 100 µl medium (10% FBS) with primary anti-CALR antibodies (Abcam, ab2907, 1:250), or plain medium (10% FBS) for secondary antibody controls, and incubated on ice for 30 minutes. The samples were washed, and resulting cell pellets were resuspended in 100 µl medium (10% FBS) with secondary antibodies (Molecular Probes by Life Technologies (ThermoFisher Scientific #A-21206), Alexa Fluor 488, 1:500). The samples were incubated on ice for 30 minutes, and washed. The samples were resuspended in PBS and transferred to flow cytometry tubes. 1 µl propidium iodine (1.667 mg/ml) was added to the samples 2 minutes prior to flow cytometry (BD LSR II, BD Biosciences), for live/dead staining. Flow cytometric analysis was conducted in FlowJo v10. Ecto-CALR signals were calculated by $[(\text{signal}_{\text{treated}} - \text{background}_{\text{treated}})/(\text{signal}_{\text{mock}} - \text{background}_{\text{mock}})]$, where the secondary antibody control signals constitute the background values. Median Alexa Fluor 488 values were used as outputs from the flow cytometry.

4.7 Statistics

For measurements with ≥ 3 replicates, results are presented with standard error of the mean (SEM) error bars. Dots in bar charts indicate individual experiments. *p* values (two-tailed, one-sample Student's *t* test for pairs involving normalization value; two-tailed, paired-samples Student's *t* test for the remaining pairs) were calculated with IBM SPSS Statistics v28, with significance level set to 0.05. $^{*}p \leq 0.05$, $^{**}p \leq 0.01$, $^{***}p \leq 0.001$.

Data availability statement

The raw data supporting the conclusions of this article will be made available upon request to the corresponding author.

Author contributions

Conceptualization: RS, AEM, SH. Experiments: AEM, SH, KK. Data analysis: AEM, SH, KK, RS. Supervision: RS, SH. Critical review of work: All authors. Writing – original draft preparation: AEM, RS. Writing – editing: All authors. Funding acquisition: RS. All authors contributed to the article and approved the submitted version.

Funding

This work was funded by grants from the South-Eastern Norway Health Authorities (2018010) and the Norwegian Cancer Society (198018).

Acknowledgments

We thank Inger Øynebråten and Alexandre Corthay for helpful discussions and critical reading of the manuscript. We also thank Trond Stokke for helpful suggestions regarding barcode-staining with Hoechst 33342, and the Flow Cytometry Core Facility at the Norwegian Radium Hospital, Oslo University Hospital for training and useful support. Figures 1A, 2A, 3A, S2A and S3A contain elements from *SMART Servier Medical Art* by Laboratoires Servier.

Conflict of interest

The authors declare that the research was conducted in the absence of any commercial or financial relationships that could be construed as a potential conflict of interest.

Publisher's note

All claims expressed in this article are solely those of the authors and do not necessarily represent those of their affiliated organizations, or those of the publisher, the editors and the reviewers. Any product that may be evaluated in this article, or claim that may be made by its manufacturer, is not guaranteed or endorsed by the publisher.

Supplementary material

The Supplementary Material for this article can be found online at: https://www.frontiersin.org/articles/10.3389/fimmu.2023.1138920/full#supplementary-material

References

1. Powell SN, DeFrank JS, Connell P, Eogan M, Preffer F, Dombkowski D, et al. Differential sensitivity of p53(-) and p53(+) cells to caffeine-induced radiosensitization and override of G2 delay. *Cancer Res* (1995) 55(8):1643–8. doi: 10.1016/0360-3016(95)97825-L

2. Russell KJ, Wiens LW, Demers GW, Galloway DA, Plon SE, Groudine M. Abrogation of the G2 checkpoint results in differential radiosensitization of G1 checkpoint-deficient and G1 checkpoint-competent cells. *Cancer Res* (1995) 55(8):1639–42.

3. Buisson R, Niraj J, Rodrigue A, Ho CK, Kreuzer J, Foo TK, et al. Coupling of homologous recombination and the checkpoint by ATR. *Mol Cell* (2017) 65(2):336–46. doi: 10.1016/j.molcel.2016.12.007

4. Iliakis G, Wang Y, Guan J, Wang H. DNA Damage checkpoint control in cells exposed to ionizing radiation. *Oncogene* (2003) 22(37):5834–47. doi: 10.1038/sj.onc.1206682

5. Castedo M, Perfettini JL, Roumier T, Andreau K, Medema R, Kroemer G. Cell death by mitotic catastrophe: a molecular definition. *Oncogene* (2004) 23(16):2825–37. doi: 10.1038/sj.onc.1207528

6. Rundle S, Bradbury A, Drew Y, Curtin NJ. Targeting the ATR-CHK1 axis in cancer therapy. *Cancers* (2017) 9(5), 1–25. doi: 10.3390/cancers9050041

7. Syljuåsen RG, Hasvold G, Hauge S, Helland A. Targeting lung cancer through inhibition of checkpoint kinases. *Front Genet* (2015) 6:70. doi: 10.3389/fgene.2015.00070

8. Barnieh FM, Loadman PM, Falconer RA. Progress towards a clinically-successful ATR inhibitor for cancer therapy. *Curr Res Pharmacol Drug Discovery* (2021) 2, 100017. doi: 10.1016/j.crphar.2021.100017

9. Dillon MT, Boylan Z, Smith D, Guevara J, Mohammed K, Peckitt C, et al. PATRIOT: a phase I study to assess the tolerability, safety and biological effects of a specific ataxia telangiectasia and Rad3-related (ATR) inhibitor (AZD6738) as a single agent and in combination with palliative radiation therapy in patients with solid tumours. *Clin Trans Radiat Oncol* (2018) 12:16–20. doi: 10.1016/j.ctro.2018.06.001

10. Charpentier M, Spada S, Van Nest SJ, Demaria S. Radiation therapy-induced remodeling of the tumor immune microenvironment. *Semin Cancer Biol* (2022) 86(Pt 2):737–47. doi: 10.1016/j.semcancer.2022.04.003

11. Chan Wah Hak CML, Rullan A, Patin EC, Pedersen M, Melcher AA, Harrington KJ. Enhancing anti-tumour innate immunity by targeting the DNA damage response and pattern recognition receptors in combination with radiotherapy. *Front Oncol* (2022) 12:971959. doi: 10.3389/fonc.2022.971959

12. Golden EB, Frances D, Pellicciotta I, Demaria S, Helen Barcellos-Hoff M, Formenti SC. Radiation fosters dose-dependent and chemotherapy-induced immunogenic cell death. *Oncoimmunology* (2014) 3:e28518. doi: 10.4161/onci.28518

13. Fucikova J, Kepp O, Kasikova L, Petroni G, Yamazaki T, Liu P, et al. Detection of immunogenic cell death and its relevance for cancer therapy. *Cell Death disease* (2020) 11(11):1013. doi: 10.1038/s41419-020-03221-2

14. Jarosz-Biej M, Smolarczyk R, Cichoń T, Kułach N. Tumor microenvironment as a "Game changer" in cancer radiotherapy. *Int J Mol Sci* (2019) 20(13), 1–19. doi: 10.3390/ijms20133212

15. Galluzzi L, Vitale I, Aaronson SA, Abrams JM, Adam D, Agostinis P, et al. Molecular mechanisms of cell death: recommendations of the nomenclature committee on cell death 2018. *Cell Death differentiation* (2018) 25(3):486–541. doi: 10.1038/s41418-017-0012-4

16. Krysko DV, Garg AD, Kaczmarek A, Krysko O, Agostinis P, Vandenabeele P. Immunogenic cell death and DAMPs in cancer therapy. *Nat Rev Cancer* (2012) 12(12):860–75. doi: 10.1038/nrc3380

17. Kepp O, Senovilla L, Vitale I, Vacchelli E, Adjemian S, Agostinis P, et al. Consensus guidelines for the detection of immunogenic cell death. *Oncoimmunology* (2014) 3(9):e955691. doi: 10.4161/21624011.2014.955691

18. Matzinger P. Tolerance, danger, and the extended family. *Annu Rev Immunol* (1994) 12:991–1045. doi: 10.1146/annurev.iy.12.040194.005015

19. Vendetti FP, Karukonda P, Clump DA, Teo T, Lalonde R, Nugent K, et al. ATR kinase inhibitor AZD6738 potentiates CD8+ T cell-dependent antitumor activity following radiation. *J Clin Invest* (2018) 128(9):3926–40. doi: 10.1172/JCI96519

20. Dillon MT, Bergerhoff KF, Pedersen M, Whittock H, Crespo-Rodriguez E, Patin EC, et al. ATR inhibition potentiates the radiation-induced inflammatory tumor microenvironment. *Clin Cancer Res* (2019) 25(11):3392–403. doi: 10.1158/1078-0432.CCR-18-1821

21. Sheng H, Huang Y, Xiao Y, Zhu Z, Shen M, Zhou P, et al. ATR inhibitor AZD6738 enhances the antitumor activity of radiotherapy and immune checkpoint inhibitors by potentiating the tumor immune microenvironment in hepatocellular carcinoma. *J immunother Cancer* (2020) 8(1), 1–13. doi: 10.1136/jitc-2019-000340

22. Hsieh RC, Krishnan S, Wu RC, Boda AR, Liu A, Winkler M, et al. ATR-mediated CD47 and PD-L1 up-regulation restricts radiotherapy-induced immune priming and abscopal responses in colorectal cancer. *Sci Immunol* (2022) 7(72):eabl9330. doi: 10.1126/sciimmunol.abl9330

23. Lopez-Pelaez M, Young L, Vazquez-Chantada M, Nelson N, Durant S, Wilkinson RW, et al. Targeting DNA damage response components induces enhanced STING-dependent type-I IFN response in ATM deficient cancer cells and drives dendritic cell activation. *Oncoimmunology* (2022) 11(1):2117321. doi: 10.1080/2162402X.2022.2117321

24. Feng X, Tubbs A, Zhang C, Tang M, Sridharan S, Wang C, et al. ATR inhibition potentiates ionizing radiation-induced interferon response *via* cytosolic nucleic acid-sensing pathways. *EMBO J* (2020) 39(14):e104036. doi: 10.15252/embj.2019104036

25. Chen J, Harding SM, Natesan R, Tian L, Benci JL, Li W, et al. Cell cycle checkpoints cooperate to suppress DNA- and RNA-associated molecular pattern recognition and anti-tumor immune responses. *Cell Rep* (2020) 32(9):108080. doi: 10.1016/j.celrep.2020.108080

26. Eek Mariampillai A, Hauge S, Øynebråten I, Rødland GE, Corthay A, Syljuåsen RG. Caspase activation counteracts interferon signaling after G2 checkpoint abrogation by ATR inhibition in irradiated human cancer cells. *Front Oncol* (2022) 12:981332. doi: 10.3389/fonc.2022.981332

27. Pitt JM, Kroemer G, Zitvogel L. Immunogenic and non-immunogenic cell death in the tumor microenvironment. *Adv Exp Med Biol* (2017) 1036:65–79. doi: 10.1007/978-3-319-67577-0_5

28. Martins I, Wang Y, Michaud M, Ma Y, Sukkurwala AQ, Shen S, et al. Molecular mechanisms of ATP secretion during immunogenic cell death. *Cell Death differentiation* (2014) 21(1):79–91. doi: 10.1038/cdd.2013.75

29. Panaretakis T, Kepp O, Brockmeier U, Tesniere A, Bjorklund AC, Chapman DC, et al. Mechanisms of pre-apoptotic calreticulin exposure in immunogenic cell death. *EMBO J* (2009) 28(5):578–90. doi: 10.1038/emboj.2009.1

30. Xiong Y, Tang YD, Zheng C. The crosstalk between the caspase family and the cGAS–STING signaling pathway. *J Mol Cell Biol* (2021) 13(10):739–47. doi: 10.1093/jmcb/mjab071

31. Fang Y, Peng K. Regulation of innate immune responses by cell death-associated caspases during virus infection. *FEBS J* (2022) 289(14):4098–111. doi: 10.1111/febs.16051

32. Werthmöller N, Frey B, Wunderlich R, Fietkau R, Gaipl US. Modulation of radiochemoimmunotherapy-induced B16 melanoma cell death by the pan-caspase inhibitor zVAD-fmk induces anti-tumor immunity in a HMGB1-, nucleotide- and T-

cell-dependent manner. *Cell Death disease* (2015) 6(5):e1761. doi: 10.1038/cddis.2015.129

33. Kazama H, Ricci JE, Herndon JM, Hoppe G, Green DR, Ferguson TA. Induction of immunological tolerance by apoptotic cells requires caspase-dependent oxidation of high-mobility group box-1 protein. *Immunity* (2008) 29(1):21–32. doi: 10.1016/j.immuni.2008.05.013

34. Rodriguez-Ruiz ME, Buqué A, Hensler M, Chen J, Bloy N, Petroni G, et al. Apoptotic caspases inhibit abscopal responses to radiation and identify a new prognostic biomarker for breast cancer patients. *Oncoimmunology* (2019) 8(11):e1655964. doi: 10.1080/2162402X.2019.1655964

35. Han C, Liu Z, Zhang Y, Shen A, Dong C, Zhang A, et al. Tumor cells suppress radiation-induced immunity by hijacking caspase 9 signaling. *Nat Immunol* (2020) 21(5):546–54. doi: 10.1038/s41590-020-0641-5

36. Huang Q, Li F, Liu X, Li W, Shi W, Liu FF, et al. Caspase 3-mediated stimulation of tumor cell repopulation during cancer radiotherapy. *Nat Med* (2011) 17(7):860–6. doi: 10.1038/nm.2385

37. Gardella S, Andrei C, Ferrera D, Lotti LV, Torrisi MR, Bianchi ME, et al. The nuclear protein HMGB1 is secreted by monocytes *via* a non-classical, vesicle-mediated secretory pathway. *EMBO Rep* (2002) 3(10):995–1001. doi: 10.1093/embo-reports/kvf198

38. Bell CW, Jiang W, Reich CF3rd, Pisetsky DS. The extracellular release of HMGB1 during apoptotic cell death. *Am J Physiol Cell Physiol* (2006) 291(6):C1318–25. doi: 10.1152/ajpcell.00616.2005

39. Wang H, Bloom O, Zhang M, Vishnubhakat JM, Ombrellino M, Che J, et al. HMG-1 as a late mediator of endotoxin lethality in mice. *Sci (New York NY)* (1999) 285(5425):248–51. doi: 10.1126/science.285.5425.248

40. Wang H, Vishnubhakat JM, Bloom O, Zhang M, Ombrellino M, Sama A, et al. Proinflammatory cytokines (tumor necrosis factor and interleukin 1) stimulate release of high mobility group protein-1 by pituicytes. *Surgery* (1999) 126(2):389–92. doi: 10.1016/S0039-6060(99)70182-0

41. Chen R, Kang R, Tang D. The mechanism of HMGB1 secretion and release. *Exp Mol Med* (2022) 54(2):91–102. doi: 10.1038/s12276-022-00736-w

42. Qin S, Wang H, Yuan R, Li H, Ochani M, Ochani K, et al. Role of HMGB1 in apoptosis-mediated sepsis lethality. *J Exp Med* (2006) 203(7):1637–42. doi: 10.1084/jem.20052203

43. Tsubota M, Miyazaki T, Ikeda Y, Hayashi Y, Aokiba Y, Tomita S, et al. Caspase-dependent HMGB1 release from macrophages participates in peripheral neuropathy caused by bortezomib, a proteasome-inhibiting chemotherapeutic agent, in mice. *Cells* (2021) 10(10), 1–19. doi: 10.3390/cells10102550

44. Hufnagel S, Xu H, Colemam MF, Valdes SA, Liu KA, Hursting SD, et al. 4-(N)-Docosahexaenoyl 2', 2'-difluorodeoxycytidine induces immunogenic cell death in colon and pancreatic carcinoma models as a single agent. *Cancer chemother Pharmacol* (2022) 89(1):59–69. doi: 10.1007/s00280-021-04367-2

45. Petrazzuolo A, Perez-Lanzon M, Martins I, Liu P, Kepp O, Minard-Colin V, et al. Pharmacological inhibitors of anaplastic lymphoma kinase (ALK) induce immunogenic cell death through on-target effects. *Cell Death disease* (2021) 12(8):713. doi: 10.1038/s41419-021-03997-x

46. Gameiro SR, Jammeh ML, Wattenberg MM, Tsang KY, Ferrone S, Hodge JW. Radiation-induced immunogenic modulation of tumor enhances antigen processing and calreticulin exposure, resulting in enhanced T-cell killing. *Oncotarget* (2014) 5(2):403–16. doi: 10.18632/oncotarget.1719

47. Rødland GE, Hauge S, Hasvold G, Bay LTE, Raabe TTH, Joel M, et al. Differential effects of combined ATR/WEE1 inhibition in cancer cells. *Cancers* (2021) 13(15), 1–22. doi: 10.3390/cancers13153790

48. Kaminskyy VO, Hååg P, Novak M, Végvári Á, Arapi V, Lewensohn R, et al. EPHA2 interacts with DNA-PK(cs) in cell nucleus and controls ionizing radiation responses in non-small cell lung cancer cells. *Cancers* (2021) 13(5), 1–21. doi: 10.3390/cancers13051010

49. Obeid M, Tesniere A, Ghiringhelli F, Fimia GM, Apetoh L, Perfettini JL, et al. Calreticulin exposure dictates the immunogenicity of cancer cell death. *Nat Med* (2007) 13(1):54–61. doi: 10.1038/nm1523

50. Liu C, Wang X, Qin W, Tu J, Li C, Zhao W, et al. Combining radiation and the ATR inhibitor berzosertib activates STING signaling and enhances immunotherapy *via* inhibiting SHP1 function in colorectal cancer. *Cancer Commun (London England)* (2023) 43(4):435–54. doi: 10.1002/cac2.12412

51. Patin EC, Dillon MT, Nenclares P, Grove L, Soliman H, Leslie I, et al. Harnessing radiotherapy-induced NK-cell activity by combining DNA damage-response inhibition and immune checkpoint blockade. *J immunother Cancer* (2022) 10(3), 1–13. doi: 10.1136/jitc-2021-004306

52. Alimzhanov M, Soulard P, Zimmermann A, Schroeder A, Mehr KT, Amendt C, et al. ATR inhibitor M6620 enhances anti-tumor efficacy of the combination of the anti-PD-L1 antibody avelumab with platinum-based chemotherapy. *Cancer Res* (2019) 79(13_Supplement):2269. doi: 10.1158/1538-7445.AM2019-2269

53. Ngoi NYL, Peng G, Yap TA. A tale of two checkpoints: ATR inhibition and PD-(L)1 blockade. *Annu Rev Med* (2022) 73:231–50. doi: 10.1146/annurev-med-042320-025136

54. Kong Y, Ma Y, Zhao X, Pan J, Xu Z, Zhang L. Optimizing the treatment schedule of radiotherapy combined with anti-PD-1/PD-L1 immunotherapy in metastatic cancers. *Front Oncol* (2021) 11:638873. doi: 10.3389/fonc.2021.638873

55. Sato H, Okonogi N, Nakano T. Rationale of combination of anti-PD-1/PD-L1 antibody therapy and radiotherapy for cancer treatment. *Int J Clin Oncol* (2020) 25(5):801–9. doi: 10.1007/s10147-020-01666-1

56. Colton M, Cheadle EJ, Honeychurch J, Illidge TM. Reprogramming the tumour microenvironment by radiotherapy: implications for radiotherapy and immunotherapy combinations. *Radiat Oncol (London England)* (2020) 15(1):254. doi: 10.1186/s13014-020-01678-1

57. Vendetti FP, Pandya P, Clump DA, Schamus-Haynes S, Tavakoli M, diMayorca M, et al. The schedule of ATR inhibitor AZD6738 can potentiate or abolish antitumor immune responses to radiotherapy. *JCI Insight* (2023) 8(4), 1–19. doi: 10.1172/jci.insight.165615

Frontiers in Immunology

Explores novel approaches and diagnoses to treat immune disorders.

The official journal of the International Union of Immunological Societies (IUIS) and the most cited in its field, leading the way for research across basic, translational and clinical immunology.

Discover the latest Research Topics

See more →

Frontiers

Avenue du Tribunal-Fédéral 34
1005 Lausanne, Switzerland
frontiersin.org

Contact us

+41 (0)21 510 17 00
frontiersin.org/about/contact